UNDERSTANDING UPPER CRUSTAL SILICIC MAGMATIC SYSTEMS USING THE TEMPORAL, COMPOSITIONAL AND THERMAL RECORD IN ZIRCON

By

Lily Lowery Claiborne

Dissertation

Submitted to the Faculty of the

Graduate School of Vanderbilt University

in partial fulfillment of the requirements

for the degree of

DOCTOR OF PHILOSOPHY

in

Environmental Engineering

May, 2011

Nashville, Tennessee

Approved:

Dr. Calvin F. Miller

Dr. David J. Furbish

Dr. John C. Ayers

Dr. Guilherme A.R. Gualda

Dr. Frank Parker

Dr. James Clarke

To my infinitely supportive mother, Margia Nelle McCulloch

and

To my husband and my son, Andrew and Joe, my reasons for everything

ACKNOWLEDGEMENTS

This work would not have been possible without the financial support of the National Science Foundation, grants EAR-0409876, EAR-0107094, and EAR0635922 and the NSF-funded Center for the Integration of Research, Teaching, and Learning (CIRTL).

I am especially indebted to Dr. Calvin Miller, who provided intellectual and professional guidance to me on this work from start to finish, and who went above and beyond to provide me with every possible opportunity to succeed. He has taught me, by example, what a good scientist and mentor should be, and I will spend the rest of my career striving to become half as admirable, respected, giving and knowledgeable as he is.

I am grateful to Dr. Guil Gualda, who consistently required me to look at things with renewed skepticism. I am grateful to Dr. Michael Clynne, Dr. Ed Wolfe, Dr. Joseph Wooden, Dr. Kari Cooper, Barry Walker, Ashley Bromley, and Danny Flanagan, all of whom collaborated with me on this work and lent me either their expertise, their time and energy, their facilities, or all of the above. Each member of my dissertation committee has provided valuable insights and perspectives throughout this work, particularly Dr. David Furbish and Dr. John Ayers.

Most importantly, I must thank my family. They have sacrificed for me to follow this passion. I would like to thank my husband for making things work when I was away or too busy and for requiring me to retain a balanced life and thereby, my sanity. These last months would have been dark and difficult, but for my new baby son who provides me unsurpassed joy. Finally, I owe a great debt of gratitude (among other things) to my mother, who has unendingly given her support, her time, and anything else she can think of to help make this happen.

TABLE OF CONTENTS

Page

LIST OF TABLES

LIST OF FIGURES

CHAPTER I

INTRODUCTION

1. Overview

Recent studies have established that melts and crystals erupted from many of the world's arc volcanoes are generally relatively young, with often only a few thousand years passing between petrogenesis of a magma at its deep source and eruption of that magma (Jicha et al., 2009; Clark et al., 1998; Zellmer et al., 2005). This leads to a model of arc volcanic systems in which magmas are produced at depth, move upward toward the surface relatively rapidly, and are only stored for short periods beneath the volcano prior to eruption. This timescale contrasts significantly with well established, extended timescales of larger volcanic (Wilson and Charlier, 2009; Bacon and Lowenstern, 2005; Simon and Reid, 2005) and plutonic systems (Walker et al., 2007; Miller et al., 2007) in which magmas appear to accumulate and interact in the crust over hundreds of thousands to millions of years, apparently suggesting a fundamental difference in the behavior of relatively small arc volcanoes and larger magmatic systems. These short timescales also appear in sharp contrast to the extended lifetimes of these volcanic centers and may be prohibitive of processes that are thought to occur in evolving magmas prior to eruption, including magma mixing and fractional crystallization.

The mineral zircon provides a uniquely appropriate tool to address this paradox. As a consequence of extremely low diffusivities and solubility in melts and fluids and its resistance to recrystallization, zircon is well known as an extremely robust geochronometer. This reputation is primarily based upon its reliability for dating relatively old, high-temperature processes by U-Pb dating, but the same characteristics make it an attractive target for dating pre-eruptive

processes in young volcanic systems through ^{238}U-^{230}Th disequilibria. Minimal diffusion (Cherniak et al., 1997a; Cherniak et al., 1997b) also makes possible preservation of multiple ages of growth in single grains, and improved microbeam techniques permit *in situ* ^{238}U-^{230}Th as well as U-Pb dating. Zircon crystals also preserve the elemental zoning record of environments in which they crystallized. Very recently, development of improved elemental analysis by ion probe (SHRIMP-RG) (Mazdab and Wooden, 2006), refined interpretations of Ti and Hf abundance patterns (Claiborne et al., 2006), and a sensitive new Ti-in-zircon geothermometer (Watson and Harrison, 2005) have made possible a far clearer reading of the environmental record of zircon growth. Combining the full elemental record with *in situ* geochronology provides a powerful tool for interpreting the history of magma systems and rates of processes therein – initial crystallization, melt evolution, storage, recharging and rejuvenation, entrainment, isolation of and mechanical communication between portions of a system, and so on.

My primary objectives in this work are to better understand

(1) the timescales and processes by which silicic magma is transported, stored, and evolves within the upper crust.

(2) the growth, destruction, and transport of zircon within these upper crustal magma systems, and the record of magmatic conditions and processes preserved within zircon crystals.

(3) the evolution of an especially important system in terms of scientific progress and human impact - the one that has formed Mount St. Helens

My previous research evaluated age distributions and Hf and Ti zoning in zircons from a composite batholith of Miocene age in Nevada (Claiborne et al., 2006; Walker et al., 2007). My results suggest that there is great promise for additional elemental zoning study of this plutonic system and for applying similar methods to the erupted parts of young magmatic system. Three considerations compelled me to attempt such a study. First, I believe that there is much to be learned through investigating systems from different perspectives – although both are

magmatic products, volcanic and plutonic rocks are widely understood to provide different sorts of information, because of rate and environment of solidification. The question is, do zircons reveal similar or different sorts of histories in the plutonic and volcanic realms, and what does this tell us about magmatic processes and plutonic-volcanic connections? Second, while Hf and Ti zoning in zircons can provide useful information on magmatic processes (Claiborne et al., 2006), a more complete study of zircon elemental composition, including rare earth elements, from both plutonic and volcanic environments can provide more detailed information on magmatic conditions, compositions, and coeval crystallization. Third, plutonic zircons are loaded with information, but although they are valued for the age information they can provide, the precision of these ages falls short of what is necessary to understand the timescales, and therefore the nature, of the processes that led to their growth (and dissolution). At present, absolute uncertainty of *in situ* U-Pb zircon ages is invariably $>10^5$ years, even for high quality analyses of young (millions of years) grains. Our zoning studies suggest that fluctuations in conditions during zircon growth occur on considerably finer time scales. Using ^{238}U-^{230}Th disequilibria dating on very young zircons (<~50 ka), uncertainties on the order of 10^4 yrs are anticipated and under the best circumstances better precision can be achieved (e.g. Charlier et al., 2003, 2005), providing much better resolution of timing and rates of magmatic processes.

Finally, Mount St. Helens (MSH), as a young, iconic volcano with a recently discovered older history, provides an ideal case to test the efficacy of the zircon record in relating the history of an active magmatic center and a system where my results can achieve maximum impact and significance. Its infamous 1980 eruption has attracted many of the world's foremost volcanologists and volcanic petrologists, and they have provided a trove of data and interpretations on the volcano's recent history (<4 ka) that serves as context for the information in the zircons. Because it was only recently recognized, the older history of the volcano (4-300

ka; Clynne et al., 2009) is far less well characterized, and this work contributes to the general understanding of that older history. This study not only dates important but otherwise inaccessible events in the history of this system, but also provides a record of otherwise hidden thermal and compositional fluctuations and of mechanical exchange between different portions of the system.

2. Geologic Setting and Mount St. Helens Volcanism

Mount St. Helens lies in the Cascade Range of southwestern Washington (Figure 1), a volcanic arc resulting from the subduction of the eastward moving Juan de Fuca Plate beneath the westward moving North American Plate (Weaver and Baker, 1988). Crustal thickness has been estimated as 40-46 km throughout the Cascade arc (Mooney and Weaver, 1989), and the southern Washington Cascades lie on a crustal block with particularly high conductivity, resulting in designation of this block as the southern Washington Cascades conductor (Stanley et al., 1987). Mount St. Helens lies above the western edge of this conductive zone (Weaver, 1989; Figure 2), and it has been recently suggested that this zone could represent a melt-bearing portion of the middle crust that feeds the southern Washington Cascade volcanoes (Hill et al., 2009; Figure 2). Mount St. Helens is uniquely located on the St. Helens Shear Zone (Weaver and Smith, 1983) at a location where slight offset in the zone results in local crustal extension (Weaver, 1989), facilitating the magmatism.

Researchers have recently established that the MSH magmatic system has been erupting for at least 300,000 years (Table 1), over which time volcanism has migrated 10 km eastward from Goat Mountain to the location of the current edifice (Clynne et al., 2008; Figure 1). The dominantly erupted dacites appear to be lower crustal melts generated in response to intrusion of mantle basalts, which are also occasionally erupted, and relatively sparse

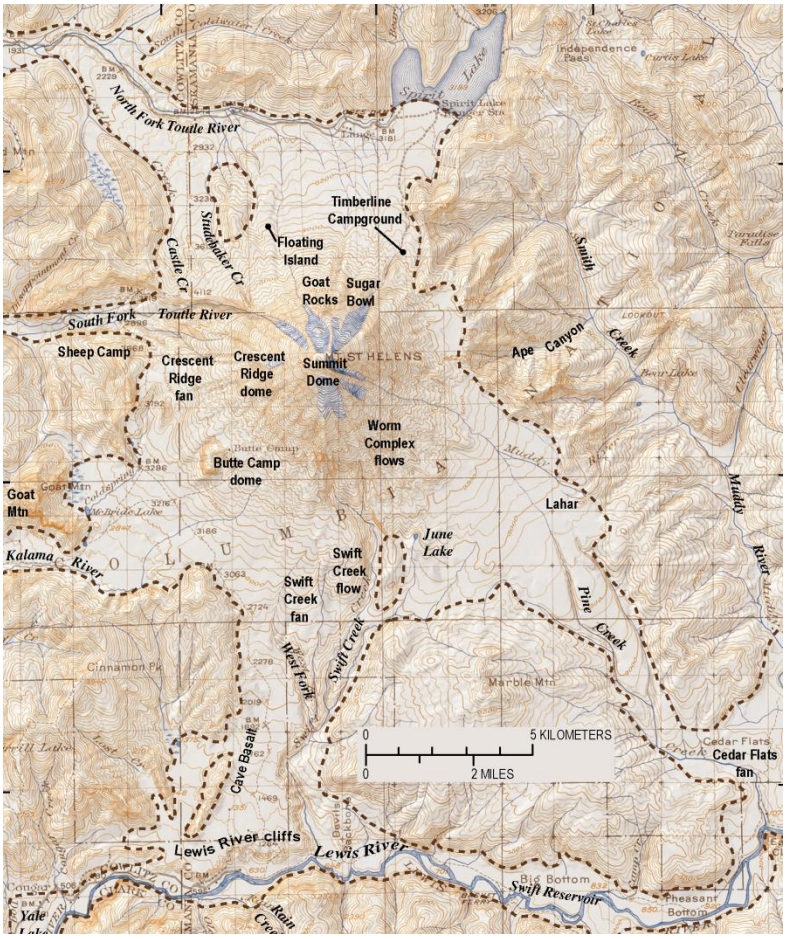

Figure 1: Topographic map of the Mount St. Helens area (pre-1980) with an inset showing its location in southwestern Washington. Note Goat Mountain and Butte Camp dome, early eruptive centers for the magmatic system that has more recently created the current Mount St. Helens volcanic edifice. *From Clynne et al. (2009).*

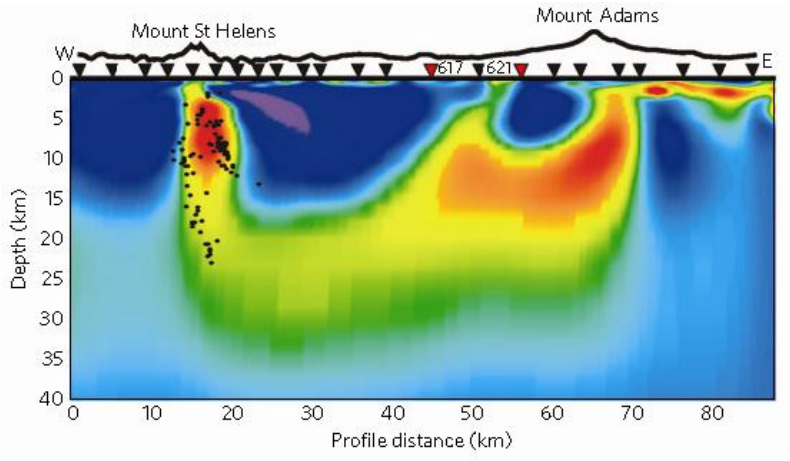

Figure 2: Model of mid-crustal conductor. High conductivity is shown in warm colors (red), low conductivity is shown in blue. Black dots show the location of earthquake hypocenters from the 1980 eruption of Mount St. Helens. *From Hill et al. (2009)*

Table 1: Eruptive history of Mount St. Helens, based on Clynne et al. (2009). **domes and airfall tephras in all episodes, pyroclastic flows in most*

Stage and Age	Period and Age	Erupted products*
Spirit Lake Stage 3,900–0 years	Modern Eruptive Period (1980–2006 CE)	dacite-silicic andesite
	Goat Rocks Eruptive Period (1800–1857 CE)	dacite, silicic andesite lava
	Kalama Eruptive Period (1479–1720 CE)	dacite, andesite lava,
	Sugar Bowl Eruptive Period (1,200–1,150 ybp)	dacite-rhyodacite
	Castle Creek Eruptive Period (2,550–1,895 ybp)	basalt lava, andesite lava, dacite
	Pine Creek Eruptive Period (3,000–2,550 ybp)	dacite, andesite lava
	Smith Creek Eruptive Period (3,900–3,300 ybp)	dacite
Dormant Interval 12.5–3.9 ka		
Swift Creek Stage 16–12.5 ka		dacite-silicic andesite
Dormant Interval 18–16 ka		
Cougar Stage 28–18 ka		dacite, andesite lava
Dormant Interval 35–28 ka		
Ape Canyon Stage (younger) ~160–35 ka		dacite-rhyodacite-silicic andesite
Dormant Interval ~250-160 ka		
Ape Canyon Stage (older) ~300-250 ka		dacite-rhyodacite-silicic andesite

intermediate compositions are produced by mixing of the two end members (Pallister et al., 2008; Smith and Leeman, 1993; Smith and Leeman, 1987). Trends in geochemistry and mineral assemblages suggest that the earlier erupted magmas were generally fractionated, cool, and wet with no evidence for interaction with more primitive magmas (Clynne et al., 2008). As the system matured, the mafic input and influence increased, and the dacitic magmas became hotter, drier and showed more evidence of interaction with mafic end members (Clynne et al., 2008).

Geophysical studies of the crust and petrologic studies of MSH's recently erupted products provide clues to the size, shape, conditions, and timing of processes in the modern magma reservoir. Uranium-series disequilibria of glasses indicate that melts are generated within a few thousand years of eruption, and feldspars appear to have grown from days to several thousands of years before eruption (Cooper and Donnelly, 2008; Cooper and Reid, 2003; Volpe and Hammond, 1991). The complex compositional zoning and multiple populations of pyroxene, amphiboles and plagioclase indicate that magma mixing, crystal recycling on the scale of thousands of years (Streck et al., 2008), and convection in the chamber are common (Cooper and Donnelly, 2008; Cooper and Reid, 2003; Rutherford and Devine, 2008). Iron-titanium oxides indicate storage at magmatic temperatures from 820°C to 940°C (Rutherford and Devine, 2008; Rutherford et al., 1985). Many of the smallest crystals (microlites) form in the conduit due to decompression and degassing during ascent and eruption (Blundy and Cashman, 2001), and so record only this final event in the magma's history. Seismic and petrologic (Volpe and Hammond, 1991) studies indicate that melt-rich magma is stored in a widened conduit at 5 to 12 km depth (Pallister et al., 2008; Gardner et al., 1995). The above information creates a vivid model of the upper part of the modern magmatic system: magmas generated in the lower crust ascend into a widened conduit at 5 to 12 km depth, approximately 4 km^3 in volume, in which

they convect, mingle and partially crystallize in the short timescales before eruption as well as recycle phenocrysts from crystal mushes that are stored around and beneath the reservoir on the scale of thousands of years (Pallister et al., 2008; Figure 3). However, the older portion (>4 ka) of the recently established 300,000 year eruptive history is less clearly understood, and how the magmatic system initially formed and evolved through time into its current state has not been deeply investigated.

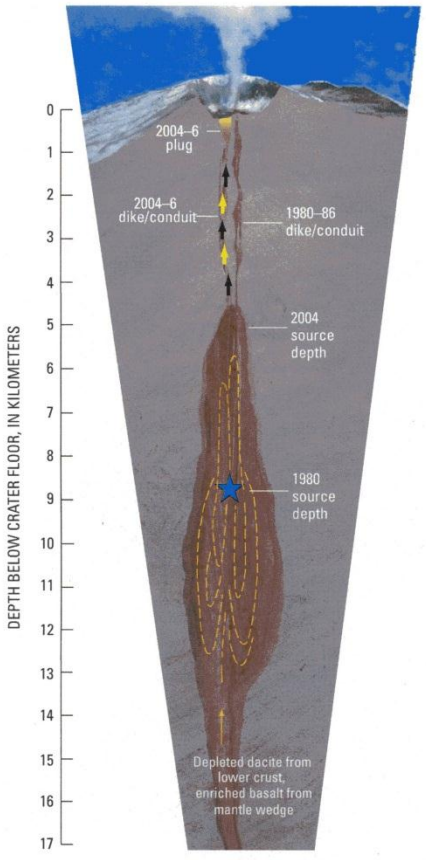

Figure 3: Schematic showing proposed modern magma reservoir beneath Mount St. Helens volcano, based on compilation of geophysical and petrologic data from recently erupted products. Yellow lines represent paths of convecting magma *(from Pallister et al., 2008).*

3. Zircon

3.1. Zircon growth and dissolution

The systematics of zircon saturation and Zr diffusivity in felsic melts are fairly well established (Watson and Harrison, 1983; Harrison and Watson, 1983; Hanchar and Watson, 2003), and as a consequence approximate rates of growth and dissolution can be computed (cf. Bacon and Lowenstern, 2005). To characterize dissolution rates, Watson (1996) defines the parameter $U_0(Dt/r_0^2)$ where U_0 is undersaturation of melt in zircon (ppm), D is diffusivity (cm2/s), t is time (s), and r_0 is initial radius of the zircon. For values of this parameter >4 to 5, dissolution of all reasonable-sized zircons is complete; between 2 and 4, depending on size, dissolution is minor to extensive; and for values <1-2, all except very small zircons remain largely intact. This has important implications for zircon behavior in plutono-volcanic magma systems with (anticipated) fluctuations in temperature and variations in water content (which strongly influences diffusivity). For example, take a zircon with 50 micron radius, initially residing in a zircon-saturated melt at T = 750°C (Zr = 100 ppm); zircon and enclosing melt experience a rapid and substantial increase in temperature. This zircon will survive for approximately 100,000 years (Watson's parameter = 4.6) at T = 770°C (U_0= 25 ppm) if melt H_2O has 3 wt%. If instead T rises to 900°C (U_0 now = 400 ppm) and H_2O = 6 wt%, complete dissolution of the same zircon transpires in about 20 years. Furthermore, although the process and mathematics of crystal growth are essentially simply a "mirror image" of dissolution *at the same conditions*, under normal natural circumstances growth will be much slower than dissolution. This is because degree of oversaturation will generally be much less than degree of undersaturation, and D falls rapidly with decreasing T. Because melts typically reach saturation in zircon at <~850°C (Watson, 1996; Miller et al., 2003) and $|-U_0|$ is likely to be <~10 ppm (unless cooling is very

rapid, which effectively precludes zircon growth), zircons will generally require a minimum thousands years to achieve lengths of ~100 microns (cf. Watson, 1996). Growth at such rates suggests residence in a more or less stable magma chamber, probably in a crystal mush: in typical intermediate to moderately felsic magmas, like the MSH dacites, zircon saturation is not reached until crystal fraction is fairly high. This seems to imply that zircon growth occurs within an environment that is more "plutonic" than "volcanic," and that erupted zircons may represent disruption and entrainment of plutonic mushes (cf. Vazquez and Reid, 2002; Bacon and Lowenstern, 2005; Simon and Reid, 2005; or Cooper and Reid, 2003, regarding major phases).

3.2. Zircon Geochronology: U-Pb dating, ^{238}U-^{230}Th disequilibria, and (U-Th)/He double dating

When zircon crystallizes, it fractionates U from its daughter products in the melt, incorporating U in relative abundance, and essentially none of its daughter products (including Pb, Th, or He). Uranium, Pb and Th have extremely low diffusivities in zircon (Cherniak et al., 1997a; 1997b), and are therefore locked in at the time of crystallization. Measuring the abundances of these isotopes, therefore, allows us to determine the age of crystallization of a given zircon, or even zircon zone, with the use of spot analysis techniques.

For zircons older than ~ 300ka, U-Pb dating gives the most reliable results. ^{238}Uranium decays to ^{206}Pb following the equation $^{206}Pb = {}^{206}Pb_0 + {}^{238}U\,(e^{\lambda t}-1)$ where $^{206}Pb_0$ is the initial ^{206}Pb present in the zircon at the time of crystallization, λ is the decay constant, and t represents time. ^{206}Pb should be essentially zero in zircon, although we measure the abundance of nonradiogenic ^{204}Pb and use the known natural ratio of $^{204}Pb/^{206}Pb$ to make any necessary corrections. Similarly, ^{235}U decays to ^{206}Pb following the equation $^{207}Pb = {}^{207}Pb_0 + {}^{235}U\,(e^{\lambda t}-1)$. By measuring both systems, we are provided with a cross-check on the zircon age.

For zircons younger than ~300ka, ^{238}U-^{230}Th disequilibria dating gives the most precise results. Unlike Pb isotopes, which are the stable decay product of the various U isotopes, ^{230}Th is an intermediate, radioactive daughter product of ^{238}U. At the time of zircon crystallization, fractionation of U from Th results in an activity ratio of $(^{238}U/^{230}Th) \neq 1$, or disequilibrium between the two. Activity is essentially a measure of the amount of decay occurring at a given time. It is defined by the decay constant times the number of parent atoms (λN). Over the course of approximately six half-lives of the radioactive daughter (corresponding to approximately 350,000 years for ^{230}Th), the activity ratio returns to one as the daughter accumulates and the system reaches secular equilibrium, where the relative abundances of the two species will no longer change as decay progresses (see Figure 4). During this time period before secular equilibrium is reached, by measuring the relative abundances of the isotopes and calculating the activity ratio, we can determine the time since the fractionation, (in this case, crystallization) of the zircon (see Figure 4).

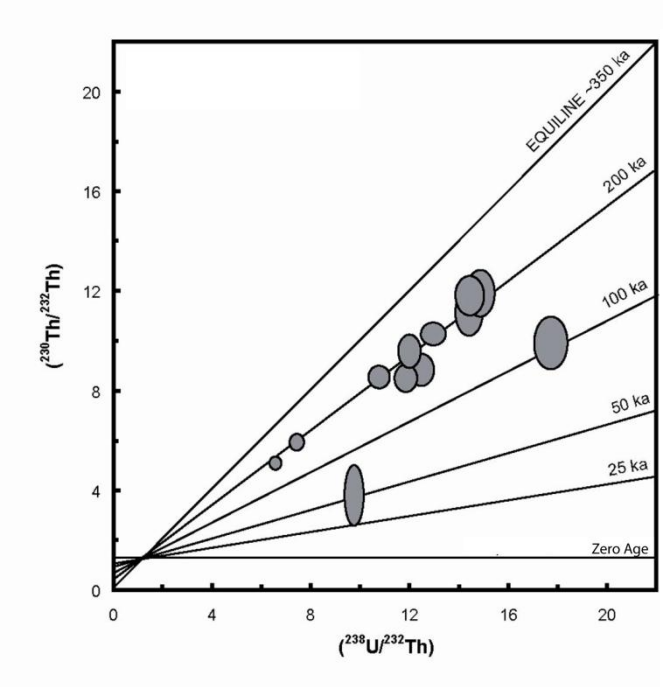

Figure 4: Isochron diagram showing systematics of the U-Th disequilibria dating system. The parentheses are indicative of activity ratios. The dark lines are reference lines of various ages. The horizontal line represents a zero age (with no ^{230}Th yet produced). The equiline, with a slope of 1, represents the time at which the ^{238}U-^{230}Th system reaches equilibrium. Each ellipse represents a hypothetical SHRIMP analysis of a zircon grain. This data set would indicate zircon ages of approximately 50, 100 and 180-200 ka.

3.3. Titanium-in-zircon thermometry

Recent work by Watson and Harrison (2005), Watson et al. (2006) and Ferry and Watson (2007) has demonstrated that incorporation of Ti into zircon depends on temperature, and the activities of TiO_2 and SiO_2 in the melt. Given appropriate geochemical constraints, the Ti concentration of zircon can therefore be used to estimate the magma temperature at the time of crystallization. Watson et al. (2006) and Watson and Harrison (2005) described the dependence of Ti concentration in zircon on crystallization temperature, and defined a thermometer based on experimental results and well-characterized natural samples. This initial form of the thermometer assumed that the melt from which the zircon grows was saturated in quartz, but allowed for variability in a_{TiO2}. Ferry and Watson (2007) revised the thermometer calculation to allow for undersaturation in both rutile and quartz by incorporating a_{TiO2} and a_{SiO2}, following the equation: $T(K) = (-4800\pm86)/(\log Ti(ppm)+\log a_{SiO2}-\log a_{TiO2}-(5.711\pm0.072))$, where Ti (ppm) is concentration of Ti in a zircon domain that crystallized from a magma with the specified activities of $aSiO_2$ and $aTiO_2$.

Accurate calculation of temperature requires knowledge of the activity of TiO_2 (a_{TiO_2}) and SiO_2 (a_{SiO_2}) in the melt at the time of crystallization (Figure 5). Without this constraint, Ti concentration in zircon can be indicative of variations in melt composition at a constant (or varying) temperature. The necessity for a_{TiO_2} and a_{SiO_2}constraints can prove an impediment to use of the thermometer, as zircon studies have shown that individual grains often exhibit complex histories with growth from different melts at different times; in general, zircons often were not in equilibrium with the melt or glass that was their final host (Miller and Wooden, 2004; Bacon and Lowenstern, 2005; Walker et al., 2007). Evolution of the melt during crystallization of a magma or events such as rejuvenation and magma mixing will likely result in

changes in a_{TiO_2} and a_{SiO_2}. However, expected simultaneous changes in a_{TiO_2} and a_{SiO_2} have counter-effects on the thermometer, with one balancing the effect of the other, and growth of Ti-bearing minerals may roughly buffer a_{TiO_2} during melt evolution (Watson et al., 2006; Ferry and Watson, 2007).

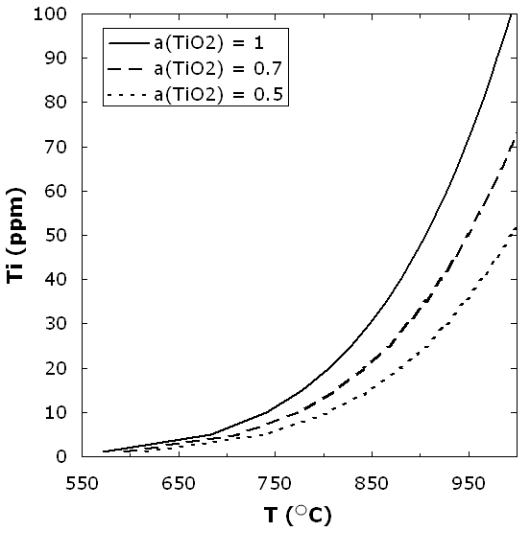

Figure 5: Ti content of zircon as a function of $a(TiO_2)$ and temperature, assuming $a(SiO_2)$=1. Based on Ferry and Watson (2007).

3.4. Hafnium and Trace Element Composition of Zircon

Growth and dissolution of accessory phases, including zircon, act as a primary control over the trace element budget of the magmas (e.g. Wark and Miller, 1993; Hoskin and Schaltegger, 2003; Claiborne et al., 2006). The trace element composition of these minerals, then, can reflect the trace element budget in the melt at the time of crystallization. During zircon growth, elements partition into the zircon structure primarily by occupying the 8-fold or 4-fold coordinated sites of tetravalent Zr or Si, respectively. Hf, a tetravalent cation with radius 0.83 Å, is nearly identical in size and charge to zirconium and the two behave nearly identically. Zircon, therefore, is essentially a zircon-hafnon solid solution (Figure 6), with most natural zircons containing between 1 and 2 wt% HfO_2 (Ahrens and Erlank, 1969; Heaman et al., 1990; Bea et al., 2006; Belousova et al., 2002; Hoskin and Schaltegger, 2003; Claiborne et al., 2006). As zircon is the primary reservoir for the crust's Hf, growth of zircon controls the Hf composition of any melt. As zircon grows both the Zr and Hf concentrations in the magma will decrease. However, this growth preferentially incorporates Zr over Hf and therefore leads to a decrease in the Zr/Hf of the remaining melt. This process leads to increasing Hf concentration in growing zircon crystals (Claiborne et al., 2006).

Trace elements found in reasonably measureable quantities in natural zircon include U, Th, Ti, REE, Sc, Y and P. Like Zirconium, Th, U, Ti, and Ce^{+4} are primarily tetravalent with 8-coordinated atoms of ionic radii 1.05 Å, 1.00 Å, 0.74 Å, and 0.97 Å, respectively (Faure, 1986). The lanthanide rare earth elements are primarily trivalent (with the exception of Ce, which can also be tetravalent, and Eu, which is primarily divalent, depending on oxidation conditions) and

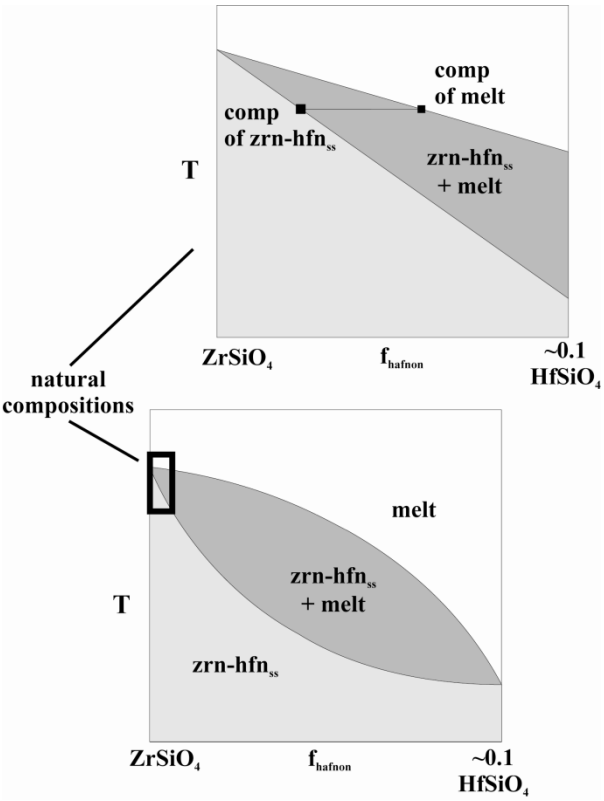

Figure 6: Schematic phase diagram showing crystallization of zircon-hafnon solid solution. *From Claiborne et al. (2006)*

decrease in atomic radius from 1.16 Å (La) to 0.98 Å (Lu) with increasing atomic number due to the Lanthanide Contraction. The REE Ho has the same radius as Y (1.02 Å) and the same charge, so Y behaves in a nearly identical manner to middle to heavy REE. Sc is a trivalent cation, with 8-fold coordination radius 0.87 Å.

Substitution of these trivalent trace elements, including REE, into zircon involves coupled substitution for charge compensation. The decreasing size of the REE with increasing atomic number results in the heavy REE partitioning more strongly into the Zr site than the larger light REE. The primary charge-compensating mechanism for substitution of REE into zircon may be the xenotime ($(Y,REE)PO_4$) substitution, in which Y^{3+} or REE^{3+} replace Zr^{4+} in the dodecahedral site and P^{5+} (radius 0.17 Å) replaces Si^{4+} (radius 0.26 Å) in the tetrahedral site (Finch and Hanchar, 2003; Harley and Kelly, 2007). However, composition of natural zircon does not show a ratio of unity between REE and P, suggesting that some more complex charge-balance mechanisms are also in effect (Hoskin and Schaltegger, 2003). Strain at the Si site caused by the significant size difference between the Si and P cations results in inability of the zircon structure to incorporate sufficient P to balance all the REE (Finch and Hanchar, 2003). Potential alternative charge balance mechanisms may include OH^- exchange for O^{2-} or coupled substitution of other ions (Nb^{5+}, Ta^{5+}) in the Zr^{4+} site (Hoskin and Schaltegger, 2003). Currently, no evidence has been recorded for interstitial REE, although interstitial charge compensators such as Al^{3+} and H^+ may play an essential role in REE substitution (Hoskin and Schaltegger, 2003).

The abundance of these trace elements in the zircon is indicative of their abundance in the magmas from which the zircon grew. The zircon compositions, therefore, record events that affect the melt composition including melt rejuvenation, mixing, and fractionation, coeval growth of other REE-rich accessory minerals, and possibly fluctuation in fO_2. It is difficult to accurately calculate melt compositions, however, as experimentally measured trace element

partition coefficients vary significantly with experimental conditions and may not reflect equilibrium crystallization (Luo and Ayers, 2009).

4. Components of the Thesis

I begin by addressing the geochemical nature of zircons from a plutonic system, the Miocene-aged Spirit Mountain batholith in southern Nevada. These zircons have been previously characterized geochronologically, and the field and geochemical relations of the batholith are well constrained (Walker et al., 2007; Claiborne et al., 2006), so it provides an ideal system in which to test the geochemical and thermal record in the zircons, particularly the less-well understood zircon-trace element systematics and further our understanding of plutonic magmatic systems. This work is reported in chapter II and has been published in *Contributions to Mineralogy and Petrology* (Claiborne et al., 2010a).

Because the relatively large uncertainties on the U-Pb ages of this Miocene-aged system limit our ability to resolve magmatic (geochemical and/or geothermal) events on relevant time scales, and considering suggestions that the magmatic systems and processes that result in plutons may be very different from the magmatic systems of volcanoes (Coleman and Glazner, 2004), I selected a young volcanic system (Mount St. Helens, WA) to further test the efficacy of the zircon record and to further constrain our understanding of upper crustal magmatic systems. I use U-series disequilibria dating, U-Pb dating and trace element analysis of zircons to unravel the history of the magmatic plumbing system of Mount St. Helens. Chapter III summarizes the fundamental findings of this work, focusing primarily on the age spectra and the Hf and Ti findings, and has been published in *Geology* (Claiborne et al., 2010b). The details of this study, including the detailed geochronology, the remaining trace elements, and whole rock isotopic and geochemical analyses performed to contextualize the zircon data, along with more

nuanced implications are reported in chapter IV, which is in preparation for submittal in 2011 to *Journal of Petrology.*

Because of my use of U-Series disequilibria dating in my Mount St. Helens project and my own struggles with explaining the nuances of the process to students and colleagues alike, I became aware of an apparent difficulty in understanding this geochronologic tool among the geologic community. Existing diagrams aimed at explaining the system and its use in dating were not accurate and implied some characteristics inconsistent with the nature of the radioactive decay chain. In an attempt to clearly illustrate the U-Series decay process and its use in dating, I chose to connect this difficult concept with a more intuitive process, and created diagrams showing buckets filling with and losing fluid as analogies for buildup and decay of radiogenic isotopes in the decay chain. The behavior of the two systems (the hydrostatics and radioactive decay) is mathematically identical and allows close analogous treatment. This led to development of a new laboratory activity using beakers of fluid and the fundamentals of hydrostatics to teach basic radioactive decay and radiometric dating. This activity can be modified to accurately mimic the U-series system and disequilibria dating, similar to our original diagrams. I tested the effect of the basic version of this activity on student learning during two consecutive semesters in each of five sections of EES111, the laboratory section of EES101, Dynamic Earth. The laboratory activity and our evaluation of its effectiveness are reported in chapter V, which has been submitted for publication with Calvin Miller as co-author to *Journal of Geoscience Education* and is currently in review at the time of this writing.

In chapter VI, I draw conclusions surrounding my main objectives, describe remaining questions that will further our understanding of upper crustal magmatic systems, and advise on future use of zircon as a record of magmatic events and processes.

5. References

Ahrens, L.H. and Erlank, A.J. (1969) Hafnium In: Wedepohl KH (ed) *Handbook of Geochemistry*, 2-5, sections B-O. Springer, Berlin.

Bacon, C.R. and Lowenstern, J.B. (2005) Late Pleistocene granodiorite source for recycled zircon and phenocrysts in rhyodacite lava at Crater Lake, Oregon. *Earth and Planetary Science Letters,* **233,** 277-293.

Bacon, C.R., Persing, H.M., Wooden, J.L. and Ireland, T.R. (2000) Late Pleistocene granodiorite beneath Crater Lake caldera, Oregon, dated by ion microprobe. *Geology*, **28**, 467-470.

Bea, F., Montero, P. and Ortega, M. (2006) A LA-ICPMS evaluation of Zr reservoirs in common crustal rocks: Implications for Zr and Hf geochemistry and zircon-forming processes. *Canadian Mineralogist*, **44**, 693-714.

Belousova, E.A., Griffin, W.L., O'Reilly, S.Y. and Fisher, N.I. (2002) Igneous zircon: trace element composition as an indicator of source rock type. *Contributions to Mineralogy and Petrology*, **143**, 602-622.

Blundy, J. and Cashman, K.V. (2001) Ascent-driven crystallisation of dacite magmas at Mount St. Helens, 1980-1986. *Contributions to Mineralogy and Petrology,* **140**, 631-650.

Charlier, B.L.A, Peate, D.W., Wilson, C.J.N, Lowenstern, J.B., Storey, M. and Brown, S.J.A. (2003) Crystallisation ages in coeval silicic magma bodies; 238U- 230Th disequilibrium evidence from the Rotoiti and Earthquake Flat eruption deposits, Taupo volcanic zone, New Zealand. *Earth and Planetary Science Letters,* **206**, 441-457.

Charlier, B.L.A., Wilson, C.J.N., Lowenstern, J.B., Blake S., Van Calsteren, P.W. and Davidson, J.P. (2005) Magma generation at al large, hyperactive silicic volcano (Taupo, New Zealand) revealed by U-Th and U-Pb systematics in zircons. *Journal of Petrology*, **46**, 3-32.

Cherniak, D.J., Hanchar, J.M. and Watson, E.B. (1997) Diffusion of tetravalent cations in zircon. *Contributions to Mineralogy and Petrology*, **127**, 383-390.

Cherniak, D.J., Hanchar, J.M. and Watson, E.B. (1997) Rare-earth diffusion in zircon. *Chemical Geology*, **134**, 289-301.

Claiborne, L.L., Miller, C.F., Walker, B.A., Wooden, J.L., Mazdab, F.K. and Bea, F. (2006) Tracking magmatic processes through Zr/Hf rations in rocks and Hf and Ti zoning in zircons: An example from the Spirit Mountain batholith, Nevada. *Mineralogical Magazine*, **70**, 517-543.

Claiborne, L. L., Miller, C.F., Flanagan, D.M., Clynne, M.A., Wooden, J.L. (2010b) Zircon reveals protracted magma storage and recycling beneath Mount St. Helens, *Geology*, v. 38, no. 11, p. 1011–1014.

Claiborne, L.L., Miller, C.F., Wooden, J.L. (2010a) Trace element composition of igneous zircon: a thermal and compositional record of the accumulation and evolution of a large silicic batholith, Spirit Mountain, Nevada. *Contributions to Mineralogy and Petrology*, v. 160, p. 511–531.

Claiborne, L. L., Furbish, D.J., Miller, C.F. (2006) Determining mechanics of segregation of small crystals from melt using modeling and SHRIMP-RG trace element analysis of zircons: Application to the Spirit Mountain batholith, Nevada, *Eos Transactions AGU*, **87(52)** Fall Meeting Supplement, V54B-02.

Clark, S.K., Reagan, M.K. and Plank, T. (1998) Trace element and U-series systematics for 1963-1965 tephras from Irazú Volcano, Costa Rica: Implications for magma generation processes and transit times. *Geochimica et Cosmochimica Acta,* **62**, 2689-2699.

Clynne , M.A., Calvert, A.T., Wolfe, E.W., Evarts, R.C., Fleck, R.J. and Lanphere, M.A. (2008) The Pleistocene Eruptive History of Mount St. Helens, Washington, from 300,000 to 12,000 Years Before Present , chap 28 *of* Sherrod, D.R., Scott, W.E. and Stauffer, P.H., eds., A volcano rekindled: the renewed eruption of Mount St. Helens, 2004-2006: U.S. Geological Survey Professional paper 1750, p. 593-627.

Cooper, K.M. and Donnelly, C.T. (2008) 238U-230Th-226Ra Disequilibria in Dacite and Plagioclase from the 2004–2005 Eruption of Mount St. Helens, chap 36 *of* Sherrod, D.R., Scott, W.E. and Stauffer, P.H., eds., A volcano rekindled: the renewed eruption of Mount St. Helens, 2004-2006: U.S. Geological Survey Professional paper 1750, p. 827- 846.

Cooper, K. M. and Reid, M.R. (2003) Re-examination of crystal ages in recent Mount St. Helens lavas: implications for magma reservoir processes. *Earth and Planetary Science Letters,* **213,** 149-167.

Ferriss, E.D.A., Essene, E.J. and Becker, U. (2008) Computational study of the effect of pressure on the Ti-in-zircon thermometer. *European Journal of Mineralogy*, **20,** 745-755.

Ferry, J.M. and Watson, E.B. (2007) New thermodynamic models and revised calibrations for the Ti-in-zircon and Zr-in-rutile thermometers. Contributions to Mineralogy and Petrology, **154**, 429-437.

Finch, R.J. and Hanchar, J.M. (2003) Structure and chemistry of zircon and zircon-group minerals In: Hanchar JM, Hoskin PWO (eds) *Zircon, reviews in mineralogy and geochemistry*, **53**. Mineralogical Society of America, Washington, pp 1-26.

Gardner, J.E., Rutherford, M., Carey, S. and Sigurdsson, H. (1995) Experimental constraints on pre-eruptive water contents and changing magma storage prior to explosive eruptions of Mount St. Helens volcano. *Bulletin of Volcanology,* **57**, 1–17.

Gualda, G.A.R., Pamukcu, A.S., Claiborne, L.L. and Rivers, M.L. (in review) Quantitative 3D petrography using x-ray tomography, (3) Documenting accessory phases with differential absorption tomography. *Geosphere.*

Hanchar, J.M. and Watson, E.B. (2003) Zircon saturation thermometry, in: *Zircon* (J.M. Hanchar and P.W.O. Hoskin, editors). Reviews in Mineralogy and Geochemistry, **53**, Mineralogical Society of America, Virginia and the Geochemical Society, Washington, D.C, pp. 89-110.

Harley, S.L. and Kelly, N.M. (2007) Zircon: tiny but timely. *Elements*, **3**, 13-18.

Harrison, T.M. and Watson, E.B. (1983) Kinetics of zircon dissolution and zirconium diffusion in granitic melts of variable water content. *Contributions to Mineralogy and Petrology*, **84**, 66-72.

Heaman, L.M., Bowins, R. and Crocket, J.H. (1990) The chemical composition of igneous zircon suites: implications for geochemical tracer studies. *Geochimica et Cosmochimica Acta*, **54**, 1597-1607.

Hill, G.J., Caldwell, T.G., Heise, W., Chertkoff, D.G., Bibby, H.M., Burgess, M.K., Cull, J.P., Cas, R.A.F. (2009) Distribution of melt beneath Mount St Helens and Mount Adams inferred from magnetotelluric data. *Nature Geoscience*, **2**, 785-789.

Hoskin, P.W.O, Schaltegger, U. (2003) The composition of zircon and igneous and metamorphic petrogenesis, In: Hanchar, J.M., Hoskin, P.W.O. (eds) *Zircon, reviews in mineralogy and geochemistry*, **53**. Mineralogical Society of America, Washington, pp 27-62.

Jicha, B.R., Johnson, C.M., Hildreth, W., Beard, B.L., Hart, G.L., Shirey, S.B. and Singer, B.S. (2009) Discriminating assimilants and decoupling deep- vs. shallow-level crystal records at Mount Adams using 238U-230Th disequilibria and Os isotopes. *Earth and Planetary Science Letters,* **277**, 38-49.

Lowenstern, J.B., Persing, H.M., Wooden, J.L., Lanphere, M.A., Donnelly-Nolan, J.M. and Grove, T.L. (2000) U-Th dating of single zircons from young granitoid xenoliths; new tools for understanding volcanic processes. *Earth and Planetary Science Letters,* **183**, 291-302.

Luo, Y. and Ayers, J.C. (2009) Experimental measurements of zircon/melt trace element partition coefficients. *Geochimica et Cosmochimica Acta,* **73**, 3656-3679.

Mazdab, F.K. and Wooden, J.L. (2006) Trace element analysis of accessory and rock forming minerals by ion microprobe (SHRIMP-RG). *Eos Trans* AGU **87**, V33A-0630.

Miller, C.F., McDowell, S.M. and Mapes, R.W. (2003) Hot and cold granites? Implications of zircon saturation temperatures and preservation of inheritance. *Geology*, **31**, 529-532.

Miller, J.S., Matzel, J.E.P., Miller, C.F., Burgess, S.D. and Miller, R.B. (2007) Zircon growth and recycling during the assembly of large, composite arc plutons. *Journal of Volcanology and Geothermal Research,* **167**, 282-299.

Miller, J.S. and Wooden, J.L. (2004) Residence, resorption and recycling of zircons in Devils Kitchen rhyolite, Coso Volcanic field, California. *Journal of Petrology*, **45**, 2155-2170.

Mooney, W.D. and Weaver, C.S. (1989) Regional crustal structure and tectonics of the Pacific coastal states', California, Oregon, and Washington. *Geological Society of America Memoirs*, **172,** 129-161.

Pallister, J.S., Thornber, C.R., Cashman, K.V., Clynne, M.A., Lowers, H.A., Mandeville, C.W., Brownfield, I.K. and Meeker, G.P. (2008) Petrology of the 2004-2006 Mount St. Helens Lava Dome – Implications for Magmatic Plumbing and Eruption Triggering, chap 30 *of* Sherrod, D.R., Scott, W.E. and Stauffer, P.H., eds., A volcano rekindled: the renewed eruption of Mount St. Helens, 2004-2006: U.S. Geological Survey Professional paper 1750, pp. 647-702.

Reid, M.R. (2008) How long does it take to supersize an eruption? *Elements*, **4(1)**, 23-28.

Rutherford, M.J. and Devine, J.D. (2008) Magmatic Conditions and Processes in the Storage Zone of the 2004-2006 Mount St. Helens Dacite, chap 31 *of* Sherrod, D.R., Scott, W.E. and Stauffer, P.H., eds., A volcano rekindled: the renewed eruption of Mount St. Helens, 2004-2006: U.S. Geological Survey Professional paper 1750, pp. 703-725.

Rutherford, M.J., Sigurdsson, H., Carey, S. and Davis, A. (1985) The May 18, 1980, eruption of Mount St. Helens, 1; melt composition and experimental phase equilibria. *Journal of Geophysical Research*, **90**, 2929–2947.

Schmitt, A.K., Stockli, D.F. and Hausback, B.P. (2006) Eruption and magma crystallization ages of Las Tres Viergenes (Baja California) constrained by combined $^{230}Th/^{238}U$ and (U-Th)/He dating of zircon. *Journal of Volcanology and Geothermal Research*, **158**, 281-295.

Simon, J.I and Reid, M.R. (2005) The pace of rhyolite differentiation and storage in an 'archetypical' silicic magma system, Long Valley, California. *Earth and Planetary Science Letters,* **235**, 123-140.

Smith, D. R. and Leeman, W.P. (1993) The origin of Mount St. Helens andesites. *Journal of Volcanology and Geothermal Research,* **55,** 271-303.

Smith, D. R. and Leeman, W.P. (1987) Petrogenesis of Mount St. Helens dacitic magmas. *Journal of Geophysical Research,* **92**, 10313-10334.

Stanley, W.D., Finn, C. and Plesha, J.L. (1987) Tectonics and conductivity structures in the southern Washington Cascades. *Journal of Geophysical Research*, **92**, I0,179-10,193.

Streck, M.J., Broderick, C.A., Thornber, C.R., Clynne, M.A. and Pallister, J.S. (2008) Plagioclase populations and zoning in dacite of the 2004-2005 Mount St. Helens eruption; constraints for magma origin and dynamics, chap 34 *of* Sherrod, D.R., Scott, W.E. and Stauffer, P.H., eds., A volcano rekindled: the renewed eruption of Mount St. Helens, 2004-2006: U.S. Geological Survey Professional paper 1750, pp. 791-808.

Vazquez, J.A. and Reid, M.R. (2002) Time scales of magma storage and differentiation of voluminous high-silica rhyolites at Yellowstone caldera, Wyoming. *Contributions to Mineralogy and Petrology,* **144**, 274-285.

Volpe, A.M. and Hammond, P.E. (1991) ^{238}U-^{230}Th-^{226}Ra disequilibria in young Mount St. Helens rocks: constraint for magma formation and crystallization. *Earth and Planetary Science Letters,* **107**, 475-486.

Walker, B.A., Miller, C.F., Claiborne, L.L., Wooden, J.L. and Miller, J.S. (2007) Geology and geochronology of the Spirit Mountain batholith, southern Nevada: Implications for timescales and physical processes of batholith construction. *Journal of Volcanology and Geothermal Research,* **167**, 239-262.

Wark, D.A. and Miller, C.F. (1993) Accessory mineral behavior during differentiation of a granite suite: monazite, xenotime and zircon in the Sweetwater Wash pluton, southeastern California, USA. *Chemical Geology*, **110**, 49-67.

Watson EB (1996) Dissolution, growth and survival of zircons during crustal fusion: kinetic principles, geological models, and implications for isotopic inheritance. *Special Paper – Geological Society of America*, **31**, 43-56.

Watson EB (1980) Some experimentally determined zircon-liquid partition coefficients for the rare-earth elements. *Geochimica et Cosmochimica Acta*, **44**, 895-897.

Watson, E.B., Wark, D.A. and Thomas, J.B. (2006) Crystallization thermometers for zircon and rutile. *Contributions to Mineralogy and Petrology*, **151**, 413-433.

Watson, E.B. and Harrison, T.M. (2005) Zircon thermometer reveals minimum melting conditions on earliest Earth. *Science*, **308**, 841-844.

Watson, E.B. and Harrison, T.M. (1983) Zircon saturation revisited—temperature and composition
effects in a variety of crustal magma types. *Earth and Planetary Science Letters,* **64(2)**, 295- 304.

Weaver, C.S. (1989) Seismicity of the Cascade Range and adjacent areas. In: L.J. Muffler, C.S. Weaver and D.D. Blackwell (Editors), Geological, Geophysical, and Tectonic Setting of the Cascade Range. U.S. Geological Survey, Open-File Report, **89-178**: 74-93.

Weaver, C.S. and Baker, G.E. (1988) Geometry of the Juan de Fuca plate beneath Washington - evidence from seismicity and the 1949 South Puget Sound earthquake. *Bulletin of the Seismological Society of America*, **78**, 264-275.

Weaver, C.S. and Smith, S.W. (1983) Regional tectonic and earthquake hazard implications of a crustal fault zone in southwestern Washington. *Journal of Geophysical Research*, **88**, 10,371-10,383.

Wilson, C.J.N. and Charlier, B.L.A. (2009) Rapid rates of magma generation at contemporaneous magma systems, Taupo Volcano, New Zealand: Insights from U-Th model-age spectra in zircons. *Journal of Petrology,* **50**, 875-907.

Zellmer, G.F., Annen, C., Charlier, B.L.A., George, R.M.M., Turner, S.P. and Hawkesworth, C.J. (2005) Magma evolution and ascent at volcanic arcs: constraining petrogenetic processes through rates and chronologies. *Journal of Volcanology and Geothermal Research,* **140**, 171-191.

CHAPTER II

TRACE ELEMENT COMPOSITION OF IGNEOUS ZIRCON: A THERMAL AND COMPOSITIONAL RECORD OF THE ACCUMULATION AND EVOLUTION OF A LARGE SILICIC BATHOLITH, SPIRIT MOUNTAIN, NEVADA

Abstract

Hafnium, U, Th, and REE content of zircons from the Spirit Mountain batholith in southern Nevada correlate with calculated temperatures from the Ti-in-zircon thermometer to support field and petrologic evidence of rejuvenation of crystal mush and melt extraction events during the two million year accumulation of the granitoid batholith. Marked variation in zircon composition from sample to sample, from grain to grain within individual samples, and from zone to zone within individual grains documents in detail a history of fluctuating conditions with repeated episodes of replenishment, reheating, crystal mush rejuvenation, fractional crystallization, and melt segregation. The zircons exhibit compositional and thermal variability indicative of variations in host melt composition due to (1) melt rejuvenation, mixing, and fractionation (2) coeval growth of other REE-rich accessory minerals, and possibly (3) fO_2.

1. Introduction

It has become evident that many plutonic and volcanic systems accumulate and evolve over protracted periods of time, with complex histories that require frequent replenishment in order to attain the extended histories recorded in crystal populations (Wiebe and Hawkins 2004; Davies et al. 1994; Reid et al. 1997; Brown and Fletcher 1999; Schmitt et al. 2003; Vazquez and Reid 2002; Charlier et al. 2005; Miller and Wooden 2004; Glazner et al. 2004; Coleman et al. 2004; Walker et al. 2007). In these repeatedly replenished systems, temperature, quantity, composition and location of melt must fluctuate through time as zones of crystal mush and rigid sponge (Hildreth 2004) are reheated and potentially rejuvenated by introduction of new melt, mix with other magmas, crystallize and fractionate. Crystals within these systems are often recycled by entrainment in new magma (Miller and Wooden 2004; Bacon and Lowenstern 2005; Walker et al. 2007) potentially causing dissolution followed by crystallization, and recording these fluctuating conditions throughout the growth history of the crystal (e.g. Davidson et al. 2007; Vazquez & Reid 2002; Harper et al. 2004; Claiborne et al. 2006; Hanchar and Miller 1993). Zoned crystals, then, document the sequence and timing of changing environments within the magmatic system and can provide clues to the magmatic processes involved in accumulation and evolution of magmatic systems with protracted histories.

Due to its refractory nature and low elemental diffusivities (e.g. Cherniak et al. 1997a; Cherniak et al. 1997b; Cherniak and Watson 2003) and resulting ability to retain its compositional zoning through time and varying conditions, zircon is particularly invaluable for investigating the evolution of long-lived and complex magmatic silicic systems. Growth and dissolution of accessory phases, including zircon, act as a primary control over the trace element budget of the magmas (e.g. Wark and Miller 1993; Hoskin and Schaltegger 2003; Claiborne et al. 2006). The trace element composition of these minerals, then, can reflect the trace element

budget in the melt at the time of crystallization. The recent development of methods for the Sensitive High Resolution Ion Microprobe – Reverse Geometry (SHRIMP-RG) that enable high-precision in situ analysis of trace element composition of zones within zircons, including Ti, Hf, and rare earth elements (REE) (Mazdab and Wooden 2006), combined with SHRIMP-RG in situ U-Pb dating and careful application of the Ti-in-zircon thermometer (Watson et al. 2006; Ferry and Watson 2007), allows unprecedented insight into both the utility of the temporal-thermal-compositional record retained in igneous zircon and the long term evolution of silicic crustal systems (Claiborne et al. 2006; Bolhar et al. 2008; Marks et al. 2008; Bindeman et al. 2006; Vazquez et al. 2008). In this study we seek to evaluate the integrity of zircon elemental compositions as tracers of magmatic processes by integrating the zircon record with existing information for a well-characterized plutonic system, and then apply that record to refine our understanding of the accumulation and evolution of large silicic systems.

The Spirit Mountain Batholith (SMB) in southern Nevada provides an ideal example of one of these long-lived silicic systems, with zircons (U-Pb SHRIMP studies) documenting nearly two million years of magma accumulation and evolution (Walker et al. 2007). Field evidence as well as zircon geochronology suggests repeated episodes of recharge, fractionation, and some magma mixing (Walker et al. 2007). A relatively large, high-silica leucogranite cap overlies a large volume of cumulate granite, both of which apparently accumulated over the lifetime of the magmatic system, as injections of new magma rejuvenated crystal mushes and as fractionated melt segregated from the continuously accumulating pockets of crystal mush and amassed in the roof zone (Walker et al. 2007; Claiborne et al. 2006; i.e Bachmann and Bergantz 2004). In this context, the term "cumulate" is used to indicate a magma or resultant rock from which some portion of the interstitial melt has been extracted, leaving a crystal-rich residue or cumulate. Zircons selected from samples of both the fractionated leucogranites and the

cumulate granites to quartz monzonites were analyzed by SHRIMP-RG, and provide detailed information revealing the thermal-compositional history of the magmatic processes involved in the construction of the patchwork batholith.

1.1. Zircon Growth and Trace Element Composition

Zircon growth in a magma requires sufficiently low temperatures and sufficiently high Zr content for saturation, and relatively low rates of diffusion in the melt require that these conditions be maintained for some extended period of time (Watson 1996). Large uniform zones in zircons represent episodes of growth in a saturated environment and reflect magmatic conditions and composition (Hoskin 2000; Fowler et al. 2002). Due to relatively slow growth rates (Watson 1996), zircon crystals likely behave as essentially inert when they encounter rapid (moment to thousands of year) changes in melt conditions, failing to record either rapid fluctuations or events such as those thought to trigger volcanic eruptions (Sparks et al. 1977; Pallister et al. 1992; Eichelberger and Izbekov 2000; Wark et al. 2007). Oscillatory zoning represents kinetic effects at the crystal-melt interface, dependent on ordering in the melt by polymerization and often promoting local supersaturation and disequilibrium, rather than rapid changes in the composition or conditions in the bulk melt (Hoskin 2000; Hoskin and Schaltegger 2003; Fowler et al. 2002; Shore and Fowler 1996; Putnis et al. 1992). Current limitations on analysis introduced by the spot size of in situ analytical instruments make it difficult to delineate trace element compositions of individual oscillatory zones, particularly those less than a few microns thick. However, analyses of entire bands of oscillatory zoning are likely representative of the average composition and conditions of the magma at the time of crystal growth.

Because hafnium is nearly identical in size and charge to zirconium, the two behave nearly identically. Zircon, therefore, is essentially a zircon-hafnon solid solution, with most natural

zircons containing between 1 and 2 wt% HfO_2 (Ahrens and Erlank 1969; Heaman et al. 1990; Bea et al. 2006; Belousova et al. 2002; Hoskin and Schaltegger 2003; Claiborne et al. 2006). As zircon is the primary reservoir for the crust's Hf, growth of zircon controls the Hf composition of any melt. As zircon grows both the Zr and Hf concentrations in the magma will decrease. However, this growth preferentially incorporates Zr over Hf and therefore leads to a decrease in the Zr/Hf of the remaining melt. This process leads to increasing Hf concentration in growing zircon crystals that corresponds to increasing fractionation of the magma (Claiborne et al. 2006). Trace elements found in reasonably measureable quantities in natural zircon include U, Th, Ti, REE, Sc, Y and P. Zircons are generally heavy rare earth enriched and light rare earth depleted with negative Eu anomalies and strong positive Ce anomalies (Hoskin and Schaltegger 2003; Claiborne et al. 2006).

Recent work by Watson and Harrison (2005), Watson et al. (2006) and Ferry and Watson (2007) has demonstrated that incorporation of Ti into zircon depends primarily on temperature, and that Ti concentration of zircon can therefore be used to estimate the magma temperature at the time of crystallization. Accurate calculation of temperature requires knowledge of the activity of TiO_2 ($a$$TiO_2$) and SiO_2 ($a$$SiO_2$) in the melt at the time of crystallization. This can prove an impediment to use of the thermometer, as zircon studies have shown that individual grains often exhibit complex histories with growth from different melts at different times; in general, zircons often were not in equilibrium with the melt or glass that was their final host (Miller and Wooden 2004; Bacon and Lowenstern 2005; Walker et al. 2007). Evolution of the melt during crystallization of a magma or events such as rejuvenation and magma mixing will likely result in changes in $a$$TiO_2$and $a$$SiO_2$. However, expected simultaneous changes in $a$$TiO_2$ and $a$$SiO_2$ have counter-effects on the thermometer, with one balancing the effect of the other, and growth of Ti-bearing minerals may roughly buffer $a$$TiO_2$ during melt evolution (Watson et al. 2006; Ferry

and Watson 2007). Therefore, careful consideration of the history of the magma and the system in question can allow application of the thermometer with reasonable confidence (see methods section for further discussion).

2. Geologic Background

2.1. The Spirit Mountain Batholith

The Spirit Mountain batholith formed during the Miocene as part of an extensive episode of magmatism prior to and during crustal extension in the northern Colorado River Extensional Corridor of southernmost Nevada (Figure 1) (Walker et al. 2007; Faulds et al. 1995; Gans and Bohrson 1998; Howard et al. 1996). Uplift and 40 to 50° westward tilting (Faulds et al. 1992) exposed a cross section of the batholith from the roof to deep levels, providing a 250 km^2 record of the construction of a composite silicic intrusive system (Figure 2; Walker et al. 2007). Field relations suggest that the batholith accumulated by repeated injection of subhorizontal sheets from which crystal poor, fractionated melt commonly was extracted and ascended toward the roof zone, leaving a crystal rich cumulate behind to amalgamate with existing crystal mush. In situ U-Pb dating of zircons by SHRIMP-RG indicates a nearly two million year history for this accumulation process (~17.5 to 15.3 Ma). Zircons from single samples commonly exhibit much of the total age range, suggesting that new pulses of magma recycled existing zircons by incorporating less solidified portions of the existing intrusion (Walker et al. 2007).

Walker et al. (2007) subdivide the Spirit Mountain batholith into the *Spirit Mountain granite* (~16-17 Ma, described below), which is volumetrically dominant and the subject of this

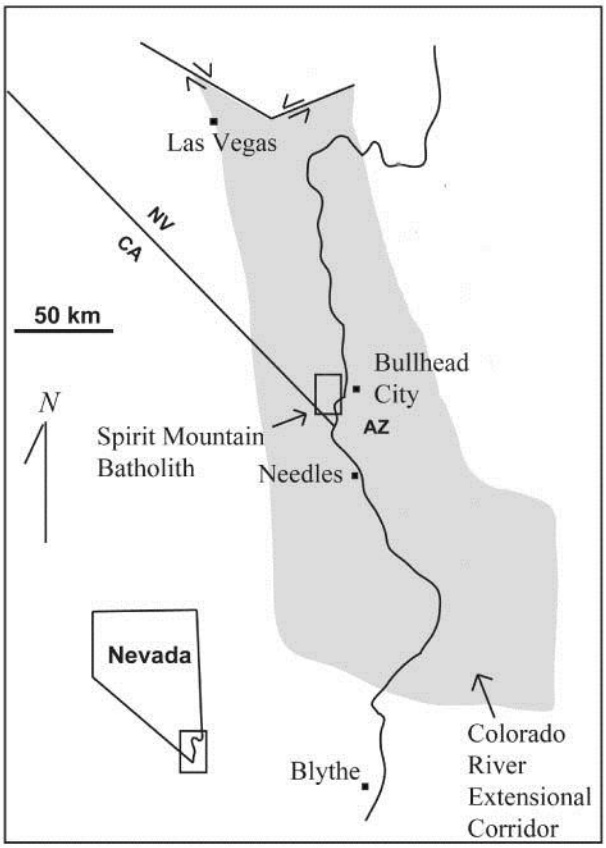

Figure 1: Map showing the study location, the Spirit Mountain batholith in the Colorado River Extensional Corridor of southern Nevada and western Arizona.

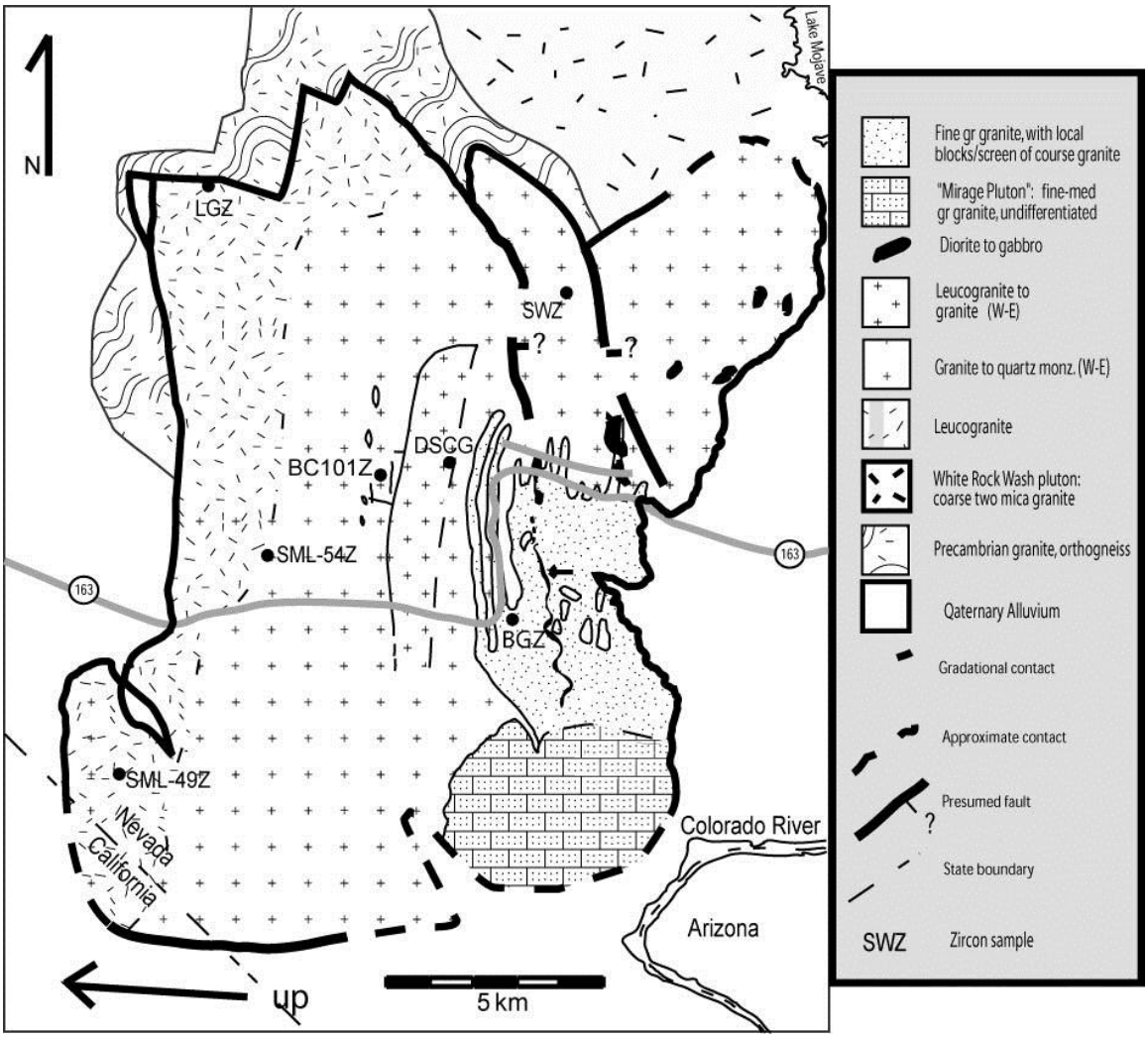

Figure 2: Geologic map of the Spirit Mountain batholith showing locations of samples used in this study (modified from Walker et al. 2007).

study, and several other smaller units that range from slightly older to slightly younger. Here, we briefly describe these other units. Based upon field relations, a felsic granite *roof unit* (~17.4 Ma) exposed along one portion of the roof appears to be the oldest unit. It is intruded by even more felsic leucogranites of the Spirit Mountain granite. The north-striking, E-dipping *Newberry Mountains dike swarm* marks the final stage of Spirit Mountain magma emplacement at ~15.3 Ma. It includes abundant rhyolite porphyries and subordinate intermediate to felsic dikes that brittlely cut all the other units. The other units all intrude deeper parts of the Spirit Mountain granite and are 16.0 Ma or slightly younger in age. The *Mirage granite* is relatively fine grained and comprises a discrete pluton. *Dioritic sheets*, which constitute a very small fraction of the total batholith, are the only direct manifestation of mafic input, although small mafic enclaves are common throughout the older, coarse cumulate granites and quartz monzonites of the Spirit Mountain granite. Sheets of *fine-grained granite* have compositions and textures consistent with granitic replenishments, essentially quenched *in situ* without fractionation. Full descriptions of the various rock units, field relationships, and zircon geochronology can be found in Walker et al. (2007).

The cross-sectional view of the Spirit Mountain granite afforded by tilting reveals a fairly consistent textural and compositional sequence from west to east (top to bottom) that is broken up by younger intrusions that generally repeat the stratigraphy of the larger body. This unit, which constitutes almost 90% of the batholith, grades from a high silica leucogranite at the roof (up to 79 wt.% SiO_2) through granites into quartz monzonite at the lowest exposed levels (down to 61 wt.% SiO_2). These rocks contain a uniform mineral assemblage, with variable modal abundances, that includes alkali feldspar, plagioclase, quartz, biotite, sphene, zircon, apatite, oxides and allanite or chevkinite (fluorite is sparsely present in leucogranites). They exhibit increasingly prominent magmatic foliation with depth, manifested most strongly by alkali

feldspars that define an initially sub-horizontal fabric. Individual intrusions within the Spirit Mountain granite, where identifiable, also appear to have been originally sub-horizontal, with vertical to sub-vertical dikes feeding the base of these sheets and transporting segregated melt upward from the top. Enclaves of fine grained diorite are common in the lower half of the granite unit, and increase in both size and abundance with depth. Our studies (Walker et al. 2007; Claiborne et al. 2006) support previous work (Hopson et al. 1994), suggesting that the extensive, foliated, coarser-grained granite represents residual cumulate and the high-silica leucogranite adjacent to the roof represents complementary fractionated melt. However, complex age and field relations suggest that the batholith formed by repeated episodes of intrusion, fractionation accompanying crystal growth, and segregation of interstitial melt (Walker et al. 2007; Claiborne et al. 2006). These segregated melts were repeatedly injected into the roof zone as dike-fed sheets, eventually accumulating the >55 km^2 leucogranite cap, leaving melt-poor cumulate residues in the lower portions of the body (Walker et al. 2007; Claiborne et al. 2006).

2.2. Petrology, Geochemistry & Zircon Saturation Temperatures

The leucogranites are composed of ~40-50% whilte alkali feldspar, 30-40% quartz, 10-30% sodic plagioclase, ~1% biotite, and accessory apatite, allanite, sphene, zircon, fluorite and opaque oxides. They range in SiO_2 from 76 to 79 wt%, with very low Sr and Ba concentrations (mostly 5-50 ppm and 20-100 ppm, respectively), strong light to middle REE depletions (up to a factor of 10) compared to other granitoids in the batholith, large negative Eu anomalies (Walker et al. 2007), and low Zr/Hf (Claiborne et al. 2006), all of which suggest that these high-silica leucogranites are the product of fractional crystallization (Table 1). The leucogranite grades with depth into a coarser, less felsic granite with pink alkali feldspars, increasing biotite

Table 1 Whole rock geochemistry of samples from the Spirit Mountain batholith used in this study. Oxides are reported in wt. % and elements are reported in ppm (from Walker et al. 2007).

sample ID	*SML49Z (leuco-granite)*	*LGZ (leuco-granite)*	*SML54Z (transitional/ leucogranite)*	*BC101Z (cumulate)*	*DSCG (cumulate)*	*SWZ (cumulate)*	*BGZ (fine grained granite)*
SiO_2	77.37	76.80	75.57	70.84	68.88	63.19	73.83
Al_2O_3	12.46	12.65	13.09	14.77	15.53	17.64	14.23
Fe_2O_3	0.68	0.92	1.19	2.37	2.94	4.10	1.56
MnO	0.05	0.05	0.05	0.06	0.06	0.09	0.04
MgO	0.09	0.10	0.28	0.69	0.85	1.35	0.34
CaO	0.43	0.67	0.78	1.71	2.18	2.73	1.48
Na_2O	4.08	3.92	3.67	4.06	4.00	4.70	3.63
K_2O	4.69	4.75	5.12	4.95	4.84	5.07	4.62
TiO_2	0.12	0.13	0.20	0.43	0.53	0.87	0.23
P_2O_5	0.04	0.02	0.05	0.13	0.18	0.27	0.05
Rb	204	236	157	131	98	83	169
Sr	17	27	89	272	356	551	243
Ba	37	92	326	886	1323	1850	1009
Cs	0.7	0.7	0.8	1.0	0.7	0.3	0.8
Ta	3.2	3.33	1.5	1.74	1.73	1.11	0.84
Nb	43.8	38.3	23.4	24.3	22.0	19.2	15.3
Tl	0.88	0.86	0.82	0.82	0.51	0.38	0.63
Hf	4.2	4.1	4.2	5.8	7.7	12.3	4.4
Zr	99	83	127	229	312	557	150
Y	19	18	16	28	43	26	19
V	< 5	5	11	29	37	57	15
Th	20.8	19.1	17.1	17.4	9.26	8.91	14.8
U	2.89	2.67	1.34	1.81	1.26	1.09	1.14
Ga	20	31	18	28	20	22	27
La	36	46.7	36.5	106	73.3	103	54.1
Ce	63	77.7	73.2	187	153	210	101
Pr	5.77	6.39	7.81	17.8	16.7	21.7	9.75
Nd	15.7	17.9	23.7	60.0	57.0	79.5	34.5
Sm	2.49	2.76	3.93	9.41	10.0	12.0	6.07
Eu	0.202	0.235	0.546	1.52	1.64	2.41	1.04
Gd	1.65	2.16	2.52	7.06	7.83	7.86	4.35
Tb	0.38	0.43	0.47	1.18	1.30	1.15	0.75
Dy	2.48	2.60	2.61	5.98	7.14	5.65	3.86
Ho	0.58	0.58	0.55	1.16	1.34	1.00	0.78
Er	2.15	2.18	1.81	3.64	4.15	3.06	2.46
Tm	0.387	0.400	0.298	0.534	0.636	0.442	0.372
Yb	2.62	2.67	1.89	3.06	3.80	2.92	2.29
Lu	0.395	0.404	0.272	0.393	0.460	0.414	0.337
Sn	1	1	1	2	2	1	<1
Be	3	6	2	3	2	2	2
Ge	1.7	2.3	1.4	1.1	1.2	1.0	1.4
Bi		0.8		0.8	1.5	0.2	0.2
Th/U	7.20	7.15	12.76	9.62	7.37	8.20	13.01
Zr/Hf	23.57	20.46	30.24	39.55	40.42	45.12	34.12

abundance and decreasing abundance of quartz. This coarse granite, which extends downward for ~3 km, averages ~20-35% plagioclase, 30-40% alkali feldspar, 15-30% quartz, 5-8% biotite, up to 1% sphene and accessory apatite, allanite, zircon and opaque oxides. The coarse grained granite grades downward into magmatically foliated quartz monzonite that is poorer in quartz and richer in biotite. The quartz monzonite is coarse-grained, with 40-50% alkali feldspar, 30-35% plagioclase, 10-15% biotite, 5-15% quartz, up to ~1% sphene and accessory apatite, allanite, zircon and opaque oxides. These less felsic granites are enriched in light REE (up to 600 times chondrite) and exhibit small Eu anomalies relative to the leucogranites and flat middle to heavy REE/chondrite patterns (Table 1), suggesting they represent the cumulate residues of fractional crystallization (Walker et al. 2007).

Textures, field relations and petrography suggest that the fine grained granite unit (represented by sample BGZ) may represent something like the primary input liquid into the batholith, and that the leucogranites (represented by samples LGZ and others, (Walker et al., 2007)) likely represent interstitial liquid segregated from cumulate mush. The zircon saturation temperatures calculated using Harrison and Watson (1983) for these two units, 785°C and 734°C, respectively (Table 2), may represent reasonable constraints on zircon growth in these two types of melts essential to the assembly of the Spirit Mountain batholith. However, depending on the amount of crystallization that occurred in these prior to zircon growth, the temperatures may be overestimates. Because the cumulate granite compositions do not closely resemble melt compositions, zircon saturation temperatures cannot be calculated for these rocks, but can be assumed to be between the saturation temperatures of the primary input magma (BGZ) and the most felsic, evolved fractionates (leucogranties).

Table 2: Zircon and rutile saturation temperatures and their factors for calculation for samples with assumed near-liquid compositions (equations from Watson and Harrison 1983 and Hayden and Watson 2007; whole rock geochemical data from Walker et al. 2007). Samples are listed in order of increasing silica content, and all samples are leucogranites, with >76 wt% SiO_2, except BGZ, which is a fine grained granite with 73.83 wt% SiO_2 (Walker et al. 2007). M and FM are factors that account for zircon and rutile solubility dependence on melt composition (Watson and Harrison 1983, Miller et al. 2003, and Hayden and Watson 2007). Shaded rows indicate samples with zircons included in this study.

Sample	*Zr (ppm)*	*M factor*	*zircon saturation T (°C)*	*Ti (ppm)*	*FM factor*	*rutile saturation T (°C)*
BGZ	150	1.39	785	1352	1.68	782
LGZ	83	1.41	734	753	1.57	734
SML52	137	1.39	777	970	1.57	756
BW47	47	1.35	696	331	1.43	673
SML63C	186	1.36	806	1249	1.61	777
SML47	83	1.39	736	847	1.54	745
SML49Z	99	1.40	749	693	1.52	728
SML76	123	1.41	767	428	1.53	690
SML132	93	1.41	744	428	1.53	690
SML74	111	1.39	759	706	1.52	730
SML130	92	1.39	744	706	1.52	730
BW24	152	1.32	792	965	1.48	757
SML129Z	116	1.38	764	739	1.51	734
SML73	128	1.38	772	739	1.51	734
SML69	68	1.39	721	513	1.49	705
SML71	131	1.39	773	773	1.53	737
SML120Z	202	1.39	811	773	1.53	737
SML67	114	1.32	766	607	1.43	720
SML78	96	1.35	750	501	1.45	704
SML133	165	1.35	796	501	1.45	704

3. Methods

3.1. Sample Preparation and Analytical Methods

Six samples from the Spirit Mountain granite unit were selected for detailed zircon trace element analysis (see Figure 2 for sample locations). Samples SWZ, DSCG, and BC101Z were selected as representative cumulates based on texture, chemical composition, mineralogy and field relations. DSCG was collected from a relatively young portion of the unit (see Figure 2). Samples LGZ and SML49Z were selected as representative leucogranites using the same criteria. Sample SML54Z represents a transitional granite, intermediate in composition, texture, and location between cumulates and leucogranites (Figure 2).

Each ~5 kg sample was crushed to pass through a 500 µm mesh. An initial density separation was performed using hydraulic separation, followed by density separation with heavy liquids of density 2.85, magnetic separation and hand picking of at least 100 zircon grains per sample from the least magnetic fraction. Thirty to fifty zircons from each sample were then mounted in epoxy and ground near the center of the grains and polished. Due to variable sizes of crystals on any given mount, uniform polishing reveals different depths in different sized grains. Imaged and analyzed “cores” or “centers” of grains, therefore, often represent the center of the cross-sectional surface that was revealed, not necessarily the very center of the grain. Grains were then imaged in reflected light on a petrographic microscope and by cathodoluminescence (CL) on the JEOL JSM 5600 scanning electron microscope at the USGS/Stanford Microanalytical Laboratory.

The zircons were analyzed using the USGS/Stanford Sensitive High Resolution Ion Microprobe, Reverse Geometry (SHRIMP-RG). Spots for trace element analyses were selected based on zoning visible in CL images and in an attempt to avoid inclusions visible in reflected

light images, with preference for locations that had been previously analyzed for U-Pb ages. In these cases, mounts were repolished and coated following U-Pb analyses. Variations in technique between the first and second trace element analysis session were due to the evolving state of the methodologies (Mazdab and Wooden 2006). In the first of two sessions (samples LGZ and SWZ only, Sept. 2005), the trace element routine included $^{31}P^{+}$, $^{40}Ca^{+}$, $^{48}Ti^{+}$, $^{49}Ti^{+}$, $^{56}Fe^{+}$, $^{89}Y^{+}$, $^{172}Yb^{16}O^{+}$, $^{180}Hf^{16}O^{+}$, $^{232}Th^{16}O^{+}$ and $^{238}U^{16}O^{+}$, in addition to $^{30}Si^{+}$, $^{96}Zr^{+}$ and $^{90}Zr_2{}^{16}O^{+}$ reference peaks. $^{49}Ti^{+}$ was selected over more abundant $^{48}Ti^{+}$ for calculation of concentrations to avoid interference from $^{96}Zr^{+}$. For the second session (all six samples, March 2006), $^{45}Sc^{+}$, $^{139}La^{+}$, $^{140}Ce^{+}$, $^{146}Nd^{+}$, $^{147}Sm^{+}$, $^{153}Eu^{+}$, $^{157}Gd^{16}O^{+}$, $^{159}Tb^{16}O^{+}$, $^{163}Dy^{16}O^{+}$, $^{165}Ho^{+}$, $^{167}Er^{16}O^{+}$, $^{169}Tm^{16}O^{+}$, and $^{175}Lu^{16}O^{+}$ were added to the analytical routine, thus completing the suite of rare earth elements. The analyses included Pr, but results were considered unreliable due to potential hydride interference from the $^{140}Ce^{1}H^{+}$ peak. For Yb, Gd, Tb, Dy, Er, Tm, Lu, Hf, Th and U, the oxide peaks rather than the element peaks were used due to their greater ion production during sputtering. In the first session, each measurement consisted of one block of three cycles. During the second session, we generally ran two cycles and in a few cases one. Each cycle represents a sequential stepping through the entire mass range from low to high mass. Data reduction involved averaging raw counts for all cycles and then normalizing to the average $^{30}Si^{+}$ count rate. This normalization minimizes variations caused both by drift in the primary current and by time-dependent ionization phenomena related to sputtering. Normalized count rates from the unknowns were compared to comparable measurements of standard zircon CZ3 which were calibrated against a set of synthetic REE and Ti-bearing zircons to determine absolute elemental concentrations. These synthetic zircons were grown using a technique modified from Hanchar et al. (2001) and were independently analyzed by electron microprobe (Mazdab and Wooden 2006).

3.2. Application of the Ti-in-zircon thermometer

Watson et al. (2006) and Watson and Harrison (2005) described the dependence of Ti concentration in zircon on crystallization temperature, and defined a thermometer based on experimental results and well characterized natural samples. This initial form of the thermometer assumed that the melt from which the zircon grows was saturated in quartz, but allowed for variability in $a\mathrm{TiO_2}$. Ferry and Watson (2007) revised the thermometer calculation to allow for under saturation in rutile and quartz by incorporating $a\mathrm{TiO_2}$ and $a\mathrm{SiO_2}$, following the equation $T(K) = \frac{-4800 \pm 86}{\log Ti(ppm) + \log a_{SiO_2} - \log a_{TiO_2} - (5.711 \pm 0.072)}$ (Ferry and Watson 2007). Accurate application of this thermometer requires knowledge of $a\mathrm{TiO_2}$ and $a\mathrm{SiO_2}$ at the time of zircon crystallization. This can be an impediment to use of this tool, as it can be difficult to constrain activities at the time of zircon growth. Zircons often were not in equilibrium with their final host magma, and crystallization will likely cause $a\mathrm{TiO_2}$ and $a\mathrm{SiO_2}$ to change throughout the evolution of a magma. Careful consideration of the system specific melt compositions and mineral assemblages, effects of melt evolution during crystallization or mixing on these activities and the effect of changes in activity with time on the thermometer can allow useful application of the Ti-in-zircon thermometer, even when activities cannot be definitively identified from the rocks themselves. In these cases of undersaturation in either quartz or rutile, unless it can be determined that a volcanic zircon is cognate to a glass with which it is in contact and for which $a\mathrm{TiO_2}$ and/or $a\mathrm{SiO_2}$ are known, calculated temperatures must be considered estimates.

The configuration of the temperature equation is such that a similar magnitude overestimate or underestimate of both activities, which is the likely case for our compositions, will cancel out resulting errors in T estimate (Ferry and Watson 2007). Overestimating the $a\mathrm{SiO_2}$ will result in an overestimate of temperature, while overestimating the $a\mathrm{TiO_2}$ will result in an underestimate of temperature. Textures of the cumulates suggest that significant amounts of

crystallization occurred before the magmas saturated in quartz, although considering zircon saturation temperatures it may be that much of the zircon grew coeval with quartz. The evolved nature of even the putative primary magmas (BGZ) necessitates a relatively high $a\mathrm{SiO_2}$. As we cannot be certain how these compositions varied and considering the ubiquity of quartz in these samples, we have held $a\mathrm{SiO_2}$ constant at 1, thus maximizing temperature estimate. Co-existing Ti-bearing phases (sphene and potentially ilmenite) indicate $a\mathrm{TiO_2}$ was not low (Hayden and Watson 2007; their table 4), although few natural magmas are rutile saturated. Rutile saturation temperature were calculated using the equation of Hayden and Watson (2007) and compared with zircon saturation temperatures (Harrison and Watson 1983; Miller et al. 2003; Hanchar and Watson 2003) for samples with assumed near-liquid compositions, such as the leucogranites and putative primary input melt BGZ (Table 2). This comparison suggests that these magmas were near rutile saturation at reasonable temperatures for zircon growth, supporting our assumption of a relatively high $a\mathrm{TiO_2}$, which we held constant at 0.7. Calculated T_{TiZ} for samples LGZ and SWZ have been amended from those previously reported in Claiborne et al. (2006), reflecting recalibration of the Watson et al. (2006) thermometer by Ferry and Watson (2007). The new, revised temperatures are slightly higher, by approximately 5-15°C and are considered in the data interpretations but are not re-reported herein.

A moderate pressure dependence of the Ti-in-zircon thermometer has been suggested by Ferry and Watson (2007) and Ferriss et al. (2008) (-5 to 10°C/kb). This implies that calculated temperatures from the Ferry and Watson formulation (calibrated at 10 kb) could be tens of degrees too high for the shallow crust and tens of degrees too low at very deep crust or upper mantle pressures. Because the Spirit Mountain batholith was emplaced in the upper crust, this suggest that our calculated temperatures may be systematically too high. However, it is unlikely that the large *relative* differences in temperature that we estimate are not real, and the

generally responsible magmatic temperature range would still apply even with a downward correction.

4. Results

4.1 Zircon Zoning in CL Images

Zircons are abundant in both leucogranite and cumulate samples, and identified grains range in size up to our maximum retrievable size, 500 microns in length. Grains are generally euhedral, prismatic, and often contain mineral and/or melt inclusions. Cathodoluminescence (CL) imaging of the zircons reveals distinct euhedral zoning, visible as discrete zones and as bands of oscillatory zoning. Different samples have populations with distinctly similar zoning patterns, although it was not possible to definitively match zoning stratigraphy or characteristics among grains from the same samples or among grains of the same age. Although we do not ultimately base our interpretations on the appearance of the zoning or take zoning as a proxy for composition, relative brightness of zones does appear to correlate with Ti, Hf, U, Th and REE concentrations, with dark zones that exhibit low Ti and REE and high Hf, U, and Th, and bright zones that exhibit high Ti and REE and low Hf, U, and Th.

Zircons from all three of the cumulate samples are mostly fairly bright in CL, and most of these grains have at least thin rims that are moderate to bright (Figure 3). These cumulate samples often exhibit internal resorption surfaces identified by truncated zoning often associated with curved zone boundaries and embayments, particularly where bright rims or interior zones surround darker centers. Melt and mineral inclusions are most commonly found in these bright zones adjacent to resorption surfaces (Figure 3). Nearly all the grains in the three leucogranite samples exhibit very dark rims, with rim thickness varying from thin (<30 microns)

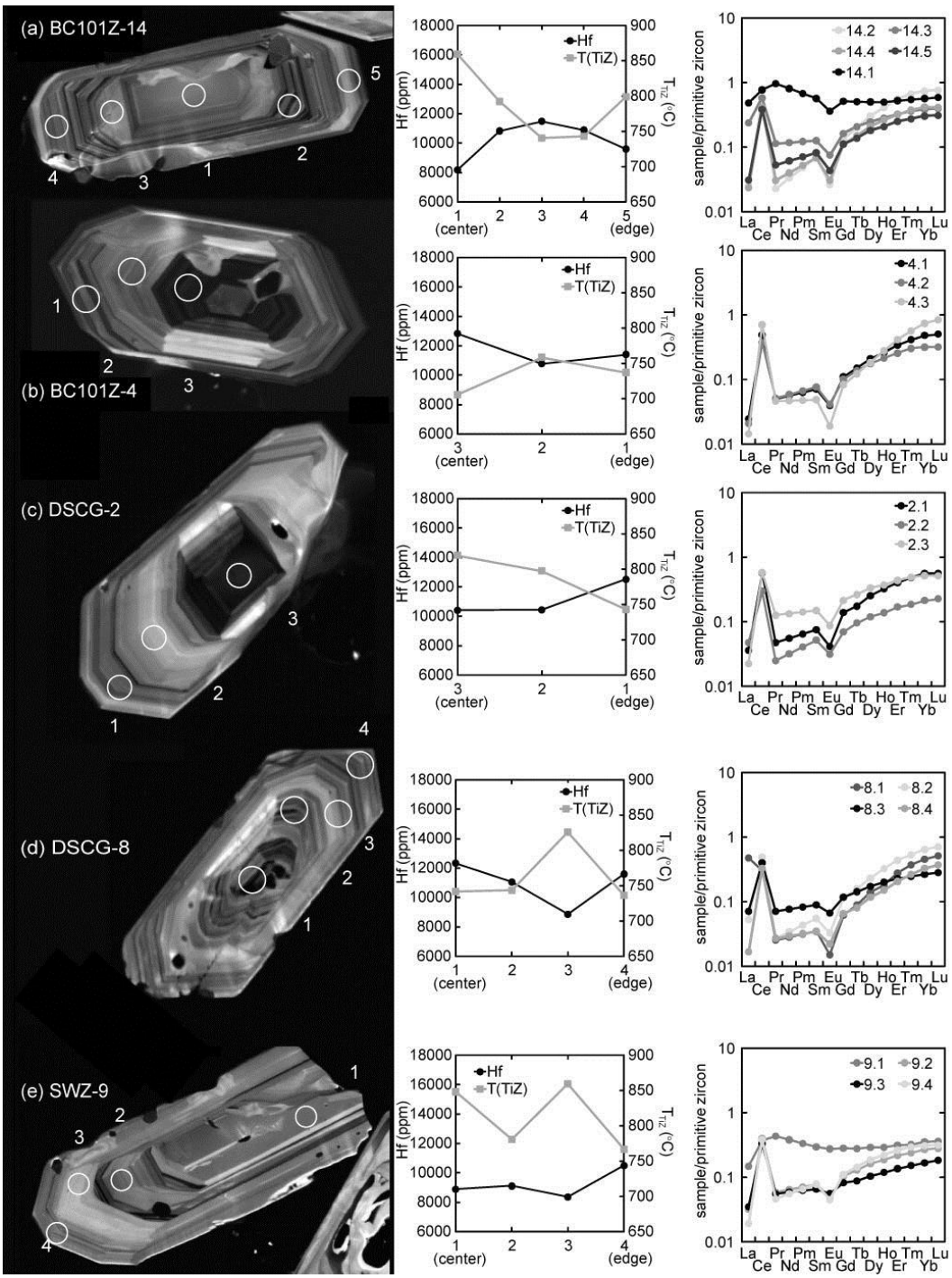

Figure 3: Cathodoluminescence images of zircon grains from each sample showing zoning typical of that sample. (a, b, c, d, e) are zircons from cumulate samples. Circles represent locations of SHRIMP-RG trace element analyses and are approximately 15 microns in diameter. Each grain is accompanied by corresponding Hf and Ti profiles and 'primitive' zircon normalized REE patterns (zircon REE were normalized to zircon analysis LGZ-8.1, which shows an especially unevolved composition, allowing clearer distinction of REE variations). Shading on REE lines increases in darkness with decreasing Hf, such that black lines represent the least fractionated, highest Ti analysis of any given grain.

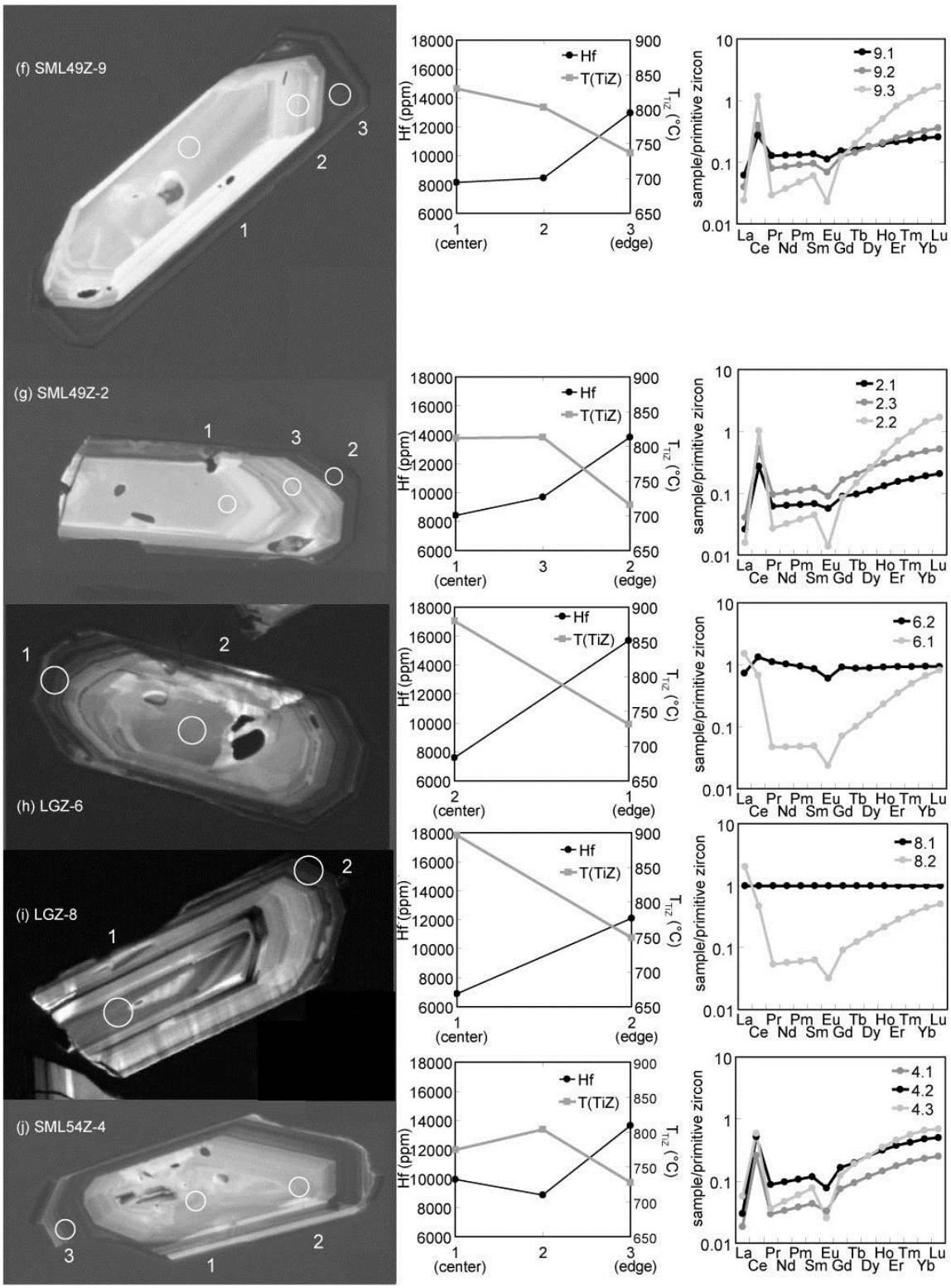

Figure 3 (cont'd): Cathodoluminescence images of zircon grains from each sample showing zoning typical of that sample. (f, g, h, i, j) are zircons from leucogranite and transitional samples.

in the transitional sample, SML54Z to moderate to very thick (up to 60 microns) in the more silicic leucogranites, LGZ and SML49Z (Figure 3). Most grains in all the leucogranite samples have medium to bright centers, although some grains in sample LGZ do have very dark centers. Appendix 3 describes zircon zones in spots analyzed by SHRIMP-RG, corresponding geochemical and geochronologic data (where available), and calculated T_{TiZ}.

4.2. Hf, Ti, and T_{TiZ} in Zircon

Appendix A provides a summary of Hf and trace element compositions of 171 analyses of 58 zircons from 4 samples from the Spirit Mountain granite. Data from two additional samples from this study (98 analyses, 41 zircons) were reported in Claiborne et al. (2006), and are not included in Appendix A, but are included in graphical representations of the data set. Zircons from the Spirit Mountain granite contain 6900 to 16700 ppm Hf (0.75 to 1.82 wt% HfO_2). Titanium and T_{TiZ} decrease and U and Th increase systematically with increasing Hf (Figure 4, 5). The leucogranite samples have higher maximum Hf concentrations than cumulates (16700 ppm and 15000 ppm, respectively), primarily from analyses of the ubiquitous dark rims, and span the entire range of Hf values for all samples (Figure 4, Appendix A). Low Hf from leucogranite samples are primarily from grain centers. Cumulate interior and rim Hf concentrations overlap nearly completely in range (7273 to 15037 ppm and 7847 to 14711 ppm, respectively), although the minimum Hf concentrations of cumulate rims is slightly higher than that of the interiors. Intragrain fluctuations in Hf are common and will be discussed further.

Titanium concentration and calculated temperatures from the Ti-in-zircon thermometer (T_{TiZ}) are inversely correlated with Hf; as Hf increases, Ti and T_{TiZ} decrease. Titanium concentrations in zircons from the Spirit Mountain batholith range from 3.3 to 36.1 ppm, yielding T_{TiZ} ranging from 680 to 925°C with similar variation within samples and up to 100°C

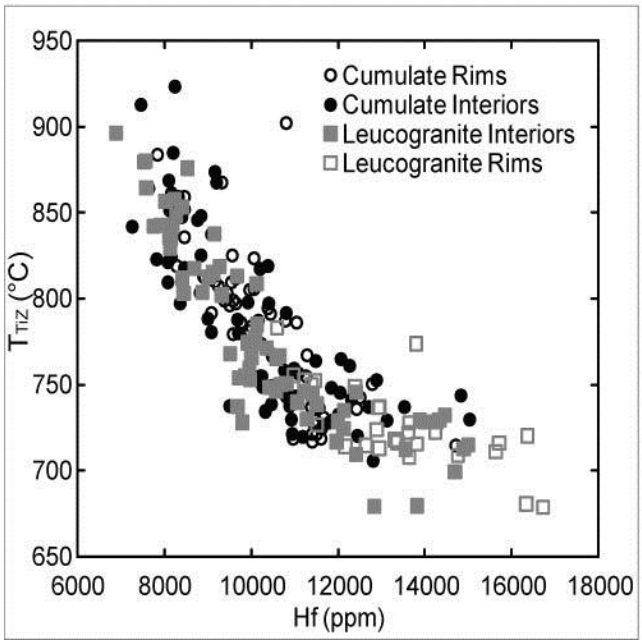

Figure 4: Hafnium concentration vs. Ti concentration in zircons. Dashed lines represent estimated temperatures for a given Ti concentration, calculated from the Ti-in-zircon thermometer (Ferry and Watson 2007) assuming *a*TiO2=0.7 and *a*SiO2=1.

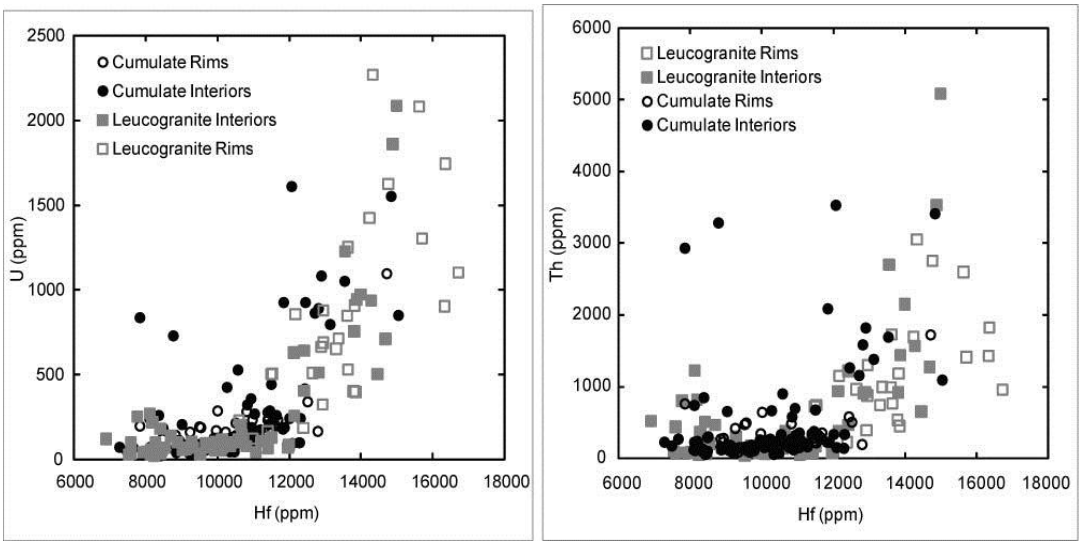

Figure 5: (a) Hafnium concentration vs. U concentration in zircons (b) Hafnium concentration vs. Th concentration in zircons.

variation within grains. Histograms of Ti concentration and resulting T_{TiZ} for each sample (Figure 6) show that all six samples from both cumulates and leucogranite mainly yield temperatures between 700 and 850°C, with 33% of analyses showing temperatures greater than 800°C. Zircon analyses from cumulate samples yield no temperatures less than 700°C, and generally have a larger percentage of high calculated temperatures than the leucogranites. Unlike the other cumulate samples that exhibit a broad distribution of temperatures between 700 and 950°C, sample BC101Z has a fairly restricted range, with most temperatures between 700 and 800°C and only 15% of analyses above that. The transitional sample and both leucogranites samples have at least one analysis each below 700°C. The transitional sample is bimodal, with a peak population between 700 and 750°C and another between 800 and 850°C. Both leucogranites are distinctly unimodal, with a main temperature population between 700 and 750°C. The two leucogranite samples exhibit very different ranges, with analyses from LGZ yielding temperatures spanning the entire range up to 925°C, and sample SML49Z containing greater than 75% of its temperatures between 700 and 750°C, and no temperatures above 850°C.

The sample-to-sample variation in composition of zircon populations described above is relatively subtle, particularly between samples of similar lithology. In contrast, intragrain and grain-to-grain variability within each sample are striking. In some cases, the variability within single grains spans much of the compositional range of the entire sample suite. Individual zircon grains exhibit variation in T_{TiZ} and Hf (and U, Th, REE) corresponding to visible zones in CL images (Figure 3). In grains from samples where several spots were analyzed, most exhibit fluctuations rather than monotonic change from core to rim. In grains where two or less spots were analyzed, patterns of variation are similar to those revealed more fully in grains with three or more analyzed spots. Zircons from cumulate sample SWZ have generally bright, high temperature, low Hf cores, surrounded by darker interior zones with lower T_{TiZ} and higher Hf

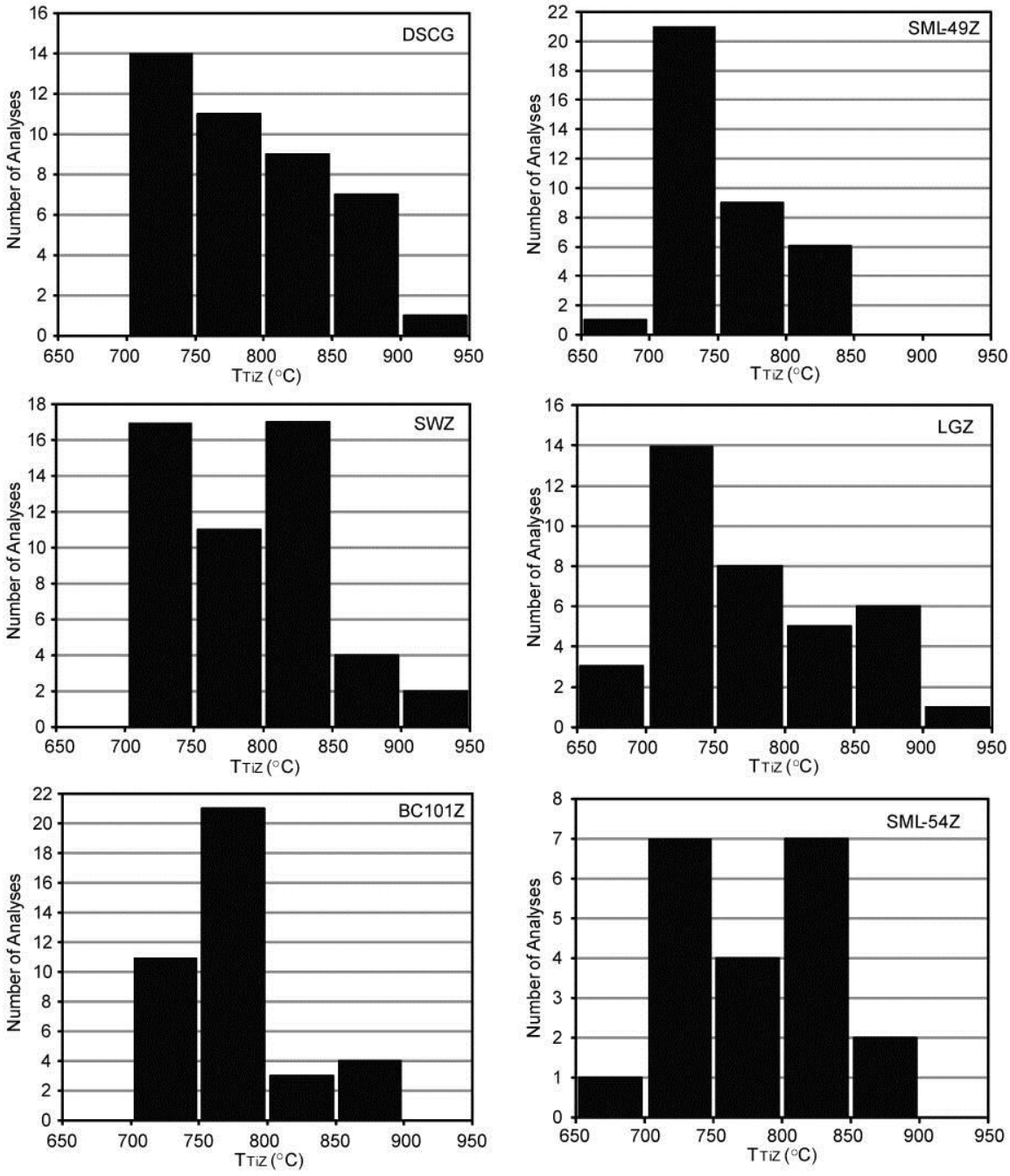

Figure 6: Histograms showing distribution of temperatures from Ti-in-zircon thermometry for each sample.

which are then surrounded by bright, higher T_{TiZ}, low Hf rims 20 to 50 µm thick (Figure 3). The other two cumulate samples are not as uniform in compositional zoning patterns. Both BC101Z and DSCG contain some zircons with moderately dark cores that exhibit low T_{TiZ} and high Hf and some grains that have bright cores with higher T_{TiZ} and lower Hf. Most zircons from both of these samples, however, do exhibit fluctuations in T_{TiZ} and Hf from core to rim of up to 100°C and 5000 ppm Hf (Figure 3).

Nearly all of the zircons from both leucogranite samples have thick (20 to 60 µm), very dark rims visible in CL images that are quite distinct from any cumulate sample and correspond to relatively low T_{TiZ} (680 to 750°C) and high Hf (10500 to 17500 ppm) (Figure 3). The cores and interiors of grains from the two samples are more variable, however. All zircons analyzed from SML49Z exhibit general core to rim cooling and fractionation, with cores of T_{TiZ} between 725 and 835°C and 7500 to 11000 ppm Hf surrounded by the previously mentioned thick, "cool," fractionated rims (Figure 3). Zircons from sample LGZ are more variable, some exhibiting low temperatures and high Hf throughout with core to rim cooling and fractionation, some with bright cores showing relatively high T_{TiZ} and low Hf, and some with dark interior zones with lower T_{TiZ} and higher Hf than either the core or rim (Figure 3).

Because the interior and rim data for the transitional sample was nearly identical to the leucogranite interior and rim data, and it was so similar compositionally and mineralogically to the leucogranites, it is treated in geochemical plots and in remaining discussions as a leucogranite. The zircons in the transitional sample also all exhibit dark rims, although thinner than in the other leucogranites (1 to 30 microns), with very low temperatures and high Hf (680 to 730°C and 12500 to 15000 ppm, respectively). The cores of these zircons are mostly bright, with moderate to high T_{TiZ} and moderate to low Hf. A few cores are dark with low T_{TiZ} and high

Hf. Many grains from this sample have a bright interior zone that has higher T_{TiZ} and lower Hf than either the core or rim (Figure 3).

4.3. Uranium and Thorium in Zircon

Uranium varies from 20 to 4750 ppm, with 80% of analyses between 20 and 300 ppm and only 3 above 2300 ppm (Figure 7a). Th varies from 40 to 23,300 ppm, with 70% of analyses between 40 and 400 ppm, and 4 above 3500 ppm (Figure 7b). Both U and Th remain fairly uniform and low at low Hf (less than 10000 or 12000 ppm Hf, respectively), then generally increase with increasing Hf (Figure 5). Thorium/uranium is greater than 1, ranging from ~1 to ~4.5, with the most extreme enrichment in Th relative to U corresponding to low Hf and high T_{TiZ} (Figure 8a,b). The leucogranite samples have higher maximum U and Th than zircons from the cumulate samples. All leucogranite rims are in the upper ranges for both (greater than 100 ppm U and 200 ppm Th). The rims of the leucogranite samples have the highest U, while the interiors have the highest Th (approached by some cumulate analyses). Leucogranite rims have lower Th for the same U as leucogranite interiors or cumulate samples, apparently marking slightly different Th/U trends (Figure 8a,b).

4.4. Rare Earth Elements in Zircon

The chondrite-normalized REE patterns of natural zircons are very strongly enriched in heavy REE relative to light REE and have positive Ce and negative Eu anomalies (Figure 9). Within suites of related zircons, the similarities may be even stronger. These common characteristics dominate the appearance of chondrite-normalized patterns and mask meaningful variability. To reveal important differences among the Spirit Mountain zircon compositions, we normalize to the concentrations in a typical "primitive" (high T_{TiZ}, low Hf) zircon zone (Figure 3).

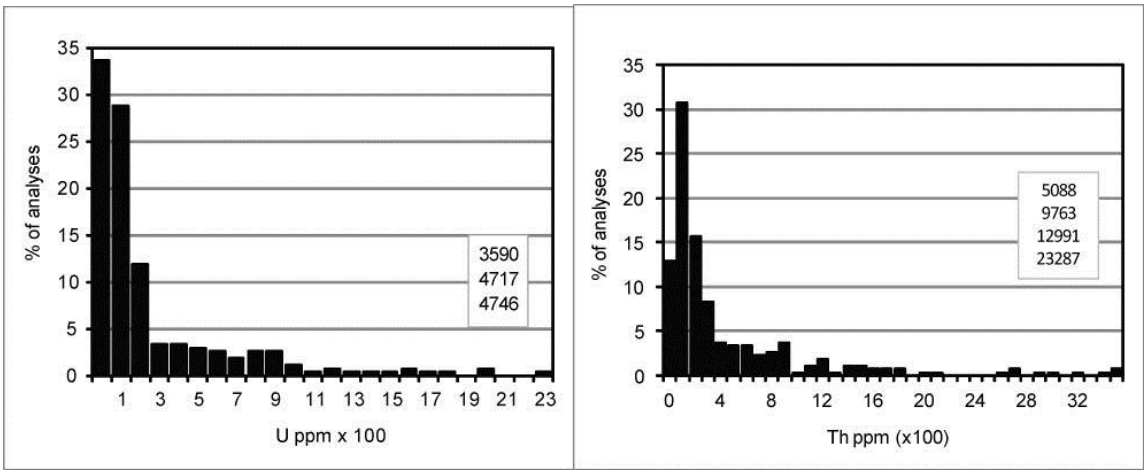

Figure 7: Histograms showing distribution of (a) Uranium concentrations and (b) Thorium concentrations in zircons from all six samples. Numbers in boxes represent results that plot outside the scale of the histograms.

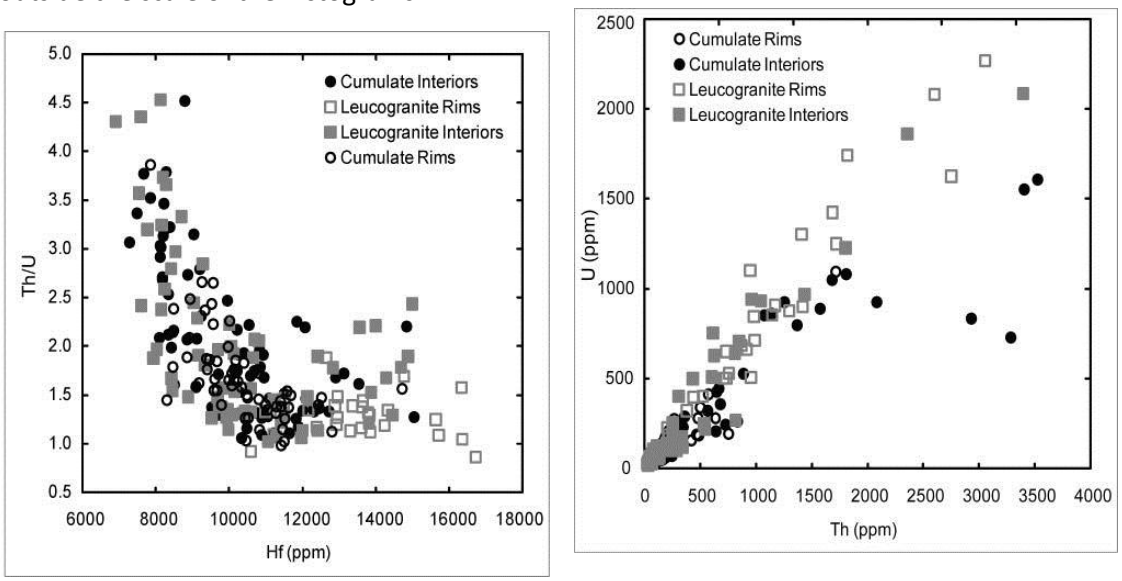

Figure 8: (a) Hafnium concentration vs. Th/U in zircons. (b) Uranium vs. Thorium concentration in zircons.

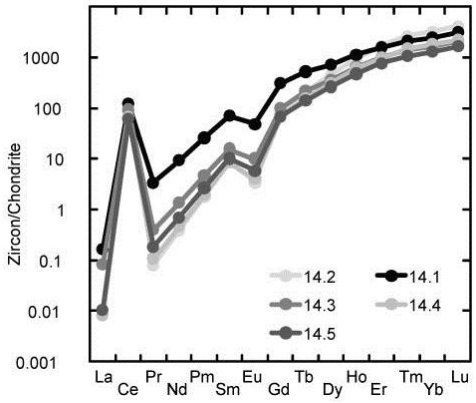

Figure 9: Chondrite-normalized REE plot for sample BC101Z grain 14; corresponds to Fig3a.

This reveals that like Hf, T_{TiZ}, Th, and U, REE concentrations and patterns in zircon vary significantly from sample to sample, from grain to grain within a sample, and even within individual grains. This enrichment in heavy REE relative to light REE increases with fractionation and lower T_{TiZ} (Figure 3, 10a) resulting in variation in heavy REE such as Lu by a factor of 10 (Figure 10b). Middle rare earth elements such as Sm and Gd vary by two orders of magnitude from 0.3 to 30 ppm, increasing with increasing T_{TiZ} and decreasing Hf (Figure 10c). Light rare earth element concentrations, exemplified by La, often show relative enrichment that we regard as highly unlikely for natural zircon (Figure 3d,h,i). These high concentrations may be dominated by minute inclusions of light REE-rich mineral inclusions (e.g. allanite, chevkinite - both present in Spirit Mountain granites) or small melt inclusions. Any light REE-rich mineral or melt inclusion could potentially strongly influence the analyses of the naturally low concentration of light REE in zircon without significantly affecting the concentrations of the more abundant heavy REE, Hf, U, Th, and Ti. In analyses where presence of light REE-rich inclusions are not suspected, La concentrations vary by two orders of magnitude, from ~0.001 to 0.1 ppm (Appendix A). Primitive zircon-normalized REE patterns for fractionated samples commonly illustrate heavy REE enrichment and middle REE depletion, indicated by a steep negative slope between the heavy and middle REE and shallower or flat slope between the middle REE and light REE (Figure 3b spot 4.3; Figure 3d spots 8.1,8.4).

The zircons from the Spirit Mountain granite exhibit a negative Eu anomaly and positive Ce anomaly in chondrite-normalized REE plots (Figure 9). The magnitude of the Eu anomaly increases with increasing fractionation and decreasing T_{TiZ} (Figure 10d). Most of the change in the Eu anomaly is in the interiors, both cumulate and leucogranite. The maximum Eu/Eu* values, 0.4 – 0.5, are represented by 5 interior analyses, otherwise Eu/Eu* values below 0.4 are most characteristic of the maximum Eu/Eu* measured for these samples. The positive Ce

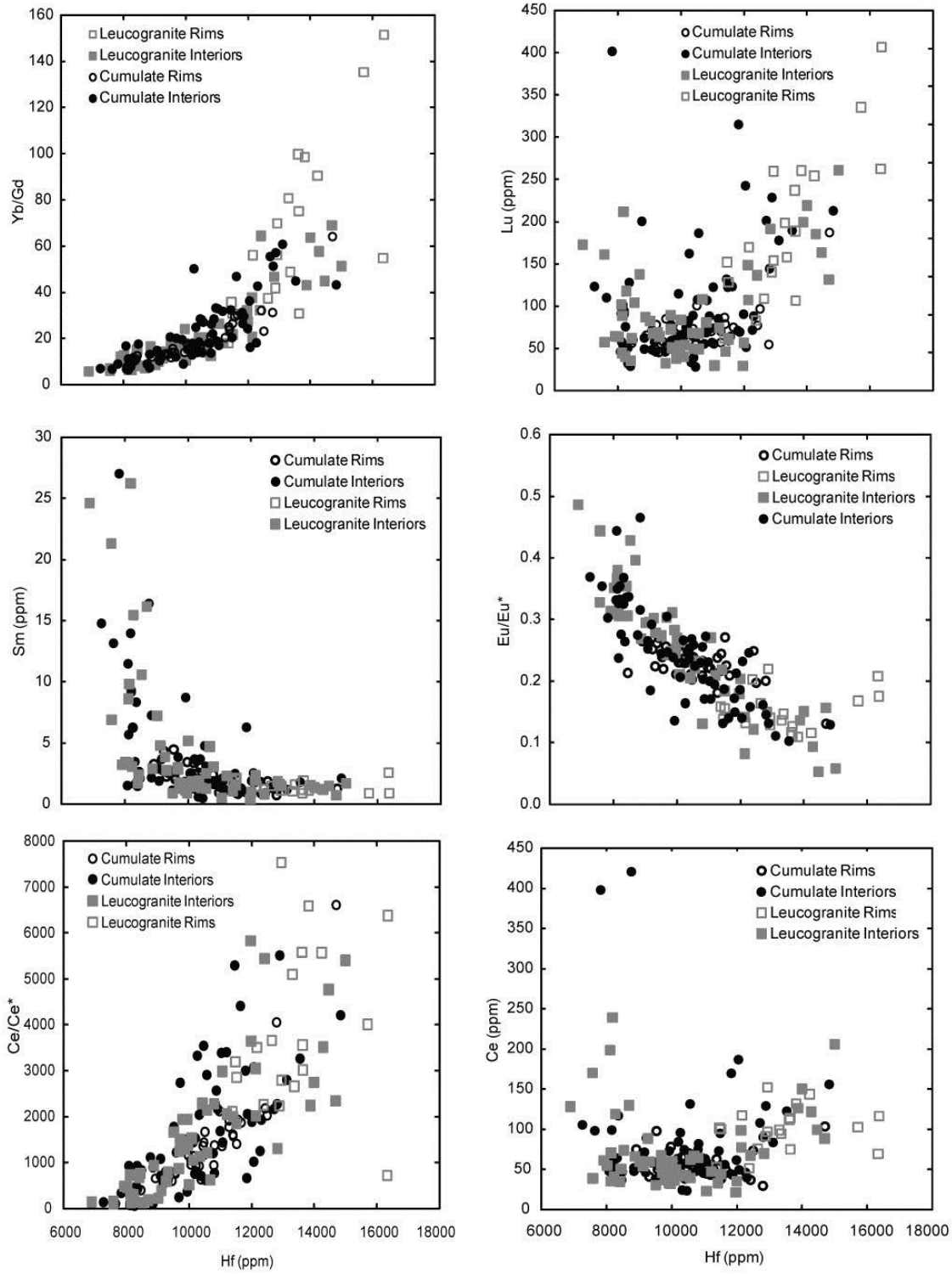

Figure 10: (a) Hafnium concentrations vs. Y/Gd in zircons illustrates variation in heavy REE vs. light REE with fractionation (b) Hafnium concentrations vs. Lu concentrations in zircons (c) Hafnium concentrations vs. Sm concentrations in zircons (d) Hafnium concentrations vs. Eu/Eu*, or Eu anomaly, in zircons (e) Hafnium concentrations vs. Ce/Ce*, or Ce anomaly, in zircons (f) Hafnium concentrations vs. Ce concentrations in zircons.

anomaly also increases with increasing fractionation and decreasing T_{TiZ} (Figure 10e). At high Hf the magnitude of the Ce anomaly increases sharply, primarily in the leucogranite rims, corresponding to increasing U, Th and heavy REE (Figure 10e). The Ce concentration appears to correlate weakly with fractionation (Figure 10f).

Comparison of the total 3+ ions in each analysis ($Sc^{3+}+Y^{3+}+REE^{3+}$) to P as a molar ratio reveals the ratio is nearly always greater than unity: that is, the substitution of 3+ cations for 4+ Zr is only partly charge-balanced by substitution of P^{5+} for Zr^{4+} ('xenotime substitution'). The amount of 3+ ions incorporated at any spot increases with P in a scattered, but grossly linear trend, and total 3+/P increases with increasing Hf and decreasing $T_{TiZ,}$ with maxima defined by leucogranite rims (Figure 11). The highest concentrations of P (ppm) and total 3+ ions are in spots with very low Hf and high T_{TiZ}.

5. Discussion

5.1. Ti-in-zircon Thermometer

It has been suggested (Fu et al., 2008) that further application of the Ti-in-zircon thermometer in natural systems with careful consideration of petrologic context is necessary to determine whether Ti-in-zircon is a reliable indicator of temperature. This is particularly true considering that our data, along with other studies (Miller and Wooden 2004; Bacon and Lowenstern 2005; Walker et al. 2007; Miller et al. 2007), suggest that it is common for zircons to finally reside in melt with which they are not cognate. This study, in which we can use the geochronology and trace element composition of the zircon along with extensive field observations and petrologic data, allows us to fit Ti-in-zircon temperatures into previously established zircon histories and test the thermometer.

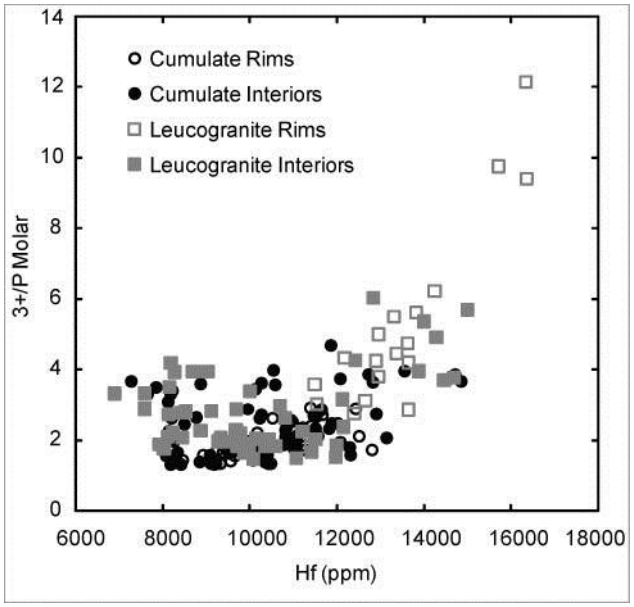

Figure 11: Hafnium concentrations vs. (the sum of all 3+ ions)/P to illustrate departure from the 'xenotime' substitution.

All calculated Ti-in-zircon temperatures, including maxima and minima, are reasonable for felsic magmas and for zircon growth. A discussion of relationships between zircon saturation and calculated T_{TiZ} can be found in the following section on zircon growth. Calculated T_{TiZ} from zoned zircons document sequences of changing thermal environments during growth that were previously suggested by field, petrologic and geochronologic relations (Walker et al., 2007). These temperatures also correlate well with zircon trace element data that also support such a history. The higher temperatures and common fluctuations recorded in zircons from the cumulate samples and the ubiquitous low temperature, fractionated rims on zircons in the leucogranites support at least the relative validity of the calculated temperature variations. Since the Ti-in-zircon record appears to correlate with all the other records, we feel confident that our assumptions were in fact, reasonable and the calculated temperatures are useful.

The ubiquity of sphene in all samples indicates relatively high $a\mathrm{TiO_2}$. If our assumed $a\mathrm{TiO_2}$ (0.7) is either an over or underestimate, the relative variations in temperature recorded by the zoned zircons remain intact and the resulting conclusions are robust. Ferry and Watson (2007) argue that $a\mathrm{TiO_2}$ and $a\mathrm{SiO_2}$ will likely vary together and therefore counterbalance their respective effects on the thermometer. As we have used a fixed value for both and calculations result in temperatures and relative temperatures that are reasonable in field, petrologic, and geochemical context, we again feel confident that these calculated temperatures are useful.

In addition to the issue of changing or unknown activity of $\mathrm{TiO_2}$ and $\mathrm{SiO_2}$, potential problems that have been associated with the thermometer include possible errors in calibration, pressure dependence (Tomkins et al. 2007; Anderson et al. 2007; Ferriss et al. 2008), subsolidus resetting of Ti composition, non-Henry's Law substitution of Ti into the zircon structure (Fu et al. 2008), and disequilibrium crystallization from melts (Fu et al. 2008). We argue that sufficient experimental (Watson and Harrison 2005; Watson et al. 2006; Ferry and Watson 2007; Hayden

and Watson 2007) and natural studies have been performed in field, geochemical and petrologic context that show well constrained and reasonable results (Claiborne et al. 2006; Reid et al. 2006; Vazquez et al. 2006; Reid and Vazquez 2006; Bea et al. 2007; Bromley et al. 2007; Miller et al. 2007; Leslie et al. 2007; Bolhar et al. 2008; Hiess et al. 2008) that calibration of the model apparently does not produce substantial error. Pressure dependence of the thermometer if applied to the Spirit Mountain batholith could result in temperatures that are tens of degrees lower than are reported herein (Ferriss et al. 2008; Ferry and Watson, 2007), but does not affect our conclusions regarding relative temperature changes or move the temperatures out of a range reasonable for felsic magmas. Cathodoluminescence images show magmatic textures for all grains, with no evidence for recrystallization. The retention of distinct trace element zoning tracked by our SHRIMP data indicates no diffusional, sub-solidus re-equilibration of Ti has occurred. Finally, at the low Ti concentrations under consideration, it is reasonable to assume Henry's Law substitution and neglect potential kinetic effects. Since our data do fit well with previously established petrologic and geochronologic models and with other geochemical indicators, we argue that these assumptions are reasonable and well founded in this case. If for other studies, the resultant temperatures do not make petrologic sense, then it may be necessary to reconsider one or more of these assumptions for each specific case.

5.2. Zircon growth and dissolution

A comparison of calculated zircon saturation temperatures with T_{TiZ} for the putative 'primary' magma represented by sample BGZ and the 'crystal-poor fractionated melt' represented by sample LGZ reveals some discrepancy. The highest Ti-in-zircon temperatures, from cumulate samples, are ~140°C higher than the calculated saturation temperature for what is assumed to be the batholith input composition. Only two T_{TiZ} from the rims of leucogranites that are assumed to have grown directly from segregated melt are appreciably higher (~50°C)

than the zircon saturation temperature for crystal-poor LGZ, and one of these rims appears to be generally more 'primitive' and therefore we would expect a higher T_{TiZ}. Harrison et al. (2007) found that in plutonic rocks, it is common for ~50% of T_{TiZ} to be greater than calculated zircon saturation temperatures. Normal crystallization of zircon-undersaturated melt will increase its zircon saturation temperature, as Zr concentration and 'M' value in the remaining melt increases. Since none of these natural samples, particularly the cumulate samples, was likely devoid of crystals when zircon began growing, it is expected that these zircon saturation temperatures calculated from bulk rock compositions will be underestimates. Plausibly, unusually high T_{TiZ} zones could reflect growth in Zr-rich melt pockets formed during reheating of zircon-rich cumulate mush. Alternatively, they might be derived from grains that grew at elevated T in fractionated mafic magma - perhaps restributed by disaggregation of enclaves.

Zircons from Spirit Mountain batholith do not exhibit a monotonic decrease in T_{TiZ} following the onset of crystallization, as would be predicted by simple crystallization and cooling (Harrison et al. 2007). Rather, the complexity in zoning suggests that the zircon population of each sample grew either in a complex magmatic environment with fluctuating conditions or during separate, repeated episodes of crystallization. Both scenarios are supported by ubiquitous resorption surfaces and embayments within zircon grains that suggest zircon-saturated magmas were repeatedly rejuvenated or mixed with hotter, zircon undersaturated magmas. These surfaces are commonly surrounded by bright zones with higher T_{TiZ}, suggesting that the rejuvenation or mixing allowed zircon to saturate at a higher temperature than previously. In order to achieve zircon growth at these higher temperatures, the Zr concentration in the melt must have increased (along with the other elements that comprise the 'M' factor). This could occur as rejuvenation dissolves zircon-rich cumulate, increasing the temperature required for saturation to temperatures that would normally result in total zircon

dissolution (>800°C). Some change in zircon saturation temperature might also be expected with introduction of a new magma with a different composition, although the large volumes of chemically, modally similar granite with a large age range (Walker et al. 2007) suggests that the composition of input magmas, with the exception of apparently low-volume mafic magma, were likely very similar throughout the lifetime of the batholith. Some bright, high T_{TiZ} zones surround darker cooler zones with no evidence of resorption. This could be attributable to buffering of zircon grains as inclusions in phenocrysts during periods of rejuvenation and dissolution, which would be an important consideration in interpreting any zircon data. These un-resorbed zircon grains apparently only contacted the higher temperature melt once the melt had re-saturated in zircon at the higher temperature. Alternatively, cores of cumulate zircons could represent grains injected into the system with input magmas, and could have grown at greater depth.

Ideally, we would like to correlate age and trace elements, including Hf, Ti and T_{TiZ}, in order to discuss timescales of growth and dissolution processes as well as a specific chronology of events during the assembly of the batholith and the resulting timescales. However, due to the relatively large errors on the geochronologic data, inherent to U-Pb systematics in zircons of this age, no significant correlations can be made.

5.3. Composition of Igneous Zircon: Implications for Magma Evolution

As there is also no evidence of re-equilibration or recrystallization, we assume the zircon geochemistry is indicative of its incorporation of constituents at the time of growth. Incorporation of dispersed elements into zircon should directly reflect melt composition according to an appropriate Henry's Law partition coefficient. However, partition coefficients for zircon are the subject of ongoing research and debate, in part because they are sensitive to changes in melt composition, oxygen fugacity and water content; furthermore, kinetic effects including boundary layer formation and disequilibrium crystallization can influence uptake of

elements and effective partition coefficients (Kds) (Watson 1980; Watson 1996; Hanchar and van Westrenen 2007). Because of this, and due to difficulties in attaining useful experimental data, Kds for REE incorporation during zircon growth from felsic melts are highly variable from study to study and may be unreliable (Luo and Ayers in revision). Partition coefficients for elements in higher abundance in zircon such as U and Th are more straightforward and are utilized below.

Systematic variation in trace element composition with temperature (T_{TiZ}) and degree of fractionation (as indicated by Hf) and covariance of T_{TiZ} with Hf that correlates with sample bulk rock chemistry and petrology, geochronology, and field relations together suggest that the composition of these zircons generally corresponds to real variation in melt composition. The close fit of our zircon data to petrologic context gives us confidence that zircon composition can be relied on to determine complexity in magmatic history and track evolution and fluctuations in magma temperature and composition, in spite of uncertainties in specific Kds. Certainly the general pattern of partition coefficient change is correct for zircon which means that the zircon composition can be used to generally interpret gross changes in magma composition (i.e. the high Yb/Gd ratios in zircon rims must reflect a melt pattern with flat or even negative slope for the heavy REE).

Relatively high Th/U (>1 with high maxima) is a common characteristic of zircon from the Mesozoic igneous rocks of the Mojave terrane, reflecting high magmatic Th/U that appears to be related to the regional lithosphere, although Th/U of these zircons is especially high. The ratio is especially high (up to 4.5) in zones that grew from higher temperature, less evolved melt, and drops rapidly with decreasing Hf and T_{TiZ}, leveling off at ~1.5 in zones that exhibit a cooler, evolved signature. These "cool" zones are richest in both U and Th. The initial sharp drop in this ratio is common in zircon, probably reflecting greater incompatibility of U than Th with

crystallizing assemblage, and suggesting a lack of early accessory mineral crystallization, as coeval crystallization of sphene, allanite and/or chevkinite would result in a decrease in both elements. More puzzling is the leveling off of the ratio in evolved portions of the zircon with high U and Th, suggesting that the two elements were both highly and equally incompatible with the most evolved mineral assemblages.

Published zircon/melt partition coefficients for U and Th vary by well over an order of magnitude (e.g. Mahood and Hildreth 1983; LaTourrette et al. 1991; Bea et al. 1994; Rubatto et al. 2007; cf. Blundy and Wood 2003; Charlier and Zellmer 2000; Wilson et al. 2006). These experimental and empirical studies appear to show a systematic increase in Kd with falling temperature, with values reaching 200-400 for U and 50-100 for Th at temperatures below 800°C. Using these Kds and evolved zircon compositions from leucogranite samples, concentrations of U and Th in the more evolved melts should be ~4 and ~20 ppm, respectively. This compares with typical U and Th concentrations of ~2-8 ppm and 17-68 ppm in fine-grained leucogranites that are considered to approximate the compositions of crystal-poor segregated melts from which these evolved zircon zones grew. Taking the fine-grained granites (sample BGZ) as representative of the input magma that formed the batholith (~1.5 ppm U, ~14 ppm Th), both the U-enriched zircon zones and the whole-rock leucogranite U concentrations appear to require at least 80% fractional crystallization to form the typical highly evolved melts and ~90% to form the most extreme compositions. These rim zones thus have quite reasonable compositions. Common concentrations of U and Th of ~50 and 150 ppm, respectively, found in zircons from all samples may represent growth following initial zircon saturation; using likely partition coefficients for T = 800-900°C of greater than 50 and 15 (see references above), these values suggest melt concentrations less than 1 and 10 ppm, respectively, similar to the measured concentrations of the input magma.

Miller and Wooden (2004) and Bindeman et al. (2008) suggest that melts with the highest U and Th concentrations indicated by zircon compositions from rhyolites that they studied (Coso, California, and Yellowstone) may reflect extreme fractional crystallization (>95%) and represent late stage, uneruptible melt, and thus that zircon with this composition documents growth in a specifically plutonic environment. Miller and Wooden (2004) point out that these late melts would be restricted by their low volumes and Zr concentrations to produce a very limited volume of zircon. It appears that rims on Spirit Mountain leucogranite zircons reflect similar, but somewhat less extreme, fractionation and an appropriately larger volume.

Rare earth element compositions of zircons in this study are in a very general sense typical for igneous zircon (Hoskin and Schaltegger, 2003) in that they are highly enriched in the heaviest REE, with enrichment decreasing systematically with decreasing atomic number. The exceptions to this regular pattern of increasing enrichment with atomic number, as with most zircons from granitic compositions, are positive Ce and negative Eu anomalies. Sharp increase in heavy REE enrichment and light REE depletion with fractionation are likely a function of extreme variation (increase or decrease, respectively) of concentrations of those elements in the melt as the melt composition becomes highly fractionated. Variations in zircon REE patterns probably reflect coeval crystallization of accessory minerals in which REE behave compatibly, (i.e. sphene, allanite and chevkinite). Growth of these minerals modifies REE patterns in the melt, and therefore in the growing zircon. The steeply positive middle to heavy REE accompanied by relatively flat light to middle REE visible in primitive zircon-normalized REE plots document a relative middle REE depletion and may indicate zircon growth coeval with sphene, which preferentially incorporates the middle REE (e.g. Glazner et al. 2008).

The modest Eu/Eu* values observed here suggest parental magmas that either had experienced significant feldspar fractionation before zircon reached saturation or had an initial

negative Eu anomaly as the result of being derived from a feldspar-rich source. The variation in the Eu anomaly for rims from both cumulates and leucogranites is small. The implication is that the Eu anomaly is being somewhat buffered in the rims, likely due to growth of coeval accessory minerals, including sphene. As expected, the leucogranite rims have a more negative anomaly than the cumulate rims, supporting the more fractionated character of the leucogranite melts. The implication is that the Eu anomaly is being somewhat buffered in the rims, likely due to growth of coeval accessory minerals, including sphene. As with other elements, the overlap of Eu/Eu* cumulate interior analyses and leucogranite rim analyses suggests that parts of the cumulate zircons did grow from melts as fractionated as those from which the leucogranite rims grew, but in general were in equilibrium with a less fractionated melt for their final stage of growth. This observation is consistent with the model for the extraction of the leucogranite melts from what became the cumulates, and that the cumulates are the product of repeated injections of less fractionated magma.

The ubiquitous positive Ce anomaly is the result of compatibility of Ce^{4+} with zircon, a consequence of its similar ionic radius and identical charge to Zr^{4+}. This contrasts to the trivalent light REE, which are mismatched with Zr in both charge and radius and are highly incompatible with zircon. It has been suggested that the magnitude of the anomaly is controlled by the oxygen fugacity of the magma and that it thus can be used to provide information on the fO_2. However, while the Ce anomaly in the zircons varies by a factor of more than 50, we see no independent evidence of changes in melt fO_2. We argue that while the Ce^{+3}/Ce^{+4} of the melt may likely be primarily controlled by the fO_2 (Hoskin and Schaltegger 2003), partitioning of Ce^{3+} and Ce^{+4} among coexisting phases may be more influential. The increasing Ce anomaly in zircon may be explained by highly compatible behavior of trivalent LREE during growth of other accessory minerals (allanite, chevkinite, sphene, apatite), but relatively incompatible behavior of

Ce^{+4}, which is likely compatible only with zircon and therefore would not decrease as much as other LREE and might actually increase in concentration as crystallization progresses. This behavior would be analogous to that demonstrated for Eu^{+2}/Eu^{+3} in clinopyroxene in highly fractionated melts (Ayers, 1993).

5.4. Spirit Mountain batholith: Construction and evolution of a large silicic system

The major and trace element geochemistry of zircons from the Spirit Mountain batholith appears to record the same history of protracted accumulation, repeated reheating and rejuvenation of zones within crystal mushes and episodic fractionation and melt segregation events, that is suggested by the petrology, field relations and U-Pb geochronology. Zircons from cumulate samples appear to have grown from relatively high temperature, less evolved melts (either in the cumulate pile or at some greater depth) and the ubiquitous evidence for resorption followed by growth at higher temperatures attests to their presence in a melt experiencing repeated inputs of new, hot magma. Zircons from leucogranites often contain cores that share this history with the cumulate zircons, representing grains that were carried along with the extracted, crystal-poor melt during segregation events (Claiborne et al. 2006). Rims on all leucogranite grains and cores of some appear to have grown entirely from highly evolved, cooler melt, presumably following the segregation event and injection of the extracted melt into the roof zone.

The extreme melt evolution recorded in some zircons requires significant crystallization and could potentially be used as an indicator of plutonic or near-solid conditions that are past the rheological limits for eruptibility or melt extraction (Bindeman et al., 2008; Miller and Wooden, 2004, Ayers, 1993). Zircons from the leucogranite samples from the Spirit Mountain batholith do attain these extreme compositions, particularly in rims and do record crystallization in highly evolved melts requiring significant crystallization. However, both cores and rims of

grains in the leucogranite record this, suggesting that from the time of interstitial melt extraction and throughout the entirety of new zircon growth, these conditions prevailed. This extracted melt was definitively below the eruptible rheological limit at the time of extraction and presumably for some time after. Similarly, no zircons from the cumulate samples that were presumably growing both prior to and after reaching the rheological limit show this signature, though they are irrefutably plutonic in nature. Although extreme composition zircons must have grown from highly evolved melts that had at some point undergone significant crystallization, considering this set of plutonic data along with the unreliability of zircon/trace element partition coefficients, it does not appear reasonable to use zircon compositions to divide definitively *plutonic* from definitively *volcanic* zircons.

Constraining the timescales of the magmatic processes through which a large magma body like the Spirit Mountain batholith accumulates and evolves are essential to a better understanding of these processes. Zircon growth rates are poorly understood, but age analyses of cores and rims on individual grains suggest that individual grains record events hundreds of thousands of years apart. We cannot definitively determine whether these grains record extended histories through constant slow growth punctuated by periods of dissolution, or record episodes of growth hundreds of thousands of years apart. With U-Pb SHRIMP age dating of zircons, errors are often on the order of hundreds of thousands of years, and these do not allow us to resolve the timing of heating or melt extraction events, although the complexity of the system over its lifetime appears irrefutable. As established by Walker et al. (2007), it is apparent that the Spirit Mountain batholith did accumulate over two million years and that repeated episodes of intrusion and heating followed by crystallization and melt segregation throughout that history built the body into its current form.

6. Conclusions

Hafnium, U and Th, and REE content of zoned zircons from the Spirit Mountain batholith correlate with calculated temperatures from the Ti-in-zircon thermometer as well as with field and petrologic evidence of rejuvenation of crystal mush and melt extraction events during the two million year accumulation of this patchwork batholith. While the timescales of specific events cannot be resolved, it is apparent that multiple rejuvenation and reheating events affected zircon grains within individual samples and that each sample contains grains that experienced different histories. These zircons document changes in the trace element budget of the magmas, potentially recording crystallization of other phases that exert control over this budget, such as sphene, allanite and chevkinite, and tracking general evolution of the magma with reheating, crystallization and segregation events. These zircons therefore tell a story of a large body with melt fraction and composition varying in both time and space, recycling these refractory zircon crystals during repeated episodes of intrusion, rejuvenation and interstitial melt extraction.

7. Acknowledgments

This work was supported by National Science Foundation grants EAR-0409876 and EAR-0107094. Frank K. Mazdab was instrumental in developing methods for analysis of trace elements in zircon using the SHRIMP-RG that we used in this study. We would like to thank BJ Walker for spending time in the field and in discussion working with us on puzzling out the history of the Spirit Mountain batholith. Discussions with Jonathan Miller regarding behavior of zircon in magmatic systems contributed to this work. Discussions with Ashley Bromley, Guil Gualda, Mark Ghiorso and Bruce Watson contributed to our understanding of the behavior of $a\mathrm{TiO_2}$ and its influence on the Ti-in-zircon thermometer.

8. References

Ahrens LH, Erlank AJ (1969) Hafnium In: Wedepohl KH (ed) Handbook of Geochemistry, 2-5, sections B-O. Springer, Berlin.

Anderson BE, Essene EJ, Becker U (2007) Ti substitution in zircon. Geochim Cosmochim Acta 71:A27

Bachmann O, Bergantz GW (2004) On the origin of crystal-poor rhyolites: extracted from batholithic
crystal mushes. J Petrol 45:1565-1582

Bacon CA, Lowenstern JB (2005) Late Pleistocene granodiorite source for recycled phenocrysts in rhyodacite lava at Crater Lake, Oregon. Earth Planet Sci Lett 233:277-293

Bea F, Montero P, Gonzalez-Lodiero F, Talavera C (2007) Zircon inheritance reveals exceptionally fast crustal magma generation processes in Central Iberia during the Cambro-Ordovician. J Petrol 48:2327-2339

Bea F, Montero P, Ortega M (2006) A LA-ICPMS evaluation of Zr reservoirs in common crustal rocks: Implications for Zr amd Hf geochemistry and zircon-forming processes. Can Mineral 44:693-714

Bea F, Pereira MD, Stroh A (1994) Mineral/leucosome trace element partitioning in a peraluminous migmatite (a laser ablation-ICP-MS study). Chem Geol 117:291-312

Belousova EA, Griffin WL, O'Reilly SY, Fisher NI (2002) Igneous zircon: trace element composition as an indicator of source rock type. Contrib Mineral Petrol 143:602-622

Bindeman IN, Fu B, Kita NT, Valley JW (2008) Origin and evolution of silic magmatism at Tellowstone based on ion microprobe analysis and isotopically zoned zircons. J Petrol 49:163-193

Blundy J,Wood B (2003) Partitioning of trace elements between crystals and melts. Earth Planet Sci Lett 210:383-397

Bolhar R, Weaver SD, Palin JM, Cole JW, Paterson LA (2008) Systematics of zircon crystallization in the Cretaceous Separation Point suite, New Zealand, using U/Pb isotopes, REE and Ti geothermometry. Contrib Mineral Petrol 156:133-160

Bromley SA, Miller CF, Claiborne LL, Wooden JL, Mazdab FK (2007) Record of Hybridization Preserved in Zircon, Aztec Wash Pluton, NV. Eos Trans AGU 88:V51C-0705

Brown SJA, Fletcher IR (1999) SHRIMP U-Pb dating of the pre-eruption growth history of zircons from the 340 ka Whakamaru Ignimbrite, New Zealand: Evidence for >250 k.y. magma residence times. Geol 27:1035-1038

Charlier B, Zellmer G (2000) Some remarks on U-Th mineral ages from igneous rocks with prolonged crystallization histories. Earth Planet Sci Lett 183:457-469.

Charlier BLA, Wilson CJN, Lowenstern JB, Blake S, Van Calsteren PW, Davidson JP (2005) Magma generation at al large, hyperactive silicic volcano (Taupo, New Zealand) revealed by U-Th and U-Pb systematics in zircons. J Petrol 46:3-32

Cherniak DJ, Watson EB (2003) Diffusion in zircon In: Hanchar JM, Hoskin PWO (eds) Zircon, reviews in mineralogy and geochemistry, vol 53. Mineralogical Society of America, Washington, pp 113-144

Cherniak DJ, Hanchar JM, Watson EB (1997) Diffusion of tetravalent cations in zircon. Contrib Mineral Petrol 127:383-390

Cherniak DJ, Hanchar JM, Watson EB (1997) Rare-earth diffusion in zircon. Chem Geol 134:289-301

Claiborne LL, Miller CF, Walker BA, Wooden JL, Mazdab FK, Bea F (2006) Tracking magmatic processes through Zr/Hf rations in rocks and Hf and Ti zoning in zircons: An example from the Spirit Mountain batholith, Nevada. Mineral Mag 70:517-543

Claiborne LL, Furbish DJ, Miller CF (2006) Determining mechanics of segregating small crystals from melt using modeling and SHRIMP-RG trace element analysis of zircons: An example from the Spirit Mountain Batholith, Nevada. Eos Trans AGU 87:V54B-02

Coleman DS, Gray W, Glazner AF (2004) Rethinking the emplacement and evolution of zoned plutons: Geochronologic evidence for incremental assembly of the Tuolumne Intrusive Suite, California. Geol 32:433-436

Davidson JP, Morgan DJ, Charlier BLA (2007) Isotopic Microsampling of Magmatic Rocks. Elem 3: 253-259

Davies GR, Halliday AN, Mahood GA, Hall CM (1994) Isotopic constrains on the production-rates, crystallization histories and residence times of pre-caldera silicic magmas, Long Valley, California. Earth Planet Sci Lett 125:17-37

Eichelberger JC, Izbekov PE (2000) Eruption of andesite triggered by dyke injection; contrasting cases at Karymsky Volcano, Kamchatka and Mt Katmai, Alaska. Philos Trans R Soc Lond 358:1465-1485

Faulds JE, Geissman JW, Shafiqullah M (1992) Implications of paleomagnetic data on Miocene extension near a mjor accommodation zone in the Basin and Range province, northwestern Arizona and southern Nevada. Tectonics 11:204-227

Faulds JE, Feuerbach DL, Reagan MK, Metcalf RV, Gans P, Walker JD (1995) The Mount Perkins Block, northwestern Arizona: an exposed cross section of an evolving, pre-extensional to synextensional magmatic system. J Geophys Res, Solid Earth Planet 100:15249-15266

Ferriss, E.D.A., Essene, E.J. and Becker, U. (2008) Computational study of the effect of pressure on the Ti-in-zircon thermometer. Eur J. Mineral 20: 745-755

Ferry JM, Watson EB (2007) New thermodynamic models and revised calibrations for the Ti-in-zircon and Zr-in-rutile thermometers. Contrib Mineral Petrol 154:429-437

Finch RJ, Hanchar JM (2003) Structure and chemistry of zircon and zircon-group minerals In: Hanchar JM, Hoskin PWO (eds) Zircon, reviews in mineralogy and geochemistry, vol 53. Mineralogical Society of America, Washington, pp 1-26

Ferriss EDA, Essene EJ, Becker U (2008) Computational study of the effect of pressure on the Ti-in-zircon geothermometer. Eur J Mineral 20:745-755

Fowler A, Prokoph A, Stern R, Dupuis C (2002) Organization of oscillatory zoning in zircon: Analysis, scaling, geochemistry, and model of a zircon from Kipawa, Quebec, Canada. Geochim Cosmochim Acta 66:311-328

Fu B, Page FZ, Cavosie AJ, Fournelle J, Kita NK, Lackey JS, Wilde SA, Valley JW (2008) Ti-in-zircon thermometry: applications and limitations. Contrib Mineral Petrol 156:197-215

Gans PB, Bohrson WA (1998) Suppression of volcanism during rapid extension in the Basin and Range province, United States. Sci 279:66-68

Glazner AF, Coleman DS, Bartley JM (2008) The tenuous connection between high-silica rhyolites and granodiorite plutons. Geol 36:183-186

Glazner AF, Bartley JM, Coleman DS, Gray W, Taylor RZ (2004) Are plutons assembled over millions of years by amalgamation from small magma chambers. GSA Today 14:4-11

Hanchar JM, van Westrenen W (2007) Rare earth element behavior in zircon-melt systems. Elem 3:37-42

Hanchar JM, Watson EB (2003) Zircon saturation thermometry In: Hanchar JM, Hoskin PWO (eds) Zircon, reviews in mineralogy and geochemistry, vol 53. Mineralogical Society of America, Washington, pp 89-112

Hanchar JM, Miller CF (1993) Zircon zonation patterns as revealed by cathodoluminescence and backscattered electron images: Implications for interpretation of complex crustal histories. Chem Geol 110:1-13

Harley SL, Kelly NM (2007) Zircon: tiny but timely. Elem 3:13-18

Harper BE, Miller CF, Koteas GC, Cates NL, Wiebe RA, Lazzareschi DS, Cribb JW (2004) Granites, dynamic magma chamber processes and pluton construction: the Aztec Wash pluton, Eldorado Mountains, Nevada, USA. Trans R Soc Edinb – Earth Sci 95: 277-295

Harrison TM, Watson EB, Aikman AB (2007) Temperature spectra of zircon crystallization in plutonic rocks. Geol 35:635-368

rrison TM, Watson EB (1983) Kinetics of zircon dissolution and zirconium diffusion in granitic melts of variable water content. Contrib Mineral Petrol 84:67-72

Hayden LA, Watson EB (2007) Rutile saturation in hydrous silicate melts and its bearing on Ti-thermometry of quartz and zircon. Earth Planet Sci Lett 258:561-568

Heaman LM, Bowins R, Crocket JH (1990) The chemical composition of igneous zircon suites: implications for geochemical tracer studies. Geochim Cosmochim Acta 54:1597-1607

Hiess J, Nutman AP, Bennett VC Holden P (2008) Ti-in-zircon thermometry applied to contrasting Archean metamorphic and igneous systems. Chem Geol 247:323-388

Hildreth W (2004) Volcanological perspectives on Long Valley, Mammoth Mountain, and Mono Craters: several contiguous but discrete systems. J Volcanol Geotherm Res 136:169-198

Hopson, C.A., Gans, P.B., Baer, E., Blythe, A.E., Calvert, A. and Pinnow, J. (1994) Spirit Mountain Pluton, southern Nevada; a progress report. Geol Soc Am Abstr Program 26:60

Hoskin PWO (2000) Patterns of chaos: Fractal statistics and the oscillatory chemistry of zircon. Geochim Cosmochim Acta 64:1905-1923

Hoskin PWO, Schaltegger U (2003) The composition of zircon and igneous and metamorphic petrogenesis In: Hanchar JM, Hoskin PWO (eds) Zircon, reviews in mineralogy and geochemistry, vol 53. Mineralogical Society of America, Washington, pp 27-62

Howard KA, Wooden JL, Simpson RW, Pease VL (1996) Extension-related plutonism along the Colorado River extensional corridor. Geol Soc Am Abstr Program 28:450

La Tourrette TZ, Burnett DS, Bacon CR (1991) Uranium and minor-element partitioning in Fe-Ti oxides and zircon from partially melted granodiorite, Crater Lake, Oregon. Geochim Cosmochim Acta 55:457-469

Leslie S, Miller J, Miller C, Wooden J, Faulds J (2007) Magmatic construction of the Searchlight magmatic system (Eldorado-Newberry Mountains, Nevada) as revealed through zircon geochemistry and Ti-in-zircon geothermometry. Eos Trans. AGU 88:V51C-0707

Luo Y, Ayers JC (in revision) Experimental measurements of zircon/melt trace element partition coefficients. Geochim Cosmochim Acta

Mahood GA, Hildreth W (1983) Large partition coefficients for trace elements in high-silica rhyolites. Geochim Cosmochim Acta 47:11-30

Marks MAW, Coulson AM Schilling J, Jacob DE, Schmitt AK, Markl G (2008) The effect of titanite and other HFSE-rich mineral (Ti-bearing andradite, zircon, eudialyte) fractionation on the geochemical evolution of silicate melts. Chem Geol 257:153-172

Mazdab FK, Wooden JL (2006) Trace element analysis of accessory and rock forming minerals by ion microprobe (SHRIMP-RG). Eos Trans AGU 87:V33A-0630

Miller CF, McDowell SM, Mapes RW (2003) Hot and cold granites? Implications of zircon saturation and preservation of inheritance. Geol 31:529-532

Miller JS, Matzel JEP, Miller CF, Burgess SD, Miller RB (2007) Zircon growth and recycling during the assembly of large, composite arc plutons. J Volcanol Geotherm Res 167:282-299

Miller JS, Matzel J, Wooden JL, Burgess S, Mazdab FK, Mundil R (2007) Zircon age spectra, zircon crystallization temperature, and the growth of the half dome and cathedral peak granodiorites, Sierra Nevada batholith, California. Geol Soc Am Abstr Program 39: 527

Miller JS, Wooden JL (2004) Residence, resorption and recycling of zircons in Devils Kitchen rhyolite, Coso Volcanic field, California. J Petrol 45:2155-2170

Pallister JS, Hoblitt RP, Reyes AG (1992) A basalt trigger for the 1991 eruptions of Pinatubo volcano? Nature 356:426-428

Putnis A, Fernandez-Diaz L, Prieto M (1992) Experimentally produced oscillatory zoning in the (Ba,Sr)SO4 solid solution. Nat 358:743-745

Reid MR, Vazquez JA (2006) Crystal-scale t-T-X records in zircons from the Youngest Toba Tuff, Sumatra, Indonesia, Eos Trans. AGU 87:V54B-01.

Reid, M.R., Vazquez, J.A., Simon, J.I., Schmitt, A.K. (2006) Zircon geothermometry and the Bishop Tuff: Evidence for remobilization of crystal mush or for temperature-independent Ti partitioning? Eos Trans. AGU 87:V51E-1712.

Reid MR, Coath CD, Harrison TM, McKeegan KD (1997) Prolonged residence times for the youngest rhyolites associated with Long Valley Caldera: (super 230) Th- (super 238) U ion microprobe dating of young zircons. Earth Planet Sci Lett 150:27-39

Rubatto D, Hermann J (2007) Experimental zircon/melt and zircon/garnet trace element partitioning and implications for the geochronology of crustal rocks. Chem Geol 241:38-61

Schmitt AK, Lindsay JM, de Silva S, Trumbull RB (2003) U-Pb zircon
chronostratigraphy of early-Pliocene ignimbrites from La Pacana, North Chile: Implication for the formation of stratified magma chambers. J Volcanol Geotherm Res 120:43-53

Shore M, Fowler AD (1996) Oscillatory zoning in minerals: a common phenomenon. Can Mineral 34:1111-1126

Sparks SRJ, Sigurdsson H, Wilson L (1977) Magma mixing: a mechanism for triggering acid explosive eruptions. Nat 267:315-318

Tomkins HS, Powell R, Ellis DJ (2007) The pressure dependence of the zirconium-in-rutile thermometer. J Metamorph Geol 25:703-713

Vazquez JA, Reid MR, Kyriazis SF (2006) Differentiation and thermal history of the post-collapse magma reservoir at Yellowstone caldera as revealed by combining the temperature-age-compositional history of zircons. Eos Trans. AGU, 87:V51E-1713

Vazquez JA, Kyriazis S, Reid MR, Sehler R, Ramos F (2008) Thermochemical evolution of young rhyolites at Yellowstone: evidence for a cooling but periodically replenished postcaldera magma reservoir. J Volcanol Geotherm Res (in press)

Vazquez JA, Reid MR (2002) Timescales of magma storage and differentiation of voluminous high-silica rhyolites at Yellowstone caldera, Wyoming. Contrib Mineral Petrol 144:274-285

Walker BA, Miller CF, Claiborne LL, Wooden JL, George B (2007) Batholith construction: New insights concerning timescales and physical processes from the Spirit Mountain Batholith, southern Nevada. J Volcanol Geotherm Res 167:239-262

Wark DA, Hildreth W, Spear FS, Cherniak DJ, Watson EB (2007) Pre-eruption recharge of the Bishop magma system. Geol 35:235-238

Wark DA, Miller CF (1993) Accessory mineral behavior during differentiation of a granite suite: monazite, xenotime and zircon in the Sweetwater Wash pluton, southeastern California, USA. Chem Geol 110:49-67

Watson EB (1996) Dissolution, growth and survival of zircons during crustal fusion: kinetic principles, geological models, and implications for isotopic inheritance. Special Paper - Geol Soc Am 31:43-56

Watson EB, Harrison TM (2005) Zircon thermometer reveals minimum melting conditions on earliest Earth. Sci 308:841-844

Watson EB, Wark DA, Thomas JB (2006) Crystallization thermometers for zircon and rutile. Contrib Mineral Petrol 151:413-433

Watson EB (1980) Some experimentally determined zircon-liquid partition coefficients for the rare-earth elements. Geochim Cosmochim Acta 44:895-897

Wiebe RA, Hawkins DP (2004) Multiple replenishments in an evolving silicic magma chamber: The Vinalhaven intrusive complex, Maine, USA. Geochim Cosmochim Acta 68:A672

CHAPTER III

ZIRCON REVEALS PROTRACTED MAGMA STORAGE AND RECYCLING BENEATH MOUNT ST. HELENS

Abstract

Current data and models for Mount St. Helens volcano suggest relatively rapid transport from magma genesis to eruption, with no evidence for protracted storage or recycling of magmas. However, we show here that complex zircon age populations extending back hundreds of thousands of years from eruption age indicate that magmas regularly stall in the crust, cool and crystallize beneath the volcano, and are then rejuvenated and incorporated by hotter, young magmas on their way to the surface. Estimated dissolution times suggest that entrained zircon generally resided in rejuvenating magmas for no more than about a century. Zircon elemental compositions reflect the increasing influence of mafic input into the system through time, recording growth from hotter, less evolved magmas tens of thousands of years prior to appearance of mafic magmas at the surface or changes in whole rock geochemistry and petrology and providing a new, time-correlated record of this evolution independent of the eruption history. Zircon data thus reveal the history of the hidden, long-lived intrusive portion of the Mount St. Helens system, where melt and crystals are stored for up to hundreds of thousands of years and interact with fresh influxes of magmas that traverse the intrusive reservoir before erupting.

1. Introduction

Constraining timescales of magmatic processes at arc volcanoes is essential to understanding how magmas are transported, stored, and interact in the crust and what may trigger volcanic eruptions. Recent studies of Mount St. Helens have established that melts and major phase crystals erupted from this iconic arc system are generally relatively young, suggesting that only a few thousand years pass between generation and eruption of the magmas (Cooper and Donnelly, 2008; Cooper and Reid, 2003; Volpe and Hammond, 1991). This is in contrast to models of many other continental arc volcanic systems, where mafic magmas may be generally young, but intermediate to silicic magmas appear to have experienced more protracted and complex histories (Zellmer et al., 2005). Evidence from the Aleutian Arc (Bacon et al., 2007), the Aegean Arc (Zellmer and Turner, 2007; Bachmann et al., 2007), the Taupo Volcanic Zone (Charlier et al., 2003) and large volcanoes in the Cascade Arc (Bacon & Lowenstern, 2005; Reagan et al., 2003) suggest that these magmas require more extended timescales (10s to 100s of k.y.) for fractionation and accumulation, or may often be stored for these timescales and then remobilized before eruption. These protracted histories also correspond to the plutonic record, where zircon U-Pb studies indicate that accumulation and evolution of silicic magmatic bodies in the crust require hundreds of thousands to millions of years (Miller et al., 2007; Walker et al., 2007).

Zircon provides a uniquely appropriate tool to address questions of duration and conditions of magma storage and evolution in young volcanic systems, through combined ^{238}U-^{230}Th disequilibria dating and elemental analysis of growth zones by ion probe. Uranium-Thorium analysis of young zircon yields uncertainties of thousands to tens of thousands of years that allow us to investigate timescales of magmatic processes (e.g., Bacon and Lowenstern, 2005; Charlier et al., 2003), and corresponding elemental compositions provide an

unprecedented time-correlated record of the evolving growth environment (e.g. Claiborne et al., 2010, 2006a). Using the USGS-Stanford Sensitive High Resolution Ion Microprobe – Reverse Geometry (SHRIMP-RG), we have applied these combined methods to zircons extracted from erupted products that span the 300,000 year eruptive history of Mount St. Helens. Our unique dataset illuminates the previously hidden intrusive component of the Mount St. Helens system, where magmas and their crystals are stored for as much as hundreds of thousands of years before being entrained by erupting magmas, and where magmatic processes and interactions begin that manifest themselves in surface products tens of thousands of years later.

2. Mount St. Helens Background

Recent research has established that Mount St. Helens has been erupting for nearly 300 k.y., over which time volcanism has migrated 10 km eastward to the location of the current edifice (Clynne et al., 2008). The dominantly erupted dacites appear to be lower crustal melts generated in response to intrusion of mantle basalts, which are also occasionally erupted, and relatively sparse intermediate compositions are produced by mixing of the two end members (Pallister et al., 2008; Smith and Leeman, 1993, 1987). Trends in geochemistry and mineral assemblages suggest that the earlier erupted magmas were generally relatively silicic, cool, and wet, with no evidence for interaction with more primitive magmas (Clynne et al., 2008). As the system matured, mafic input apparently increased, and beginning ~20 ka the erupted dacitic magmas became hotter and drier and showed more evidence of interaction with mafic end members (Clynne et al., 2008).

Geophysical studies of the crust and petrologic studies of Mount St. Helens' recently erupted products provide clues to the size, shape, conditions, and timing of processes in the modern magma reservoir. Uranium-series disequilibria of glasses indicate that melts are

generated within a few thousand years of eruption, and feldspars appear to have grown from days (Blundy and Cashman, 2001) to <20 k.y. before eruption (Cooper and Donnelly, 2008; Cooper and Reid, 2003; Volpe and Hammond, 1991). The complex compositional zoning and multiple populations of pyroxene, amphibole and plagioclase indicate that magma mixing, crystal recycling on the scale of thousands of years, and convection in the chamber are common (Cooper and Donnelly, 2008; Cooper and Reid, 2003; Rutherford and Devine, 2008; Streck et al., 2008). Iron-titanium oxides indicate storage at temperatures from 820 °C to 940 °C (Rutherford and Devine, 2008; Rutherford et al., 1985). Seismic and petrologic studies indicate that melt-rich magma is stored in a widened conduit at 5–12 km depth (Pallister et al., 2008; Gardner et al., 1995). The above information creates a vivid model of the upper part of the modern magmatic system: magmas generated in the lower crust ascend into a widened conduit at 5–12 km depth, ~4 km^3 in volume, in which they convect, mingle and partially crystallize in the short timescales before eruption as well as recycle phenocrysts from crystal mushes that have been stored on the scale of thousands of years (Pallister et al., 2008).

3. Methods

We used the SHRIMP-RG at the Stanford-USGS Microanalytical Center to measure U-Th and U-Pb isotopes and trace elements in zircons following Bacon and Lowenstern (2005), Walker et al. (2007), Claiborne et al. (2006a, 2010), and Mazdab and Wooden (2006). These data provided crystallization ages and chemical composition of zircon from eighteen erupted units that span the eruptive history of Mount St. Helens, nine of which comprise a study focusing on one eruptive period (9–16 ka). Uranium-Thorium data were collected for samples erupted less than 300 ka; U-Pb data were collected for the sample erupted ~300 ka and for spots proved older than 300 ka by U-Th analyses. Since the zircon is not cognate to the melt in which it

erupted (see discussion), we cannot directly use whole rock or glass ($^{230}Th/^{232}Th$) to establish the initial ratio. We chose an initial ($^{230}Th/^{232}Th$) of 1.2, reported in Cooper and Donnelly (2008) for the 2004–2006 eruption and within 0.15 of all previously published values (Cooper and Reid, 2003; Volpe and Hammond, 1991; Bennett et al., 1982), as a likely average for the Mount St. Helens dacites. Likely variability of this ratio introduces uncertainty on the scale of thousands of years into our model ages, particularly those with low U/Th, but this is not sufficiently large to affect our main conclusions. We use Ti concentration to constrain temperature, following the Ti-in-zircon thermometer (Ferry and Watson, 2007), assigning $\alpha_{SiO2} = 1$ and $\alpha_{TiO2} = 0.7$. Quartz is a common phenocryst in the more silicic lavas, and we interpret most zircon growth to have occurred at or near quartz saturation. Compositions of Mount St. Helens glasses suggest high a_{TiO2} (>0.5), calculated following Hayden and Watson (2007; cf. Claiborne et al., 2006a, 2010). Assuming too high a_{TiO2} or too low a_{SiO2} results in underestimation of temperature, and an error of 0.2 in activity estimates yields an error of ~30 °C; this uncertainty does not affect our main conclusions.

4. Results

Uranium-Thorium and U-Pb analyses of 325 spots on zircon collected from 17 samples ranging from the oldest known (~300 ka) to most recent (December 2005) eruptions provide a contrasting but complementary and more complex view of magma storage and interaction beneath Mount St. Helens than previously established. All samples have multiple age populations, including ages at least 150 k.y. older than their eruption age (Fig. 1,2). Age groups, which range from ~6–600 ka, generally appear in multiple, but not all, samples. Younger ages generally dominate over older, but it is common for the youngest identified ages for a sample to be at least 10s of k.y. older than the eruption age; only 3 of 17 samples contain ages within error

(~5-20 k.y.) of eruption age as defined by $^{40}Ar/^{39}Ar$, K-Ar or radiocarbon (Clynne et al., 2008). Ten of the analyses reveal xenocrystic zircons that range from 12 to 96 Ma; these are most common in the earlier eruptions.

Just as the zircons from any one sample are a composite of many ages, many of the zircons themselves record more than one growth episode. In grains large enough for multiple U-Th analyses, the magmatic ages vary from core to rim by as much as 200 k.y. Age and compositional variations usually correspond to zones visible in cathodoluminescence images of the zircon grains (Fig. 3) that are sometimes separated by resorption surfaces. Rounded external morphology suggests that most zircons from some samples suffered resorption prior to eruption, whereas all zircons from some other units are euhedral.

Concentrations of Ti and Hf correlate inversely (Fig. 4). Older zircon is more restricted in composition, with lower Ti (~3–10 ppm) and higher Hf (~11,000–14,000 ppm) than the younger zircon, which ranges to a maximum of ~40 ppm Ti and a minimum of ~6200 ppm Hf. A distinct increase in variability and in maximum Ti and minimum Hf corresponds to zircon ages beginning ~100 ka (Fig. 4).

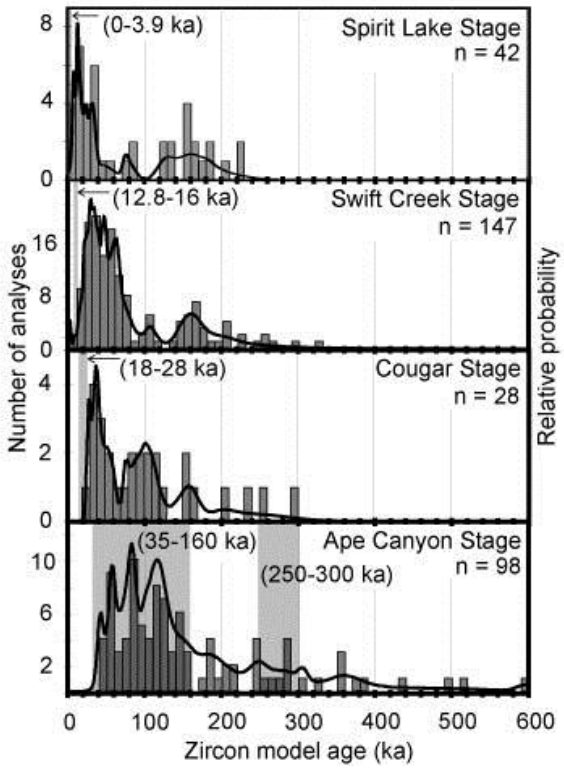

Figure 1: Probability density and histograms of zircon model ages. Each of the four panels contains a histogram for samples erupted during one of Mount St. Helens' four eruptive periods, as described in Clynne et al. (2008). The black lines represent the probability density curves and the shaded areas show the age of the relevant eruptive period, listed in parentheses. Clynne et al. (2008) describes a possible hiatus in Ape Canyon stage activity from ~160 to 250 ka.

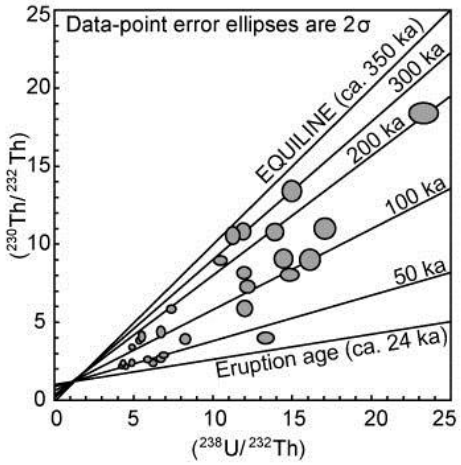

Figure 2: (^{230}Th/^{232}Th) as a function of (^{238}U/^{232}Th) in zircon from one sample. Each gray ellipse represents the ± 2σ error of one analysis. Representative isochrons are included for reference. The equiline represents the age at which the U-Th system reaches equilibrium (~350 ka) and is no longer useful for geochronology. This unit yielded a calibrated radiocarbon age of 24.3 ± 0.5 ka (Clynne et al., 2008).

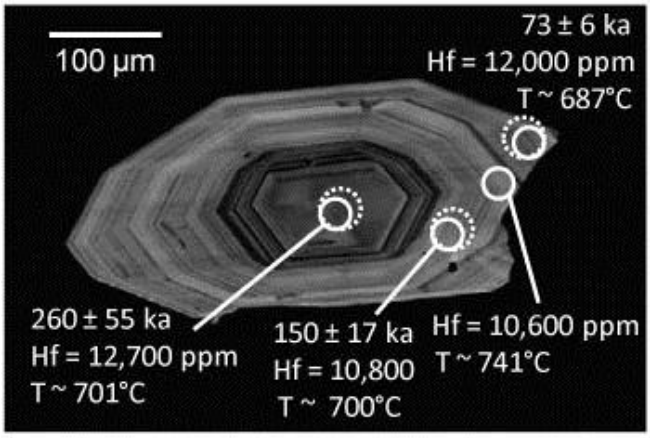

Figure 3: Cathodoluminescence image of an exceptionally large zoned zircon showing multiple SHRIMP analysis locations and corresponding age and trace element data. The dashed circles represent U-Series analyses and the solid circles represent trace element analyses. The uncertainties on the age data are ± 2σ.

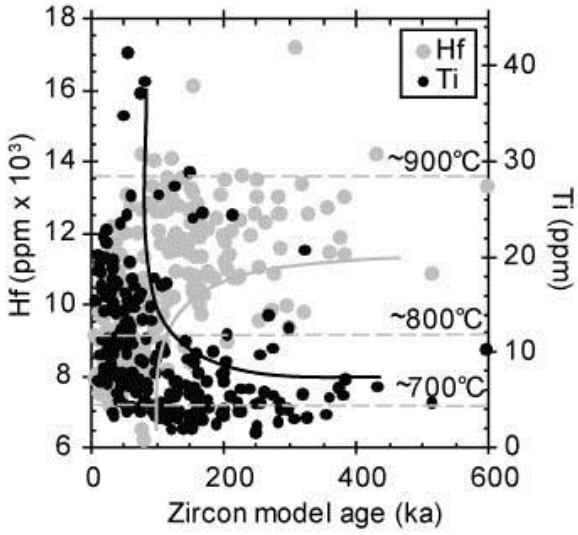

Figure 4: Hf and Ti concentration in zircons from Mount St. Helens as a function of zircon age. Analytical error for Ti and Hf concentrations is smaller than the symbols. See Figure 2 for typical 2σ uncertainties on age data. The gray and black curves show the boundaries of the fields containing >95% of Hf and >90% of Ti concentrations, respectively. The horizontal dashed lines represent approximate temperatures for the given Ti ppm from Ti-in-zircon thermometry (Ferry and Watson, 2007).

5. Discussion and Conclusions

As the only mineral identified as more than a few thousand years older than its eruption, zircon records a different, more extended part of the Mount St. Helens magmatic history than any other phase. This could be due to its relatively slow growth and dissolution (Watson, 1996), low diffusivities (Cherniak et al., 1997) and resulting ability to survive reheating events intact while other phases are dissolved or have their age and chemical systems reset. Furthermore, zircon is sufficiently small that it will behave as a physical tracer in the melt (Claiborne et al., 2006b), segregating from rejuvenated, crystal-rich, sluggishly mobile mushes with interstitial melt while the major phases coeval with the zircon remain locked in the "rigid sponge" (rheologically solid, melt-poor, Hildreth, 2004) portion of the magma system. These characteristics may distinguish its behavior during magmatic processes, resulting in zircon and major phases in the same volcanic rock that potentially have very different histories.

The oldest magmatic ages (500–600 ka) likely reflect the initiation of the Mount St. Helens magmatic system, ~300 k.y. before the first known eruption. The increase in abundance of ages with time may suggest higher rates of zircon crystallization as the magmatic system matured, but paucity of older ages (including xenocrysts) must be treated carefully; it may represent loss of zircon crystals through time by heating and dissolution, or natural bias in sampling as a consequence of focused ascent within younger portions of the system. Regardless, dominant age populations probably represent episodes of increased crystallization. Zircon saturation temperatures (Watson and Harrison, 1983) calculated from whole rock compositions suggest saturation at ~740–780 °C for melts with compositions equivalent to our samples, broadly consistent with dominant estimated Ti-in-zircon temperatures (Ferry and Watson, 2007, Fig. 4). Close coincidence between whole-rock saturation temperature and actual temperature

of initiation of growth is not necessarily expected because whole rocks are not equivalent to melt compositions (c.f. Harrison et al., 2007). Furthermore, the magmas that transported Mount St. Helens zircons to the surface are not the ones in which they crystallized (see discussion). At the probable thermal interval of dominant zircon growth for Mount St. Helens dacites based on both thermometers, these magmas would have been crystal-rich mushes or immobile, rigid sponges, indicating that episodes of zircon growth correspond to cooling and crystallization events in the sub-volcanic system. These could correspond to post-eruptive cooling or intrusive events during periods of reduced replenishment and eruption, but magnitudes of uncertainties on eruption ages and zircon ages and the possibility of unidentified eruptive units prohibit direct correlation on a large scale.

The crystal-rich storage zone suggested by our data has been repeatedly remobilized by hot, young magmas that reheat, mix and incorporate older Mount St. Helens magmas shortly before eruption (e.g. Charlier et al., 2003; Bacon and Lowenstern, 2005; Zellmer & Turner, 2007; Zellmer et al., 2003). The zircon ages present in any eruption would then partly depend on the physical distribution of zircon populations in the storage zone relative to the path that the replenishing magma took on its way to eruption, resulting in complex age populations that vary from eruption to eruption. The paucity of eruption-age zircon is likely a consequence of erupting magmas that were undersaturated in zircon. The fact that the entrained/recycled zircons have not been completely dissolved constrains the amount of time they have been in contact with the undersaturated melt to less than ~100 years (following the models of Watson (1996) and assuming grains with radii of ~50 μm in undersaturated melt with 4 wt% water at ~900 °C; c.f. Zellmer et al. (2003)), constraining the timescale between rejuvenation and eruption and corroborating other evidence that the Mount St. Helens erupted magmas are not stored in the upper crust for long periods of time prior to eruption (Cooper and Donnelly, 2008).

Using Hf as an indicator of fractionation (Claiborne et al., 2006a) and Ti as a proxy for temperature (Ferry and Watson, 2007), variations in zircon geochemistry clearly illustrate that the early melts from which zircon grew were generally cool (most ≤750 °C) and relatively silicic. These were followed by more variable but generally hotter (most ~720 °C to 850 °C), less fractionated melts (Fig. 4), presumably a consequence of the increasing mafic input through time recognized by Clynne et al. (2008). However, zircon records modification of the magmatic system at ~100ka, ~80 k.y. before increased thermal influx manifested itself in the whole rock and major phase chemistry of erupted products. We interpret this to mean that higher thermal flux was introduced to the intrusive portion of the system and influenced magmas stored there for 10s of k.y. before erupting magmas were significantly modified. The zircon record is also unique in that much of this geochemical and thermal history is commonly revealed in grains from a single sample.

Zircon data from Mount St. Helens reveal an intrusive body beneath the edifice with a melt fraction that varies in volume and location through time from solid rock through melt-rich zones. The locations of these melt-rich or crystal mush zones not only affect the distribution of zircon ages in any one sample, but could potentially dictate the path erupting magmas take through the crust. Except for the eruption process, this model is remarkably similar to processes thought to occur in incrementally assembled plutonic bodies and larger volcanic systems (Bacon and Lowenstern, 2005; Charlier et al., 2003; Walker et al., 2007). While the major mineral phases in Mount St. Helens rocks document the 'volcanic' aspects of the system (convection, mixing, and decompression and degassing of the magma just prior to and during eruption), zircon records its intrusive behavior: the input, interaction, repeated rejuvenation and slow, cool crystallization of unerupted magma that reflects the growth of a volcanic center. The information from these zircons indicates that each erupted magma interacts with older,

rejuvenated parts of the system on its relatively rapid journey from source to eruption, and suggests that active plutonic bodies are essential components of the magmatic plumbing systems of small, arc volcanoes such as Mount St. Helens.

6. Acknowledgements

We thank John Pallister, Kari Cooper, and Jake Lowenstern for participating in enlightening discussions and sharing resources, Ed Wolfe for guidance in the field, and Charlie Bacon and Jorge Vazquez at the U.S.G.S. and Georg Zellmer, Brian Jicha and an anonymous reviewer whose suggestions improved this paper. This work was supported by NSF grant EAR0635922.

7. References

Bachmann, O., Charlier, B.L.A., and Lowenstern, J.B., 2007, Zircon crystallization and recycling in the magma chamber of the rhyolitic Kos Plateau Tuff (Aegean arc): Geology, v. 35, p. 73-76, doi:10.1130/G23151A.1.

Bacon, C.R., Sisson, T.W., and Mazdab, F.K., 2007, Young cumulate complex beneath Veniaminof caldera, Aleutian arc, dated by zircon in erupted plutonic blocks: Geology, v. 35, p. 491-494, doi:10.1130/G23446A.1.

Bacon, C.R., and Lowenstern, J.B., 2005, Late Pleistocene granodiorite source for recycled zircon and phenocrysts in rhyodacite lava at Crater Lake, Oregon: Earth and Planetary Science Letters, v. 233, p. 277–293, doi:10.1016/j.epsl.2005.02.012.

Bennett, J.T., Krishnaswami, S., Turekian, K.K., Melson, W.G., and Hopson, C.A., 1982, The uranium and thorium decay series nuclides in Mt. St. Helens effusives: Earth and Planetary Science Letters, v. 60, p. 61-69, doi:10.1016/0012-821X(82)90020-6.

Blundy, J., and Cashman, K., 2001, Ascent-driven crystallisation of dacite magmas at Mount St. Helens, 1980–1986: Contributions to Mineralogy and Petrology, v. 140, p. 631–650.

Charlier, B.L.A., Peate, D.W., Wilson, C.J.N., Lowenstern, J.B., Storey, M., and Brown, S.J.A., 2003, Crystallisation ages in coeval silicic magma bodies: ^{238}U-^{230}Th disequilibrium evidence from the Rotoiti and Earthquake Flat eruption deposits, Taupo Volcanic Zone, New Zealand: Earth and Planetary Science Letters, v. 206, p. 446-457, doi:10.1016/S0012-821X(02)01109–3.

Cherniak, D.J., Hanchar, J.M., and Watson, E.B., 1997, Diffusion of tetravalent cations in zircon: Contributions to Mineralogy and Petrology, v. 127, p. 383–390, doi:10.1007/s004100050287.

Claiborne, L.L., Miller, C.F., Wooden, J.L., and Mazdab, F.K., 2010, Trace element composition of igneous zircon: Temporal, thermal, and compositional record of magmatic processes in the Spirit Mountain Batholith, Nevada: Contributions to Mineralogy and Petrology, In press, doi:10.1007/s00410-010-0491-5.

Claiborne, L.L., Miller, C.F., Walker, B.A., Wooden, J.L., Mazdab, F.K., and Bea, F., 2006a, Tracking magmatic processes through Zr/Hf ratios in rocks and Hf and Ti zoning in zircons: an example from the Spirit Mountain batholith, Nevada: Mineralogical Magazine, v. 70, p. 517–543, doi:10.1180/0026461067050348.

Claiborne, L.L., Furbish, D.J., and Miller, C.F., 2006b, Determining mechanics of segregating small crystals from melt using modeling and SHRIMP-RG trace element analysis of zircons: an example from the Spirit Mountain Batholith, Nevada: Eos (Transactions, American Geophysical Union), v. 87, abs. V54B–02.

Clynne, M.A., Calvert, A.T., Wolfe, E.W., Evarts, R.C., Fleck, R.J., and Lanphere, M.A., 2008, The Pleistocene Eruptive History of Mount St. Helens, Washington, from 300,000 to 12,000 Years Before Present, *in* Sherrod, D.R., Scott, W.E., and Stauffer, P.H., eds., A volcano rekindled: the renewed eruption of Mount St. Helens, 2004–2006: U.S. Geological Survey Professional paper 1750, p. 593–627.

Cooper, K.M., and Donnelly, C.T., 2008, ^{238}U-^{230}Th-^{226}Ra Disequilibria in Dacite and Plagioclase from the 2004–2005 Eruption of Mount St. Helens, *in* Sherrod, D.R., Scott, W.E., and Stauffer, P.H., eds., A volcano rekindled: the renewed eruption of Mount St. Helens, 2004–2006: U.S. Geological Survey Professional paper 1750, p. 827–846.

Cooper, K.M., and Reid, M.R., 2003, Re-examination of crystal ages in recent Mount St. Helens lavas: implications for magma reservoir processes: Earth and Planetary Science Letters, v. 213, p. 149–167, doi:10.1016/S0012-821X(03)00262-0.

Ferry, J.M., and Watson, E.B., 2007, New thermodynamic models and revised calibrations for the Ti-in-zircon and Zr-in-rutile thermometers: Contributions to Mineralogy and Petrology, v. 154, p. 429–437, doi:10.1007/s00410-007-0201-0.

Gardner, J.E., Rutherford, M., Carey, S., and Sigurdsson, H., 1995, Experimental constraints on pre-eruptive water contents and changing magma storage prior to explosive eruptions of Mount St. Helens volcano: Bulletin of Volcanology, v. 57, p. 1–17.

Harrison, T.M., Watson, E.B., and Aikman, A.B., 2007, Temperature spectra of zircon crystallization in plutonic rocks: Geology, v. 35, p. 635–638, doi:10.1130/G23505A.1.

Hayden, L.A., and Watson, E.B., 2007, Rutile saturation in hydrous silicate melts and its bearing on Ti-thermometry of quartz and zircon: Earth and Planetary Science Letters, v. 258, p. 561–568, doi:10.1016/j.epsl.2007.04.020.

Hildreth, W., 2004, Volcanological perspectives on Long Valley, Mammoth Mountain, and Mono Craters: several contiguous but discrete systems: Journal of Volcanology and Geothermal Research, v. 136, p. 169–198, doi:10.1016/j.jvolgeores.2004.05.019.

Pallister, J.S., Thornber, C.R., Cashman, K.V., Clynne, M.A., Lowers, H.A., Mandeville, C.W., Brownfield, I.K., and Meeker, G.P., 2008, Petrology of the 2004–2006 Mount St. Helens Lava Dome – Implications for Magmatic Plumbing and Eruption Triggering, *in* Sherrod, D.R., Scott, W.E., and Stauffer, P.H., eds., A volcano rekindled: the renewed eruption of Mount St. Helens, 2004–2006: U.S. Geological Survey Professional paper 1750, p. 647–702.

Mazdab, F.K., and Wooden, J.L., 2006, Trace element analysis of accessory and rock forming minerals by ion microprobe (SHRIMP-RG) [abs]: Eos (Transactions, American Geophysical Union), v. 87, abs. V33A–0630.

Miller, J.S., Matzel, J.E.P., Miller, C.F., Burgess, S.D., and Miller, R.B., 2007, Zircon growth and recycling during the assembly of large, composite arc plutons: Journal of Volcanology and Geothermal Research, v. 167, p. 282–299, doi:10.1016/j.jvolgeores.2007.04.019.

Reagan, M.K., Sims, K.W.W., Erich, J., Thomas, R.B., Cheng, H., Edwards, R.L., Layne, G., and Ball, L., 2003, Time-scales of differentiation from mafic parents to rhyolite in North American continental arcs: Journal of Petrology, v. 44, p. 1703-1726, doi:10.1093/petrology/egg/057.

Rutherford, M.J., and Devine, J.D., 2008, Magmatic Conditions and Processes in the Storage Zone of the 2004–2006 Mount St. Helens Dacite, *in* Sherrod, D.R., Scott, W.E., and Stauffer, P.H., eds., A volcano rekindled: the renewed eruption of Mount St. Helens, 2004–2006: U.S. Geological Survey Professional paper 1750, p. 703–725.

Rutherford, M.J., Sigurdsson, H., Carey, S., and Davis, A., 1985, The May 18, 1980, eruption of Mount St. Helens, 1; melt composition and experimental phase equilibria: Journal of Geophysical Research, v. 90, p. 2929–2947, doi:10.1029/JB090iB04p02929.

Smith, D.R., and Leeman, W.P., 1993, The origin of Mount St. Helens andesites: Journal of Volcanology and Geothermal Research, v. 55, p. 271–303, doi:10.1016/0377-0273(93)90042-P.

Smith, D.R., and Leeman, W.P., 1987, Petrogenesis of Mount St. Helens dacitic magmas: Journal of Geophysical Research, v. 92, p. 10313–10334, doi:10.1029/JB092iB10p10313.

Streck, M.J., Broderick, C.A., Thornber, C.R., Clynne, M.A., and Pallister, J.S., 2008, Plagioclase populations and zoning in dacite of the 2004–2005 Mount St. Helens eruption; constraints for magma origin and dynamics, *in* Sherrod, D.R., Scott, W.E., and Stauffer, P.H., eds., A volcano rekindled: the renewed eruption of Mount St. Helens, 2004–2006: U.S. Geological Survey Professional paper 1750, p. 791–808.

Volpe, A.M., and Hammond, P.E., 1991, ^{238}U-^{230}Th-^{226}Ra disequilibria in young Mount St. Helens rocks: Constraint for magma formation and crystallization: Earth and Planetary Science Letters, v. 107, p. 475–486, doi:10.1016/0012-821X(91)90094-X.

Walker, B.A., Miller, C.F., Claiborne, L.L., Wooden, J.L., and Miller, J.S., 2007, Geology and geochronology of the Spirit Mountain batholith, southern Nevada: Implications for timescales and physical processes of batholith construction: Journal of Volcanology and Geothermal Research, v. 167, p. 239–262, doi:10.1016/j.jvolgeores.2006.12.008.

Watson, E.B., 1996, Dissolution, growth and survival of zircons during crustal fusion: kinetic principles, geological models, and implications for isotopic inheritance: Geological Society of America. Special Paper, v. 31, p. 43–56.

Watson, E.B., and Harrison, T.M., 1983, Zircon saturation revisited: temperature and composition effects in a variety of crustal magma types: Earth and Planetary Science Letters, v. 64, p. 295–304, doi:10.1016/0012-821X(83)90211-X.

Zellmer G.F. and Turner S.P., 2007, Arc dacite genesis pathways: evidence from mafic enclaves and their hosts in Aegean lavas: Lithos, v. 95, p. 346-362, doi:10.1016/j.lithos.2006.08.002.

Zellmer, G.F., Annen, C., Charlier, B.L.A., George, R.M.M., Turner, S.P., and Hawkesworth, C.J., 2005, Magma evolution and ascent at volcanic arcs: constraining petrogenetic processes through rates and chronologies: Journal of Volcanology and Geothermal Research, v. 140, p. 171–191, doi:10.1016/j.jvolgeores.2004.07.020.

Zellmer G.F., Sparks R.S.J., Hawkesworth C.J., and Wiedenbeck M., 2003, Magma emplacement and remobilisation timescales beneath Montserrat: insights from Sr and Ba zonation in plagioclase phenocrysts: Journal of Petrology, v. 44, p. 1413-1431, doi:10.1093/petrology/44.8.1413.

CHAPTER IV

GEOCHRONOLOGY AND GEOCHEMISTRY OF ZIRCON FROM MOUNT ST. HELENS

1. Introduction

While zircon geochronology provides evidence for the timescales of magmatic storage and processes, zircon geochemistry provides information about the compositions and potentially the temperatures of the magmas from which they grew. Changes in magma composition and temperature result from physical and thermal processes such as injection of new magmas and rejuvenation, crystal fractionation and/or transport, and melt segregation from crystal mushes, and so these zircon compositions provide a record of these important processes. By obtaining time-correlated compositional data, as we have done here, we can begin to understand not only what these processes are and how they function, but also the timescales on which they operate, and can begin to reconstruct a chronological history of the Mount St. Helens sub-volcanic magmatic system.

2. Methods

Forty-two samples were collected representing thirty-nine eruptive units spanning the eruptive history of Mount St. Helens (Table 1), with a focus on compositions most likely to yield zircon (based on mineral assemblage and/or geochemistry) but including sufficient variety to encompass all potential zircon carrying

Table 1: List of samples included in this study[a]. Samples are listed in chronological order by eruption. Horizontal lines delineate eruptive stages, with Ape Canyon followed by Cougar, followed by Spirit Lake.

Sample #	Location [b]	Eruption Age [c,d] (method)	Eruptive unit [d]	Distinguishing Minerals [e]	Zircon grains yielded
SHL06-3Z	46° 8.847' N 122° 16.958' W	272 ± 0.9 ka[f] (groundmass Ar-Ar)	Goat Mountain Dome (dacite)	Quartz, biotite	100s
SHL08-36EZ	45° 59.182' N 122° 33.474' W	263±19 ka (plagioclase Ar-Ar)	Cape Horn Creek Dacite	Quartz, biotite, cummingtonite	10s
SHL08-37Z	45° 57.860' N 122° 29.020' W	247±12 ka (plagioclase Ar-Ar)	Green Mountain Dacite	Quartz, biotite, cummingtonite	10s
SHL06-8Z	45° 10.168' N 122° 14.719' W	107±39 ka (plag & WR Ar-Ar)	Butte Camp Dome	Hypersthene	None
SHL08-29Z		74±9 ka – MAX (plag Ar-Ar)	AC Lahar – North Shore Lake Merwin	Quartz, biotite, opacite	100s
SHL08-26Z	46° 12.356' N 122° 5.036' W	54±10 ka – MAX (plag Ar-Ar)	Ape Canyon PF	Quartz, biotite, cummingtonite	10s
SHL08-30Z		49.5±1.0 ka (radiocarbon)	AC Pumice Lahar – North Shore Lake Merwin	Quartz, biotite	10s
SHL06-4Z	46° 8.473' N 122° 15.425' W	34.9±4.6 ka (groundmass Ar-Ar)	Dacite of McBride Lake	Quartz, biotite	100s
SHL06-5Z		34.9±7.1 ka[f] (Ar-Ar)	Unnamed Ape Canyon dacite	Quartz, biotite	100s
SHL08-20Z	46° 3.855' N 122° 15.616' W	28.8±1.4 ka (radiocarbon)	Pre-Debris Avalanche Dacite Cougar Dacite Lahar	orthopyroxene	None
SHL08-17Z	46° 9.141' N 122° 9.638' W	27.9±1.7 ka (whole rock Ar-Ar)	Dacite of June Lake	Hypersthene	None
SHL08-35Z	46° 3.617' N 122° 13.772' W	NA	Minor dacite in Cougar and AC aged lahars	Hypersthene	100s
SHL08-18Z/484A	46° 3.906' N 122° 12.447' W	>24.3 ka (stratigraphy & radiocarbon)	Debris Avalanche Dacite	Hydrothermally altered	10s
SHL08-21Z	46° 5.094' N 122° 12.292' W	24.3±0.5 ka (radiocarbon)	Two Pumice PF (white pumice)	Hypersthene	10s
SHL06-10WZ		24.3±0.5 ka (radiocarbon)	Two Pumice PF [d] (white pumice)	Augite, hypersthene	None
SHL06-10BZ		24.3±0.5 ka (radiocarbon)	Two Pumice PF (brown pumice)	Augite, hypersthene	None
SHL08-19Z	46° 3.264' N 122° 12.882' W	23.5±0.1ka (radiocarbon)	Cougar White Pumice	Hypersthene	None
SHL08-27Z	46° 12.356' N 122° 5.036' W	23.5±0.1ka (radiocarbon)	Cougar White Pumice	Hypersthene	None
SHL08-42Z	46° 8.644' N	17.8±2.7 ka	Andesite of	Augite,	None

	122° 11.214' W	(WR Ar-Ar)	Swift Creek	hypersthene	
SHL08-34Z	46° 16.870' N 122° 4.735' W	3510 ybp	Yn pumice	Hornblende rims on cummingtonite	100s
SHL08-49AZ	46° 10.429' N 122° 8.286' W	Pine Creek Age (~2.5 ka)	Mush Inclusion in Pine Creek Dacite		10s
SHD08-9Z		Sugarbowl Age (~1.2 ka)	Sugarbowl Dome Rhyolite	Hypersthene	2
SHL08-9Z		1480-1500 AD (dendrochronology)	Unnamed Kalama dacite	Pyroxene	None
SHL08-28Z	46° 11.030' N 122° 13.361' W	1500-1647 AD	Older Summit Dome Dacite	Double terminated quartz, biotite	None
SHL06-11Z	46° 13.850' N 122° 8.953' W	1980	Cryptodome Dacite	Orthopyroxene	1
SHL08-33Z	46° 13.896' N 122° 9.037' W	1980 AD	Cryptodome Dacite	Orthopyroxene	5
SH325-2		December 20, 2005	Spine 7 dacite	Orthopyroxene	10s

[a] samples from the Swift Creek eruptive stage are not listed here. See Flanagan et al. (in prep).
[b] datum for location coordinates is North American 1927.
[c] unless otherwise noted, eruption ages for Ape Canyon and Cougar age eruptions are from Clynne et al., 2008. Spirit Lake eruption ages are from Mullineaux (1996) and Crandell (1987).
[d] PF = pyroclastic flow, WR = whole rock
[e] All samples also contain plagioclase, hornblende, magnetite and ilmenite, and apatite.
[f] unpublished data, M.A. Clynne, USGS

compositions. Fifteen of those samples were collected from the Swift Creek stage for a simultaneous study focusing on that eruptive stage and will be neglected for the course of this chapter. Please see Flanagan (2010) and Flanagan et al. (in prep) for the detailed results of that study.

Whole rock powders for all samples yielding zircon or of particular compositional interest were sent to Activation Laboratory for geochemical analysis. Thin sections were prepared for these selected samples and studied by petrographic microscope to confirm that mineral assemblage and petrography matched unit descriptions from the literature. Three of these thin sections were studied using a Scanning Electron Microscope with EDS to identify the oxide minerals. Zircon saturation temperatures were calculated following Harrison and Watson (1983) from whole rock compositions for our samples, and from whole rock and glass compositions reported in the literature.

Approximately 5kg of each sample was crushed to pass through a 500 μm mesh. Zircons were separated from other minerals by density and magnetism using a hydraulic table, heavy liquids (density 2.85), and a Franz magnetic separator. Zircons were manually picked from the heavy, non-magnetic fraction on a binocular microscope. All identified zircon grains up to ~ 100 grains were picked per sample. Zircons were mounted in epoxy (up to approximately fifty per sample, depending on yield). Epoxy mounts were ground down to expose the near-centers of the grains, polished and then rinsed in acid and gold-coated. Grains were photographed in reflected light on a petrographic microscope and by cathodoluminescence (CL) on the JEOL JSM 5600 scanning electron microscope at the USGS/Stanford Microanalytical Laboratory.

Trace element, U-Th and U-Pb analyses were conducted using the sensitive high resolution ion microprobe, reverse geometry (SHRIMP-RG) at the Stanford-USGS Microanalytical Laboratory in seven sessions spanning six years. During this time analytical methods evolved,

particularly for the relatively novel process of analysis of zircon trace element compositions by SHRIMP, resulting in variations in methods described below. Analysis spot locations were selected in an attempt to avoid inclusions and cracks in grains visible in reflected light images and to analyze representative zircon zones and features as well as particularly interesting grain attributes visible in CL images, including resorption surfaces and sector zoning.

Trace element analyses and data reduction were conducted following methods detailed in Claiborne et al., 2010a. Trace element analyses were conducted before age analyses, because the smaller pits resulting from the trace element analyses would not interfere with the larger beam required for U-Series analyses. Trace element spot size averaged ~15µm and each measurement consisted of one cycle (stepping through the entire mass range from low to high mass once). In addition to standard zircon CZ3 (Claiborne et al., 2010a), normalized count rates from the unknowns were compared to zircon Madagascar Green (MAD) which was calibrated against the well characterized CZ3 to determine absolute elemental concentrations.

Minute glass and mineral inclusions may be present in zircons and included in SHRIMP analyses, and invisible cracks in the grains may serve as pathways for sub-solidus concentration of certain elements by diffusion (Fe, Ti; Harrison and Schmitt, 2007; Hoffman et al., 2009) and thereby contribute to inaccuracy in reported zircon trace element concentrations. However, extremely low natural concentrations of some trace elements in the zircons allow us to identify this kind of contamination and exclude these analyses from our datasets. Iron concentrations more than one order of magnitude higher than the zircon standards likely indicate the presence of magnetite, ilmenite, or a crack in the grain, all of which would also contribute Ti and thereby result in overestimation of temperature by Ti-in-zircon thermometry; we have excluded these analyses. Presence of significant Ca, Na, K, Al, and/or P can be attributed to glass and/or apatite inclusions and analyses one order of magnitude higher than the zircon standard in these

elements have also been excluded. Light REE (La and Nd) concentrations in zircon are particularly sensitive to the presence of LREE-enriched accessory mineral inclusions such as allanite and monazite, because the light REE are so low in zircon. These inclusions, however, are unlikely to significantly affect the relatively high concentrations of middle and heavy REE or other trace elements in the zircons, so we have not excluded these data, but instead do not rely on light REE analyses to be accurate representations of zircon compositions. The analytical routine included Pr, but the results are considered unreliable due to potential hydride interference from the $^{140}Ce^{1}H^{+}$ peak (Claiborne et al., 2010a). Due to the previously discussed unreliability of LREE, we calculate Pr and instead calculate it as a log-linear projection of the slope from Sm to Nd rather than a 2/3 average between La and Nd. For the same reason and because Pr is calculated, we also use log-linear projection of that slope to determine Ce* for plotting and calculation of Ce anomaly, rather than the traditional midpoint between La and Pr.

Watson et al. (2006) and Ferry and Watson (2007) quantified the interdependency of the activities of TiO_2 and SiO_2 ($a$$TiO_2$ and $a$$SiO_2$, respectively) in the melt and melt temperature on partitioning of Ti into the zircon structure in the Ti-in-zircon thermometer. Use of Ti concentrations in zircon as a thermometer requires assumption of some constant $a$$TiO_2$ and $a$$SiO_2$ in the melt. In the case of a closed system or open systems where evidence suggests newly injected magmas are similar in composition to existing magmas (Claiborne et al., 2010a), this might be a safe assumption, and glass or melt inclusions could be measured or mineral assemblage considered to determine the activities of the two species, resulting in an accurate calculated zircon crystallization temperature. However, we must be very careful in situations where different magmas may be interacting, changing the melt composition along with temperature, as it may be $a$$TiO_2$ and $a$$SiO_2$ that are changing instead of, or along with, temperature.

We use Ti concentration to estimate temperatures, reporting various Ti-in-zircon temperatures based on various $a\mathrm{TiO_2}$ and $a\mathrm{SiO_2}$. Quartz is a common phenocryst in the more silicic lavas of MSH, and calculated zircon saturation temperatures suggest most zircon growth to have occurred at or near quartz saturation, so we consider $a\mathrm{SiO_2}$=1.0 as the most likely composition. Compositions of MSH glasses (Gardner et al., 1995) suggest high $a\mathrm{TiO_2}$ (>0.5) at and below zircon saturation temperatures, calculated by the method of Hayden and Watson, 2007; (cf. Claiborne et al., 2006; 2010a,b; see results and discussion sections for further explanation of these assumptions). Coeval ilmenite also suggests high $a\mathrm{TiO_2}$ and might also have buffered $a\mathrm{TiO_2}$ in the melt during zircon growth. For these reasons, and those further detailed in the discussion section, we chose $a\mathrm{TiO_2}$=0.7 as the most likely composition at the time of zircon growth. Assuming too high $a\mathrm{TiO_2}$ or too low $a\mathrm{SiO_2}$ results in underestimation of temperature, and an error of 0.2 in activity estimates yields an error of ~30°C; this uncertainty does not affect the main conclusions. We also consider the possibility that variations in Ti are due to changes in magma composition and use Ti concentration to constrain potential variation in magma composition ($a\mathrm{TiO_2}$), assigning a constant temperature. Recent work has quantified a pressure dependence of the thermometer of 50-100°C/GPa (Ferry and Watson, 2007; Ferriss et al., 2008), adding additional uncertainty to temperature estimates for systems where pressure is unknown or potentially changing. For these reasons, we do not entirely rely upon absolute temperatures, but consider relative temperatures within the system, within samples, and particularly within grains as potentially meaningful, and also consider temperature estimates at various activity and pressures to infer constraints on temperature.

Uranium-Th SHRIMP isotope analyses were conducted following the methods based on Lowenstern et al. (2000) and described in Wilson and Charlier (2009). Uranium-Th isotope analyses were placed directly over trace element spots where possible, and when the grain was

of sufficient size, multiple U-Th spots were put on one grain. The beam spot size varied from ~30 to ~40 μm, depending on the beam strength during any given session. The U-Series isotopes in all the standards analyzed should be in secular equilibrium, given the antiquity of the samples (Madagascar green (MAD), concentration standard CZ3, age standard R33, and age standard VP10). Deviation in calculated ($^{230}Th/^{238}U$) from unity for these standards is indicative of internal fractionation of the isotopes or ionization issues within the instrument, so we applied a correction factor for each mount that brought the average standard ($^{230}Th/^{238}U$) for that mount to unity. This correction factor varied from 0.902 to 1.11. During one session, a correlation between the Th/U correction factor and UO/U was noticed with implausible variation in UO/U, and a correction was applied to enforce a linear UO/U that also resulted in (230^{Th})/(238U) average of unity in the standards.

Uranium-Th data were processed using Isoplot 3.00 (Ludwig, 2003). Uranium-series isochrons with slope≥ 1 were assumed to have reached secular equilibrium and were excluded from this dataset. Model ages were calculated from the slope of a two point isochron between the data point and an initial (^{230}Th)/(^{232}Th) on the equiline. Age populations were determined using Isoplot's Unmix feature, based on Sambridge and Compston's (1994) mixture modeling and applied to the isochron slopes. The number of age components were varied until a minimum misfit was found, and the ages matched peaks in the cumulative probability density plots. Model ages and isochrons are strongly dependent on the chosen initial value, particularly for data points with low (^{238}U)/(^{232}Th). We selected an average of initial values for Mount St. Helens, 1.2 (Cooper & Donnelly, 2009). Model ages ≥ 300ka were excluded from plots of age vs. composition, as these analyses were within error of the equiline, and therefore exhibited an infinite upper error.

Uranium-Pb analyses were conducted on zircons from samples that were understood to have erupted >250 ka and on zircon zones (spots) from younger samples that were found to be in U-Th secular equilibrium. When re-analyzing a U-Th analysis location for U-Pb, the mount was first polished slightly to minimize the pit from the U-Th analysis which could otherwise interfere with ionization and sputtering, and was then recoated in gold. Uranium-Pb spot size was approximately 20 μm. U-Pb ages reported herein are the ^{230}Th corrected ^{206}Pb/^{238}U age, due to the potentially significant effect of initial ^{230}Th produced ^{206}Pb in such young samples with so little radiogenic Pb. Uranium-Pb data were also reduced using Isoplot 3.00 (Ludwig, 2003) to create histograms, probability density functions, and using Unmix to identify multiple age populations. Where U-Th and U-Pb for the same spot were not in agreement, the age with the smaller reported error was used and the other excluded.

A set of ten samples ranging in age and composition were selected for whole rock U and Th isotope analysis. Procedures for chemical separation and multi collector-inductively coupled plasma-mass spectrometer (MC-ICP-MS) analyses are described in detail in Cooper and Donnelly, 2008. Briefly, rock chips from these samples were cleaned in ultrasonicators in sequential baths of acetone, peroxide, oxalic acid, hydrochloric acid and distilled water and were then powdered. Rock dissolution and chemical separation of U and Th were conducted at University of California, Davis in class-100 laboratory facilities. Powders were dissolved in concentrated hydrofluoric + nitric acids, which were then evaporated, and the sample dissolved in hydrochloric acid. Each sample solution was then split in two aliquots: one, spiked with ^{233}U and ^{229}Th, for concentration measurement by isotope dilution (ID), and a second for U and Th isotope composition (IC) analysis. The elements of interest (U and Th) were then separated from the rock matrix solutions and from one another using Eichrom TRU™ resin and anion and cation exchange resin. Concentrations and compositions were then measured on the Nu Plasma

MC-ICP-MS at the University of California Davis. Rock standard TML was processed and analyzed in parallel with samples.

3. Results

Zircons were successfully extracted from seventeen of the twenty seven samples that were processed, with yield varying from 1 to hundreds of grains for each sample (Table 1). Zircons were mostly small (~50μm) to medium (~250 μm) in size and fairly euhedral, although some samples did contain both rounded and euhedral grains, and a few samples did contain grains up to ~500μm. Zoning varied from conventional magmatic zoning, with or without oscillatory zones, to unzoned (Figure 1). Many samples contained a few sparse, elongate grains with dark, unzoned interiors and bright rims (Figure 1) that tended to have anomalously low U/Th and gave relatively young ages for the given sample.

Figure 2 illustrates the petrographic variation in samples for this study, ranging from andesite to rhyolite, with primarily dacites (it should be noted that the andesite did not yield any zircon). All oxide minerals assessed during Scanning Electron Microscope reconnaissance contained primarily either Fe or Fe and Ti, suggesting all samples contained both magnetite and ilmenite (Appendix B). Major element trends (Table 2, Figure 2) show decrease in MgO, FeO, Al_2O_3, and CaO and increase in K_2O and Na_2O with increasing silica (trace element data available in Appendix C). As has been previously noted for Mount St. Helens rocks (Clynne et al., 2008), these dacites are particularly low in K_2O. Uranium concentration increases from 0.7 to 1.9 ppm with increasing SiO_2, and Th increases from 1.8 to 3.4 ppm from low to relatively high SiO_2, although the trend is not pronounced. Th/U ranges from 1.3 to 3.0, with >90% limited to 2 to

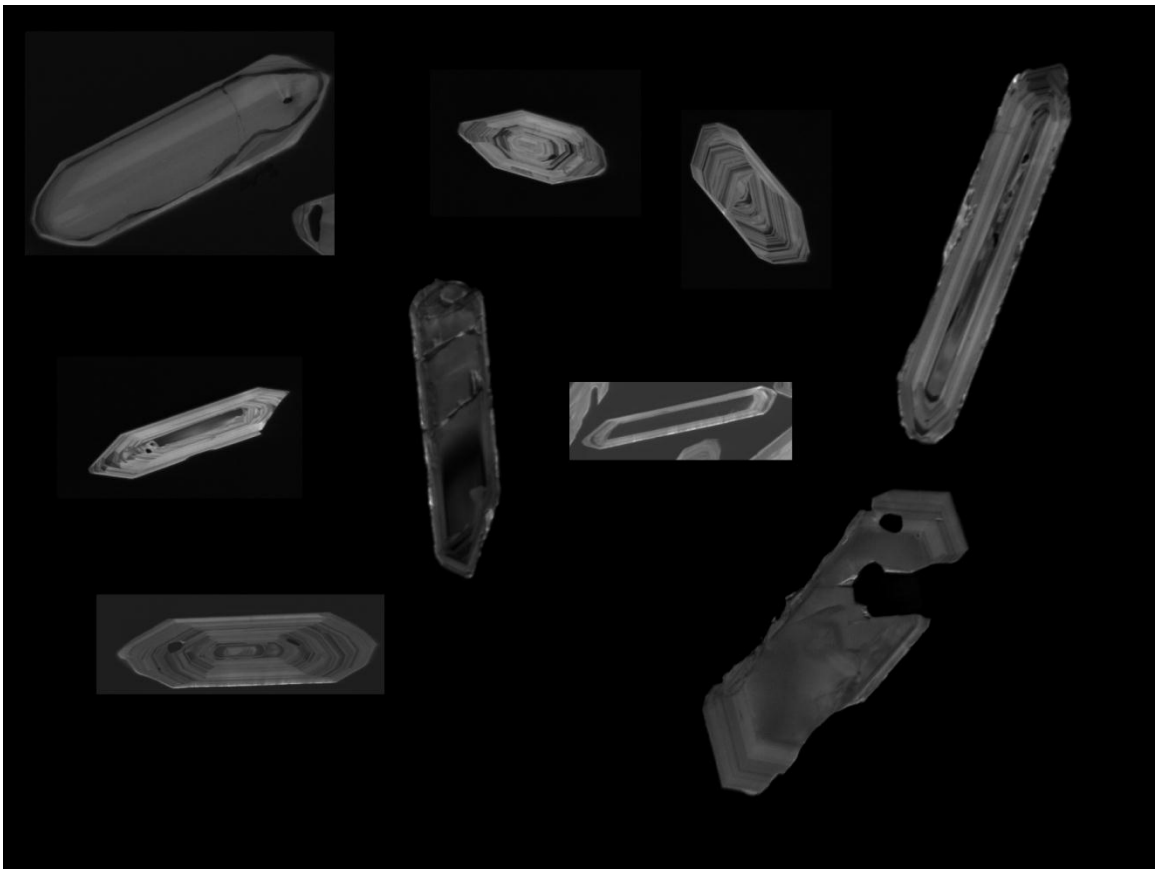

Figure 1: Cathodoluminescence images of polished zircons from this study showing typical varieties of zoning patterns. Zircons are not to scale relative to one another.

Table 2: Whole rock major element geochemistry for samples included in this study. For trace element compositions, please see Appendix C.

sample	SiO_2 wt%	Na_2O wt%	K_2O wt%	Al_2O_3 wt%	MgO wt%	Fe_2O_3 wt%	CaO wt%	MnO wt%	TiO_2 wt%	P_2O_5 wt%
SHL06-3Z	66.06	4.42	1.49	16.94	1.67	3.40	4.48	0.07	0.56	0.17
SHL06-4Z	62.75	4.41	1.26	17.46	2.50	4.44	5.40	0.08	0.75	0.20
SHL06-5Z	66.50	4.35	1.53	16.08	1.82	4.14	4.14	0.08	0.65	0.16
SHL06-8Z	63.91	4.30	1.55	16.72	2.09	5.17	5.00	0.08	0.76	0.15
SHL06-9Z	62.75	4.41	1.26	17.46	2.50	4.28	5.40	0.08	0.75	0.20
SHL06-10BZ	64.15	4.50	1.35	17.52	1.96	4.49	4.91	0.08	0.62	0.13
SHL06-10WZ	61.97	4.30	0.56	20.68	1.56	4.32	5.12	0.07	1.09	0.06
SHL06-11Z	63.86	4.17	1.24	17.80	1.80	4.44	4.14	0.09	0.78	0.10
SHL06-12Z	61.97	4.30	0.56	20.68	1.56	3.67	5.12	0.07	1.09	0.06
SHL08-18Z	65.02	4.40	1.46	17.87	1.71	4.06	3.94	0.02	0.64	0.11
SHL08-21Z	64.37	4.29	1.35	17.34	2.17	3.38	4.87	0.09	0.74	0.23
SHL08-26Za	63.76	4.23	1.4	16.83	1.2	3.98	4.07	0.064	0.48	0.08
SHL08-26Zc	64.55	4.27	1.37	16.9	1.28	3.93	4.13	0.068	0.518	0.1
SHL08-27Z	63.76	4.43	1.57	16.83	1.6	4.72	4.08	0.077	0.627	0.14
SHL08-28Z	60.67	4.23	1.3	17.91	2.59	5.97	5.63	0.093	0.785	0.16
SHL08-29Z	59.93	4.43	1.03	17.76	2.41	4.68	5.85	0.11	1.23	0.25
SHL08-30Z	61.38	4.01	1.19	17.11	1.73	5.78	3.98	0.087	0.747	0.1
SHL08-33Z	63.12	4.43	1.33	17.24	1.93	4.7	4.83	0.075	0.608	0.13
SHL08-34Z	67.70	4.64	1.67	16.64	1.15	4.21	3.81	0.07	0.47	0.15
SHL08-35Z	64.65	4.47	1.39	17.48	1.84	5.38	4.87	0.07	0.60	0.15
SHL08-36EZ	66.52	4.52	1.48	17.37	1.31	4.68	4.12	0.07	0.51	0.14
SHL08-37Z	60.13	4.17	0.54	20.07	1.51	4.46	4.97	0.065	1.06	0.06
SHL08-42Z	60.47	4.52	1.28	17.82	3.02	5.79	5.92	0.02	0.84	0.21
SHL08-49AZ	66.52	4.52	1.48	17.37	1.31	6.97	4.12	0.07	0.51	0.14
SH325-2	66.47	4.40	1.41	17.40	1.32	4.28	4.25	0.07	0.53	0.10
SHD08-9Z	71.00	4.87	2.05	15.52	0.77	3.12	2.77	0.013	0.347	0.13

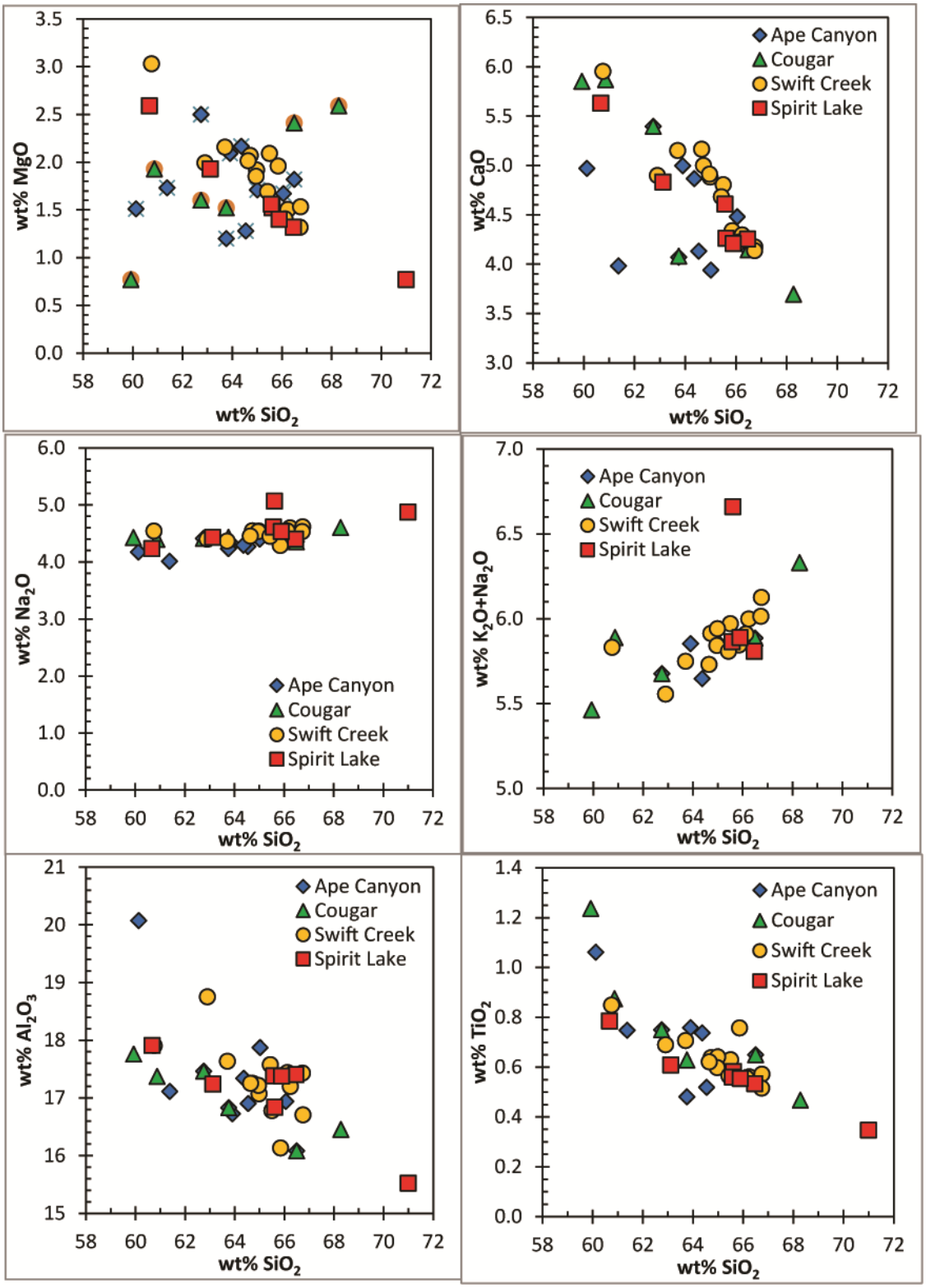

Figure 2: Whole rock geochemistry for selected samples from this study. Data available in Table 2 and Appendix C.

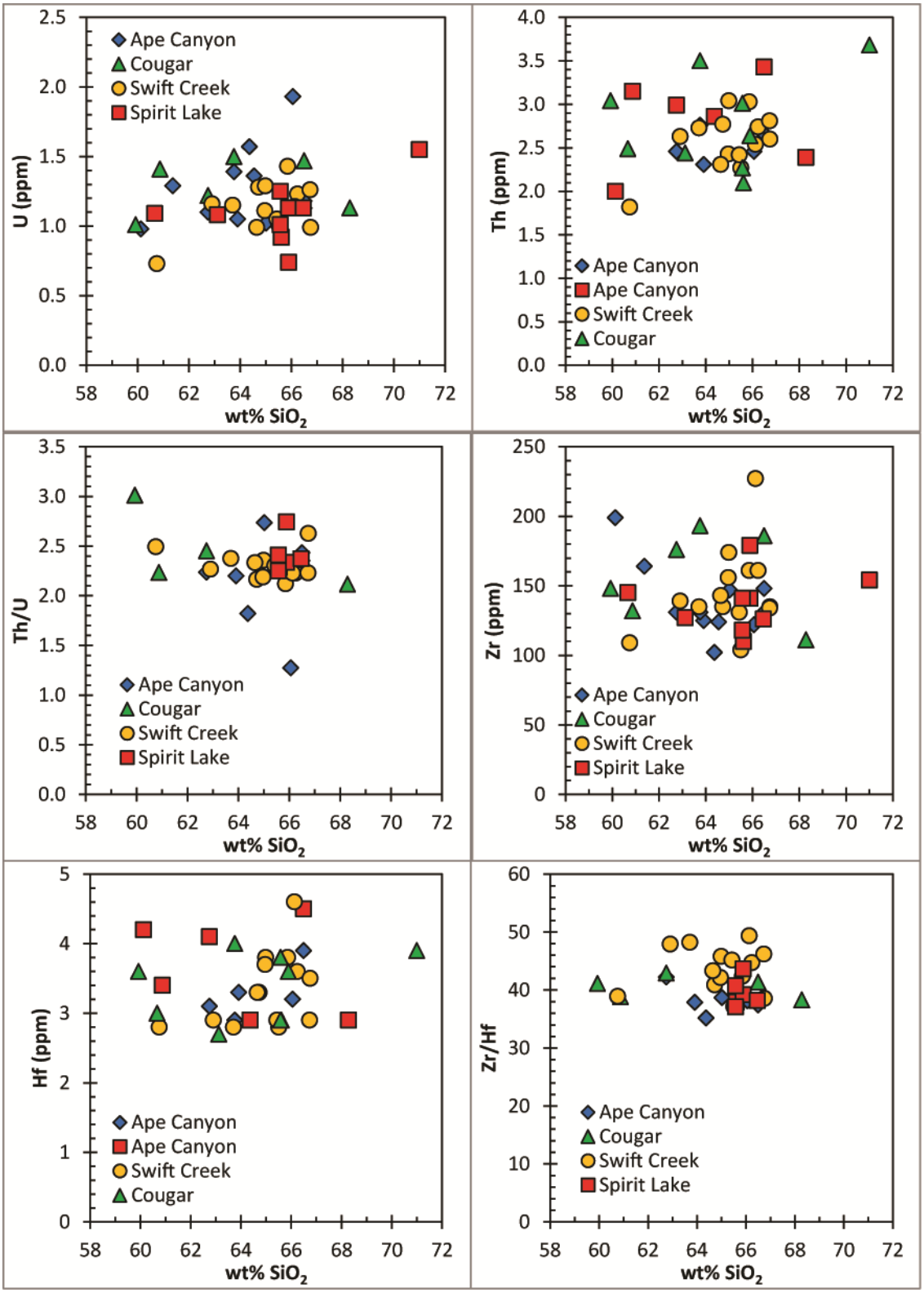

Figure 2 (cont'd): Whole rock geochemistry for selected samples from this study. Data available in Table 2 and Appendix C.

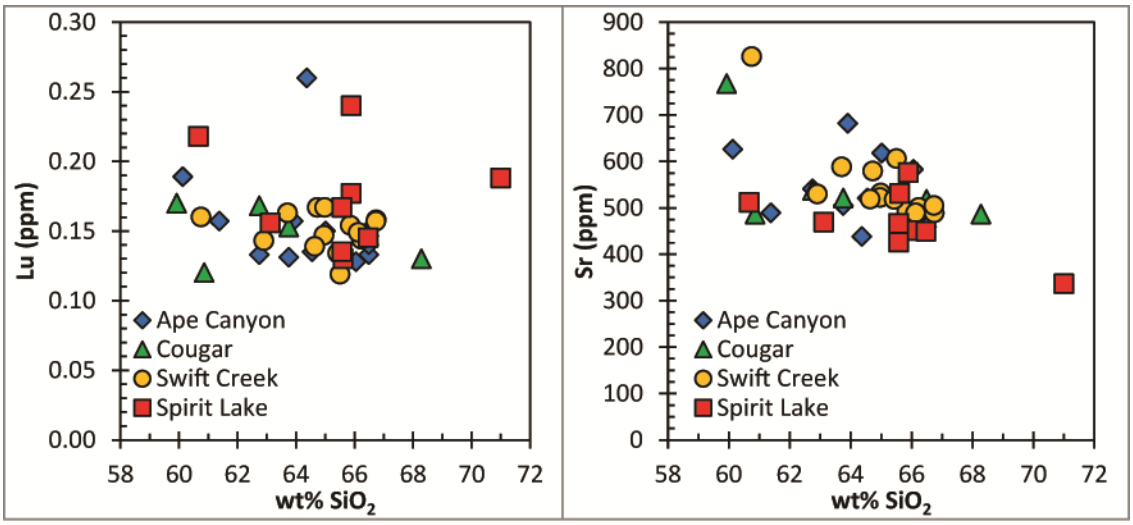

Figure 2 (cont'd): Whole rock geochemistry for selected samples from this study. Data available in Table 2 and Appendix C.

2.5, with little variation with SiO_2. TiO_2 varies tightly inversely with SiO_2, decreasing from 1.2 to 0.5 wt% with increasing SiO_2. Zirconium concentration varies from ~100 to 225 ppm, and does not correlate with SiO_2. Zr/Hf varies from 35 to 49, with slightly lower values more common for Ape Canyon samples and the highest values common in the Swift Creek samples, and does not appear to correlate directly with Hf concentration. Strontium varies inversely with SiO_2 from 826 to 426 ppm.

Zircon saturation temperatures calculated from whole rock compositions range from 717 to 784°C (Table 3). Zircon saturation temperatures calculated from both whole rock and glass compositions taken from the literature, where major element geochemistry in conjunction with Zr concentrations is available, also fall within this range (Gardner et al., 1995; Smith and Leeman, 1992; Table 4). It should be noted that these data from the literature mostly pertain to recent eruptions, during the Spirit Lake Stage. Rutile saturation temperatures calculated from whole rock compositions for these samples range from 819 to 904°C (Table 3). This range also encompass rutile

saturation temperatures calculated from whole rock data from the literature, where major element and TiO_2 concentrations are available (Gardner et al., 1995; Smith and Leeman, 1992; Clynne et al., 2008). Where glass compositions including TiO_2 (Gardner et al., 1995), and magma temperature estimates (Smith and Leeman, 1992) are available, calculated melt $aTiO_2$ (based on Hayden and Watson 2007) ranges from 0.13 in the highest temperature melts (~950°C) up to 0.60 in the lowest temperature melts (~850°C) (Table 4), decreasing with decreasing temperature.

Measured ($^{230}Th/^{232}Th$) range from 1.11 to 1.32 for selected samples from this study, with the exception of Sample SHL08-36EZ with ($^{230}Th/^{232}Th$) of 1.7 (Figure 3, Table 5). With the exception of the one outlier, these values fall within the previously reported range for Mount St.

Table 3: Whole rock Ti and Zr compositions and calculated zircon (T-zrc) and rutile (T-rtl) saturation temperatures of samples included in this study. Zircon saturation temperatures calculated following Harrison and Watson (1983) and rutile saturation temperatures calculated following Hayden and Watson (2007).

sample	Ti (ppm)	Zr (ppm)	T-zrc(°C)	T-rtl (°C)
SHL06-3Z	3338	122	748	834
SHL06-4Z	4492	131	740	844
SHL06-5Z	3888	148	763	841
SHL06-8Z	4543	125	737	841
SHL06-9Z	4492	141	747	845
SHL06-10BZ	3708	176	772	832
SHL06-10WZ	6554	186	798	912
SHL06-11Z	4663	118	756	866
SHL06-12Z	6554	141	775	918
SHL08-18Z	3845	111	751	850
SHL08-21Z	4416	132	752	859
SHL08-26Za	2880	131	760	821
SHL08-26Zc	3108	124	756	829
SHL08-27Z	3762	193	787	836
SHL08-28Z	4710	145	745	834
SHL08-29Z	7409	131	734	893
SHL08-30Z	4482	164	781	848
SHL08-33Z	3648	127	745	828
SHL08-34Z	2828	110	743	817
SHL08-35Z	3599	147	756	823
SHL08-36EZ	3084	102	738	823
SHL08-37Z	6360	199	804	907
SHL08-42Z	5069	148	738	835
SHL08-49AZ	3084	179	781	804
SH325-2	3200	126	756	830
SHD08-9Z	2082	154	777	800

Table 4: $a\mathrm{TiO_2}$ calculations at various temperatures based on glass compositions from Gardner et al. (1995) and temperatures from Smith and Leeman (1992). Calculated $a\mathrm{TiO_2}$ for each sample that uses the temperature closest to the eruption temperature for that sample is in bold.

unit	Eruptive Period	sample	Eruption T	Ti (ppm)	aTiO2 at 750°C	aTiO2 at 800°C	aTiO2 at 850°C	aTiO2 at 900°C	aTiO2 at 950°C
T	Goat Rocks	MSH357-1	915-965	2880	2.61	1.50	0.90	**0.57**	**0.37**
T	Goat Rocks	MSH357-2	915-965	3060	2.76	1.58	0.95	**0.60**	**0.39**
T	Goat Rocks	MSH325-1	915-965	3060	2.71	1.56	0.94	**0.59**	**0.39**
We	Kalama	MSH364-1	840-850	1500	1.53	0.88	**0.53**	0.33	0.22
We	Kalama	MSH365-4	840-850	1500	1.59	0.91	**0.55**	0.35	0.23
We	Kalama	MSH370-2	840-850	1620	1.73	0.99	**0.60**	0.38	0.25
Wn	Kalama	MSH313-1	840-845	1380	1.42	0.82	**0.49**	0.31	0.20
Wn	Kalama	MSH313-2	840-845	1440	1.51	0.87	**0.52**	0.33	0.21
Wn	Kalama	MSH320-1	840-845	1200	1.25	0.72	**0.43**	0.27	0.18
Wn	Kalama	MSH320-3	840-845	1200	1.25	0.71	**0.43**	0.27	0.18
Wn	Kalama	MSH320-4	840-845	1200	1.25	0.72	**0.43**	0.27	0.18
Pu	Pine Creek	MSH372-1	NA	1800	1.83	1.05	0.63	0.40	0.26
Pu	Pine Creek	MSH372-3	NA	2100	2.08	1.19	0.72	0.45	0.30
Pu	Pine Creek	MSH372-13	NA	1800	1.82	1.05	0.63	0.40	0.26
Pu	Pine Creek	MSH363-2	NA	1920	1.91	1.10	0.66	0.42	0.27
Ps	Pine Creek	MSH368-1	NA	2400	2.50	1.43	0.86	0.54	0.35
Ye	Smith Creek	MSH367-3	880-945	900	0.97	0.56	0.34	**0.21**	**0.14**
Ye	Smith Creek	MSH367-4	880-945	840	0.91	0.52	0.31	**0.20**	**0.13**
Yn	Smith Creek	MSH334-1	855-905	1140	1.21	0.69	**0.42**	**0.26**	0.17
Yn	Smith Creek	MSH334-2	855-905	1200	1.28	0.74	**0.44**	**0.28**	0.18
Yn	Smith Creek	MSH340-4	855-905	900	0.97	0.56	**0.34**	**0.21**	0.14
Yn	Smith Creek	MSH340-6	855-905	960	1.03	0.59	**0.36**	**0.22**	0.15
Yn	Smith Creek	MSH338-1	855-905	960	1.04	0.60	**0.36**	**0.23**	0.15
Yn	Smith Creek	MSH338-3	855-905	780	0.83	0.48	**0.29**	**0.18**	0.12
Yn	Smith Creek	MSH336-4	855-905	1080	1.14	0.65	**0.39**	**0.25**	0.16
Yn	Smith Creek	MSH336-6	855-905	1080	1.16	0.66	**0.40**	**0.25**	0.16
Yb	Smith Creek	MSH309-9	830-860	1260	1.29	0.74	**0.44**	0.28	0.18
Yb	Smith Creek	MSH309-3	830-860	1020	1.06	0.61	**0.37**	0.23	0.15
Yb	Smith Creek	MSH341-1	830-860	1800	1.72	0.99	**0.60**	0.37	0.24
Yb	Smith Creek	MSH518-2	830-860	1080	1.16	0.67	**0.40**	0.25	0.17
Yb	Smith Creek	MSH518-3	830-860	1200	1.35	0.77	**0.47**	0.29	0.19

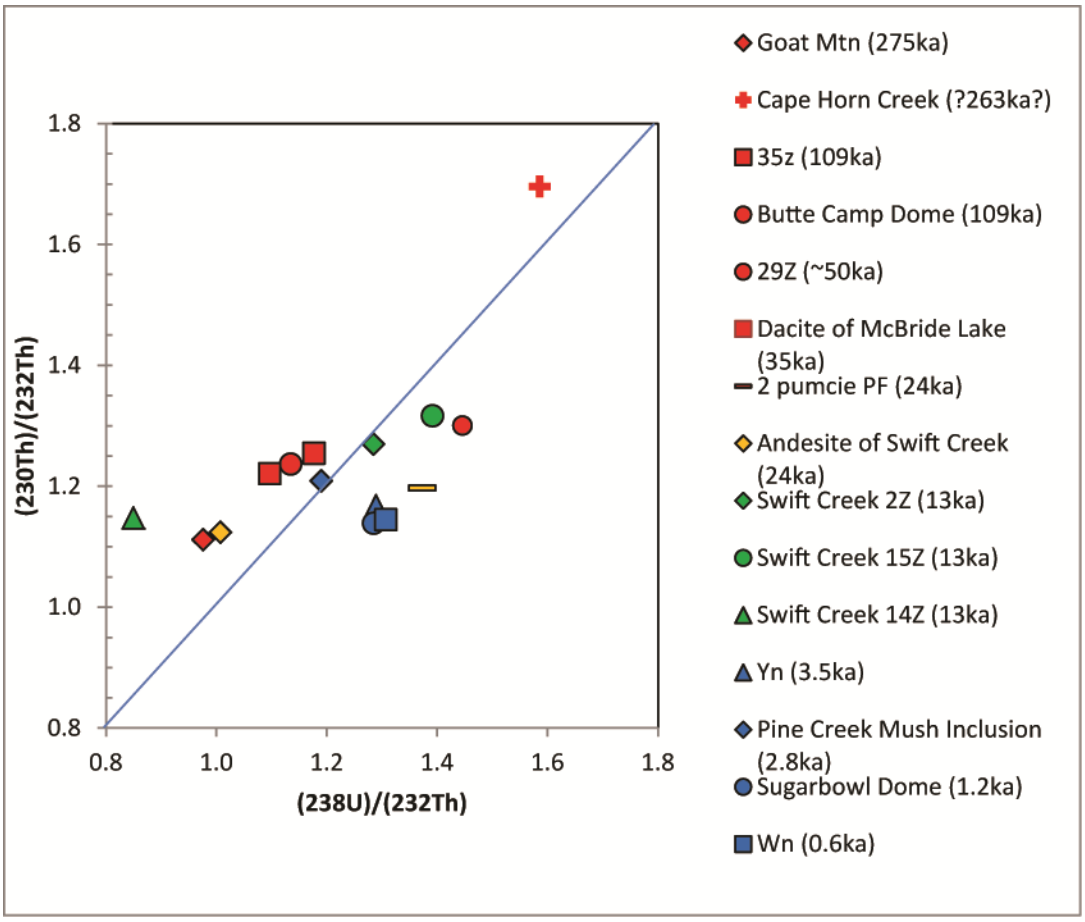

Figure 3: Whole rock isotope compositions from ten selected samples from this study. Rocks erupted during the Ape Canyon eruptive stage are in red, Cougar are in yellow, Swift Creek are in green, and Spirit Lake are in blue. The approximate eruption age is listed in parentheses beside each sample name. The diagonal line within the plot area represents the equiline, with slope=1.

Table 5: Whole rock Uranium and Thorium isotopic compositions and concentrations for ten selected samples from this study, including three samples from the Swift Creek stage from Flanagan (2010).

sample	Th (ppm)	U (ppm)	(^{230}Th/^{232}Th)	±1σ	(^{238}U/^{232}Th)	±1σ
Ape Canyon						
SHL06-3Z WR #2	2.42	0.78	1.111	0.001	0.976	0.003
SHL08-36EZ WR	2.92	1.53	1.696	0.001	1.586	0.006
SHL08-35Z WR	3.05	1.18	1.255	0.001	1.177	0.006
SHL06-8Z WR #2	2.06	0.98	1.300	0.002	1.446	0.006
SHL08-29Z WR	2.81	1.05	1.237	0.001	1.134	0.006
SHL06-4Z WR	2.73	0.99	1.221	0.001	1.097	0.006
Cougar						
SHL08-42Z WR	3.02	1.00	1.120	0.002	1.007	0.006
SHL08-21Z WR	2.85	1.29	1.197	0.001	1.373	0.006
Swift Creek						
SHD08-2Z WR	1.85	0.78	1.270	0.001	1.285	0.006
SHD08-15Z WR	2.30	1.05	1.317	0.001	1.391	0.006
SHD08-14Z WR	1.59	0.44	1.147	0.002	0.850	0.005
Spirit Lake						
SHL08-34Z WR	2.13	0.90	1.167	0.001	1.290	0.006
SHL08-49AZ WR	2.18	0.86	1.209	0.002	1.190	0.006
SHD08-9Z WR	3.86	1.64	1.139	0.001	1.285	0.006
SHL06-12Z WR	2.85	1.23	1.144	0.001	1.307	0.006

Helens magmas. The magmas exhibit both ^{230}Th excess and deficiency, and only two samples (one Swift Creek aged and one Spirit Lake aged) appear to fall on the equiline. Three Spirit Lake samples cluster together in both (^{230}Th/^{232}Th) and (^{238}U/^{232}Th), and all three Swift Creek samples and the three younger Ape Canyon samples fall in linear trends that may be representative of isochrons. Calculating back to the date of eruption, two of the Ape Canyon samples reveal what appear to be unreasonable initial (^{230}Th/^{232}Th), suggesting a problem with that data.

Zircon geochronology (U-Th and U-Pb) results are available in full in Appendix D and are summarized in Figure 4. Zircon surface geochronology results are available in full in Appendix e, but will not be discussed in this paper. In all samples, zircon ages range at least 100 ka older

than the eruption age. Sample SHL08-49AZ, interpreted to represent an inclusion of sub-volcanic crystal mush (Clynne et al., personal communication), has a more restricted age dispersion, with all but two analyses falling between 10 and 34 ka. Where eruption ages are very well established, zircon ages are rarely within error of eruption age. Where eruption ages are more questionable, particularly for the older Ape Canyon units (SHL08-3Z, SHL08-36EZ, SHL08-37PZ), the zircon ages often range to younger than the eruption age. These three samples all exhibited high total Ar gas measurements during Ar-Ar dating (Clynne et al., 2008), potentially indicating the presence of some older component of plagioclase that could skew the Ar age to older than reality. Some age populations are repeated among samples, for example 6 samples have populations between ~110 and 115 ka), two at ~79ka, two at ~69ka, and two at ~183ka.

Zircon geochemistry results are available in full in Appendix F and are summarized in Figure 5. Zircon Hf concentrations range from ~7150 to ~17175 ppm, becoming more variable and ranging to lower values with decreasing age. Titanium concentrations in the zircons range from 1.8 to 26.6 ppm, inversely correlated with Hf. Thorium varies from ~10 to ~1030 ppm, mostly below 300 ppm and U ranges from 25 to ~2800, with most values below 1000 ppm.

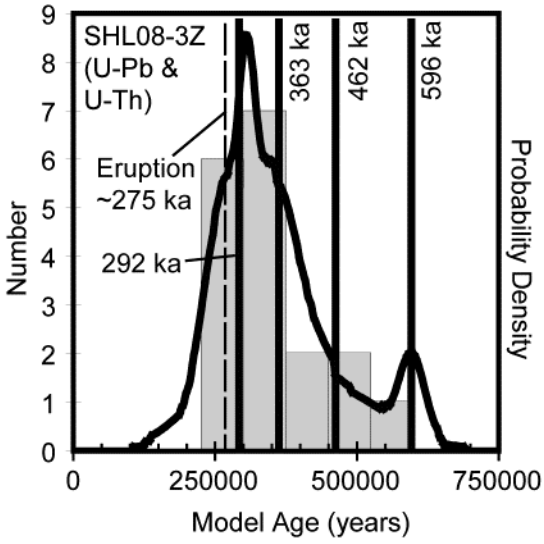

Figure 4a: Histogram of U-Pb and U-Th zircon model ages for sample SHL08-3Z. The black curve represents the cumulative probability density, the black vertical lines represent zircon age populations, and the dashed line represents the eruption age, as listed in Table 1.

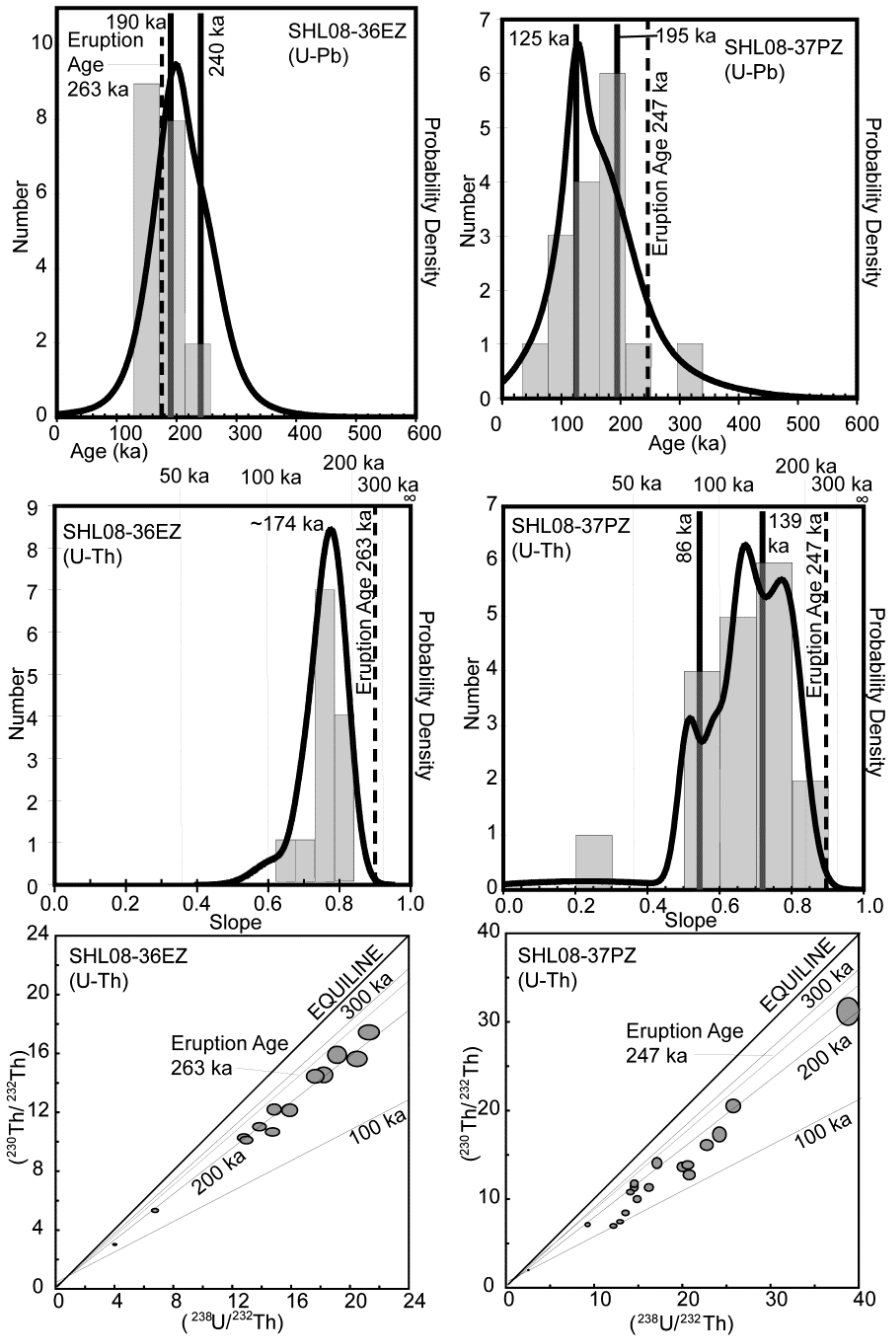

Figure 4b: Histograms of U-Pb zircon ages *(top)* and U-Th isochron slopes *(middle)* for samples SHL08-36EZ and SHL08-37PZ. The black curve represents the cumulative probability density, the black vertical lines indicate zircon age populations, and the dashed line indicates the published eruption age. The vertical gray lines on the middle diagrams indicate ages for various slopes, for reference. *(bottom)* Uranium-Thorium isochron diagrams for SHL08-36EZ and SHL08-37PZ. The gray ellipses represent 2σ error. Lines provided to illustrate reference ages.

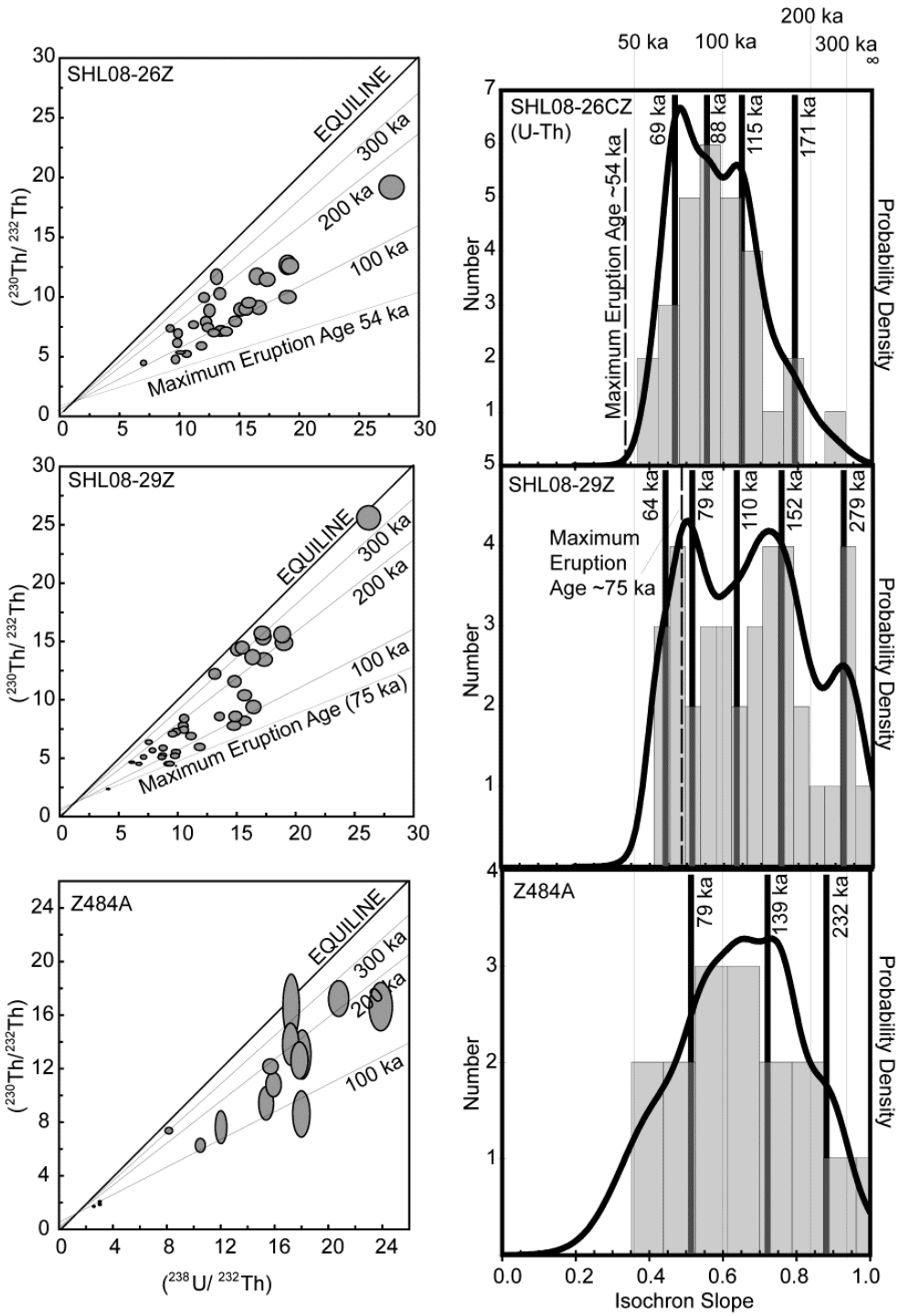

Figure 4c: *(left)* U-Th isochrons diagrams. The gray ellipses represent 2σ error. Lines provided to illustrate reference ages. *(right)* Histograms of U-Th isochron slopes. The light vertical lines provide ages at various slopes for reference. The black curve represents the probability density, the black vertical lines indicate age populations, and the vertical dashed line indicates the published eruption age.

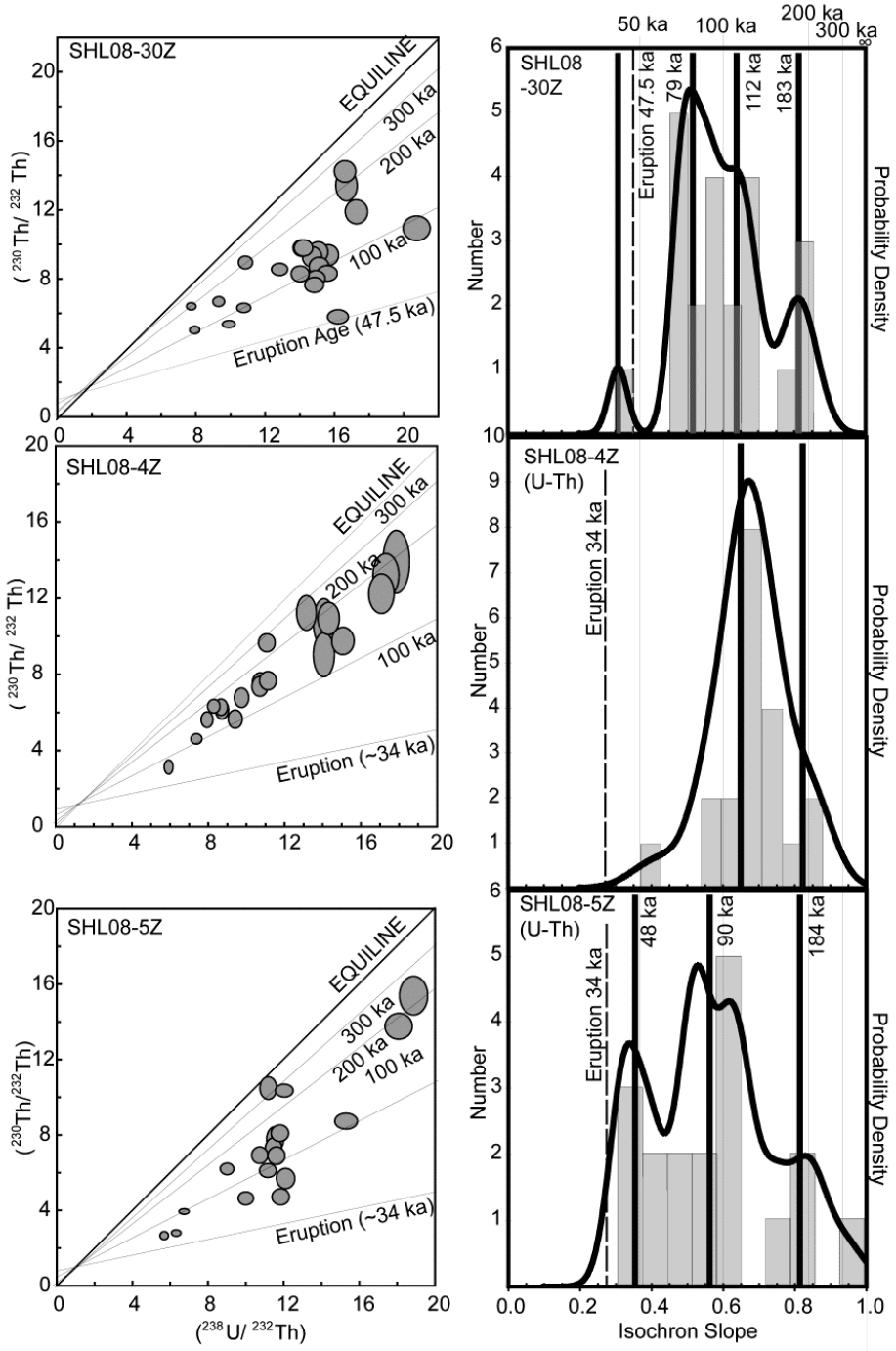

Figure 4d: *(left)* U-Th isochrons diagrams. The gray ellipses represent 2σ error. Lines provided to illustrate reference ages. *(right)* Histograms of U-Th isochron slopes. The light vertical lines provide ages at various slopes for reference. The black curve represents the probability density, the black vertical lines indicate age populations, and the vertical dashed line indicates the published eruption age.

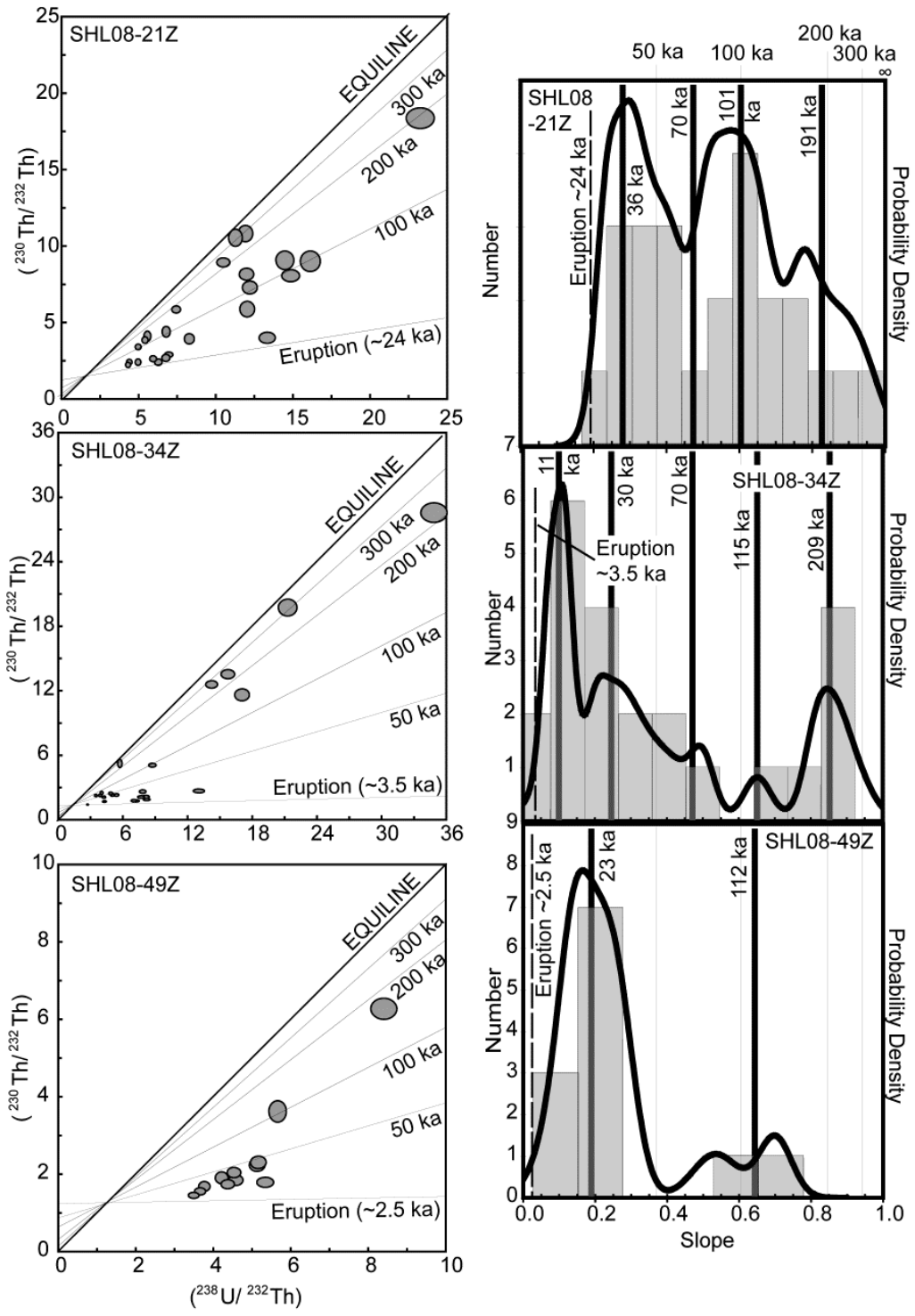

Figure 4e: *(left)* U-Th isochrons diagrams. The gray ellipses represent 2σ error. Lines provided to illustrate reference ages. *(right)* Histograms of U-Th isochron slopes. The light vertical lines provide ages at various slopes for reference. The black curve represents the probability density, the black vertical lines indicate age populations, and the vertical dashed line indicates the published eruption age.

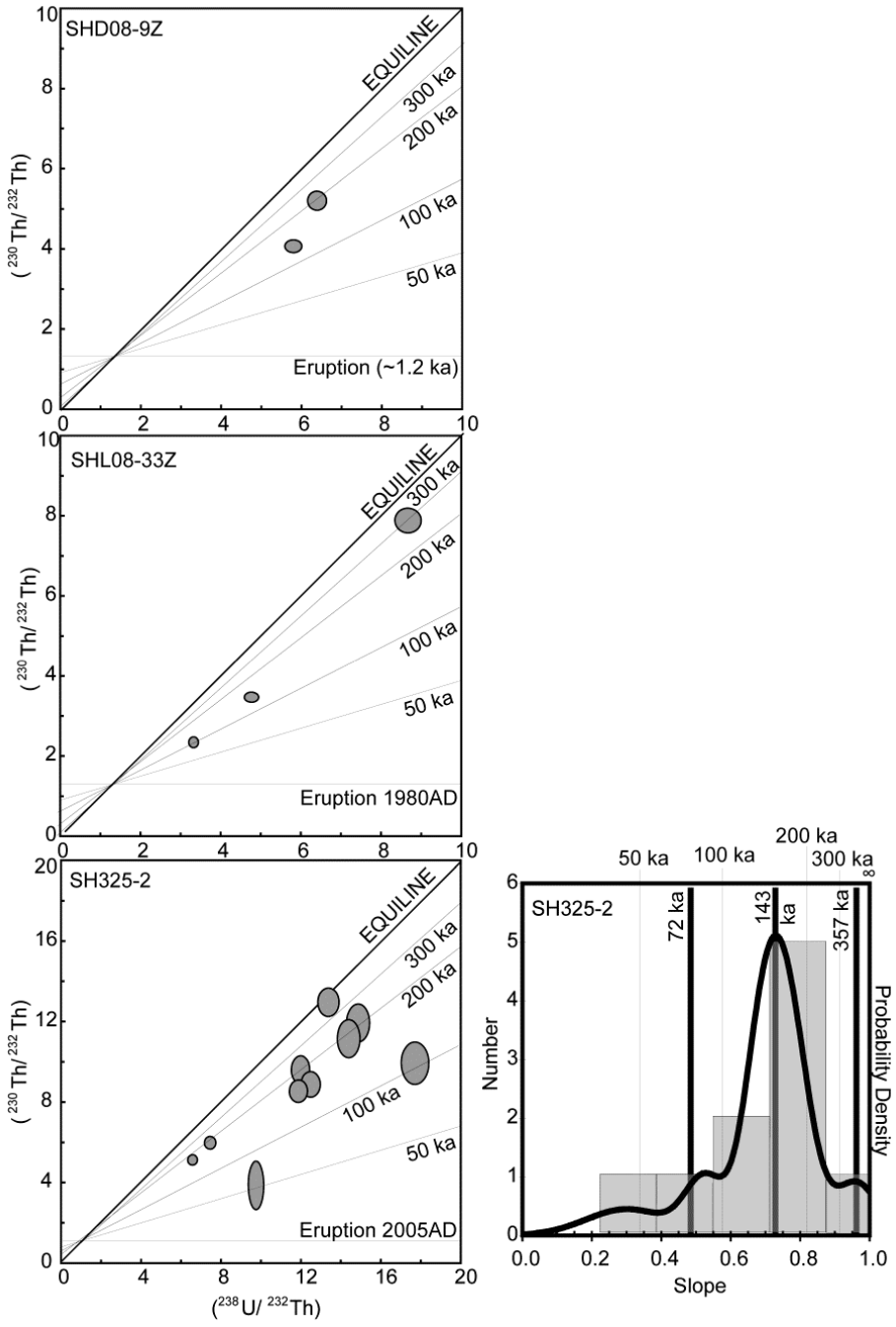

Figure 4f: *(left)* U-Th isochrons diagrams. The gray ellipses represent 2σ error. Lines provided to illustrate reference ages. *(right)* Histograms of U-Th isochron slopes for sample SH325-2. The light vertical lines provide ages at various slopes for reference. The black curve represents the probability density, the black vertical lines indicate age populations, and the vertical dashed line indicates the published eruption age. Histograms were not created for samples with less than five data points.

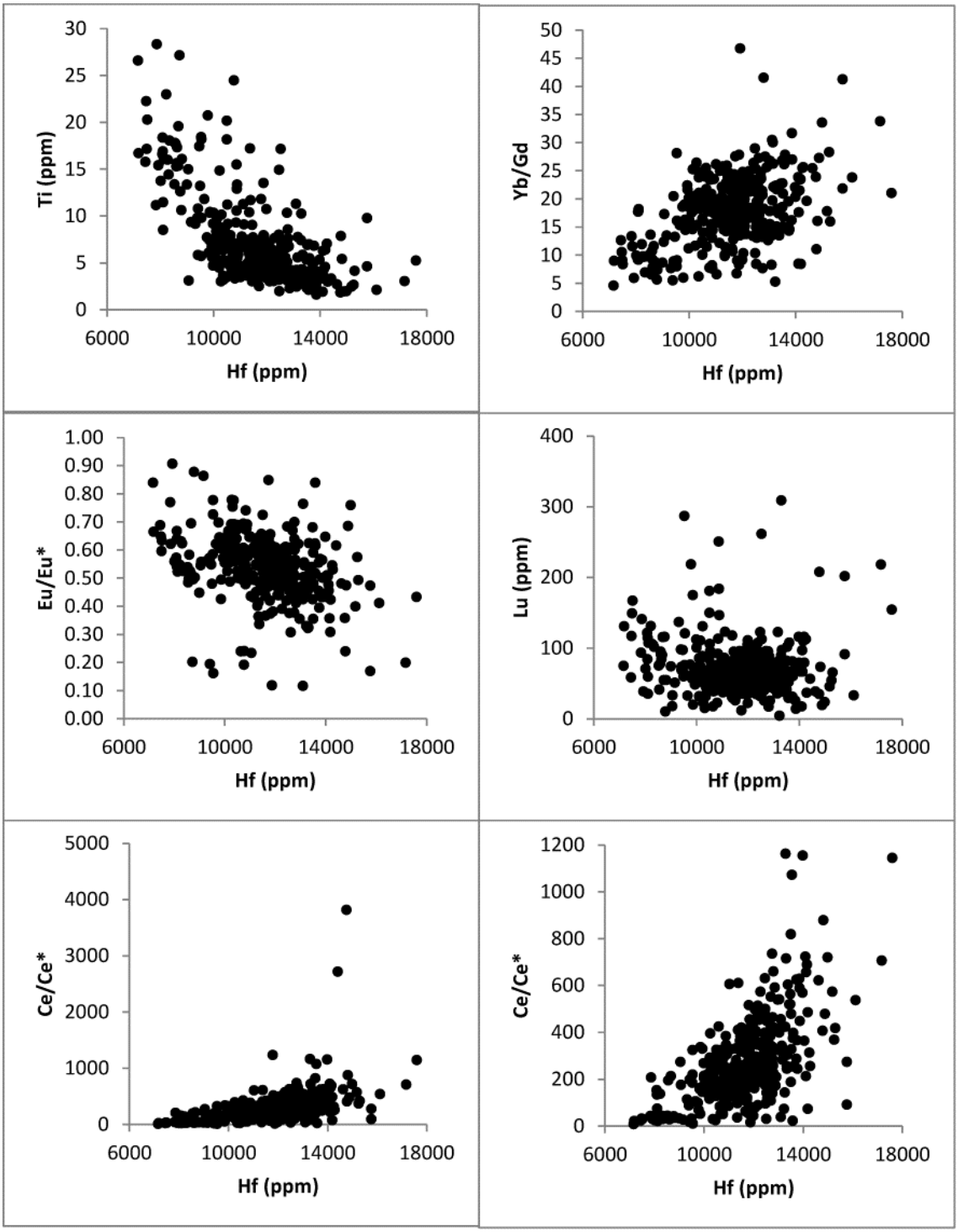

Figure 5a: Zircon geochemistry vs. zircon Hf concentration for all samples. In cases where data is tightly clustered, we have plotted the data a second time with an expanded scale (i.e. Ce/Ce*). These data are available in Appendix F.

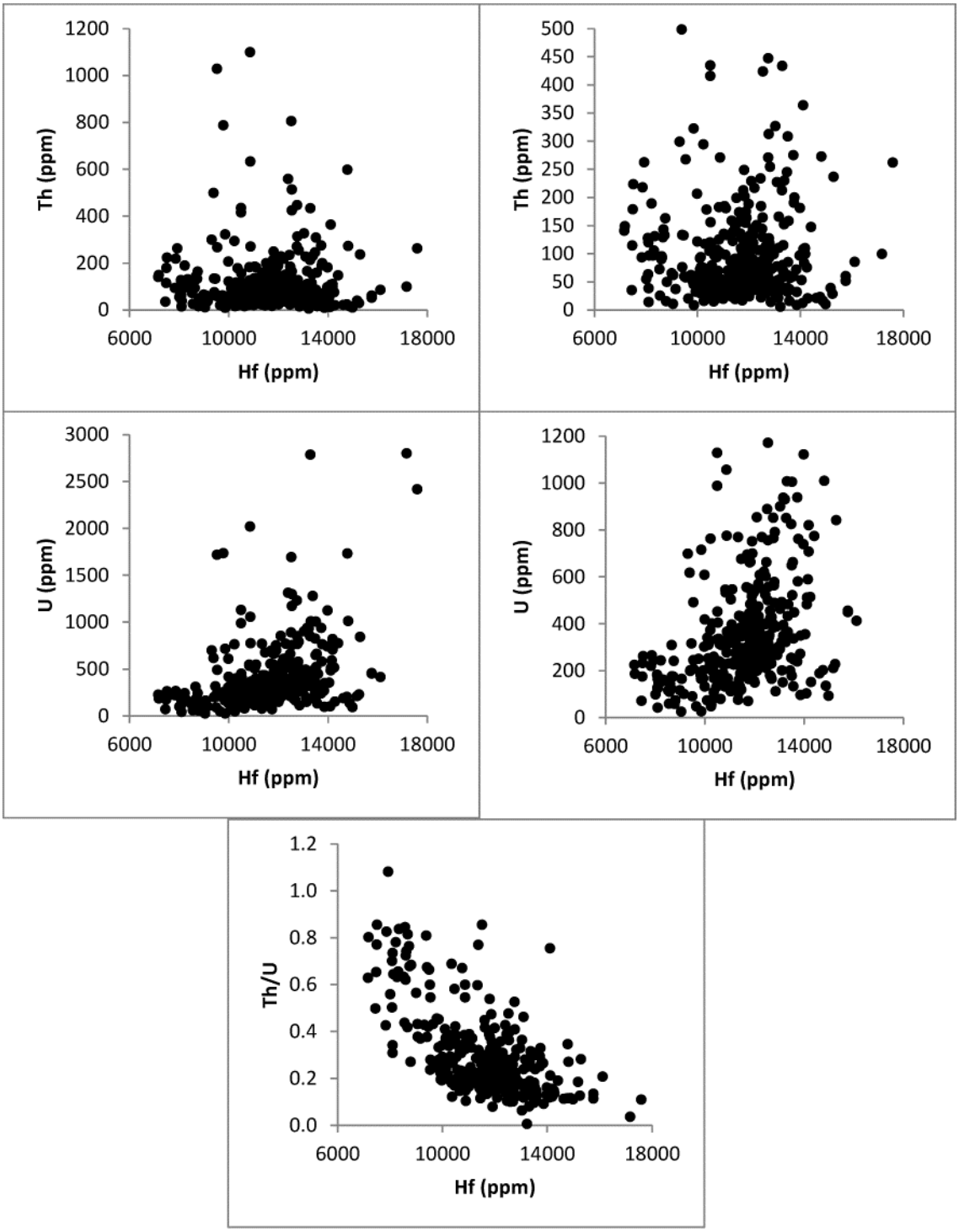

Figure 5a (cont'd): Zircon geochemistry vs. zircon Hf concentration for all samples. In cases where data is tightly clustered, we have plotted the data a second time with an expanded scale (i.e. Th & U). These data are available in Appendix F.

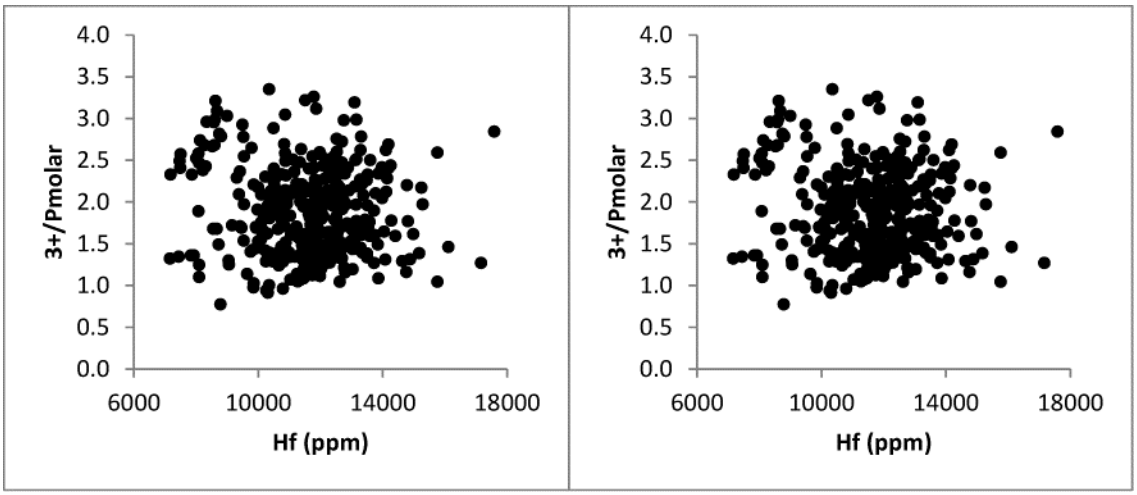

Figure 5a (cont'd): Zircon geochemistry vs. zircon Hf concentration for all samples. In cases where data is tightly clustered, we have plotted the data again with an expanded scale. These data are available in Appendix F.

Neither Th nor U correlate with Hf, but Th/U is tightly inversely correlated with Hf, decreasing with fractionation and with zircon age. HREE (represented here by Lu) does not correlate closely with Hf, and concentrations range from ~5 to ~ 300 ppm. HREE/MREE (represented here by Yb/Gd) increases from ~5 to ~45 with increasing Hf, indicating an increase in the steepness of chondrite normalized REE patterns with fractionation. Cerium anomaly increases from ~7 to ~1150 with increasing fractionation. Europium anomaly varies from ~0.9 to ~0.1, showing a slight decrease with increasing Hf, although zircons with both low and high Hf exhibit nearly the full range of Eu/Eu*. The molar total of 3+ atoms/molar P varies from ~0.8 to ~3.5. Each sample tends to exhibit compositions spanning most of the range for all samples, excluding SHL08-49AZ and SH325-2, which have more restricted compositions (Figure 6).

Older zircons exhibit a restricted range of most compositions, while younger zircons reveal more varied concentrations of most elements, beginning ~60 to 100 ka (Figure 7). At this time, Hf and Yb/Gd range to lower values, and Ti, Th, HREE (Lu), and Th/U range into higher values. Cerium anomaly is not closely correlated with age, although a series of zircons mostly from two samples (SHL08-49Z and SHL08-34Z) range in age from ~60 to 6 ka and exhibit a very

low and fairly uniform Ce anomaly (20-40, but mostly 28-30). Europium anomaly becomes more variable, both higher and lower, as zircon age decreases. Uranium behaves uniquely relative to time, as the older zircons show the widest range of compositions, and they become generally lower and much more restricted in range beginning around 60 ka.

Figure 8 shows Rare Earth Elements plotted for each sample by core, interior, and rims. REE/Chondrite trends follow expected patterns: enriched in HREE and depleted in LREE, with positive Ce anomaly and negative Eu anomalies. Normalizing REE to a zircon from this system allows us to see more internal variation (also shown in Figure 8). Rims tend to exhibit a more

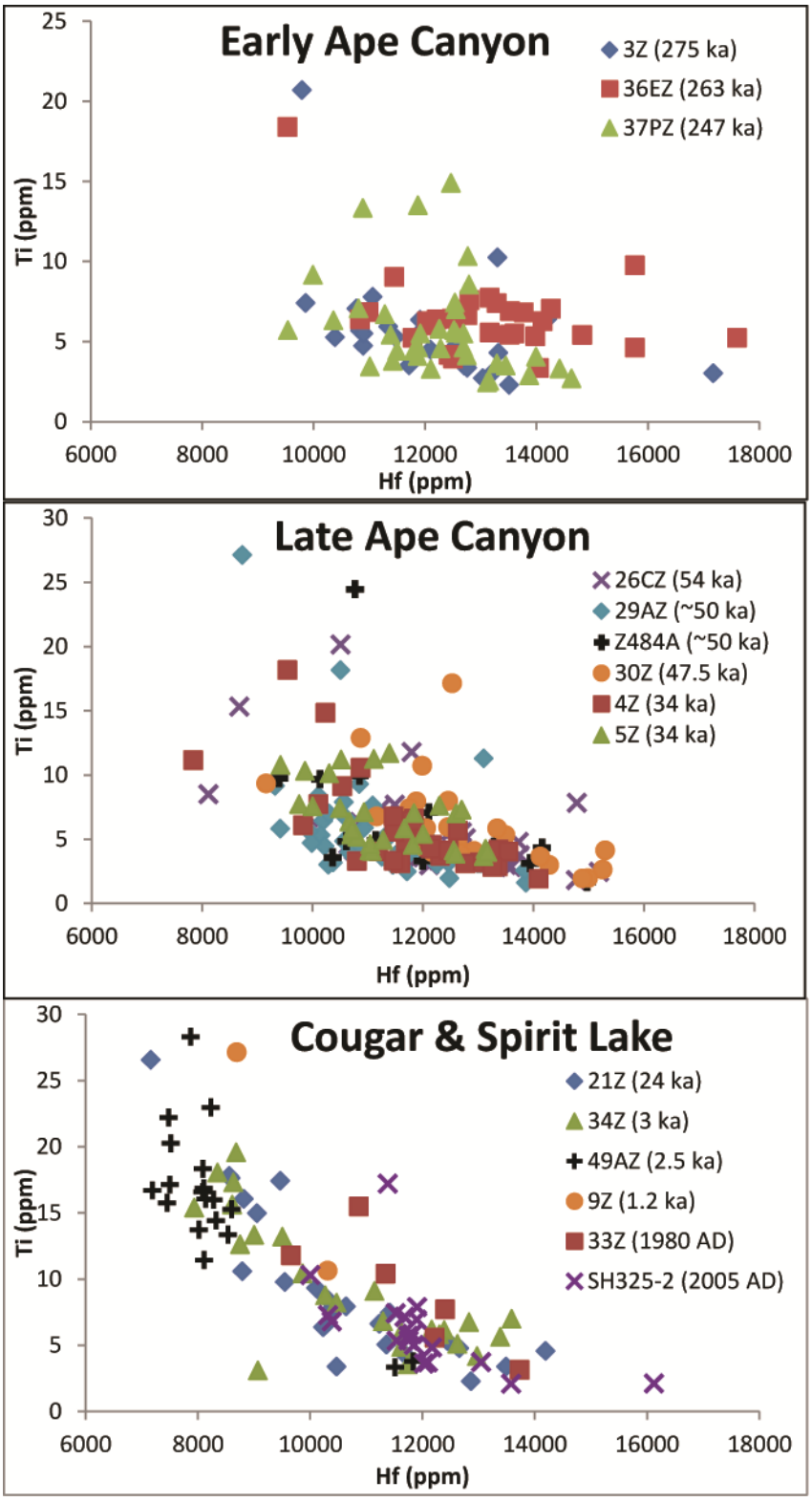

Figure 6: Zircon geochemistry by sample. Each panel contains data for zircons from rocks erupted during the Eruptive period listed. See Table 1 for sample information. Age of eruption is listed in parentheses for each sample.

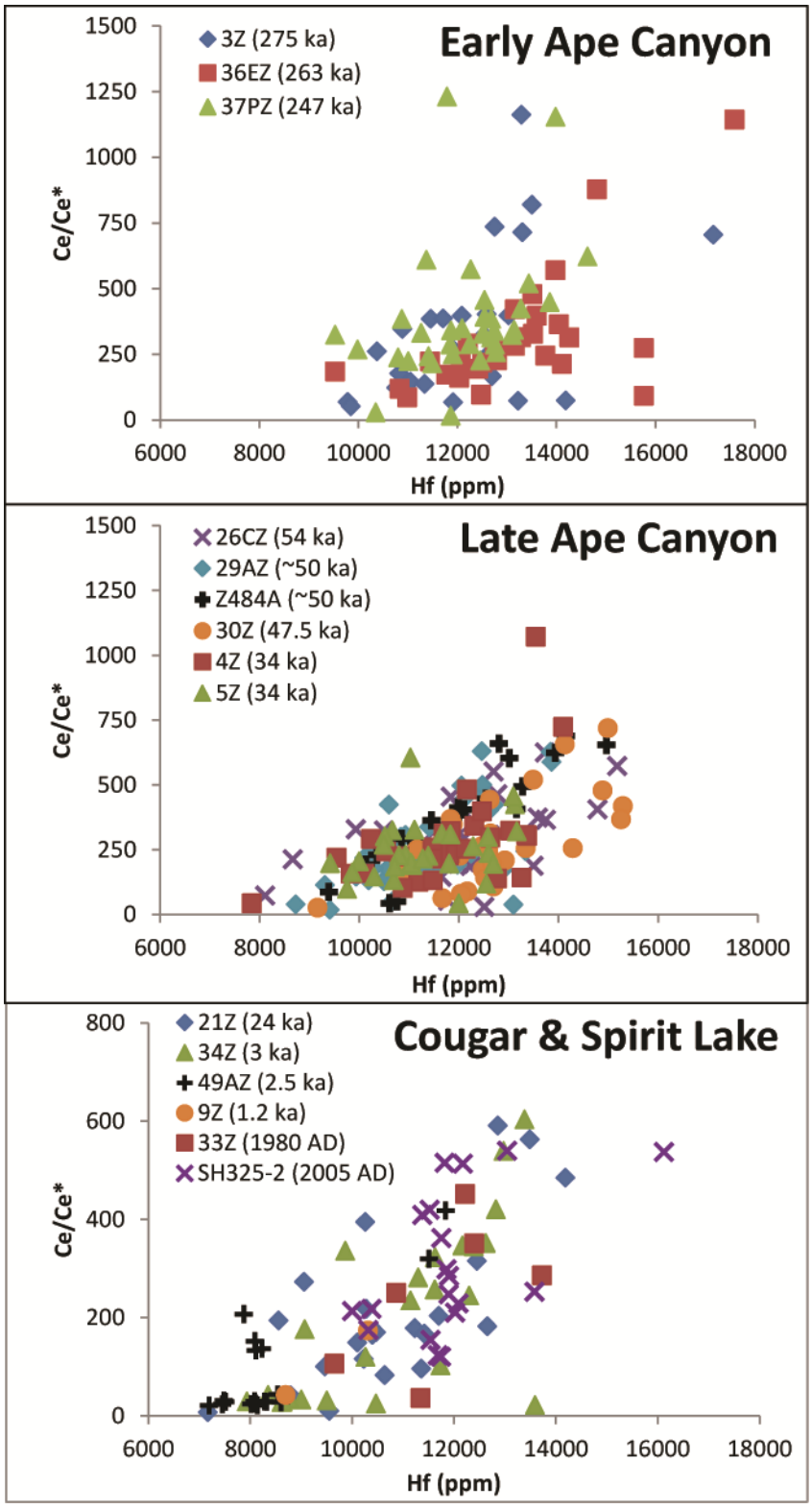

Figure 6 (cont'd): Zircon geochemistry by sample. Each panel contains data for zircons from rocks erupted during the Eruptive period listed. See Table 1 for sample information. Age of eruption is listed in parentheses for each sample.

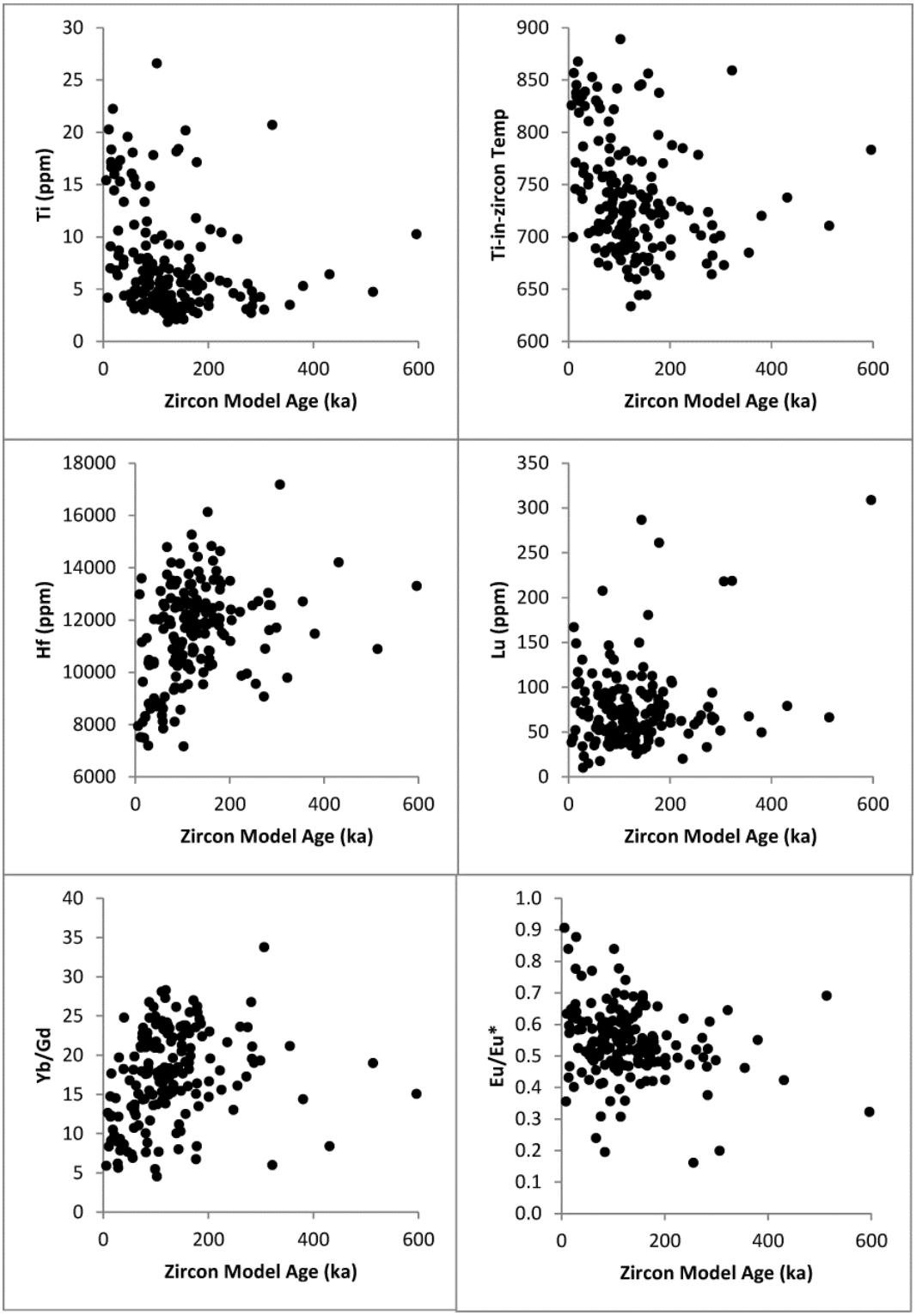

Figure 7: Zircon geochemistry vs. zircon model age for all samples. Error of geochemical data is within the size of the data point. For errors on model ages, see error ellipses in Figure 4. Ti-in-zircon estimates here assume αTiO_2=0.7 and αSiO_2=1.0. Data is available in Appendices 3 and 4.

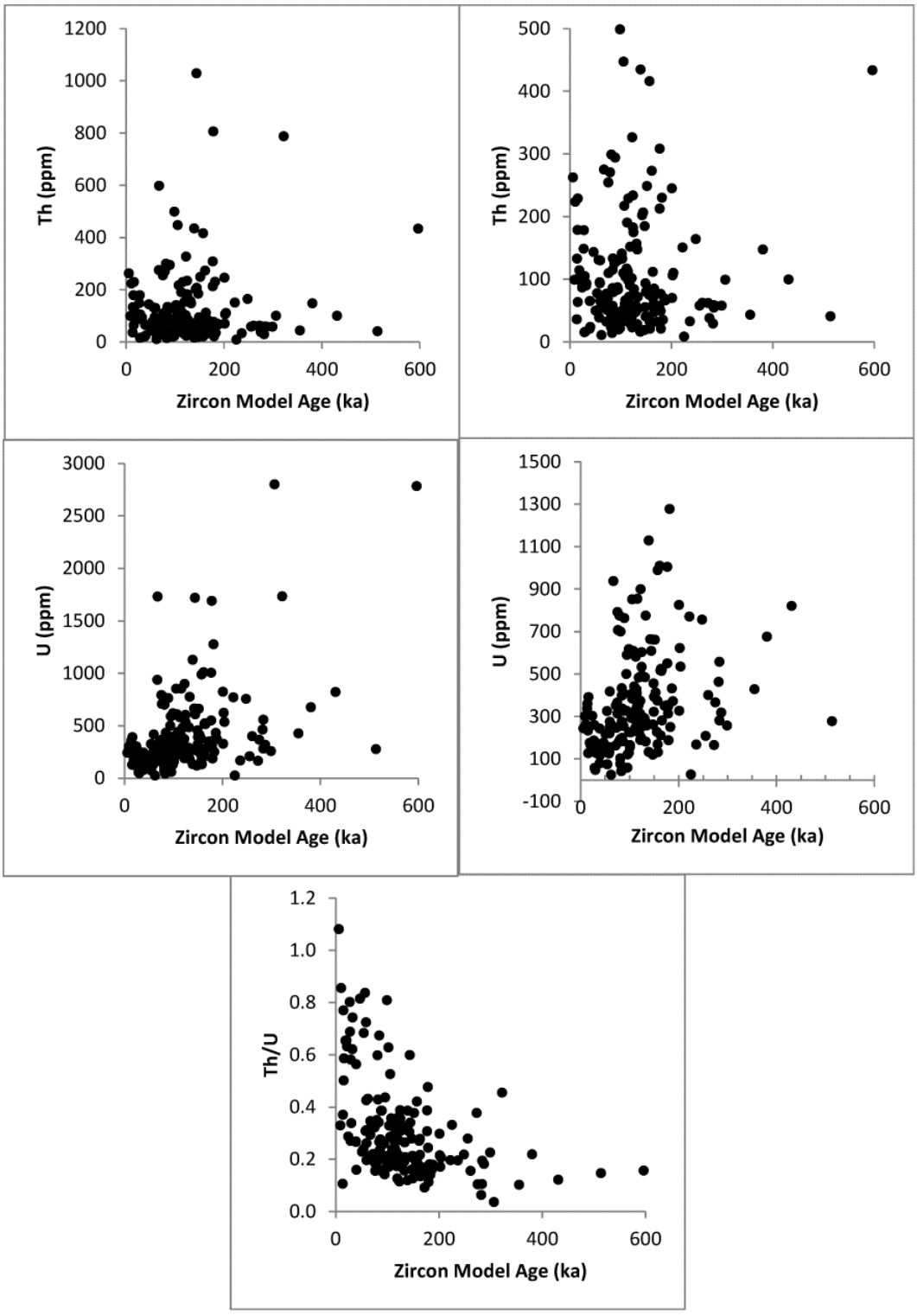

Figure 7 (cont'd): Zircon geochemistry vs. zircon model age for all samples. Error of geochemical data is within the size of the data point. For errors on model ages, see error ellipses in Figure 4. Where data clustered, we plotted it a second time with a restricted scale. Data is available in Appendices 3 and 4.

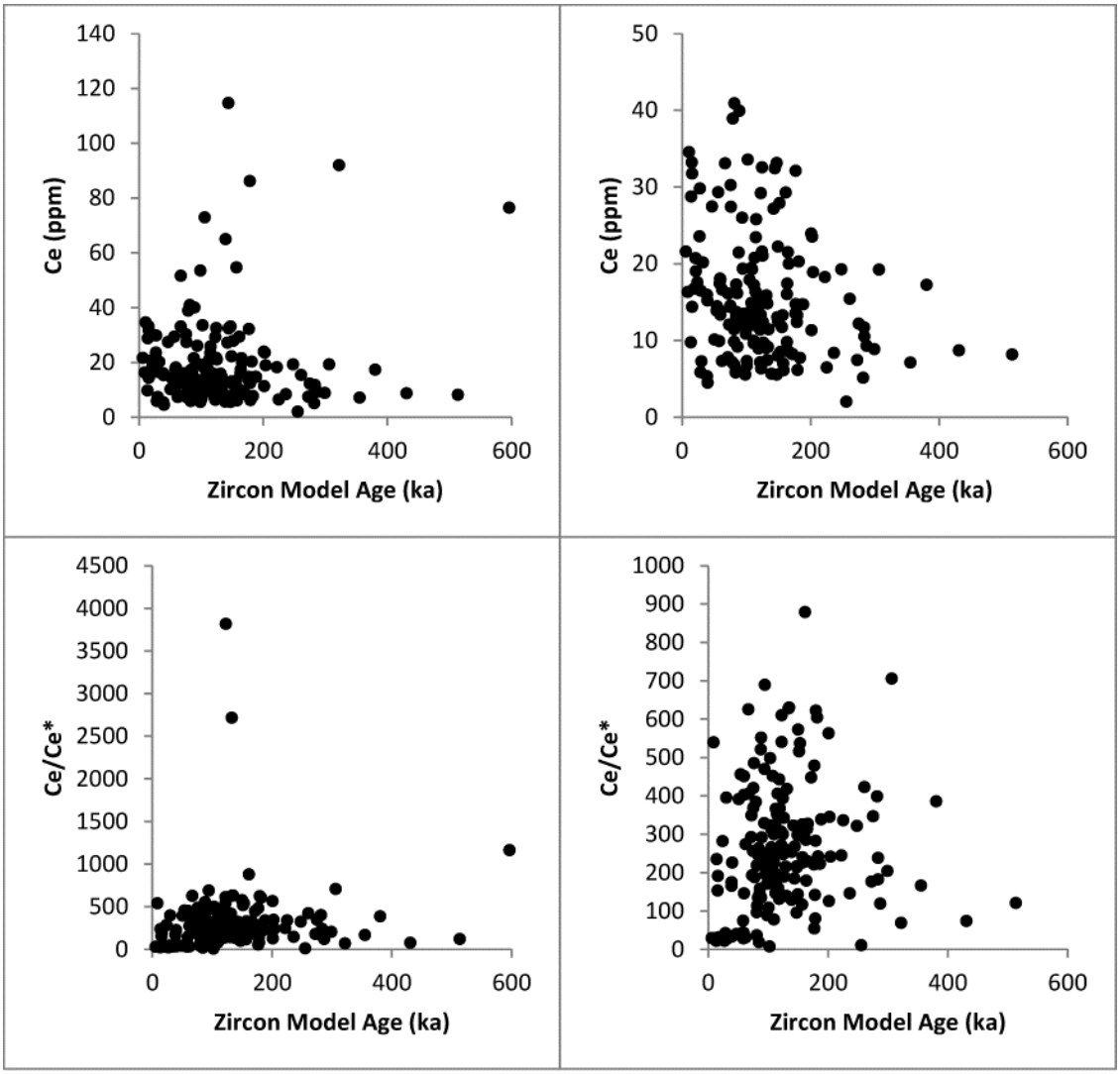

Figure 7 (cont'd): Zircon geochemistry vs. zircon model age for all samples. Error of geochemical data is within the size of the data point. For errors on model ages, see error ellipses in Figure 4. Where data clustered, we plotted it a second time with a restricted scale. Data is available in Appendices 3 and 4.

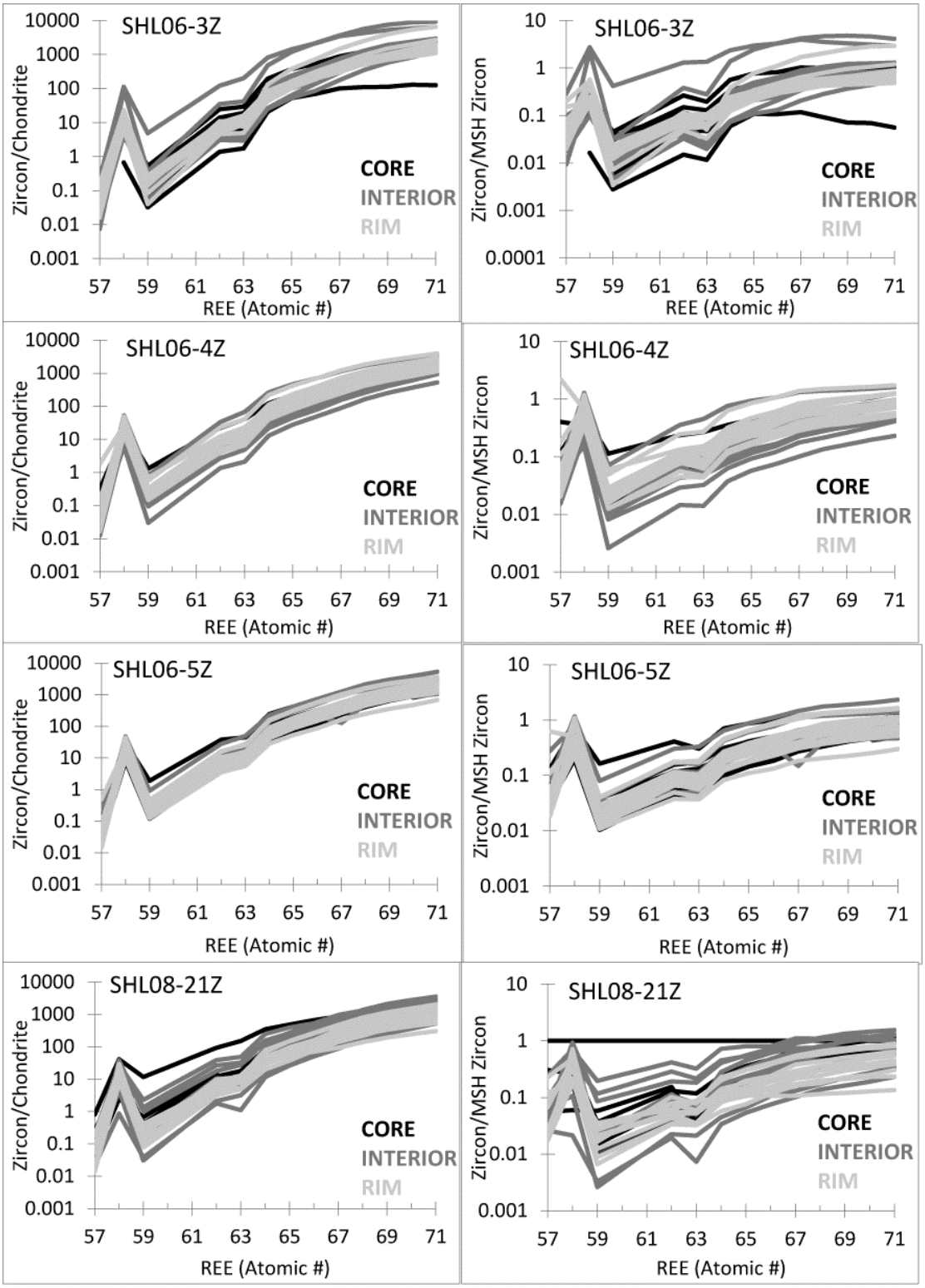

Figure 8: *(left)* REE/Chondrite for each sample. Each line represents one analysis, and is color coded to indicate whether it was a zircon core, interior or rim. *(right)* REE/MSH Zircon for each sample. The normalizing zircon was from sample SHL08-21Z.

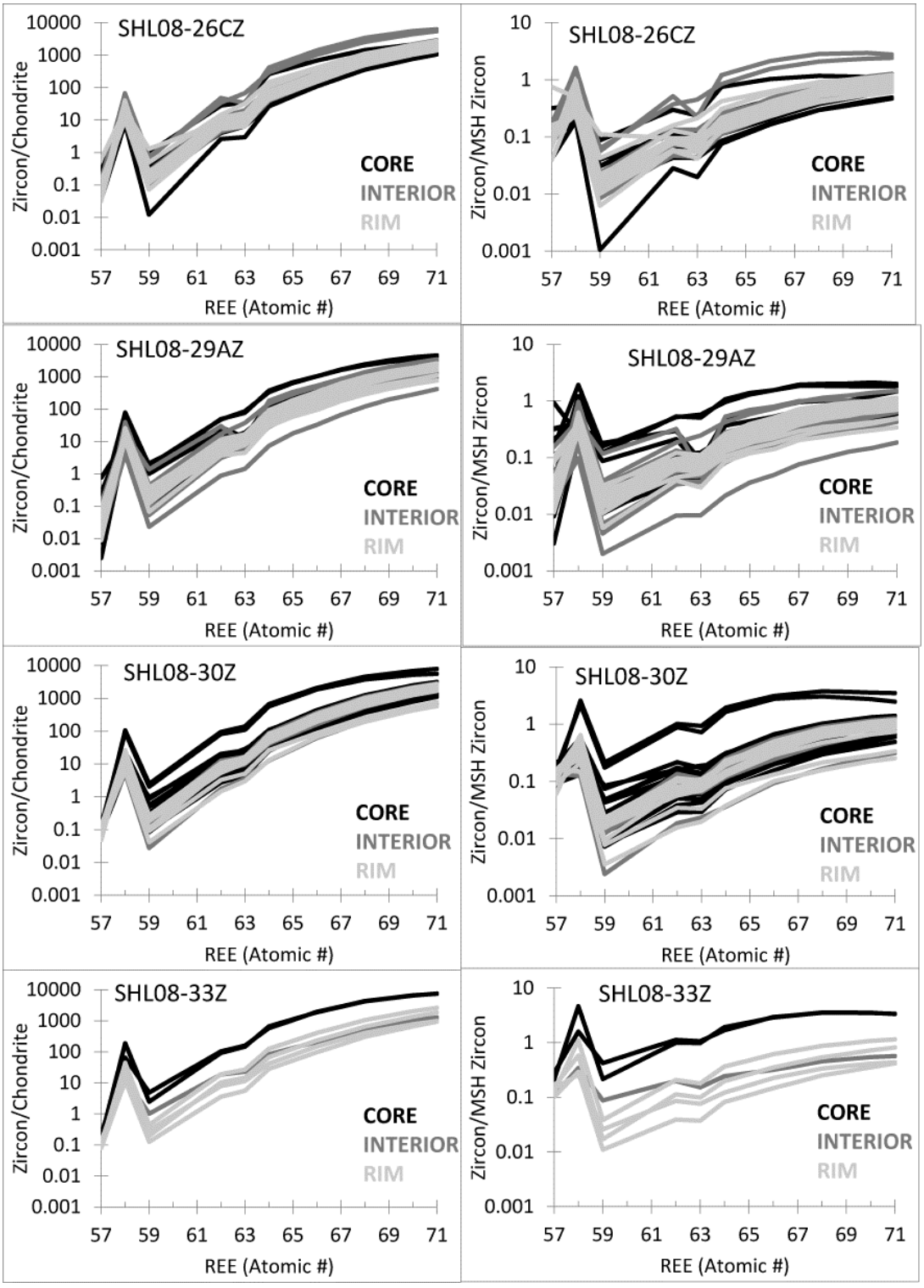

Figure 8 (cont'd): *(left)* REE/Chondrite for each sample. Each line represents one analysis, and is color coded to indicate whether it was a zircon core, interior or rim. *(right)* REE/MSH Zircon for each sample. The normalizing zircon was from sample SHL08-21Z.

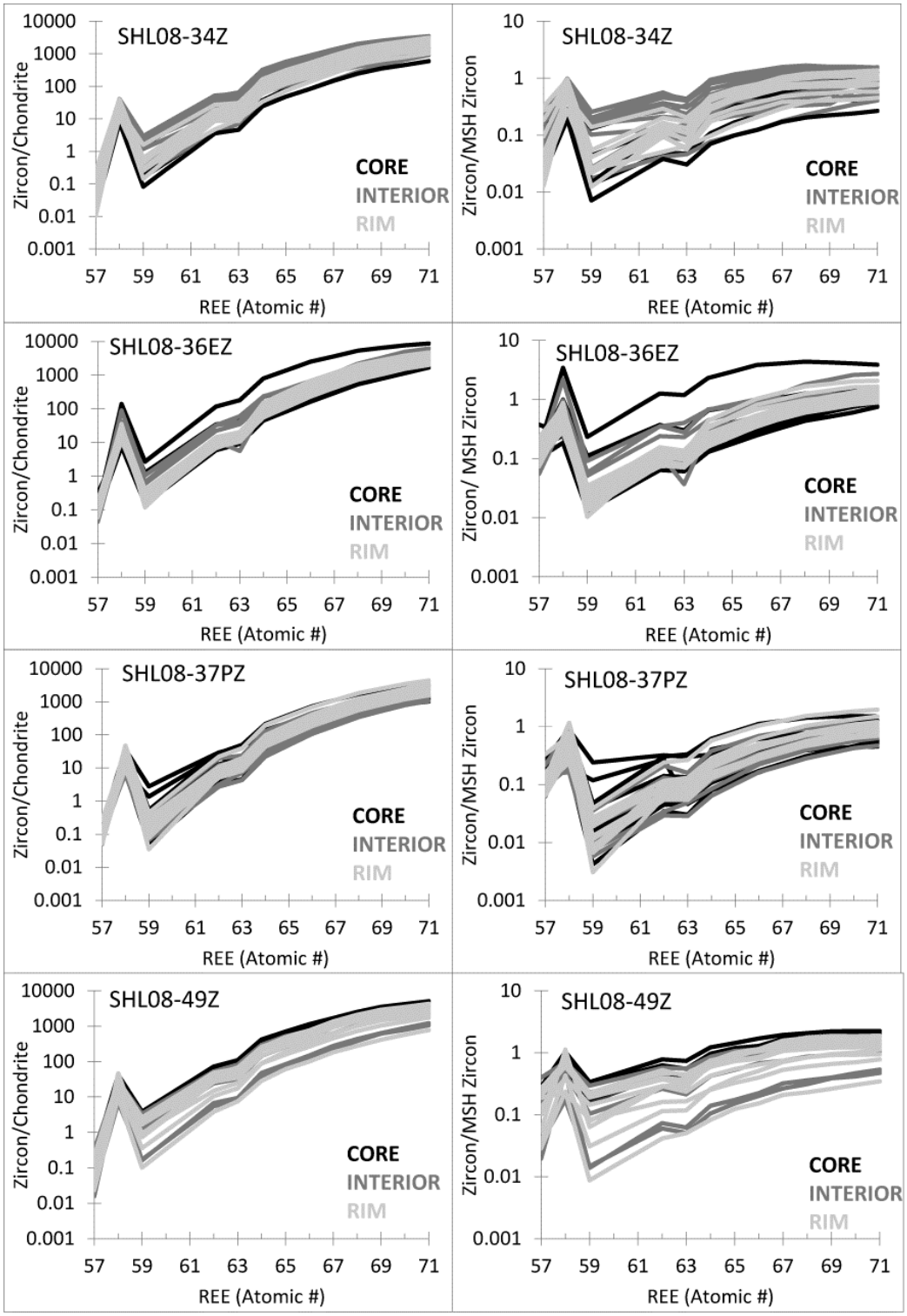

Figure 8 (cont'd): *(left)* REE/Chondrite for each sample. Each line represents one analysis, and is color coded to indicate whether it was a zircon core, interior or rim. *(right)* REE/MSH Zircon for each sample. The normalizing zircon was from sample SHL08-21Z.

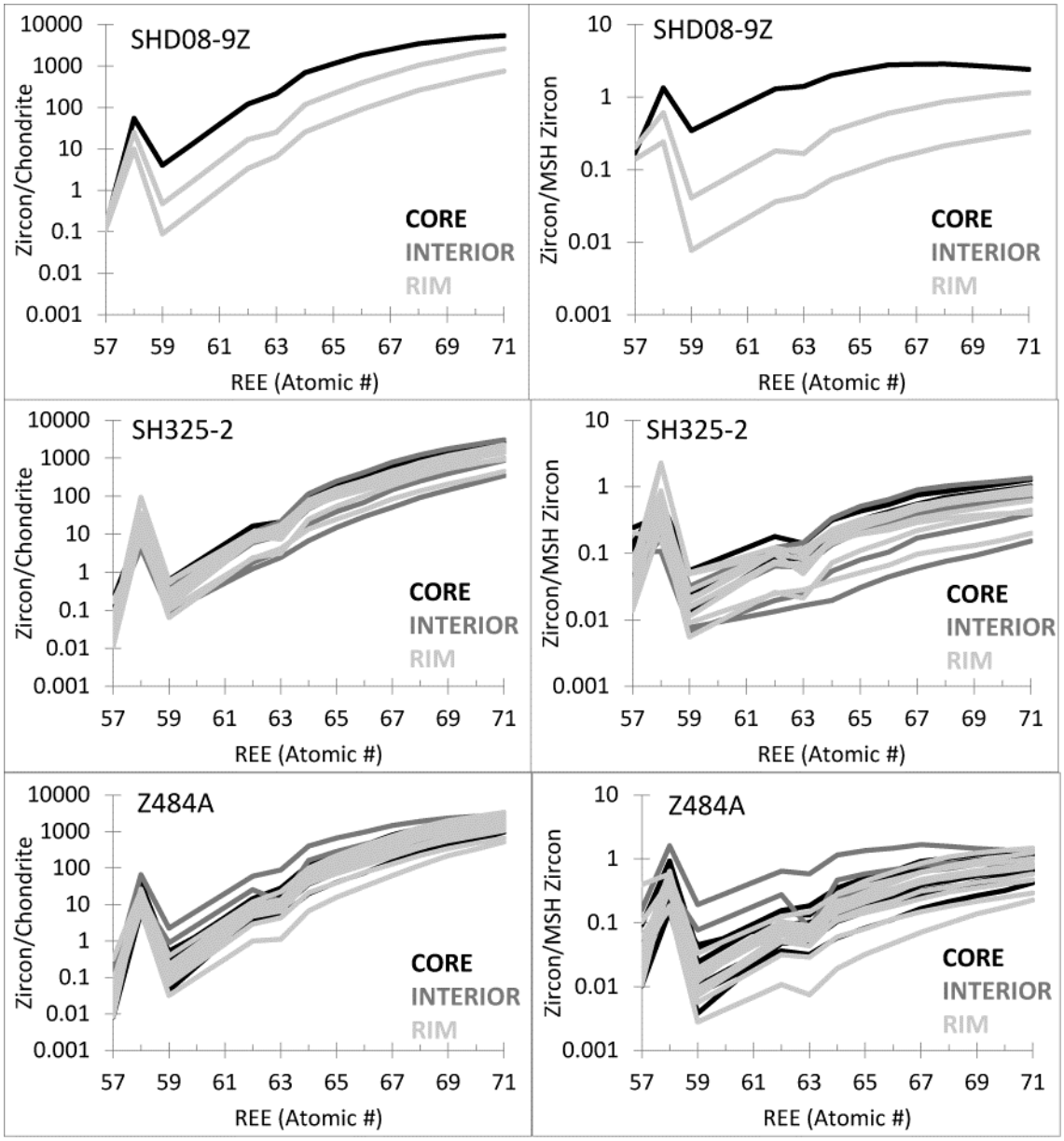

Figure 8 (cont'd): *(left)* REE/Chondrite for each sample. Each line represents one analysis, and is color coded to indicate whether it was a zircon core, interior or rim. *(right)* REE/MSH Zircon for each sample. The normalizing zircon was from sample SHL08-21Z.

restricted REE composition than interiors and cores, and are often also lower in REE. Figure 9 shows core, interior, and rim compositions for all samples included in this study. Generally, the compositions overlap for most chemical components with rims being slightly more restricted in composition than cores and interiors. This is especially true for Yb/Gd, which is significantly more restricted in composition and is generally lower in rims than interiors and cores.

Estimated zircon temperatures based on the Ti-in-zircon thermometer at various $aSiO_2$ and αTiO_2 are reported in Figure 10 and Table6. At αSiO_2=1.0 and αTiO_2=0.7, calculated zircon temperatures range from 624°C to 897°C, with sample averages ranging from 714°C to 839°C. Figure 11 shows variations in αTiO_2 required to account for changes in measured zircon Ti concentrations, assuming aSiO2=1.0 and constant temperature. At 700°C, αTiO_2 varies from 0.27 to 4.42, with an average of 0.62. At 800°C, αTiO_2 varies from 0.09 to 1.54 with an average of 1.15. At 900°C, αTiO_2 varies from to 0.04 to 0.64, with an average of 0.17.

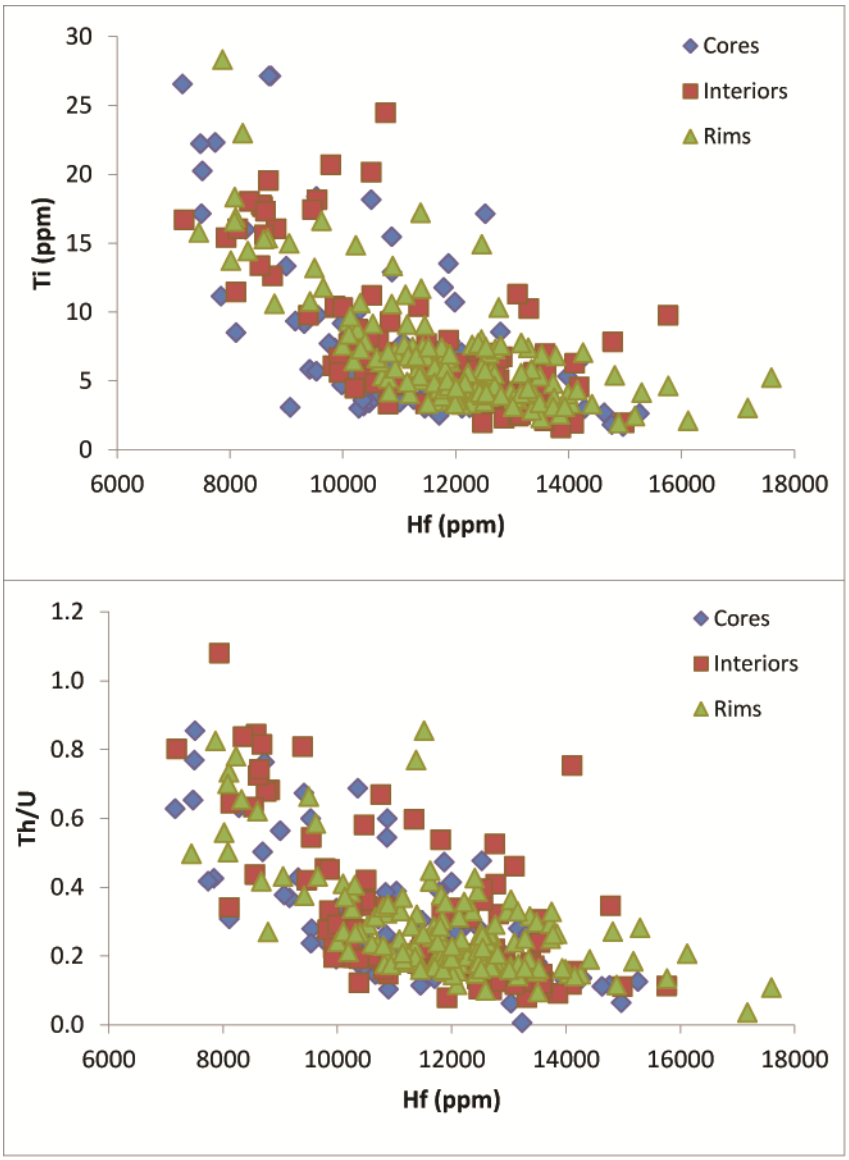

Figure 9: Zircon geochemistry vs. Hf for all zircon cores, interiors, and rims.

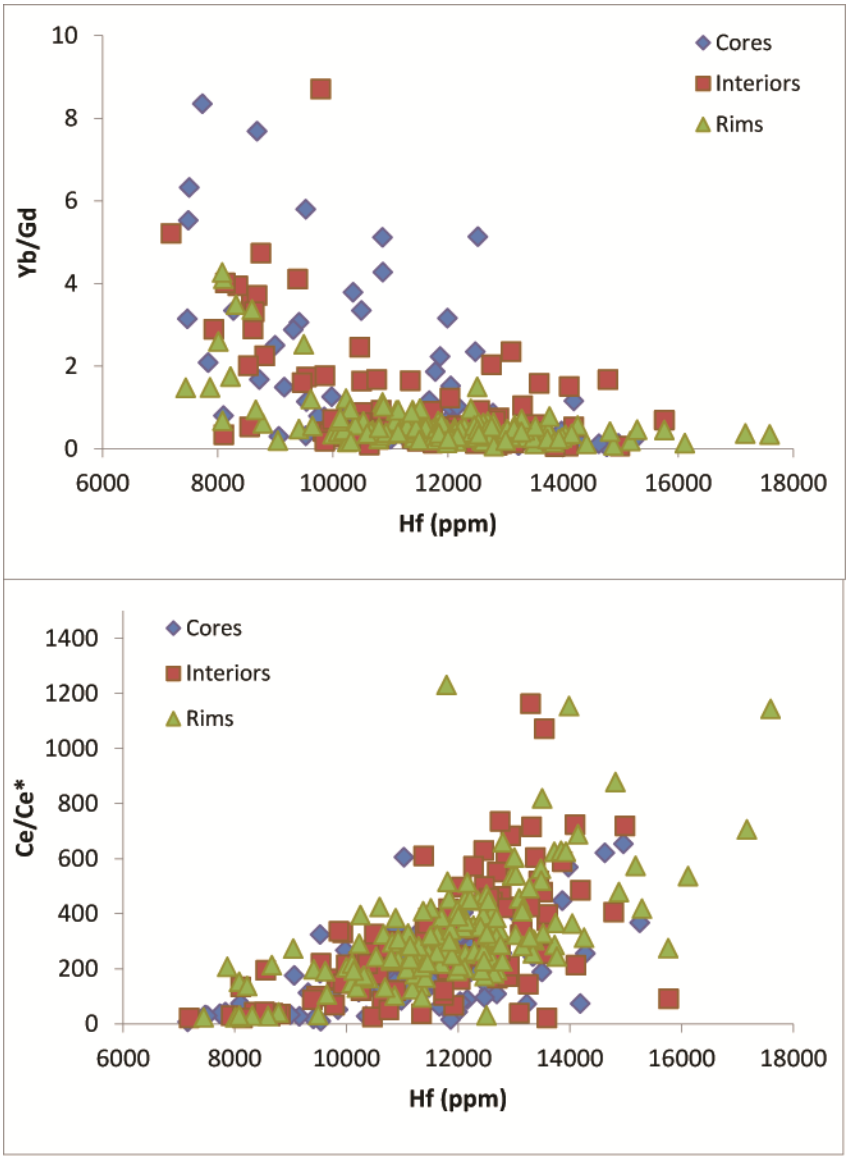

Figure 9 (cont'd): Zircon geochemistry vs. Hf for all zircon cores, interiors, and rims.

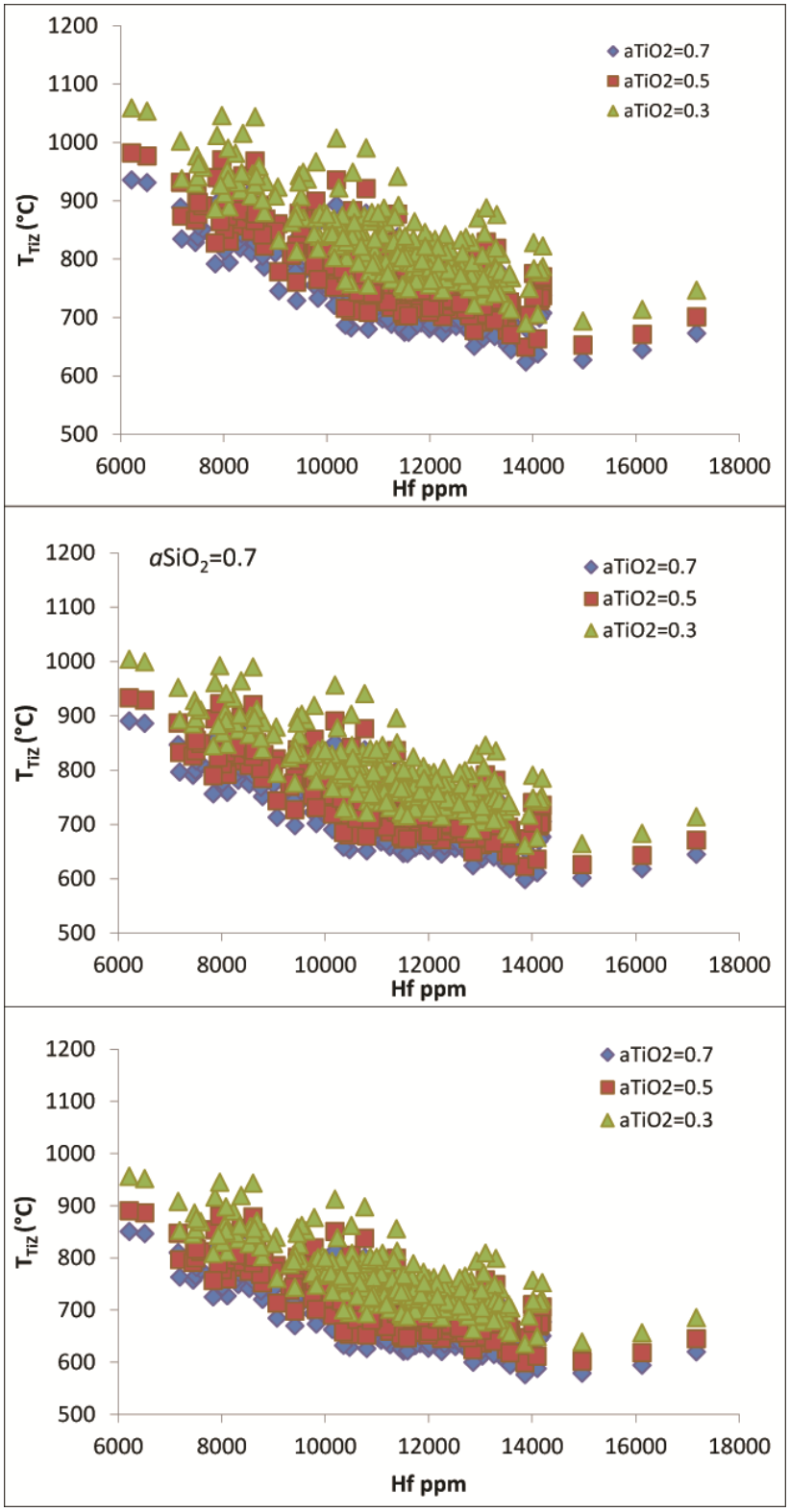

Figure 10: Ti-in-zircon temperatures (T_{TiZ}) calculated for various aTiO$_2$, assuming *(top)* aSiO$_2$=1.0, *(middle)* aSiO$_2$=0.7, and *(bottom)* aSiO$_2$=0.5.

Table 6: Calculated Ti-in-zircon temperature ranges and averages at various αSiO_2 and αTiO_2 for samples in this study. Samples are listed in chronological order by eruption. Block highlighted in gray represents values considered most reasonable (see discussion).

Sample	aSiO2=1.0				aSiO2=0.7			
	aTiO2=0.7		aTiO2=0.5		aTiO2=0.7		aTiO2=0.5	
	Range	Avg	Range	Avg	Range	Avg	Range	Avg
SHL06-3Z	650-859	718	677-899	749	624-819	687	649-856	716
SHL08-36EZ	681-845	736	709-885	769	652-806	704	679-843	734
SHL08-37PZ	656-822	721	683-860	752	629-785	690	654-820	719
SHL08-26CZ	637-844	718	663-883	748	611-805	688	636-842	715
SHL08-29Z	624-891	714	649-934	745	599-849	684	622-889	712
Z484A	627-879	722	652-921	753	602-837	691	625-876	720
SHL08-30Z	638-837	720	664-876	751	612-799	689	637-835	718
SHL08-4Z	637-844	717	663-883	748	611-805	687	635-842	716
SHL08-5Z	689-796	736	718-832	768	660-761	704	687-794	734
SHL08-21Z	651-889	759	677-931	793	624-847	726	649-886	757
SHL08-34Z	674-852	763	702-892	797	646-813	730	673-850	761
SHL08-49Z	681-897	821	709-940	859	652-854	784	679-894	819
SHD08-9Z	712-891	839	742-934	878	681-849	800	710-889	836
SHL08-33Z	675-826	760	703-864	794	647-789	727	674-824	758
SH325-2	644-838	726	670-877	756	618-800	694	643-836	724

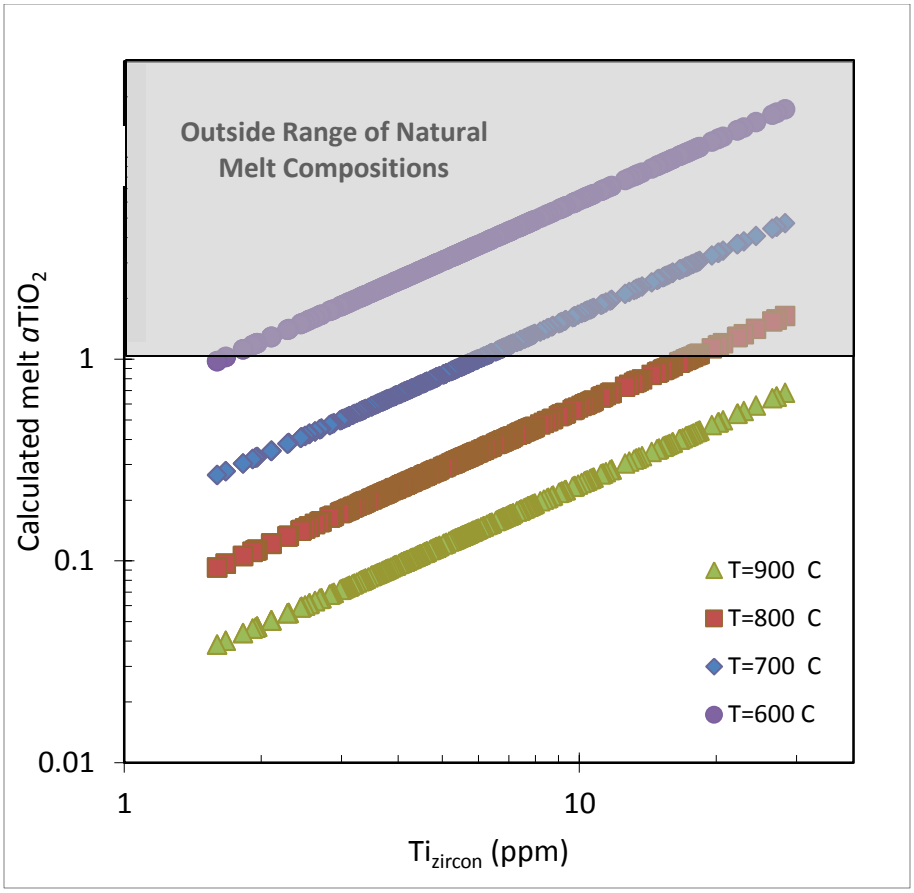

Figure 11: Calculated melt $aTiO_2$ at three constant temperatures, based on zircon Ti concentrations and assuming $aSiO_2$=1.0.

4. Discussion and Conclusions

4.1. Zircon Ages

We analyzed whole rocks to determine their U-Th isotopic compisitions in order to constrain the initial ratios of the magmas from which the zircons grew. However, since it appears that the zircons are not cognate to the melts in which they were erupted (see discussion below), we cannot directly apply these values to the zircons from these samples. They do serve to inform us about the normal range of values for Mount St. Helens magmas. Since most of these values fall within the range of all values in the literature and have an

average close to our previously selected value of 1.2, we have chosen to use an initial ($^{230}Th/^{232}Th$) of 1.2 in our calculations.

The lack of eruption age zircon in most samples, combined with significantly higher eruption temperatures than zircon saturation temperatures or Ti-in-zircon temperatures all suggests that the zircons are not cognate to the melts in which they are erupted. Calculations based on Watson 1996, assuming an average Zr concentration of 135 ppm and an average major element composition for MSH dacites (averages for samples from this study, Table 3), indicate that a 50 micron zircon would dissolve in an 850°C melt in <100 years with 6 wt% H_2O and <1000 years with 3 wt% H_2O (Figure 12). This suggests that a maximum of 1000 years, probably much less, must have passed from entrainment of the zircons in the upward migrating melt and eruption.

For most cases where zircon ages are within error of or younger than the eruption age established by Ar-Ar dating (Clynne et al., 2008), inaccuracies in the proposed eruption age are likely. The three samples with zircon ages definitively younger than the established eruption age are the three earliest erupted samples. For these three early Ape Canyon samples (SHL06-3Z, SHL08-36EZ, and SHL08-37PZ), the total Ar gas measured during Ar-Ar dating gave a much older age than the isochron or plateau age (Clynne et al., 2008), suggesting the presence of some portion of older plagioclase that could skew the Ar-Ar ages to older than reality. For sample SHL08-37Z, the isochron age was not selected as the preferred age, but was in fact, much younger than the plateau age and is within error of the youngest eruption age. This is consistent with the youngest zircons ages representing a newly constrained maximum eruption age for these samples. These younger ages are also permitted by the stratigraphic relations of these samples. In general, considering the lack of zircon ages as young as the eruption in most

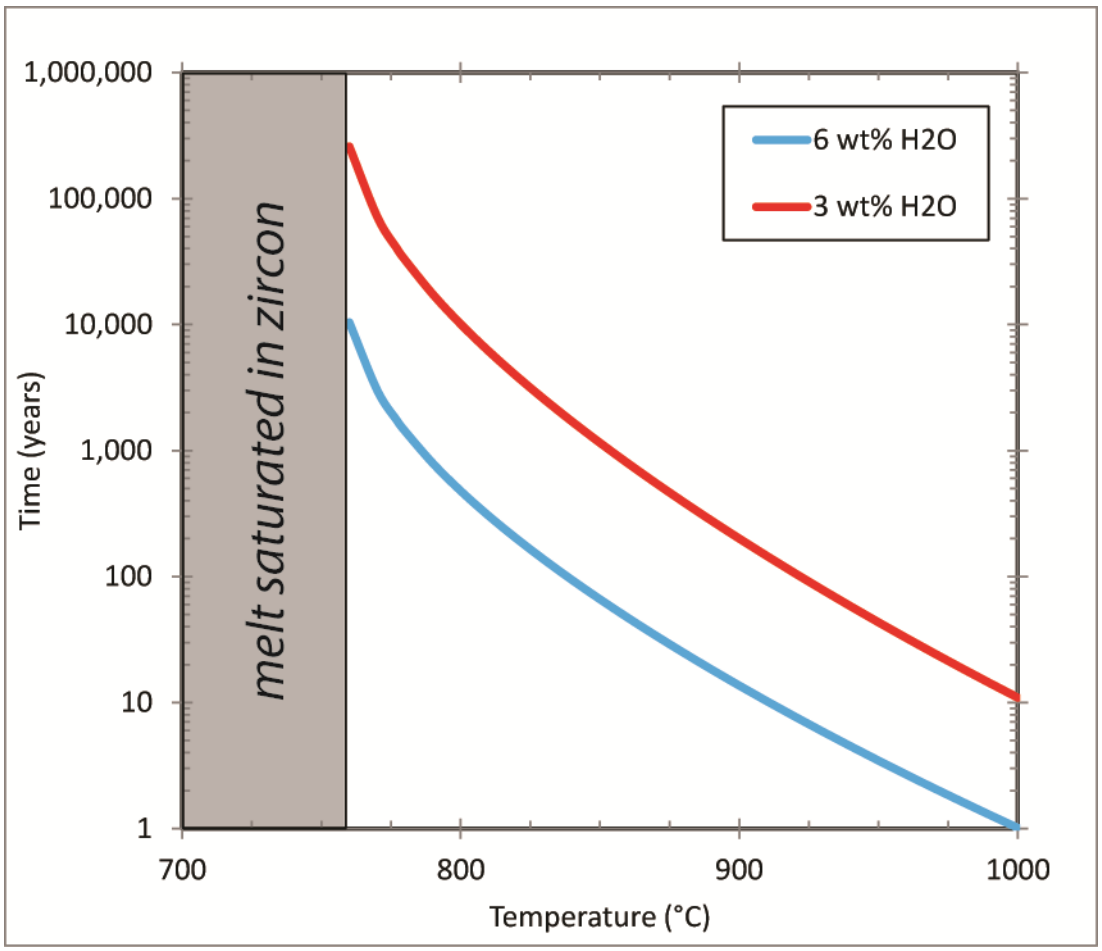

Figure 12: Dissolution rates for a 50µm zircon in a dacitic melt with 135 ppm Zr (compositions are average for samples from this study) at 3 and 6 wt% H_2O. Calculated based on Watson (1996).

other MSH samples, it seems prudent to always consider zircons as providing a constraint on the maximum possible eruption age, and assume that the actual eruption age is something less than that.

That zircon age populations are repeated from sample to sample, but are not present in all samples suggests two possibilities. First, they could indicate episodes of widespread zircon crystallization in the sub-volcanic system. At the relatively low expected temperatures of zircon saturation, this would also imply widespread crystallization of major phases. Young, hot magmas on the way to eruption would then be likely to entrain crystals of this age. The second

possibility is that crystallization during these periods is not particularly widespread, but various eruptive episodes repeatedly tap the same part of the sub-volcanic system and entrain portions of it. This could suggest something about the geometry and/or evolution of the magmatic plumbing system beneath MSH.

4.2. Zircon compositions & temperatures

Glass compositions and eruption temperatures from the literature for Mount St. Helens provide $a\mathrm{TiO_2}$ estimates (Table 4) much lower than we use here. Temperatures of zircon saturation and inferred zircon growth temperatures are much lower than the eruption temperatures of these melts, so we cannot use $a\mathrm{TiO_2}$ calculated at those higher temperatures. It is not valid to use these same compositions and extrapolate to a lower temperature (such as those assumed for zircon growth), because at a lower temperature, the magma would have contained a different mineral assemblage and the melt would have had a different composition, resulting in a different $a\mathrm{TiO_2}$. So, while we have considered glass compositions as constraints and to understand the changes in melt $a\mathrm{TiO_2}$ with composition and temperature, we cannot apply them to zircon growth. As $a\mathrm{TiO_2}$ does increase with decreasing temperature, we can assume higher $a\mathrm{TiO_2}$ than that estimated from glasses at their eruption temperatures (average = 0.38, Table 4). Where reported in the literature, the oxide mineral assemblage consists of magnetite and ilmenite, a $\mathrm{TiO_2}$ rich phase (Geschwind and Rutherford, 1992, Pallister et al., 2008; Rutherford and Devine, 2008), which also requires a relatively high $a\mathrm{TiO_2}$. For these reasons, we choose to use $a\mathrm{TiO_2} = 0.7$. At the temperatures of zircon saturation, MSH dacite magmas would likely be saturated in quartz, so we also assume $a\mathrm{SiO_2}=1$. Figure 11 illustrates that varying $a\mathrm{TiO_2}$ while holding temperature constant results in $a\mathrm{TiO_2}$ would require impossible (>1) $a\mathrm{TiO_2}$ to account for the zircon Ti concentrations. As no rutile has been noted in Mount St.

Helens rocks, this suggests that the Ti variations in zircon cannot be due only to compositional changes, but must also (and primarily) be due to temperature variation. Whether due primarily to temperature, or to a combination of temperature and compositional change, the increase and wider range of Ti in zircon after approximately 100ka suggests input of hot, presumably more mafic magma into the system. This had been recognized in surface products at approximately 20ka, during the Cougar Eruptive Stage (Clynne et al., 2008), but apparently began at depth ~80 kyr prior to that.

Other compositional indicators also reflect this increasing complexity of the magmatic system 60-100ka that can be attributed to injection of mafic magmas. Hf in zircon is an indicator of fractionation (Claiborne et al., 2006), and the lower and wider ranging Hf concentrations in younger zircon, along with higher Ti and HREE (Lu), support this interpretation (Figure 7). Increase in Th/U reflects a distinct decrease in U concentration at approximately 60ka. More varied Eu anomaly, both higher and lower, suggests that the magmas from which the zircon grew had experienced varied degrees of feldspar growth and fractionation, both more and less than in the earlier magmas. This spread may also be indicative of variable oxygen fugacity, like the Ce anomaly. Consistent variation of 3+/P molar above unity indicates that the xenotime substitution is insufficient to account for all trivalent ions in the tetravalent Zr sites.

Lack of correlation between zircon Ce anomaly and time suggests varied oxygen fugacity in the sub-volcanic system throughout its history. However, nearly uniform and very low Ce anomaly in a subset of some zircons ranging in age from ~42 to ~6 ka, from two samples (SHL08-34Z and SHL08-49Z) erupted close together in time (3150 ybp and 2500 ybp) suggest that a pocket of reduced magma crystallized throughout that time and then contributed zircons to both eruptions. The younger of these two samples, SHL08-49Z, is interpreted to be an inclusion of crystal mush from the sub-volcanic system, entrained and erupted during Pine Creek eruptive

stage (~2.5 ka). This suggests that this reduced magma was, in fact, a crystal mush that was sustained above solidus for the ~ 40kyr from the growth of the oldest reduced zircon (~42 ka) through eruption 2.5ka.

The Pine Creek 'mush inclusion' is a particularly interesting sample, as it may give us a glimpse of a stage of magmatic processes (nearer solidification) that is rarely recorded in volcanic rocks and minerals. Zircons from this sample have a more restricted composition than any other sample (including Hf, REE, and Ce anomaly), excluding two zircons that are apparently much older and very different in composition from the rest. Excluding the two older grains, the zircons only range back to ~50 ka, interpreted as a timescale of crystal mush residence in the sub-volcanic system (a minimum in this case, as we cannot predict how long it might have continued if not erupted). This limited composition and more restricted age-range support its provenance as a cognate set of crystals. Interestingly, the mush inclusion zircons have a much higher average Ti concentration and resulting Ti-in-zircon temperature than any other sample. Unfortunately, because this sample is particularly crystal rich, we cannot compare Ti-in-zircon temperatures to zircon saturation temperatures, as the saturation temperature calculation is most accurate for crystal-free or crystal-poor compositions (Harrison and Watson, 1983). However, assuming that this is in fact a crystal mush, possibly growing as one package, we can assume no compositional (or $a\mathrm{TiO_2}$) changes to the melt from mixing (also supported by restricted composition), and therefore that the Ti concentration variations are due entirely to temperature. In the 50 kyr that this package of crystal mush resided in the sub-volcanic system, suggest that these zircons grew over 200°C temperature variation. This might be expected on the margins of a system where hot, young magmas are repeatedly injected, making their way quickly from source to eruption. However, it is not reasonable that zircon would be stable in

one composition across this temperature range, so something else must also contribute to the Ti variation.

4.3. Implications for Zircon as a Record of magmatic Processes

Zircon appears to be a unique record of the intrusive portion of the volcanic system. This could be due to its small size, resulting in different physical behavior than larger, major phase minerals (e.g. behaving as a tracer in melts that are segregating from crystal mushes after rejuvenation). It may also be unique due to low diffusion rates that allow it to remain intact and retain its geochemical signatures through time and through heating events, unlike major phases. There is also the possibility that it is not, in fact, unique, and that other phases may also be stored, recycled, and record these long term events. There are hints from plagioclase disequilibria (Cooper and Donnelly 2008, Cooper and Reid 2003) and plagioclase Ar-Ar dating (Clynne et al., 2008) that there may be an old component included, but when mixed into the abundant young plagioclase, it is difficult to recognize.

While zircon is often used to date older eruptions and to calibrate Ar-Ar eruption ages, the wide ranges of zircon ages found in each sample for this study suggests that this may not be a particularly valid application of zircon ages. However, zircon ages can certainly provide constraints on maximum eruption age, and for the case of Mount St. Helens resulted in identification of inaccurate plagioclase Ar-Ar eruption ages and provided new, more accurate constraints on maximum eruption ages.

4.4. Implications for Mount St. Helens magmatic system

As discussed in the previous chapter and supported by the detailed geochronology and geochemistry herein, zircons indicate the presence of an intrusive complex beneath the volcano,

where magmas are intruded, stored, crystallize and cool, and may then be rejuvenated and mixed into erupting magmas as they traverse this storage zone. These stored magmas may represent the stranded remnants of magma batches that were mostly erupted, magmas intruded into the system during a period of quiescence and relative stability, and/or magmas intruded into the system without the necessary characteristics to drive eruption themselves. The wide ranging ages in most samples (at least 100 kyr, and often more than 200 kyr older than eruption) and sometimes in individual zircon crystals, require storage of the zircons for these extended timescales. The 50 kyr range of ages in the crystal mush inclusion presents the possibility that magmas may be stored for at least this long as a crystal mush, without fully solidifying. This mush was apparently sampled by a large, violent eruption in 3150 ybp that fully disaggregated the mush, leaving only zircons, then again in ~2500 ybp by a smaller, less violent eruption that retained it as a cohesive mush inclusion. Other than this suggestion of a minimum-mush timescale, no direct evidence is available to determine whether the zircons are stored for those 100s of kyr in crystal mush or solid rock.

Without being able to definitively identify the state of the stored magmas, it is prudent to compare this to known systems with similarly long timescales identified in zircons. It is now widely accepted that plutons are often assembled incrementally over long timescales, with melt location and volume varying through time as new magmas are continually injected into various parts of the system, causing local rejuvenation followed by cooling and crystallization (Walker et al., 2007; Miller et al., 2007; Coleman et al., 2004). This scenario is supported by the MSH zircon data, and it seems likely that the zircons are recording the building of a proto-pluton beneath the active volcano, where melt location and volume are transient, and the melt fraction waxes and wanes with rates of injection, eruptive activity, and composition and temperature of injected magmas.

While surface products began to show the influence of mafic magmas approximately 20ka, the zircon data suggest that hot, dry, mafic magmas were intruded into the sub-volcanic system beginning ~60-100 ka, mixing with existing cooler dacites and creating more compositional complexity. Magmas that moved through this zone from ~ 100 to 20 ka on the way to eruption apparently didn't interact with these mafic magmas, but only with the modified dacites, as only the zircons hint at the presence of the mafic magmas until 20 ka when less felsic, hotter, dryer magmas and magmas showing textures and compositions indicative of mixing began to erupt. Interestingly, it does not appear that these mafic magmas directly affected the oxygen fugacity of the system, as the Ce anomaly in the zircons generally does not change systematically with time. One apparent pocket of highly reduced melt does make an appearance at this time, given the restricted and low Ce anomaly in zircons ranging in age from 100ka to present in samples erupted ~3500-2500 ybp. However, this low fO_2 was not as widespread as the other effects of mafic magmas, as there are also abundant high Ce anomalies at this time, recording oxidizing conditions.

5. References

Claiborne, L.L., Miller, C.F., Wooden, J.L., and Mazdab, F.K., 2010, Trace element composition of igneous zircon: Temporal, thermal, and compositional record of magmatic processes in the Spirit Mountain Batholith, Nevada: Contributions to Mineralogy and Petrology, (in press).

Claiborne, L.L., Miller, C.F., Walker, B.A., Wooden, J.L., Mazdab, F.K., and Bea, F., 2006, Tracking magmatic processes through Zr/Hf rations in rocks and Hf and Ti zoning in zircons: an example from the Spirit Mountain batholith, Nevada. Mineralogical Magazine: v. 70, p. 517-543.

Clynne , M.A., Calvert, A.T., Wolfe, E.W., Evarts, R.C., Fleck, R.J. and Lanphere, M.A., 2008, The Pleistocene Eruptive History of Mount St. Helens, Washington, from 300,000 to 12,000 Years Before Present, *in* Sherrod, D.R., Scott, W.E., and Stauffer, P.H., eds., A volcano rekindled: the renewed eruption of Mount St. Helens, 2004-2006: U.S. Geological Survey Professional paper 1750, p. 593-627.

Cooper, K.M. and Donnelly, C.T., 2008, ^{238}U-^{230}Th-^{226}Ra Disequilibria in Dacite and Plagioclase from the 2004–2005 Eruption of Mount St. Helens, *in* Sherrod, D.R., Scott, W.E., and Stauffer, P.H., eds., A volcano rekindled: the renewed eruption of Mount St. Helens, 2004-2006: U.S. Geological Survey Professional paper 1750, p. 827-846.

Cooper, K. M. and Reid, M.R., 2003, Re-examination of crystal ages in recent Mount St. Helens lavas: implications for magma reservoir processes: Earth and Planetary Science Letters, v. 213**,** p. 149-167.

Crandell, D.R., 1987, Deposits of pre-1980 pyroclastic flows and lahars from Mount St. Helens Volcano, Washington: U.S. Geological Survey Professional Paper 1444, 91 p.

Coleman DS, Gray W, Glazner AF (2004) Rethinking the emplacement and evolution of zoned plutons: Geochronologic evidence for incremental assembly of the Tuolumne Intrusive Suite, California. Geol 32:433–436

Ferriss, E.D.A., Essene, E.J. and Becker, U. (2008) Computational study of the effect of pressure on the Ti-in-zircon geothermometer: European Journal of Mineralogy, v. 20, p, 745-755.

Ferry, J.M. and Watson, E.B., 2007, New thermodynamic models and revised calibrations for the Ti-in-zircon and Zr-in-rutile thermometers: Contributions to Mineralogy and Petrology, v. 154, p. 429-437.

Flanagan, D.M., 2009, Zircon from Swift Creek Stage eruptions record the assembly and evolution of an intrusive magmatic complex beneath Mount St. Helens. M.S. Thesis, Vanderbilt University.

Flanagan, D.M., Miller, C.F., Claiborne, L.L., Clynne, M.A., Wooden, J.L., in prep, Zircon from Swift Creek stage eruptions records the assembly and evolution of an intrusive magmatic complex beneath Mount St. Helens, Journal of Volcanology and Geothermal Research.

Gardner, J.E., Rutherford, M., Carey, S., and Sigurdsson, H., 1995, Experimental constraints on pre-eruptive water contents and changing magma storage prior to explosive eruptions of Mount St Helens volcano: Bulletin of Volcanology, v. 57, p. 1–17.

Geschwind, C.H., and Rutherford, M.J., 1992, Cummingtonite and the evolution of the Mount St. Helens (Washington) magma system: An experimental study: geology, v. 20, p. 1011-1014.

Harrison, T.M., and Schmitt, A.K., 2007, High sensitivity mapping of Ti distributions in Hadean zircons: Earth Planet Sci Lett, v. 261(1–2), p. 9–19. doi:10.1016/j.epsl.2007.05.016

Hayden L.A. and Watson E.B., 2007, Rutile saturation in hydrous silicate melts and its bearing on Ti-thermometry of quartz and zircon: Earth and Planetary Science Letters, v. 258, p. 561-568.

Hofmann AE, Valley JW, Watson EB, Cavosie AJ, Eiler JM (2009) Sub-micron scale distributions of trace elements in zircon. Contrib Mineral Petrol. doi:10.1007/s00410-009-0385-6

Lowenstern, J.B., Persing, H.M., Wooden, J.L., Lanphere, M.A., Donnelly-Nolan, J. & Grove, T.L. (2000) U-Th dating of single zircons from young granitoid xenoliths: new tools for understanding volcanic processes: Earth and Planetary Science Letters, v. 183, p. 291-302.

Miller, J.S., Matzel, J.E.P., Miller, C.F., Burgess, S.D., and Miller, R.B., 2007, Zircon growth and recycling during the assembly of large, composite arc plutons: Journal of Volcanology and Geothermal Research, v. 167, p. 282–299, doi: 10.1016/j.jvolgeores.2007.04.019.

Mullineaux, D.R., 1996, Pre-1980 tephra fall deposits erupted from Mount St. Helens, Washington: U.S. Geological Survey Professional Paper 1563, 99 p.

Pallister, J.S., Thornber, C.R., Cashman, K.V., Clynne, M.A., Lowers, H.A., Mandeville, C.W., Brownfield, I.K. and Meeker, G.P. (2008) Petrology of the 2004-2006 Mount St. Helens Lava Dome – Implications for Magmatic Plumbing and Eruption Triggering, chap 30 *of* Sherrod, D.R., Scott, W.E. and Stauffer, P.H., 20 eds., A volcano rekindled: the renewed eruption of Mount St. Helens, 2004-2006: U.S. Geological Survey Professional paper 1750, pp. 647-702.

Rutherford, M.J., and Devine , J.D., 2008, Magmatic conditions and processes in the storage zone of the 2004-2006 Mount St. Helens dacite, chap 31 *of* Sherrod, D.R., Scott, W.E. and Stauffer, P.H., 20 eds., A volcano rekindled: the renewed eruption of Mount St. Helens, 2004-2006: U.S. Geological Survey Professional paper 1750.

Sambridge, M.S., and Compston, W., 1994, Mixture modeling of multi-component data sets with application to ion-probe zircon ages: Earth Planet. Sci. Lett. V. 128, p. 373-390.

Walker, B.A., Miller, C.F., Claiborne, L.L., Wooden, J.L., and Miller, J.S., 2007, Geology and geochronology of the Spirit Mountain batholith, southern Nevada: Implications for timescales and physical processes of batholith construction: Journal of Volcanology and Geothermal Research, v. 167, p. 239–262, doi: 10.1016/j.jvolgeores.2006.12.008.

Watson, E.B., Wark, D.A., Thomas, J.B. (2006) Crystallization thermometers for zircon and rutile: Contrib Mineral Petrol, v. 151, p. 413–433. doi:10.1007/s00410-006-0068-5

Watson, E.B., 1996, Dissolution, growth and survival of zircons during crustal fusion: kinetic principles, geological models, and implications for isotopic inheritance: Special Paper, Geological Society of America, v. 31, p. 43-56.

Watson, E.B. and Harrison, T.M., 1983, Zircon saturation revisited: temperature and composition effects in a variety of crustal magma types: Earth and Planetary Science Letters, v. 64, p. 295-304.

Wilson, C.J.N. and Charlier, B.L.A., 2009, Rapid rates of magma generation at contemporaneous magma systems, Taupo Volcano, New Zealand: Insights from U-Th model-age spectra in zircons. Journal of Petrology, v. 50, p. 875-907.

CHAPTER V

TEACHING RADIOACTIVE DECAY AND RAIOMETRIC DATING: AN ANALOG ACTIVITY BASED ON FLUID DYNAMICS

Abstract

We present a new laboratory activity for teaching radioactive decay using hydrodynamic processes as an analog and an evaluation of its efficacy in the classroom. A fluid flowing from an upper beaker into a lower beaker (shampoo in this case) behaves mathematically identically to radioactive decay, mimicking the exponential decay process, dependent on the amount of fluid in the upper beaker (representing the amount of parent isotopes) and the size of the hole in the beaker (representing the decay constant). Students measure the fluid depth with time for several "runs" with varied conditions, then graph their results, create decay equations, manipulate these equations and use them to "date" another experiment. They then apply their new understanding to make predictions regarding complications involved in the decay process and its use in dating (such as daughter loss). Student quiz performance improved from before to after the activity, indicating improved student learning. Student comments and questions indicated deep understanding and a new curiosity about the process and its application.

1. Introduction

Understanding the process of radioactive decay and its use in radiometric dating is necessary to understanding basic foundations of modern science and is essential knowledge for educated citizenry concerned about current controversies over evolution, the age of the earth and the use of radioactive decay as an energy source. It is, therefore, an important concept for students in secondary through graduate level science courses to fully internalize. However, due

to its very small scale, mathematical treatment, general unfamiliarity, and misconceptions instilled by the media, the topic is fundamentally difficult for students to grasp (Prather, 2005). Commonly, lectures accompanied by demonstrations are employed to teach this topic, using games with dice, cards or poker chips (McGeachy, 1988; Kowalski, 1981; Clinikier, 1980), computer simulations (Jesse, 2003), electrical circuitry (Wunderlich & Peastrel, 1978; Evans, 1974), or melting ice (Wise, 1990) to mimic the process of decay and explain the concept of half-life. While these activities may demonstrate the randomness and/or exponential nature of decay, they do not allow students to engage with the process in order to explore the controlling factors in a way that may instill a deep understanding.

We present here a newly developed hands-on laboratory activity for teaching radioactive decay and radiometric dating, and an evaluation of the activity's effectiveness. In this lesson, hydrodynamic principles and processes serve as an analog for radioactive decay processes. Using analogies in teaching, such as the one employed here, has been shown to be a highly effective teaching strategy (Duit, 1991). The use of analogy makes this lesson particularly effective at instilling an intuitive understanding of this complex, unfamiliar process and its uses by guiding students as they relate radioactive decay to more familiar, intuitive and approachable processes of fluid flow. The fundamentals that are learned can be adapted to appropriately address any level classroom, from elementary through upper level graduate courses. We have found it effective at all levels of university education. n the analogy employed herein, students observe the drainage of fluid from a container with a hole in its base into another container (Figure 1), and they recognize that this process can be described qualitatively and quantitatively in exactly the same way as decay of radioactive parent isotopes and resulting production of daughter isotopes. This allows students to observe, record, and manipulate the process in a way impossible with real radioactive materials. They can see the exponential decrease of flow

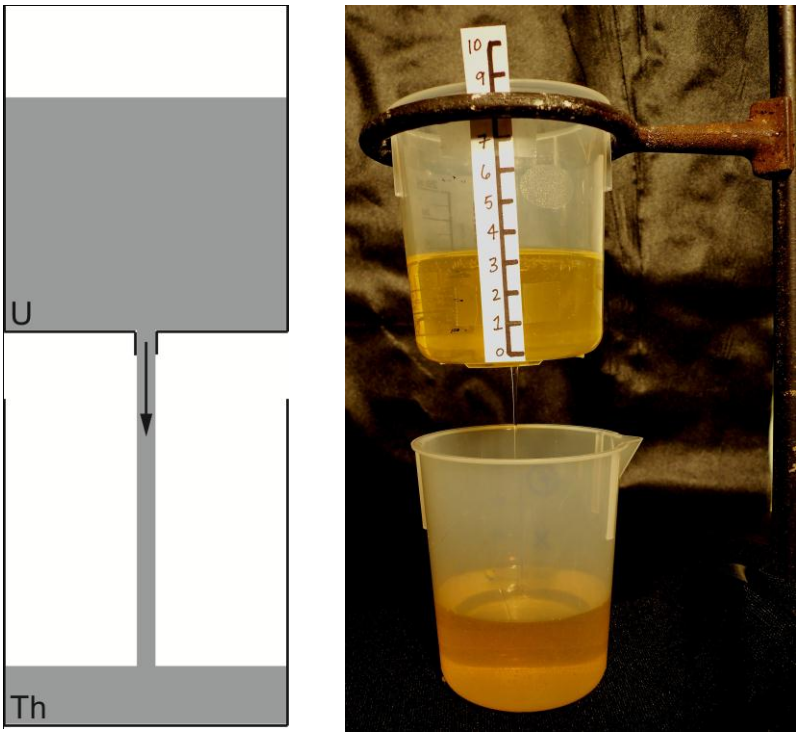

Figure 1: (a) *left* Schematic of buckets representing radioactive decay of the parent uranium (fluid in the upper bucket) to the daughter thorium (fluid in the lower bucket), modified from Bourdon et al., 2003. (b) *right* photo of apparatus set up for radioactive decay lesson.

from the upper beaker to lower with time (Figure 2a), and so clearly envision the exponential decay of radioactive isotopes and the meaning of "half-lives" (Figure 2b). Students closely observe, measure, graph, and think about the behavior of the fluid flow and then define the factors that control the process, extract and manipulate the controlling equations, and make predictions regarding changes to the initial conditions. They are then asked to transfer this conceptual understanding to the process of radioactive decay. This connection to familiar concepts and the ability to measure and manipulate the process promotes a deep understanding of the decay process and its use in geochronology.

2. Theoretical Framework

2.1. Teaching with analogs

New ideas are best constructed by building upon a basis of previously acquired knowledge or by relating the unfamiliar to the familiar (Duit, 1991). This makes analogies particularly useful in teaching, as we use a concrete or familiar "source" concept to essentially serve as a picture or metaphor that explains an abstract or unfamiliar "target" concept (Dupin & Joshua, 1989; Duit, 1991). While the use of analogies in teaching has been shown to enhance student conceptual understanding, some inherent pitfalls must be avoided in order for the exercise to be effective (Harrison & Treagust, 1993). The source concept or analog must be familiar to the student, corresponding attributes between the source concept and target concept must be explored, unshared attributes between the source concept and target concept must be explicitly discussed, and the instructor must ensure that the students see the source concept in the intended manner (Thagard, 1992; Duit, 1991; Orgill & Bodner, 2006).

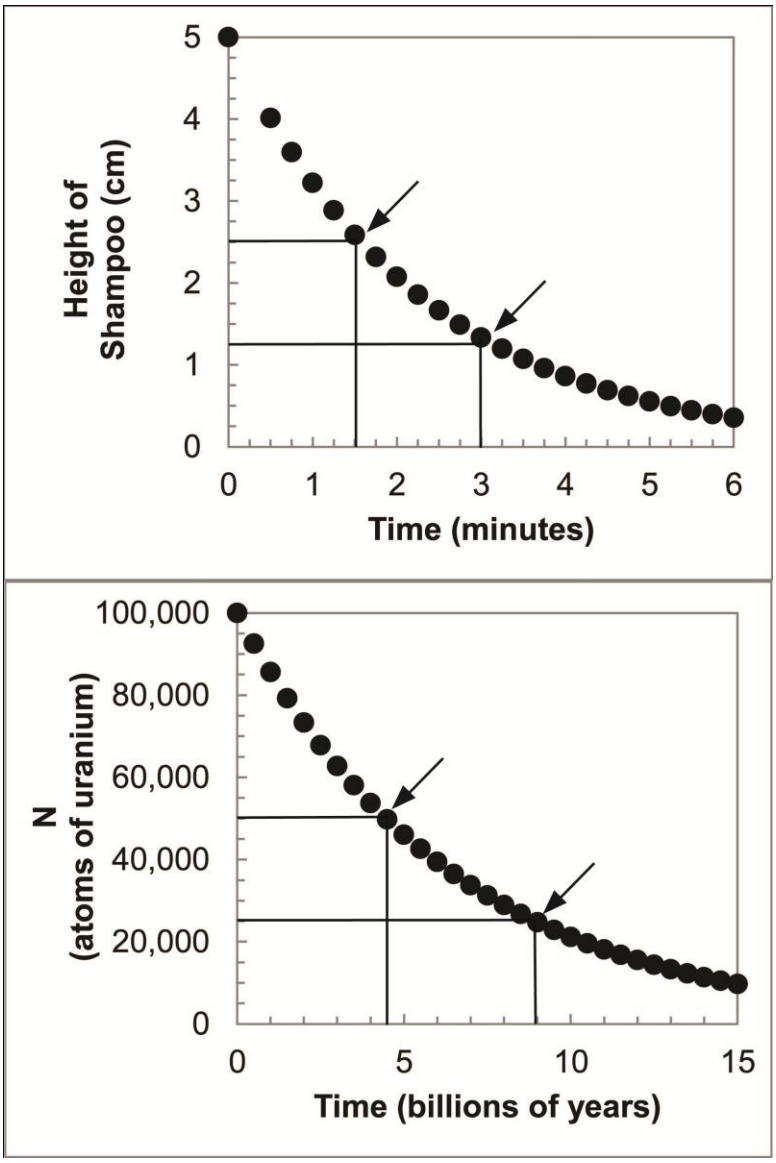

Figure 2: (a) *top* Shampoo depth vs. time, illustrating exponential nature of the fluid flow. The arrows indicate the apparent half-life of the fluid, 1.5 minutes. (b) *bottom* Number of parent atoms (N) vs. time for ^{238}U using a decay constant of $1.55 \times 10^{-10} y^{-1}$ (Faure and Mensing, 2005), illustrating exponential nature of decay. The arrows indicate the half-life of ^{238}U, 4.468 billion years (Faure and Mensing, 2005).

In order to prevent these sorts of problems from rendering analogical lessons ineffective, several researchers have developed explicit guidelines for teaching with analogies. We have based our lesson on two of these sets of guidelines that we believe best fit classroom practices and the practicalities of the analog activity we had in mind. Dupin and Joshua (1989) describe guidelines for a "modeling analogy" which we believe applies to our analog well, as it uses a hands-on physical model to relay the source concept. The modeling analogy should have the following five characteristics (Dupin & Joshua, 1989):

1. It serves as a picture or metaphor to put a new concept in concrete form.
2. It must have a "descriptive function" which helps students to understand the target concept and to recognize that the explanation is plausible.
3. It must be less complex than the target concept.
4. It does not have to constitute a real situation. It can be idealized to encourage thorough experiments so that students think deeply about the target concept.
5. The analogical system must have great structural similarity to the target concept, such that it is adaptable to different teaching situations and depths of understanding.

Glynn (1991) proposed the following Teaching With Analogy (TWA) model that has proven highly effective (Harrison and Treagust, 1993), and on which we based the framework of our lesson:

1. Introduce target concept to be learned
2. Cue the students' memory of the analogous situation
3. Identify the relevant features of the analog
4. Map the similarities between the analog and the target concepts
5. Identify the comparisons for which the analogy breaks down
6. Draw conclusions about the target concepts

2.2. Fundamentals: Radioactive Decay

Radioactive decay occurs when an unstable isotope, known as the 'parent' isotope, emits radiation through loss of an ionizing particle from its nucleus. This transforms the isotope into a new, 'daughter' isotope, often a different element. For example, nuclei of ^{238}U iare unstable and by emitting alpha particles, decay into ^{234}Th (Faure and Mensing, 2005). While the

timing of the loss of a particle from an individual unstable nucleus is random, over long periods of time and with large numbers of nuclei, the rate of decay is measurable and constant, and the decay process can be represented mathematically by the following equation

$$\frac{dN}{dt} = -\lambda N$$

where *N* is the amount of parent isotope, *t* represents time, λ is the decay constant for the given isotopic system. Note that the decay rate of parent to daughter is constant for each isotopic system, and is essentially a proportion per unit time. For example, the rate of decay (decay constant) of ^{238}U is 1.55×10^{-10}/year (Faure and Mensing, 2005). This is an exponential relationship, as shown by Figure 2b and the solution to the above equation:

$$N(t) = N_0 e^{-\lambda t},$$

where N_0 is the initial amount of parent. Because of the timescales involved and this exponential nature of the process, it is useful to consider decay rates in terms of half-life, or the amount of time it takes for half of the parent material to decay (Figure 2b). For example, the half-life of ^{238}U is 4.468 billion years (Faure and Mensing, 2005).

In radiometric dating, we measure the amount of parent and daughter isotope in a material and, since the decay rates of radioactive isotopes are known, we can use the above equation to calculate the time that has passed since the product of decay (daughter) began to accumulate. The incorporation of non-radioactively produced 'daughter' isotopes at the formation of the material can occur in natural systems and necessitates careful corrections to obtain accurate results. The loss of daughter isotopes at some time after the formation of the material can also occur, for example, if the material is heated sufficiently, and can be used to determine dates of thermal events that cause the loss.

2.3. Fundamentals: A Hydrodynamic Analog for Radioactive Decay

The experiment carried out in this lesson allows students to explore a simple, intuitive hydrodynamic principle in order to develop a qualitative and quantitative understanding of radioactive decay. The experimental analog consists of one beaker with a small hole in the base suspended above another beaker (Figure 1). Fluid flow from the upper beaker to the lower beaker is controlled by the size of the hole and the hydrostatic pressure being exerted by the column of fluid above. Rate of flow, and thus change in height of fluid in the upper beaker with time, is directly proportional to both the height of fluid in the beaker at any given time and the area of the hole in the bottom of the beaker. This can be stated as:

$$\frac{dh}{dt} = -\propto h$$

where *h* is the height of fluid in the upper beaker, *t* is time, α is a flow coefficient that includes the density and viscosity of the fluid, the acceleration due to gravity, the cross sectional area of the beaker, and the area of the hole. The value is negative because the height of fluid in the upper beaker is decreasing.

Radioactive decay is analogous to the flow of fluid out of the beaker, because the rate of loss of parent isotope is directly proportional to the amount of parent present (the height of fluid) and the decay constant (the flow coefficient α). The equation for radioactive decay is therefore mathematically identical to the equation for fluid flow shown above:

$$\frac{dN}{dt} = -\lambda N$$

where *N* is the amount of parent isotope, *t* is time, and λ is the decay constant for the specific isotope, and the value is negative because the amount of parent is decreasing. When solved, these two equations remain mathematically identical and illustrate the exponential nature of each:

$$h(t) = h_0 e^{-\propto t} \qquad N(t) = N_0 e^{-\lambda t}$$

where the subscript *0* indicates the initial condition. It is this mathematically identical behavior of the two phenomena that allows us to use fluid flow as an analog for radioactive decay (Figure 2). For example, varying the initial height of fluid in the experiment will cause the system to behave similarly to varying the amount of initial parent material in a radioactively decaying system. Varying the area of the hole or the viscosity of the fluid changes the flow coefficient (α), which is analogous to dealing with different isotopic systems that have different decay constants (λ); a larger hole will result in loss of more fluid in a given time, just as a larger decay constant will result in more decay in a given time. For purposes of the experiment, it is simplest and most intuitive to consider the area of the hole as the determining factor for the "decay constant" of the draining fluid, because it is easy to see and measure the size of the hole and to create holes with different areas. It would be difficult and less intuitive to try to quantify viscosity, and it is simplest to use the same fluid with the same viscosity throughout the experiment.

3. Methods

3.1. Student Population

We implemented this study in Dynamic Earth 111 in the Department of Earth and Environmental Sciences at Vanderbilt University, the lab component of the department's introductory geology course (Dynamic Earth 101). Each lab section has approximately 20 students, and Dynamic Earth 101 is a co-requisite for the lab section. The students range from freshmen to seniors and are dominantly taking the course to fulfill general education requirements for a laboratory science course, although anyone interested in majoring the in

Earth and Environmental Sciences also begins with these two courses, resulting in a wide variety of skill, experience, and interest levels in each lab section.

3.2. Framework for Educational Study

This study was performed during two consecutive semesters, with a similar format, but with slight changes in the activity and the assessment during the second semester intended to improve the learning experience. Materials and data reported herein are from the second iteration of the study. Students first attended a lecture on the topic of radioactive decay and radiometric dating. The next week, they were asked to complete a pretest at the beginning of their laboratory session (the pre/post-test is available in supplemental material). The pretest covered basic concepts, involved some critical thinking, and requested a statement of confidence in the student's understanding of the topic. They then completed the analog activity in groups of 3-5 (see below for full description of the activity; the student handout is available in supplemental material). They discussed the laboratory assignment in their groups, answering some discussion questions related to the activity that range from basic knowledge to higher-order thinking, including evaluation and prediction. They ended the lab session by completing a post-test that was identical to the pretest. The results from these assessments were then evaluated and compared to determine the impact of the activity and to identify remaining points of confusion and misconceptions.

4. LESSON PLAN

The student handout with instructions, material lists, and follow up questions is available in Appendix G.

The analog activity employed 4 beakers of the same size (we used 250mL), two of these beakers should have a hole in the base and vertical depth scales on the side (centimeters). We used plastic beakers and a drill to form the holes; the exact size of the holes does not matter as long as one is larger than the other. Each group will also need play-doh to make a stopper for the holes, baby shampoo (fill one beaker), stopwatches, a spatula and access to Microsoft Excel. Baby shampoo was chosen as our fluid due to its appropriate viscosity and ease in cleanup.

The activity takes approximately an hour and a half. Students selected the beaker with the smaller hole and positioned it above the hole-less beaker using the beaker stand (Figure 1). Students plugged the hole and poured a pre-determined amount of shampoo into the upper beaker. They were told that for the experiment, the shampoo in the upper beaker represents the parent isotope, and the flow represents the decay of the parent to produce the daughter isotope (shampoo in the lower beaker). When they were ready to begin the experiment, they unplugged the hole and allowed the shampoo to flow into a lower beaker (Figure 1) for a pre-determined amount of time (at least six minutes, depending on the viscosity of the shampoo), measuring and recording the liquid depth every thirty seconds. After they recorded the changes in liquid depth, questions on the lab handout guided the students to relate this process to the amount of decay and its dependence on the amount of parent available (depth of liquid) and the decay constant (size of the hole in the beaker). Students performed several runs of the experiment with different initial amounts of shampoo (5 cm and 10 cm) and upper beakers with different sized holes. Before each run, students cleaned out the beakers using the spatula, emptying all the shampoo back into its main container before starting a new run. Variation in the initial amount of shampoo mimicked variation in initial amounts of parent material that result in different amounts of decay, although the proportion of material decayed in a given time remained uniform. For example, students could identify the half-life (the length of time

until half of the liquid had been lost from the upper beaker) and see that it was the same regardless of how much shampoo there was to begin with. The effect of variation in the area of the hole illustrated how variations in decay constant specific to different parent isotopes yield different rates of destruction of parent and production of daughter. The instructor asked students throughout the experiment what observations they were making regarding the process, and discussed what they were seeing and how it related to real radioactive decay, particularly to the concept of half-life.

It is important for the instructor to clarify points of the experiment that are not identical to the target concept. In the case of the shampoo, it is not possible to measure the amount of "daughter" product accurately for comparison with amount of parent because as the shampoo flows into the lower beaker it increases in volume due to the incorporation of bubbles. It is also important to make sure that the students understand that decay doesn't "slow down" like the fluid velocity. Rather, the decay rate is a constant proportion, but as there is less material to decay, the amount of decay decreases. We covered this material in conversations with individual groups as they completed the activity. It is also important to test the viscosity of the fluid chosen before each use, as the properties (primarily the viscosity) may change from semester to semester and therefore may affect the results of the experiment. Viscosity tends to increase as shampoo dehydrates over time; if so, the experiment still works fine, but the fluid will flow more slowly and take longer to complete.

Following the completion of the experiments, the students were asked to name the three things that controlled the amount of 'decay' that had occurred – the amount of shampoo in the upper beaker (parent), the size of the hole (decay constant), and the time. From their recorded data, they created and explored depth vs. time graphical representations in Excel (Figure 2a), extracting the general equation for radioactive decay from their own data (using

Excel and the exponential equation display). They dissected these equations, defining what each number represented, concluding that the numbers in the equation that described their data represented the three things that they had identified as controlling 'parent' loss and 'daughter' gain – the amount of initial parent, the decay constant, and the time – thus describing the decay process. They were asked to rearrange the equation to solve for time, so that it could be used in finding the age of something. As this mathematical manipulation proved to be frustrating to many students, the instructor provided guidance with the math according to the students' individual needs.

For the final step of the activity, each group began a run of the experiment with the same initial depth and same size hole as the first run of the experiment. However, rather than letting it run to completion as before, they plugged the hole at some time of their choosing. They wrote the time on a card and placed it face down beside their experiment. Each group then switched tables and used the decay equation they had created from their first run to 'date' the other group's experiment.

Following the completion of the activity, the groups were asked discussion questions designed to address their comprehension, including predicting the behavior of the system in various scenarios that were more complex than their experiments (such as the presence of initial parent or the loss of daughter product). They were asked to provide suggestions for how to deal with these issues when trying to use radioactive isotopes for dating.

5. EVIDENCE OF STUDENT LEARNING

The first test of student success was the formative assessment involving students 'dating' one another's experiments using the equations they had created from their own experiments. This was largely successful, and gave students a meaningful understanding of how

radiometric dating works along with confidence in their understanding. In the cases where the students were not at first successful with their calculations, it provided an opportunity for them to review their work and their understanding, find mistakes or misconceptions and correct those errors themselves before trying again and finding success.

Comparing the results of students' pre and post-tests indicates improvement in their understanding (Figure 3a) and confidence (Figure 3b) in their grasp of the concepts following this activity. Interestingly, on an individual basis, high confidence levels did not always correlate with high levels of understanding; Students' confidence in their understanding of the concepts increased even more significantly than their performance. The lower number questions on the quiz covered more basic concepts and the higher number questions involved higher level, critical thinking (see Appendix G). Question number 5 specifically required them to take their understanding of the decay process and think critically to determine possible sources of error or inconsistencies. For this question, most of the students tended to reproduce statements that were the conclusion of their experiment, rather than think about the problem with which they were presented. We expected the correct answers for this question to improve significantly from pre to post test, but they did not. Adding some variations to the experiment that deal with inconsistencies and wording the question more carefully may lead to better student success with these specific ideas.

In addition to the assessment results that indicate improvement in understanding, the students' comments and questions during the lab indicated they were thinking deeply about the process involved and were making new connections between the process itself and its products (Table 1). They were clearly able to transfer the concepts illustrated by the analog fluid experiment to the process of radioactive decay and dating, and they seemed to enjoy teasing out the details that were either the same or different in the analog experiment and the original

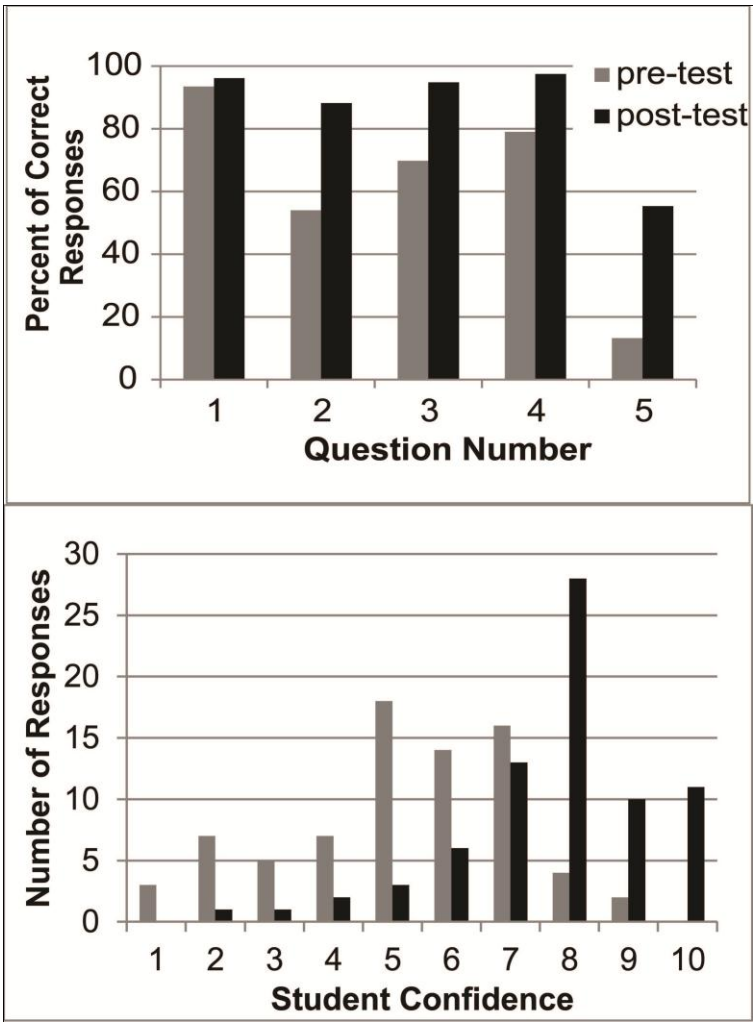

Figure 3: (a) Student performance on the pretest vs. post-test reported as number of correct responses. (b) Self-reported student confidence on the pretest vs. post-test.

concept. These comments and questions demonstrated the learning that was occurring; for example, student comment #5 in Table 1 showed that the student understood the process of decay well enough to work out on his own how one could use radioactive isotopes to determine the age of a natural material where you didn't know the amount of initial parent. These student comments and questions also created opportunities for teaching the higher order concepts and the more complex details of the process and its uses to students who had become genuinely curious. For example, comment #7 allowed us to discuss uncertainty and error and what a meaningful result of an experiment can look like, which was an unexpected teaching moment.

TABLE 1: Student comments and questions and aspect of target concept addressed.

Student Comment/Question	Aspect of Target Concept Addressed
(1) "It slows down as it goes, so as there is less parent material, there is less decay, right?"	Exponential nature of decay
(2) "So, is the decay constant like a proportion of the amount of parent that's there?"	Decay constant, half-life, exponential nature of decay
(3) "If the decay constant depends on what the parent material is, does that mean different parent materials decay at different rates, like different kinds of liquids would go through at different speeds?"	Controls on the rate of decay of a given material
(4) "When it's running out of shampoo, it drips kind of sporadically. Would radioactive decay do the same thing?"	The random nature of decay that is invisible until the very end of the decay process
(5) "If we didn't know the amount of parent we'd started with, could we just measure the amount of parent and the amount of daughter and figure out how long it had been going?"	Radiometric dating in natural materials
(6) "Will it make a difference if there's still some shampoo in the lower beaker when we start?"	Radiometric dating – corrections for presence of initial daughter
(7) "We calculated 2 minutes 17 seconds, and they had recorded 2 minutes 39 seconds! It didn't work!"	Uncertainty and error and what meaningful results can look like

The gains in student understanding could come from simple reinforcement of the concept, learning about radioactive decay again and in a different way, rather than being specifically related to the nature of the analog activity. However, the student comments do show a deeper understanding of the process and its uses than the instructors had previously been able to instill in students and suggest that the exercise was largely successful and particularly effective.

6. Lesson Plan Variations for Advanced Students (U-Series Disequilibria)

The activity described in this paper was inspired by attempts to explain uranium-series disequilibria dating to advanced students (and more senior geoscientists). Uranium-series disequilibria dating is founded on the fact that uranium decays to form a series of radioactive daughter products that eventually decay to produce lead, the stable daughter product (Figure 4a,b). When decay of uranium begins in a natural substance and there are none of these intermediate products in the material, or they are present in the 'wrong' proportions, the system is in 'disequilibrium' (Figure 4a). As decay progresses and the amount of each intermediate radioactive isotope builds up, the system eventually reaches 'secular equilibrium,' where the amount of decay of the parent (known as the 'activity') and production of the daughter matches the amount of decay of the daughter (its activity), and the amount of each intermediate isotope no longer changes with time (Figure 4b). This equilibrium state is reached when:

$$\lambda_P N_P = \lambda_{ID} N_{ID}$$

Where λ is the decay constant, *N* is the number of atoms, and the *P* and *ID* indicate Parent and Intermediate Daughter, respectively. By measuring the degree of disequilibrium, we can determine the amount of time that has passed since the material was formed and decay began:

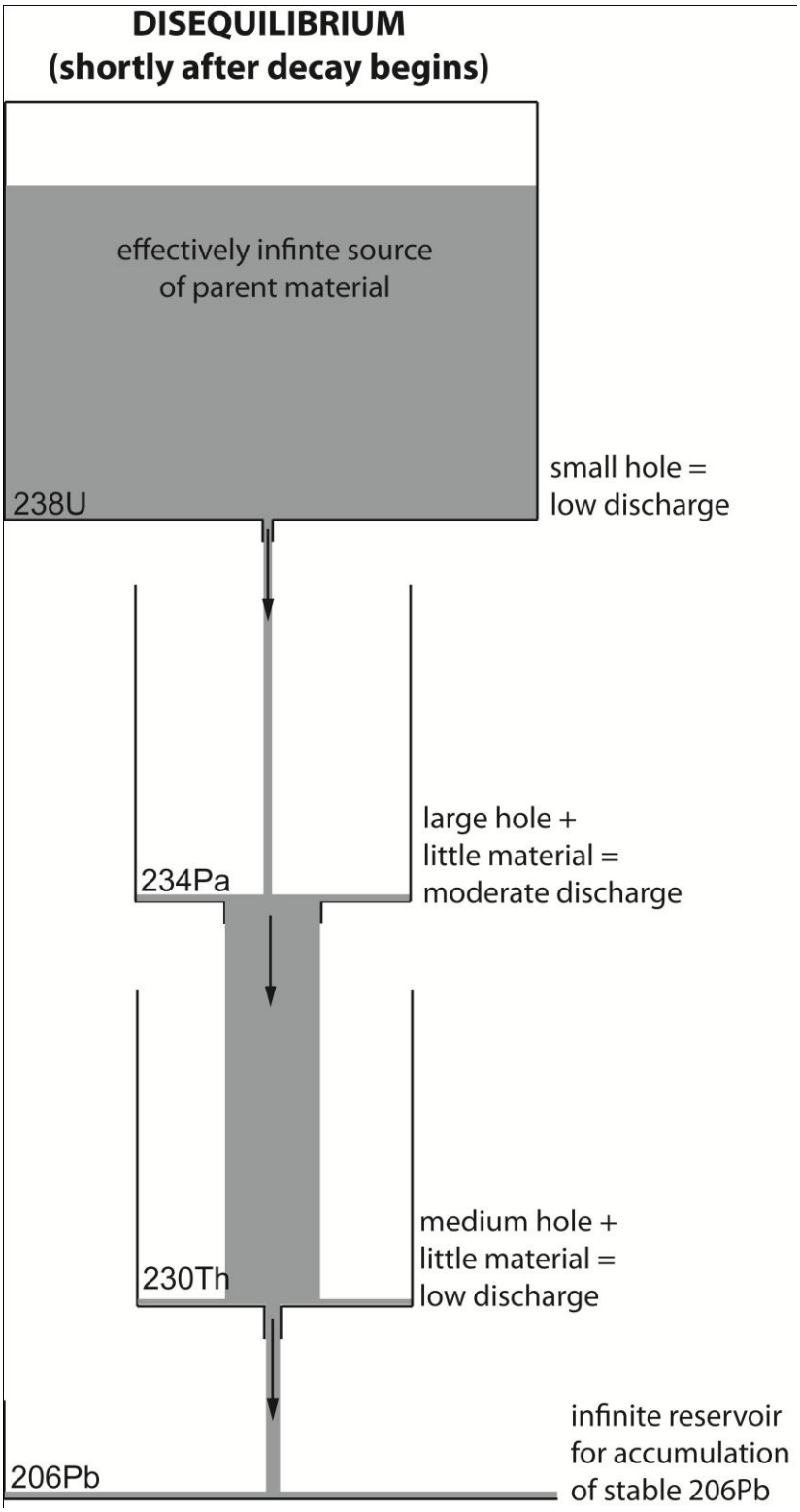

Figure 4: (a) Schematic illustrating U-series decay as a set of buckets, with the system out of secular equilibrium, modified from Bourdon et al., 2003.

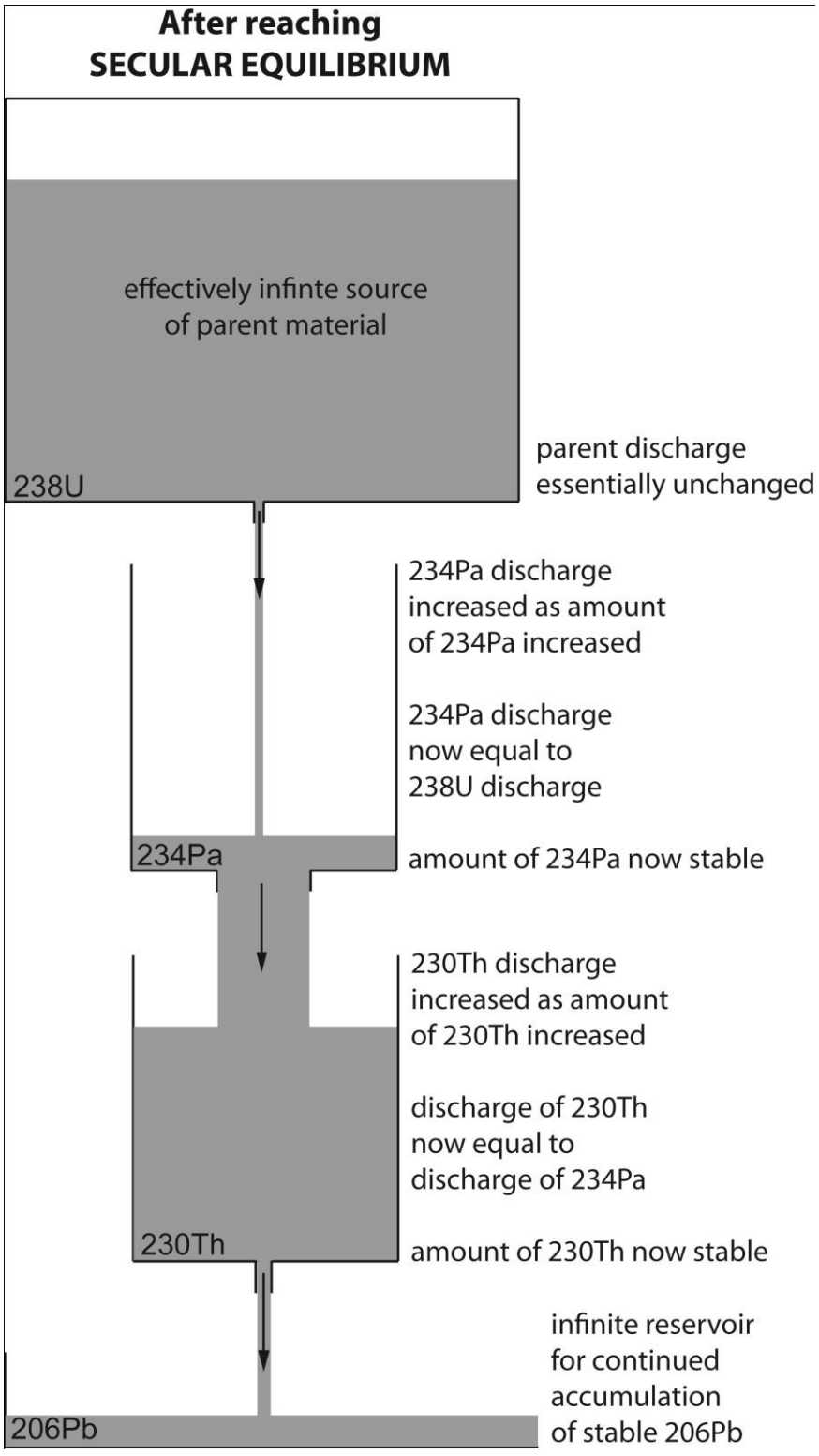

Figure 4 (cont'd): (b) Schematic illustrating U-series decay as a set of buckets, with the system in secular equilibrium, modified from Bourdon et al., 2003.

Figure 4 (cont'd): (c) Photo of apparatus set up for U-Series decay lesson.

the farther from equilibrium, the younger; the closer to equilibrium, the older. Once the system effectively reaches secular equilibrium (ratios of isotopes are within analytical uncertainty of matching the equation above), the relative amounts of each isotope are constant, it is impossible to determine the amount of time that has passed and the intermediate U-series isotopes are no longer useful in dating.

To teach the U-series decay process and disequilibria dating, we use a similar apparatus and the same principles, but with multiple beakers with various sized holes suspended in a column (Figure 4c). The top beaker represents the initial parent and should contain a sufficiently large amount of fluid that the flow does not slow down significantly during the experiment. The bottom beaker represents the final, stable daughter product, with beakers in between representing the intermediate, unstable parent/daughter products in the decay process. The flow of shampoo from any given upper beaker to lower beaker behaves identically to the previously described experiment, controlled by the size of the hole and the pressure exerted by the column of fluid. In this case, however, the experimenter can initiate the experiment in 'disequilibrium' ('wrong' levels of shampoo) and observe it as it approaches equilibrium. After some time passes, if the mass of shampoo in the uppermost beaker ('U') is large enough that the level doesn't change much during the experiment, the entire system reaches equilibrium, where the amount being added from above to each 'intermediate' beaker in the series is identical to the amount being lost out its base. Thus, the heights of fluid in the intermediate beakers stabilize at a level that is inversely proportional to the area of the hole in its base (its 'decay constant'), mimicking the U-series system reaching secular equilibrium.

7. Conclusions

Teaching using analogs can enhance understanding of difficult, non-intuitive, unfamiliar concepts by relating them to more intuitive, familiar concepts, if the analog is sufficiently similar to the target concept. Rate of loss of a fluid from a beaker by flow from a hole in its base (a process that is familiar to students) is mathematically identical to the process by which radioactive isotopes decay. The lab activity described herein allows students to take advantage of the structural similarities of these two processes by studying and manipulating familiar and easily visualized hydrodynamic principles and processes and relating them to the less accessible principles and processes of radioactive decay. This activity instills in students a much deeper, more intuitive understanding of the concepts involved in radioactive decay and radiometric dating than lectures and demonstrations can achieve, resulting in their ability to make predictions regarding complications to the process and to apply this understanding to radiometric dating activities. The results of this study illustrate the effectiveness of this analog activity as a powerful teaching tool for an important, but very difficult and often misunderstood concept integral to many basic sciences. Along with improved conceptual understanding, the activity provides observational and mathematical empowerment to students, with the potential to carry over into other challenges and enhance their confidence and success across disciplines and outside of academia.

8. Acknowledgements

This activity was designed and tested during a Teaching as Research project funded by the National Science Foundation-sponsored Center for the Integration of Teaching and Learning and guided by Derek Bruff at the Vanderbilt University Center for Teaching. Thanks to the other Vanderbilt Teaching as Research Fellows for guidance and support during this project and to the teaching assistants and students in Dynamic Earth 111 who participated so enthusiastically in

the study. Thanks to David Furbish, Vanderbilt University earth fluid physicist, who detailed the mathematical similarity of the fluid flow and radioactive decay for us. Research funded by National Science Foundation grant EAR0635922 inspired this work and supported the authors while it was undertaken.

9. References

Bourdon, B., Turner, S., Henderson, G.M., and Lundstrom, C.C., 2003, Introduction to U-Series geochemistry. *In* Bourdon, B., Henderson., G.M., Lundstrom, C.C., and Turner, S.P. (Eds.), Reviews in Mineralogy and Geochemistry, v. 52: Uranium-Series geochemistry: Washington DC, The Mineralogical Society, p. 1-21.

Clinikier, L.M., 1980, Teaching principles of radioactive dating and population growth without calculus: American Journal of Physics, v. 48, p. 211-213.

Duit, R., 1991, On the role of analogies and metaphors in learning science: Science Education, v. 75(6), p. 649-672.

Dupin, J.J. and Joshua, S., 1989, Analogies and "modeling analogies" in teaching: some examples in basic electricity: Science Education, v. 73(2), p. 207-224.

Evans, G.R., 1974, Radioactive decay chains – an electronic analogue: Physics Education, v. 9, p. 487-489.

Faure, G. and Mensing, T.M., 2005, Isotopes: Principles and Applications, 3rd edition: New Jersey, John Wiley & Sons, 897 p.

Glynn, S.M. *(*1991*).* Explaining science concepts: A teaching-with-analogies model*. In* Glynn, S., Yeany, R., andBritton, B. (Eds.), The psychology of learning science: New Jersey, Erlbaum, p. 219-240.

Harrison, A.G. and Treagust, D.F., 1993, Teaching with analogies: a case study in grade-10 optics: Journal of Research in Science Teaching, v. 30(10), p. 1291-1307.

Jesse, K.E., 2003, Computer simulation of radioactive decay: The Physics Teacher, v. 41, p. 542-543.

Kowalski, L., 1981, Simulating radioactive decay with dice: The physics teacher, v. 19, p. 113.

McGeachy, F., 1988, Radioactive decay – an analog: The Physics Teacher, v. 26, p. 28-29.

Orgill, M.K. and Bodnar, G.M., 2006, An Analysis of the effectiveness of analogy used in college-level biochemistry textbooks: Journal of Research in Science Teaching, v. 43, p. 1040-1060.

Prather, E., 2005, Students' beliefs about the role of atoms in radioactive decay and half-life: Journal of Geoscience Education, v. 53, p. 345-354.

Thagard, P., 1992, Analogy, explanation, and education: Journal of Research in Science Teaching, v. 29, p. 537-544.

Wise, D.U., 1990, Using melting ice to teach radiometric dating: Journal of Geological Education, v. 38, p. 38-40.

Wunderlich, F.J. and Peastrel, M., 1978, Electronic analog of radioactive decay: American Journal of Physics, v. 46, p. 189-190.

CHAPTER VI

CONCLUSIONS

Combined in situ zircon geochronology and geochemistry can provide an unprecedented record of the magmatic processes and timescales involved in transport, storage, interaction and eruption of silicic magmas in the upper crust. While this tool is effective and informative for both plutonic and volcanic magmatic systems of all ages, it is particularly useful for evaluating timescales of these processes for young volcanic systems, where U-Th disequilibria dating with its high resolution can be applied. In the case of volcanic systems, zircon records a different part of the magmatic history than the major phases, essentially providing information on the extended sub-volcanic, intrusive zones of these systems where magmas stall, cool and crystallize, rather than the days to thousands of years prior to eruption in melt-rich magmas that are recorded in most volcanic minerals. Therefore, to elucidate the comprehensive magmatic system of any volcano, it is necessary to evaluate the record from major phases and zircons.

The zircon record at Mount St. Helens has revealed the previously hidden intrusive portion of the magmatic system. Mount St. Helens is underlain by a proto-pluton: an actively forming incrementally assembled intrusion with melt volume and location that changes in time, where magmas are stored for as much as hundreds of thousands of years. Young, hot magmas moving through rapidly on their way to eruption interact with materials in this intrusive zone, rejuvenating and recycling them, and erupting often within 100 years of these events. While no

definitive evidence has been found to determine how those materials are stored (rock or melt-bearing crystal mush), the zircon data suggest that crystal mushes may reside in the system for at least 50 thousand years. Major changes in the input into the magmatic system may happen tens of thousands of years before they are manifest in the surface products. Since this model of incremental assembly is similar to what is suggested for many plutonic bodies, it may be that modest-sized arc volcanoes are often underlain by these intrusive zones, and they eventually become small to medium-sized plutons.

APPENDIX A

TRACE ELEMENT COMPOSITION OF ZIRCON FROM SPIRIT MOUNTAIN

Appendix A: Trace element composition from SHRIMP-RG analyses, calculated T_{TiZ}, and descriptions of zoning visible in CL images for zircons from the Spirit Mountain batholith. Data are grouped by grain, listed from core (top) to rim (bottom). All concentrations are listed as parts per million. Italicized data are suspect due to high P, relative Ca and/or Fe that may be indicative of inclusions. Ages of spots reflect SHRIMP-RG U-Pb geochronology (Walker et al. 2007). Zr/Hf calculated using an approximate reasonable concentration for Zr of 477600 ppm. T_{TiZ} was calculated using the equation of Ferry and Watson (2007) and a_{TiO2}=0.7 and a_{SiO2}=1.0. Rel. Ca and Fe represent calculated values relative to the standard. Pr was calculated, not measured, using a log-linear projection from the measured Sm and Nd values for each analysis.

Analyzed spot	Spot Description	Age (Ma±2σ)	Hf	U	Th	Th/U	Zr/Hf	Ti	T_{TiZ}	Y	Sc	P	Rel. Ca	Rel. Fe
BC101-1LGC		16.8±0.7	9149	103	253	2.5	48.1	11.8	797	2460	23.0	424	1.44	0.94
BC101-1E2			10381	117	154	1.3	42.4	7.7	755	788	17.4	224	1.73	1.09
BC101-1LGI			10128	108	144	1.3	43.4	8.1	759	898	18.6	263	1.59	0.79
BC101-1.5			11054	241	322	1.3	39.8	6.1	732	1261	24.2	267	0.98	0.75
BC101-1.6R		14.8±0.6	7789	30	64	2.1	56.5	20.8	859	916	45.1	342	0.73	0.46
BC101-1E			*11032*	*436*	*341*	*0.8*	*39.9*	*143.7*	*1139*	*1176*	*64.3*	*257*	*18.38*	*25.37*
BC101-2.2C			6696	70	214	3.1	65.7	17.8	842	2375	53.1	335	1.31	0.84
BC101-2.3I			7443	54	113	2.1	59.1	13.2	809	594	21.0	211	1.20	0.83
BC101-2.4I		16.5±0.3	10878	177	222	1.3	40.4	5.8	728	875	22.1	201	1.93	1.01
BC101-2.5T2			9512	116	183	1.6	46.2	9.1	771	1161	28.3	301	3.46	0.81
BC101-2.1T			10178	112	150	1.3	43.2	10.6	786	859	23.2	243	1.35	1.15
BC101-3.4C	*med-dark unzoned core*	*16.7±0.4*	*7836*	*49*	*125*	*2.5*	*56.1*	*12.8*	*806*	*1157*	*36.9*	*216*	*2.49*	*1.13*
BC101-3.2I		*16.3±0.3*	*10472*	*419*	*964*	*2.3*	*42.0*	*6.5*	*739*	*1373*	*24.8*	*263*	*1.50*	*0.91*
BC101-3.5T2	*med-dark zoned tip*		*10828*	*326*	*509*	*1.6*	*40.6*	*6.3*	*735*	*1057*	*34.6*	*210*	*2.87*	*1.95*
BC101-3.3R	*med dark o-zoned rim*		*11101*	*226*	*299*	*1.3*	*39.6*	*5.2*	*719*	*690*	*43.4*	*777*	*365.61*	*0.06*
BC101-3.1T			*10545*	*241*	*402*	*1.7*	*41.7*	*5.8*	*728*	*664*	*41.4*	*159*	*14.80*	*1.45*
BC101-4.3C	very dark, euh zoned core	16.8±0.3	11800	887	1580	1.8	37.3	4.5	706	1485	48.9	223	1.63	1.13
BC101-4.2I	fairly bright int, euh zoned		9912	105	137	1.3	44.4	8.0	758	880	20.6	248	1.15	0.72
BC101-4.1R	med-dark o-zoned rim	15.7±0.4	10489	234	336	1.4	41.9	6.4	737	1203	30.5	217	1.75	1.27
BC101-5.1I	medium zoned interior		11120	95	140	1.5	39.5	8.5	765	801	20.2	218	0.67	0.49
BC101-5.2R	medium-bright zoned rim	15.1±0.5	8805	70	156	2.2	49.9	15.3	825	861	32.9	329	1.37	1.19
BC101-6.1I	bright, unzoned interior		7562	61	195	3.2	58.1	20.4	857	1693	42.2	260	1.42	0.92
BC101-7.1I	med, weakly zoned interior		9442	84	160	1.9	46.6	7.7	755	1396	23.0	263	1.19	1.16
BC101-7.2R	dark inner rim	16.1±0.2	13544	1096	1719	1.6	32.5	5.0	714	1667	49.6	244	1.81	2.00
BC101-8.2I	fairly dark o-zoned interior	17.1±0.4	9107	125	198	1.6	48.3	7.7	754	962	20.9	280	2.43	0.95
BC101-8.1R	med-dark o-zoned rim	16.4±0.5	9658	111	164	1.5	45.5	8.8	767	1003	19.4	284	2.70	0.96

BC101-9.4C	gray unzoned core		9406	86	151	1.7	46.7	7.7	754	1068	21.7	212	1.51	0.73
BC101-9.3I	med dark unzoned interior		9315	104	182	1.8	47.2	9.4	775	1031	19.5	158	2.13	0.89
BC101-9.2IR	dark inner rim		9738	528	895	1.7	45.2	8.6	766	2638	82.0	395	1.13	0.67
BC101-9.1R	bright outer rim		11784	165	186	1.1	37.3	7.3	750	587	29.7	189	1.52	2.31
BC101-10.2C	gray, ozoned core		7704	260	839	3.2	57.1	11.8	797	2479	73.2	624	1.20	1.44
BC101-10.3I	dark euh o-zoned interior		12465	1048	1688	1.6	35.3	6.4	737	2119	51.4	288	1.13	1.25
BC101-10.1R	gray o-zoned rim		10746	232	348	1.5	40.9	5.9	731	987	25.3	191	1.24	0.99
BC101-11.2I	dark zoned interior/core		10207	160	234	1.5	43.1	7.8	756	1307	23.1	313	1.23	0.69
BC101-11.1R	very light interior rim		8584	36	85	2.4	51.2	22.2	867	779	35.6	307	1.37	0.95
BC101-11.3R	dark zoned outer rim		9613	119	151	1.3	45.7	11.1	791	1012	29.8	291	1.08	0.82
BC101-12.3C	*small, light unzoned core*		*11169*	*103*	*143*	*1.4*	*39.4*	*22.5*	*868*	*844*	*20.8*	*265*	*2.44*	*51.21*
BC101-12.4C	same spot as 12.3C		11303	100	135	1.4	38.9	8.2	761	1115	27.6	320	0.50	1.39
BC101-12.2I	medium dark o-zoned int		10584	444	670	1.5	41.5	8.4	764	1774	32.1	406	3.98	3.03
BC101-12.1T	med-dark o-zoned tip		9959	281	483	1.7	44.1	6.8	743	1086	48.4	256	2.42	1.45
BC101-13.1C	light unzoned center		9697	145	322	2.2	45.3	7.2	749	1952	22.0	244	2.88	1.11
BC101-13.2IR	*med-dark o-zoned inner rim*	*16.3±0.4*	*11128*	*273*	*396*	*1.4*	*39.5*	*6.3*	*736*	*1312*	*24.7*	*276*	*5.02*	*1.29*
BC101-13.3R	*light o-zoned outer rim*		*9387*	*104*	*162*	*1.6*	*46.8*	*10.4*	*784*	*1044*	*38.9*	*315*	*8.44*	*1.10*
BC101-14.1C	med-light unzoned resorbed core		7534	72	227	3.1	58.4	20.7	859	1973	63.0	312	2.24	1.36
BC101-14.3I	light unzoned interior		9952	132	258	2.0	41.7	6.6	740	1868	33.6	359	1.77	0.96
BC101-14.2IR	dark OZ inner rim		10550	287	363	1.3	44.2	11.2	792	1176	32.9	294	2.11	1.70
BC101-14.4IR	med-dark OZ IR	16.5±0.3	10015	186	236	1.3	43.9	6.7	742	1058	18.0	287	1.97	1.30
BC101-14.5R	light OZ euhedral outer rim		8830	90	150	1.7	49.8	11.9	798	900	26.0	277	1.70	0.91

Analyzed spot	Spot Description	Age (Ma±2σ)	La	Ce	Pr	Nd	Sm	Eu	Gd	Tb	Ho	Dy	Er	Tm	Yb	Lu
BC101-1LGC		16.8±0.7	0.0062	72.8	0.13	1.99	8.69	1.12	73.2	25.73	108.5	278.1	443	87.6	643	114.3
BC101-1E2			0.0021	44.6	0.05	0.28	1.49	0.36	14.2	5.67	31.7	70.5	149	34.9	291	56.6
BC101-1LGI			0.0016	46.3	0.06	0.31	1.52	0.37	15.6	6.09	32.5	74.2	154	36.0	293	56.8
BC101-1.5			0.0024	61.2	0.09	0.38	1.92	0.37	19.5	8.01	46.9	104.6	236	56.3	471	90.5
BC101-1.6R		14.8±0.6	0.0046	36.8	0.06	0.74	2.63	0.54	22.9	8.31	36.7	90.4	162	37.1	288	56.2
BC101-1E			*4.4196*	*72.9*	*0.63*	*2.14*	*2.18*	*0.45*	*17.3*	*7.30*	*42.5*	*92.3*	*185*	*47.5*	*380*	*87.1*
BC101-2.2C			0.0470	105.2	0.33	5.18	14.75	4.49	93.2	29.37	103.9	288.4	421	85.8	660	122.9
BC101-2.3I			0.0042	47.3	0.06	0.42	1.55	0.49	13.1	4.63	23.8	53.5	109	25.6	221	45.5
BC101-2.4I		16.5±0.3	0.0140	44.0	0.04	0.18	1.00	0.19	11.1	4.81	31.6	68.3	160	40.1	346	70.6
BC101-2.5T2			0.0555	65.3	0.07	0.65	2.58	0.59	22.6	9.42	44.7	107.3	205	45.5	351	66.0
BC101-2.1T			0.0045	45.0	0.06	0.36	1.65	0.37	16.0	6.63	32.9	76.2	154	35.3	290	55.3
BC101-3.4C	*med-dark unzoned core*	*16.7±0.4*	*0.0072*	*43.7*	*0.13*	*1.20*	*4.38*	*1.34*	*36.3*	*11.70*	*48.0*	*123.3*	*207*	*43.6*	*355*	*68.2*
BC101-3.2I		*16.3±0.3*	*0.0025*	*75.8*	*0.06*	*0.37*	*1.94*	*0.35*	*20.1*	*8.93*	*52.5*	*110.4*	*257*	*60.0*	*507*	*97.7*
BC101-3.5T2	*med-dark zoned tip*		*0.1109*	*59.3*	*0.08*	*0.30*	*1.25*	*0.32*	*13.1*	*5.49*	*35.7*	*73.5*	*189*	*48.4*	*450*	*92.5*
BC101-3.3R	*med dark o-zoned rim*		*6.3224*	*70.6*	*1.21*	*4.88*	*2.69*	*0.39*	*11.4*	*3.61*	*23.0*	*47.8*	*127*	*33.7*	*324*	*75.7*
BC101-3.1T			*0.0082*	*45.8*	*0.05*	*0.25*	*0.90*	*0.22*	*9.6*	*4.22*	*22.8*	*49.7*	*121*	*31.8*	*305*	*68.6*
BC101-4.3C	very dark, euh zoned core	16.8±0.3	0.0016	90.0	0.06	0.33	1.20	0.19	13.4	6.18	47.0	85.1	269	71.3	687	143.9
BC101-4.2I	fairly bright int, euh zoned		0.0023	47.8	0.07	0.41	1.88	0.42	16.5	6.93	36.5	82.7	166	38.7	297	55.2
BC101-4.1R	med-dark o-zoned rim	15.7±0.4	0.0027	62.4	0.06	0.40	1.74	0.40	17.8	7.59	44.1	98.1	220	52.2	446	86.1
BC101-5.1I	medium zoned interior		0.0094	48.8	0.06	0.44	1.75	0.41	16.8	6.95	33.4	78.6	156	33.7	272	51.5
BC101-5.2R	medium-bright zoned rim	15.1±0.5	0.0034	55.5	0.07	0.61	2.22	0.55	21.6	8.24	36.9	90.5	168	37.4	300	53.4
BC101-6.1I	bright, unzoned interior		0.0305	59.1	0.26	3.59	9.15	2.81	63.6	21.08	76.8	204.9	321	65.0	497	94.1
BC101-7.1I	med, weakly zoned interior		0.0032	52.6	0.06	0.74	3.60	0.81	32.6	12.65	59.5	145.8	263	57.5	446	82.3
BC101-7.2R	dark inner rim	16.1±0.2	0.0043	102.9	0.06	0.21	1.28	0.18	13.7	7.02	54.8	99.9	329	92.9	883	187.0
BC101-8.2I	fairly dark o-zoned interior	17.1±0.4	0.0188	52.8	0.05	0.39	1.85	0.44	17.2	7.52	38.8	89.0	179	41.7	334	63.7
BC101-8.1R	med-dark o-zoned rim	16.4±0.5	0.0024	49.4	0.06	0.44	1.98	0.40	18.5	7.99	41.0	89.6	182	41.0	322	56.7
BC101-9.4C	gray unzoned core		0.0013	48.3	0.04	0.37	1.88	0.54	20.1	8.56	45.1	106.6	203	45.6	358	68.5
BC101-9.3I	med dark unzeoned interior		0.0033	42.1	0.06	0.42	2.55	0.54	24.4	9.87	46.3	113.1	213	46.8	368	66.0
BC101-9.2IR	dark inner rim		0.0016	131.2	0.06	0.57	3.11	0.80	37.3	16.89	100.1	223.1	508	121.7	1002	186.0
BC101-9.1R	bright outer rim		0.0033	29.5	0.04	0.11	0.74	0.16	8.1	3.63	22.5	48.6	114	28.5	253	54.3

BC101-10.2C	grazy, ozoned core		0.0188	116.6	0.18	2.26	8.33	2.07	68.3	24.33	101.4	256.7	433	90.2	702	128.0
BC101-10.3I	dark euh o-zoned interior		0.0342	121.9	0.05	0.39	1.80	0.21	21.3	10.22	71.8	142.1	390	103.0	952	189.4
BC101-10.1R	gray o-zoned rim		0.0025	49.8	0.06	0.28	1.27	0.28	13.0	5.97	35.7	78.3	179	44.4	390	74.9
BC101-11.2I	dark zoned interior/core		0.0013	59.1	0.05	0.45	2.11	0.40	24.5	10.35	50.9	124.4	243	51.6	419	74.2
BC101-11.1R	very light interior rim		0.0059	41.1	0.06	0.59	2.27	0.47	18.1	6.92	30.1	77.9	134	27.8	235	45.1
BC101-11.3R	dark zoned outer rim		0.0014	51.0	0.04	0.40	1.89	0.41	18.2	7.41	42.3	90.4	189	43.5	336	63.1
BC101-12.3C	*small, light unzoned core*		*0.0032*	*36.0*	*0.06*	*0.29*	*1.39*	*0.36*	*16.9*	*6.82*	*33.6*	*82.1*	*167*	*39.1*	*332*	*70.5*
BC101-12.4C	same spot as 12.3C		0.0023	46.3	0.05	0.40	1.83	0.49	20.0	8.48	42.6	98.9	201	44.0	362	71.3
BC101-12.2I	medium dark o-zoned int		0.0057	94.4	0.07	0.54	2.50	0.55	32.8	13.18	77.7	177.7	370	86.8	662	122.3
BC101-12.1T	med-dark o-zoned tip		0.0042	54.0	0.05	0.39	1.67	0.43	19.0	7.25	41.5	92.3	198	46.6	397	76.4
BC101-13.1C	light unzoned center		0.0123	69.9	0.09	1.11	4.75	1.20	41.8	17.02	76.9	187.8	340	75.1	581	107.5
BC101-13.2IR	*med-dark o-zoned inner rim*	*16.3±0.4*	*0.0667*	*60.9*	*0.04*	*0.34*	*1.78*	*0.25*	*17.9*	*8.58*	*50.5*	*110.2*	*248*	*57.5*	*476*	*90.9*
BC101-13.3R	*light o-zoned outer rim*		*0.1223*	*56.3*	*0.07*	*0.60*	*2.21*	*0.43*	*19.5*	*8.02*	*40.4*	*93.0*	*183*	*41.6*	*335*	*65.4*
BC101-14.1C	med-light unzoned resorbed core		0.0530	98.8	0.38	5.68	13.93	3.63	82.7	25.43	84.5	234.1	339	69.1	528	101.5
BC101-14.3I	light unzoned interior		0.0028	72.5	0.04	0.23	1.73	0.26	21.3	10.02	69.5	141.1	358	85.3	690	131.6
BC101-14.2IR	dark OZ inner rim		0.0263	74.6	0.08	0.83	3.10	0.76	26.4	10.52	48.0	115.2	209	45.9	362	68.5
BC101-14.4IR	med-dark OZ IR	16.5±0.3	0.0026	53.2	0.03	0.28	1.68	0.31	17.9	7.60	45.0	98.2	208	48.2	393	71.5
BC101-14.5R	light OZ euhedral outer rim		0.0034	49.3	0.04	0.43	2.02	0.44	18.0	6.93	35.2	84.6	163	34.9	284	53.4

Analyzed Spot	Spot Description	Age (Ma±2σ)	Hf	U	Th	Th/U	Zr/Hf	Ti	T_{TiZ}	Y	Sc	P	Rel. Ca	Rel. Fe
DSCG-1.3C	light zoned interior		8950	67	87	1.3	49.1	9.9	780	799	36.6	259	3.09	1.84
DSCG-1.2IR	dark o-zoned outer rim	15.6±0.5	9978	322	576	1.8	44.1	7.6	754	1314	39.3	305	3.03	2.06
DSCG-1.1T	light zoned tip		8701	81	151	1.9	50.5	12.5	803	988	33.0	291	2.10	1.38
DSCG-2.3C	*very dark unzoned core*	*16.6±0.3*	*13848*	*527*	*815*	*1.5*	*31.8*	*7.3*	*749*	*1714*	*46.1*	*266*	*10.19*	*5.66*
DSCG-2.2I	light zoned interior		9593	65	83	1.3	45.8	11.8	797	534	24.8	226	4.38	2.06
DSCG-2.1T	medium-dark zoned tip	16.7±0.4	11512	340	501	1.5	38.2	6.8	742	1389	29.6	343	2.67	2.01
DSCG-3.2C	light unzoned core	16.0±0.8	7047	68	255	3.8	62.4	21.6	864	2206	53.3	344	3.10	1.69
DSCG-3.3IR	*dark o-zoned inner rim*		*10340*	*206*	*238*	*1.2*	*42.5*	*7.2*	*748*	*1151*	*64.9*	*292*	*24.59*	*1.73*
DSCG-2.3C2/3.1T	light zoned tip		9570	102	196	1.9	45.9	14.5	819	1473	43.8	494	2.26	1.67
DSCG-4.4C	*light zoned long core*	*15.8±0.6*	*6915*	*65*	*313*	*4.8*	*63.6*	*26.8*	*890*	*2467*	*89.2*	*447*	*5.88*	*2.01*
DSCG-4.3IR	light zoned inner rim, outside core		7483	33	100	3.0	58.8	19.3	851	1110	44.1	256	2.48	1.43
DSCG-4.2R	med-dark zoned rim (4.1T)		9683	212	268	1.3	45.4	7.2	749	1333	53.3	274	4.20	2.09
DSCG-4.1T	*med-dark zoned tip*		*11664*	*328*	*541*	*1.6*	*37.7*	*8.1*	*759*	*1043*	*45.6*	*294*	*6.10*	*2.56*
DSCG-5.5C	dark unzoned core	16.2±0.4	11706	863	1149	1.3	37.6	6.4	737	2042	73.2	289	3.88	3.24
DSCG-5.6I	*med-dark unzoned patch*		*11038*	*100*	*116*	*1.2*	*39.8*	*4.8*	*712*	*487*	*31.6*	*103*	*11.04*	*1.26*
DSCG-5.4IR	*light zoned, outside core*		*9673*	*130*	*226*	*1.7*	*45.5*	*9.3*	*774*	*1067*	*27.4*	*330*	*4.70*	*1.63*
DSCG-5.3IR	*same as 5.2 IR*	*15.7±0.4*	*12535*	*240*	*333*	*1.4*	*35.1*	*19.4*	*852*	*559*	*47.9*	*144*	*8.66*	*14.76*
DSCG-5.2IR	*med-dark zoned inner rim*		*12264*	*188*	*238*	*1.3*	*35.9*	*6.3*	*736*	*539*	*36.4*	*562*	*212.96*	*0.00*
DSCG-5.1T	light zoned tip		9330	118	196	1.7	47.1	10.2	782	1042	32.1	356	1.77	1.55
DSCG-6.2C	dark, zoned resorbed core	18.0±0.2	11872	1079	1810	1.7	37.0	7.5	753	2433	78.8	476	3.51	3.11
DSCG-6.1T	med-dark o-zoned tip	15.7±0.3	11444	415	580	1.4	38.4	6.3	735	749	73.2	152	3.72	2.54
DSCG-7.1C	dark, euhedral zoned core		13665	1551	3408	2.2	32.2	6.8	744	2482	62.1	359	3.20	2.97
DSCG-7.2IR	*med-dark euh zone, outside core*		*8943*	*230*	*605*	*2.6*	*49.2*	*11.8*	*797*	*1657*	*40.8*	*428*	*2.59*	*132.40*
DSCG-7.3IR	med-dark o-zoned inner rim		9401	117	254	2.2	46.8	14.2	817	1326	40.3	399	2.77	2.84
DSCG-7.4T	med-dark zoned tip		10385	140	194	1.4	42.3	8.7	767	1061	26.1	321	3.24	2.54
DSCG-8.1C	*euh. Zoned dark core*		*11336*	*242*	*322*	*1.3*	*38.8*	*6.7*	*741*	*940*	*32.3*	*330*	*2.74*	*3.87*
DSCG-8.2IR	med-dark o-zone		10162	266	342	1.3	43.3	6.8	743	1592	44.8	413	2.52	2.77
DSCG-8.3IR	light euhedral zoned inner rim		8149	72	149	2.1	54.0	15.3	825	776	28.6	301	3.36	2.37
DSCG-8.4T	med dark ozoned tip		10656	208	322	1.5	41.3	6.3	736	691	30.1	182	2.80	2.22
DSCG-9.1C	dark zoned core		7214	833	2932	3.5	61.0	15.0	823	8791	124.3	1264	2.45	3.67

DSCG-9.2IR	med-light zoned inner rim		8452	51	143	2.8	52.0	23.4	873	1030	40.2	421	2.98	1.56
DSCG-9.4IR	*dark o-zoned inner rim*		*10304*	*153*	*243*	*1.6*	*42.7*	*8.2*	*760*	*712*	*23.6*	*234*	*14.45*	*2.12*
DSCG-9.3R	light zoned outer rim		9270	99	171	1.7	47.4	15.1	823	962	35.4	348	3.32	3.23
DSCG-10.1C	dark unzoned core		12088	796	1372	1.7	36.4	5.9	729	1620	57.2	441	2.13	2.43
DSCG-10.2IR			8379	86	178	2.1	52.5	17.1	837	1059	39.7	444	2.59	2.12
DSCG-11.1C	dark unzoned core		10907	926	2084	2.3	40.3	7.2	748	4745	48.7	509	2.10	3.89
DSCG-11.2I	dark o-zoned interior		11105	1607	3528	2.2	39.6	7.0	745	2952	66.2	419	1.73	3.04
DSCG-11.3R	bright o-zoned rim		10107	233	326	1.4	43.5	5.2	718	859	24.7	182	2.09	1.81
DSCG-12.2I	med-dark o-zoned center		8920	100	171	1.7	49.3	10.8	788	1419	26.6	384	2.81	1.77
DSCG-12.1R	bright o-zoned rim		9573	130	237	1.8	45.9	11.4	794	1245	32.9	346	2.62	2.83
DSCG-13.1C	dark, unzoned euhedral center		7606	28	108	3.8	57.8	35.0	923	1355	45.6	365	2.90	1.73
DSCG-13.2I	gray o-zoned interior		7530	48	128	2.7	58.4	21.2	861	972	41.6	395	1.45	0.92
DSCG-13.3T	dark o-zoned tip/rim		9265	95	151	1.6	47.5	12.8	805	821	29.2	309	2.19	2.01
DSCG-14.1I	*gray unzoned interior*		*11205*	*113*	*133*	*1.2*	*39.2*	*6.7*	*741*	*699*	*15.5*	*189*	*1.95*	*2.58*
DSCG-14.2R	*bright o-zoned rim*		*8884*	*114*	*163*	*1.4*	*49.5*	*12.5*	*803*	*1476*	*51.7*	*407*	*1.77*	*1.66*
DSCG-15.2I	bright zoned interior		7749	23	46	2.0	56.7	18.7	847	414	27.9	182	1.67	1.15
DSCG-15.1R	dark o-zoned rim		9410	162	266	1.6	46.7	9.3	773	1226	40.8	343	1.47	1.54
DSCG-16.1C	*very dark core*		*10502*	*4717*	*23287*	*4.9*	*41.9*	*11.7*	*797*	*6182*	*128.5*	*552*	*2.16*	*5.83*
DSCG-16.2R	bright o-zoned rim		9939	152	222	1.5	44.2	10.7	787	1347	35.4	361	2.20	2.35
DSCG-17.1C	*very dark core*		*11913*	*4746*	*12991*	*2.7*	*36.9*	*11.7*	*797*	*5582*	*162.6*	*468*	*9.15*	*10.27*
DSCG-17.2R	med-dark o-zoned rim		9368	116	215	1.9	46.9	10.7	787	1320	29.9	307	4.31	2.04
DSCG-18.1R	med-dark, faint o-zoned rim	15.4±0.4	10603	166	209	1.3	41.5	5.3	721	619	40.7	133	2.46	1.70
DSCG-19.1IR	dark o-zoned euh interior	16.1±0.3	10059	358	684	1.9	43.7	5.9	730	953	57.9	212	2.58	1.99
DSCG-20.2I	bright, weakly zoned interior		7669	49	125	2.5	57.3	20.5	858	815	42.8	271	2.47	1.17
DSCG-20.1R	med-dark, o-zoned rim		10508	243	335	1.4	41.8	5.3	721	989	44.8	225	2.45	1.60
DSCG-21.1C	dark unzoned euhedral core	16.2±0.8	7555	49	170	3.5	58.2	25.8	885	1939	45.4	373	2.36	1.38
DSCG-21.2I	bright, weak o-zoned interior		8490	37	85	2.3	51.8	22.3	868	715	37.6	295	2.66	1.42

	Spot Description	Age (Ma±2σ)	La	Ce	Pr	Nd	Sm	Eu	Gd	Tb	Ho	Dy	Er	Tm	Yb	Lu
DSCG-1.3C	light zoned interior		0.0089	42.3	0.05	0.23	1.52	0.39	15.0	6.31	32.7	73.7	157	34.7	299	59.0
DSCG-1.2IR	dark o-zoned outer rim	15.6±0.5	0.0050	81.7	0.06	0.40	1.92	0.42	21.1	8.96	54.2	115.6	257	63.5	555	106.3
DSCG-1.1T	light zoned tip		0.0046	58.9	0.07	0.77	2.64	0.70	23.6	8.45	40.4	98.1	173	37.0	310	57.7
DSCG-2.3C	*very dark unzoned core*	*16.6±0.3*	*0.0597*	*69.9*	*0.05*	*0.34*	*1.58*	*0.17*	*15.2*	*7.61*	*57.7*	*109.7*	*324*	*91.3*	*877*	*197.0*
DSCG-2.2I	light zoned interior		0.0052	38.1	0.05	0.22	1.27	0.32	11.3	4.83	23.2	55.7	109	23.6	199	38.9
DSCG-2.1T	medium-dark zoned tip	16.7±0.4	0.0040	72.8	0.05	0.39	1.85	0.42	22.5	8.78	54.5	118.5	259	61.0	520	96.6
DSCG-3.2C	light unzoned core	16.0±0.8	0.0591	98.0	0.36	5.08	13.1	4.04	92.0	27.33	97.7	267.3	391	77.4	604	110.1
DSCG-3.3IR	*dark o-zoned inner rim*		*0.4246*	*56.2*	*0.14*	*0.77*	*1.69*	*0.37*	*15.7*	*6.95*	*42.5*	*90.5*	*221*	*53.4*	*487*	*101.6*
DSCG-2.3C2/3.1T	light zoned tip		0.0025	74.6	0.07	0.95	3.68	0.88	35.0	13.36	63.1	156.9	285	62.9	486	88.9
DSCG-4.4C	*light zoned long core*	*15.8±0.6*	*0.1314*	*140.6*	*0.65*	*9.41*	*20.2*	*5.83*	*115.5*	*34.01*	*113.0*	*318.3*	*420*	*82.4*	*590*	*111.2*
DSCG-4.3IR	light zoned inner rim, outside core		0.0188	50.1	0.14	2.17	5.70	1.70	38.7	12.02	45.3	120.0	188	39.5	297	57.4
DSCG-4.2R	med-dark zoned rim (4.1T)		0.0016	57.4	0.04	0.35	1.57	0.42	18.4	8.77	51.6	110.9	253	59.4	519	100.2
DSCG-4.1T	*med-dark zoned tip*		*0.0121*	*61.7*	*0.05*	*0.35*	*1.62*	*0.53*	*17.0*	*7.48*	*40.4*	*86.2*	*191*	*46.8*	*406*	*82.4*
DSCG-5.5C	dark unzoned core	16.2±0.4	0.0327	107.4	0.06	0.38	1.26	0.25	17.1	7.29	62.3	118.7	356	100.9	951	201.3
DSCG-5.6I	*med-dark unzoned patch*		*0.0040*	*26.4*	*0.04*	*0.11*	*0.60*	*0.20*	*6.6*	*2.62*	*16.1*	*34.8*	*88*	*23.6*	*238*	*56.8*
DSCG-5.4IR	*light zoned, outside core*		*0.0041*	*63.4*	*0.06*	*0.53*	*2.54*	*0.65*	*24.6*	*9.35*	*45.6*	*106.7*	*208*	*46.6*	*365*	*65.4*
DSCG-5.3IR	*same as 5.2 IR*	*15.7±0.4*	*2.2404*	*54.0*	*0.27*	*0.76*	*0.79*	*0.20*	*6.7*	*2.74*	*19.2*	*38.7*	*112*	*32.3*	*320*	*77.4*
DSCG-5.2IR	*med-dark zoned inner rim*		*3.0502*	*46.8*	*0.43*	*1.59*	*0.88*	*0.21*	*6.9*	*2.77*	*17.7*	*35.1*	*103*	*28.6*	*287*	*65.8*
DSCG-5.1T	light zoned tip		0.0017	54.0	0.05	0.49	2.20	0.51	20.6	8.44	44.2	106.3	203	44.5	364	65.8
DSCG-6.2C	dark, zoned resorbed core	18.0±0.2	0.0081	128.8	0.07	0.31	1.79	0.25	19.0	9.27	70.6	132.9	415	115.2	1087	228.4
DSCG-6.1T	med-dark o-zoned tip	15.7±0.3	0.0058	36.7	0.03	0.19	0.91	0.25	10.0	3.82	26.1	55.2	129	35.8	320	76.7
DSCG-7.1C	dark, euhedral zoned core		0.0027	155.7	0.05	0.43	2.12	0.30	23.9	10.45	77.5	158.8	428	111.3	1032	212.7
DSCG-7.2IR	*med-dark euh zone, outside core*		*0.0108*	*98.2*	*0.07*	*0.96*	*4.23*	*0.96*	*37.7*	*14.20*	*66.1*	*165.0*	*282*	*59.2*	*462*	*83.8*
DSCG-7.3IR	med-dark o-zoned inner rim		0.0031	84.4	0.06	0.97	3.70	0.95	31.6	11.63	56.1	133.0	239	50.7	407	72.8
DSCG-7.4T	med-dark zoned tip		0.0018	50.3	0.04	0.31	1.49	0.31	18.2	7.35	41.4	92.9	194	45.2	371	70.2
DSCG-8.1C	*euh. Zoned dark core*		*0.0523*	*39.1*	*0.03*	*0.20*	*0.86*	*0.15*	*9.9*	*4.47*	*30.7*	*64.9*	*178*	*47.1*	*423*	*87.9*
DSCG-8.2IR	med-dark o-zone		0.0058	63.1	0.04	0.24	1.35	0.33	18.3	8.00	55.0	108.2	284	68.0	602	122.3
DSCG-8.3IR	light euhedral zoned IR		0.0078	51.6	0.07	0.54	2.19	0.67	19.0	7.17	34.0	81.0	146	31.3	248	48.7

DSCG-8.4T	med dark ozoned tip		0.0018	42.1	0.05	0.21	0.85	0.22	10.5	4.05	25.4	54.6	133	33.5	307	63.5
DSCG-9.1C	dark zoned core		0.0882	397.0	0.53	8.42	26.9	8.38	263.6	92.51	370.6	980.3	1549	306.3	2353	401.5
DSCG-9.2IR	med-light zoned inner rim		0.0083	71.3	0.09	1.04	3.67	0.63	29.6	9.97	42.5	109.2	179	37.8	307	57.7
DSCG-9.4IR	*dark o-zoned inner rim*		*0.5671*	*39.3*	*0.14*	*0.69*	*1.10*	*0.25*	*11.8*	*4.49*	*26.6*	*59.3*	*132*	*32.4*	*276*	*51.3*
DSCG-9.3R	light zoned outer rim		0.0068	53.4	0.07	0.54	2.49	0.55	21.4	8.33	38.3	94.1	183	40.4	329	62.8
DSCG-10.1C	dark unzoned core		0.0080	83.0	0.06	0.28	1.18	0.15	13.6	5.93	51.6	99.8	312	84.7	829	177.8
DSCG-10.2IR			0.0058	64.6	0.08	0.78	2.88	0.73	27.0	10.14	49.5	119.7	225	48.2	380	71.2
DSCG-11.1C	dark unzoned core		0.0478	169.6	0.16	1.92	6.28	0.98	63.5	28.33	164.2	350.5	825	195.9	1679	314.8
DSCG-11.2I	dark o-zoned interior		0.0079	186.1	0.08	0.60	2.56	0.43	33.3	14.05	99.9	205.8	529	135.1	1204	242.1
DSCG-11.3R	bright o-zoned rim		0.0029	45.3	0.03	0.22	0.96	0.23	10.3	4.54	31.2	64.3	162	39.2	343	70.3
DSCG-12.2I	med-dark o-zoned center		0.0158	50.0	0.11	1.33	3.88	1.16	34.9	12.44	57.7	137.3	253	54.3	420	77.5
DSCG-12.1R	bright o-zoned rim		0.0288	65.3	0.07	0.84	3.01	0.71	27.9	10.67	49.7	124.2	229	48.8	407	73.2
DSCG-13.1C	dark, unzoned euhedral center		0.0269	40.7	0.25	3.08	6.26	1.60	50.2	16.36	62.3	166.8	261	51.9	398	75.2
DSCG-13.2I	gray o-zoned interior		0.0039	51.5	0.09	1.09	3.40	0.74	26.8	9.37	39.9	102.4	179	37.6	296	54.1
DSCG-13.3T	dark o-zoned tip/rim		0.0025	46.6	0.03	0.37	1.21	0.38	16.6	6.51	34.9	84.3	161	36.6	292	55.0
DSCG-14.1I	*gray unzoned interior*		*0.0674*	*28.3*	*0.03*	*0.10*	*0.70*	*0.15*	*7.8*	*3.70*	*24.5*	*52.1*	*134*	*32.5*	*285*	*55.5*
DSCG-14.2R	*bright o-zoned rim*		*0.0380*	*58.6*	*0.07*	*0.62*	*3.04*	*0.73*	*26.3*	*10.69*	*57.8*	*130.8*	*272*	*59.6*	*498*	*95.2*
DSCG-15.2I	bright zoned interior		0.0028	36.7	0.04	0.43	1.45	0.47	12.6	4.47	17.6	45.3	81	17.1	142	28.6
DSCG-15.1R	dark o-zoned rim		0.0065	57.9	0.04	0.60	2.47	0.58	22.4	9.59	48.2	105.6	213	48.3	387	72.4
DSCG-16.1C	*very dark core*		*0.0371*	*577.2*	*0.17*	*2.33*	*8.02*	*1.18*	*80.7*	*33.72*	*214.8*	*437.3*	*1153*	*288.9*	*2608*	*515.9*
DSCG-16.2R	bright o-zoned rim		0.0129	62.6	0.04	0.61	2.41	0.53	24.7	10.62	52.0	122.2	247	54.5	438	80.2
DSCG-17.1C	*very dark core*		*0.2282*	*515.6*	*0.18*	*1.48*	*4.63*	*0.48*	*40.8*	*19.56*	*155.9*	*270.8*	*975*	*272.8*	*2826*	*600.0*
DSCG-17.2R	med-dark o-zoned rim		0.0578	62.8	0.10	0.80	3.35	0.76	28.7	10.70	54.1	127.4	250	54.3	424	75.0
DSCG-18.1R	med-dark, faint o-zoned rim	15.4±0.4	0.0041	38.7	0.04	0.25	0.98	0.29	10.5	3.68	23.2	51.9	115	28.7	276	59.4
DSCG-19.1IR	dark o-zoned euh interior	16.1±0.3	0.0025	64.9	0.05	0.33	1.63	0.43	14.4	5.61	34.2	78.4	181	43.9	410	87.7
DSCG-20.2I	bright, weakly zoned interior		0.0074	63.5	0.09	1.03	3.48	1.00	25.4	7.82	33.9	84.2	142	31.0	256	50.1
DSCG-20.1R	med-dark, o-zoned rim		0.0036	51.8	0.05	0.35	1.65	0.42	16.6	6.75	36.9	83.4	184	44.5	399	79.0
DSCG-21.1C	dark unzoned euhedral core	16.2±0.8	0.0248	50.3	0.23	3.69	9.31	2.77	69.2	22.00	81.0	223.8	330	65.9	511	90.4
DSCG-21.2I	bright, weak o-zoned interior		0.0127	46.1	0.06	0.72	2.71	0.70	19.6	7.30	31.7	78.0	134	28.4	236	46.0

Analyzed Spot	Spot Description	Age (Ma±2σ)	Hf	U	Th	Th/U	Zr/Hf	Ti	T_{TiZ}	Y	Sc	P	Rel. Ca	Rel. Fe
SML49Z-1.1C	*med-dark unzoned core, resorbed*	*16.5±0.5*	*7866*	*189*	*520*	*2.8*	*55.9*	*10.1*	*782*	*2595*	*41.5*	*650*	*201*	*0.01*
SML49Z-1.3I	light o-zoned interior around core		10327	104	151	1.5	42.6	7.0	746	1190	20.8	273	1.41	1.03
SML49Z-1.2R	dark o-zoned euh rim, resorbing core		10573	503	715	1.4	41.6	7.5	752	2140	52.3	315	1.43	1.13
SML49Z-2.1C	bright euhedral unzoned interior	15.9±1.0	7753	33	55	1.7	56.7	13.5	812	513	33.6	104	1.20	0.97
SML49Z-2.3IR			8916	94	138	1.5	49.3	13.7	813	1210	58.4	293	1.91	1.75
SML49Z-2.2T	dark rim	16.2±0.2	12724	907	1175	1.3	34.6	5.0	715	2631	106.4	260	0.79	0.98
SML49Z-3.1I	bright, unzoned euhedral interior		8316	56	137	2.4	52.9	13.6	813	1481	31.6	194	1.35	1.45
SML49Z-3.2R	euh, o-zoned gray rim	18.3+0.8	11406	186	218	1.2	38.5	7.2	748	1086	38.3	214	1.06	1.13
SML49Z-4.1C	gray unzoned center/core/interior	16.1±0.6	9213	76	169	2.2	47.7	8.6	766	1409	27.3	220	1.19	1.14
SML49Z-4.2T	very dark euh zoned rim		12307	714	992	1.4	35.7	5.0	716	1823	54.8	223	1.21	1.28
SML49Z-5.1C	light unzoned core	15.4±0.4	9843	143	295	2.1	44.7	7.3	750	1882	23.5	324	1.35	1.00
SML49Z-5.3IR	light, zoned inner rim		9744	100	133	1.3	45.1	7.0	746	724	16.4	208	1.48	0.92
SML49Z-5.2R	very dark zoned euhedral corner/rim	16.5±0.3	12250	652	737	1.1	35.9	5.1	718	1936	85.5	201	1.77	1.23
SML49Z-6.2IR	dark unzoned interior		7475	270	1225	4.5	58.8	16.8	835	1984	81.5	515	1.45	1.17
SML49Z-6.3IR	light, zoned inner rim		9082	73	115	1.6	48.4	7.7	755	598	21.8	193	1.41	1.14
SML49Z-6.1R	very dark euh zoned outer rim	16.8±0.2	11816	511	910	1.8	37.2	3.3	679	2009	43.0	178	1.45	1.30
SML49Z-7.3C	light unzoned core		8764	30	38	1.3	50.2	8.8	768	501	20.8	136	1.48	0.92
SML49Z-7.2IR	light, zoned thick inner rim		9168	103	139	1.4	48.0	8.0	759	851	25.6	271	1.62	1.13
SML49Z-7.4IR	same spot as 7.2IR		8947	97	135	1.4	49.1	7.6	754	822	24.9	234	0.73	0.71
SML49Z-7.1R	very dark euhedral outer rim, zoned		12532	846	985	1.2	35.1	5.4	722	1979	95.5	249	1.44	1.22
SML49Z-8.1C	med-dark unzoned center	16.2±0.4	9017	68	94	1.4	48.8	5.8	728	870	19.2	198	1.37	0.97
SML49Z-8.5C	same spot as 8.1C		10511	66	81	1.2	41.8	6.9	744	628	20.1	203	1.29	1.12
SML49Z-8.2IR	*dark, thick zoned inner rim*		*10129*	*473*	*652*	*1.4*	*43.4*	*6.3*	*736*	*2522*	*58.6*	*366*	*6.12*	*1.70*
SML49Z-8.4IR	same as 8.2IR		11169	631	936	1.5	39.4	5.5	724	1939	39.3	319	1.58	1.06
SML49Z-8.3R	very dark zoned outer rim	16.0±0.2	12551	1251	1723	1.4	35.0	4.6	707	1922	61.8	253	1.44	1.04
SML49Z-9.1C	light unzoned long center		7495	29	68	2.4	58.7	16.0	829	762	33.7	149	1.42	0.94
SML49Z-9.2IR	light, euhedral zoned thick inner rim		7779	54	84	1.6	56.5	12.5	803	844	49.9	227	1.23	1.04
SML49Z-9.3R	very dark euhdral zoned corner/rim	16.3±0.2	11925	877	1299	1.5	36.9	6.3	737	2731	104.4	306	1.33	1.07
SML49Z-10.3C	*light unzoned resorbed core*		*10436*	*78*	*87*	*1.1*	*42.1*	*5.5*	*724*	*1449*	*12.1*	*391*	*22.51*	*2.44*
SML49Z-10.4C	same as 10.3C		11041	84	96	1.1	39.8	5.8	728	787	15.8	222	1.35	0.83

SML49Z-10.5IR	very dark zoned inner rim		11432	405	462	1.1	38.5	4.7	709	1320	54.8	170	1.11	0.90
SML49Z-10.2IR	*med-dark zoned IR*		*9496*	*326*	*652*	*2.0*	*46.3*	*5.6*	*726*	*3416*	*26.7*	*286*	*49.45*	*0.01*
SML49Z-10.1R	very dark euhedral zoned corner	16.2±0.3	10610	504	738	1.5	41.4	5.7	726	1910	39.1	333	1.45	1.16
SML49Z-10.6IR	light zoned inner rim		11019	68	72	1.1	39.9	5.1	717	328	8.4	120	1.31	0.84
SML49Z-11.1C	med-dark unzoned resorbed core		9189	69	79	1.1	47.9	7.5	753	603	17.2	196	1.41	1.32
SML49Z-11.2IR	*light euhedral zoned inner rim*		*7845*	*51*	*79*	*1.5*	*56.0*	*10.9*	*789*	*800*	*38.4*	*237*	*3.28*	*1.08*
SML49Z-11.3R	dark euhedral zoned rim		11919	687	873	1.3	36.9	4.9	713	1683	59.4	245	1.57	1.16
SML49Z-12.1IC	large light euhedral unzoned center	17.6±0.8	8923	87	172	2.0	49.3	6.4	737	1347	24.5	235	1.13	0.80
SML49Z-12.2T	dark euhedral zoned rim		11204	855	1146	1.3	39.2	4.9	714	1979	67.2	249	1.20	0.89
SML49Z-13.1IC	med, unzoned euh center		9951	78	161	2.1	44.2	7.4	750	1749	13.2	328	1.36	1.10
SML49Z-13.2IR	med o-zoned inner rim		9603	98	132	1.3	45.8	7.2	748	745	16.8	193	1.26	0.95
SML49Z-13.3T	dark euh zoned rim	16.1±0.5	11639	508	957	1.9	37.8	5.0	714	1330	37.3	234	1.38	1.50

Analyzed Spots	Spot Description	Age (Ma±2σ)	La	Ce	Pr	Nd	Sm	Eu	Gd	Tb	Ho	Dy	Er	Tm	Yb	Lu
SML49Z-1.1C	*med-dark unzoned core*	*16.5±0.5*	*3.2482*	*134.8*	*0.81*	*6.19*	*13.70*	*2.96*	*91.5*	*31.75*	*125.0*	*324.0*	*539*	*110.9*	*859*	*154.8*
SML49Z-1.3I	light o-zoned interior		0.0079	47.5	0.03	0.35	2.26	0.48	22.1	9.41	48.5	110.9	222	49.3	395	74.3
SML49Z-1.2R	dark o-zoned euhedral rim		0.0029	101.2	0.04	0.39	2.08	0.32	23.5	10.82	75.8	147.4	384	95.8	840	168.6
SML49Z-2.1C	bright euhedral unzoned interior	15.9±1.0	0.0029	34.8	0.04	0.45	1.66	0.57	14.4	4.86	22.2	52.5	99	21.7	178	35.4
SML49Z-2.3IR			0.0045	67.4	0.05	0.73	2.99	0.89	26.7	10.23	51.6	120.3	239	54.2	449	88.8
SML49Z-2.2T	dark rim	16.2±0.2	0.0017	131.9	0.02	0.23	1.10	0.14	13.6	7.37	74.7	117.8	454	126.7	1338	289.0
SML49Z-3.1I	bright, unzoned euhedral interior		0.0093	59.8	0.11	2.14	7.19	1.87	52.1	16.79	66.9	171.4	274	56.6	439	82.0
SML49Z-3.2R	euh, o-zoned gray rim	18.3+0.8	0.0024	51.5	0.02	0.25	1.22	0.27	13.8	6.59	40.7	79.8	203	49.3	445	92.1
SML49Z-4.1C	gray unzoned center	16.1±0.6	0.0065	60.4	0.07	1.18	5.15	1.33	43.4	15.19	66.0	167.7	286	58.9	461	83.3
SML49Z-4.2T	very dark euh zoned rim		0.0030	94.5	0.03	0.36	1.59	0.25	17.2	7.90	60.0	113.2	334	89.2	838	175.0
SML49Z-5.1C	light unzoned core	15.4±0.4	0.0048	66.6	0.06	1.07	4.68	1.08	43.6	17.05	83.1	193.8	361	76.8	604	107.6
SML49Z-5.3IR	light, zoned inner rim		0.0020	39.4	0.01	0.23	1.23	0.29	12.9	5.11	28.7	62.5	133	31.2	265	48.8
SML49Z-5.2R	very dark zoned euhedral rim	16.5±0.3	0.0033	98.7	0.02	0.21	1.03	0.16	12.7	6.64	61.0	104.7	366	105.1	1028	220.4
SML49Z-6.2IR	dark unzoned interior		0.0133	198.6	0.15	2.33	8.58	2.95	69.7	23.71	93.6	241.6	374	74.5	552	101.2
SML49Z-6.3IR	light, zoned inner rim		0.0038	40.3	0.03	0.31	1.31	0.40	12.0	4.48	23.8	55.2	109	23.9	202	37.8
SML49Z-6.1R	very dark euh zoned outer rim	16.8±0.2	0.0021	69.5	0.04	0.47	1.80	0.30	19.8	8.98	64.2	126.5	369	97.3	924	191.2
SML49Z-7.3C	light unzoned core		0.0028	30.3	0.01	0.19	0.88	0.25	9.0	3.54	19.1	43.2	90	20.0	164	32.1
SML49Z-7.2IR	light, zoned thick inner rim		0.0028	47.6	0.03	0.31	1.69	0.42	15.9	6.35	34.1	77.0	154	34.9	284	52.7
SML49Z-7.4IR	same spot as 7.2IR		0.0026	45.7	0.04	0.35	1.71	0.40	14.8	6.06	32.6	73.3	147	32.7	257	50.3
SML49Z-7.1R	very dark euhedral rim, zoned		0.0026	111.2	0.02	0.20	0.90	0.13	12.1	6.49	62.6	102.7	409	119.2	1213	263.2
SML49Z-8.1C	med-dark unzoned center	16.2±0.4	0.0059	36.8	0.02	0.23	1.25	0.34	13.6	6.07	31.1	67.6	145	31.9	257	49.4
SML49Z-8.5C	same spot as 8.1C		0.0035	32.7	0.02	0.20	1.05	0.24	10.4	4.28	24.1	55.4	122	28.0	243	46.2
SML49Z-8.2IR	*dark, thick zoned inner rim*		*0.1574*	*114.7*	*0.08*	*0.60*	*2.19*	*0.36*	*21.8*	*10.25*	*81.1*	*149.8*	*430*	*106.0*	*983*	*193.8*
SML49Z-8.4IR	same as 8.2IR		0.0080	98.4	0.03	0.38	1.91	0.29	20.0	9.35	63.6	128.6	336	83.5	752	148.0
SML49Z-8.3R	very dark zoned outer rim	16.0±0.2	0.0079	114.1	0.04	0.29	1.15	0.14	12.8	6.30	55.9	94.7	339	96.1	962	209.3
SML49Z-9.1C	light unzoned long center		0.0068	34.9	0.06	0.92	3.33	1.13	24.7	8.40	33.4	83.5	139	28.8	230	44.1
SML49Z-9.2IR	light, euhedral zoned IR		0.0044	50.5	0.04	0.60	2.36	0.69	19.9	7.17	35.3	82.3	161	36.4	302	61.9
SML49Z-9.3R	very dark euhedral zoned rim	16.3±0.2	0.0027	151.8	0.03	0.26	1.49	0.23	19.6	10.16	86.3	153.2	521	142.7	1367	288.1
SML49Z-10.3C	*light unzoned resorbed core*		*1.7205*	*46.2*	*1.03*	*7.62*	*13.04*	*1.24*	*45.8*	*15.51*	*58.9*	*148.3*	*222*	*47.1*	*363*	*62.2*
SML49Z-10.4C	same as 10.3C		0.0026	34.9	0.02	0.14	0.94	0.21	10.7	5.08	31.2	65.6	151	35.0	293	56.1

SML49Z-10.5IR	very dark zoned inner rim		0.0023	67.2	0.02	0.15	0.79	0.11	9.6	5.03	41.2	70.0	230	63.4	615	136.0
SML49Z-10.2IR	*med-dark zoned IR*		*2.2786*	*100.4*	*1.34*	*9.83*	*19.79*	*2.01*	*82.0*	*28.81*	*130.0*	*291.3*	*523*	*117.2*	*909*	*169.2*
SML49Z-10.1R	very dark euhedral zoned corner	16.2±0.3	0.0010	100.2	0.02	0.41	2.12	0.36	23.9	10.78	70.0	141.8	356	85.9	739	142.4
SML49Z-10.6IR	light zoned inner rim		0.0018	21.5	0.02	0.06	0.38	0.08	4.6	2.05	13.4	27.3	68	17.1	146	29.0
SML49Z-11.1C	med-dark unzoned core		0.0035	32.1	0.02	0.22	0.89	0.24	9.6	3.86	24.5	51.3	119	27.4	232	46.1
SML49Z-11.2IR	*light euhedral zoned inner rim*		*0.0480*	*41.9*	*0.04*	*0.49*	*1.69*	*0.49*	*15.5*	*6.03*	*30.0*	*70.4*	*139*	*30.5*	*257*	*49.9*
SML49Z-11.3R	dark euhedral zoned rim		0.0024	97.0	0.02	0.30	1.13	0.19	14.2	6.70	54.5	96.8	312	83.9	801	171.0
SML49Z-12.1IC	light euhedral unzoned center	17.6±0.8	0.0037	56.6	0.03	0.55	2.84	0.70	27.4	10.51	51.0	119.5	231	50.1	390	72.1
SML49Z-12.2T	dark euhedral zoned rim		0.0050	116.9	0.04	0.34	1.46	0.21	15.9	7.72	62.0	110.4	346	93.5	891	188.3
SML49Z-13.1IC	med, unzoned euhedral center		0.0021	64.6	0.03	0.44	3.02	0.46	37.1	15.44	73.2	181.5	311	63.3	467	80.4
SML49Z-13.2IR	med o-zoned inner rim		0.0026	42.1	0.02	0.23	1.28	0.28	13.2	5.40	29.5	67.9	143	32.4	269	49.3
SML49Z-13.3T	dark euhedral zoned rim	16.1±0.5	0.0020	75.8	0.02	0.26	1.47	0.26	16.0	7.09	48.7	98.8	260	66.7	600	120.5

Analyzed Spots	spot description	Age (Ma±2σ)	Hf	U	Th	Th/U	Zr/Hf	Ti	T_{TiZ}	Y	Sc	P	Rel. Ca	Rel. Fe
SML54Z-1.1I	gray, euh zoned interior		8403	59	136	2.3	52.3	13.9	815	1253	38.6	229	1.33	1.74
SML54Z-1.2R	dark euh rim		15035	902	1421	1.6	29.2	3.3	680	2077	166.3	102	1.55	1.76
SML54Z-2.1I	bright weakly zoned interior		6986	33	81	2.4	62.9	21.7	864	1098	39.6	196	1.20	1.95
SML54Z-3.1C	weakly zoned, resorbed core		8010	138	461	3.3	54.9	14.3	817	2946	73.6	383	1.67	1.76
SML54Z-3.2I	gray unzoned interior		8542	105	298	2.8	51.5	14.4	819	1121	38.2	308	1.37	1.35
SML54Z-3.3T	very dark rim	16.1±0.5	15056	1743	1821	1.0	29.2	5.3	720	2351	412.1	177	1.59	1.62
SML54Z-4.1C	gray, unzoned center		9143	53	68	1.3	48.1	9.4	774	587	26.4	170	1.04	1.15
SML54Z-4.2IR	euh, weakly zoned inner rim, gray		8174	100	148	1.5	53.8	12.5	804	1327	64.0	314	1.29	1.51
SML54Z-4.3T	dark euh zoned tip	16.1±0.5	12560	529	762	1.4	35.0	5.7	728	1517	28.4	282	1.69	3.47
SML54Z-5.1C	gray irregularly zoned interior		10188	43	44	1.0	43.2	6.5	740	399	13.7	143	1.39	1.32
SML54Z-5.2IIR	bright o-zoned euh inner inner rim		9543	79	104	1.3	46.1	9.1	771	1044	30.1	299	2.91	1.26
SML54Z-5.3IR	darker gray o-zoned euh inner rim	16.1±0.5	9743	118	186	1.6	45.1	8.6	765	1075	28.2	311	1.36	1.70
SML54Z-6.1C	resorbed core		7622	100	367	3.7	57.7	18.8	848	2524	57.9	328	1.31	1.23
SML54Z-6.2IR	*gray o-zoned euh inner rim*	*16.1±0.5*	*8555*	*118*	*301*	*2.5*	*51.4*	*15.3*	*825*	*1048*	*36.1*	*406*	*56.79*	*0.00*
SML54Z-7.1C	resorbed dark core	17.2±0.2	12778	944	1441	1.5	34.4	5.8	729	2189	58.1	299	1.33	1.47
SML54Z-7.2IR	light gray o-zoned inner rim		10596	129	168	1.3	41.5	6.5	738	876	20.4	231	1.24	1.32
SML54Z-7.3T	very dark euh tip		11864	663	921	1.4	37.1	5.5	723	1385	99.3	194	1.27	1.43
SML54Z-8.1IC	gray, unzoned euh center		7586	20	52	2.6	58.0	20.5	858	610	36.8	156	1.23	1.11
SML54Z-8.2T	med-dark gray o-zoned tip	16.4±0.5	10492	166	221	1.3	41.9	7.3	750	1230	16.1	348	1.31	1.42
SML54Z-9.1C	gray unzoned euh center		7506	58	189	3.2	58.6	16.7	834	1776	37.8	258	1.28	1.23
SML54Z-9.2IR	gray euh o-zoned inner rim	17.0±0.3	8592	69	125	1.8	51.2	12.4	802	972	36.9	253	1.41	1.40
SML54Z-9.3T	dark euhedral rim		14463	1302	1410	1.1	30.4	5.0	716	1889	364.8	141	1.50	1.62
SML54Z-10.1C	*dark, zoned rounded core*	*17.2±0.2*	*12012*	*695*	*887*	*1.3*	*36.6*	*9.4*	*774*	*1993*	*58.2*	*705*	*3.16*	*3.56*
SML54Z-10.2R	*med-dark, euhedral, o-zoned rim*		*10123*	*145*	*216*	*1.5*	*43.4*	*8.0*	*759*	*973*	*19.1*	*293*	*2.33*	*2.78*

	spot description	Age (Ma±2σ)	La	Ce	Pr	Nd	Sm	Eu	Gd	Tb	Ho	Dy	Er	Tm	Yb	Lu
SML54Z-1.1I	gray, euhedral zoned interior		0.0088	54.3	0.08	1.23	4.77	1.27	35.6	12.66	51.5	133.5	223	44.9	356	67.6
SML54Z-1.2R	dark euhedral rim		0.0037	69.4	0.06	0.76	2.57	0.51	21.8	8.30	59.0	108.7	357	108.1	1192	291.4
SML54Z-2.1I	bright weakly zoned interior		0.0236	38.9	0.14	2.49	6.88	2.49	42.4	12.44	46.0	119.6	181	38.1	296	57.2

SML54Z-3.1C	weakly zoned, resorbed core		0.0554	129.8	0.34	5.11	16.14	5.53	111.9	35.49	127.2	348.1	514	102.4	791	137.3
SML54Z-3.2I	gray unzoned interior		0.0082	88.4	0.06	1.15	3.86	1.10	31.7	11.18	50.9	123.8	219	45.8	360	68.5
SML54Z-3.3T	very dark rim	16.1±0.5	0.0025	116.3	0.02	0.19	0.89	0.18	11.4	5.65	62.8	93.9	434	144.9	1733	451.3
SML54Z-4.1C	gray, unzoned center		0.0020	32.9	0.02	0.24	1.07	0.33	12.0	4.75	24.5	56.3	113	26.4	216	43.0
SML54Z-4.2IR	euh, weakly zoned inner rim, gray		0.0033	66.1	0.04	0.68	2.88	0.78	26.8	9.94	52.7	119.4	241	53.1	446	86.7
SML54Z-4.3T	dark euhedral zoned tip	16.1±0.5	0.0062	74.9	0.03	0.33	1.89	0.25	19.9	9.57	59.6	118.8	296	71.6	616	118.3
SML54Z-5.1C	gray irregularly zoned interior		0.0018	23.1	0.01	0.09	0.49	0.15	5.8	2.49	15.0	32.5	76	18.1	152	29.3
SML54Z-5.2IIR	bright o-zoned euh inner rim		0.0334	42.9	0.03	0.40	1.87	0.47	20.3	8.12	44.0	103.9	202	45.0	367	67.9
SML54Z-5.3IR	darker gray o-zoned euh inner rim	16.1±0.5	0.0547	62.0	0.05	0.54	2.49	0.57	22.6	8.97	47.7	106.1	214	45.6	377	67.6
SML54Z-6.1C	resorbed core		0.0597	118.6	0.34	5.38	15.43	4.67	101.6	31.10	110.1	298.7	435	85.4	648	117.3
SML54Z-6.2IR	*gray o-zoned euh inner rim*	*16.1±0.5*	*0.9270*	*80.5*	*0.24*	*1.79*	*3.53*	*0.93*	*29.2*	*10.60*	*46.8*	*116.2*	*202*	*41.6*	*346*	*63.2*
SML54Z-7.1C	resorbed dark core	17.2±0.2	0.0043	125.9	0.03	0.44	1.51	0.26	22.5	10.31	74.3	143.1	409	103.8	968	198.8
SML54Z-7.2IR	light gray o-zoned inner rim		0.0083	44.3	0.03	0.29	1.53	0.29	15.2	6.19	35.5	81.0	173	39.2	331	60.6
SML54Z-7.3T	very dark euh tip		0.0087	90.9	0.03	0.39	1.65	0.38	16.8	7.11	48.8	100.8	269	72.0	705	155.8
SML54Z-8.1IC	gray, unzoned euhedral center		0.0054	40.8	0.05	0.97	3.03	0.98	22.6	7.46	26.9	74.6	122	25.3	204	40.2
SML54Z-8.2T	med-dark gray o-zoned tip	16.4±0.5	0.0021	52.5	0.02	0.33	1.91	0.34	21.8	9.17	51.3	117.5	236	51.5	394	68.8
SML54Z-9.1C	gray unzoned euh center		0.0192	70.3	0.21	3.47	9.80	2.56	64.7	20.10	76.6	201.6	309	62.3	484	88.0
SML54Z-9.2IR	gray euhedral o-zoned inner rim	17.0±0.3	0.0042	59.6	0.05	0.69	2.73	0.73	23.6	8.82	41.8	102.1	187	40.7	336	63.7
SML54Z-9.3T	dark euhedral rim		0.0018	102.4	0.03	0.23	0.90	0.17	10.5	4.91	53.0	81.0	372	117.8	1419	372.2
SML54Z-10.1C	*dark, zoned rounded core*	*17.2±0.2*	*0.0818*	*65.3*	*0.03*	*0.31*	*1.33*	*0.21*	*15.8*	*7.86*	*64.3*	*120.4*	*368*	*97.1*	*935*	*188.6*
SML54Z-10.2R	*med-dark, euhedral, o-zoned rim*		*0.0738*	*49.8*	*0.03*	*0.38*	*1.72*	*0.36*	*17.2*	*7.17*	*40.4*	*90.7*	*184*	*41.7*	*336*	*60.1*

APPENDIX B

SEM SPECTRA FOR OXIDE MINERALS FROM MOUNT ST. HELENS

APPENDIX B

SEM SPECTRA FOR OXIDE MINERALS FROM MOUNT ST. HELENS

SHL08-34Z

2/11/2011 12:44:33 PM

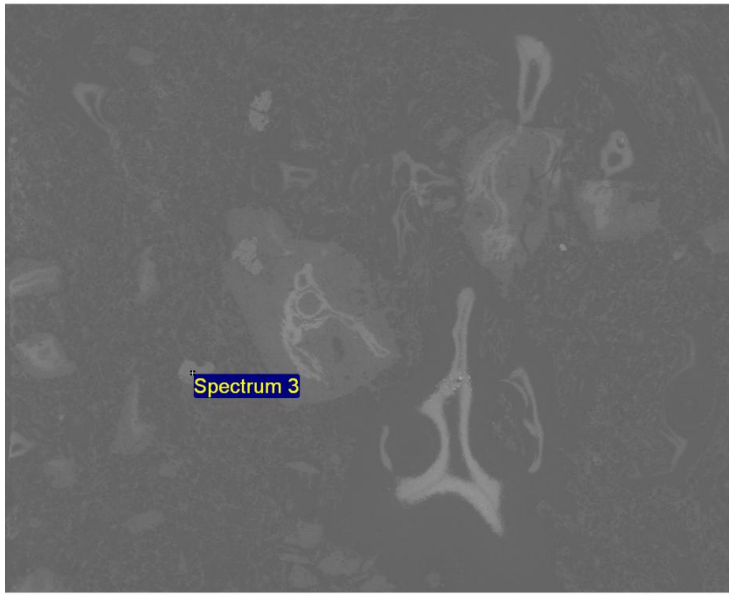

Element	App Conc.	Intensity Corrn.	Weight%	Weight% Sigma	Atomic%
O K	13.94	0.7357	24.50	2.79	51.09
Mg K	0.67	0.6388	1.35	0.63	1.85
Ti K	20.86	0.9617	28.05	2.06	19.53
Fe K	32.32	0.9066	46.10	2.82	27.53
Totals			100.00		

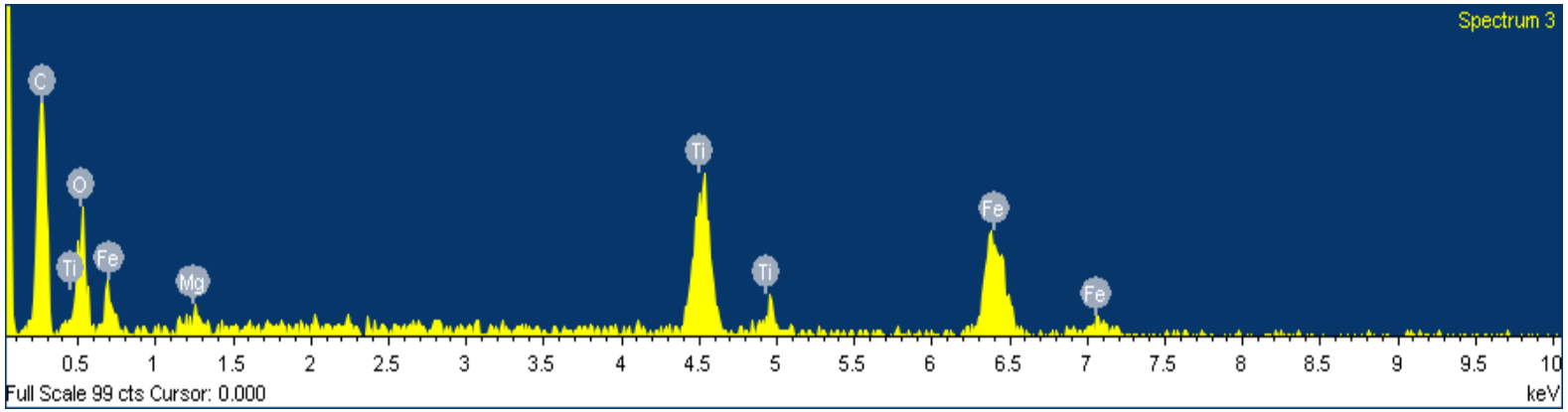

SHL08-34Z

2/11/2011 12:44:56 PM

Element	App Conc.	Intensity Corrn.	Weight%	Weight% Sigma	Atomic%
O K	2.66	1.7443	13.46	1.96	35.20
Fe K	9.42	0.9629	86.54	1.96	64.80
Totals			100.00		

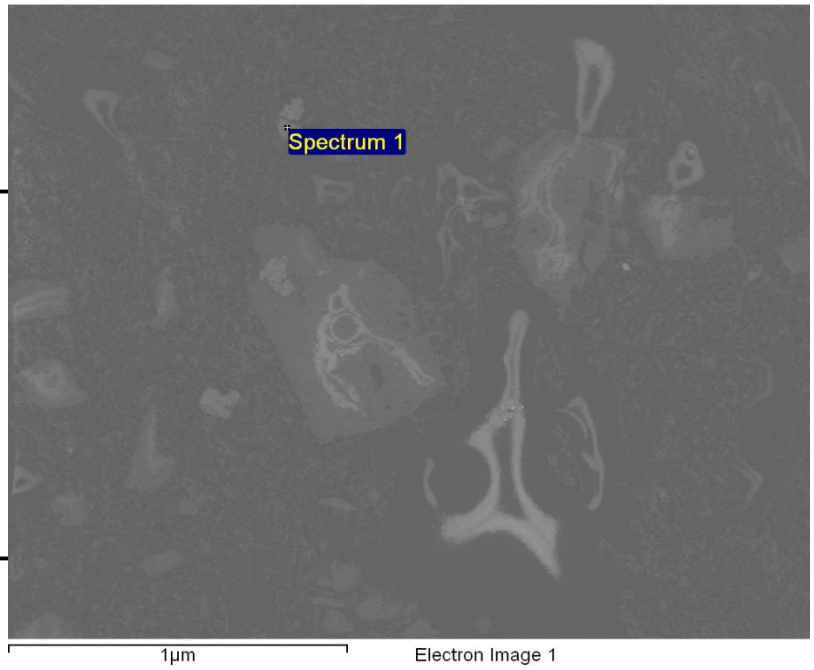

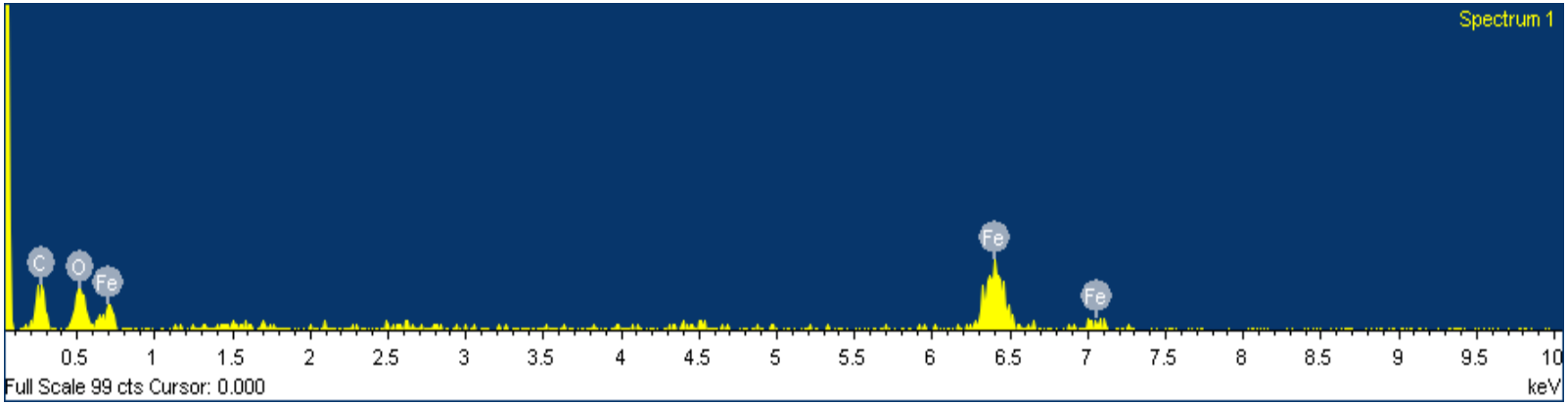

SHL08-34Z

2/11/2011 12:45:06 PM

Element	App Conc.	Intensity Corrn.	Weight%	Weight% Sigma	Atomic%
O K	10.73	1.4594	9.44	1.86	26.13
Al K	0.95	0.6937	1.76	0.65	2.88
Ti K	3.19	1.0305	3.97	1.20	3.67
Fe K	63.91	0.9672	84.84	2.22	67.31
Totals			100.00		

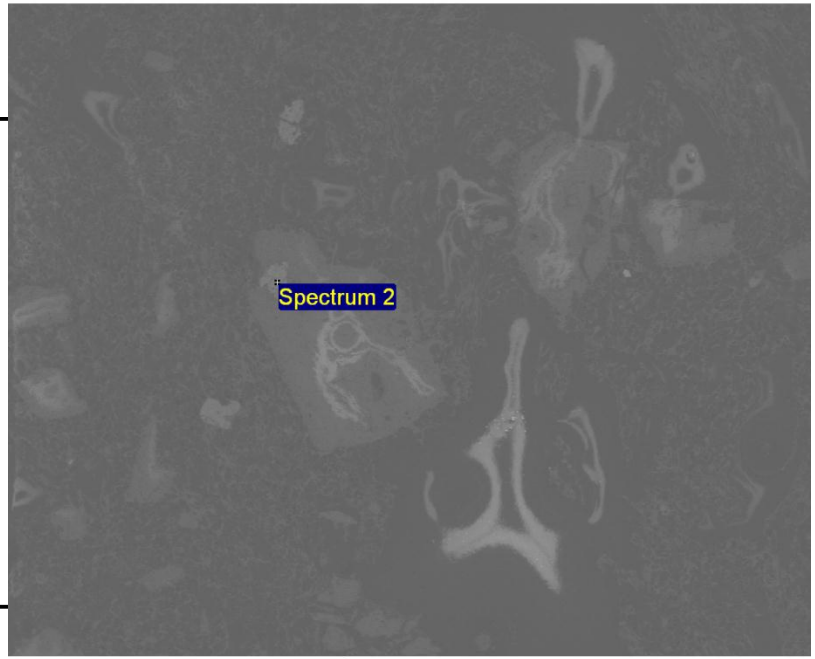

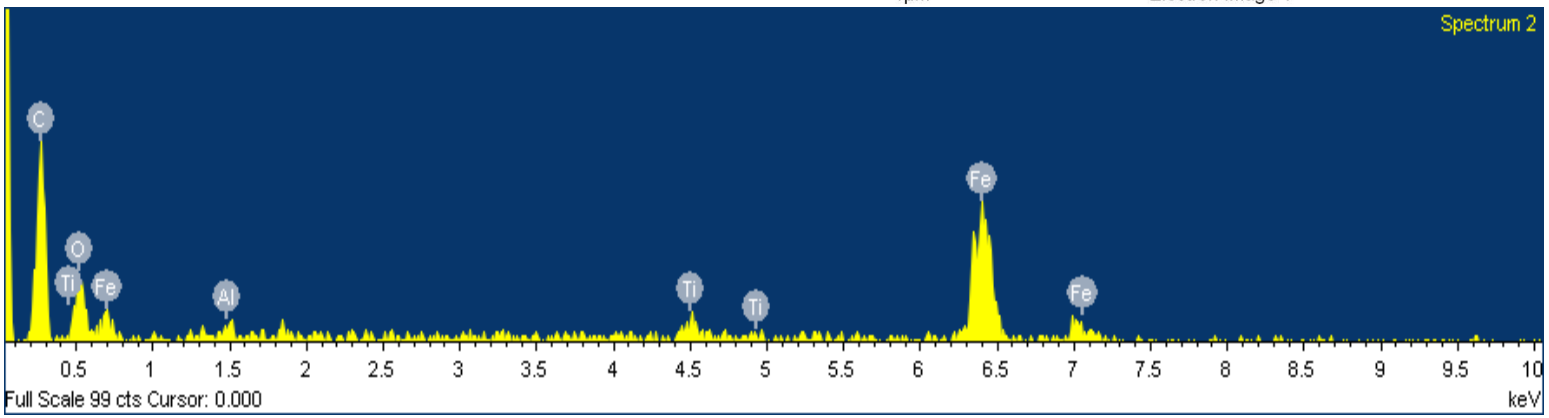

SHL08-34Z

2/11/2011 12:47:27 PM

Element	App Conc.	Intensity Corrn.	Weight%	Weight% Sigma	Atomic%
O K	7.23	1.3215	16.16	2.43	40.43
Si K	2.14	0.7428	8.49	1.35	12.10
Cu L	20.30	0.7952	75.35	2.62	47.47
Totals			100.00		

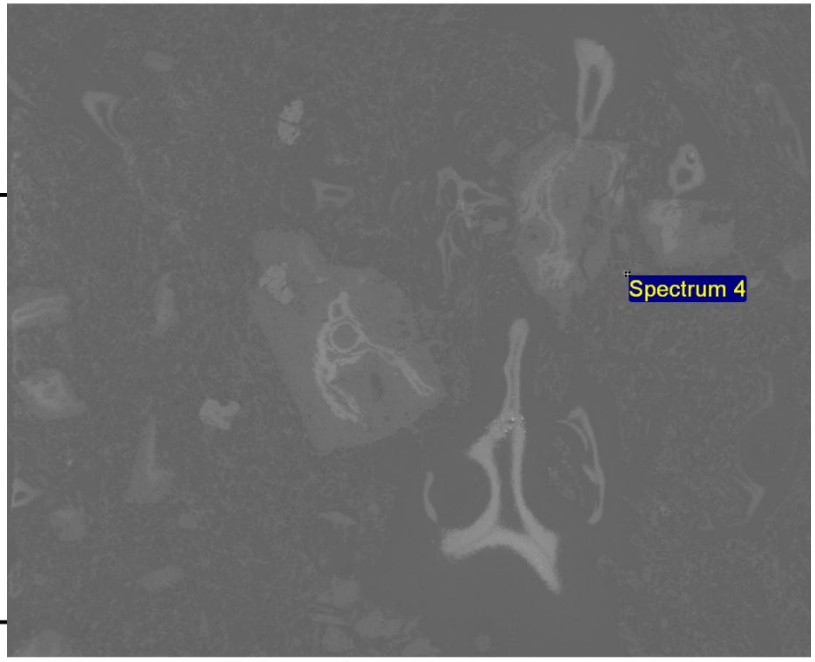

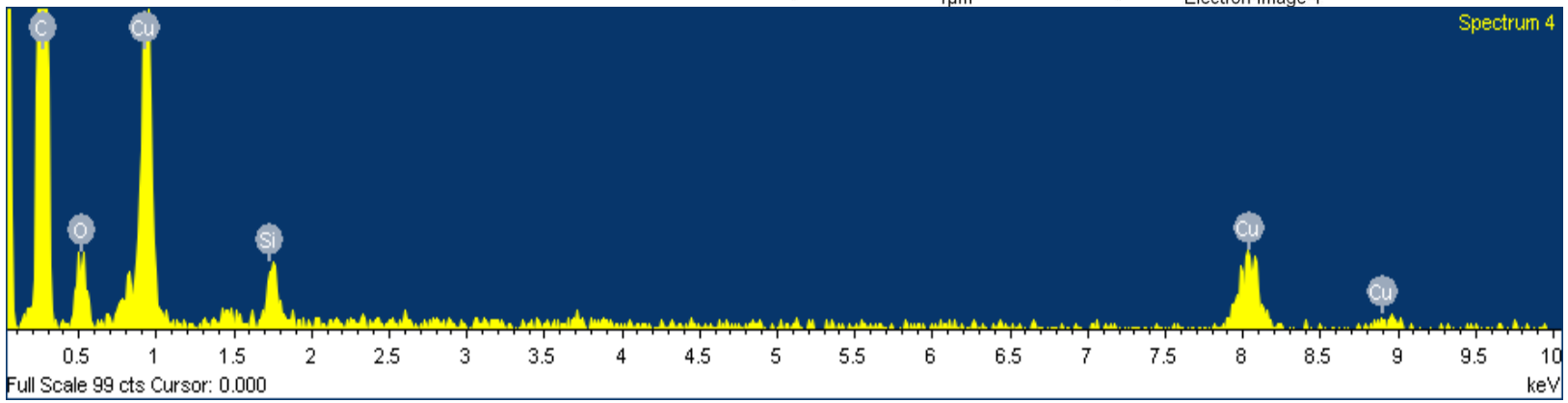

SHL08-34Z

Element	App Conc.	Intensity Corrn.	Weight%	Weight% Sigma	Atomic%
Totals			.00		

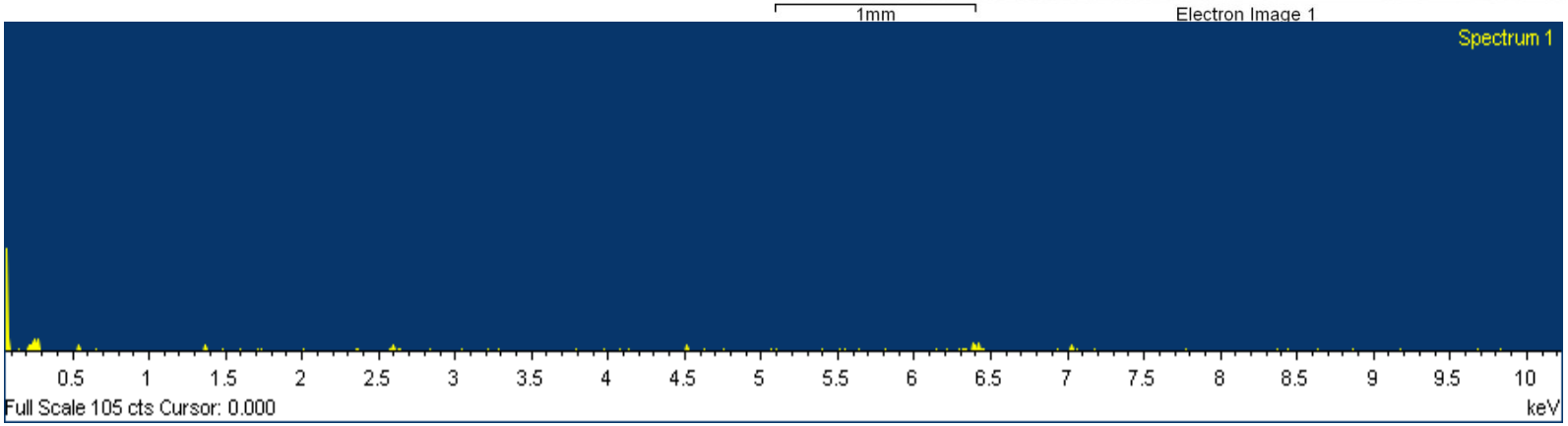

SHL08-34Z

Element	App Conc.	Intensity Corrn.	Weight%	Weight% Sigma	Atomic%
O K	18.15	1.7345	11.91	2.41	32.06
Fe K	74.88	0.9670	88.09	2.41	67.94
Totals			100.00		

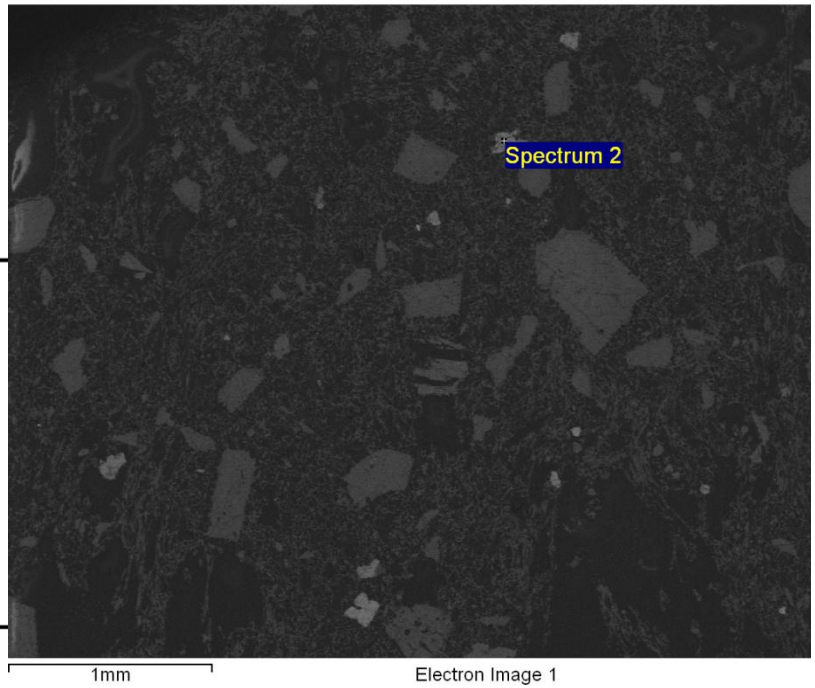

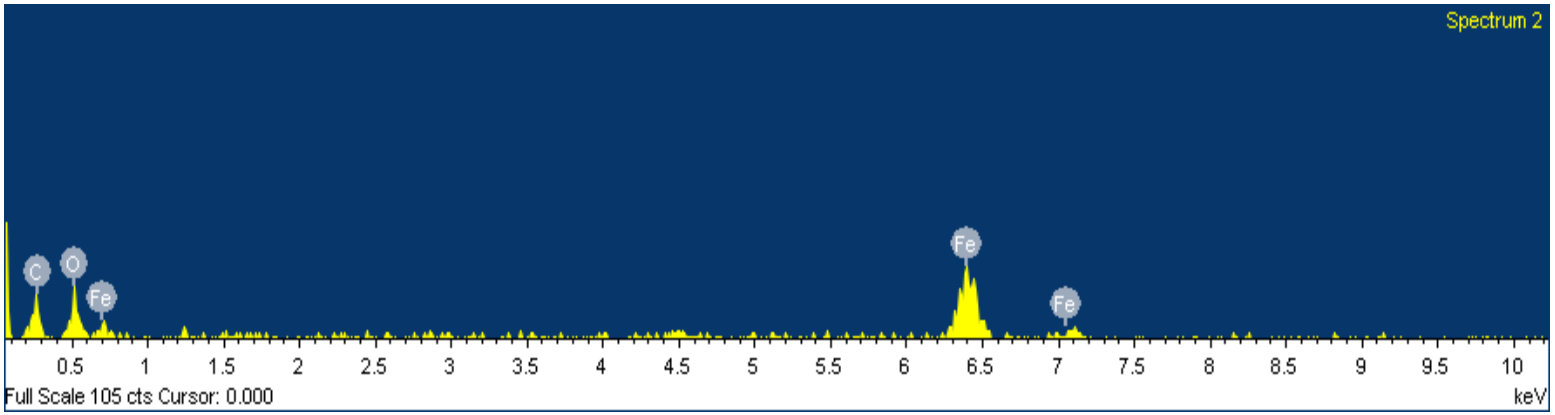

SHL08-34Z

2/11/2011 1:08:07 PM

Element	App Conc.	Intensity Corrn.	Weight%	Weight% Sigma	Atomic%
O K	13.57	0.8335	20.62	3.14	46.38
Ti K	17.89	0.9802	23.13	2.32	17.37
Fe K	40.98	0.9232	56.25	3.31	36.25
Totals			100.00		

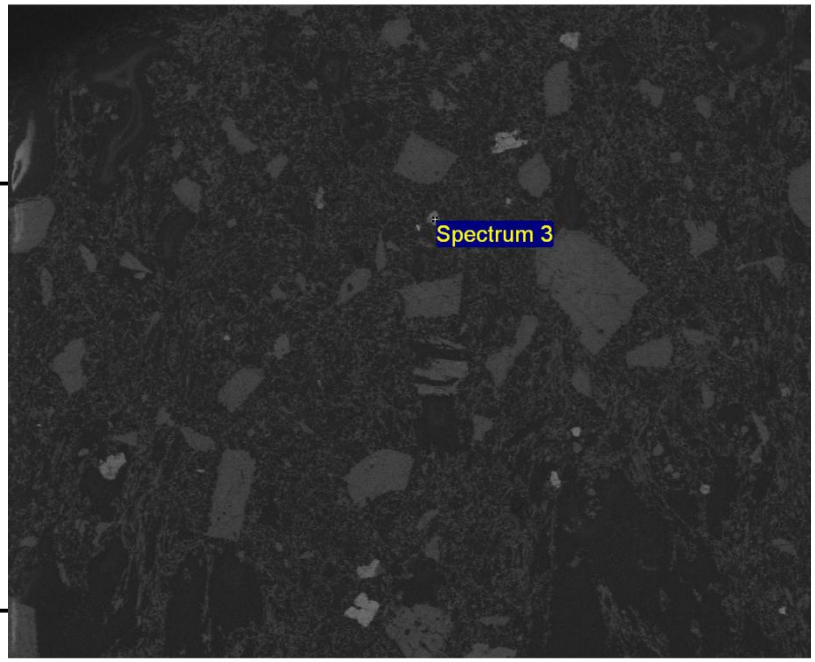

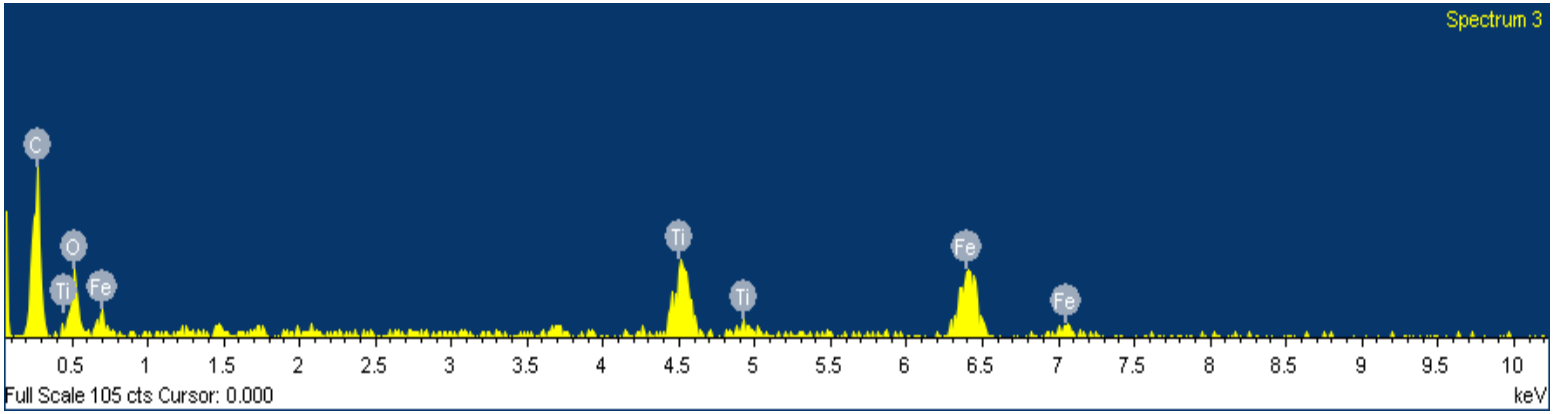

SHL08-34Z

2/11/2011 1:08:14 PM

Element	App Conc.	Intensity Corrn.	Weight%	Weight% Sigma	Atomic%
O K	30.17	1.2161	55.58	2.92	68.56
Al K	3.64	1.0161	8.02	1.26	5.87
Si K	15.67	0.9636	36.40	2.64	25.58
Totals			100.00		

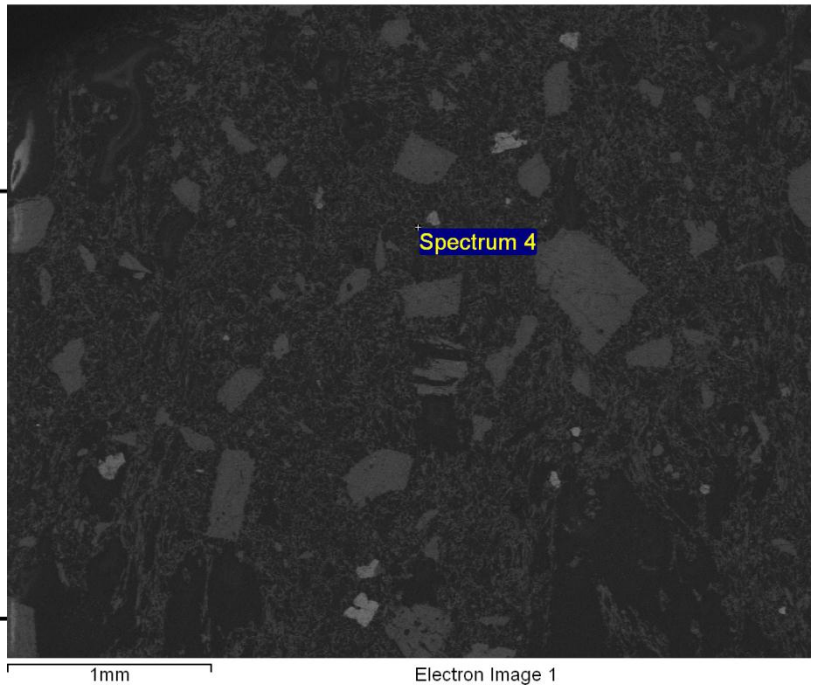

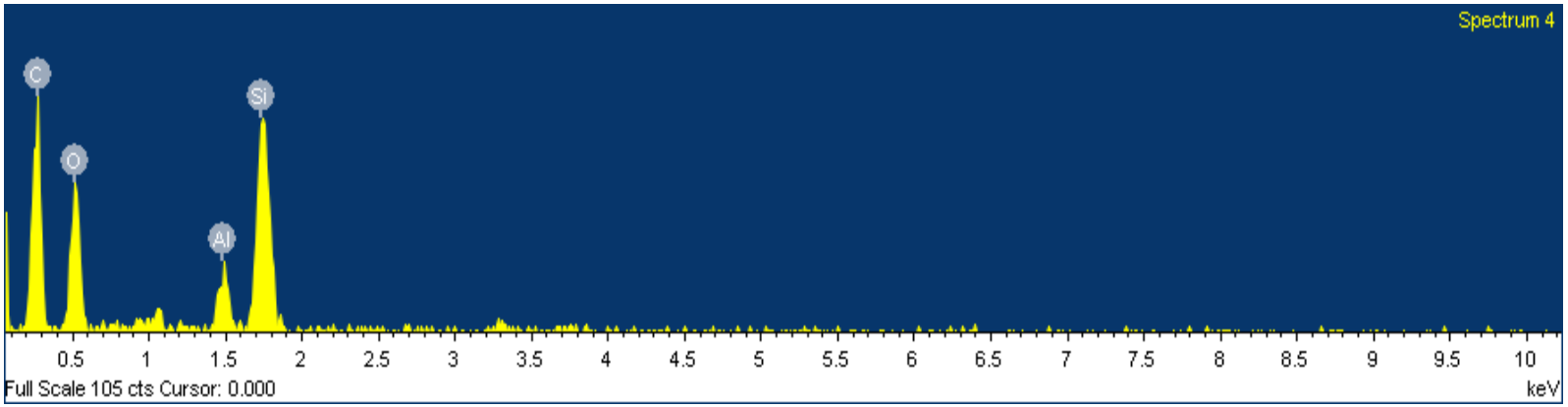

SHL08-34Z

2/11/2011 1:08:29 PM

Element	App Conc.	Intensity Corrn.	Weight%	Weight% Sigma	Atomic%
O K	16.98	0.7911	23.25	2.15	50.06
Ti K	22.67	0.9708	25.29	1.51	18.19
Fe K	43.46	0.9144	51.46	2.17	31.75
Totals			100.00		

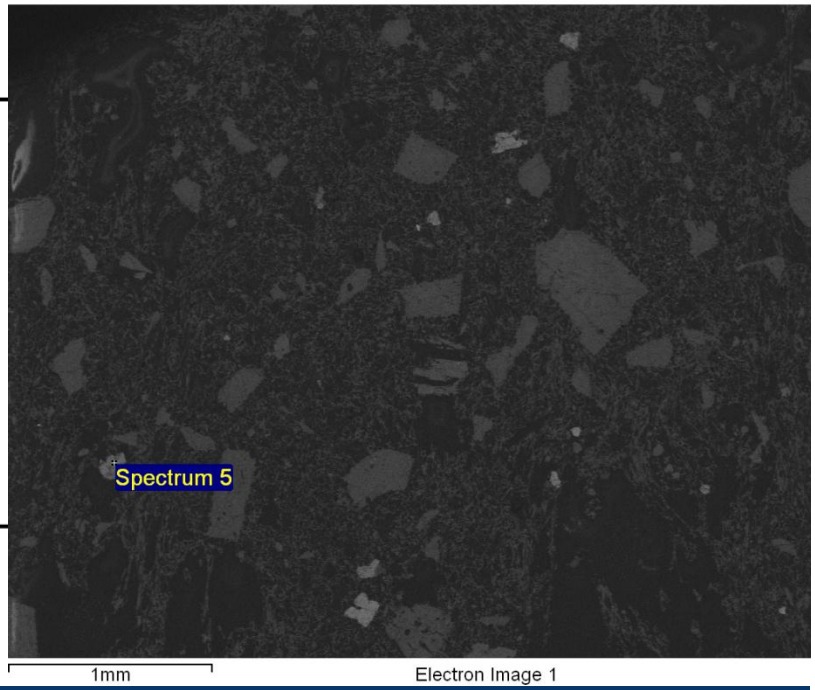

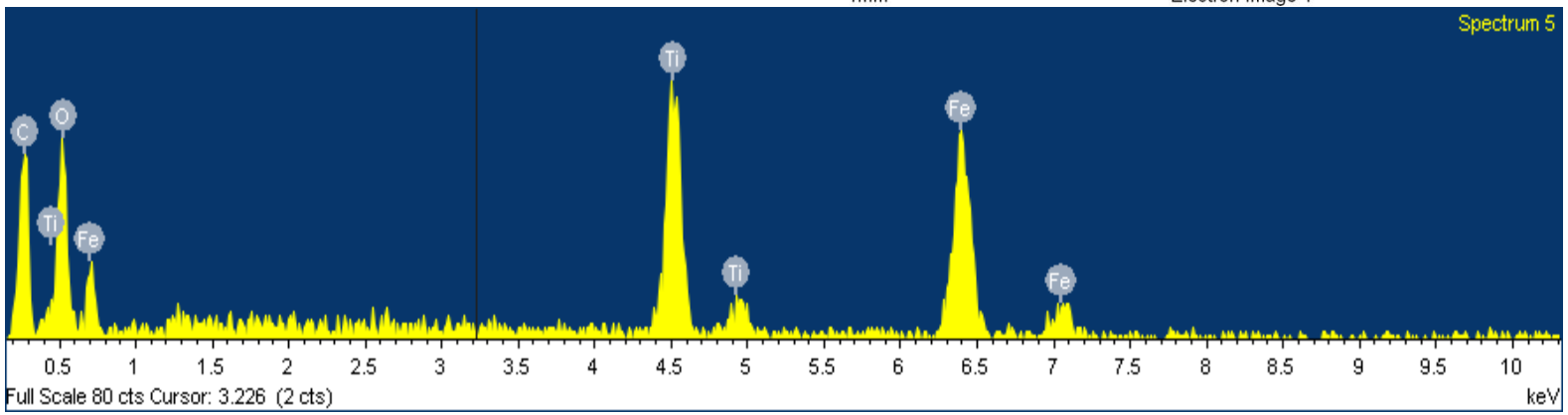

SHL08-34Z

2/11/2011 1:08:39 PM

Element	App Conc.	Intensity Corrn.	Weight%	Weight% Sigma	Atomic%
O K	17.62	0.8341	27.22	1.86	55.34
Ti K	17.48	0.9617	23.43	1.27	15.91
Fe K	34.71	0.9063	49.35	1.87	28.75
Totals			100.00		

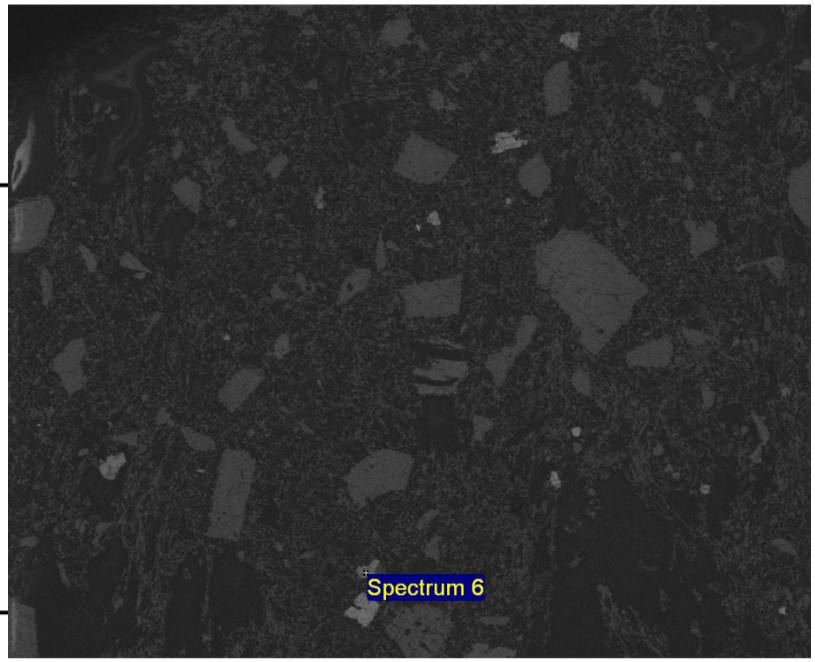

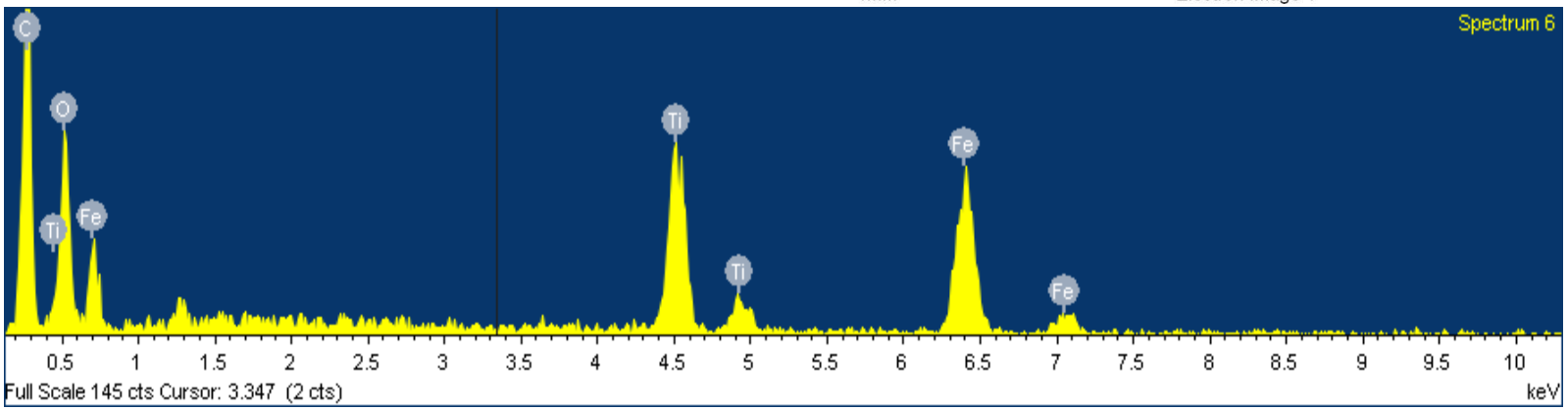

SHL08-34Z

2/11/2011 1:08:49 PM

Element	App Conc.	Intensity Corrn.	Weight%	Weight% Sigma	Atomic%
O K	11.28	1.4668	8.82	0.92	24.92
Al K	0.52	0.6895	0.86	0.27	1.45
Ti K	3.56	1.0347	3.95	0.61	3.72
Fe K	73.06	0.9702	86.37	1.11	69.91
Totals			100.00		

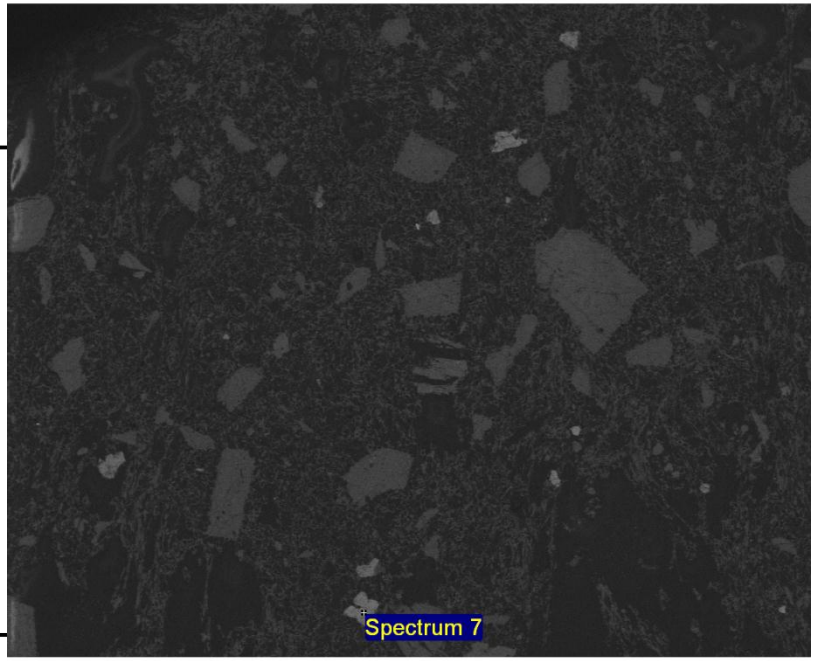

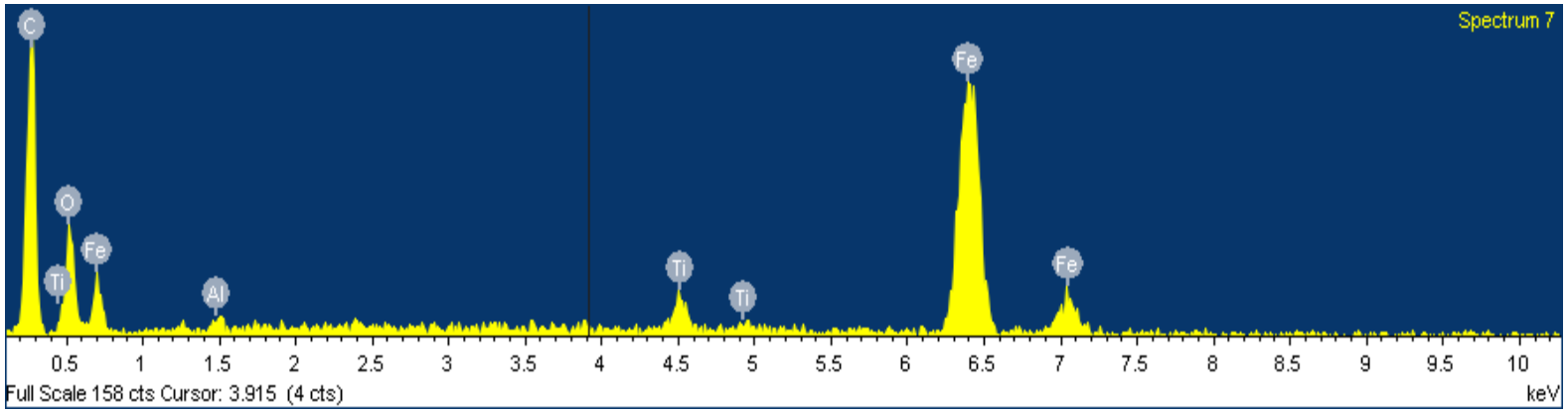

SHL08-34Z

2/11/2011 1:08:58 PM

Element	App Conc.	Intensity Corrn.	Weight%	Weight% Sigma	Atomic%
O K	27.12	1.5772	23.80	1.63	51.39
Al K	0.89	0.7121	1.74	0.46	2.22
Ti K	2.23	0.9926	3.11	0.73	2.24
Fe K	47.96	0.9306	71.35	1.76	44.14
Totals			100.00		

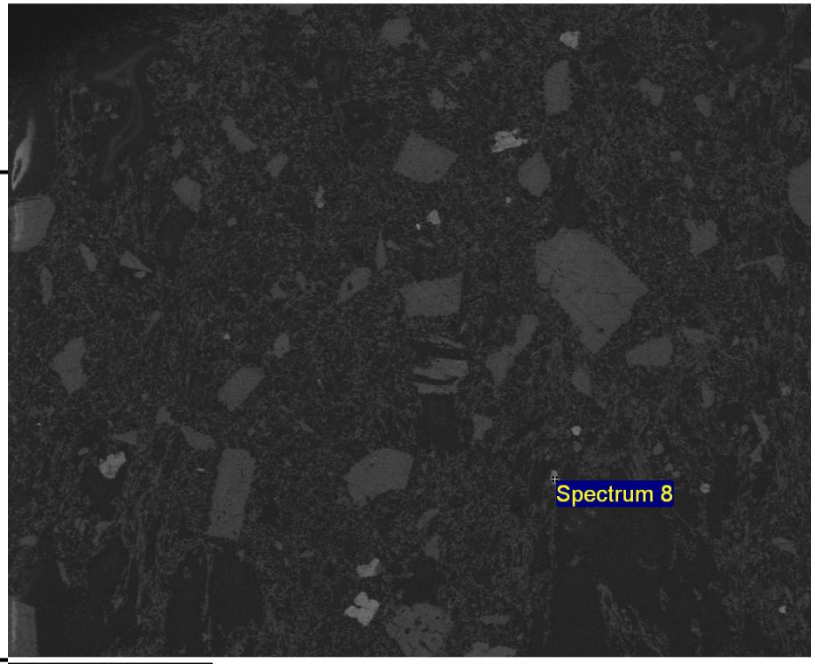

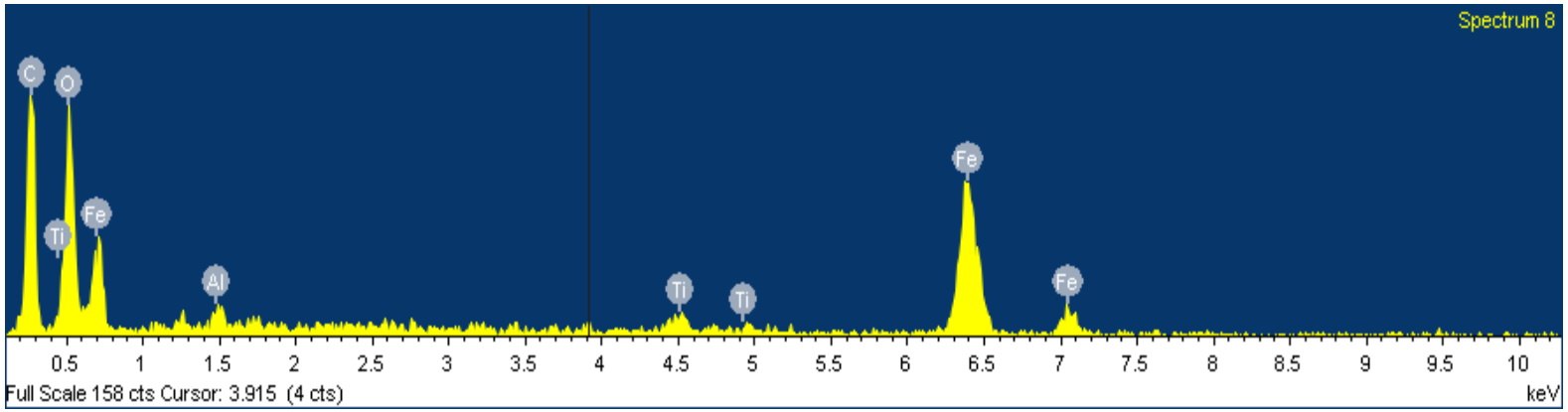

SHL08-34Z

2/11/2011 1:09:04 PM

Element	App Conc.	Intensity Corrn.	Weight%	Weight% Sigma	Atomic%
O K	14.72	1.4919	11.32	1.33	30.68
Ti K	3.46	1.0302	3.85	0.82	3.49
Fe K	71.31	0.9649	84.83	1.52	65.84
Totals			100.00		

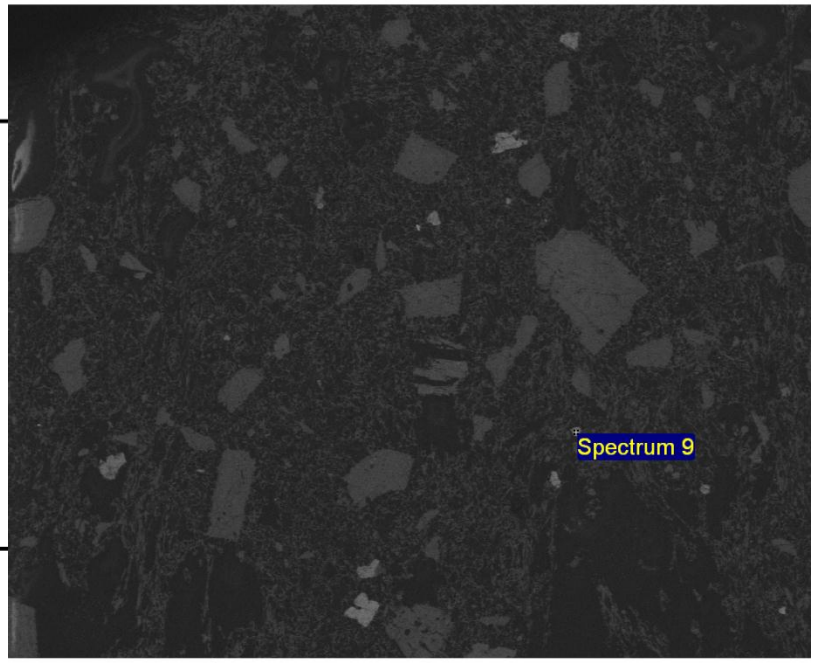

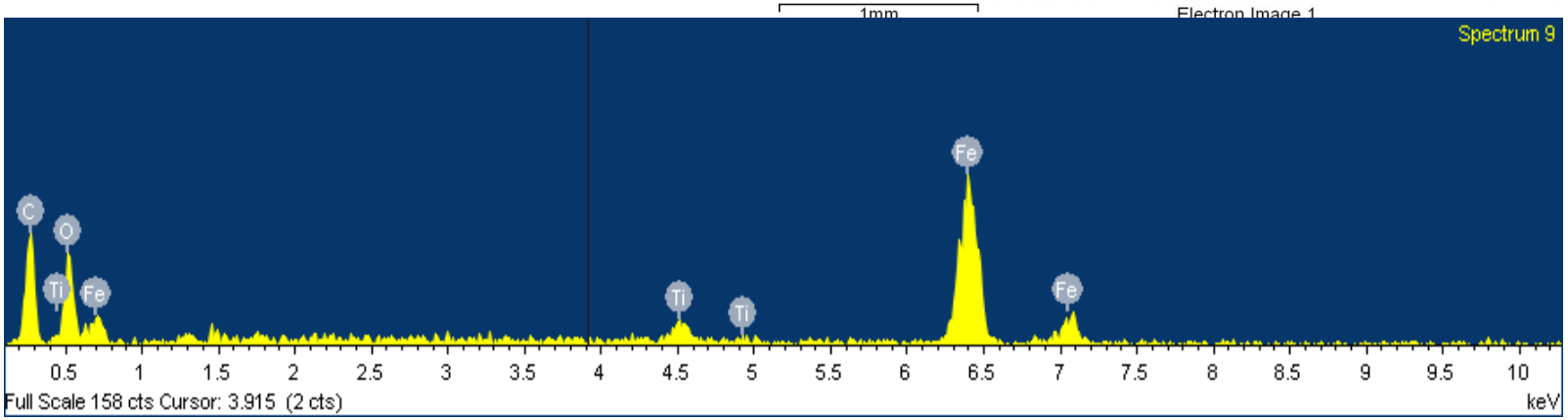

SHL08-34Z

2/11/2011 1:09:11 PM

Element	App Conc.	Intensity Corrn.	Weight%	Weight% Sigma	Atomic%
O K	8.11	0.7525	20.69	2.97	46.28
Ti K	13.79	0.9765	27.13	2.19	20.27
Fe K	24.97	0.9195	52.18	2.99	33.45
Totals			100.00		

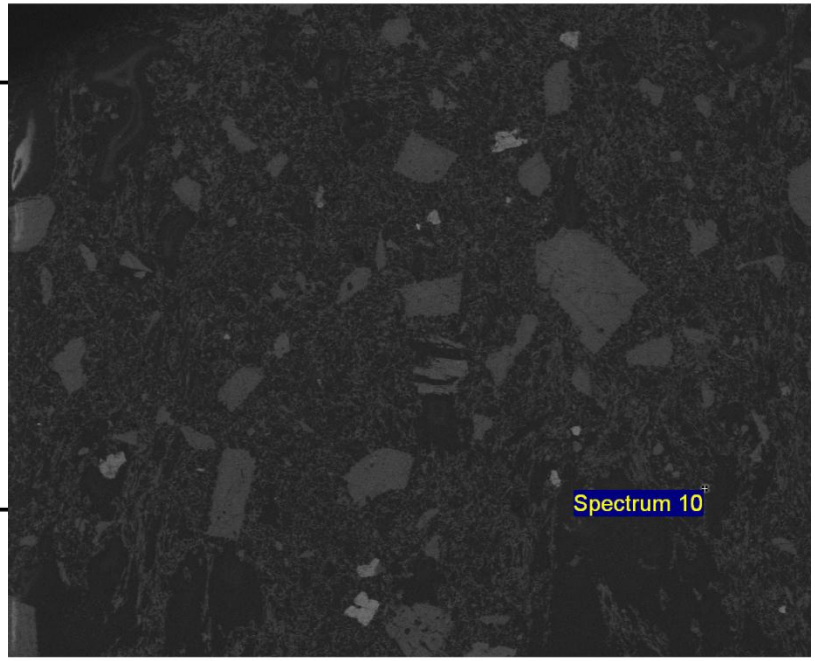

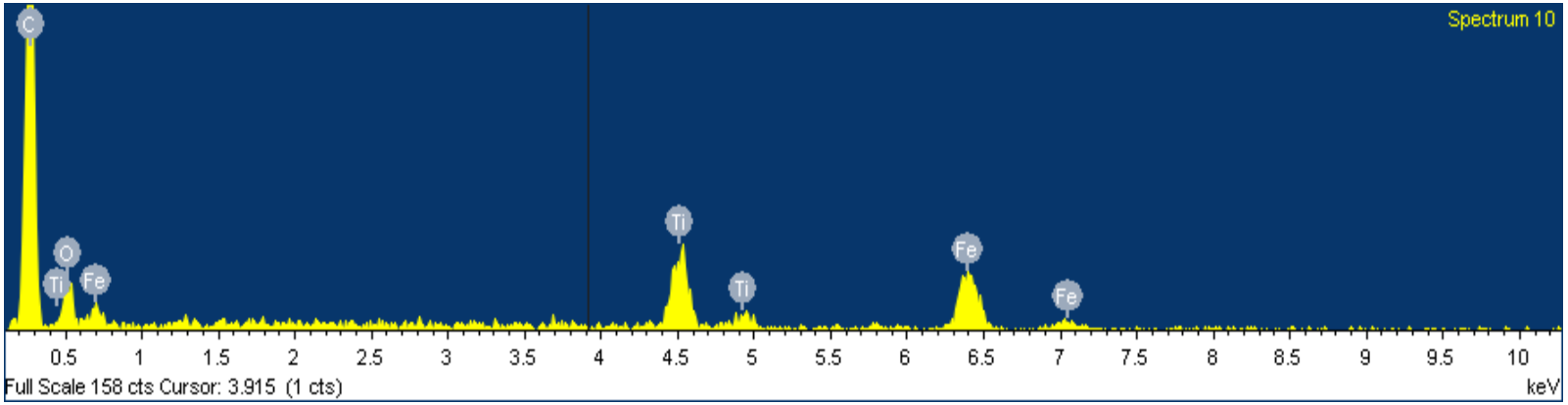

SHL08-34Z

2/11/2011 1:09:17 PM

Element	App Conc.	Intensity Corrn.	Weight%	Weight% Sigma	Atomic%
O K	30.96	1.5984	25.54	1.42	53.87
Al K	0.71	0.7127	1.32	0.39	1.65
Ti K	2.24	0.9892	2.99	0.59	2.11
Fe K	49.28	0.9269	70.15	1.53	42.38
Totals			100.00		

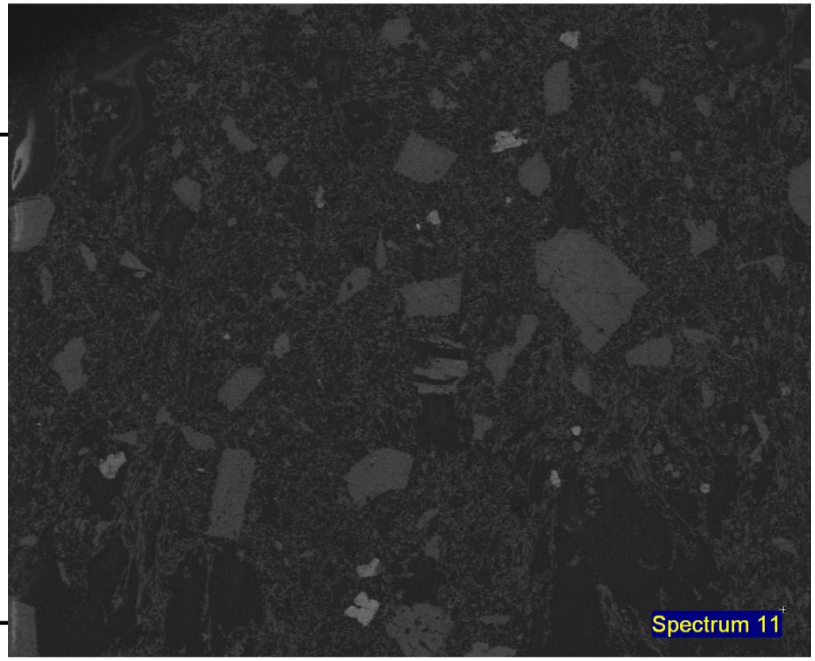

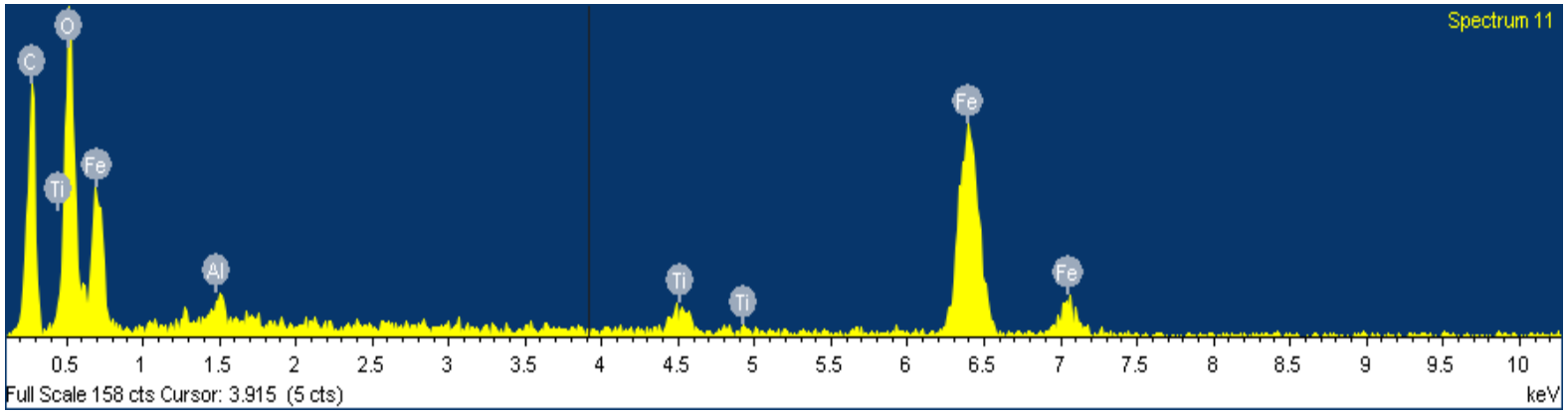

SHL06-3Z

2/11/2011 1:30:41 PM

Element	App Conc.	Intensity Corrn.	Weight%	Weight% Sigma	Atomic%
O K	32.73	1.7926	20.84	1.50	47.88
Fe K	65.45	0.9434	79.16	1.50	52.12
Totals			100.00		

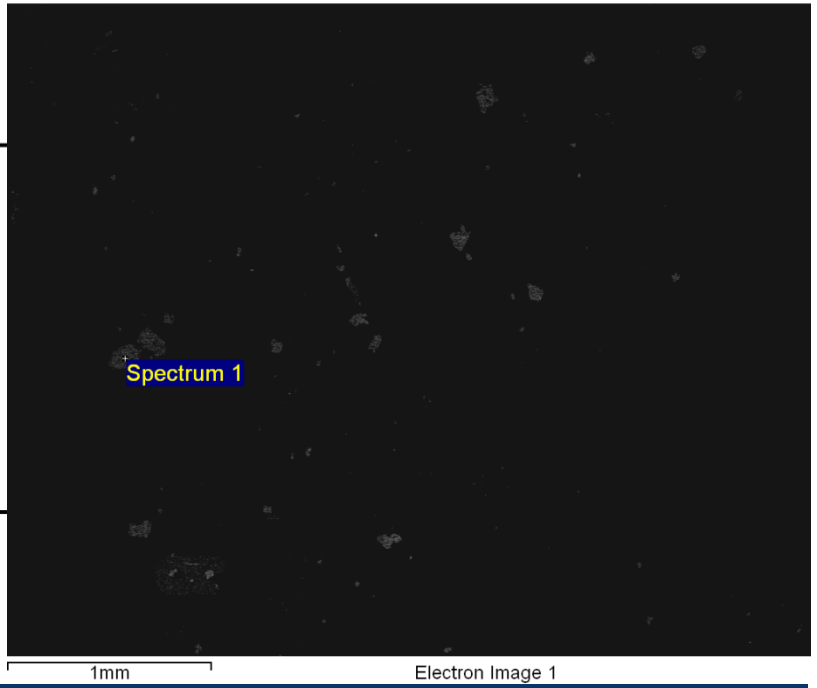

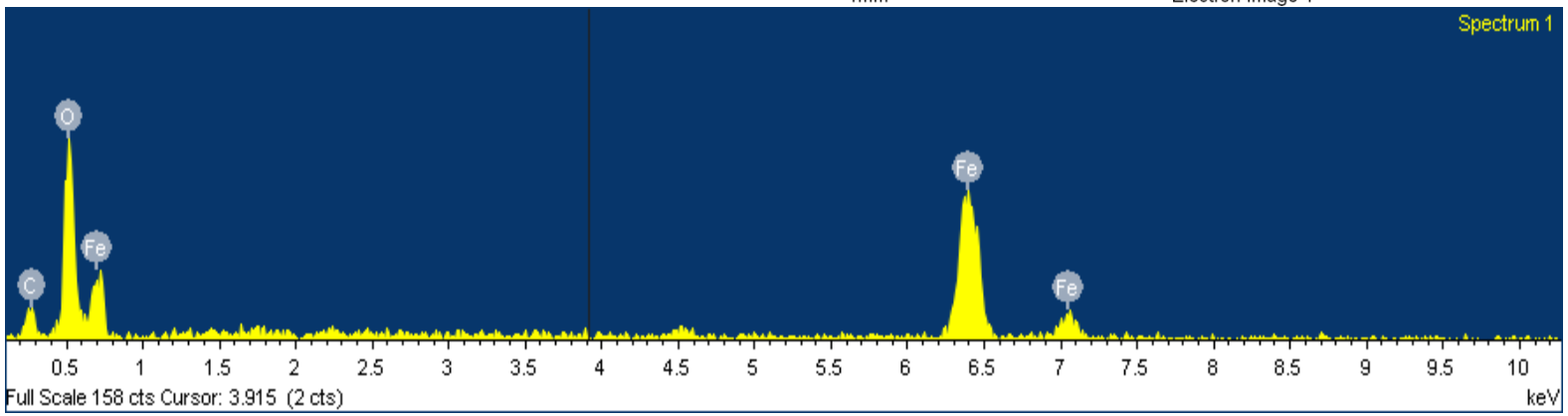

SHL06-3Z

Element	App Conc.	Intensity Corrn.	Weight%	Weight% Sigma	Atomic%
O K	21.84	0.8314	30.88	2.15	59.61
Ti K	19.19	0.9516	23.70	1.43	15.28
Fe K	34.67	0.8972	45.42	2.11	25.11
Totals			100.00		

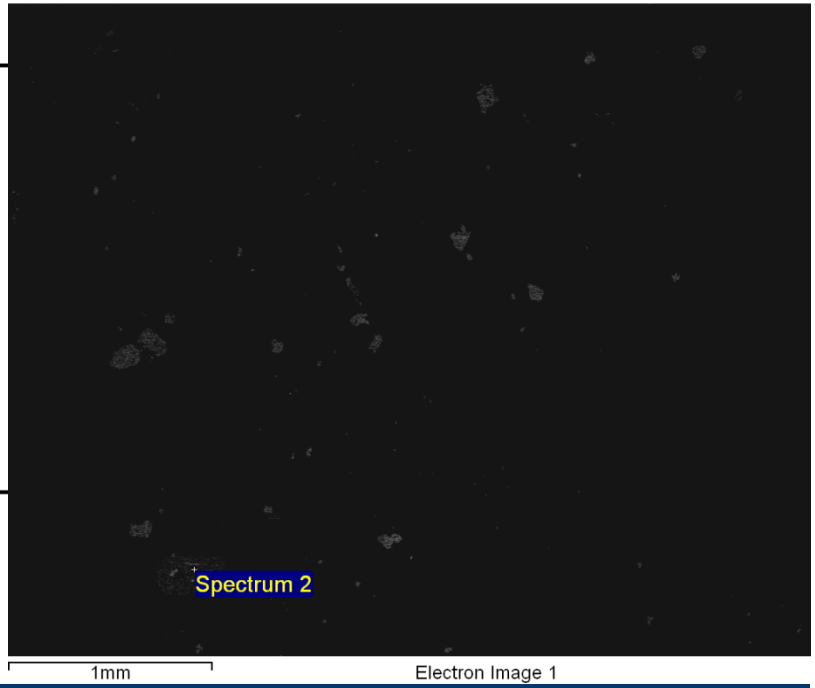

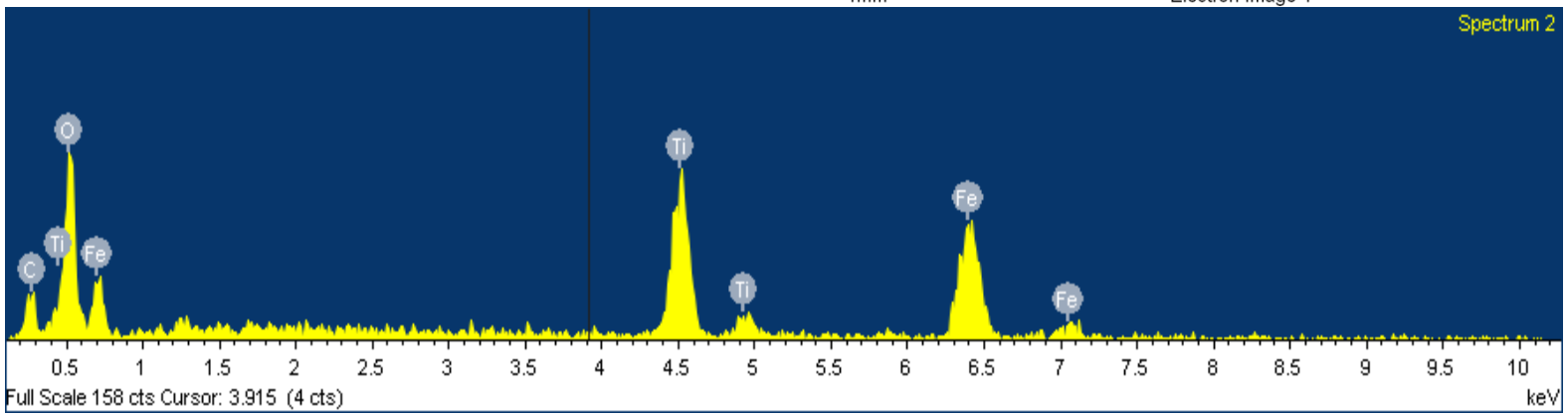

SHL06-3Z

2/11/2011 1:30:56 PM

Element	App Conc.	Intensity Corrn.	Weight%	Weight% Sigma	Atomic%
O K	15.57	0.4887	42.39	2.80	62.79
P K	19.59	1.4371	18.15	1.38	13.88
Ca K	30.11	1.0158	39.46	2.20	23.33
Totals			100.00		

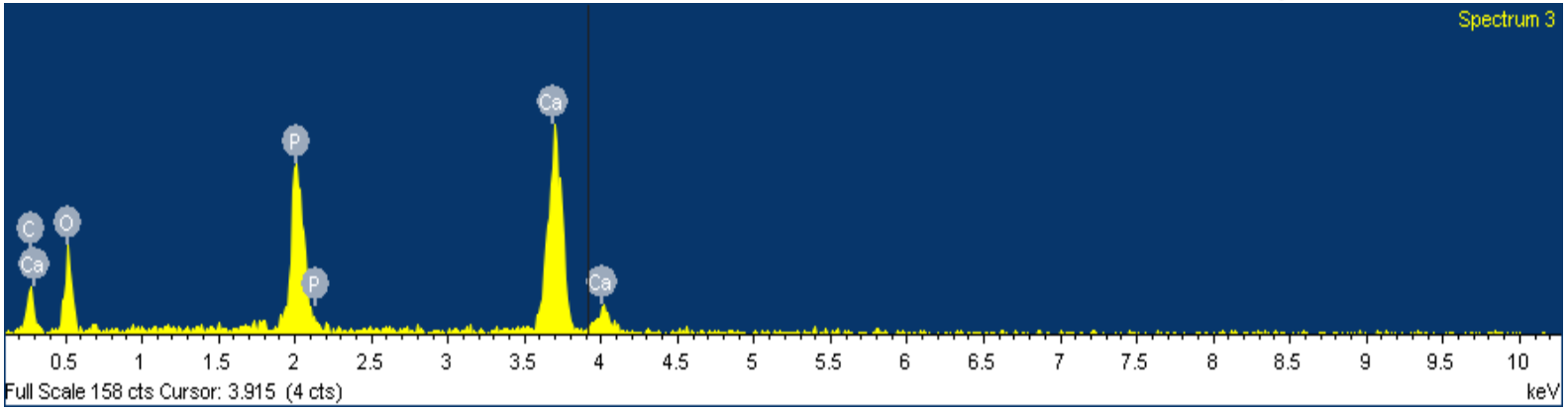

SHL06-3Z

2/11/2011 1:31:04 PM

Element	App Conc.	Intensity Corrn.	Weight%	Weight% Sigma	Atomic%
O K	45.80	1.4800	42.40	2.57	68.69
Al K	1.74	0.7759	3.08	0.66	2.96
Si K	3.69	0.8554	5.92	0.87	5.46
Ti K	2.83	0.9189	4.22	1.04	2.29
Fe K	28.28	0.8732	44.39	2.69	20.60
Totals			100.00		

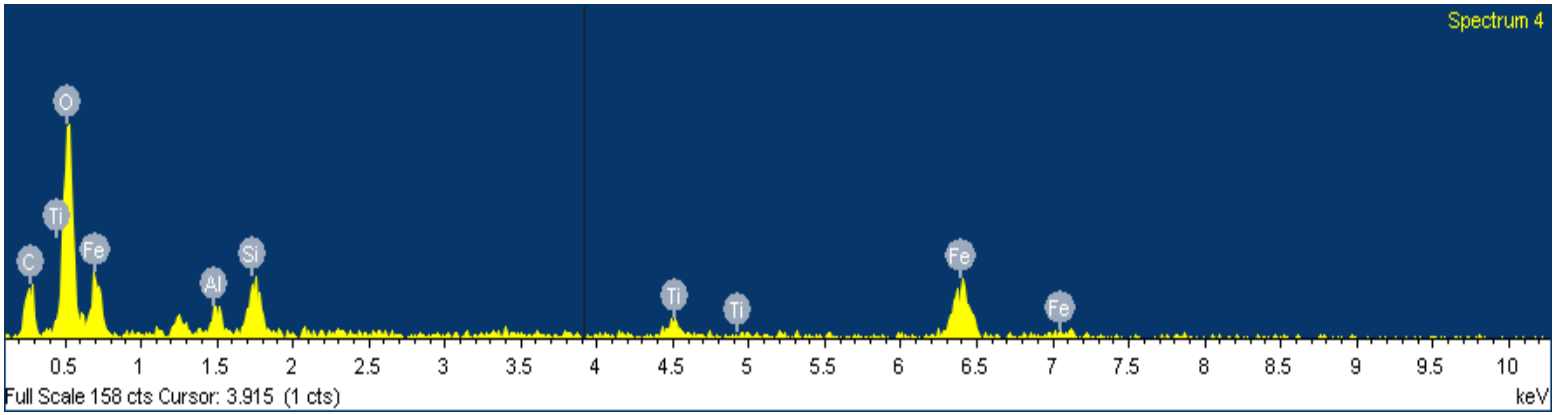

SHL06-3Z

2/11/2011 1:31:11 PM

Element	App Conc.	Intensity Corrn.	Weight%	Weight% Sigma	Atomic%
O K	36.66	1.8382	27.51	2.31	56.98
Fe K	48.68	0.9266	72.49	2.31	43.02
Totals			100.00		

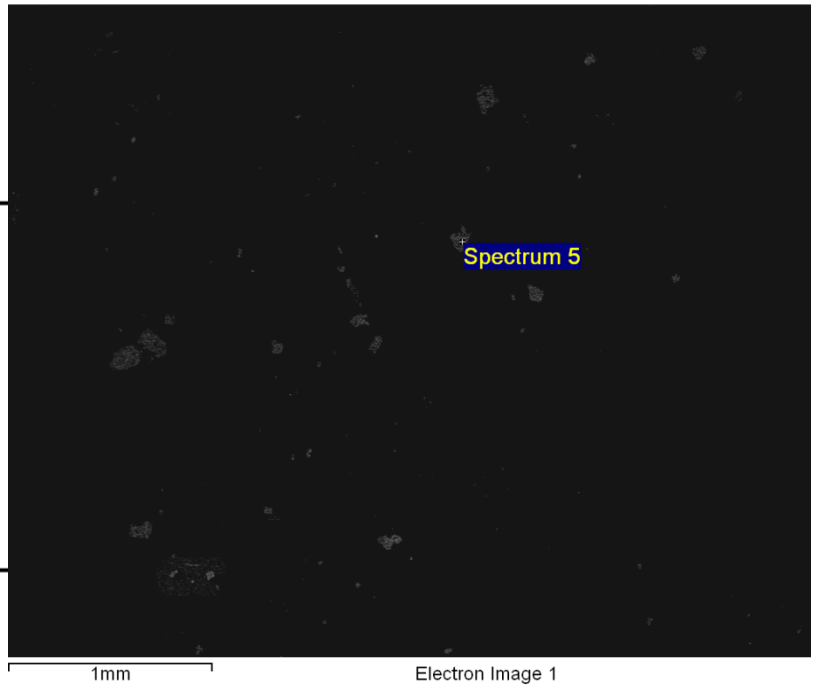

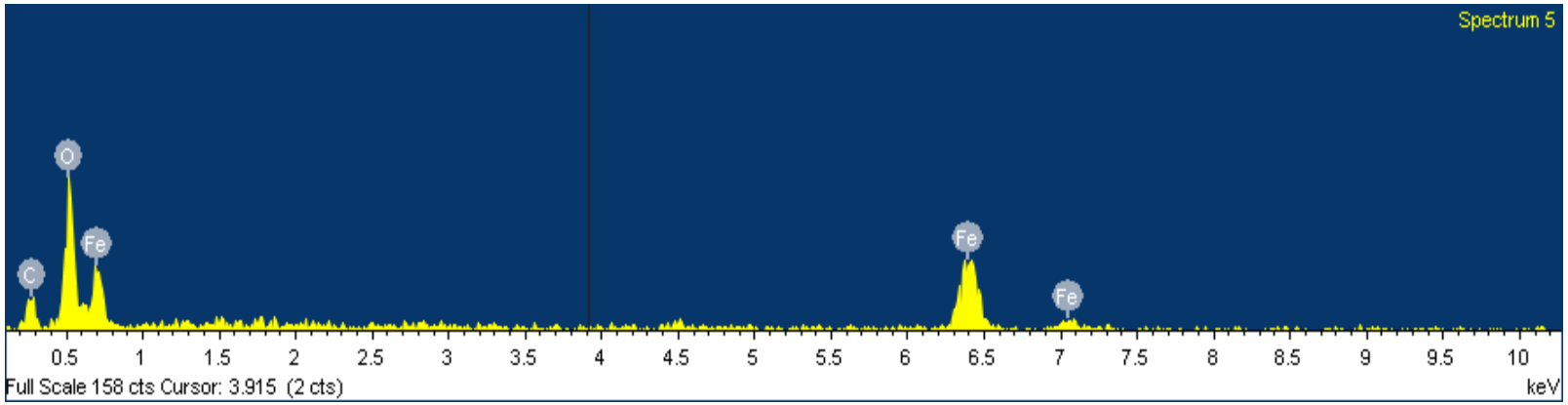

SHL06-3Z

2/11/2011 1:41:02 PM

Element	App Conc.	Intensity Corrn.	Weight%	Weight% Sigma	Atomic%
O K	35.81	1.8081	23.17	1.75	51.28
Fe K	61.56	0.9376	76.83	1.75	48.72
Totals			100.00		

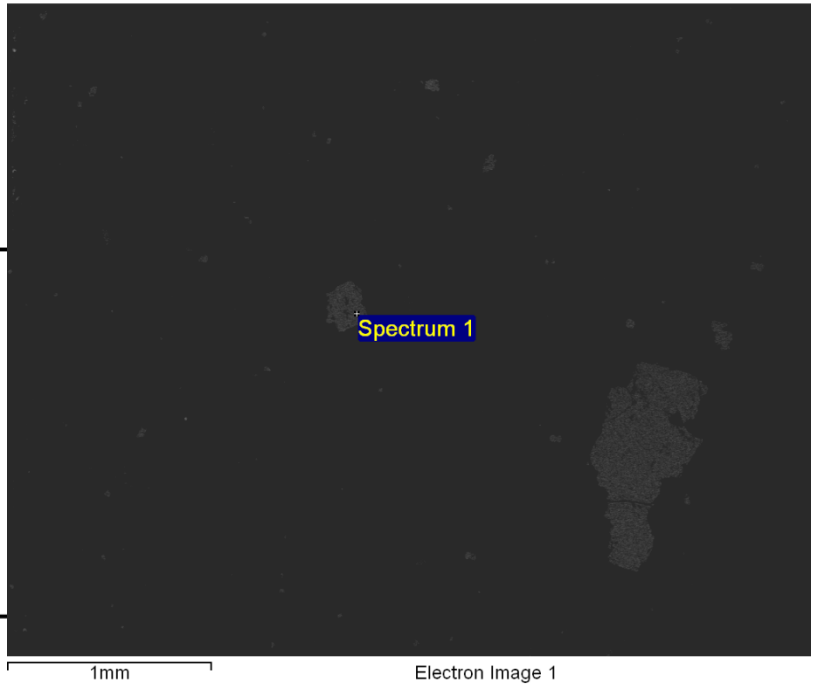

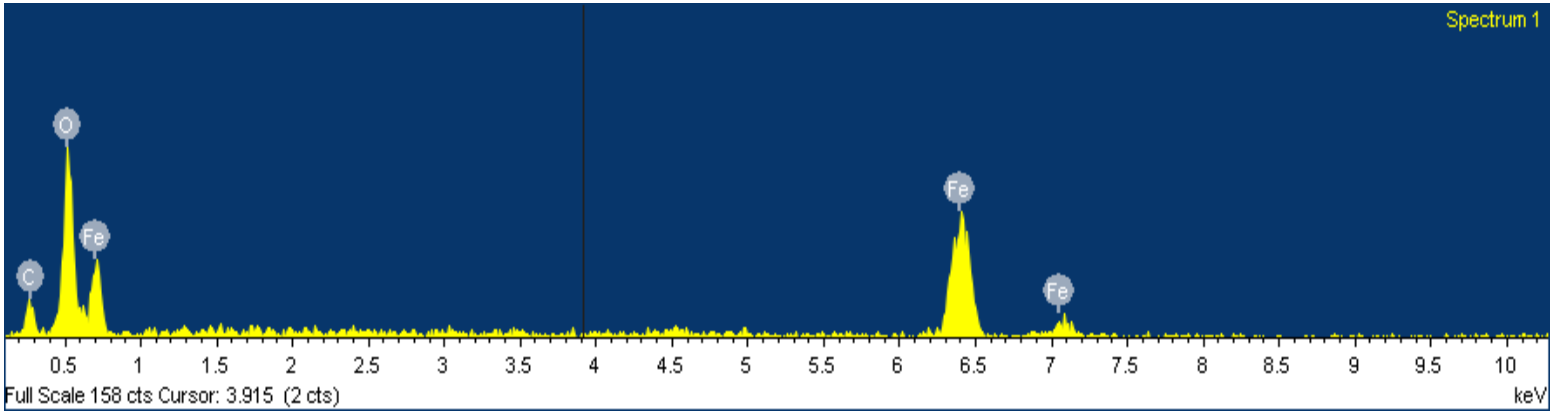

SHL06-3Z

2/11/2011 1:41:24 PM

Element	App Conc.	Intensity Corrn.	Weight%	Weight% Sigma	Atomic%
O K	35.45	1.5405	25.20	1.48	53.82
Ti K	3.76	0.9916	4.15	0.65	2.96
Fe K	59.87	0.9286	70.65	1.56	43.22
Totals			100.00		

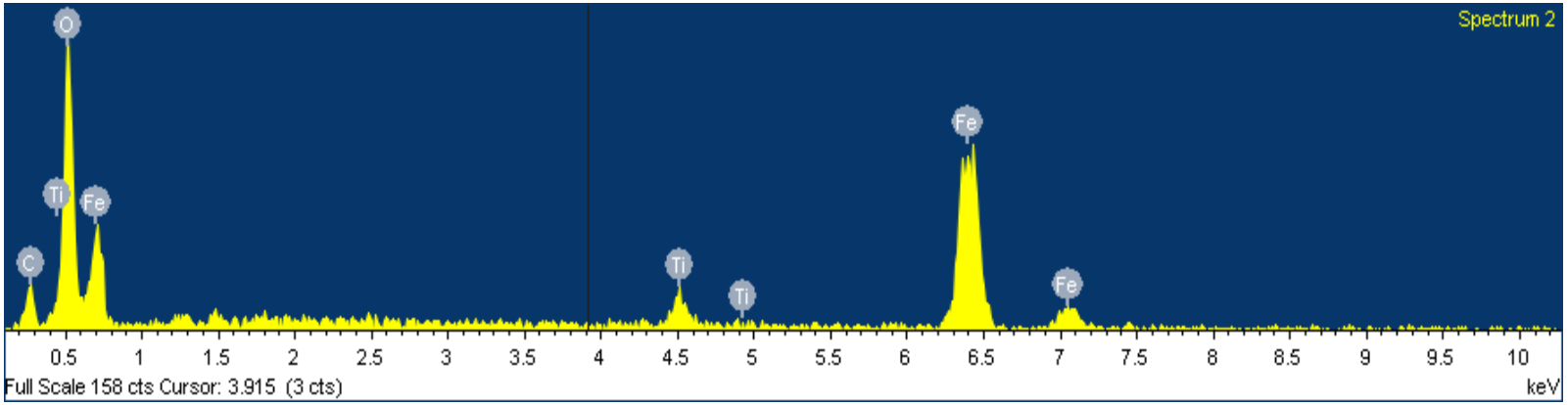

SHL06-3Z

2/11/2011 1:41:29 PM

Element	App Conc.	Intensity Corrn.	Weight%	Weight% Sigma	Atomic%
O K	25.60	0.9395	37.80	2.50	60.50
Si K	14.42	0.9375	21.32	1.36	19.44
Ca K	2.39	1.0511	3.15	0.67	2.01
Ti K	6.23	0.8767	9.85	1.18	5.26
Fe K	17.18	0.8542	27.88	2.39	12.79
Totals			100.00		

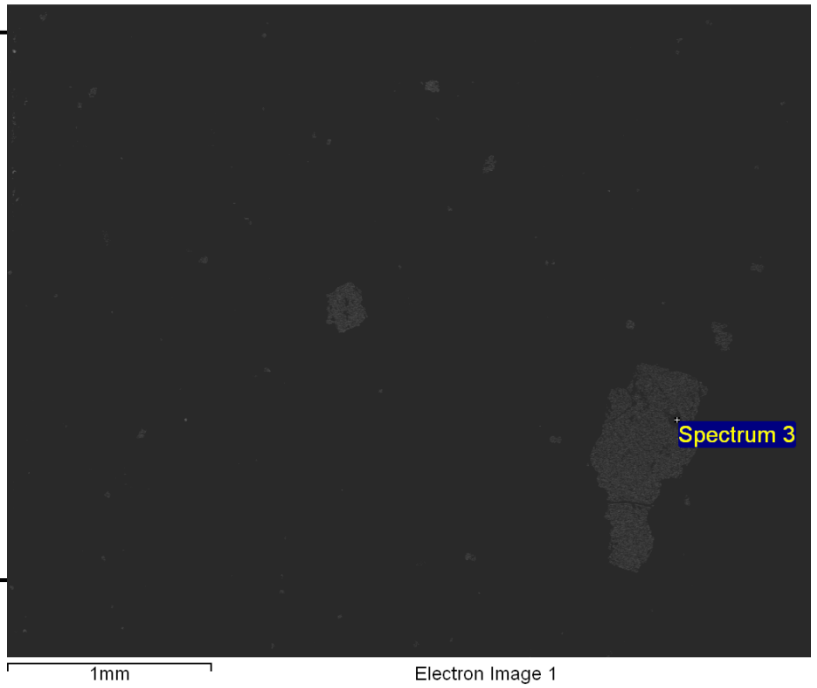

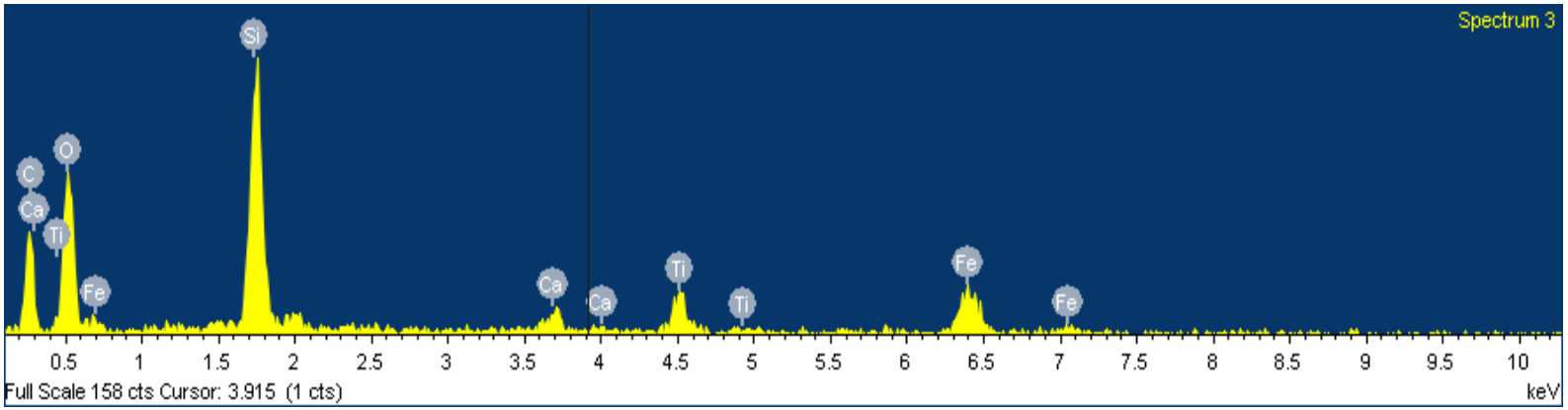

SHL06-3Z

2/11/2011 1:41:37 PM

Element	App Conc.	Intensity Corrn.	Weight%	Weight% Sigma	Atomic%
O K	37.90	1.8295	26.26	1.86	55.42
Fe K	54.05	0.9298	73.74	1.86	44.58
Totals			100.00		

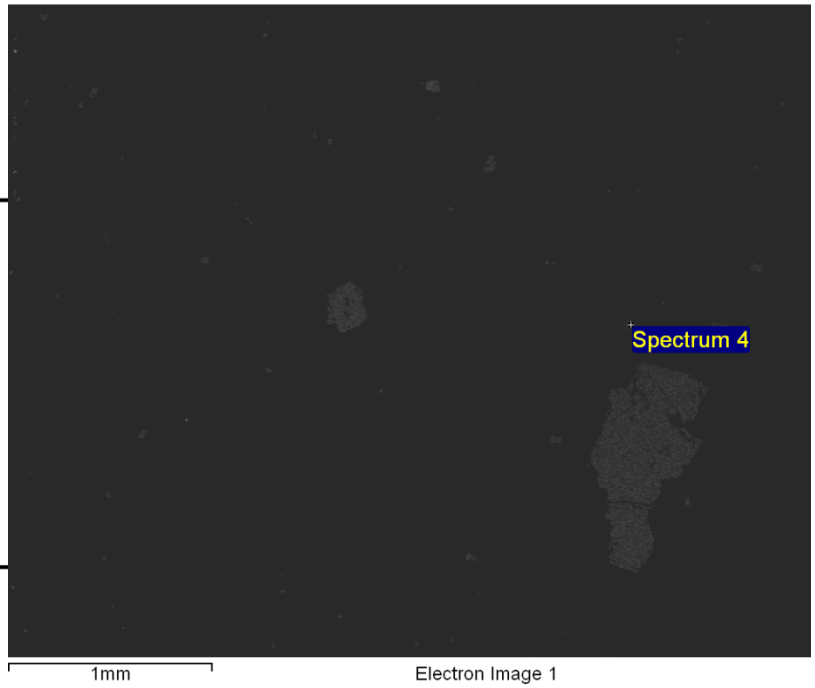

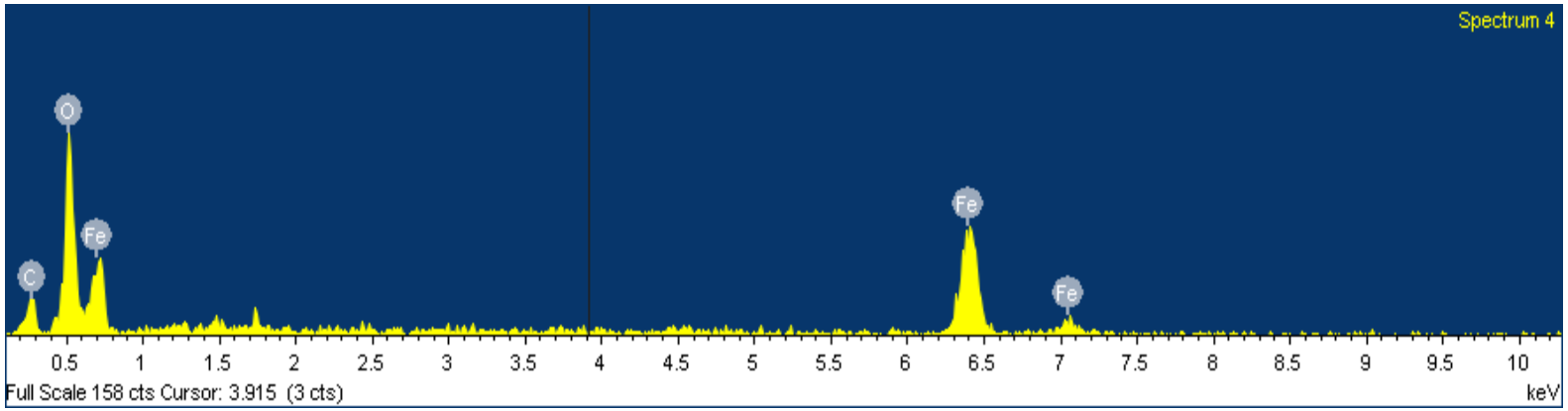

SHL06-3Z

2/11/2011 1:59:36 PM

Element	App Conc.	Intensity Corrn.	Weight%	Weight% Sigma	Atomic%
O K	43.16	1.2592	49.38	2.12	66.83
Na K	2.01	0.9268	3.12	0.74	2.94
Al K	4.88	0.8997	7.81	0.82	6.26
Si K	12.84	0.9004	20.55	1.28	15.84
K K	3.04	1.0436	4.20	0.71	2.33
Fe K	8.54	0.8236	14.94	1.90	5.79
Totals			100.00		

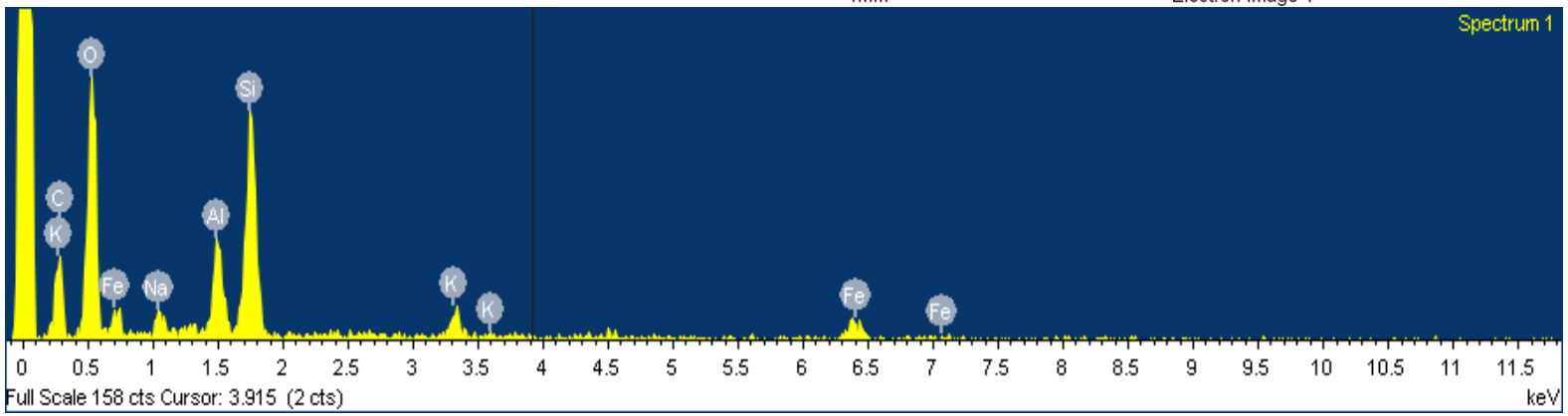

SHL06-3Z

2/11/2011 1:59:41 PM

Element	App Conc.	Intensity Corrn.	Weight%	Weight% Sigma	Atomic%
O K	50.10	1.9580	43.22	2.58	72.65
Fe K	29.86	0.8883	56.78	2.58	27.35
Totals			100.00		

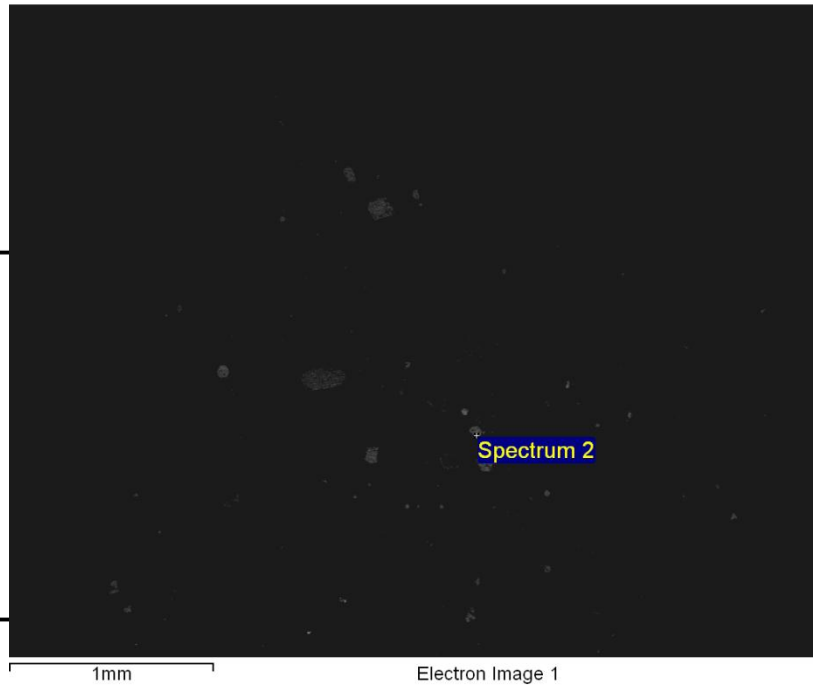

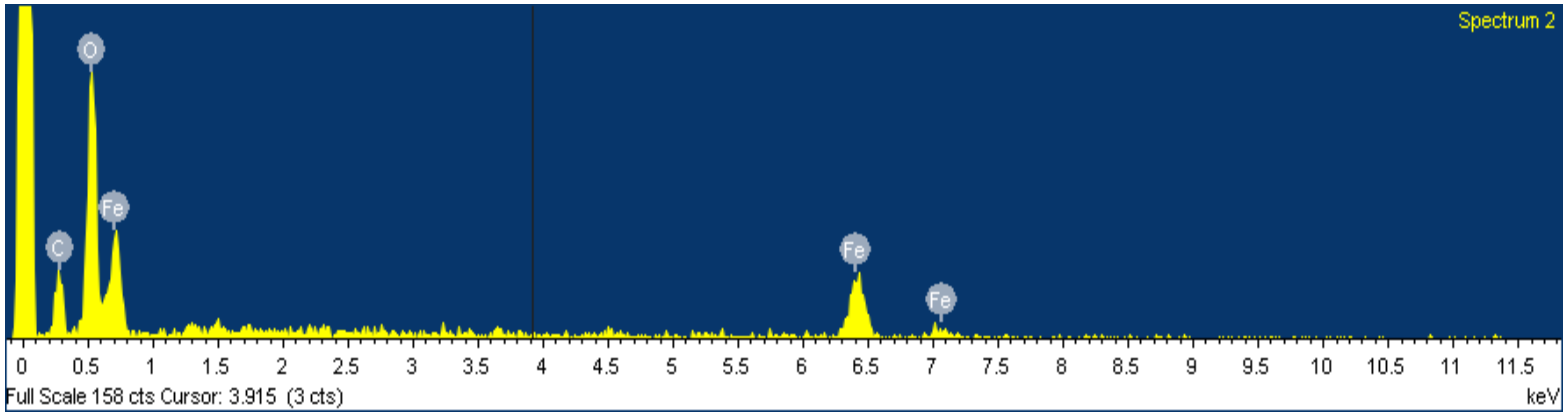

SHL06-3Z

2/11/2011 1:59:46 PM

Element	App Conc.	Intensity Corrn.	Weight%	Weight% Sigma	Atomic%
O K	40.89	1.8582	30.22	1.82	60.18
Fe K	46.75	0.9197	69.78	1.82	39.82
Totals			100.00		

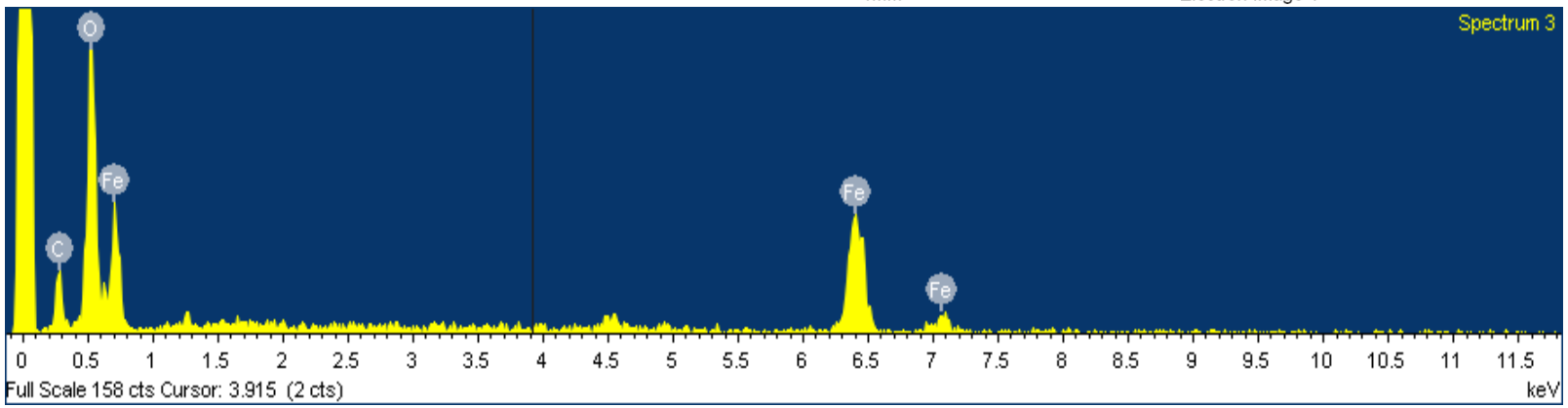

SHL06-3Z

2/11/2011 1:59:58 PM

Element	App Conc.	Intensity Corrn.	Weight%	Weight% Sigma	Atomic%
O K	25.19	0.6103	53.26	2.35	72.06
P K	18.56	1.4129	16.95	1.29	11.84
Ca K	23.15	1.0019	29.79	1.80	16.09
Totals			100.00		

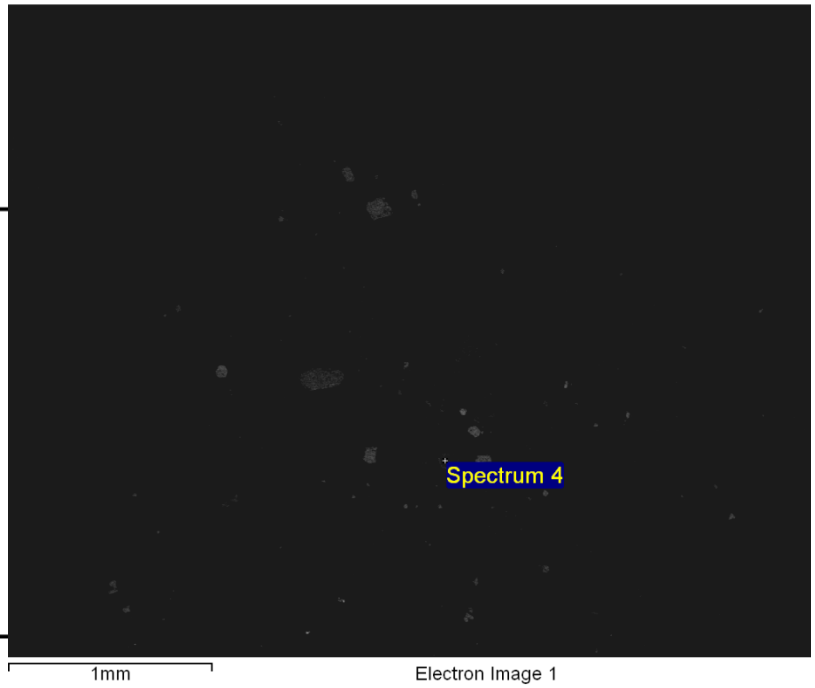

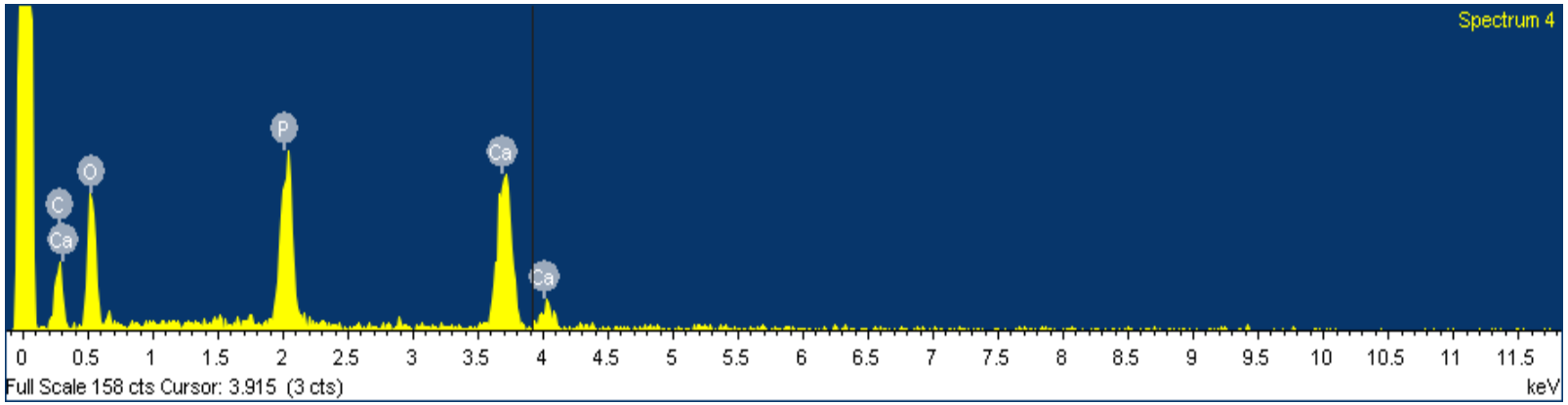

SHL06-3Z

2/11/2011 2:00:04 PM

Element	App Conc.	Intensity Corrn.	Weight%	Weight% Sigma	Atomic%
O K	26.89	0.7993	37.32	2.72	66.07
Ti K	21.37	0.9330	25.40	1.83	15.02
Fe K	29.60	0.8804	37.28	2.54	18.91
Totals			100.00		

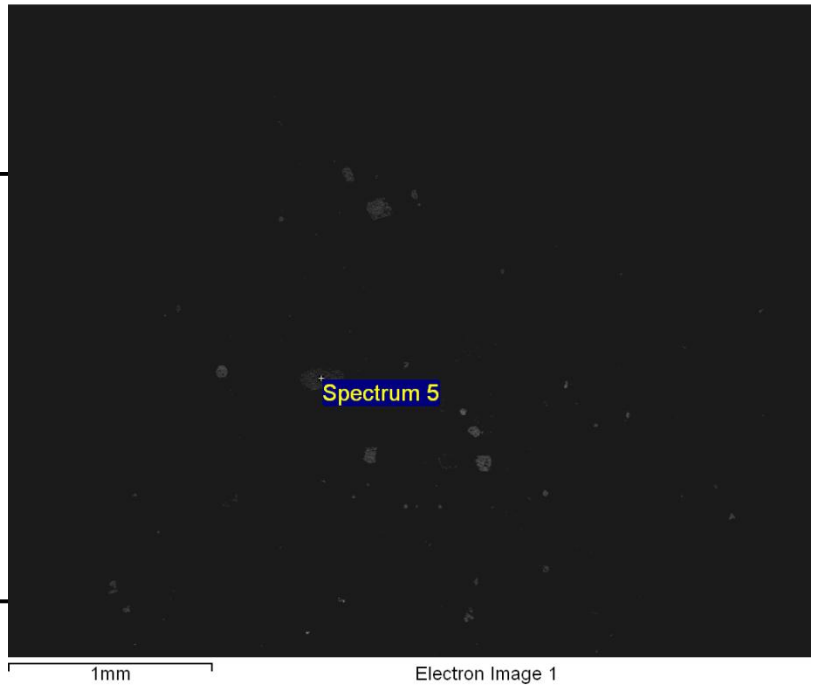

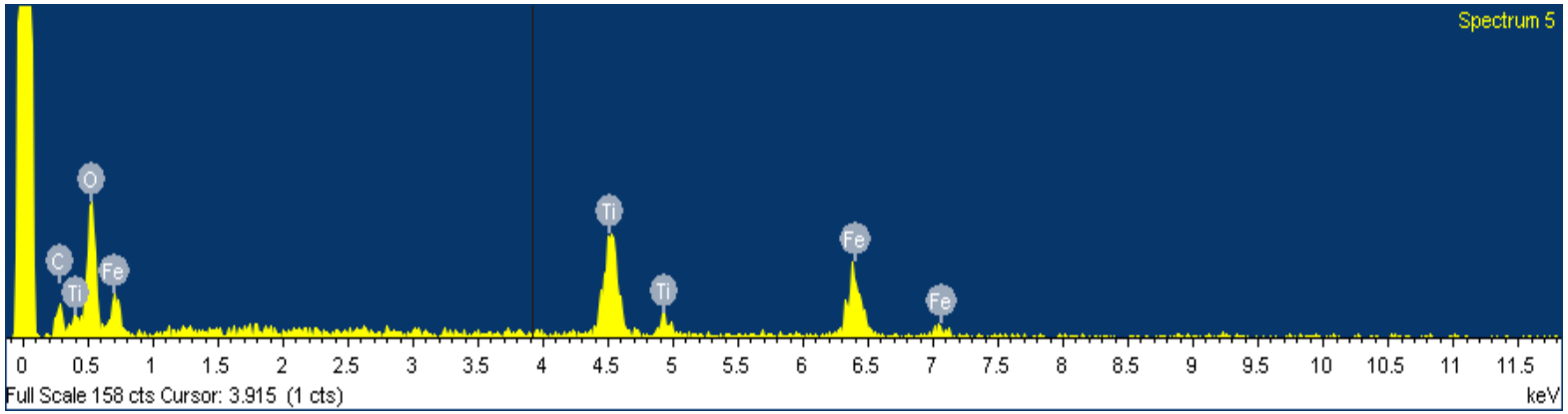

SHL06-3Z

2/11/2011 2:00:15 PM

Element	App Conc.	Intensity Corrn.	Weight%	Weight% Sigma	Atomic%
O K	36.73	1.8088	23.28	2.12	51.44
Fe K	62.69	0.9373	76.72	2.12	48.56
Totals			100.00		

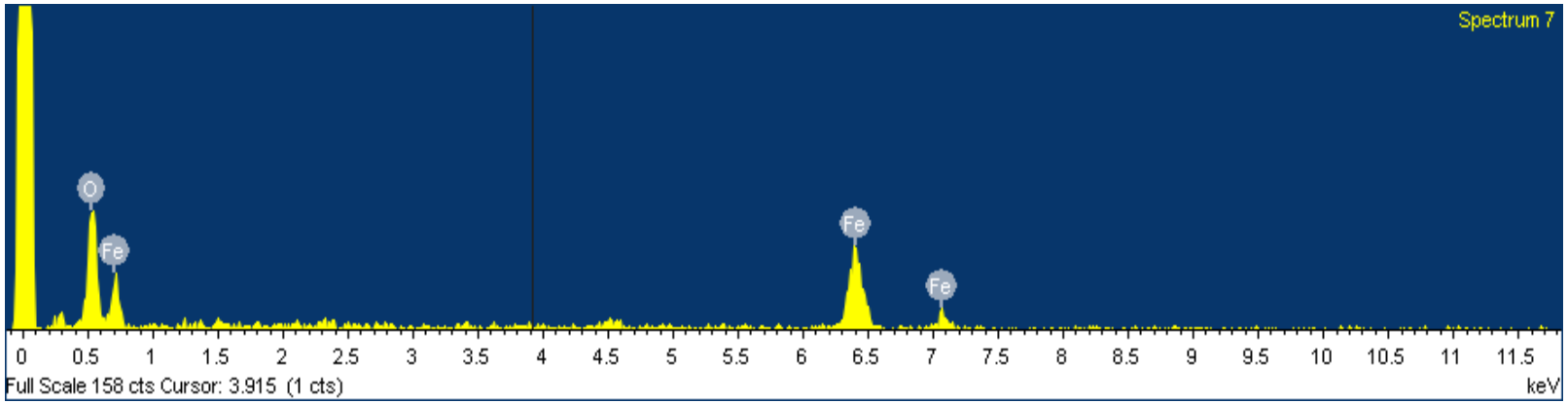

SHL06-3Z

2/11/2011 2:00:22 PM

Element	App Conc.	Intensity Corrn.	Weight%	Weight% Sigma	Atomic%
O K	32.24	1.8024	22.34	3.01	50.10
Fe K	58.42	0.9397	77.66	3.01	49.90
Totals			100.00		

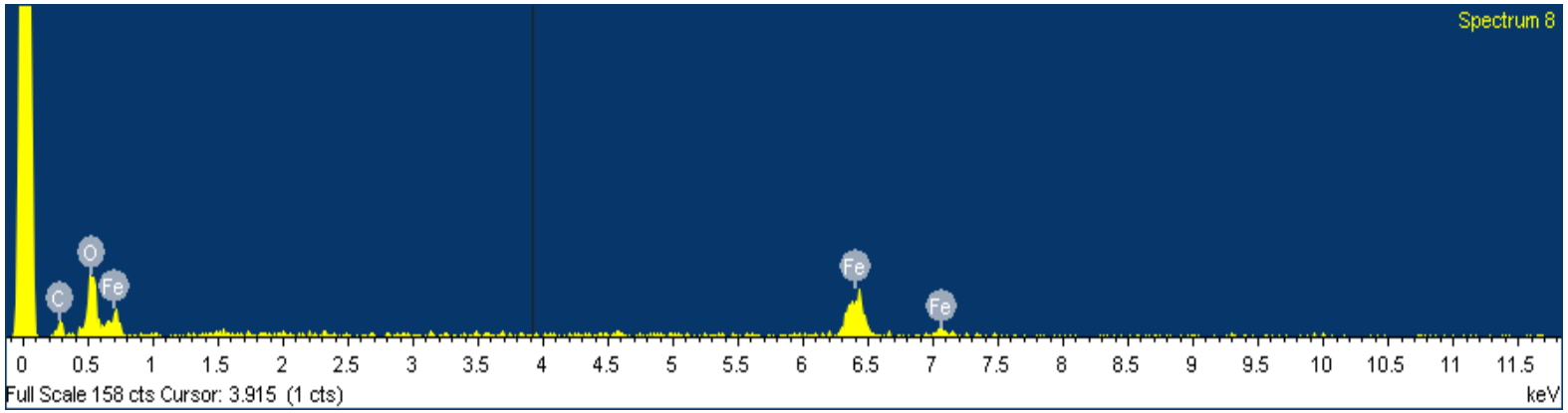

SHL06-3Z

2/11/2011 2:00:29 PM

Element	App Conc.	Intensity Corrn.	Weight%	Weight% Sigma	Atomic%
O K	38.24	1.5549	30.44	2.19	60.19
Ti K	3.42	0.9772	4.34	0.93	2.87
Fe K	48.21	0.9154	65.22	2.29	36.94
Totals			100.00		

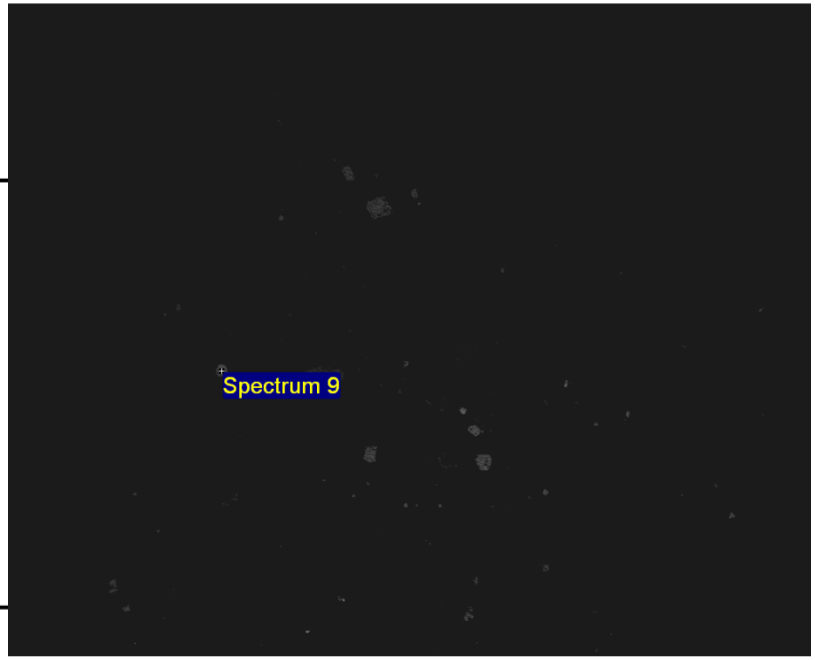

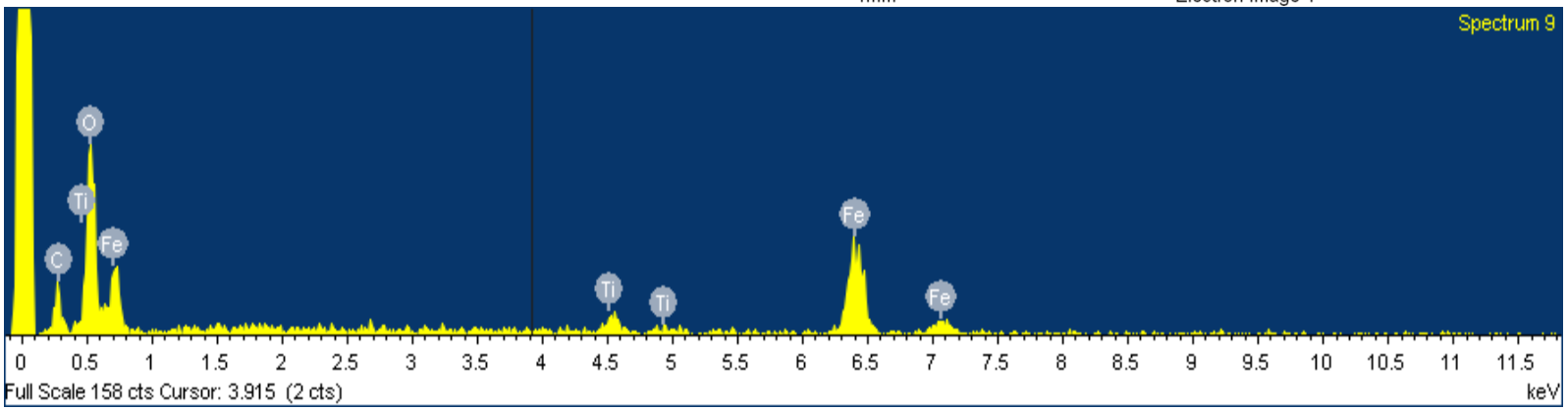

SHD08-2ZA

2/11/2011 2:36:53 PM

Element	App Conc.	Intensity Corrn.	Weight%	Weight% Sigma	Atomic%
O K	28.64	1.8545	29.79	3.42	59.70
Fe K	33.49	0.9210	70.21	3.42	40.30
Totals			100.00		

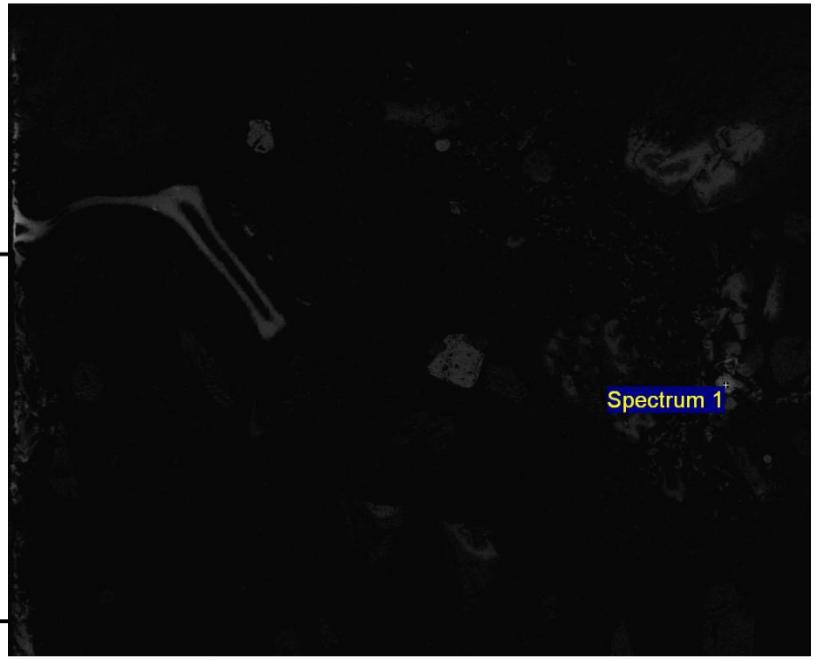

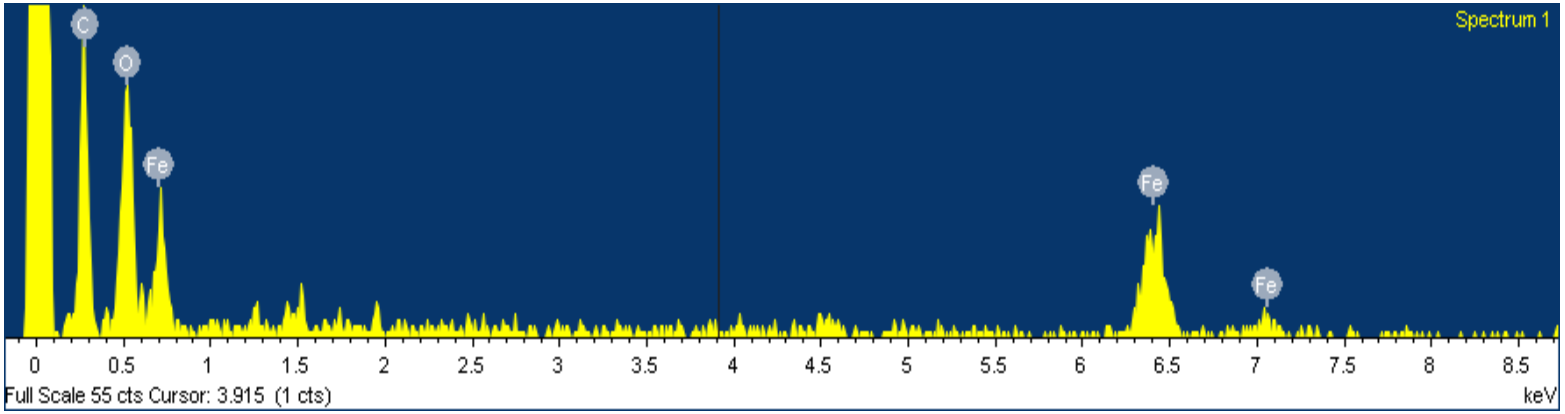

SHD08-2ZA

2/11/2011 2:37:29 PM

Element	App Conc.	Intensity Corrn.	Weight%	Weight% Sigma	Atomic%
O K	28.62	1.5532	20.99	2.02	46.68
Mg K	0.61	0.5878	1.18	0.64	1.73
Al K	1.16	0.7084	1.86	0.57	2.46
Si K	0.49	0.8171	0.68	0.49	0.86
Ti K	2.56	0.9945	2.94	1.01	2.18
Fe K	59.32	0.9343	72.34	2.32	46.09
Totals			100.00		

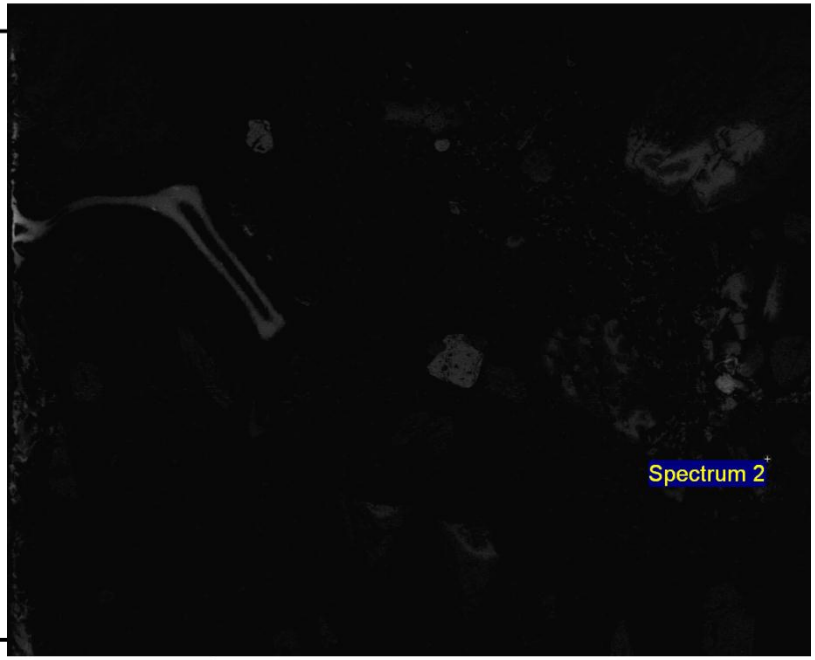

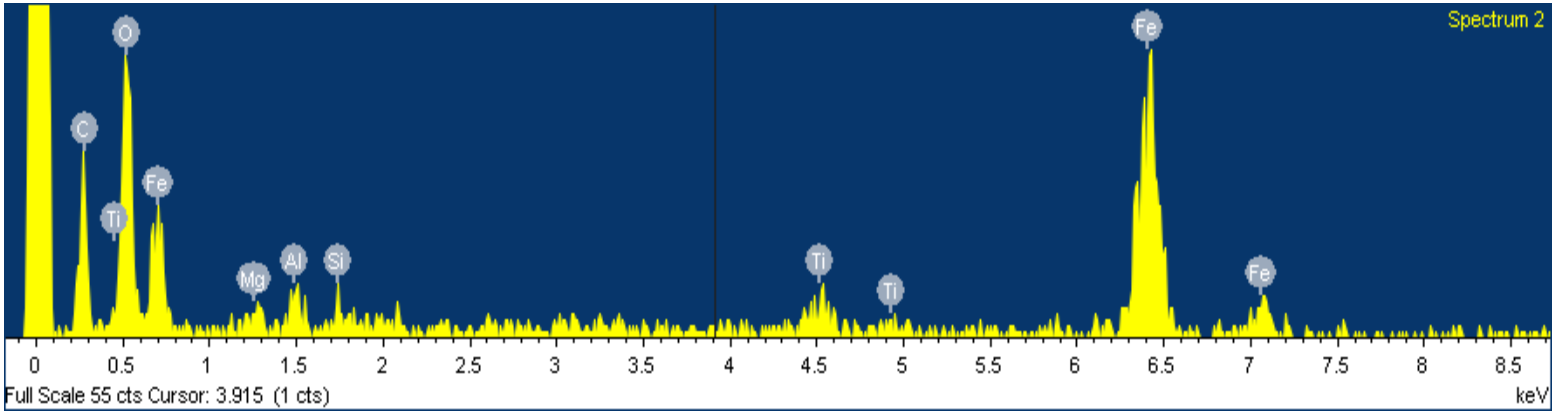

SHD08-2ZA

2/11/2011 2:37:48 PM

Element	App Conc.	Intensity Corrn.	Weight%	Weight% Sigma	Atomic%
O K	28.46	1.4456	27.72	3.38	56.90
Ti K	4.20	0.9817	6.02	1.76	4.13
Fe K	43.30	0.9207	66.26	3.70	38.97
Totals			100.00		

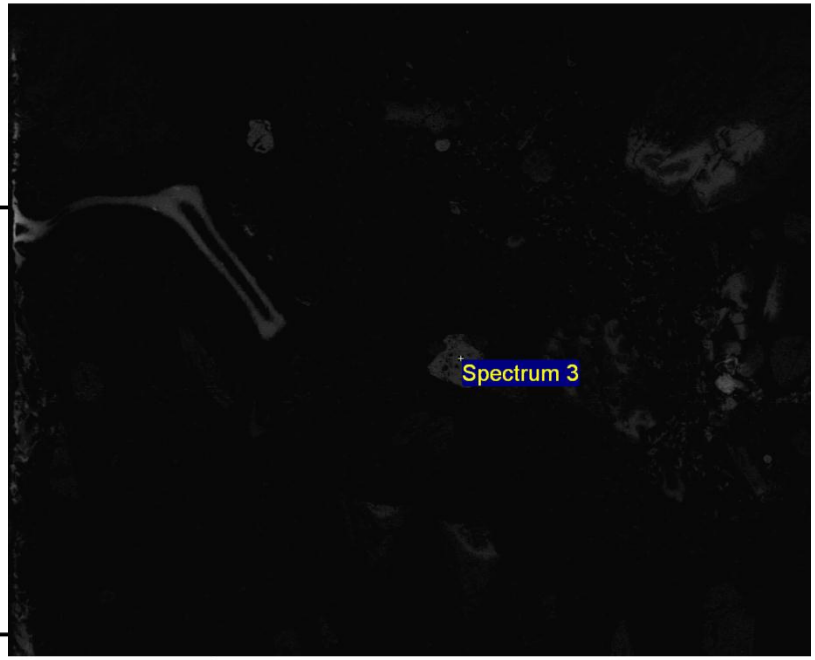

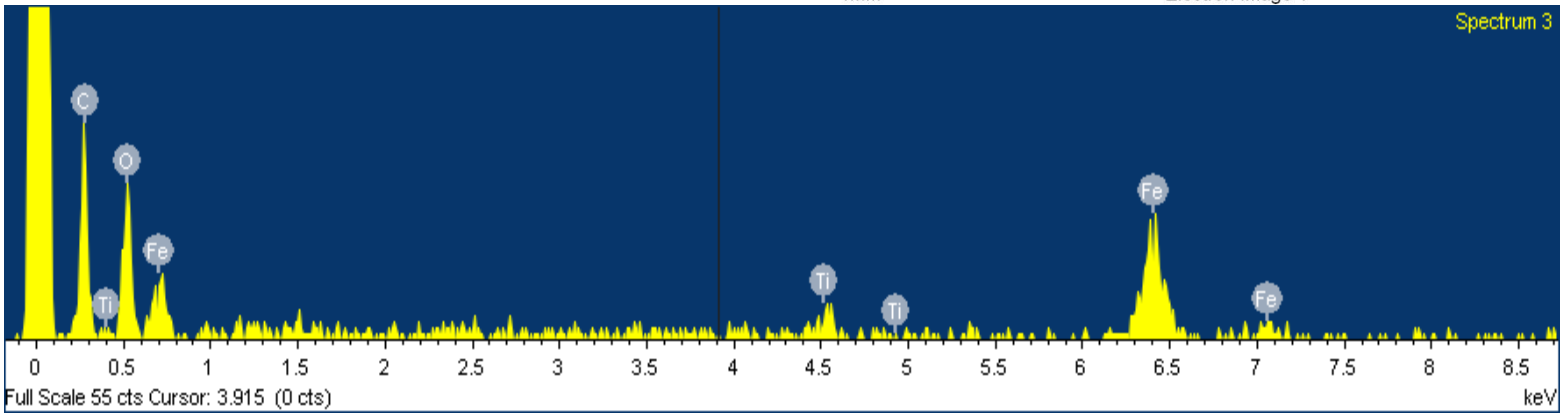

SHD08-2ZA

2/11/2011 2:37:53 PM

Element	App Conc.	Intensity Corrn.	Weight%	Weight% Sigma	Atomic%
O K	8.35	1.7164	9.00	5.46	25.66
Fe K	47.97	0.9749	91.00	5.46	74.34
Totals			100.00		

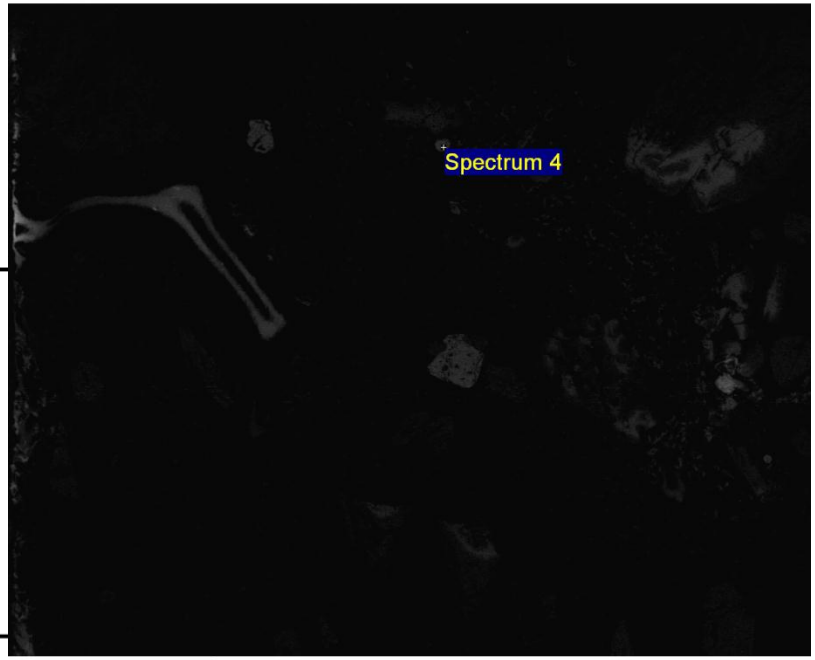

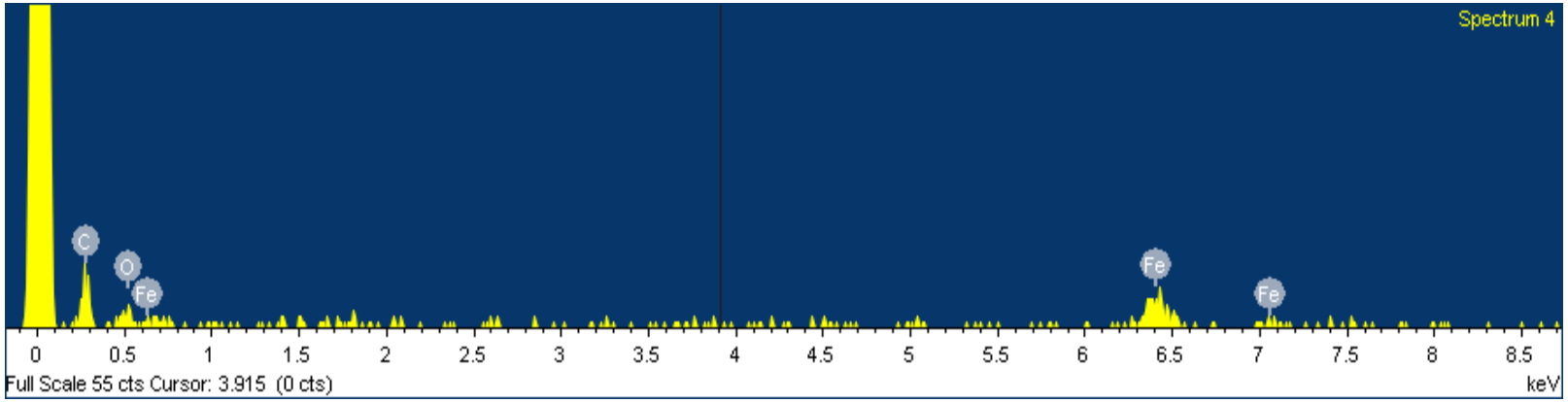

SHD08-2ZA

2/11/2011 2:38:00 PM

Element	App Conc.	Intensity Corrn.	Weight%	Weight% Sigma	Atomic%
O K	11.82	1.7119	8.26	3.54	23.91
Fe K	74.89	0.9769	91.74	3.54	76.09
Totals			100.00		

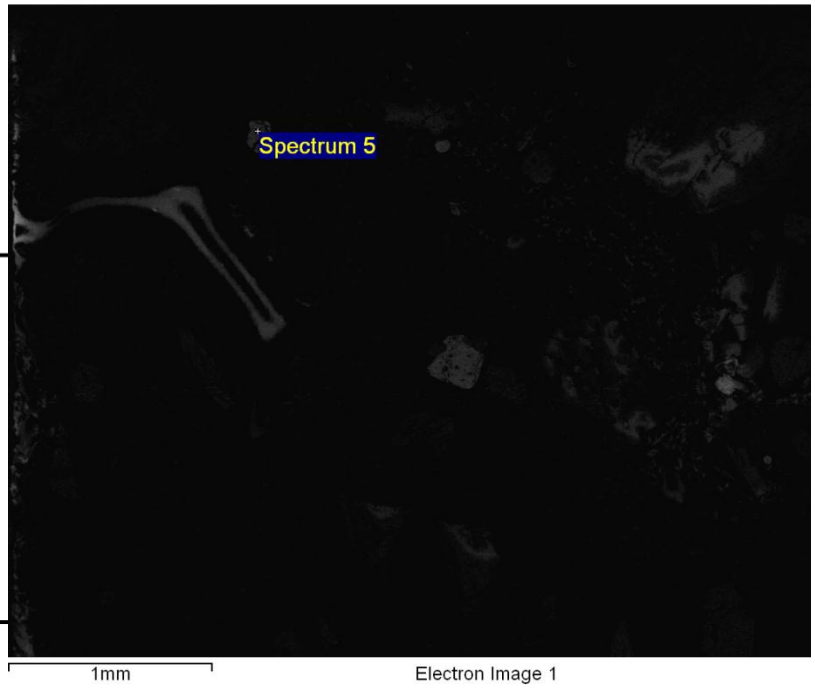

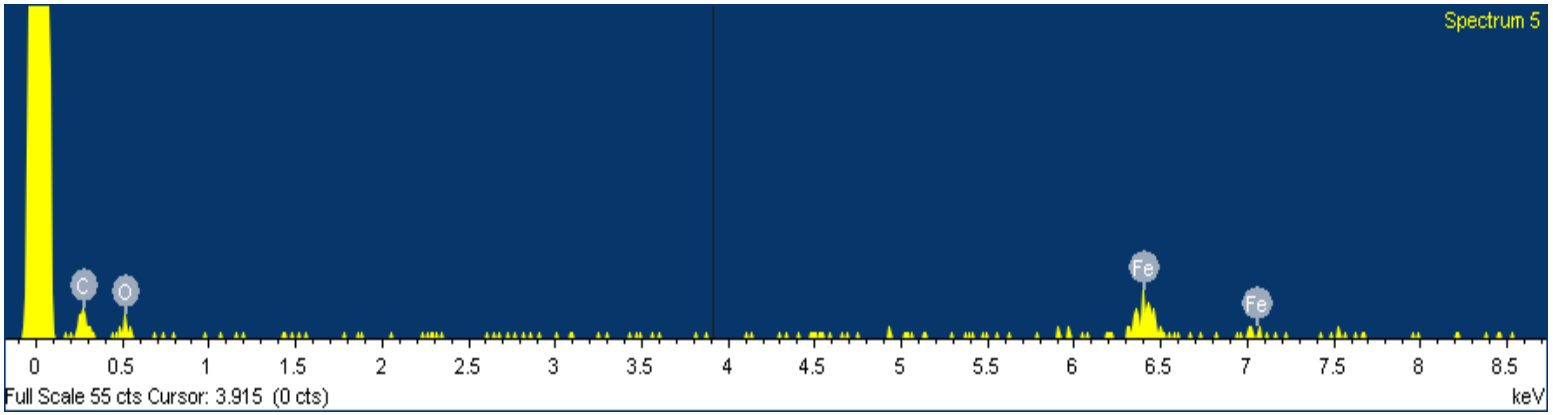

SHL08-21Z

2/11/2011 3:24:22 PM

Element	App Conc.	Intensity Corrn.	Weight%	Weight% Sigma	Atomic%
O K	28.02	1.5391	23.29	3.00	51.23
Ti K	3.13	0.9970	4.02	1.56	2.95
Fe K	53.05	0.9336	72.70	3.25	45.82
Totals			100.00		

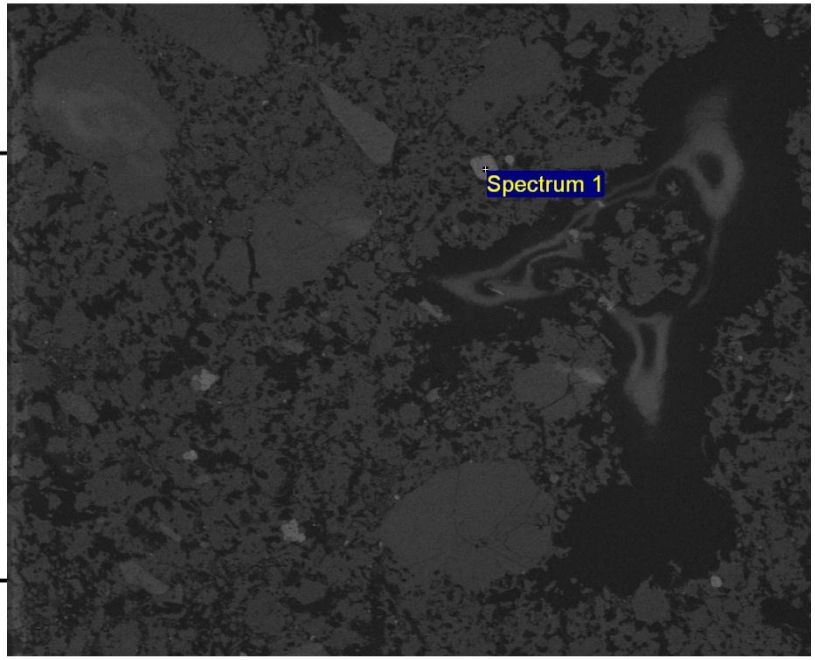

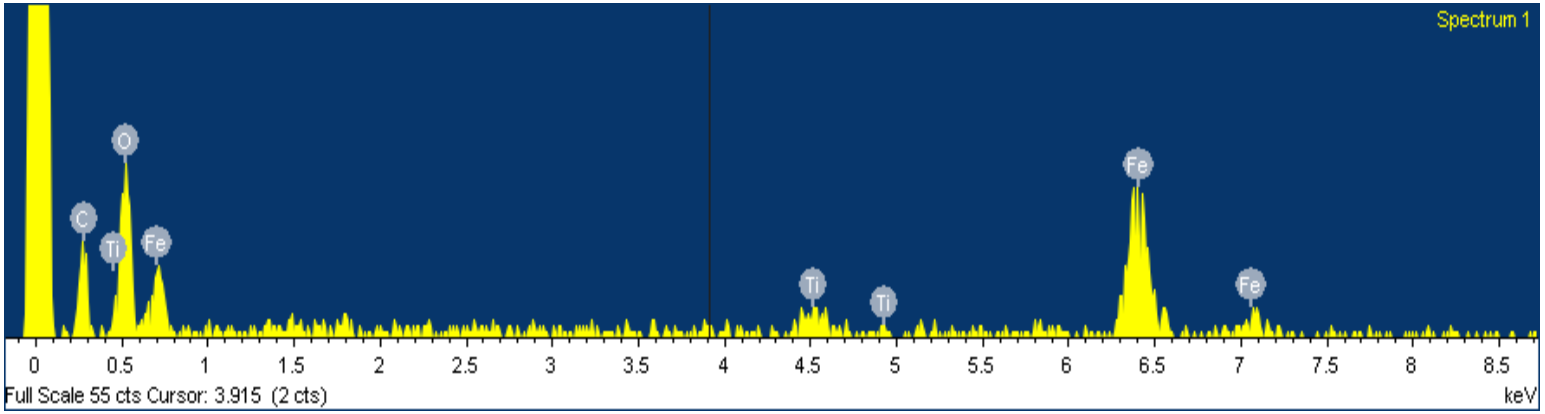

SHL08-21Z

2/11/2011 3:24:35 PM

Element	App Conc.	Intensity Corrn.	Weight%	Weight% Sigma	Atomic%
O K	18.22	1.4167	12.94	2.14	33.93
Ti K	5.49	1.0231	5.40	1.15	4.73
Fe K	77.81	0.9592	81.66	2.36	61.34
Totals			100.00		

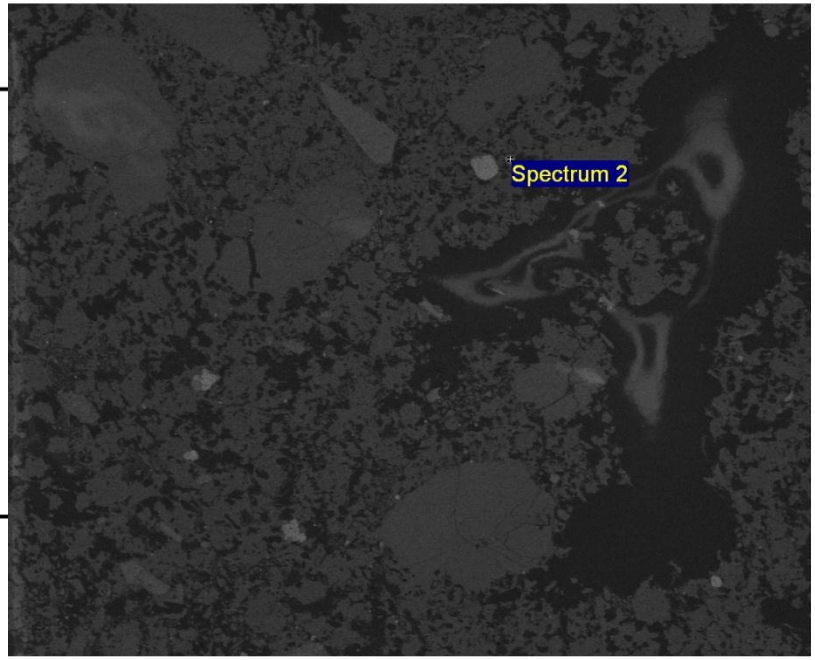

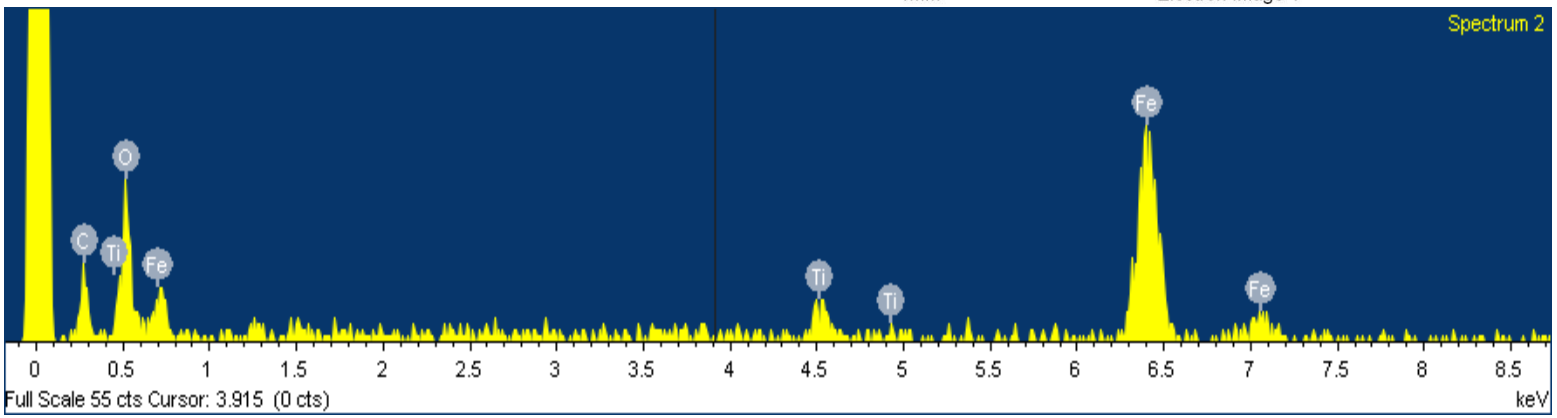

SHL08-21Z

2/11/2011 3:24:42 PM

Element	App Conc.	Intensity Corrn.	Weight%	Weight% Sigma	Atomic%
O K	24.07	1.4115	20.77	2.15	47.47
Ti K	5.03	1.0004	6.13	1.20	4.68
Fe K	56.28	0.9381	73.10	2.36	47.86
Totals			100.00		

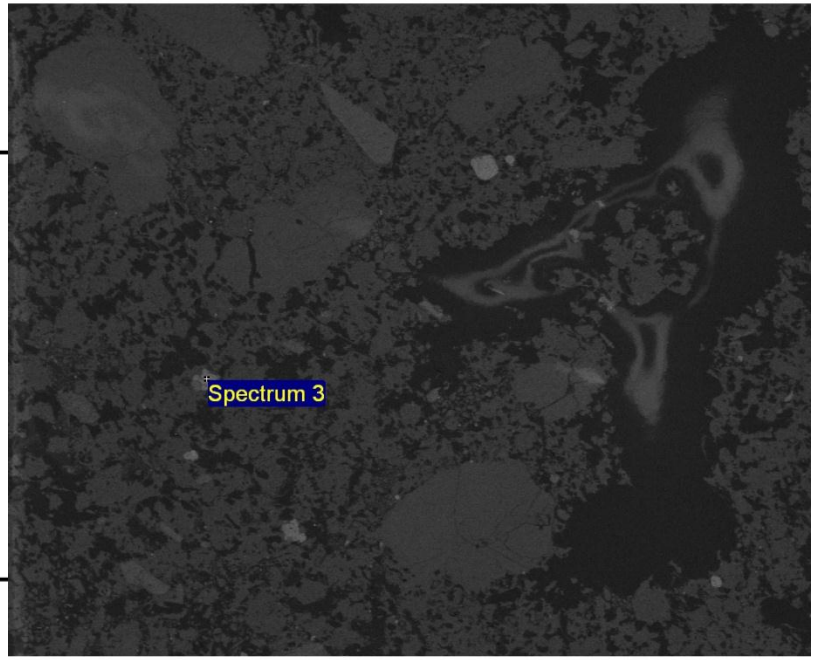

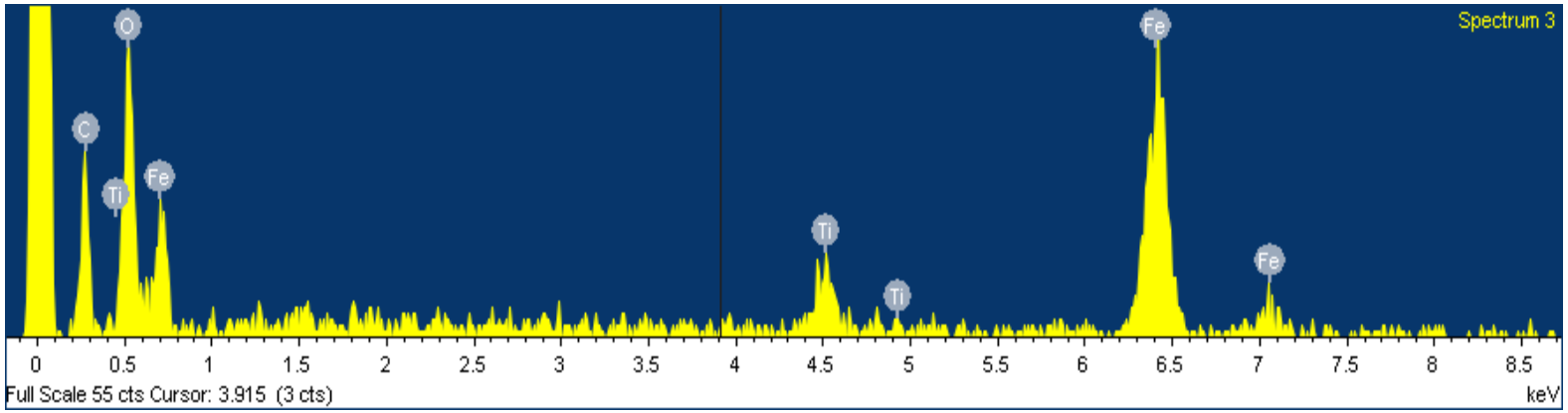

SHL08-21Z

2/11/2011 3:24:49 PM

Element	App Conc.	Intensity Corrn.	Weight%	Weight% Sigma	Atomic%
O K	40.80	1.4247	35.84	2.17	60.18
Na K	1.58	0.7124	2.78	0.82	3.24
Al K	2.75	0.7830	4.39	0.67	4.37
Si K	6.49	0.8524	9.53	0.87	9.11
Ti K	2.42	0.9174	3.30	0.87	1.85
Fe K	30.96	0.8776	44.17	2.34	21.24
Totals			100.00		

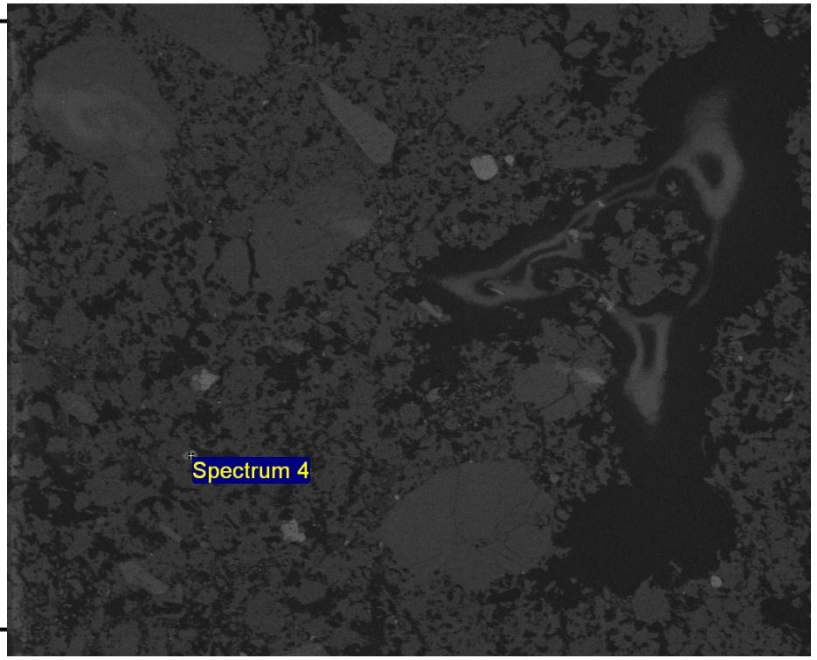

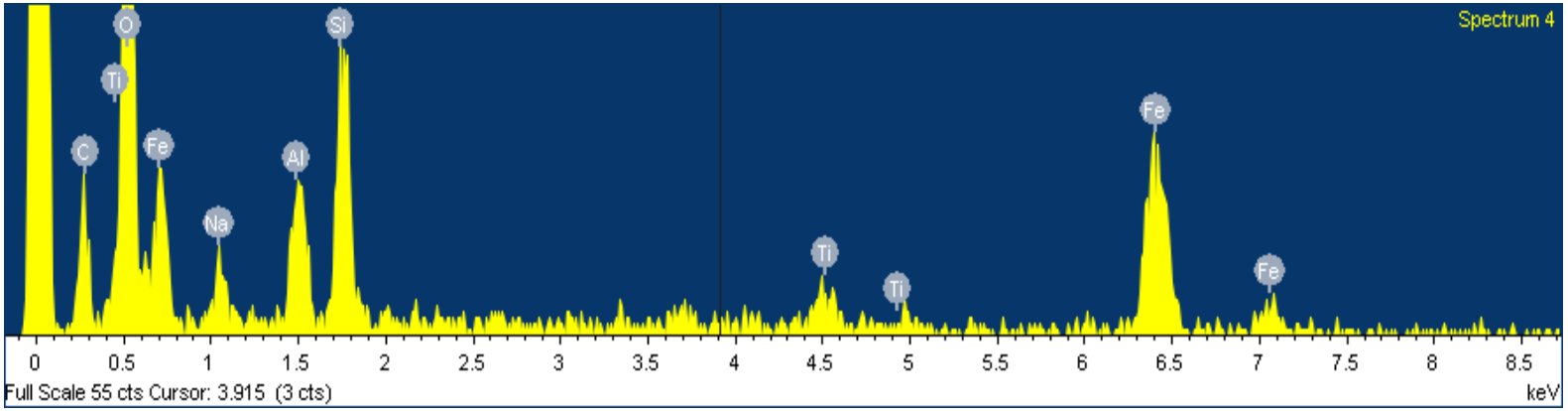

SHL08-21Z

2/11/2011 3:24:56 PM

Element	App Conc.	Intensity Corrn.	Weight%	Weight% Sigma	Atomic%
O K	22.95	0.8058	32.48	2.22	58.57
Na K	0.68	0.7042	1.10	0.53	1.38
Mg K	0.54	0.6724	0.92	0.45	1.09
Al K	0.60	0.7864	0.88	0.36	0.94
Si K	4.07	0.8848	5.24	0.61	5.38
Ti K	18.61	0.9272	22.88	1.45	13.78
Fe K	28.22	0.8812	36.51	2.14	18.86
Totals			100.00		

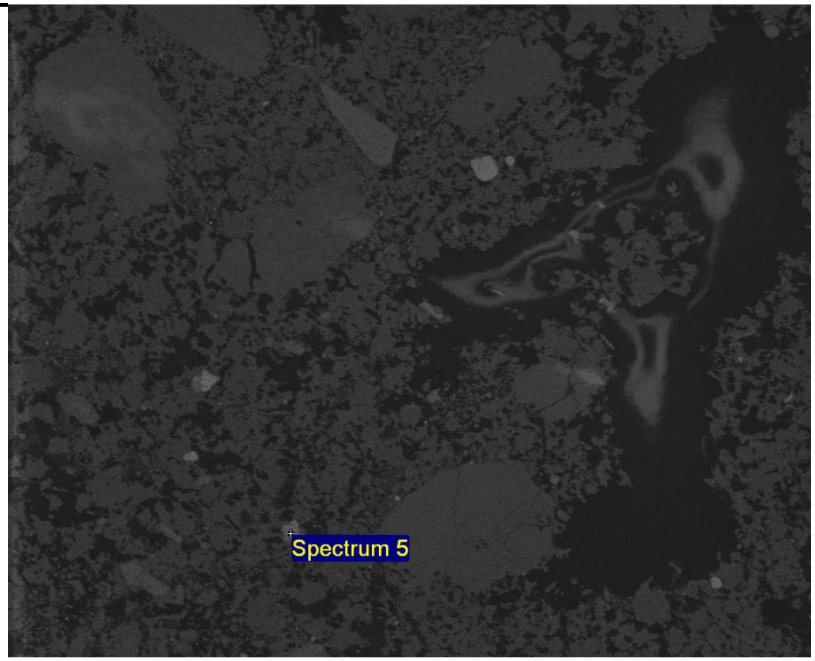

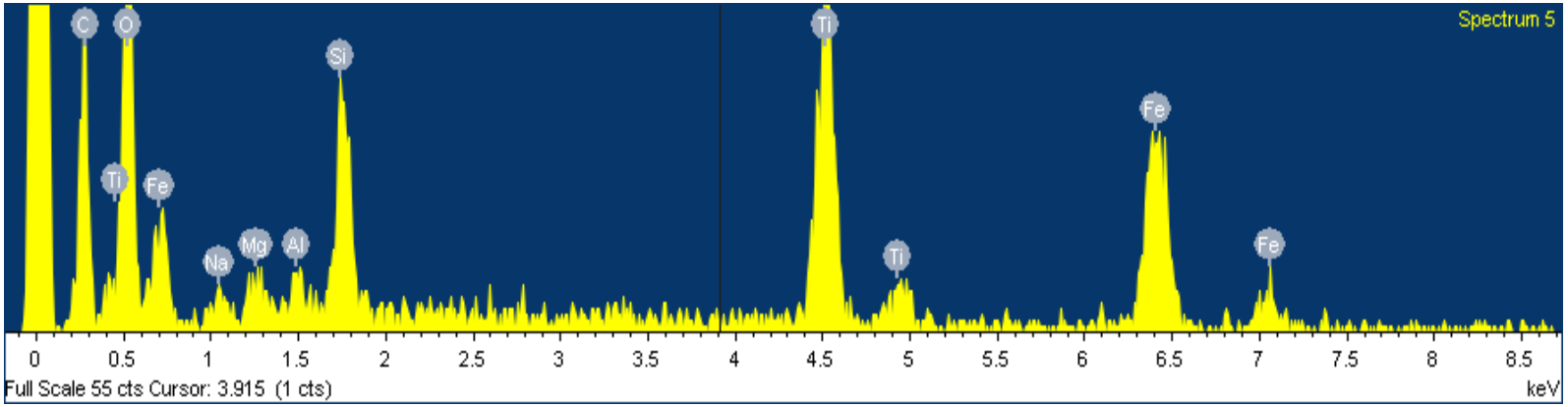

SHL08-21Z

2/11/2011 3:25:03 PM

Element	App Conc.	Intensity Corrn.	Weight%	Weight% Sigma	Atomic%
O K	20.69	1.4226	16.06	1.36	39.20
Mg K	0.31	0.5764	0.60	0.37	0.96
Al K	0.47	0.7025	0.75	0.36	1.08
Si K	0.29	0.8211	0.39	0.32	0.55
P K	0.31	1.2648	0.27	0.32	0.34
Ti K	4.69	1.0090	5.13	0.78	4.19
Fe K	65.91	0.9479	76.80	1.60	53.69
Totals			100.00		

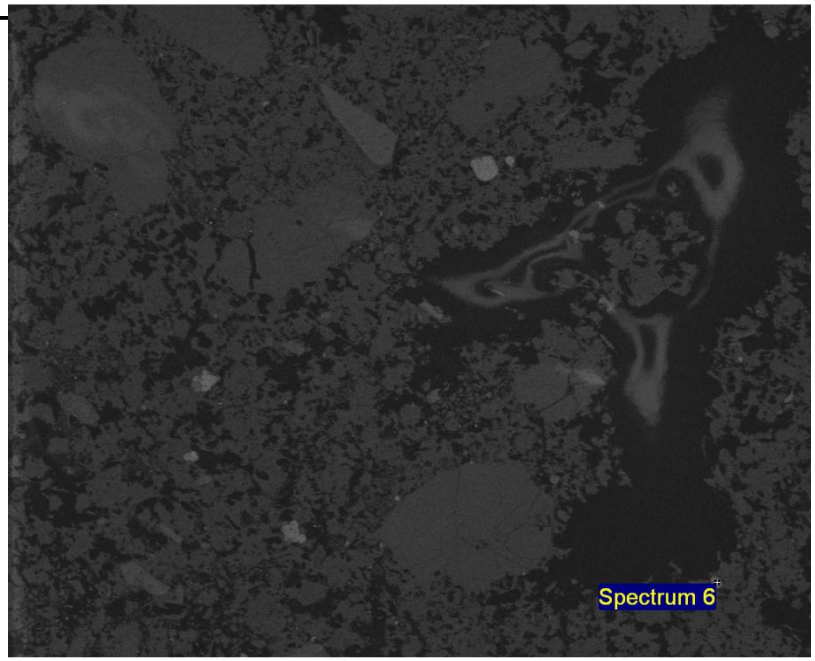

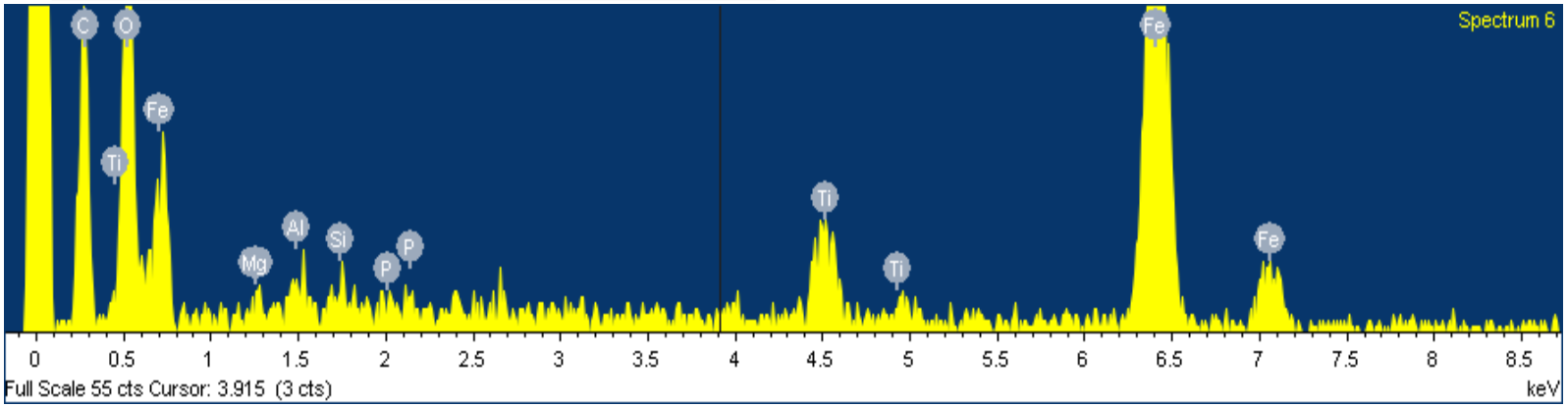

SHL08-21Z

2/11/2011 3:25:12 PM

Element	App Conc.	Intensity Corrn.	Weight%	Weight% Sigma	Atomic%
O K	32.07	1.0543	49.16	2.04	63.06
Na K	1.75	1.1486	2.46	0.58	2.20
Al K	4.06	1.0148	6.47	0.73	4.92
Si K	23.03	0.9788	38.03	1.74	27.79
K K	2.41	0.9995	3.89	0.81	2.04
Totals			100.00		

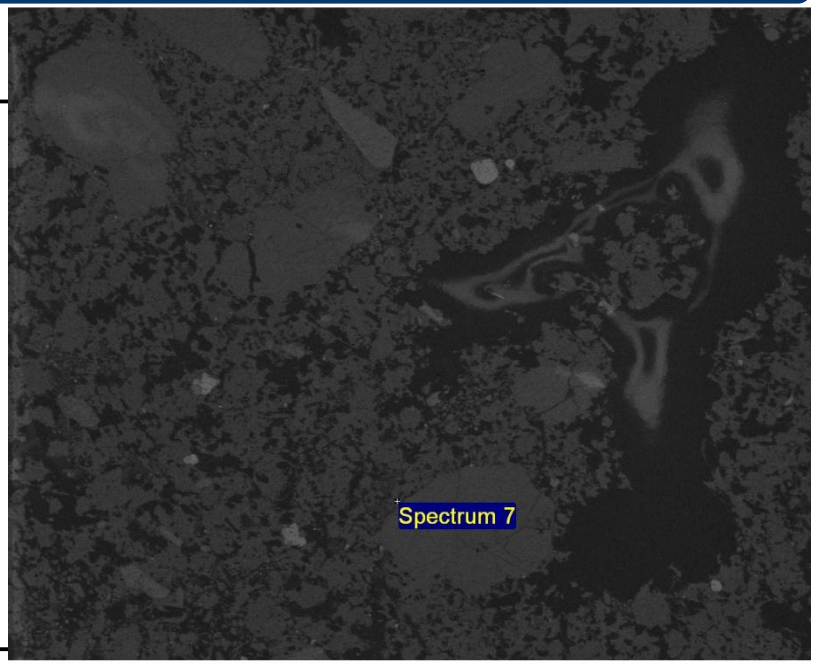

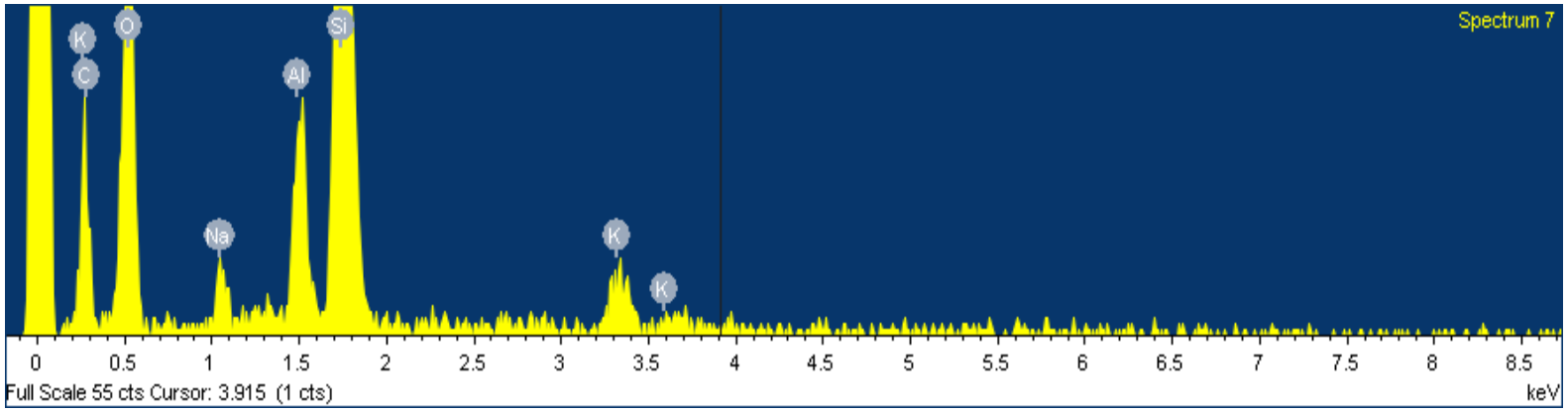

SHL08-21Z

2/11/2011 3:57:28 PM

Element	App Conc.	Intensity Corrn.	Weight%	Weight% Sigma	Atomic%
O K	19.96	1.7618	16.20	2.73	40.29
Fe K	55.99	0.9556	83.80	2.73	59.71
Totals			100.00		

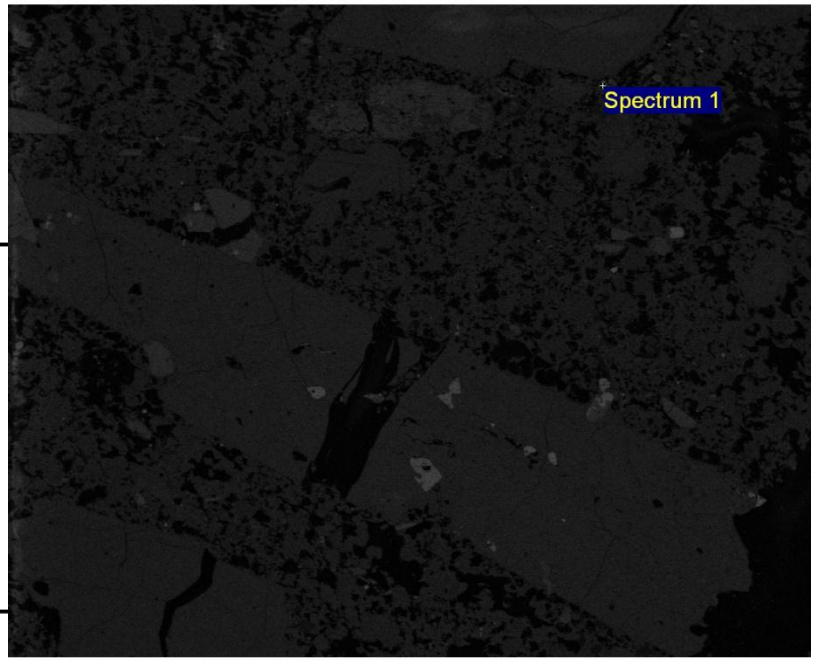

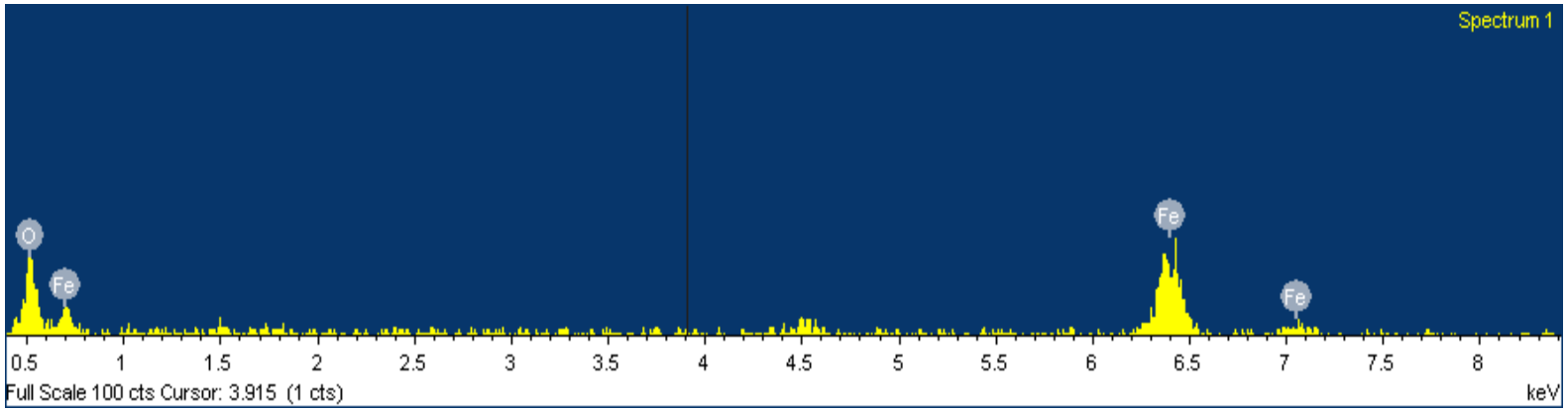

SHL08-21Z

Element	App Conc.	Intensity Corrn.	Weight%	Weight% Sigma	Atomic%
O K	19.34	1.4084	13.72	1.25	35.44
Ti K	5.75	1.0206	5.63	0.75	4.86
Fe K	77.27	0.9569	80.65	1.41	59.70
Totals			100.00		

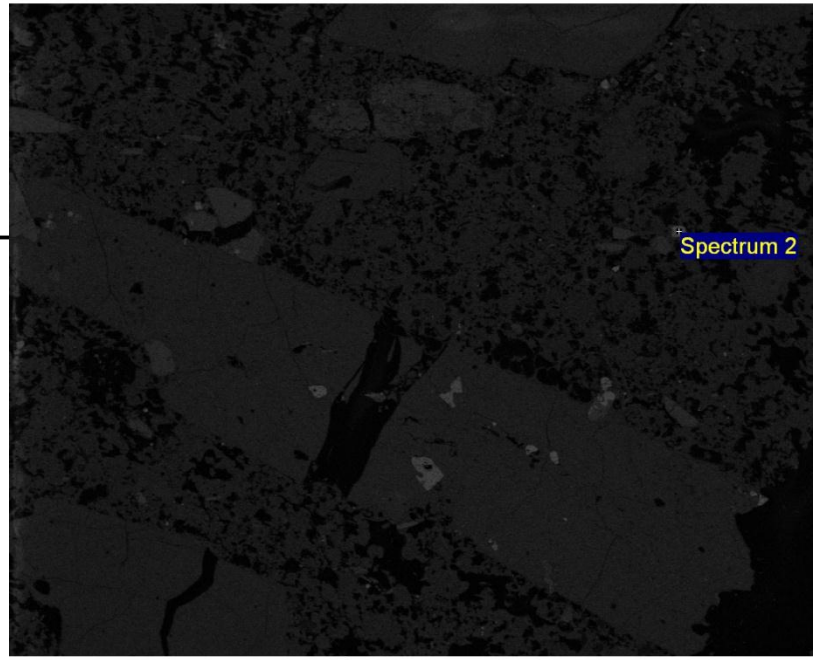

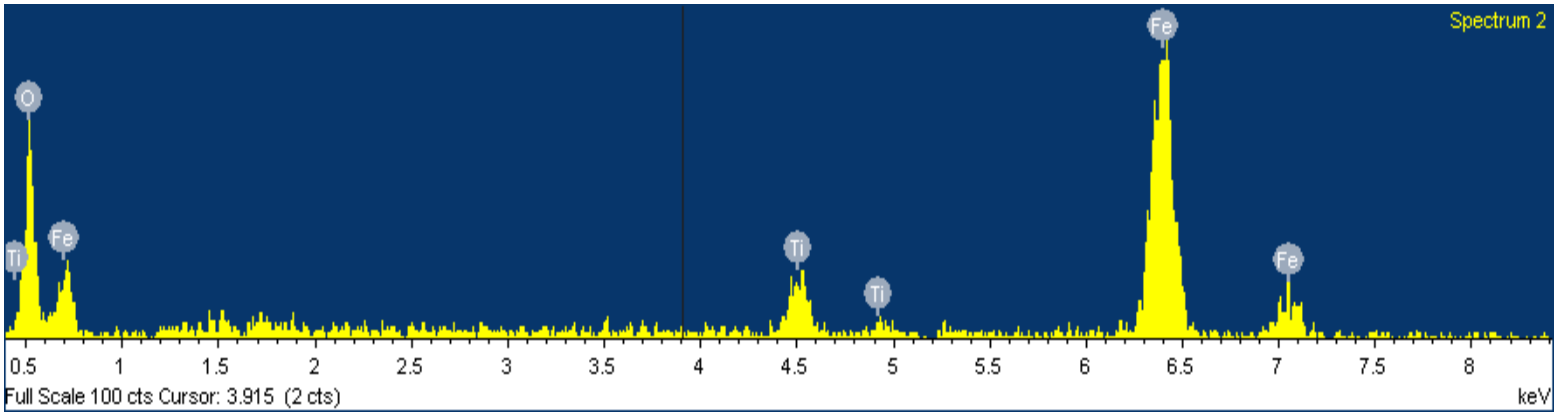

SHL08-21Z

2/11/2011 3:57:42 PM

Element	App Conc.	Intensity Corrn.	Weight%	Weight% Sigma	Atomic%
O K	15.11	1.2725	44.08	3.94	64.61
Al K	0.68	0.8323	3.02	1.31	2.63
Si K	6.83	0.8892	28.44	2.79	23.74
Cu L	3.66	0.5544	24.46	4.24	9.02
Totals			100.00		

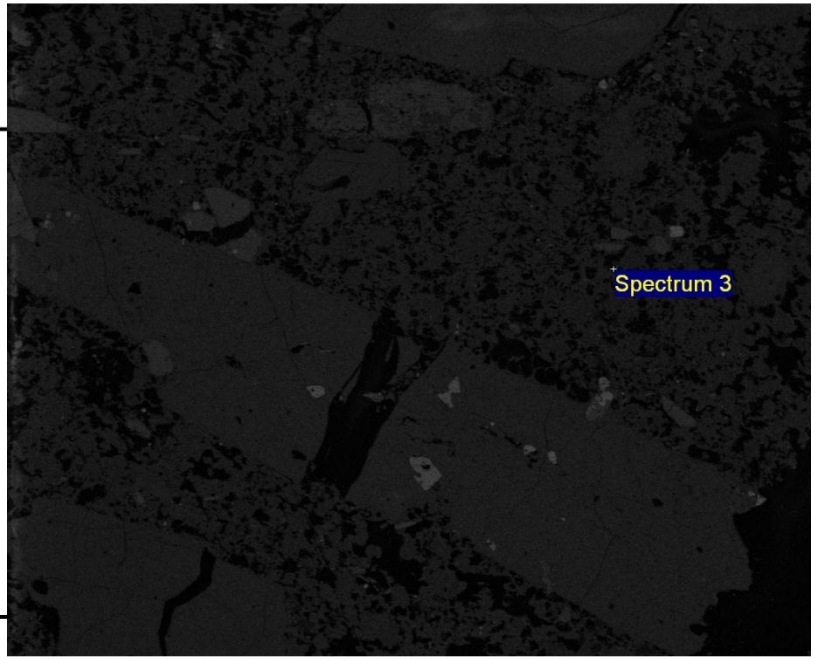

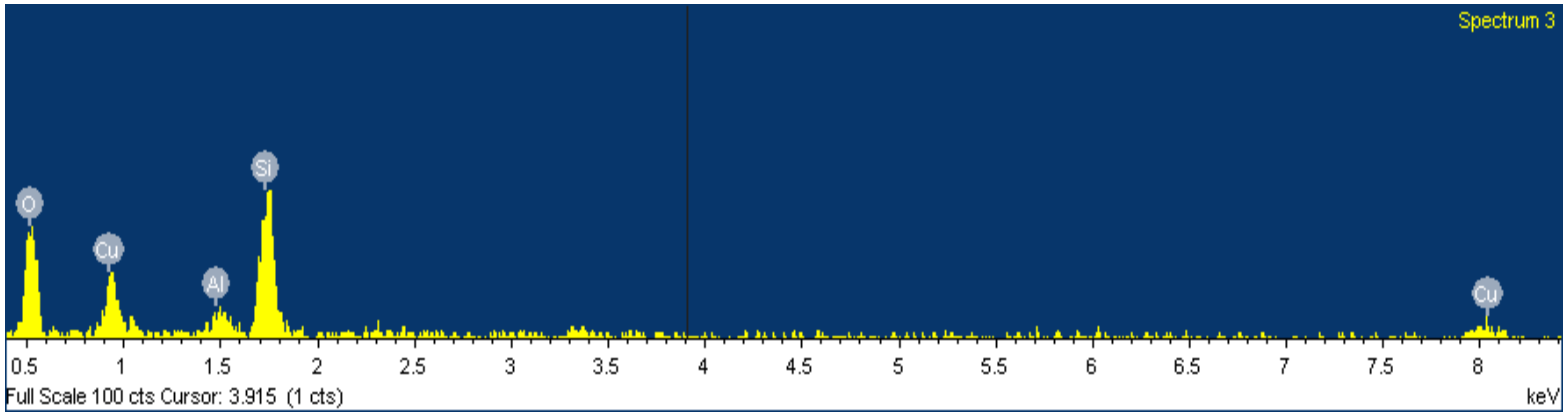

SHL08-21Z

2/11/2011 3:57:50 PM

Element	App Conc.	Intensity Corrn.	Weight%	Weight% Sigma	Atomic%
O K	15.22	1.3806	13.81	1.20	35.30
Al K	0.60	0.7009	1.07	0.37	1.62
Ti K	4.87	1.0169	5.99	0.77	5.12
Fe K	60.32	0.9547	79.13	1.40	57.96
Totals			100.00		

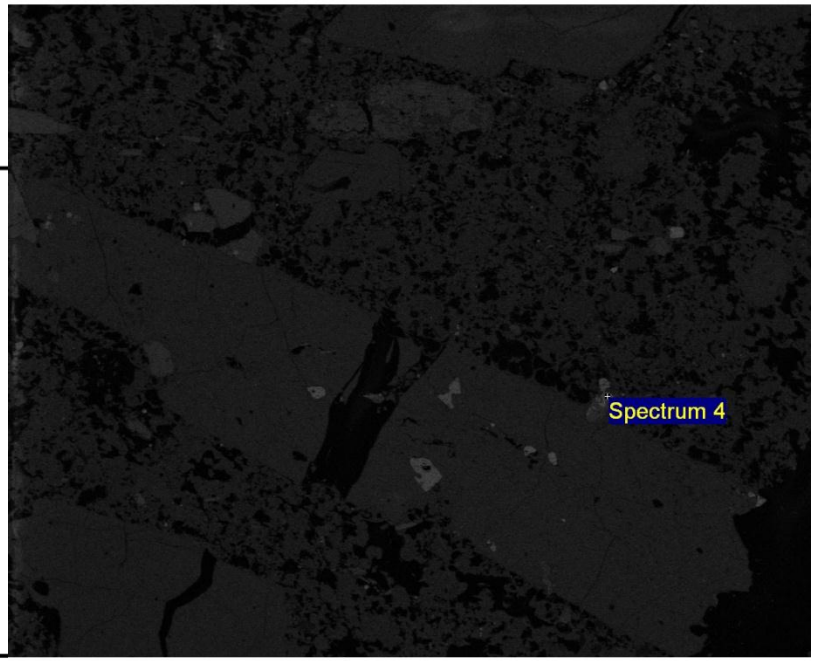

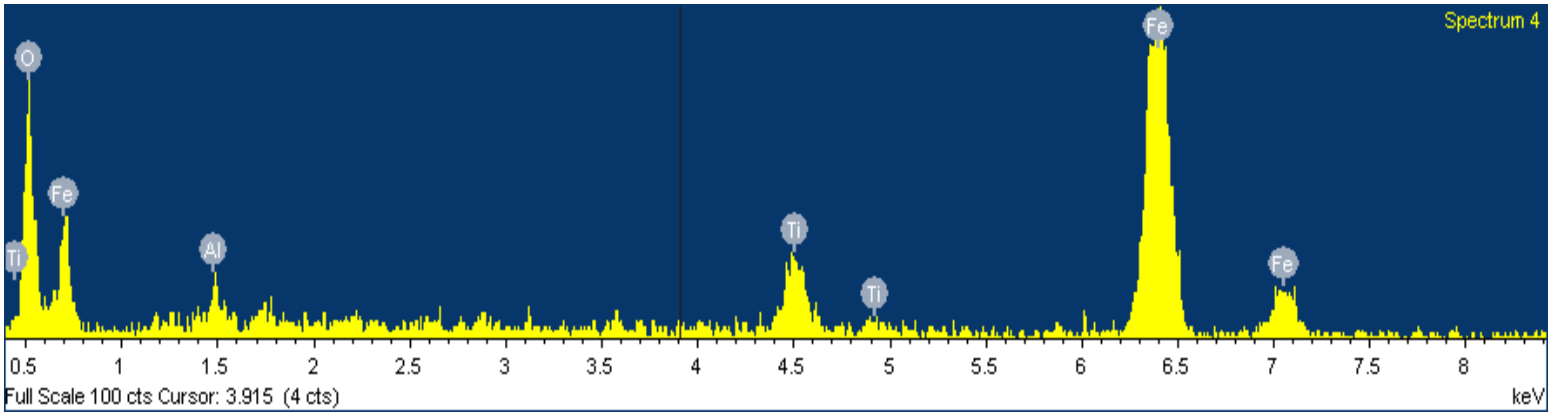

SHL08-21Z

2/11/2011 3:58:12 PM

Element	App Conc.	Intensity Corrn.	Weight%	Weight% Sigma	Atomic%
O K	18.56	1.4486	16.38	1.19	40.12
Al K	0.46	0.7015	0.83	0.33	1.21
Ti K	3.89	1.0122	4.91	0.66	4.02
Fe K	57.83	0.9493	77.88	1.34	54.65
Totals			100.00		

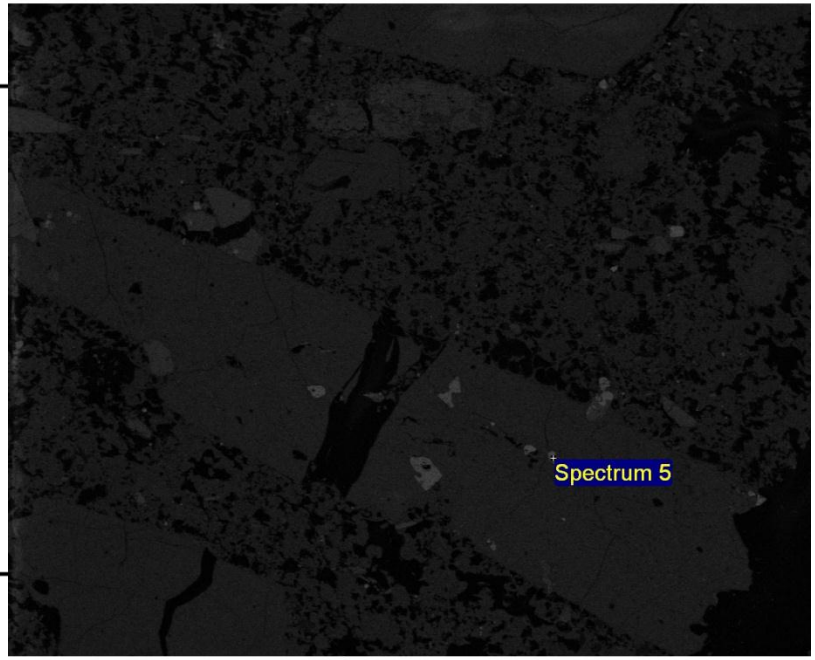

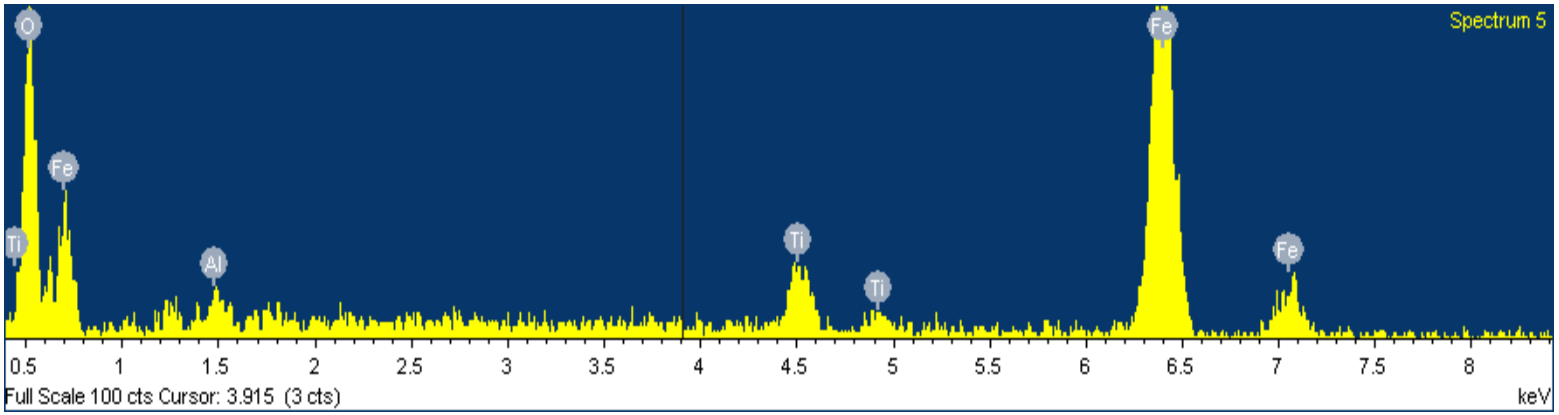

SHL08-21Z

2/11/2011 3:58:19 PM

Element	App Conc.	Intensity Corrn.	Weight%	Weight% Sigma	Atomic%
O K	15.79	0.7390	26.39	2.03	53.39
Mg K	0.88	0.6442	1.69	0.44	2.25
Ti K	21.58	0.9559	27.88	1.41	18.84
Fe K	32.15	0.9015	44.04	1.92	25.52
Totals			100.00		

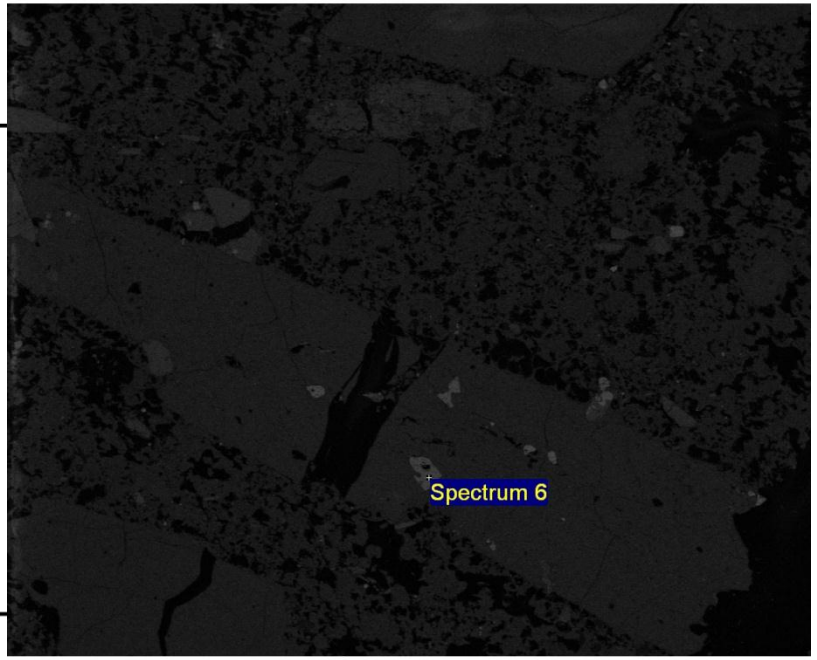

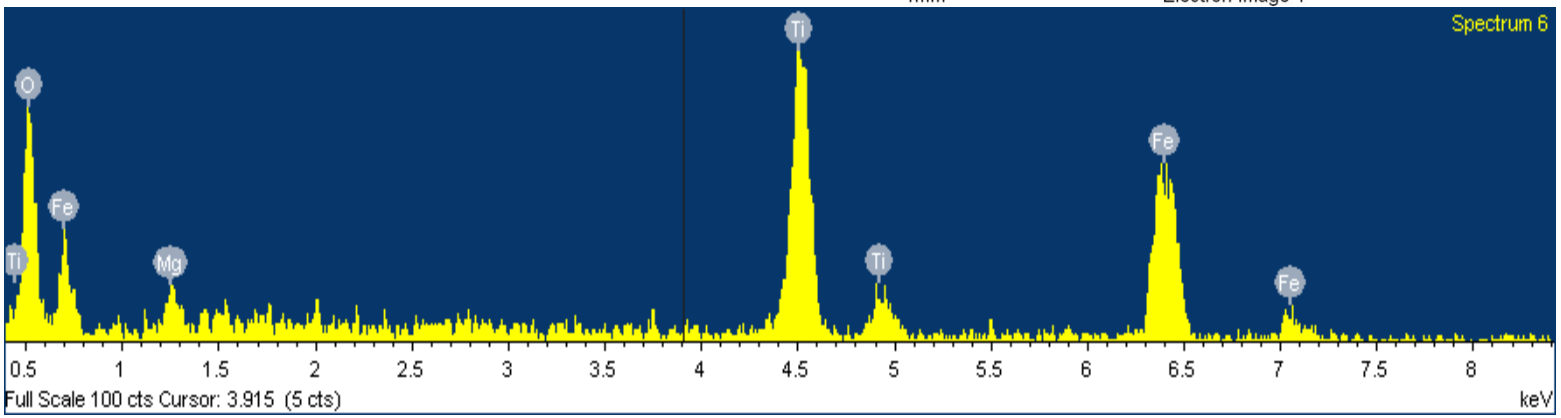

SHL08-21Z

2/11/2011 3:58:27 PM

Element	App Conc.	Intensity Corrn.	Weight%	Weight% Sigma	Atomic%
O K	15.96	0.7502	28.80	2.39	56.35
Mg K	0.78	0.6478	1.63	0.56	2.09
Ti K	19.21	0.9501	27.36	1.66	17.88
Fe K	27.97	0.8963	42.22	2.27	23.67
Totals			100.00		

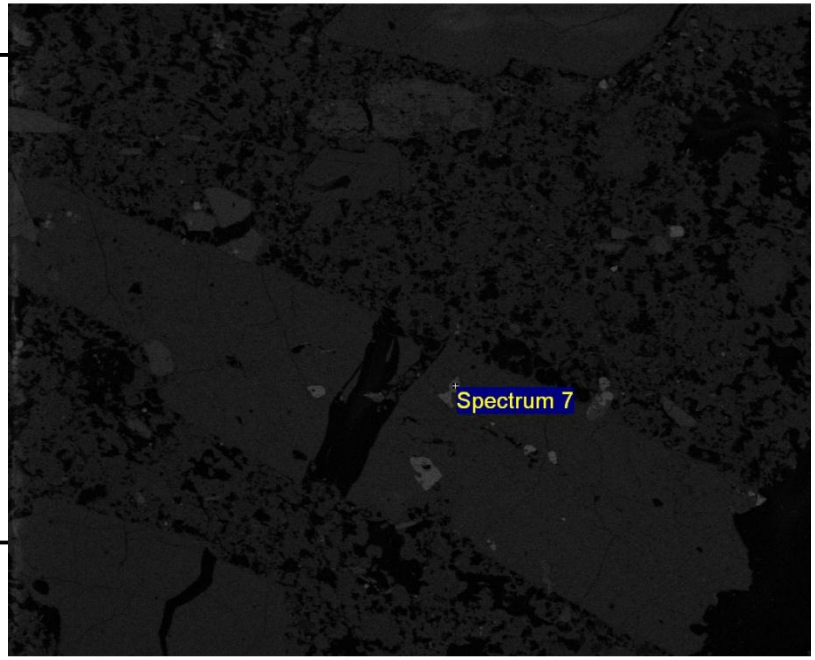

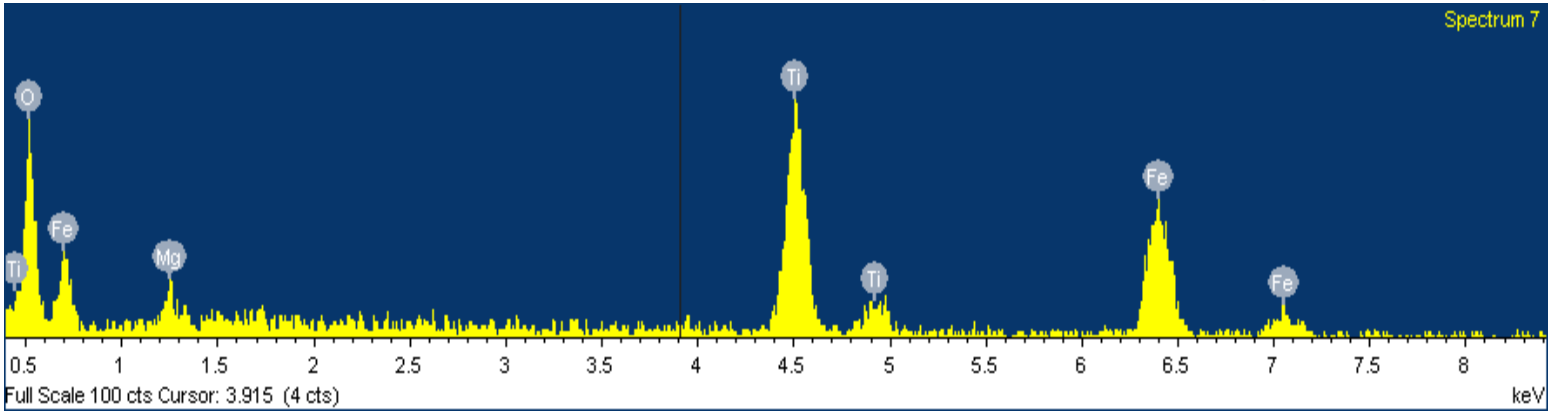

SHL08-21Z

2/11/2011 3:58:37 PM

Element	App Conc.	Intensity Corrn.	Weight%	Weight% Sigma	Atomic%
O K	40.26	1.5592	30.61	1.45	59.21
Mg K	0.46	0.6044	0.89	0.37	1.14
Al K	0.93	0.7238	1.53	0.35	1.75
Si K	0.57	0.8290	0.81	0.31	0.89
Ti K	3.01	0.9687	3.68	0.56	2.38
Fe K	47.97	0.9105	62.48	1.55	34.63
Totals			100.00		

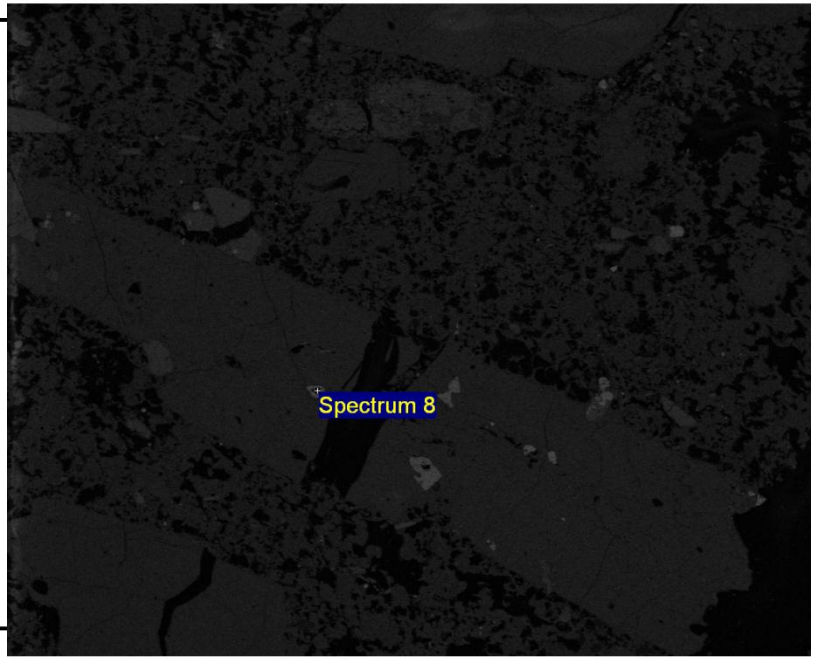

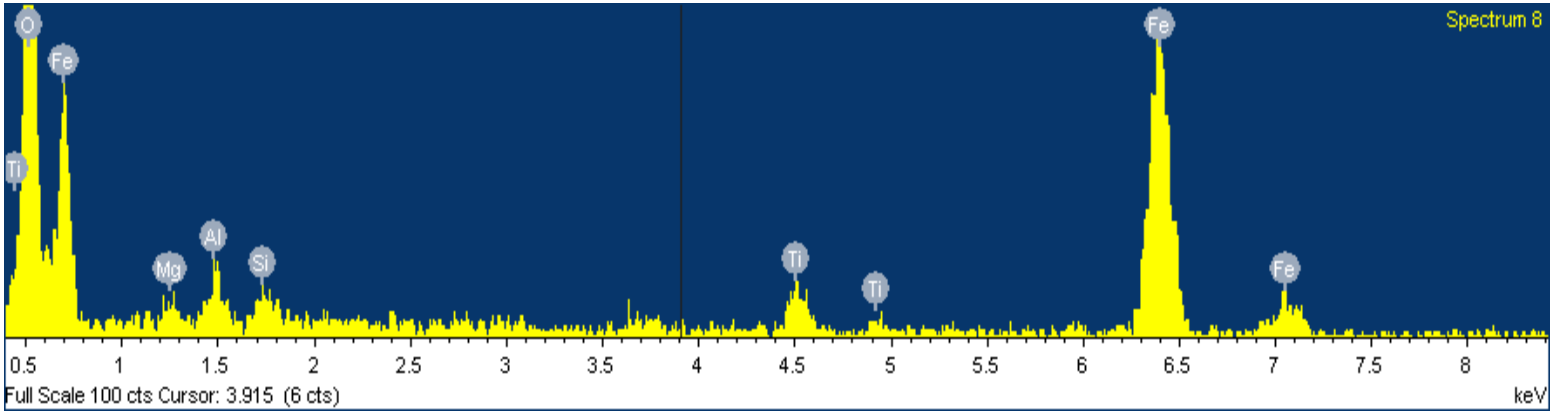

SHL08-21Z

Element	App Conc.	Intensity Corrn.	Weight%	Weight% Sigma	Atomic%
O K	17.79	1.4950	13.94	1.54	35.94
Ti K	3.50	1.0227	4.01	0.92	3.46
Fe K	67.08	0.9578	82.05	1.74	60.61
Totals			100.00		

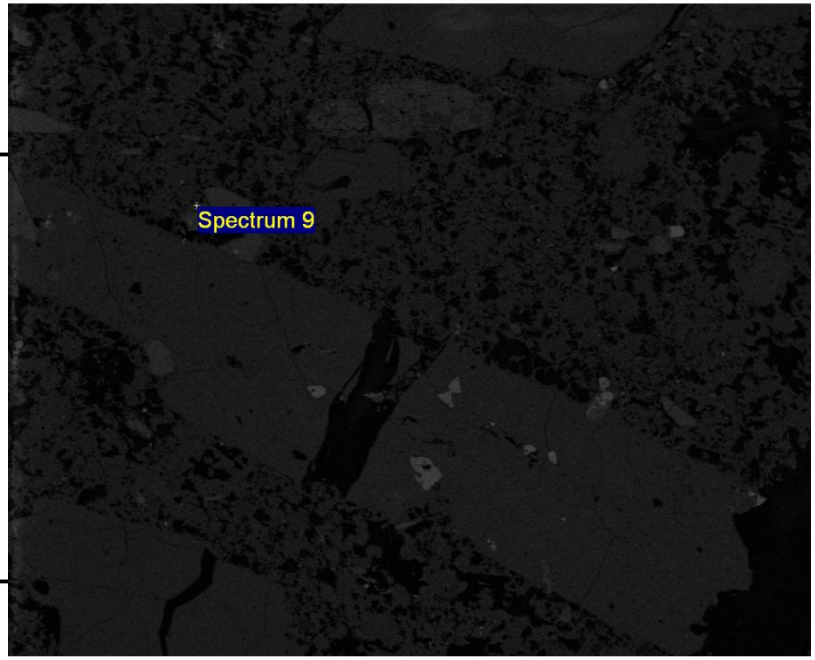

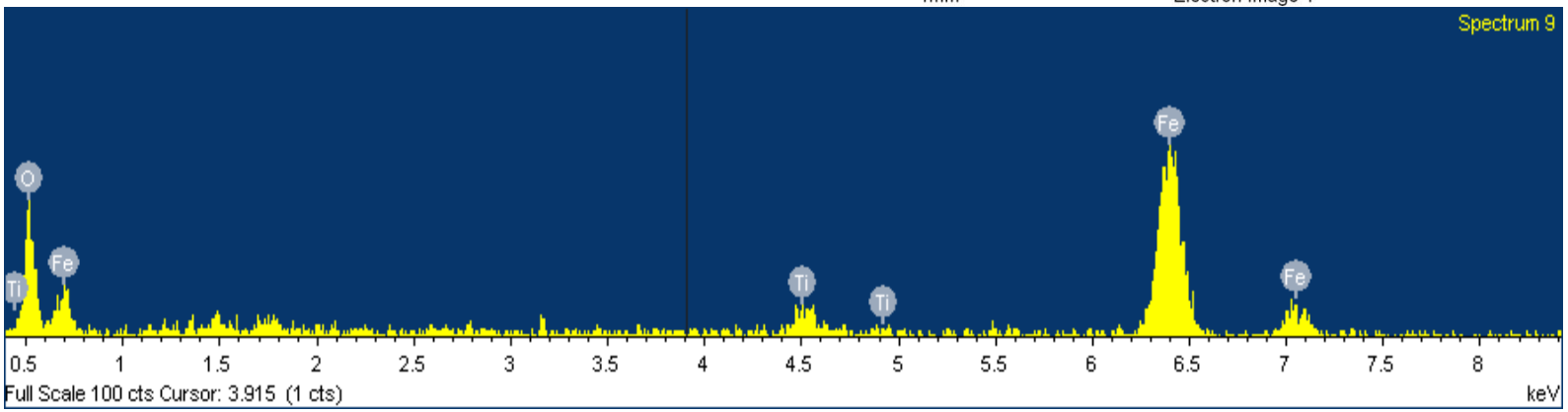

APPENDIX C

WHOLE ROCK TRACE ELEMENT GEOCHEMISTRY, MOUNT ST. HELENS

Appendix C: Whole rock trace element geochemistry, Mount St. Helens. Concentrations are listed in ppm, and <# indicates the concentration was below the detection limit.

sample	Ba	Be	Co	Cr	Cs	Cu	Ga	Ge	Hf	Nb	Ni	Rb	S
SHL06-3Z	428	2	9.2	15.8	2.3	19	19	1	3.2	6.3	15	39	0.004
SHL06-4Z	360	2	8.2	17	1.4	36	18	0.7	3.1	6	20	27	0.007
SHL06-5Z	347	1	11.9	17.2	1.4	16	19	0.9	3.9	5.6	12	35	0.001
SHL06-8Z	345	1	17.5	24.7	1.3	27	18	0.8	3.3	4.8	24	24	0.003
SHL06-9Z	368	2	12.3	14.6	1.8	26	19	0.8	3.6	6.5	10	37	0.003
SHL06-10BZ	366	2	22.7	30.1	1.1	90	15	0.7	4.1	9.7	19	24	0.005
SHL06-10WZ	396	2	14.8	14.2	1.5	25	19	0.8	4.5	11.2	12	31	0.008
SHL06-11Z	312	1	13.4	8.1	1.3	34	17	0.8	2.9	4.1	10	27	0.003
SHL06-12Z	392	2	18.1	11.8	1.9	113	17	0.8	3.8	5.7	6	36	0.006
SHL08-18Z	363	3	10	22	0.8	23	19	1	2.9	5.6	12	36	0.002
SHL08-21Z	415	3	8	21	2.2	4	19	1	3.4	6.9	8	40	0.002
SHL08-26Za	352	1	7.4	8.4	2	13	20	1.3	2.9	4.9	8	37	0.002
SHL08-26Zc	328	1	7.9	40.4	1.9	5	20	1.4	2.7	5.7	8	33	0.004
SHL08-27Z	398	2	9.6	11.5	1.7	3	20	1.3	4	12.2	15	36	0.002
SHL08-28Z	286	1	17.3	15.1	1.3	43	20	1.3	3	5.6	18	28	0.003
SHL08-29Z	398	1	11	20	1.3	16	16	1.1	3.5	6.4	16	34	0.002
SHL08-30Z	297	1	12.1	11.3	1.7	9	20	1.4	3.6	6.4	10	28	0.005
SHL08-33Z	311	1	12.1	13.1	1.4	22	19	1.4	2.7	3.9	11	31	0.005
SHL08-34Z	324	3	10	16	1.4	5	21	0.9	2.9	5.4	7	30	0.004
SHL08-35Z	351	1	14	21	1	12	16	0.8	3.8	5.3	16	26	0.002
SHL08-36EZ	336	3	10	17	2.3	19	21	1.1	2.9	6.4	10	33	0.007
SHL08-37Z	159	1	10.1	20.4	1	15	22	1.2	4.2	7.3	11	12	0.003
SHL08-42Z	370	3	17	28	0.8	24	21	1.1	3.6	9.6	25	23	0.002
SHL08-49AZ	295	2	16	8	0.8	36	18	1	4.1	19	8	20	0.011
SH325-2	347	1	13	14.8	1.3	32	16	0.8	3.3	4.3	10	29	0.003
SHD08-9Z	474	3	6	7	2.6	21	19	1	3.9	7.4	3	55	0.001

sample	Sc	Sr	Ta	Th	Tl	U	V	Y	Zn	Zr	La	Ce
SHL06-3Z	7.1	583	0.5	2.46	0.19	1.93	50	9	54	122	11.5	28.1
SHL06-4Z	6.4	541	0.4	2.46	0.13	1.1	86	10	54	131	12.4	27.3
SHL06-5Z	8.5	492	0.4	2.66	0.07	1.13	62	9	50	148	12.1	25.6
SHL06-8Z	12.1	682	0.4	2.31	0.33	1.05	101	11	54	125	12.3	27.2
SHL06-9Z	8.8	451	0.6	2.64	0.3	1.13	56	12	54	141	15	29.9
SHL06-10BZ	10	537	0.8	2.99	0.07	1.22	72	12	61	176	16.5	35.2
SHL06-10WZ	7.3	518	0.8	3.43	0.18	1.47	48	11	64	186	16	36.5
SHL06-11Z	9.5	466	0.3	2.27	0.24	1.01	76	10	52	118	9.37	20.5
SHL06-12Z	7	426	0.4	3.01	0.31	1.25	41	12	51	141	12.9	26.5
SHL08-18Z	8	486	0.4	2.39	0.46	1.13	77	11	58	111	14.6	27.9
SHL08-21Z	6.4	486	0.5	3.15	0.28	1.41	45	7	57	132	17.9	29.5
SHL08-26Za	6.11	505	0.36	2.76	0.23	1.39	49	8	53	131	12.3	25
SHL08-26Zc	6.52	521	0.36	2.66	0.22	1.36	54	9	55	124	12.6	25.5
SHL08-27Z	6.42	521	0.79	3.5	0.2	1.5	54	8	63	193	14.5	27.7
SHL08-28Z	11.7	512	0.36	2.49	0.11	1.09	111	13	60	145	13.4	27.2
SHL08-29Z	9	459	0.5	2.87	0.2	1.18	75	10	62	131	17	34.9
SHL08-30Z	7.64	489	0.47	3.06	0.18	1.29	77	10	70	164	12.3	22.5
SHL08-33Z	8.63	469	0.29	2.44	0.2	1.08	80	10	55	127	13.6	26.1
SHL08-34Z	6.6	531	0.4	2.1	0.34	0.92	60	8	61	110	12.7	26
SHL08-35Z	9.5	618	0.4	2.79	0.23	1.02	103	10	61	147	16.8	36
SHL08-36EZ	7.7	438	0.6	2.86	0.39	1.57	72	10	61	102	12	24.2
SHL08-37Z	10.3	626	0.43	2	0.08	0.98	83	11	47	199	9.13	20.8
SHL08-42Z	12	767	0.7	3.04	0.19	1.01	115	12	72	148	18.8	37.7
SHL08-49AZ	13.6	576	1.2	2.03	0.33	0.74	129	18	88	179	20.7	43.9
SH325-2	9.9	449	0.3	2.68	0.09	1.13	74	10	52	126	11	22.5
SHD08-9Z	4.7	336	0.6	3.68	0.49	1.55	26	13	58	154	22	36.7

sample	Nd	Sm	Eu	Gd	Tb	Dy	Ho	Er	Tm	Yb	Lu
SHL06-3Z	13.3	3.05	0.969	2.69	0.36	1.87	0.35	1	0.144	0.91	0.128
SHL06-4Z	12.4	2.83	0.94	2.58	0.36	1.95	0.36	1.05	0.148	0.93	0.133
SHL06-5Z	11.9	2.84	0.974	2.52	0.34	1.78	0.34	0.98	0.139	0.87	0.133
SHL06-8Z	13.1	3.11	1.06	2.76	0.38	2.12	0.41	1.21	0.17	1.05	0.157
SHL06-9Z	13.1	3.12	1.03	2.94	0.43	2.33	0.46	1.36	0.191	1.16	0.177
SHL06-10BZ	16	3.56	1.12	3.08	0.44	2.38	0.44	1.24	0.176	1.09	0.168
SHL06-10WZ	15.6	3.34	1.11	3.02	0.41	2.09	0.41	1.2	0.174	1.08	0.153
SHL06-11Z	9.4	2.17	0.762	2.14	0.31	1.71	0.33	0.95	0.137	0.89	0.135
SHL06-12Z	12.3	2.93	0.861	2.57	0.38	2.12	0.41	1.19	0.172	1.12	0.167
SHL08-18Z	17	2.8	1.3	2.65	< 0.1	2.04	0.39	1.09	0.153	0.9	0.13
SHL08-21Z	12	2.4	1.1	1.9	< 0.1	1.38	0.26	0.75	0.111	0.8	0.12
SHL08-26Za	12.2	2.49	0.772	2.1	0.31	1.61	0.3	0.84	0.121	0.79	0.131
SHL08-26Zc	12.3	2.58	0.821	2.25	0.32	1.74	0.32	0.88	0.127	0.84	0.135
SHL08-27Z	11.7	2.26	0.996	1.84	0.28	1.62	0.32	0.91	0.137	0.94	0.153
SHL08-28Z	13.4	2.87	0.917	2.65	0.41	2.38	0.46	1.35	0.21	1.41	0.218
SHL08-29Z	15	3	1.1	2.82	< 0.1	2.31	0.43	1.23	0.178	1	0.14
SHL08-30Z	12.1	2.53	0.838	2.28	0.34	1.86	0.35	0.97	0.141	0.91	0.157
SHL08-33Z	11.9	2.4	0.78	2.22	0.34	1.84	0.35	0.99	0.146	0.95	0.156
SHL08-34Z	13	2.5	0.8	2.3	< 0.1	1.67	0.3	0.84	0.12	0.8	0.13
SHL08-35Z	23	2.8	1.1	2.76	< 0.1	2.14	0.41	1.19	0.171	1	0.15
SHL08-36EZ	10	2.4	1.2	2.49	< 0.1	1.98	0.36	1.03	0.151	1	0.26
SHL08-37Z	11.4	2.84	1.08	2.62	0.41	2.29	0.43	1.21	0.18	1.2	0.189
SHL08-42Z	20	3.2	1.3	2.94	< 0.1	2.27	0.43	1.2	0.172	1.1	0.17
SHL08-49AZ	27	4	1.9	4.44	< 0.1	3.75	0.74	2.12	0.298	1.7	0.24
SH325-2	10.7	2.6	0.852	2.3	0.34	1.92	0.38	1.12	0.16	0.97	0.145
SHD08-9Z	14.3	3.14	0.847	2.89	0.44	2.47	0.48	1.37	0.2	1.26	0.188

APPENDIX D

ZIRCON GEOCHRONOLOGY DATA, MOUNT ST. HELENS

Spot ID	Mount	Date Analyzed	Method	230 cor. 206/238 Age (Ma)	2 sig err 206/238 age (Ma)	U/Th Cor. Factor	UO/U Cor. Factor	Cor. (238/232)	±(238/232)	(230/232)	±(230/232)
SHL3Z-1.1	309	2007 May	U-Pb	0.322	0.033						
SHL3Z-1.2	309	2007 May	U-Pb	0.355	0.053						
SHL3Z-2.1	309	2007 May	U-Pb	0.381	0.053						
SHL3Z-2.2	309	2007 May	U-Pb	0.359	0.049						
SHL3Z-4.1	309	2007 May	U-Pb	0.374	0.041						
SHL3Z-4.2	309	2007 May	U-Pb	0.496	0.084						
SHL3Z-4.3	309	2007 May	U-Pb	0.431	0.058						
SHL3Z-5.1	309	2007 May	U-Pb	0.514	0.110						
SHL3Z-1.4DRa	414	2009 Jan	U-Pb	12.502	0.271						
SHL063Z-2.3A	***414***	***2009 Jan***	***U-Th COMP***				***NA***	***21.95***	***0.72***	***22.23***	***0.57***
SHL3Z-3.1LCa	414	2009 Jan	U-Pb	27.042	1.613						
SHL3Z-3.2DIa	414	2009 Jan	U-Pb	0.597	0.022						
SHL3Z-3.3LRa	414	2009 Jan	U-Pb	0.307	0.012						
SHL3Z-4.3LCa	414	2009 Jan	U-Pb	0.282	0.035						
SHL063Z-4.3A	***414***	***2009 Jan***	***U-Th COMP***				***NA***	***33.08***	***1.08***	***32.65***	***1.12***
SHL3Z-10.1DIa	414	2009 Jan	U-Pb	0.357	0.028						
SHL3Z-11.1LEa	***414***	***2009 Jan***	***U-Pb***	***0.244***	***0.026***						
SHL3Z-11.1A	414	2009 Jan	U-Th COMP				NA	12.46	0.41	11.50	0.29
SHL3Z-5.1DCa	414	2009 Jan	U-Pb	0.248	0.025						
SHL063Z-5.1DCA-A	***414***	***2009 Jan***	***U-Th COMP***				***NA***	***17.59***	***0.57***	***16.64***	***0.47***
SHL3Z-5.1DCa(2)	414	2009 Jan	U-Pb	16.666	0.252						
SHL3Z-6.2LCa	414	2009 Jan	U-Pb	0.286	0.037						
SHL063Z-6.2A	***414***	***2009 Jan***	***U-Th COMP***				***NA***	***16.54***	***0.54***	***15.98***	***0.41***
SHL063Z-7.1A	414	2009 Jan	U-Th COMP				NA	28.57	0.93	27.25	0.56
SHL3Z-7.3LCa	414	2009 Jan	U-Pb	22.84	0.621						

Spot ID	Mount	Date Analyzed	Method	230 cor. 206/238 Age (Ma)	2 sig err 206/238 age (Ma)	U/Th Cor. Factor	UO/U Cor. Factor	Cor. (238/232)	±(238/232)	(230/232)	±(230/232)
SHL3Z-8.5A	414	2009 Jan	U-Th COMP				NA	24.20	0.79	21.80	0.63
SHL3Z-8.1LCa	414	2009 Jan	U-Pb	0.275	0.037						
SHL3Z-9.3LIa	414	2009 Jan	U-Pb	0.283	0.032						
~~SHL063Z-9.3A~~	~~414~~	~~2009 Jan~~	~~U-Th COMP~~				~~NA~~	~~31.92~~	~~1.04~~	~~32.78~~	~~1.20~~
SHL4Z-1.1I	309	2007 May	U-Th			0.938	NA	9.75	0.31	6.82	0.42
SHL4Z-1.2I	309	2007 May	U-Th			0.938	NA	8.72	0.28	6.19	0.41
SHL4Z-10.1	309	2007 May	U-Th			0.938	NA	14.07	0.45	10.74	1.04
SHL4Z-11.1	309	2007 May	U-Th			0.938	NA	17.08	0.55	12.28	0.85
SHL4Z-12.1	309	2007 May	U-Th			0.938	NA	5.93	0.19	3.18	0.30
SHL4Z-2.1C	309	2007 May	U-Th			0.938	NA	8.67	0.28	6.32	0.35
SHL4Z-2.2T	309	2007 May	U-Th			0.938	NA	14.06	0.45	9.07	0.94
SHL4Z-3.1T	309	2007 May	U-Th			0.938	NA	8.28	0.27	6.36	0.29
SHL4Z-3.2I	309	2007 May	U-Th			0.938	NA	13.15	0.42	11.27	0.74
SHL4Z-4.1T	309	2007 May	U-Th			0.938	NA	10.71	0.34	7.41	0.42
SHL4Z-4.2C	309	2007 May	U-Th			0.938	NA	11.07	0.35	9.70	0.38
SHL4Z-4.3I	309	2007 May	U-Th			0.938	NA	10.73	0.34	7.60	0.44
SHL4Z-5.1E	309	2007 May	U-Th			0.938	NA	14.32	0.46	10.97	0.69
SHL4Z-5.2I	309	2007 May	U-Th			0.938	NA	15.06	0.48	9.79	0.59
SHL4Z-6.1C	309	2007 May	U-Th			0.938	NA	17.85	0.57	13.94	1.35
SHL4Z-7.1C	309	2007 May	U-Th			0.938	NA	17.32	0.55	13.23	0.93
SHL4Z-7.2	309	2007 May	U-Th			0.938	NA	11.13	0.36	7.70	0.39
SHL4Z-8.1C	309	2007 May	U-Th			0.938	NA	7.94	0.25	5.66	0.34
SHL4Z-8.2	309	2007 May	U-Th			0.938	NA	7.38	0.24	4.66	0.22
SHL4Z-9.1C	309	2007 May	U-Th			0.938	NA	9.42	0.30	5.70	0.39
SHL5Z-10.1I	364	2008 Jan	U-Th			0.918	NA	11.15	0.37	6.10	0.30
SHL5Z-11.1I	364	2008 Jan	U-Th			0.918	NA	11.79	0.39	8.06	0.36

Spot ID	Mount	Date Analyzed	Method	230 cor. 206/238 Age (Ma)	2 sig err 206/238 age (Ma)	U/Th Cor. Factor	UO/U Cor. Factor	Cor. (238/232)	±(238/232)	(230/232)	±(230/232)
SHL5Z-12.1C	364	2008 Jan	U-Th			0.918	NA	6.67	0.22	3.92	0.12
SHL5Z-12.2T	364	2008 Jan	U-Th			0.918	NA	12.10	0.40	5.67	0.43
SHL5Z-13.1T	364	2008 Jan	U-Th			0.918	NA	11.84	0.39	4.70	0.35
SHL5Z-13.2C	364	2008 Jan	U-Th			0.918	NA	18.94	0.62	15.37	0.84
SHL5Z-14.1I	364	2008 Jan	U-Th			0.918	NA	10.72	0.35	6.92	0.36
SHL5Z-15.1T	364	2008 Jan	U-Th			0.918	NA	6.26	0.20	2.78	0.14
SHL5Z-16.1T	364	2008 Jan	U-Th			0.918	NA	5.61	0.18	2.64	0.17
SHL5Z-17.1IR	364	2008 Jan	U-Th			0.918	NA	15.34	0.50	8.71	0.35
SHL5Z-18.1E	364	2008 Jan	U-Th			0.918	NA	18.15	0.59	13.75	0.56
SHL5Z-19.1IR	364	2008 Jan	U-Th			0.918	NA	11.60	0.38	6.87	0.38
SHL5Z-20.1T	364	2008 Jan	U-Th			0.918	NA	11.46	0.38	7.22	0.49
SHL5Z-3.1C	364	2008 Jan	U-Th			0.918	NA	11.17	0.37	10.46	0.49
SHL5Z-4.1C	364	2008 Jan	U-Th			0.918	NA	8.96	0.29	6.18	0.25
SHL5Z-6.1C	364	2008 Jan	U-Th			0.918	NA	2.36	0.08	2.06	0.04
SHL5Z-6.2T	364	2008 Jan	U-Th			0.918	NA	11.55	0.38	7.76	0.55
SHL5Z-7.1C	364	2008 Jan	U-Th			0.918	NA	8.43	0.28	6.22	0.25
SHL5Z-7.2T	364	2008 Jan	U-Th			0.918	NA	9.98	0.33	4.63	0.29
SHL5Z-9.1I	364	2008 Jan	U-Th			0.918	NA	12.02	0.39	10.33	0.29
SHL5Z-1.1	364	08-01	U-Th			0.918	NA	10.06	0.33	10.19	0.34
SHL5Z-8.1C	364	08-01	U-Th			0.918	NA	11.76	0.39	14.28	0.91
SHD9-2.3C	443	2009 Dec	U-Th			0.982		6.39	0.20	5.18	0.20
SHD9-1.3C	443	2009 Dec	U-Th			0.982		5.80	0.18	4.04	0.13
SHL21Z-13.3A	414	2009 Jan	U-Th			0.920	NA	13.28	0.44	4.01	0.30
SHL21Z-9.2A	414	2009 Jan	U-Th			0.920	NA	6.15	0.20	2.41	0.17
SHL21Z-17.1A	414	2009 Jan	U-Th			0.920	NA	6.64	0.22	2.69	0.19
SHL21Z-5.1A	414	2009 Jan	U-Th			0.920	NA	4.43	0.14	2.17	0.13
SHL21Z-12.2A	414	2009 Jan	U-Th			0.920	NA	6.82	0.22	2.90	0.15
SHL21Z-16.1A	414	2009 Jan	U-Th			0.920	NA	5.80	0.19	2.62	0.17

Spot ID	Mount	Date Analyzed	Method	230 cor. 206/238 Age (Ma)	2 sig err 206/238 age (Ma)	U/Th Cor. Factor	UO/U Cor. Factor	Cor. (238/232)	±(238/232)	(230/232)	±(230/232)
SHL21Z-6.1A	414	2009 Jan	U-Th			0.920	NA	4.81	0.16	2.42	0.18
SHL21Z-15.1A	414	2009 Jan	U-Th			0.920	NA	4.17	0.14	2.22	0.13
SHL21Z-14.1A	414	2009 Jan	U-Th			0.920	NA	8.19	0.27	3.94	0.27
SHL21Z-9.1A	414	2009 Jan	U-Th			0.920	NA	4.26	0.14	2.40	0.15
SHL21Z-7.3A	414	2009 Jan	U-Th			0.920	NA	11.98	0.39	5.89	0.42
SHL21Z-8.3A	414	2009 Jan	U-Th			0.920	NA	14.83	0.48	8.07	0.33
SHL21Z-4.1A	414	2009 Jan	U-Th			0.920	NA	16.11	0.53	9.03	0.55
SHL21Z-20.1A	414	2009 Jan	U-Th			0.920	NA	12.14	0.40	7.30	0.34
SHL21Z-10.1A	414	2009 Jan	U-Th			0.920	NA	6.66	0.22	4.39	0.29
SHL21Z-4.2A	414	2009 Jan	U-Th			0.920	NA	14.45	0.47	9.09	0.49
SHL21Z-12.1A	414	2009 Jan	U-Th			0.920	NA	4.83	0.16	3.41	0.16
SHL21Z-13.1A	414	2009 Jan	U-Th			0.920	NA	17.06	0.56	11.01	0.55
SHL21Z-3.1A	414	2009 Jan	U-Th			0.920	NA	11.93	0.39	8.17	0.32
SHL21Z-19.1A	414	2009 Jan	U-Th			0.920	NA	5.28	0.17	3.86	0.17
SHL21Z-5.2A	414	2009 Jan	U-Th			0.920	NA	5.43	0.18	4.10	0.28
SHL21Z-8.1A	414	2009 Jan	U-Th			0.920	NA	13.88	0.45	10.79	0.45
SHL21Z-11.2A	414	2009 Jan	U-Th			0.920	NA	7.31	0.24	5.86	0.20
SHL21Z-2.2A	414	2009 Jan	U-Th			0.920	NA	23.32	0.76	18.40	0.55
SHL21Z-11.1A	414	2009 Jan	U-Th			0.920	NA	10.41	0.34	8.95	0.24
SHL21Z-1.2A	414	2009 Jan	U-Th			0.920	NA	14.95	0.49	13.42	0.54
SHL21Z-7.1A	414	2009 Jan	U-Th			0.920	NA	11.85	0.39	10.83	0.44
SHL21Z-13.1A	414	2009 Jan	U-Th			0.920	NA	11.21	0.37	10.57	0.45
SHL21Z-18.1A	414	09-01	U-Th			0.920	NA	4.93	0.16	5.01	0.34
SHL21Z-21.1A	414	09-01	U-Th			0.920	NA	12.57	0.41	11.98	0.34
SHL26C-1.1C	443	2009 Dec	U-Th			0.982		13.32	0.41	10.20	0.40
SHL26C-3.2C	443	2009 Dec	U-Th			0.982		9.62	0.30	4.68	0.30
SHL26C-2.1C	443	2009 Dec	U-Th			0.982		27.69	0.85	19.12	0.81
SHL26C-4.1C	443	2009 Dec	U-Th			0.982		17.45	0.53	14.52	0.65
SHL26C-4.2T	443	2009 Dec	U-Th			0.982		13.85	0.42	7.02	0.31

Spot ID	Mount	Date Analyzed	Method	230 cor. 206/238 Age (Ma)	2 sig err 206/238 age (Ma)	U/Th Cor. Factor	UO/U Cor. Factor	Cor. (238/232)	±(238/232)	(230/232)	±(230/232)
SHL26C-5.1T	443	2009 Dec	U-Th			0.982		11.78	0.36	5.82	0.28
SHL26C-5.2C	443	2009 Dec	U-Th			0.982		12.19	0.37	7.82	0.37
SHL26C-16.1R	443	2009 Dec	U-Th			0.982		9.76	0.30	6.07	0.31
SHL26C-6.2I	443	2009 Dec	U-Th			0.982		19.18	0.59	12.52	0.53
SHL26C-7.1C	443	2009 Dec	U-Th			0.982		10.56	0.32	5.15	0.24
SHL26C-7.1C2	443	2009 Dec	U-Th			0.982		16.58	0.51	9.02	0.47
SHL26C-9.1C	443	2009 Dec	U-Th			0.982		12.00	0.37	9.87	0.34
SHL26C-9.3R	443	2009 Dec	U-Th			0.982		11.12	0.34	7.60	0.26
SHL26C-10.3R	443	2009 Dec	U-Th			0.982		15.51	0.47	8.89	0.41
SHL26C-11.1C	443	2009 Dec	U-Th			0.982		6.94	0.21	4.38	0.19
SHL26C-12.2I	443	2009 Dec	U-Th			0.982		12.33	0.38	7.38	0.30
SHL26C-12.1C	443	2009 Dec	U-Th			0.982		16.42	0.50	11.65	0.56
SHL26C-17.1I	443	2009 Dec	U-Th			0.982		15.06	0.46	8.88	0.45
SHL26C-18.1I	443	2009 Dec	U-Th			0.982		15.74	0.48	9.45	0.36
SHL26C-19.1T	443	2009 Dec	U-Th			0.982		12.82	0.39	6.91	0.26
SHL26C-20.1R	443	2009 Dec	U-Th			0.982		19.00	0.58	9.90	0.44
SHL26C-13.1C	443	2009 Dec	U-Th			0.982		12.44	0.38	8.76	0.44
SHL26C-13.2R	443	2009 Dec	U-Th			0.982		13.39	0.41	7.07	0.37
SHL26C-21.1I	443	2009 Dec	U-Th			0.982		9.83	0.30	6.86	0.33
SHL26C-14.2I	443	2009 Dec	U-Th			0.982		9.17	0.28	7.28	0.25
SHL26C-22.1R	443	2009 Dec	U-Th			0.982		14.62	0.45	7.86	0.35
SHL26C-15.1IR	443	2009 Dec	U-Th			0.982		10.02	0.31	5.27	0.11
SHL26C-15.3C	443	2009 Dec	U-Th			0.982		18.98	0.58	12.61	0.67
SHL26C-23.1R	443	2009 Dec	U-Th			0.982		17.29	0.53	11.39	0.46
SHL26C-24.1I	443	2009 Dec	U-Th			0.982		13.05	0.40	11.61	0.53
SHL29AZ-1.1C	393	2008 Aug	U-Th			0.902	0.97	18.92	0.59	15.62	0.57
SHL29Z-1.1CUPB	***393***	***2009 Jan***	***U-Pb***	***0.145***	***0.030***						
SHL29AZ-10.1I	393	2008 Aug	U-Th			0.902	0.88	10.44	0.35	7.82	0.26
SHL29AZ-11.1CA	393	2008 Aug	U-Th			0.902	0.89	7.50	0.25	6.40	0.16

Spot ID	Mount	Date Analyzed	Method	230 cor. 206/238 Age (Ma)	2 sig err 206/238 age (Ma)	U/Th Cor. Factor	UO/U Cor. Factor	Cor. (238/232)	±(238/232)	(230/232)	±(230/232)
SHL29AZ-12.1EA	393	2008 Aug	U-Th			0.902	0.94	9.81	0.31	5.55	0.19
SHL29AZ-12.2CA	393	2008 Aug	U-Th			0.902	0.93	8.72	0.28	5.91	0.20
SHL29AZ-13.1CA	393	2008 Aug	U-Th			0.902	0.93	19.06	0.62	14.90	0.52
SHL29AZ-13.2EA	393	2008 Aug	U-Th			0.902	0.95	9.74	0.31	5.24	0.18
SHL29AZ-14.1CA	393	2008 Aug	U-Th			0.902	1.14	13.53	0.36	8.61	0.29
SHL29AZ-15.1EA	393	2008 Aug	U-Th			0.902	0.95	9.30	0.29	4.57	0.17
SHL29AZ-2.2IA	393	2008 Aug	U-Th			0.902	0.93	16.39	0.53	13.68	0.51
SHL29AZ-3.2EA	393	2008 Aug	U-Th			0.902	0.96	16.46	0.52	9.42	0.47
SHL29AZ-4.1CA	393	2008 Aug	U-Th			0.902	0.93	16.29	0.53	13.42	0.42
SHL29AZ-4.2EA	393	2008 Aug	U-Th			0.902	0.94	10.50	0.34	7.46	0.24
SHL29AZ-5.2EA	393	2008 Aug	U-Th			0.902	0.98	14.90	0.46	8.59	0.37
SHL29AZ-6.1CA	393	2008 Aug	U-Th			0.902	1.01	4.02	0.12	2.39	0.04
SHL29AZ-6.2EA	393	2008 Aug	U-Th			0.902	0.92	9.15	0.30	4.56	0.16
SHL29AZ-7.2IA	393	2008 Aug	U-Th			0.902	0.97	7.82	0.24	5.70	0.18
SHL29AZ-7.3EA	393	2008 Aug	U-Th			0.902	0.93	7.06	0.23	5.14	0.15
SHL29AZ-8.1CA	393	2008 Aug	U-Th			0.902	0.99	8.60	0.26	5.11	0.16
SHL29AZ-9.1CA	393	2008 Aug	U-Th			0.902	0.97	8.67	0.27	5.27	0.19
SHL29AZ-9.3EA	393	2008 Aug	U-Th			0.902	0.94	11.86	0.38	6.00	0.25
SHL29AZ-1.1TA	392	2008 Aug	U-Th			0.907		14.78	0.49	7.82	0.31
SHL29AZ-3.4EA	392	2008 Aug	U-Th			0.907		15.61	0.52	8.24	0.32
SHL29AZ-2.2EA	392	2008 Aug	U-Th			0.907		11.12	0.37	6.93	0.25
SHL29AZ-1.2CA	392	2008 Aug	U-Th			0.907		6.03	0.20	4.68	0.08
SHL29AZ-3.2IEA	392	2008 Aug	U-Th			0.907		17.36	0.57	13.48	0.46
SHL29AZ-3.1CA	392	2008 Aug	U-Th			0.907		17.20	0.57	15.74	0.47
SHL29AZ-2.3bIA	***392***	***2008 Aug***	***U-Th***			***0.907***		***7.37***	***0.24***	***7.39***	***0.21***
SHL29Z-2.3IUPB	392	2009 Jan	U-Pb	23.519	0.694						
SHL29AZ-2.4IA	***392***	***2008 Aug***	***U-Th***			***0.907***		***6.03***	***0.20***	***5.90***	***0.14***
SHL29Z-2.4IUPB	392	2009 Jan	U-Pb	24.352	0.585						

Spot ID	Mount	Date Analyzed	Method	230 cor. 206/238 Age (Ma)	2 sig err 206/238 age (Ma)	U/Th Cor. Factor	UO/U Cor. Factor	Cor. (238/232)	±(238/232)	(230/232)	±(230/232)
SHL08-29Z-14.3c	478	2010 May	U-Th			0.949		20.51	0.65	26.22	0.83
SHL08-29Z-13.2c	478	2010 May	U-Th			0.949		4.93	0.16	6.02	0.22
SHL08-29Z-6.3c	478	2010 May	U-Th			0.949		15.92	0.50	17.82	0.67
SHL08-29Z-8.3c	478	2010 May	U-Th			0.949		19.60	0.62	21.40	0.70
SHL08-29Z-10.3c	478	2010 May	U-Th			0.949		16.09	0.51	17.16	0.53
SHL08-29Z-8.4i	478	2010 May	U-Th			0.949		29.80	0.94	31.00	0.99
SHL08-29Z-11.4i	478	2010 May	U-Th			0.949		14.84	0.47	15.13	0.51
SHL08-29Z-1.2C	478	2010 May	U-Th			0.949		28.55	0.90	28.75	0.51
SHL08-29Z-11.3c	478	2010 May	U-Th			0.949		26.30	0.83	25.61	0.84
SHL08-29Z-14.4i	478	2010 May	U-Th			0.949		15.07	0.48	14.36	0.45
SHL08-29Z-7.2c	478	2010 May	U-Th			0.949		13.05	0.41	12.36	0.38
SHL08-29Z-17.1c	478	2010 May	U-Th			0.949		15.50	0.49	14.50	0.44
SHL08-29Z-9.2c	478	2010 May	U-Th			0.949		13.14	0.42	12.25	0.36
SHL08-29Z-6.4e	478	2010 May	U-Th			0.949		17.28	0.55	15.44	0.56
SHL08-29Z-15.2i	478	2010 May	U-Th			0.949		10.52	0.33	8.43	0.28
SHL08-29Z-3.2c	478	2010 May	U-Th			0.949		14.82	0.47	11.61	0.40
SHL08-29Z-4.2c	478	2010 May	U-Th			0.949		14.14	0.45	10.66	0.35
SHL08-29Z-10.4i	478	2010 May	U-Th			0.949		9.53	0.30	7.11	0.21
SHL08-29Z-5.4e	478	2010 May	U-Th			0.949		9.82	0.31	7.30	0.24
SHL08-29Z-2.2c	478	2010 May	U-Th			0.949		15.70	0.50	10.42	0.38
SHL08-29Z-16.2i	478	2010 May	U-Th			0.949		6.66	0.21	4.55	0.12
SHL08-29Z-12.2c	478	2010 May	U-Th			0.949		2.60	0.08	1.97	0.03
SHL30C-15.1R	443	2009 Dec				0.982		7.91	0.24	5.06	0.18
SHL30C-16.1C	443	2009 Dec				0.982		15.67	0.48	9.40	0.49
SHL30C-1.2R	443	2009 Dec				0.982		14.03	0.43	8.31	0.37
SHL30C-2.1C	443	2009 Dec				0.982		16.62	0.51	14.24	0.52
SHL30C-17.1C	443	2009 Dec				0.982		15.13	0.46	8.69	0.47
SHL30C-17.2E	443	2009 Dec				0.982		14.83	0.45	7.67	0.36
SHL30C-3.3I	443	2009 Dec				0.982		9.87	0.30	5.40	0.17

Spot ID	Mount	Date Analyzed	Method	230 cor. 206/238 Age (Ma)	2 sig err 206/238 age (Ma)	U/Th Cor. Factor	UO/U Cor. Factor	Cor. (238/232)	±(238/232)	(230/232)	±(230/232)
SHL30C-3.1C	443	2009 Dec				0.982		17.28	0.53	11.91	0.57
SHL30C-4.2C	443	2009 Dec				0.982		16.21	0.50	5.82	0.35
SHL30C-5.2T	443	2009 Dec				0.982		9.28	0.28	6.70	0.22
SHL30C-6.1I	443	2009 Dec				0.982		14.22	0.43	9.82	0.39
SHL30C-7.1C	443	2009 Dec				0.982		10.84	0.33	8.96	0.31
SHL30C-7.3R	443	2009 Dec				0.982		10.74	0.33	6.34	0.23
SHL30C-8.1C	443	2009 Dec				0.982		7.70	0.24	6.43	0.17
SHL30C-10.1C	443	2009 Dec				0.982		15.07	0.46	9.57	0.49
SHL30C-10.3R	443	2009 Dec				0.982		15.60	0.48	8.34	0.37
SHL30-12.2I	443	2009 Dec				0.982		14.91	0.46	8.03	0.39
SHL30-11.2T	443	2009 Dec				0.982		13.21	0.40	8.54	0.31
SHL30-4.3R	443	2009 Dec				0.982		14.71	0.45	9.29	0.49
SHL30-13.1C	443	2009 Dec				0.982		12.83	0.39	8.56	0.29
SHL30-18.1I	443	2009 Dec				0.982		20.80	0.64	10.95	0.58
SHL30-18.2R	443	2009 Dec				0.982		14.14	0.43	9.79	0.39
SHL30-4.4C	443	2009 Dec				0.982		16.72	0.51	13.42	0.72
SHL33-3.3I	443	2009 Dec				0.982		8.69	0.27	7.87	0.25
SHL33-2.2I	443	2009 Dec				0.982		3.32	0.10	2.31	0.11
SHL33-4.2C	443	2009 Dec				0.982		1.92	0.06	1.69	0.04
SHL33-4.1T	443	2009 Dec				0.982		4.77	0.15	3.44	0.11
SHL34Z-9.1IA	393	2008 Aug	U-Th				0.98	2.69	0.08	1.28	0.05
SHL34Z-11.3IA	393	2008 Aug	U-Th				0.91	7.21	0.24	1.63	0.08
SHL34Z-13.1CA	393	2008 Aug	U-Th				0.99	6.98	0.21	1.64	0.09
SHL34Z-1.2EA	393	2008 Aug	U-Th				0.92	13.03	0.43	2.56	0.16
SHL34Z-1.1IA	393	2008 Aug	U-Th				0.95	8.11	0.26	2.01	0.12
SHL34Z-7.2EA	393	2008 Aug	U-Th				0.98	5.60	0.17	1.80	0.09
SHL34Z-3.1EA	393	2008 Aug	U-Th				0.93	7.79	0.25	2.51	0.13
SHL34Z-12.1IA	393	2008 Aug	U-Th				1.00	4.20	0.13	1.98	0.10

Spot ID	Mount	Date Analyzed	Method	230 cor. 206/238 Age (Ma)	2 sig err 206/238 age (Ma)	U/Th Cor. Factor	UO/U Cor. Factor	Cor. (238/232)	±(238/232)	(230/232)	±(230/232)
SHL34Z-6.2IA	393	2008 Aug	U-Th				1.01	3.86	0.11	2.13	0.11
SHL34Z-8.1IA	393	2008 Aug	U-Th				0.99	4.00	0.12	2.37	0.12
SHL34Z-11.1IA	393	2008 Aug	U-Th				0.97	8.70	0.27	4.95	0.15
SHL34Z-2.2IA	393	2008 Aug	U-Th				1.05	34.88	1.00	28.51	0.73
SHL34Z-5.1IA	393	2008 Aug	U-Th				0.93	15.72	0.51	13.45	0.35
SHL34Z-10.1IA	393	2008 Aug	U-Th				0.94	14.20	0.45	12.50	0.28
SHL34Z-3.3IA	393	2008 Aug	U-Th				0.94	5.69	0.18	5.12	0.31
SHL34Z-3.3EA	392	2008 Aug	U-Th			0.907		8.18	0.27	1.76	0.08
SHL34Z-4.1EA	392	2008 Aug	U-Th			0.907		7.64	0.25	1.99	0.10
SHL34Z-6.1A	392	2008 Aug	U-Th			0.907		4.24	0.14	1.57	0.06
SHL34Z-3.1IA	392	2008 Aug	U-Th			0.907		5.37	0.18	2.18	0.11
SHL34Z-5.1IA	392	2008 Aug	U-Th			0.907		5.00	0.17	2.20	0.13
SHL34Z-4.2CA	392	2008 Aug	U-Th			0.907		4.86	0.16	2.32	0.11
SHL34Z-2.1IA	392	2008 Aug	U-Th			0.907		3.46	0.11	2.11	0.09
SHL34Z-1.3EA	392	2008 Aug	U-Th			0.907		17.03	0.56	11.51	0.45
SHL34Z-1.1CA	392	2008 Aug	U-Th			0.907		21.30	0.71	19.65	0.65
SHL34Z-5.1IUPB	393	2009 Jan	U-Pb EQ	0.260	0.087						
SHL34Z-3.3IUPB	393	2009 Jan	U-Pb EQ	0.334	0.524						
SHL34Z-10.1IUPB	393	2009 Jan	U-Pb EQ	0.195	0.025						
SHL29Z-1.1CUPB	393	2009 Jan	U-Pb EQ	0.145	0.030						
SHL34Z-1.1CUPB	393	2009 Jan	U-Pb EQ	0.159	0.058						
SHL34Z-2.2IUPB	393	2009 Jan	U-Pb EQ	0.317	0.098						
SHL36E-1.5I	443	2009 Dec	U-Pb	0.203	0.037						
SHL36E-10.2I	443	2009 Dec	U-Pb	0.156	0.038						
SHL36E-12.4R	443	2009 Dec	U-Pb	0.244	0.026						
SHL36E-13.3I	443	2009 Dec	U-Pb	0.163	0.021						
SHL36E-14.4C	443	2009 Dec	U-Pb	0.187	0.020						
SHL36E-15.1	443	2009 Dec	U-Pb	0.238	0.032						
SHL36E-16.1	443	2009 Dec	U-Pb	0.245	0.035						

Spot ID	Mount	Date Analyzed	Method	230 cor. 206/238 Age (Ma)	2 sig err 206/238 age (Ma)	U/Th Cor. Factor	UO/U Cor. Factor	Cor. (238/232)	±(238/232)	(230/232)	±(230/232)
SHL36E-17.1	443	2009 Dec	U-Pb	0.226	0.050						
SHL36E-18.1C	443	2009 Dec	U-Pb	0.267	0.075						
SHL36E-18.1R	443	2009 Dec	U-Pb	0.199	0.022						
SHL36E-2.3C	443	2009 Dec	U-Pb	0.256	0.042						
SHL36E-20.1C	443	2009 Dec	U-Pb	0.166	0.112						
SHL36E-21.1C	443	2009 Dec	U-Pb	0.210	0.051						
SHL36E-3.4C	443	2009 Dec	U-Pb	0.200	0.081						
SHL36E-4.3T	443	2009 Dec	U-Pb	0.176	0.041						
SHL36E-6.1R	443	2009 Dec	U-Pb	0.189	0.048						
SHL36E-7.1I	443	2009 Dec	U-Pb	0.226	0.044						
SHL36E-8.3R	443	2009 Dec	U-Pb	0.202	0.029						
SHL36E-9.3C	443	2009 Dec	U-Pb	0.200	0.016						
SHL36E-1.6	443R	2010 May	U-Th			1.110		17.64	0.48	14.39	0.37
SHL36E-1.7	443R	2010 May	U-Th			1.110		14.84	0.40	12.14	0.31
SHL36E-10.2I	443R	2010 May	U-Th			1.110		12.46	0.34	10.35	0.30
SHL36E-12.4	443R	2010 May	U-Th			1.110		12.76	0.34	10.21	0.22
SHL36E-13.3I	443R	2010 May	U-Th			1.110		3.99	0.11	2.93	0.05
SHL36E-14.4	443R	2010 May	U-Th			1.110		6.73	0.18	5.25	0.11
SHL36E-15.2T	443R	2010 May	U-Th			1.110		12.95	0.35	10.04	0.21
SHL36E-16.2T	443R	2010 May	U-Th			1.110		14.71	0.40	10.59	0.22
SHL36E-17.2T	443R	2010 May	U-Th			1.110		20.48	0.55	15.58	0.41
SHL36E-2.4	443R	2010 May	U-Th			1.110		15.89	0.43	12.09	0.35
SHL36E-3.4	443R	2010 May	U-Th			1.110		9.29	0.25	7.05	0.11
SHL36E-4.3T	443R	2010 May	U-Th			1.110		19.11	0.52	15.86	0.47
SHL36E-6.3T	443R	2010 May	U-Th			1.110		18.21	0.49	14.49	0.43
SHL36E-7.3T	443R	2010 May	U-Th			1.110		21.27	0.58	17.39	0.41
SHL36E-8.3R	443R	2010 May	U-Th			1.110		13.82	0.37	10.95	0.22
SHL36E-9.3C	443R	2010 May	U-Th			1.110		5.05	0.14	3.97	0.06

Spot ID	Mount	Date Analyzed	Method	230 cor. 206/238 Age (Ma)	2 sig err 206/238 age (Ma)	U/Th Cor. Factor	UO/U Cor. Factor	Cor. (238/232)	±(238/232)	(230/232)	±(230/232)
SHL37P14.4R	443	2009 Dec	U-Pb	0.069	0.042						
SHL37P-15.1T	443	2009 Dec	U-Pb	0.116	0.023						
SHL37P-11.5C	443	2009 Dec	U-Pb	0.118	0.058						
SHL37P-7.5T	443	2009 Dec	U-Pb	0.119	0.070						
SHL37P-4.4R	443	2009 Dec	U-Pb	0.121	0.030						
SHL37P-8.4C	443	2009 Dec	U-Pb	0.126	0.012						
SHL37P-2.4R	443	2009 Dec	U-Pb	0.136	0.039						
SHL37P-9.3C	443	2009 Dec	U-Pb	0.151	0.027						
SHL37P-16.1R	443	2009 Dec	U-Pb	0.173	0.038						
SHL37P-7.6I	443	2009 Dec	U-Pb	0.176	0.086						
SHL37P-13.3C	443	2009 Dec	U-Pb	0.181	0.046						
SHL37P-14.3C	443	2009 Dec	U-Pb	0.189	0.066						
SHL37P-12.4I	443	2009 Dec	U-Pb	0.191	0.034						
SHL37P-18.1C	443	2009 Dec	U-Pb	0.204	0.048						
SHL37P-5.4C	443	2009 Dec	U-Pb	0.237	0.064						
SHL37P-17.1C	443	2009 Dec	U-Pb	0.317	0.091						
SHL37P-18.2	443R	2010 May	U-Th			1.110		16.48	0.45	13.70	0.51
SHL37P-7.8	443R	2010 May	U-Th			1.110		38.38	1.04	31.22	1.29
SHL37P-5.5	443R	2010 May	U-Th			1.110		13.90	0.38	11.28	0.34
SHL37P-4.5	443R	2010 May	U-Th			1.110		25.25	0.68	20.28	0.63
SHL37P-17.2	443R	2010 May	U-Th			1.110		13.90	0.38	10.96	0.42
SHL37P-2.5	443R	2010 May	U-Th			1.110		13.42	0.36	10.33	0.24
SHL37P-13.4	443R	2010 May	U-Th			1.110		8.50	0.23	6.56	0.18
SHL37P-12.5	443R	2010 May	U-Th			1.110		14.33	0.39	10.82	0.30
SHL37P-11.6	443R	2010 May	U-Th			1.110		16.96	0.46	12.50	0.39
SHL37P-7.7	443R	2010 May	U-Th			1.110		23.63	0.64	16.99	0.68
SHL37P-6.2	443R	2010 May	U-Th			1.110		22.17	0.60	15.76	0.51
SHL37P-11.7	443R	2010 May	U-Th			1.110		15.54	0.42	10.88	0.36
SHL37P-8.5	443R	2010 May	U-Th			1.110		2.82	0.08	2.15	0.03

Spot ID	Mount	Date Analyzed	Method	230 cor. 206/238 Age (Ma)	2 sig err 206/238 age (Ma)	U/Th Cor. Factor	UO/U Cor. Factor	Cor. (238/232)	±(238/232)	(230/232)	±(230/232)
SHL37P-19.1	443R	2010 May	U-Th			1.110		19.42	0.53	13.24	0.43
SHL37P-1.4	443R	2010 May	U-Th			1.110		20.03	0.54	13.47	0.38
SHL37P-14.6	443R	2010 May	U-Th			1.110		14.18	0.38	9.51	0.33
SHL37P-15.3	443R	2010 May	U-Th			1.110		20.17	0.55	12.31	0.45
SHL37P-14.5	443R	2010 May	U-Th			1.110		12.89	0.35	7.94	0.26
SHL37P-4.4	443R	2010 May	U-Th			1.110		12.24	0.33	6.90	0.18
SHL37P-9.4	443R	2010 May	U-Th			1.110		1.71	0.05	1.32	0.02
SHL37P-16.2	443R	2010 May	U-Th			1.110		11.46	0.31	6.40	0.21
SHL49AZ-6.1A	414	2009 Jan	U-Th			0.920	NA	3.66	0.12	1.42	0.07
SHL49AZ-14.1A	414	2009 Jan	U-Th			0.920	NA	3.49	0.11	1.42	0.07
SHL49AZ-7.1A	414	2009 Jan	U-Th			0.920	NA	3.65	0.12	1.52	0.08
SHL49AZ-4.3A	414	2009 Jan	U-Th			0.920	NA	5.35	0.17	1.76	0.10
SHL49AZ-4.2A	414	2009 Jan	U-Th			0.920	NA	4.38	0.14	1.71	0.10
SHL49AZ-3.1A	414	2009 Jan	U-Th			0.920	NA	3.77	0.12	1.65	0.10
SHL49AZ-10.1A	414	2009 Jan	U-Th			0.920	NA	4.59	0.15	1.81	0.11
SHL49AZ-1.1A	414	2009 Jan	U-Th			0.920	NA	4.22	0.14	1.87	0.13
SHL49AZ-15.1A	414	2009 Jan	U-Th			0.920	NA	4.54	0.15	2.01	0.11
SHL49AZ-2.1A	414	2009 Jan	U-Th			0.920	NA	5.14	0.17	2.22	0.14
SHL49AZ-12.2A	414	2009 Jan	U-Th			0.920	NA	4.45	0.15	2.06	0.13
SHL49AZ-12.3A	414	2009 Jan	U-Th			0.920	NA	5.17	0.17	2.28	0.13
SHL49AZ-11.1A	414	2009 Jan	U-Th			0.920	NA	5.67	0.19	3.59	0.23
SHL49AZ-13.1A	414	2009 Jan	U-Th			0.920	NA	8.42	0.27	6.25	0.22
SHL49AZ-13.3A	414	2009 Jan	U-Th			0.920	NA	11.20	0.37	9.37	0.24
SHL49AZ-5.1A	414	09-01	U-Th			0.920	NA	4.18	0.14	1.14	0.07
SHL49AZ-11.2A	414	09-01	U-Th			0.920	NA	5.00	0.16	1.19	0.08
SHL325.2-10.1T	309	2007 May	U-Th			0.938	NA	9.73	0.31	3.77	1.00
SHL325.2-1.3T2	309	2007 May	U-Th			0.938	NA	17.73	0.57	9.88	0.86
SHL325.2-1.1T	309	2007 May	U-Th			0.938	NA	12.48	0.40	8.81	0.53

Spot ID	Mount	Date Analyzed	Method	230 cor. 206/238 Age (Ma)	2 sig err 206/238 age (Ma)	U/Th Cor. Factor	UO/U Cor. Factor	Cor. (238/232)	±(238/232)	(230/232)	±(230/232)
SHL325.2-6.1T	309	2007 May	U-Th			0.938	NA	11.85	0.38	8.48	0.45
SHL325.2-2.1I	309	2007 May	U-Th			0.938	NA	6.53	0.21	5.04	0.21
SHL325.2-3.1C	309	2007 May	U-Th			0.938	NA	14.39	0.46	11.11	0.78
SHL325.2-6.3T	309	2007 May	U-Th			0.938	NA	7.42	0.24	5.90	0.26
SHL325.2-4.1C	309	2007 May	U-Th			0.938	NA	10.75	0.34	8.51	0.37
SHL325.2-5.2T	309	2007 May	U-Th			0.938	NA	12.96	0.41	10.24	0.38
SHL325.2-6.2C	309	2007 May	U-Th			0.938	NA	11.97	0.38	9.56	0.56
SHL325.2-1.2C	309	2007 May	U-Th			0.938	NA	14.87	0.48	11.89	0.78
SHL325.2-5.1C	309	2007 May	U-Th			0.938	NA	14.43	0.46	11.80	0.65
SHL325.2-9.1T	309	07-05	U-Th				NA	3.08	0.10	3.09	0.22
SHL325.2-8.1	309	07-05	U-Th				NA	13.03	0.42	15.52	0.82
SH325.2-7.1	309	07-05	U-Th				NA	13.37	0.43	12.93	0.58
SH325.2-7.1UPB	309	2009 Jan	U-Pb EQ	0.162	0.019						
SH325.2-9.1TUPB	309	2009 Jan	U-Pb EQ	16.366	0.816						
84A-1	JP04	2004	U-Th			1.013		15.63	0.46	12.14	0.46
84A-10.2	JP04	2004	U-Th			1.013		18.01	0.53	13.04	1.50
84A-11	JP04	2004	U-Th			1.013		20.75	0.61	17.22	1.09
84A-14	JP04	2004	U-Th			1.013		2.40	0.07	1.68	0.05
84A-14.2	JP04	2004	U-Th			1.013		2.27	0.07	1.62	0.04
84A-15	JP04	2004	U-Th			1.013		17.95	0.53	8.58	1.41
84A-2	JP04	2004	U-Th			1.013		15.87	0.47	10.78	0.75
84A-3	JP04	2004	U-Th			1.013		2.86	0.08	2.04	0.05
84A-4.1	JP04	2004	U-Th			1.013		2.87	0.08	1.82	0.05
84A-4.2	JP04	2004	U-Th			1.013		2.79	0.08	1.77	0.04
84A-5.1	JP04	2004	U-Th			1.013		12.46	0.37	7.83	1.64
84A-6	JP04	2004	U-Th			1.013		3.00	0.09	2.14	0.06
84A-7	JP04	2004	U-Th			1.013		23.89	0.71	16.62	1.47
84A-7	JP04	2004	U-Th			1.013		8.02	0.24	7.35	0.21

Spot ID	Mount	Date Analyzed	Method	230 cor. 206/238 Age (Ma)	2 sig err 206/238 age (Ma)	U/Th Cor. Factor	UO/U Cor. Factor	Cor. (238/232)	±(238/232)	(230/232)	±(230/232)
84A-8	JP04	2004	U-Th			1.013		11.93	0.35	7.60	1.01
84A-9	JP04	2004	U-Th			1.013		10.38	0.31	6.24	0.42
84A-15.2	JP04	2004	U-Th					17.18	0.51	16.61	1.99
84A-13	JP04	2004	U-Th					17.81	0.53	12.60	1.12
84A-10	JP04	2004	U-Th					15.30	0.45	9.38	1.03
84A-11.2	JP04	2004	U-Th					17.15	0.51	13.82	1.29
84A-11	JP04	2004	U-Th					14.23	0.42	14.87	0.63
84A-12.2	JP04	2004	U-Th					5.36	0.16	6.74	0.88

Spot ID	Mount	Date Analyzed	Method	Model Age (years)	Error Model + yrs	Error Model - yrs	Intcpt Equiline	Error Intcpt	Slpe	Error Slpe	Xdiff	Ex-diff	Ydiff	Ey-diff
SHL3Z-1.1	309	2007 May	U-Pb											
SHL3Z-1.2	309	2007 May	U-Pb											
SHL3Z-2.1	309	2007 May	U-Pb											
SHL3Z-2.2	309	2007 May	U-Pb											
SHL3Z-4.1	309	2007 May	U-Pb											
SHL3Z-4.2	309	2007 May	U-Pb											
SHL3Z-4.3	309	2007 May	U-Pb											
SHL3Z-5.1	309	2007 May	U-Pb											
SHL3Z-1.4DRa	414	2009 Jan	U-Pb											
SHL063Z-2.3A	***414***	***2009 Jan***	***U-Th COMP***	***#NUM!***	***#NUM!***	***#NUM!***	***1.2***	***0.12***	***1.0133***	***0.045***	***20.75***	***0.73***	***21.03***	***0.59***
SHL3Z-3.1LCa	414	2009 Jan	U-Pb											
SHL3Z-3.2DIa	414	2009 Jan	U-Pb											
SHL3Z-3.3LRa	414	2009 Jan	U-Pb											
SHL3Z-4.3LCa	414	2009 Jan	U-Pb											
SHL063Z-4.3A	***414***	***2009 Jan***	***U-Th COMP***	***470951***	***#NUM!***	***167695***	***1.2***	***0.12***	***0.9866***	***0.049***	***31.88***	***1.09***	***31.45***	***1.13***
SHL3Z-10.1DIa	414	2009 Jan	U-Pb											
SHL3Z-11.1LEa	***414***	***2009 Jan***	***U-Pb***											
SHL3Z-11.1A	414	2009 Jan	U-Th COMP	268782	80468	45823	1.2	0.12	0.9147	0.044	11.26	0.42	10.30	0.32
SHL3Z-5.1DCa	414	2009 Jan	U-Pb											
SHL063Z-5.1DCA-A	***414***	***2009 Jan***	***U-Th COMP***	***311513***	***162938***	***62664***	***1.2***	***0.12***	***0.9423***	***0.045***	***16.39***	***0.59***	***15.44***	***0.48***
SHL3Z-5.1DCa(2)	414	2009 Jan	U-Pb											
SHL3Z-6.2LCa	414	2009 Jan	U-Pb											
SHL063Z-	***414***	***2009 Jan***	***U-Th***	***360373***	***#NUM!***	***86178***	***1.2***	***0.12***	***0.9631***	***0.044***	***15.34***	***0.55***	***14.78***	***0.42***

Spot ID	Mount	Date Analyzed	Method	Model Age (years)	Error Model + yrs	Error Model - yrs	Intcpt Equiline	Error Intcpt	Slpe	Error Slpe	Xdiff	Ex-diff	Ydiff	Ey-diff
6.2A			***COMP***											
SHL063Z-7.1A	414	2009 Jan	U-Th COMP	331083	177989	64431	1.2	0.12	0.9518	0.039	27.37	0.94	26.05	0.57
SHL3Z-7.3LCa	414	2009 Jan	U-Pb											
SHL3Z-8.5A	414	2009 Jan	U-Th COMP	246689	55659	36690	1.2	0.12	0.8956	0.042	23.00	0.80	20.60	0.64
SHL3Z-8.1LCa	414	2009 Jan	U-Pb											
SHL3Z-9.3LIa	414	2009 Jan	U-Pb											
~~SHL063Z-9.3A~~	~~414~~	~~2009 Jan~~	~~U-Th COMP~~	~~#NUM!~~	~~#NUM!~~	~~#NUM!~~	~~1.2~~	~~0.12~~	~~1.0283~~	~~0.053~~	~~30.72~~	~~1.05~~	~~31.58~~	~~1.21~~
SHL4Z-1.1I	309	2007 May	U-Th	116930	19806	16759	1.2	0.12	0.6573	0.057	8.55	0.33	5.62	0.43
SHL4Z-1.2I	309	2007 May	U-Th	119014	22757	18823	1.2	0.12	0.6637	0.063	7.52	0.30	4.99	0.43
SHL4Z-10.1	309	2007 May	U-Th	147712	44026	31289	1.2	0.12	0.7415	0.086	12.87	0.47	9.54	1.05
SHL4Z-11.1	309	2007 May	U-Th	130544	23826	19547	1.2	0.12	0.6974	0.059	15.88	0.56	11.08	0.86
SHL4Z-12.1	309	2007 May	U-Th	59349	14296	12639	1.2	0.12	0.4193	0.071	4.73	0.22	1.98	0.32
SHL4Z-2.1C	309	2007 May	U-Th	126390	21690	18088	1.2	0.12	0.6857	0.057	7.47	0.30	5.12	0.37
SHL4Z-2.2T	309	2007 May	U-Th	103397	24236	19822	1.2	0.12	0.6121	0.077	12.86	0.47	7.87	0.95
SHL4Z-3.1T	309	2007 May	U-Th	142544	24174	19781	1.2	0.12	0.7289	0.054	7.08	0.29	5.16	0.32
SHL4Z-3.2I	309	2007 May	U-Th	201652	64135	40135	1.2	0.12	0.8422	0.070	11.95	0.44	10.07	0.75
SHL4Z-4.1T	309	2007 May	U-Th	115583	17811	15309	1.2	0.12	0.6530	0.052	9.51	0.36	6.21	0.44
SHL4Z-4.2C	309	2007 May	U-Th	215547	51325	34775	1.2	0.12	0.8611	0.052	9.87	0.37	8.50	0.40
SHL4Z-4.3I	309	2007 May	U-Th	121708	19636	16637	1.2	0.12	0.6719	0.054	9.53	0.36	6.40	0.45
SHL4Z-5.1E	309	2007 May	U-Th	149321	29177	23002	1.2	0.12	0.7452	0.060	13.12	0.47	9.77	0.70
SHL4Z-5.2I	309	2007 May	U-Th	105538	14939	13139	1.2	0.12	0.6196	0.049	13.86	0.50	8.59	0.60
SHL4Z-6.1C	309	2007 May	U-Th	158039	49548	33958	1.2	0.12	0.7648	0.086	16.65	0.58	12.74	1.36
SHL4Z-7.1C	309	2007 May	U-Th	149657	31610	24484	1.2	0.12	0.7460	0.064	16.12	0.57	12.03	0.94
SHL4Z-7.2	309	2007 May	U-Th	116170	16399	14255	1.2	0.12	0.6549	0.048	9.93	0.38	6.50	0.41
SHL4Z-8.1C	309	2007 May	U-Th	118618	21233	17769	1.2	0.12	0.6625	0.060	6.74	0.28	4.46	0.36
SHL4Z-8.2	309	2007 May	U-Th	89439	12240	11005	1.2	0.12	0.5592	0.047	6.18	0.27	3.46	0.25
SHL4Z-9.1C	309	2007 May	U-Th	86429	13903	12331	1.2	0.12	0.5468	0.054	8.22	0.32	4.50	0.41

Spot ID	Mount	Date Analyzed	Method	Model Age (years)	Error Model + yrs	Error Model - yrs	Intcpt Equiline	Error Intcpt	Slpe	Error Slpe	Xdiff	Ex-diff	Ydiff	Ey-diff
SHL5Z-10.1I	364	2008 Jan	U-Th	73994	8436	7830	1.2	0.12	0.4922	0.038	9.95	0.38	4.90	0.32
SHL5Z-11.1I	364	2008 Jan	U-Th	113855	14364	12693	1.2	0.12	0.6475	0.043	10.59	0.40	6.86	0.38
SHL5Z-12.1C	364	2008 Jan	U-Th	75040	8693	8052	1.2	0.12	0.4970	0.038	5.47	0.25	2.72	0.17
SHL5Z-12.2T	364	2008 Jan	U-Th	57575	8505	7890	1.2	0.12	0.4098	0.044	10.90	0.42	4.47	0.45
SHL5Z-13.1T	364	2008 Jan	U-Th	43641	6180	5849	1.2	0.12	0.3294	0.037	10.64	0.41	3.50	0.37
SHL5Z-13.2C	364	2008 Jan	U-Th	174836	35275	26619	1.2	0.12	0.7983	0.056	17.74	0.63	14.17	0.85
SHL5Z-14.1I	364	2008 Jan	U-Th	100069	13354	11897	1.2	0.12	0.6000	0.046	9.52	0.37	5.72	0.38
SHL5Z-15.1T	364	2008 Jan	U-Th	40988	6489	6125	1.2	0.12	0.3130	0.040	5.06	0.24	1.58	0.19
SHL5Z-16.1T	364	2008 Jan	U-Th	43229	8442	7836	1.2	0.12	0.3269	0.050	4.41	0.22	1.44	0.21
SHL5Z-17.1IR	364	2008 Jan	U-Th	82668	7832	7308	1.2	0.12	0.5310	0.032	14.14	0.52	7.51	0.37
SHL5Z-18.1E	364	2008 Jan	U-Th	147342	19757	16724	1.2	0.12	0.7406	0.043	16.95	0.61	12.55	0.57
SHL5Z-19.1IR	364	2008 Jan	U-Th	86077	11074	10054	1.2	0.12	0.5454	0.044	10.40	0.40	5.67	0.40
SHL5Z-20.1T	364	2008 Jan	U-Th	96634	15248	13378	1.2	0.12	0.5873	0.054	10.26	0.39	6.02	0.50
SHL5Z-3.1C	364	2008 Jan	U-Th	287568	218024	68012	1.2	0.12	0.9282	0.062	9.97	0.39	9.26	0.51
SHL5Z-4.1C	364	2008 Jan	U-Th	112159	14534	12825	1.2	0.12	0.6420	0.045	7.76	0.32	4.98	0.28
SHL5Z-6.1C	364	2008 Jan	U-Th	149586	89944	48642	1.2	0.12	0.7459	0.143	1.16	0.14	0.86	0.13
SHL5Z-6.2T	364	2008 Jan	U-Th	109732	19340	16425	1.2	0.12	0.6339	0.059	10.35	0.40	6.56	0.56
SHL5Z-7.1C	364	2008 Jan	U-Th	129245	18715	15972	1.2	0.12	0.6938	0.048	7.23	0.30	5.02	0.28
SHL5Z-7.2T	364	2008 Jan	U-Th	54087	7133	6695	1.2	0.12	0.3906	0.039	8.78	0.35	3.43	0.31
SHL5Z-9.1I	364	2008 Jan	U-Th	202682	35584	26794	1.2	0.12	0.8437	0.043	10.82	0.41	9.13	0.32
SHL5Z-1.1	364	08-01	U-Th	#NUM!	#NUM!	#NUM!	1.2	0.12	1.0152	0.057	8.86	0.35	8.99	0.36
SHL5Z-8.1C	364	08-01	U-Th	#NUM!	#NUM!	#NUM!	1.2	0.12	1.2379	0.099	10.56	0.40	13.08	0.92
SHD9-2.3C	443	2009 Dec	U-Th	159326	30153	23603	1.2	0.12	0.7675	0.056	5.19	0.23	3.98	0.23
SHD9-1.3C	443	2009 Dec	U-Th	105163	14738	12984	1.2	0.12	0.6183	0.048	4.60	0.21	2.84	0.18
SHL21Z-13.3A	414	2009 Jan	U-Th	28856	4027	3883	1.2	0.12	0.2322	0.028	12.08	0.45	2.81	0.32
SHL21Z-9.2A	414	2009 Jan	U-Th	30485	6514	6147	1.2	0.12	0.2436	0.044	4.95	0.23	1.21	0.21
SHL21Z-17.1A	414	2009 Jan	U-Th	35033	6728	6338	1.2	0.12	0.2744	0.043	5.44	0.25	1.49	0.23

Spot ID	Mount	Date Analyzed	Method	Model Age (years)	Error Model + yrs	Error Model - yrs	Intcpt Equiline	Error Intcpt	Slpe	Error Slpe	Xdiff	Ex-diff	Ydiff	Ey-diff
SHL21Z-5.1A	414	2009 Jan	U-Th	38996	9506	8744	1.2	0.12	0.3003	0.058	3.23	0.19	0.97	0.18
SHL21Z-12.2A	414	2009 Jan	U-Th	39247	5962	5653	1.2	0.12	0.3019	0.037	5.62	0.25	1.70	0.19
SHL21Z-16.1A	414	2009 Jan	U-Th	40272	7751	7237	1.2	0.12	0.3084	0.047	4.60	0.22	1.42	0.21
SHL21Z-6.1A	414	2009 Jan	U-Th	44852	10679	9727	1.2	0.12	0.3368	0.062	3.61	0.20	1.22	0.21
SHL21Z-15.1A	414	2009 Jan	U-Th	46098	11239	10190	1.2	0.12	0.3444	0.064	2.97	0.18	1.02	0.18
SHL21Z-14.1A	414	2009 Jan	U-Th	54333	8562	7939	1.2	0.12	0.3920	0.046	6.99	0.29	2.74	0.30
SHL21Z-9.1A	414	2009 Jan	U-Th	54640	12723	11394	1.2	0.12	0.3937	0.067	3.06	0.18	1.20	0.19
SHL21Z-7.3A	414	2009 Jan	U-Th	62344	8785	8130	1.2	0.12	0.4350	0.044	10.78	0.41	4.69	0.44
SHL21Z-8.3A	414	2009 Jan	U-Th	76553	7170	6728	1.2	0.12	0.5039	0.032	13.63	0.50	6.87	0.35
SHL21Z-4.1A	414	2009 Jan	U-Th	81249	10139	9277	1.2	0.12	0.5248	0.042	14.91	0.54	7.83	0.56
SHL21Z-20.1A	414	2009 Jan	U-Th	88920	10160	9294	1.2	0.12	0.5571	0.039	10.94	0.41	6.10	0.36
SHL21Z-10.1A	414	2009 Jan	U-Th	95887	17986	15439	1.2	0.12	0.5844	0.063	5.46	0.25	3.19	0.31
SHL21Z-4.2A	414	2009 Jan	U-Th	98823	12570	11271	1.2	0.12	0.5955	0.044	13.25	0.49	7.89	0.51
SHL21Z-12.1A	414	2009 Jan	U-Th	102505	19672	16663	1.2	0.12	0.6089	0.064	3.63	0.20	2.21	0.20
SHL21Z-13.1A	414	2009 Jan	U-Th	105229	12760	11424	1.2	0.12	0.6185	0.042	15.86	0.57	9.81	0.57
SHL21Z-3.1A	414	2009 Jan	U-Th	114489	13297	11852	1.2	0.12	0.6495	0.040	10.73	0.41	6.97	0.34
SHL21Z-19.1A	414	2009 Jan	U-Th	115298	20970	17584	1.2	0.12	0.6521	0.061	4.08	0.21	2.66	0.21
SHL21Z-5.2A	414	2009 Jan	U-Th	126067	31478	24405	1.2	0.12	0.6848	0.079	4.23	0.21	2.90	0.30
SHL21Z-8.1A	414	2009 Jan	U-Th	154078	22790	18845	1.2	0.12	0.7561	0.046	12.68	0.47	9.59	0.46
SHL21Z-11.2A	414	2009 Jan	U-Th	156778	26172	21096	1.2	0.12	0.7621	0.051	6.11	0.27	4.66	0.23
SHL21Z-2.2A	414	2009 Jan	U-Th	164217	19913	16836	1.2	0.12	0.7777	0.037	22.12	0.77	17.20	0.56
SHL21Z-11.1A	414	2009 Jan	U-Th	201200	35778	26904	1.2	0.12	0.8416	0.044	9.21	0.36	7.75	0.27
SHL21Z-1.2A	414	2009 Jan	U-Th	240192	68657	41827	1.2	0.12	0.8892	0.052	13.75	0.50	12.22	0.55
SHL21Z-7.1A	414	2009 Jan	U-Th	255718	92201	49268	1.2	0.12	0.9038	0.055	10.65	0.41	9.63	0.46
SHL21Z-13.1A	414	2009 Jan	U-Th	299322	269338	70954	1.2	0.12	0.9355	0.059	10.01	0.39	9.37	0.47
SHL21Z-18.1A	414	09-01	U-Th	#NUM!	#NUM!	#NUM!	1.2	0.12	1.0211	0.112	3.73	0.20	3.81	0.36
SHL21Z-21.1A	414	09-01	U-Th	323355	278685	71351	1.2	0.12	0.9482	0.048	11.37	0.43	10.78	0.36
SHL26C-1.1C	443	2009 Dec		148441	20189	17032	1.2	0.12	0.7432	0.043	12.12	0.42	9.00	0.42
SHL26C-3.2C	443	2009 Dec		58087	7886	7355	1.2	0.12	0.4125	0.041	8.42	0.32	3.48	0.32

Spot ID	Mount	Date Analyzed	Method	Model Age (years)	Error Model + yrs	Error Model - yrs	Intcpt Equiline	Error Intcpt	Slpe	Error Slpe	Xdiff	Ex-diff	Ydiff	Ey-diff
SHL26C-2.1C	443	2009 Dec		123242	13627	12114	1.2	0.12	0.6765	0.038	26.49	0.86	17.92	0.82
SHL26C-4.1C	443	2009 Dec		187056	34684	26283	1.2	0.12	0.8197	0.049	16.25	0.55	13.32	0.66
SHL26C-4.2T	443	2009 Dec		67322	6345	5997	1.2	0.12	0.4602	0.030	12.65	0.44	5.82	0.33
SHL26C-5.1T	443	2009 Dec		62629	6506	6140	1.2	0.12	0.4365	0.033	10.58	0.38	4.62	0.30
SHL26C-5.2C	443	2009 Dec		100829	12016	10824	1.2	0.12	0.6028	0.041	10.99	0.39	6.62	0.39
SHL26C-16.1R	443	2009 Dec		91842	11718	10581	1.2	0.12	0.5687	0.044	8.56	0.32	4.87	0.33
SHL26C-6.2I	443	2009 Dec		108377	11484	10390	1.2	0.12	0.6293	0.037	17.98	0.60	11.32	0.55
SHL26C-7.1C	443	2009 Dec		59829	6303	5959	1.2	0.12	0.4218	0.032	9.36	0.34	3.95	0.27
SHL26C-7.1C2	443	2009 Dec		77601	8345	7753	1.2	0.12	0.5087	0.036	15.38	0.52	7.82	0.49
SHL26C-9.1C	443	2009 Dec		177139	27483	21938	1.2	0.12	0.8025	0.044	10.80	0.39	8.67	0.36
SHL26C-9.3R	443	2009 Dec		113067	12024	10830	1.2	0.12	0.6449	0.037	9.92	0.36	6.40	0.28
SHL26C-10.3R	443	2009 Dec		84279	8561	7939	1.2	0.12	0.5378	0.035	14.31	0.49	7.69	0.42
SHL26C-11.1C	443	2009 Dec		88209	11730	10592	1.2	0.12	0.5542	0.045	5.74	0.24	3.18	0.22
SHL26C-12.2I	443	2009 Dec		88464	8899	8228	1.2	0.12	0.5552	0.035	11.13	0.40	6.18	0.32
SHL26C-12.1C	443	2009 Dec		126710	16723	14499	1.2	0.12	0.6866	0.044	15.22	0.52	10.45	0.58
SHL26C-17.1I	443	2009 Dec		88296	9862	9045	1.2	0.12	0.5545	0.038	13.86	0.48	7.68	0.46
SHL26C-18.1I	443	2009 Dec		91508	8529	7911	1.2	0.12	0.5674	0.033	14.54	0.50	8.25	0.38
SHL26C-19.1T	443	2009 Dec		73812	6731	6340	1.2	0.12	0.4913	0.030	11.62	0.41	5.71	0.29
SHL26C-20.1R	443	2009 Dec		73289	6716	6327	1.2	0.12	0.4889	0.030	17.80	0.59	8.70	0.46
SHL26C-13.1C	443	2009 Dec		122102	16926	14651	1.2	0.12	0.6731	0.047	11.24	0.40	7.56	0.45
SHL26C-13.2R	443	2009 Dec		71696	7946	7407	1.2	0.12	0.4814	0.036	12.19	0.43	5.87	0.39
SHL26C-21.1I	443	2009 Dec		116474	16196	14101	1.2	0.12	0.6558	0.047	8.63	0.32	5.66	0.35
SHL26C-14.2I	443	2009 Dec		157299	23364	19235	1.2	0.12	0.7632	0.046	7.97	0.30	6.08	0.28
SHL26C-22.1R	443	2009 Dec		74984	7308	6849	1.2	0.12	0.4968	0.033	13.42	0.46	6.66	0.37
SHL26C-15.1IR	443	2009 Dec		67498	5269	5026	1.2	0.12	0.4610	0.025	8.82	0.33	4.07	0.16
SHL26C-15.3C	443	2009 Dec		112014	14210	12572	1.2	0.12	0.6415	0.044	17.78	0.59	11.41	0.68
SHL26C-23.1R	443	2009 Dec		109548	11385	10309	1.2	0.12	0.6333	0.036	16.09	0.54	10.19	0.47
SHL26C-24.1I	443	2009 Dec		229551	65234	40556	1.2	0.12	0.8778	0.055	11.85	0.42	10.41	0.54

Spot ID	Mount	Date Analyzed	Method	Model Age (years)	Error Model + yrs	Error Model - yrs	Intcpt Equiline	Error Intcpt	Slpe	Error Slpe	Xdiff	Ex-diff	Ydiff	Ey-diff
SHL29AZ-1.1C	393	2008 Aug	U-Th	183619	28462	22557	1.2	0.12	0.8139	0.043	17.72	0.60	14.42	0.58
SHL29Z-1.1CUPB	***393***	***2009 Jan***	***U-Pb***	***145222***	***30273***	***30273***								
SHL29AZ-10.1I	393	2008 Aug	U-Th	137547	17602	15155	1.2	0.12	0.7162	0.042	9.24	0.37	6.62	0.28
SHL29AZ-11.1CA	393	2008 Aug	U-Th	191356	35762	26895	1.2	0.12	0.8266	0.048	6.30	0.28	5.20	0.20
SHL29AZ-12.1EA	393	2008 Aug	U-Th	76729	7371	6905	1.2	0.12	0.5047	0.032	8.61	0.34	4.35	0.22
SHL29AZ-12.2CA	393	2008 Aug	U-Th	107327	12300	11053	1.2	0.12	0.6258	0.040	7.52	0.31	4.71	0.23
SHL29AZ-13.1CA	393	2008 Aug	U-Th	159166	20815	17475	1.2	0.12	0.7672	0.040	17.86	0.63	13.70	0.54
SHL29AZ-13.2EA	393	2008 Aug	U-Th	69924	6695	6308	1.2	0.12	0.4729	0.031	8.54	0.33	4.04	0.22
SHL29AZ-14.1CA	393	2008 Aug	U-Th	100271	8952	8273	1.2	0.12	0.6008	0.031	12.33	0.38	7.41	0.32
SHL29AZ-15.1EA	393	2008 Aug	U-Th	58687	5760	5472	1.2	0.12	0.4158	0.030	8.10	0.32	3.37	0.20
SHL29AZ-2.2IA	393	2008 Aug	U-Th	188487	31942	24682	1.2	0.12	0.8220	0.045	15.19	0.54	12.48	0.52
SHL29AZ-3.2EA	393	2008 Aug	U-Th	84377	9088	8389	1.2	0.12	0.5382	0.037	15.26	0.53	8.22	0.48
SHL29AZ-4.1CA	393	2008 Aug	U-Th	181073	26537	21332	1.2	0.12	0.8095	0.041	15.09	0.54	12.22	0.44
SHL29AZ-4.2EA	393	2008 Aug	U-Th	122072	13774	12230	1.2	0.12	0.6730	0.039	9.30	0.36	6.26	0.27
SHL29AZ-5.2EA	393	2008 Aug	U-Th	84714	8411	7809	1.2	0.12	0.5397	0.034	13.70	0.47	7.39	0.39
SHL29AZ-6.1CA	393	2008 Aug	U-Th	59968	10203	9331	1.2	0.12	0.4226	0.052	2.82	0.17	1.19	0.13
SHL29AZ-	393	2008 Aug	U-Th	60013	5895	5593	1.2	0.12	0.4228	0.030	7.95	0.32	3.36	0.20

Spot ID	Mount	Date Analyzed	Method	Model Age (years)	Error Model + yrs	Error Model - yrs	Intcpt Equiline	Error Intcpt	Slpe	Error Slpe	Xdiff	Ex-diff	Ydiff	Ey-diff
6.2EA														
SHL29AZ-7.2IA	393	2008 Aug	U-Th	124571	15593	13642	1.2	0.12	0.6804	0.043	6.62	0.27	4.50	0.21
SHL29AZ-7.3EA	393	2008 Aug	U-Th	121795	15629	13670	1.2	0.12	0.6722	0.044	5.86	0.26	3.94	0.19
SHL29AZ-8.1CA	393	2008 Aug	U-Th	81907	8108	7548	1.2	0.12	0.5277	0.034	7.40	0.29	3.91	0.20
SHL29AZ-9.1CA	393	2008 Aug	U-Th	85926	9209	8492	1.2	0.12	0.5447	0.037	7.47	0.29	4.07	0.22
SHL29AZ-9.3EA	393	2008 Aug	U-Th	65300	6300	5956	1.2	0.12	0.4501	0.031	10.66	0.40	4.80	0.28
SHL29AZ-1.1TA	392	2008 Aug	U-Th	72922	6709	6321	1.2	0.12	0.4872	0.031	13.58	0.50	6.62	0.33
SHL29AZ-3.4EA	392	2008 Aug	U-Th	73248	6525	6157	1.2	0.12	0.4887	0.030	14.41	0.53	7.04	0.34
SHL29AZ-2.2EA	392	2008 Aug	U-Th	94165	9634	8852	1.2	0.12	0.5778	0.036	9.92	0.39	5.73	0.27
SHL29AZ-1.2CA	392	2008 Aug	U-Th	139609	19610	16618	1.2	0.12	0.7215	0.046	4.83	0.23	3.48	0.14
SHL29AZ-3.2IEA	392	2008 Aug	U-Th	155862	20155	17008	1.2	0.12	0.7601	0.040	16.16	0.59	12.28	0.48
SHL29AZ-3.1CA	392	2008 Aug	U-Th	261131	73796	43637	1.2	0.12	0.9085	0.045	16.00	0.58	14.54	0.49
SHL29AZ-2.3bIA	***392***	***2008 Aug***	***U-Th***	***#NUM!***	***#NUM!***	***#NUM!***	***1.2***	***0.12***	***1.0023***	***0.059***	***6.17***	***0.27***	***6.19***	***0.24***
SHL29Z-2.3IUPB	392	2009 Jan	U-Pb	23519400	694323	694323								
SHL29AZ-2.4IA	***392***	***2008 Aug***	***U-Th***	***393649***	***#NUM!***	***128263***	***1.2***	***0.12***	***0.9728***	***0.061***	***4.83***	***0.23***	***4.70***	***0.19***
SHL29Z-2.4IUPB	392	2009 Jan	U-Pb	24351500	584986	584986								

Spot ID	Mount	Date Analyzed	Method	Model Age (years)	Error Model + yrs	Error Model - yrs	Intcpt Equiline	Error Intcpt	Slpe	Error Slpe	Xdiff	Ex-diff	Ydiff	Ey-diff
SHL08-29Z-14.3c	478	2010 May	U-Th	#NUM!	#NUM!	#NUM!	1.2	0.12	1.2960	0.062	19.31	0.66	25.02	0.84
SHL08-29Z-13.2c	478	2010 May	U-Th	#NUM!	#NUM!	#NUM!	1.2	0.12	1.2929	0.095	3.73	0.20	4.82	0.25
SHL08-29Z-6.3c	478	2010 May	U-Th	#NUM!	#NUM!	#NUM!	1.2	0.12	1.1293	0.061	14.72	0.52	16.62	0.68
SHL08-29Z-8.3c	478	2010 May	U-Th	#NUM!	#NUM!	#NUM!	1.2	0.12	1.0979	0.054	18.40	0.63	20.20	0.71
SHL08-29Z-10.3c	478	2010 May	U-Th	#NUM!	#NUM!	#NUM!	1.2	0.12	1.0718	0.052	14.89	0.52	15.96	0.54
SHL08-29Z-8.4i	478	2010 May	U-Th	#NUM!	#NUM!	#NUM!	1.2	0.12	1.0419	0.049	28.60	0.95	29.80	0.99
SHL08-29Z-11.4i	478	2010 May	U-Th	#NUM!	#NUM!	#NUM!	1.2	0.12	1.0211	0.053	13.64	0.48	13.93	0.53
SHL08-29Z-1.2C	478	2010 May	U-Th	#NUM!	#NUM!	#NUM!	1.2	0.12	1.0071	0.039	27.35	0.91	27.55	0.52
SHL08-29Z-11.3c	478	2010 May	U-Th	392611	#NUM!	108968	1.2	0.12	0.9726	0.047	25.10	0.84	24.41	0.85
SHL08-29Z-14.4i	478	2010 May	U-Th	324877	291373	71835	1.2	0.12	0.9490	0.047	13.87	0.49	13.16	0.46
SHL08-29Z-7.2c	478	2010 May	U-Th	309812	186369	65304	1.2	0.12	0.9414	0.048	11.85	0.43	11.16	0.40
SHL08-29Z-17.1c	478	2010 May	U-Th	291024	117574	55296	1.2	0.12	0.9304	0.046	14.30	0.50	13.30	0.46
SHL08-29Z-9.2c	478	2010 May	U-Th	283909	106181	52802	1.2	0.12	0.9257	0.046	11.94	0.43	11.05	0.38
SHL08-29Z-6.4e	478	2010 May	U-Th	236553	57885	37631	1.2	0.12	0.8854	0.047	16.08	0.56	14.24	0.57
SHL08-29Z-15.2i	478	2010 May	U-Th	163535	23790	19523	1.2	0.12	0.7763	0.044	9.32	0.35	7.23	0.30
SHL08-29Z-3.2c	478	2010 May	U-Th	157712	20731	17416	1.2	0.12	0.7641	0.041	13.62	0.48	10.41	0.41

Spot ID	Mount	Date Analyzed	Method	Model Age (years)	Error Model + yrs	Error Model - yrs	Intcpt Equiline	Error Intcpt	Slpe	Error Slpe	Xdiff	Ex-diff	Ydiff	Ey-diff
SHL08-29Z-4.2c	478	2010 May	U-Th	143177	16981	14692	1.2	0.12	0.7305	0.039	12.94	0.46	9.46	0.37
SHL08-29Z-10.4i	478	2010 May	U-Th	134949	16267	14155	1.2	0.12	0.7094	0.040	8.33	0.32	5.91	0.24
SHL08-29Z-5.4e	478	2010 May	U-Th	134041	16798	14555	1.2	0.12	0.7070	0.042	8.62	0.33	6.10	0.27
SHL08-29Z-2.2c	478	2010 May	U-Th	110320	11187	10147	1.2	0.12	0.6359	0.035	14.50	0.51	9.22	0.40
SHL08-29Z-16.2i	478	2010 May	U-Th	103685	12290	11045	1.2	0.12	0.6131	0.041	5.46	0.24	3.35	0.17
SHL08-29Z-12.2c	478	2010 May	U-Th	86841	29086	22945	1.2	0.12	0.5485	0.106	1.40	0.15	0.77	0.12
SHL30C-15.1R	443	2009 Dec		93405	10565	9633	1.2	0.12	0.5749	0.039	6.71	0.27	3.86	0.21
SHL30C-16.1C	443	2009 Dec		91245	10504	9581	1.2	0.12	0.5664	0.040	14.47	0.50	8.20	0.50
SHL30C-1.2R	443	2009 Dec		88152	9208	8491	1.2	0.12	0.5539	0.036	12.83	0.45	7.11	0.39
SHL30C-2.1C	443	2009 Dec		204152	37594	27913	1.2	0.12	0.8458	0.045	15.42	0.52	13.04	0.53
SHL30C-17.1C	443	2009 Dec		84293	9706	8913	1.2	0.12	0.5379	0.039	13.93	0.48	7.49	0.48
SHL30C-17.2E	443	2009 Dec		70256	6879	6471	1.2	0.12	0.4745	0.032	13.63	0.47	6.47	0.38
SHL30C-3.3I	443	2009 Dec		72218	6624	6245	1.2	0.12	0.4838	0.030	8.67	0.32	4.20	0.21
SHL30C-3.1C	443	2009 Dec		119692	14865	13082	1.2	0.12	0.6658	0.043	16.08	0.54	10.71	0.58
SHL30C-4.2C	443	2009 Dec		40178	4265	4104	1.2	0.12	0.3078	0.027	15.01	0.51	4.62	0.37
SHL30C-5.2T	443	2009 Dec		124767	14957	13153	1.2	0.12	0.6810	0.041	8.08	0.31	5.50	0.25
SHL30C-6.1I	443	2009 Dec		118530	13257	11820	1.2	0.12	0.6623	0.039	13.02	0.45	8.62	0.40
SHL30C-7.1C	443	2009 Dec		178916	28840	22793	1.2	0.12	0.8057	0.045	9.64	0.35	7.76	0.33
SHL30C-7.3R	443	2009 Dec		84480	8204	7631	1.2	0.12	0.5387	0.033	9.54	0.35	5.14	0.26
SHL30C-8.1C	443	2009 Dec		178540	29223	23030	1.2	0.12	0.8051	0.046	6.50	0.26	5.23	0.21
SHL30C-10.1C	443	2009 Dec		101033	12151	10934	1.2	0.12	0.6036	0.042	13.87	0.48	8.37	0.50
SHL30C-10.3R	443	2009 Dec		74811	7145	6706	1.2	0.12	0.4960	0.032	14.40	0.49	7.14	0.39
SHL30-12.2I	443	2009 Dec		75333	7753	7239	1.2	0.12	0.4984	0.034	13.71	0.47	6.83	0.41
SHL30-11.2T	443	2009 Dec		103119	10215	9341	1.2	0.12	0.6111	0.035	12.01	0.42	7.34	0.33

Spot ID	Mount	Date Analyzed	Method	Model Age (years)	Error Model + yrs	Error Model - yrs	Intcpt Equiline	Error Intcpt	Slpe	Error Slpe	Xdiff	Ex-diff	Ydiff	Ey-diff
SHL30-4.3R	443	2009 Dec		99617	12176	10953	1.2	0.12	0.5984	0.042	13.51	0.47	8.09	0.50
SHL30-13.1C	443	2009 Dec		109494	10933	9937	1.2	0.12	0.6331	0.035	11.63	0.41	7.36	0.31
SHL30-18.1I	443	2009 Dec		75176	7803	7283	1.2	0.12	0.4976	0.035	19.60	0.65	9.75	0.60
SHL30-18.2R	443	2009 Dec		119109	13597	12090	1.2	0.12	0.6640	0.039	12.94	0.45	8.59	0.41
SHL30-4.4C	443	2009 Dec		169305	32275	24880	1.2	0.12	0.7878	0.054	15.52	0.53	12.22	0.73
SHL33-3.3I	443	2009 Dec		241014	67405	41368	1.2	0.12	0.8900	0.051	7.49	0.29	6.67	0.28
SHL33-2.2I	443	2009 Dec		81176	22035	18326	1.2	0.12	0.5245	0.087	2.12	0.16	1.11	0.16
SHL33-4.2C	443	2009 Dec		125320	126770	57092	1.2	0.12	0.6826	0.218	0.72	0.13	0.49	0.13
SHL33-4.1T	443	2009 Dec		107613	17635	15179	1.2	0.12	0.6267	0.056	3.57	0.19	2.24	0.16
SHL34Z-9.1IA	393	2008 Aug	U-Th	6089	10724	9764	1.2	0.12	0.0542	0.088	1.49	0.15	0.08	0.13
SHL34Z-11.3IA	393	2008 Aug	U-Th	8062	2861	2788	1.2	0.12	0.0712	0.024	6.01	0.27	0.43	0.14
SHL34Z-13.1CA	393	2008 Aug	U-Th	8685	3134	3046	1.2	0.12	0.0765	0.026	5.78	0.24	0.44	0.15
SHL34Z-1.2EA	393	2008 Aug	U-Th	13320	2145	2104	1.2	0.12	0.1148	0.017	11.83	0.44	1.36	0.20
SHL34Z-1.1IA	393	2008 Aug	U-Th	13714	3211	3119	1.2	0.12	0.1180	0.026	6.91	0.28	0.81	0.17
SHL34Z-7.2EA	393	2008 Aug	U-Th	16067	4566	4383	1.2	0.12	0.1368	0.035	4.40	0.21	0.60	0.15
SHL34Z-3.1EA	393	2008 Aug	U-Th	24281	3933	3796	1.2	0.12	0.1994	0.028	6.59	0.28	1.31	0.18
SHL34Z-12.1IA	393	2008 Aug	U-Th	32663	8323	7734	1.2	0.12	0.2585	0.054	3.00	0.17	0.78	0.16
SHL34Z-6.2IA	393	2008 Aug	U-Th	46930	11443	10356	1.2	0.12	0.3493	0.065	2.66	0.17	0.93	0.16
SHL34Z-8.1IA	393	2008 Aug	U-Th	59067	13074	11675	1.2	0.12	0.4178	0.066	2.80	0.17	1.17	0.17
SHL34Z-11.1IA	393	2008 Aug	U-Th	75710	7293	6836	1.2	0.12	0.5001	0.032	7.50	0.30	3.75	0.19
SHL34Z-2.2IA	393	2008 Aug	U-Th	181877	20823	17481	1.2	0.12	0.8109	0.033	33.68	1.01	27.31	0.74
SHL34Z-5.1IA	393	2008 Aug	U-Th	202876	31824	24612	1.2	0.12	0.8440	0.039	14.52	0.52	12.25	0.37
SHL34Z-10.1IA	393	2008 Aug	U-Th	222368	38964	28658	1.2	0.12	0.8695	0.039	13.00	0.47	11.30	0.30
SHL34Z-3.3IA	393	2008 Aug	U-Th	225485	121826	56149	1.2	0.12	0.8732	0.085	4.49	0.22	3.92	0.33

Spot ID	Mount	Date Analyzed	Method	Model Age (years)	Error Model + yrs	Error Model - yrs	Intcpt Equiline	Error Intcpt	Slpe	Error Slpe	Xdiff	Ex-diff	Ydiff	Ey-diff
SHL34Z-3.3EA	392	2008 Aug	U-Th	9193	2551	2492	1.2	0.12	0.0807	0.021	6.98	0.30	0.56	0.15
SHL34Z-4.1EA	392	2008 Aug	U-Th	14278	3077	2992	1.2	0.12	0.1226	0.024	6.44	0.28	0.79	0.15
SHL34Z-6.1A	392	2008 Aug	U-Th	14295	5724	5439	1.2	0.12	0.1227	0.045	3.04	0.18	0.37	0.13
SHL34Z-3.1IA	392	2008 Aug	U-Th	29294	5940	5634	1.2	0.12	0.2353	0.040	4.17	0.21	0.98	0.16
SHL34Z-5.1IA	392	2008 Aug	U-Th	33246	7430	6957	1.2	0.12	0.2625	0.049	3.80	0.20	1.00	0.18
SHL34Z-4.2CA	392	2008 Aug	U-Th	39726	7704	7196	1.2	0.12	0.3050	0.047	3.66	0.20	1.12	0.16
SHL34Z-2.1IA	392	2008 Aug	U-Th	56769	14279	12626	1.2	0.12	0.4054	0.073	2.26	0.17	0.91	0.15
SHL34Z-1.3EA	392	2008 Aug	U-Th	114964	12546	11252	1.2	0.12	0.6510	0.038	15.83	0.58	10.31	0.47
SHL34Z-1.1CA	392	2008 Aug	U-Th	272910	90495	48796	1.2	0.12	0.9179	0.046	20.10	0.72	18.45	0.66
SHL34Z-5.1IUPB	393	2009 Jan	U-Pb EQ	260426	87330									
SHL34Z-3.3IUPB	393	2009 Jan	U-Pb EQ	333582	524300									
SHL34Z-10.1IUPB	393	2009 Jan	U-Pb EQ	194860	24827									
SHL29Z-1.1CUPB	393	2009 Jan	U-Pb EQ	145222	30273									
SHL34Z-1.1CUPB	393	2009 Jan	U-Pb EQ	159098	57798									
SHL34Z-2.2IUPB	393	2009 Jan	U-Pb EQ	317060	98031									
SHL36E-1.5I	443	2009 Dec	U-Pb	202651	36994									
SHL36E-10.2I	443	2009 Dec	U-Pb	155643	37842									
SHL36E-12.4R	443	2009 Dec	U-Pb	243889	26493									
SHL36E-13.3I	443	2009 Dec	U-Pb	163093	21479									
SHL36E-14.4C	443	2009 Dec	U-Pb	187259	19556									
SHL36E-15.1	443	2009 Dec	U-Pb	237644	32127									
SHL36E-16.1	443	2009 Dec	U-Pb	244612	34822									
SHL36E-17.1	443	2009 Dec	U-Pb	226364	49892									
SHL36E-18.1C	443	2009 Dec	U-Pb	266991	74534									

Spot ID	Mount	Date Analyzed	Method	Model Age (years)	Error Model + yrs	Error Model - yrs	Intcpt Equiline	Error Intcpt	Slpe	Error Slpe	Xdiff	Ex-diff	Ydiff	Ey-diff
SHL36E-18.1R	443	2009 Dec	U-Pb	199204	21585									
SHL36E-2.3C	443	2009 Dec	U-Pb	256175	41730									
SHL36E-20.1C	443	2009 Dec	U-Pb	165503	112141									
SHL36E-21.1C	443	2009 Dec	U-Pb	209546	50746									
SHL36E-3.4C	443	2009 Dec	U-Pb	199605	81017									
SHL36E-4.3T	443	2009 Dec	U-Pb	175603	40735									
SHL36E-6.1R	443	2009 Dec	U-Pb	189476	48024									
SHL36E-7.1I	443	2009 Dec	U-Pb	226240	44069									
SHL36E-8.3R	443	2009 Dec	U-Pb	202161	28754									
SHL36E-9.3C	443	2009 Dec	U-Pb	199643	15935									
SHL36E-1.6	443R	2010 May	U-Th	177176	20548	17287	1.2	0.12	0.8026	0.034	16.44	0.49	13.19	0.39
SHL36E-1.7	443R	2010 May	U-Th	176657	20954	17573	1.2	0.12	0.8017	0.035	13.64	0.42	10.94	0.33
SHL36E-10.2I	443R	2010 May	U-Th	182778	25098	20394	1.2	0.12	0.8125	0.039	11.26	0.36	9.15	0.32
SHL36E-12.4	443R	2010 May	U-Th	165132	17632	15177	1.2	0.12	0.7796	0.033	11.56	0.37	9.01	0.25
SHL36E-13.3I	443R	2010 May	U-Th	105806	18433	15766	1.2	0.12	0.6205	0.059	2.79	0.16	1.73	0.13
SHL36E-14.4	443R	2010 May	U-Th	143833	18329	15690	1.2	0.12	0.7321	0.041	5.53	0.22	4.05	0.16
SHL36E-15.2T	443R	2010 May	U-Th	152440	14753	12995	1.2	0.12	0.7524	0.031	11.75	0.37	8.84	0.24
SHL36E-16.2T	443R	2010 May	U-Th	129718	10701	9745	1.2	0.12	0.6951	0.028	13.51	0.42	9.39	0.25
SHL36E-17.2T	443R	2010 May	U-Th	149677	14363	12691	1.2	0.12	0.7461	0.031	19.28	0.57	14.38	0.43
SHL36E-2.4	443R	2010 May	U-Th	147657	15204	13344	1.2	0.12	0.7413	0.034	14.69	0.45	10.89	0.37
SHL36E-3.4	443R	2010 May	U-Th	140165	13511	12022	1.2	0.12	0.7230	0.032	8.09	0.28	5.85	0.17
SHL36E-4.3T	443R	2010 May	U-Th	186456	24418	19943	1.2	0.12	0.8187	0.036	17.91	0.53	14.66	0.48
SHL36E-6.3T	443R	2010 May	U-Th	166218	19089	16243	1.2	0.12	0.7818	0.035	17.01	0.51	13.29	0.44
SHL36E-7.3T	443R	2010 May	U-Th	179337	19665	16658	1.2	0.12	0.8065	0.032	20.07	0.59	16.19	0.43
SHL36E-8.3R	443R	2010 May	U-Th	161621	16160	14074	1.2	0.12	0.7724	0.031	12.62	0.39	9.75	0.25
SHL36E-9.3C	443R	2010 May	U-Th	138991	20864	17510	1.2	0.12	0.7200	0.049	3.85	0.18	2.77	0.13
SHL37P14.4R	443	2009 Dec	U-Pb	68893	42289									
SHL37P-15.1T	443	2009 Dec	U-Pb	115976	23319									

Spot ID	Mount	Date Analyzed	Method	Model Age (years)	Error Model + yrs	Error Model - yrs	Intcpt Equiline	Error Intcpt	Slpe	Error Slpe	Xdiff	Ex-diff	Ydiff	Ey-diff
SHL37P-11.5C	443	2009 Dec	U-Pb	117910	57675									
SHL37P-7.5T	443	2009 Dec	U-Pb	118551	69596									
SHL37P-4.4R	443	2009 Dec	U-Pb	120981	30418									
SHL37P-8.4C	443	2009 Dec	U-Pb	125953	12352									
SHL37P-2.4R	443	2009 Dec	U-Pb	136167	39015									
SHL37P-9.3C	443	2009 Dec	U-Pb	151456	27264									
SHL37P-16.1R	443	2009 Dec	U-Pb	173101	38372									
SHL37P-7.6I	443	2009 Dec	U-Pb	175973	86199									
SHL37P-13.3C	443	2009 Dec	U-Pb	180502	45627									
SHL37P-14.3C	443	2009 Dec	U-Pb	188782	66095									
SHL37P-12.4I	443	2009 Dec	U-Pb	191202	34272									
SHL37P-18.1C	443	2009 Dec	U-Pb	204409	47521									
SHL37P-5.4C	443	2009 Dec	U-Pb	237124	63864									
SHL37P-17.1C	443	2009 Dec	U-Pb	316760	90757									
SHL37P-18.2	443R	2010 May	U-Th	186056	28726	22722	1.2	0.12	0.8180	0.042	15.28	0.46	12.50	0.52
SHL37P-7.8	443R	2010 May	U-Th	179840	26601	21374	1.2	0.12	0.8074	0.042	37.18	1.05	30.02	1.30
SHL37P-5.5	443R	2010 May	U-Th	172171	22073	18353	1.2	0.12	0.7933	0.038	12.70	0.39	10.08	0.36
SHL37P-4.5	443R	2010 May	U-Th	172259	20463	17227	1.2	0.12	0.7935	0.035	24.05	0.69	19.08	0.65
SHL37P-17.2	443R	2010 May	U-Th	159847	21804	18167	1.2	0.12	0.7687	0.042	12.70	0.39	9.76	0.44
SHL37P-2.5	443R	2010 May	U-Th	150033	14877	13091	1.2	0.12	0.7469	0.032	12.22	0.38	9.13	0.27
SHL37P-13.4	443R	2010 May	U-Th	144393	17349	14967	1.2	0.12	0.7335	0.039	7.30	0.26	5.36	0.21
SHL37P-12.5	443R	2010 May	U-Th	144160	14536	12826	1.2	0.12	0.7329	0.033	13.13	0.41	9.62	0.32
SHL37P-11.6	443R	2010 May	U-Th	137894	13898	12327	1.2	0.12	0.7171	0.034	15.76	0.47	11.30	0.41
SHL37P-7.7	443R	2010 May	U-Th	132910	14534	12825	1.2	0.12	0.7039	0.037	22.43	0.65	15.79	0.69
SHL37P-6.2	443R	2010 May	U-Th	129507	12184	10960	1.2	0.12	0.6946	0.032	20.97	0.61	14.56	0.53
SHL37P-11.7	443R	2010 May	U-Th	122815	11870	10705	1.2	0.12	0.6753	0.033	14.34	0.44	9.68	0.38
SHL37P-8.5	443R	2010 May	U-Th	96013	27145	21723	1.2	0.12	0.5849	0.091	1.62	0.14	0.95	0.12
SHL37P-19.1	443R	2010 May	U-Th	118061	10523	9597	1.2	0.12	0.6608	0.031	18.22	0.54	12.04	0.44
SHL37P-1.4	443R	2010 May	U-Th	115226	9347	8610	1.2	0.12	0.6519	0.029	18.83	0.55	12.27	0.40

Spot ID	Mount	Date Analyzed	Method	Model Age (years)	Error Model + yrs	Error Model - yrs	Intcpt Equiline	Error Intcpt	Slpe	Error Slpe	Xdiff	Ex-diff	Ydiff	Ey-diff
SHL37P-14.6	443R	2010 May	U-Th	111601	10770	9803	1.2	0.12	0.6401	0.034	12.98	0.40	8.31	0.36
SHL37P-15.3	443R	2010 May	U-Th	96297	8164	7596	1.2	0.12	0.5860	0.030	18.97	0.56	11.11	0.46
SHL37P-14.5	443R	2010 May	U-Th	93782	8127	7563	1.2	0.12	0.5763	0.030	11.69	0.37	6.74	0.28
SHL37P-4.4	443R	2010 May	U-Th	79403	6006	5693	1.2	0.12	0.5167	0.026	11.04	0.35	5.70	0.22
SHL37P-9.4	443R	2010 May	U-Th	28092	41889	30201	1.2	0.12	0.2268	0.246	0.51	0.13	0.12	0.12
SHL37P-16.2	443R	2010 May	U-Th	77270	6603	6226	1.2	0.12	0.5072	0.029	10.26	0.33	5.20	0.24
SHL49AZ-6.1A	414	2009 Jan	U-Th	10024	7111	6676	1.2	0.12	0.0877	0.058	2.46	0.17	0.22	0.14
SHL49AZ-14.1A	414	2009 Jan	U-Th	10961	7485	7004	1.2	0.12	0.0955	0.060	2.29	0.17	0.22	0.14
SHL49AZ-7.1A	414	2009 Jan	U-Th	15321	7692	7186	1.2	0.12	0.1309	0.059	2.45	0.17	0.32	0.14
SHL49AZ-4.3A	414	2009 Jan	U-Th	15735	5012	4792	1.2	0.12	0.1342	0.039	4.15	0.21	0.56	0.16
SHL49AZ-4.2A	414	2009 Jan	U-Th	19017	6624	6245	1.2	0.12	0.1598	0.049	3.18	0.19	0.51	0.15
SHL49AZ-3.1A	414	2009 Jan	U-Th	20989	8632	8000	1.2	0.12	0.1749	0.063	2.57	0.17	0.45	0.16
SHL49AZ-10.1A	414	2009 Jan	U-Th	21856	6739	6348	1.2	0.12	0.1814	0.049	3.39	0.19	0.61	0.16
SHL49AZ-1.1A	414	2009 Jan	U-Th	27390	8696	8054	1.2	0.12	0.2218	0.060	3.02	0.18	0.67	0.18
SHL49AZ-15.1A	414	2009 Jan	U-Th	30412	7567	7076	1.2	0.12	0.2431	0.051	3.34	0.19	0.81	0.16
SHL49AZ-2.1A	414	2009 Jan	U-Th	32543	7433	6959	1.2	0.12	0.2577	0.049	3.94	0.21	1.02	0.18
SHL49AZ-12.2A	414	2009 Jan	U-Th	33503	8595	7967	1.2	0.12	0.2642	0.056	3.25	0.19	0.86	0.17
SHL49AZ-12.3A	414	2009 Jan	U-Th	34627	7236	6787	1.2	0.12	0.2717	0.047	3.97	0.21	1.08	0.18

Spot ID	Mount	Date Analyzed	Method	Model Age (years)	Error Model + yrs	Error Model - yrs	Intcpt Equiline	Error Intcpt	Slpe	Error Slpe	Xdiff	Ex-diff	Ydiff	Ey-diff
SHL49AZ-11.1A	414	2009 Jan	U-Th	83475	15993	13947	1.2	0.12	0.5344	0.063	4.47	0.22	2.39	0.26
SHL49AZ-13.1A	414	2009 Jan	U-Th	131461	18042	15479	1.2	0.12	0.7000	0.046	7.22	0.30	5.05	0.25
SHL49AZ-13.3A	414	2009 Jan	U-Th	185568	27893	22198	1.2	0.12	0.8172	0.041	10.00	0.38	8.17	0.27
SHL49AZ-5.1A	414	09-01	U-Th	-2055	5103	4876	1.2	0.12	######	0.047	2.98	0.18	-0.06	0.14
SHL49AZ-11.2A	414	09-01	U-Th	-304	4175	4021	1.2	0.12	######	0.038	3.80	0.20	-0.01	0.14
SHL325.2-10.1T	309	2007 May	U-Th	39127	20225	17058	1.2	0.12	0.3011	0.118	8.53	0.33	2.57	1.00
SHL325.2-1.3T2	309	2007 May	U-Th	81283	13644	12127	1.2	0.12	0.5250	0.056	16.53	0.58	8.68	0.87
SHL325.2-1.1T	309	2007 May	U-Th	122806	19874	16808	1.2	0.12	0.6752	0.054	11.28	0.42	7.61	0.54
SHL325.2-6.1T	309	2007 May	U-Th	125517	19032	16202	1.2	0.12	0.6832	0.051	10.65	0.40	7.28	0.47
SHL325.2-2.1I	309	2007 May	U-Th	139157	24147	19762	1.2	0.12	0.7204	0.055	5.33	0.24	3.84	0.24
SHL325.2-3.1C	309	2007 May	U-Th	151979	33523	25613	1.2	0.12	0.7514	0.066	13.19	0.48	9.91	0.79
SHL325.2-6.3T	309	2007 May	U-Th	153500	28109	22334	1.2	0.12	0.7548	0.056	6.22	0.27	4.70	0.28
SHL325.2-4.1C	309	2007 May	U-Th	158600	26473	21291	1.2	0.12	0.7660	0.050	9.55	0.36	7.31	0.39
SHL325.2-5.2T	309	2007 May	U-Th	160086	23341	19220	1.2	0.12	0.7692	0.044	11.76	0.43	9.04	0.40
SHL325.2-6.2C	309	2007 May	U-Th	163462	34716	26301	1.2	0.12	0.7762	0.061	10.77	0.40	8.36	0.58
SHL325.2-1.2C	309	2007 May	U-Th	166445	38044	28160	1.2	0.12	0.7822	0.064	13.67	0.49	10.69	0.79

Spot ID	Mount	Date Analyzed	Method	Model Age (years)	Error Model + yrs	Error Model - yrs	Intcpt Equiline	Error Intcpt	Slpe	Error Slpe	Xdiff	Ex-diff	Ydiff	Ey-diff
SHL325.2-5.1C	309	2007 May	U-Th	176689	37595	27914	1.2	0.12	0.8017	0.058	13.23	0.48	10.60	0.66
SHL325.2-9.1T	309	07-05	U-Th	#NUM!	#NUM!	#NUM!	1.2	0.12	1.0044	0.157	1.88	0.16	1.89	0.25
SHL325.2-8.1	309	07-05	U-Th	#NUM!	#NUM!	#NUM!	1.2	0.12	1.2110	0.083	11.83	0.43	14.32	0.83
SH325.2-7.1	309	07-05	U-Th	361555	#NUM!	106098	1.2	0.12	0.9635	0.060	12.17	0.44	11.73	0.59
SH325.2-7.1UPB	309	2009 Jan	U-Pb EQ	162393	18812									
SH325.2-9.1TUPB	309	2009 Jan	U-Pb EQ	16365700	816153									
84A-1	JP04	2004	U-Th	154955	20413	17191	1.2	0.12	0.7581	0.041	14.43	0.48	10.94	0.47
84A-10.2	JP04	2004	U-Th	133097	40908	29691	1.2	0.12	0.7044	0.092	16.81	0.55	11.84	1.50
84A-11	JP04	2004	U-Th	186972	45914	32224	1.2	0.12	0.8195	0.062	19.55	0.63	16.02	1.10
84A-14	JP04	2004	U-Th	56077	23888	19589	1.2	0.12	0.4016	0.118	1.20	0.14	0.48	0.13
84A-14.2	JP04	2004	U-Th	53665	25787	20846	1.2	0.12	0.3883	0.129	1.07	0.14	0.42	0.13
84A-15	JP04	2004	U-Th	63441	18198	15594	1.2	0.12	0.4406	0.086	16.75	0.55	7.38	1.42
84A-2	JP04	2004	U-Th	115730	19214	16333	1.2	0.12	0.6535	0.056	14.67	0.49	9.58	0.76
84A-3	JP04	2004	U-Th	77350	22141	18400	1.2	0.12	0.5075	0.090	1.66	0.15	0.84	0.13
84A-4.1	JP04	2004	U-Th	50905	15954	13918	1.2	0.12	0.3726	0.085	1.67	0.15	0.62	0.13
84A-4.2	JP04	2004	U-Th	48603	15836	13828	1.2	0.12	0.3592	0.087	1.59	0.15	0.57	0.13
84A-5.1	JP04	2004	U-Th	97094	48513	33473	1.2	0.12	0.5890	0.147	11.26	0.39	6.63	1.64
84A-6	JP04	2004	U-Th	80840	21650	18060	1.2	0.12	0.5230	0.086	1.80	0.15	0.94	0.13
84A-7	JP04	2004	U-Th	124254	26323	21194	1.2	0.12	0.6795	0.069	22.69	0.72	15.42	1.48
84A-7	JP04	2004	U-Th	252572	76420	44518	1.2	0.12	0.9010	0.050	6.82	0.27	6.15	0.24
84A-8	JP04	2004	U-Th	99098	29887	23440	1.2	0.12	0.5965	0.097	10.73	0.37	6.40	1.01
84A-9	JP04	2004	U-Th	87067	13190	11767	1.2	0.12	0.5495	0.051	9.18	0.33	5.04	0.43
84A-15.2	JP04	2004	U-Th	364199	#NUM!	166921	1.2	0.12	0.9644	0.129	15.98	0.52	15.41	1.99
84A-13	JP04	2004	U-Th	126673	28294	22451	1.2	0.12	0.6865	0.072	16.61	0.54	11.40	1.13
84A-10	JP04	2004	U-Th	94867	21768	18142	1.2	0.12	0.5805	0.076	14.10	0.47	8.18	1.03
84A-11.2	JP04	2004	U-Th	171328	57465	37456	1.2	0.12	0.7917	0.085	15.95	0.52	12.62	1.29

Spot ID	Mount	Date Analyzed	Method	Model Age (years)	Error Model + yrs	Error Model - yrs	Intcpt Equiline	Error Intcpt	Slpe	Error Slpe	Xdiff	Ex-diff	Ydiff	Ey-diff
84A-11	JP04	2004	U-Th	#NUM!	#NUM!	#NUM!	1.2	0.12	1.0492	0.060	13.03	0.44	13.67	0.64
84A-12.2	JP04	2004	U-Th	#NUM!	#NUM!	#NUM!	1.2	0.12	1.3318	0.223	4.16	0.20	5.54	0.89

APPENDIX E

ZIRCON SURFACE GEOCHRONOLOGY DATA, MOUNT ST. HELENS

Spot ID	Mount	Cor. (238/232)	±(238/232)	(230/232)	±(230/232)	Model Age (yrs)	Error Model +(yrs)	Error Model -(yrs)
SHL29A-2-1.1	445	13.53	0.43	5.54	0.34	47214	5451	5191
SHL29A-2-2.1	445	10.74	0.34	4.68	0.27	49275	5898	5594
SHL29A-2-2.2	445	13.03	0.41	5.53	0.32	49553	5583	5310
SHL29A-2-3.1	445	12.71	0.40	9.49	0.39	138695	18590	15871
SHL29A-2-4.1	445	12.89	0.41	5.66	0.29	52183	5456	5195
SHL29A-2-5.1	445	19.19	0.61	13.09	0.63	117637	14530	12816
SHL29A-2-6.1	445	14.13	0.45	6.82	0.37	62068	6733	6340
SHL29A-3-1.1	445	16.99	0.54	8.40	0.41	66211	6509	6142
SHL29A-3-1.2	445	16.28	0.51	7.69	0.39	61184	6038	5721
SHL29A-3-2.1	445	16.58	0.52	9.52	0.51	84585	9595	8817
SHL29A-3-2.2	445	18.19	0.58	8.83	0.45	64840	6363	6012
SHL29A-3-3.1	445	14.79	0.47	7.89	0.53	73714	9763	8958
SHL29A-3-3.2	445	14.14	0.45	5.59	0.38	45044	5597	5323
SHL29A-3-4.1	445	13.17	0.42	8.82	0.48	109931	15188	13324
SHL29A-3-5.1	445	15.89	0.50	9.02	0.52	82656	9879	9056
SHL29A-3-6.1	445	12.45	0.39	7.50	0.42	89209	11451	10360
SHL29A-4-1.1	445	15.70	0.50	7.11	0.40	56880	6110	5785
SHL29A-4-1.2	445	16.54	0.52	10.73	0.57	105564	13329	11872
SHL29A-4-1.3	445	15.99	0.51	7.62	0.43	61864	6736	6343
SHL29A-4-2.1	445	12.18	0.39	7.91	0.59	102668	17981	15425
SHL29A-4-3.1	445	14.33	0.45	7.06	0.40	64239	7201	6753
SHL29A-4-4.1	445	14.38	0.46	6.00	0.39	49260	5895	5592
SHL29A-4-5.1	445	17.45	0.55	6.54	0.48	43278	5373	5120
SHL29A-4-5.1B	445	15.38	0.49	7.28	0.52	60928	7976	7431
SHL29A-4-6.1	445	20.05	0.63	7.52	0.42	44373	4314	4149
SHL29A-4-6.2	445	21.30	0.67	9.36	0.37	56623	4460	4284
SHL29A-4-6.2B	445	19.25	0.61	10.44	0.54	78027	8193	7619
SHL36EZ-10.1U	460	23.09	0.69	18.19	0.73	162832	22668	18748
SHL36EZ-11.1U	460	17.45	0.52	14.04	0.52	169830	24358	19888
SHL36EZ-2.1U	460	23.05	0.69	21.12	0.78	263983	81738	46134
SHL36EZ-3.1U	460	17.92	0.54	15.76	0.59	222549	47956	33166
SHL36EZ-4.2U	460	12.02	0.36	10.71	0.36	229903	53204	35569
SHL36EZ-5.1U	460	26.47	0.79	29.00	1.07	#NUM!	#NUM!	#NUM!
SHL36EZ-6.1U	460	17.92	0.54	15.43	0.54	206944	37371	27761
SHL36EZ-7.1U	460	22.68	0.68	21.34	0.76	301405	150621	60839
SHL36EZ-8.1U	460	12.17	0.36	10.76	0.29	223104	42515	30487
SHL36EZ-9.1U	460	19.02	0.57	15.14	0.58	165788	23391	19240
SHL36EZ-9.2U	460	22.01	0.66	17.78	0.72	173200	26033	20989
not glassy								
SHL08-21ZNGL-17.1	480	8.35	0.27	7.01	0.39	183242	47833	33150
SHL08-21ZNGL-16.1	480	5.21	0.17	2.99	0.16	64465	11311	10249
SHL08-	480	17.43	0.55	14.89	0.63	202364	41382	29938

21ZNGL-14.1								
SHL08-21ZNGL-15.1	480	27.28	0.87	19.87	0.71	137356	15091	13256
glassy								
SHL21ZG-1.1	480	6.30	0.20	4.12	0.24	92675	16024	13970
SHL21ZG-3.1	480	17.92	0.57	9.81	0.36	79070	6698	6311
SHL21ZG-4.1	480	5.83	0.19	3.31	0.18	66517	11028	10015
SHL21ZG-4.1R	480	17.32	0.55	10.50	0.48	93975	9957	9124
SHL21ZG-5.1	480	8.13	0.26	3.07	0.19	34394	5233	4993
SHL08-21ZG-18.1	480	14.19	0.45	8.11	0.36	82937	8536	7917
SHL08-21ZG-7.1	480	6.77	0.22	4.30	0.24	88734	14136	12514
SHL08-21ZG-8.1	480	5.62	0.18	2.85	0.15	51133	8602	7974
SHL08-21ZG-2.1	480	6.78	0.22	3.22	0.17	49044	7186	6742
SHL08-21Z-9.1	480	18.34	0.58	10.26	0.50	82059	8519	7902
SHL08-21Z-13.1	480	10.57	0.34	4.78	0.27	52493	6309	5964
SHL08-21Z-11.1	480	7.45	0.24	2.49	0.12	25317	4076	3929
SHL08-21Z-10.1	480	8.51	0.27	4.56	0.24	67192	8550	7929
SHL08-21Z-12.1	480	5.95	0.19	2.29	0.11	28347	5302	5056
glassy								
SHL08-34ZG-1.1	480	11.91	0.38	2.81	0.15	17772	2485	2430
SHL08-34ZG-2.1	480	9.39	0.30	2.92	0.17	25773	3820	3691
SHL08-34ZG-3.1	480	15.92	0.51	10.77	0.49	114655	13651	12132
SHL08-34ZG-4.1	480	8.64	0.27	1.87	0.11	10306	2652	2589
SHL08-34ZG-3.2	480	13.87	0.44	12.18	0.52	220371	54734	36290
SHL08-34ZG-5.1	480	7.76	0.25	1.95	0.13	13259	3438	3333
not glassy								
SHL34-5-1.2	480	10.41	0.33	1.86	0.15	8150	2470	2416
SHL34-1-1.1	480	6.47	0.20	1.83	0.14	13775	4549	4367
SHL34-5-3.1	480	8.23	0.26	2.15	0.14	15751	3435	3330
SHL34-1-5.2	480	10.22	0.32	2.81	0.20	21343	3618	3502
SHL34-1-3.1	480	9.18	0.29	2.98	0.21	27550	4452	4277
SHL34-5-1.1	480	10.43	0.33	3.27	0.20	27555	3817	3687
SHL34-6-1.1	480	5.02	0.16	2.68	0.16	53263	10450	9533
SHL34-5-2.1	480	10.42	0.33	4.89	0.29	55616	7031	6604
SHL34-1-4.1	480	11.07	0.35	5.16	0.30	55820	6757	6362

SHL34-1-2.1	480	16.32	0.52	7.46	0.40	58122	5975	5663
SHL34-6-2.1	480	15.42	0.49	9.83	0.58	101564	13730	12189
SHL34-5-1.2	445	10.41	0.33	1.86	0.15	8150	2470	2416
SHL34-1-1.1	445	6.47	0.20	1.83	0.14	13775	4549	4367
SHL34-5-3.1	445	8.23	0.26	2.15	0.14	15751	3435	3330
SHL34-1-5.2	445	10.22	0.32	2.81	0.20	21343	3618	3502
SHL34-1-3.1	445	9.18	0.29	2.98	0.21	27550	4452	4277
SHL34-5-1.1	445	10.43	0.33	3.27	0.20	27555	3817	3687
SHL34-6-1.1	445	5.02	0.16	2.68	0.16	53263	10450	9533
SHL34-5-2.1	445	10.42	0.33	4.89	0.29	55616	7031	6604
SHL34-1-4.1	445	11.07	0.35	5.16	0.30	55820	6757	6362
SHL34-1-2.1	445	16.32	0.52	7.46	0.40	58122	5975	5663
SHL34-6-2.1	445	15.42	0.49	9.83	0.58	101564	13730	12189

Spot ID	Mount	Intrcpt Equiline 1.2	Error Intrcpt	Slope	Error Slope	Xdiff	Exdiff	Ydiff	Eydiff
SHL29A-2-1.1	445	1.2	0.12	0.3522	0.032	12.33	0.44	4.34	0.36
SHL29A-2-2.1	445	1.2	0.12	0.3643	0.034	9.54	0.36	3.48	0.29
SHL29A-2-2.2	445	1.2	0.12	0.3660	0.032	11.83	0.43	4.33	0.34
SHL29A-2-3.1	445	1.2	0.12	0.7207	0.044	11.51	0.42	8.29	0.40
SHL29A-2-4.1	445	1.2	0.12	0.3811	0.030	11.69	0.42	4.46	0.31
SHL29A-2-5.1	445	1.2	0.12	0.6610	0.042	17.99	0.62	11.89	0.64
SHL29A-2-6.1	445	1.2	0.12	0.4349	0.034	12.93	0.46	5.62	0.39
SHL29A-3-1.1	445	1.2	0.12	0.4560	0.032	15.79	0.55	7.20	0.43
SHL29A-3-1.2	445	1.2	0.12	0.4303	0.031	15.08	0.53	6.49	0.40
SHL29A-3-2.1	445	1.2	0.12	0.5406	0.039	15.38	0.54	8.32	0.52
SHL29A-3-2.2	445	1.2	0.12	0.4491	0.031	16.99	0.59	7.63	0.46
SHL29A-3-3.1	445	1.2	0.12	0.4923	0.044	13.59	0.48	6.69	0.54
SHL29A-3-3.2	445	1.2	0.12	0.3391	0.033	12.94	0.46	4.39	0.40
SHL29A-3-4.1	445	1.2	0.12	0.6361	0.047	11.97	0.43	7.62	0.50
SHL29A-3-5.1	445	1.2	0.12	0.5324	0.041	14.69	0.52	7.82	0.53
SHL29A-3-6.1	445	1.2	0.12	0.5597	0.044	11.25	0.41	6.30	0.44
SHL29A-4-1.1	445	1.2	0.12	0.4073	0.032	14.50	0.51	5.91	0.42
SHL29A-4-1.2	445	1.2	0.12	0.6212	0.044	15.34	0.54	9.53	0.58
SHL29A-4-1.3	445	1.2	0.12	0.4338	0.034	14.79	0.52	6.42	0.45
SHL29A-4-2.1	445	1.2	0.12	0.6110	0.059	10.98	0.40	6.71	0.60
SHL29A-4-3.1	445	1.2	0.12	0.4461	0.035	13.13	0.47	5.86	0.42
SHL29A-4-4.1	445	1.2	0.12	0.3643	0.034	13.18	0.47	4.80	0.41
SHL29A-4-5.1	445	1.2	0.12	0.3283	0.032	16.25	0.57	5.34	0.49
SHL29A-4-5.1B	445	1.2	0.12	0.4289	0.040	14.18	0.50	6.08	0.53
SHL29A-4-6.1	445	1.2	0.12	0.3350	0.026	18.85	0.65	6.32	0.44
SHL29A-4-6.2	445	1.2	0.12	0.4059	0.024	20.10	0.68	8.16	0.39
SHL29A-4-6.2B	445	1.2	0.12	0.5120	0.035	18.05	0.62	9.24	0.55
SHL36EZ-10.1U	460	1.2	0.12	0.7763	0.042	21.89	0.70	16.99	0.74
SHL36EZ-11.1U	460	1.2	0.12	0.7902	0.042	16.25	0.54	12.84	0.54
SHL36EZ-2.1U	460	1.2	0.12	0.9117	0.047	21.85	0.70	19.92	0.79
SHL36EZ-3.1U	460	1.2	0.12	0.8708	0.046	16.72	0.55	14.56	0.60
SHL36EZ-4.2U	460	1.2	0.12	0.8792	0.047	10.82	0.38	9.51	0.38
SHL36EZ-5.1U	460	1.2	0.12	1.1000	0.055	25.27	0.80	27.80	1.08
SHL36EZ-6.1U	460	1.2	0.12	0.8509	0.043	16.72	0.55	14.23	0.55
SHL36EZ-7.1U	460	1.2	0.12	0.9374	0.047	21.48	0.69	20.14	0.77
SHL36EZ-	460	1.2	0.12	0.8715	0.042	10.97	0.38	9.56	0.31

8.1U									
SHL36EZ-9.1U	460	1.2	0.12	0.7823	0.042	17.82	0.58	13.94	0.60
SHL36EZ-9.2U	460	1.2	0.12	0.7966	0.043	20.81	0.67	16.58	0.73
not glassy									
SHL08-21ZNGL-17.1	480	1.2	0.12	0.8133	0.066	7.15	0.29	5.81	0.41
SHL08-21ZNGL-16.1	480	1.2	0.12	0.4459	0.055	4.01	0.20	1.79	0.20
SHL08-21ZNGL-14.1	480	1.2	0.12	0.8433	0.049	16.23	0.57	13.69	0.64
SHL08-21ZNGL-15.1	480	1.2	0.12	0.7157	0.037	26.08	0.88	18.67	0.72
glassy									
SHL21ZG-1.1	480	1.2	0.12	0.5720	0.058	5.10	0.23	2.92	0.27
SHL21ZG-3.1	480	1.2	0.12	0.5152	0.029	16.72	0.58	8.61	0.38
SHL21ZG-4.1	480	1.2	0.12	0.4562	0.052	4.63	0.22	2.11	0.22
SHL21ZG-4.1R	480	1.2	0.12	0.5771	0.037	16.12	0.56	9.30	0.50
SHL21ZG-5.1	480	1.2	0.12	0.2702	0.034	6.93	0.29	1.87	0.22
SHL08-21ZG-18.1	480	1.2	0.12	0.5321	0.035	12.99	0.47	6.91	0.38
SHL08-21ZG-7.1	480	1.2	0.12	0.5563	0.054	5.57	0.25	3.10	0.27
SHL08-21ZG-8.1	480	1.2	0.12	0.3739	0.047	4.42	0.22	1.65	0.19
SHL08-21ZG-2.1	480	1.2	0.12	0.3618	0.041	5.58	0.25	2.02	0.21
SHL08-21Z-9.1	480	1.2	0.12	0.5283	0.035	17.14	0.60	9.06	0.52
SHL08-21Z-13.1	480	1.2	0.12	0.3817	0.035	9.37	0.36	3.58	0.30
SHL08-21Z-11.1	480	1.2	0.12	0.2069	0.029	6.25	0.27	1.29	0.17
SHL08-21Z-10.1	480	1.2	0.12	0.4595	0.041	7.31	0.30	3.36	0.26
SHL08-21Z-12.1	480	1.2	0.12	0.2286	0.037	4.75	0.22	1.09	0.17
glassy									
SHL08-34ZG-1.1	480	1.2	0.12	0.1502	0.019	10.71	0.40	1.61	0.20
SHL08-34ZG-2.1	480	1.2	0.12	0.2102	0.027	8.19	0.32	1.72	0.21
SHL08-34ZG-3.1	480	1.2	0.12	0.6501	0.041	14.72	0.52	9.57	0.50
SHL08-34ZG-4.1	480	1.2	0.12	0.0901	0.022	7.44	0.30	0.67	0.16
SHL08-34ZG-	480	1.2	0.12	0.8671	0.052	12.67	0.46	10.98	0.53

3.2 SHL08-34ZG-5.1	480	1.2	0.12	0.1143	0.027	6.56	0.27	0.75	0.18
not glassy									
SHL34-5-1.2	480	1.2	0.12	0.0722	0.021	9.21	0.35	0.66	0.19
SHL34-1-1.1	480	1.2	0.12	0.1190	0.036	5.27	0.24	0.63	0.19
SHL34-5-3.1	480	1.2	0.12	0.1348	0.027	7.03	0.29	0.95	0.19
SHL34-1-5.2	480	1.2	0.12	0.1782	0.027	9.02	0.34	1.61	0.23
SHL34-1-3.1	480	1.2	0.12	0.2238	0.031	7.98	0.31	1.78	0.24
SHL34-5-1.1	480	1.2	0.12	0.2238	0.027	9.23	0.35	2.07	0.23
SHL34-6-1.1	480	1.2	0.12	0.3872	0.056	3.82	0.20	1.48	0.20
SHL34-5-2.1	480	1.2	0.12	0.4003	0.038	9.22	0.35	3.69	0.32
SHL34-1-4.1	480	1.2	0.12	0.4015	0.036	9.87	0.37	3.96	0.32
SHL34-1-2.1	480	1.2	0.12	0.4140	0.031	15.12	0.53	6.26	0.42
SHL34-6-2.1	480	1.2	0.12	0.6070	0.047	14.22	0.50	8.63	0.59
SHL34-5-1.2	445	1.2	0.12	0.0722	0.021	9.21	0.35	0.66	0.19
SHL34-1-1.1	445	1.2	0.12	0.1190	0.036	5.27	0.24	0.63	0.19
SHL34-5-3.1	445	1.2	0.12	0.1348	0.027	7.03	0.29	0.95	0.19
SHL34-1-5.2	445	1.2	0.12	0.1782	0.027	9.02	0.34	1.61	0.23
SHL34-1-3.1	445	1.2	0.12	0.2238	0.031	7.98	0.31	1.78	0.24
SHL34-5-1.1	445	1.2	0.12	0.2238	0.027	9.23	0.35	2.07	0.23
SHL34-6-1.1	445	1.2	0.12	0.3872	0.056	3.82	0.20	1.48	0.20
SHL34-5-2.1	445	1.2	0.12	0.4003	0.038	9.22	0.35	3.69	0.32
SHL34-1-4.1	445	1.2	0.12	0.4015	0.036	9.87	0.37	3.96	0.32
SHL34-1-2.1	445	1.2	0.12	0.4140	0.031	15.12	0.53	6.26	0.42
SHL34-6-2.1	445	1.2	0.12	0.6070	0.047	14.22	0.50	8.63	0.59

Spot ID	Mount	Date Analyzed	Li ppm (est)	Be ppm (est)	B ppm (est)	F ppm (est)	Na ppm (est)	Mg ppm (est)	Al ppm (est)	P ppm
SHL3Z-1.1DI	JW414	2009 Jan	0.1	4.30	0.1	11	3.2	0.5	17	242
SHL3Z-1.2LC	JW414	2009 Jan	0.1	5.76	0.2	16	3.8	0.4	19	336
SHL3Z-1.3DI	JW414	2009 Jan	0.1	1.30	0.1	14	7.5	1.0	49	99
SHL3Z-1.4DR	JW414	2009 Jan	0.0	1.86	0.2	10	2.9	0.6	17	251
SHL3Z-2.1DC	JW414	2009 Jan	0.0	13.68	0.1	14	4.0	0.8	25	415
SHL3Z-2.2LR	***JW414***	***2009 Jan***	***0.4***	***8.32***	***0.2***	***10***	***17***	***57.3***	***115***	***254***
SHL3Z-3.1LC	***JW414***	***2009 Jan***	***0.1***	***9.88***	***0.1***	***13***	***5.6***	***0.8***	***29***	***184***
SHL3Z-3.2DI	JW414	2009 Jan	0.6	166.59	0.1	15	4.4	3.4	26	1422
SHL3Z-3.3LR	JW414	2009 Jan	0.0	1.72	0.1	13	3.5	0.5	20	1285
SHL3Z-4.1LR	JW414	2009 Jan	0.0	10.99	0.1	12	3.8	0.7	23	291
SHL3Z-4.2LI	JW414	2009 Jan	0.0	3.56	0.2	14	3.3	0.4	17	214
SHL3Z-4.3LC	JW414	2009 Jan	0.0	1.08	0.0	14	3.3	0.5	22	485
SHL3Z-5.1DC	JW414	2009 Jan	0.0	0.34	0.2	10	3.0	0.5	20	94
SHL3Z-5.2LR	JW414	2009 Jan	0.0	2.68	0.4	13	3.6	0.5	18	314
SHL3Z-6.1DI	JW414	2009 Jan	0.0	2.22	0.1	13	4.0	0.6	22	364
SHL3Z-6.2LC	***JW414***	***2009 Jan***	***0.2***	***2.90***	***0.2***	***18***	***19***	***2.3***	***70***	***406***
SHL3Z-6.3DE	JW414	2009 Jan	0.0	0.89	0.1	13	2.0	0.6	12	306
SHL3Z-7.1LR	JW414	2009 Jan	0.1	0.17	0.1	19	4.2	6.1	22	278
SHL3Z-7.2DI	***JW414***	***2009 Jan***	***0.0***	***0.98***	***0.1***	***16***	***5.1***	***1.5***	***34***	***257***
SHL3Z-7.3LC	***JW414***	***2009 Jan***	***0.1***	***1.11***	***0.2***	***17***	***6.5***	***0.9***	***39***	***266***
SHL3Z-8.1LC	JW414	2009 Jan	0.0	7.21	0.2	15	4.4	0.6	19	257
SHL3Z-8.2I	JW414	2009 Jan	0.0	18.40	0.2	16	3.6	0.5	21	326
SHL3Z-8.3LC	***JW414***	***2009 Jan***	***0.1***	***15.29***	***0.1***	***14***	***5.8***	***0.7***	***27***	***306***
SHL3Z-8.4DI	***JW414***	***2009 Jan***	***0.1***	***9.60***	***0.1***	***19***	***33***	***1.3***	***140***	***404***
SHL3Z-9.1DI	JW414	2009 Jan	0.1	7.37	0.1	16	6.2	0.9	38	268
SHL3Z-9.2LC	JW414	2009 Jan	0.0	0.46	0.1	12	4.0	0.6	24	573
SHL3Z-9.3LI	JW414	2009 Jan	0.0	12.16	0.2	13	4.5	0.8	22	365

Spot ID	Mount	Date Analyzed	Li ppm (est)	Be ppm (est)	B ppm (est)	F ppm (est)	Na ppm (est)	Mg ppm (est)	Al ppm (est)	P ppm
SHL3Z-1.1DGI	JW309	2007 May		118.64	0.10	13.8			40.1	1349
SHL3Z-1.2MGI	JW309	2007 May		1.46	0.05	8.4			25.0	437
SHL3Z-2.1MGZC	***JW309***	***2007 May***		***13.29***	***0.49***	***12.7***			***394.5***	***294***
SHL3Z-2.2DGZI	JW309	2007 May		1.10	0.07	10.2			12.5	289
SHL3Z-3.1DGZT	JW309	2007 May		3.38	0.15	19.1			41.2	317
SHL3Z-3.2LGZE	JW309	2007 May		1.08	0.03	10.2			22.8	349
SHL3Z-3.3DGC	JW309	2007 May		30.81	0.03	11.5			13.7	386
SHL3Z-4.1MGI	JW309	2007 May		3.72	0.04	10.8			15.4	344
SHL4Z-1.1DGZE	JW309	2007 May		4.38	0.09	11.5			15	259
SHL4Z-1.2MGZI	JW309	2007 May		19.65	0.07	7.1			8	318
SHL4Z-10.1MGT	JW309	2007 May		31.03	0.05	11.4			12	292
SHL4Z-10.2MGZC	JW309	2007 May		10.16	0.05	10.5			18	266
SHL4Z-10.3DGZIT	JW309	2007 May		89.30	0.05	7.7			12	588
MSHL4Z-11.1DGZI	JW309	2007 May		16.02	0.04	8.9			11	330
SHL4Z-11.2DZIT	JW309	2007 May		42.20	0.06	7.7			10	374
SHL4Z-12.1MGI	JW309	2007 May		2.47	0.03	11.0			18	217
SHL4Z-2.1DGZI	JW309	2007 May		5.24	0.09	12.0			18	208
SHL4Z-2.2MGZI	JW309	2007 May		23.01	0.08	7.7			15	281
SHL4Z-	JW309	2007 May		10.13	0.06	11.6			13	216

Spot ID	Mount	Date Analyzed	Li ppm (est)	Be ppm (est)	B ppm (est)	F ppm (est)	Na ppm (est)	Mg ppm (est)	Al ppm (est)	P ppm
SHL4Z-2.3DGZE										
SHL4Z-3.1DGZT	JW309	2007 May		1.98	0.04	7.7			15	353
SHL4Z-3.2MGZE	JW309	2007 May		0.47	0.06	12.2			12	401
SHL4Z-10.2MGZC	JW309	2007 May		10.16	0.05	10.5			18	266
SHL4Z-10.3DGZIT	JW309	2007 May		89.30	0.05	7.7			12	588
SHL4Z-11.1DGZI	JW309	2007 May		16.02	0.04	8.9			11	330
SHL4Z-5.1DGZT	JW309	2007 May		3.42	0.05	8.3			12	216
SHL4Z-5.2MGZE	JW309	2007 May		27.10	0.04	9.9			10	251
SHL4Z-5.3MGI	JW309	2007 May		0.99	0.05	7.9			11	95
SHL4Z-6.1MGT	JW309	2007 May		23.76	0.44	8.8			12	265
SHL4Z-6.2MGI	JW309	2007 May		1.97	0.18	7.7			12	223
SHL4Z-7.1MGZT	JW309	2007 May		21.91	0.25	13.9			147	286
SHL4Z-7.2LGC	JW309	2007 May		18.71	0.12	11.2			17	560
SHL4Z-7.3DGI	JW309	2007 May		59.35	0.21	10.3			12	639
SHL4Z-8.1MGZT	JW309	2007 May		12.23	0.03	8.7			13	305
SHL4Z-8.2DGZI	JW309	2007 May		6.95	0.04	10.4			14	274
SHL4Z-8.3MGZI	JW309	2007 May		5.77	0.06	8.3			16	285
SHL4Z-9.1MGZT	JW309	2007 May		35.92	0.04	9.6			13	292
SHL4Z-9.2LGC	JW309	2007 May		6.52	0.04	9.2			11	376
SHL4Z-9.3MGZT	JW309	2007 May		10.52	0.05	8.8			13	250

Spot ID	Mount	Date Analyzed	Li ppm (est)	Be ppm (est)	B ppm (est)	F ppm (est)	Na ppm (est)	Mg ppm (est)	Al ppm (est)	P ppm
SHL5Z-1.1C	JW364	2008 Jan	0.7	5.9	0.0	17	2.1	0.8	9	306
SHL5Z-2.1I	JW364	2008 Jan	0.2	3.1	0.0	12	5.6	3.7	15	131
SHL5Z-2.2T	JW364	2008 Jan	0.0	6.8	0.0	14	1.6	0.5	7	295
SHL5Z-3.1C	JW364	2008 Jan	0.1	3.1	0.0	13	2.3	0.6	7	272
SHL5Z-3.2E	JW364	2008 Jan	0.0	7.8	0.0	12	2.5	0.9	8	238
SHL5Z-4.1C	JW364	2008 Jan	0.1	9.8	0.0	32	17.4	1.9	27	345
SHL5Z-4.2T	JW364	2008 Jan	0.0	3.3	0.0	20	6.7	2.3	18	227
SHL5Z-5.1T	JW364	2008 Jan	0.1	3.1	0.0	24	7.2	2.0	21	271
SHL5Z-5.2C	***JW364***	***2008 Jan***	***0.5***	***198***	***1.4***	***45***	***38.2***	***11.2***	***98***	***1380***
SHL5Z-6.1C	***JW364***	***2008 Jan***	***3.8***	***555***	***0.1***	***32***	***6.5***	***10.8***	***49***	***1937***
SHL5Z-6.2T	JW364	2008 Jan	0.0	0.1	0.0	20	5.0	2.1	19	222
SHL5Z-6.3I	JW364	2008 Jan	0.3	2.2	0.0	26	6.3	1.6	20	199
SHL5Z-7.1C	***JW364***	***2008 Jan***	***0.6***	***4.8***	***0.1***	***24***	***73.3***	***11.2***	***116***	***230***
SHL5Z-7.2T	JW364	2008 Jan	0.1	1.3	0.0	23	6.3	1.7	17	226
SHL5Z-8.1T	JW364	2008 Jan	0.0	1.4	0.0	19	6.5	2.5	24	244
SHL5Z-8.2C	JW364	2008 Jan	0.1	8.4	0.0	25	7.4	1.9	27	472
SHL5Z-1.1T	JW365	2008 Jan	0.0	0.42	0.0	6	3.3	1.1	22	228
SHL5Z-1.2I	***JW365***	***2008 Jan***	***0.0***	***7.02***	***0.1***	***9***	***239.0***	***2.2***	***309***	***312***
SHL5Z-2.1C	JW365	2008 Jan	0.0	5.81	0.1	6	17.2	4.7	39	328
SHL5Z-2.2E	JW365	2008 Jan	0.0	2.36	0.0	6	2.9	0.6	19	320
SHL5Z-3.1C	JW365	2008 Jan	0.6	2.30	0.0	12	3.1	0.3	19	265
SHL5Z-3.2R	JW365	2008 Jan	0.6	3.98	0.0	6	2.0	0.4	15	304
SHL5Z-4.1C	JW365	2008 Jan	0.0	23.31	0.0	10	2.2	0.5	13	380
SHL5Z-4.2T	JW365	2008 Jan	0.0	6.09	0.0	12	13.8	0.7	33	268
SHL5Z-5.1C	JW365	2008 Jan	0.0	0.42	0.0	7	2.7	0.4	22	366
SHL5Z-5.2T	JW365	2008 Jan	0.0	14.64	0.0	9	2.4	0.6	14	393
SHL5Z-6.1C	***JW365***	***2008 Jan***	***0.0***	***23.58***	***0.1***	***11***	***9.8***	***1.5***	***16***	***424***
SHL5Z-6.2T	JW365	2008 Jan	0.0	0.22	0.0	7	2.2	0.8	19	209

Spot ID	Mount	Date Analyzed	Li ppm (est)	Be ppm (est)	B ppm (est)	F ppm (est)	Na ppm (est)	Mg ppm (est)	Al ppm (est)	P ppm
SHL5Z-7.1T	JW365	2008 Jan	0.0	4.50	0.0	13	3.9	1.2	19	271
SHL5Z-7.2C	JW365	2008 Jan	0.0	0.62	0.0	10	2.6	0.4	25	297
SHL5Z-8.1I	JW365	2008 Jan	0.0	15.74	0.0	8	1.4	0.2	10	487
SHL5Z-8.2C	JW365	2008 Jan	0.0	0.84	0.0	10	2.4	0.7	22	308
SHL5Z-8.3T	JW365	2008 Jan	0.0	9.69	0.0	10	2.7	0.6	15	298
SHL5Z-9.1T	JW365	2008 Jan	0.0	29.66	0.0	5	2.1	0.4	13	474
SHL5Z-9.2I	JW365	2008 Jan	0.1	4.34	0.0	10	5.2	0.6	20	297
SHL5Z-9.3I	JW365	2008 Jan	0.0	9.40	0.0	4	1.4	0.4	12	638
SHL0821Z-1.1E	JW414	2009 Jan	0.038	0.04	0.2	44	10	1.4	44	254
SHL0821Z-1.2C	***JW414***	***2009 Jan***	***0.328***	***0.01***	***0.1***	***29***	***51***	***0.8***	***175***	***244***
SHL0821Z-2.1E	JW414	2009 Jan	0.160	0.00	0.1	16	19	0.6	45	155
SHL0821Z-2.2I	JW414	2009 Jan	0.009	0.06	0.1	20	2.8	0.5	16	279
SHL0821Z-3.1E	JW414	2009 Jan	0.159	0.00	0.1	24	9.0	0.6	21	227
SHL0821Z-3.2I	JW414	2009 Jan	0.024	0.00	0.1	21	3.4	0.5	23	92
SHL0821Z-4.1E	JW414	2009 Jan	0.010	0.00	0.1	18	3.1	0.5	26	257
SHL0821Z-4.2C	JW414	2009 Jan	0.003	0.01	0.1	18	3.7	0.5	27	260
SHL0821Z-5.1E	***JW414***	***2009 Jan***	***0.027***	***0.01***	***0.1***	***89***	***6.6***	***0.8***	***27***	***623***
SHL0821Z-5.2I	***JW414***	***2009 Jan***	***0.146***	***0.04***	***0.7***	***15***	***189***	***13.3***	***1242***	***143***
SHL0821Z-6.1E	JW414	2009 Jan	0.010	0.02	0.1	15	3.2	0.5	26	172
SHL0821Z-6.2I	JW414	2009 Jan	0.016	0.12	0.0	17	8.5	1.1	18	314
SHL0821Z-7.1C	JW414	2009 Jan	0.013	0.04	0.1	23	4.1	0.8	23	208
SHL0821Z-7.2I	JW414	2009 Jan	0.003	0.01	0.0	18	2.8	0.5	14	75
SHL0821Z-7.3R	JW414	2009 Jan	0.005	0.00	0.0	18	4.0	0.5	33	143
SHL0821Z-8.1C	***JW414***	***2009 Jan***	***0.834***	***0.01***	***0.1***	***19***	***19***	***1.6***	***66***	***481***
SHL0821Z-8.2I	JW414	2009 Jan	0.001	0.01	0.0	14	3.0	0.4	17	269
SHL0821Z-8.3I	JW414	2009 Jan	0.000	0.02	0.0	16	3.1	0.5	17	390
SHL0821Z-9.1I	JW414	2009 Jan	0.002	0.02	0.0	14	2.2	0.3	16	228
SHL0821Z-9.2E	JW414	2009 Jan	0.006	0.00	0.1	10	2.7	0.4	24	132
SHL0821Z-	JW414	2009 Jan	0.001	0.00	0.0	13	2.2	0.4	15	250

Spot ID	Mount	Date Analyzed	Li ppm (est)	Be ppm (est)	B ppm (est)	F ppm (est)	Na ppm (est)	Mg ppm (est)	Al ppm (est)	P ppm
10.1I										
SHL0821Z-11.1E	JW414	2009 Jan	0.002	0.00	0.0	16	3.9	0.7	18	285
SHL0821Z-11.2C	JW414	2009 Jan	0.000	0.01	0.0	12	2.6	0.4	16	523
SHL0821Z-12.1C	JW414	2009 Jan	0.022	0.01	0.1	12	3.2	0.7	55	786
SHL0821Z-12.2E	JW414	2009 Jan	0.025	0.01	0.1	14	4.3	0.5	21	279
SHL0821Z-13.1C	JW414	2009 Jan	0.511	0.01	0.1	12	14	0.6	54	367
SHL0821Z-13.2I	JW414	2009 Jan	0.037	0.06	0.1	11	2.8	0.4	19	556
SHL0821Z-13.3E	JW414	2009 Jan	0.085	0.02	0.1	12	3.1	2.2	44	177
SHL26C-1.1C	JW443	2009 Dec	0.038	0.01	0.0	6	4.4		21	310
SHL26-1.2R	JW443	2009 Dec	0.000	0.01	0.0	1	1.4		8	265
SHL-26C-2.1C	JW443	2009 Dec	0.000	0.00	0.0	1	1.0		6	263
SHL-26C-2.2R	JW443	2009 Dec	0.003	0.00	0.0	4	1.1		9	277
SHL26C-3.1R	JW443	2009 Dec	0.004	0.01	0.1	3	2.2		17	537
SHL26C-3.2C	JW443	2009 Dec	0.004	0.00	0.1	5	3.7		27	411
SHL26C-4.1C	***JW443***	***2009 Dec***	***0.014***	***0.00***	***0.1***	***6***	***20.9***		***37***	***106***
SHL26C-4.2T	JW443	2009 Dec	0.001	0.00	0.0	9	1.4		8	388
SHL26C-5.1T	JW443	2009 Dec	0.023	0.00	0.0	4	11.5		29	224
SHL26C-5.2I	JW443	2009 Dec	0.000	0.00	0.0	7	2.4		14	258
SHL26C-5.3C	JW443	2009 Dec	0.003	0.00	0.0	4	2.8		16	263
SHL26C-6.1C	***JW443***	***2009 Dec***	***0.003***	***0.00***	***0.0***	***3***	***1.8***		***7***	***287***
SHL26C-6.2I	JW443	2009 Dec	0.010	0.00	0.0	3	3.3		10	252
SHL26c-7.1C	JW443	2009 Dec	0.006	0.00	0.0	6	1.4		16	217
SHL26C-7.2T	JW443	2009 Dec	0.000	0.00	0.1	8	2.3		7	222

Spot ID	Mount	Date Analyzed	Li ppm (est)	Be ppm (est)	B ppm (est)	F ppm (est)	Na ppm (est)	Mg ppm (est)	Al ppm (est)	P ppm
SHL26C-8.1C	JW443	2009 Dec	0.000	0.00	0.1	1	1.6		9	286
SHL26C-8.2R	JW443	2009 Dec	0.000	0.00	0.0	1	1.0		9	257
SHL26C-9.1C	JW443	2009 Dec	0.003	0.02	0.0	5	1.2		7	354
SHL26C-9.2I	JW443	2009 Dec	0.002	0.00	0.0	4	1.5		7	276
SHL26C-9.3R	JW443	2009 Dec	0.000	0.00	0.0	2	1.0		6	292
SHL26C-9.4R	JW443	2009 Dec	0.000	0.00	0.0	4	5.4		19	297
SHL26C-10.1C	JW443	2009 Dec	0.000	0.00	0.0	4	1.2		8	307
SHL26C-10.2I	JW443	2009 Dec	0.001	0.00	0.0	3	1.4		6	313
SHL26c-10.3R	JW443	2009 Dec	0.004	0.00	0.1	5	3.8		13	287
SHL26C-11.1C	JW443	2009 Dec	0.004	0.00	0.0	7	4.6		17	348
SHL26C-12.1C	JW443	2009 Dec	0.004	0.00	0.0	7	3.5		15	327
SHL26C-12.2I	JW443	2009 Dec	0.001	0.00	0.0	2	4.0		14	271
SHL26C-13.1C	JW443	2009 Dec	0.002	0.00	0.1	6	3.5		19	281
SHL26c-13.2R	JW443	2009 Dec	0.003	0.00	0.1	2	3.7		20	270
SHL26C-14.2I	JW443	2009 Dec	0.002	0.03	0.0	10	3.3		12	599
SHL26C-14.1I	JW443	2009 Dec	0.003	0.00	0.1	9	3.8		16	206
SHL26C-14.3R	JW443	2009 Dec	0.000	0.00	0.0	10	3.1		14	256
SHL26C-15.1I	JW443	2009 Dec	0.014	0.02	0.0	6	3.8		13	1002
SHL26C-15.2I	JW443	2009 Dec	0.005	0.00	0.0	8	5.1		21	215
SHL26C-15.3C	JW443	2009 Dec	0.004	0.00	0.1	14	3.9		17	306
SHL29AZ-1.1T	JW392	2008 Aug	0.007	26.83	0.1	12	3.7	0.9	20	236
SHL29AZ-1.2C	JW392	2008 Aug	0.146	217.62	0.1	16	9.7	1.1	40	836
SHL29AZ-1.3I	JW392	2008 Aug	0.002	0.52	0.1	9	1.9	0.5	13	84
SHL29AZ-2.1E	JW392	2008 Aug	0.000	21.39	0.4	14	3.4	0.8	15	242
SHL29AZ-2.2E	JW392	2008 Aug	0.004	3.35	0.1	13	1.9	0.5	13	211
SHL29AZ-2.3I	***JW392***	***2008 Aug***	***0.004***	***6.54***	***0.2***	***16***	***21.1***	***13.2***	***30***	***274***
SHL29AZ-2.4I	JW392	2008 Aug	0.003	44.01	0.6	17	3.4	1.9	16	253
SHL29AZ-3.1C	JW392	2008 Aug	0.028	13.48	0.2	11	3.1	0.7	14	268
SHL29AZ-3.2IE	JW392	2008 Aug	0.022	17.32	0.1	11	2.4	0.6	15	232

Spot ID	Mount	Date Analyzed	Li ppm (est)	Be ppm (est)	B ppm (est)	F ppm (est)	Na ppm (est)	Mg ppm (est)	Al ppm (est)	P ppm
SHL29AZ-3.3IE	JW392	2008 Aug	0.007	28.03	0.1	13	2.1	0.5	16	308
SHL29AZ-3.4E	JW392	2008 Aug	0.005	14.23	0.2	8	2.9	0.8	17	230
SHL29AZ-1.1C	JW393	2008 Aug	0.0	1.64	0.1	14	6.8	1.7	38	287
SHL29AZ-1.2E	JW393	2008 Aug	0.0	30.31	0.1	13	3.5	1.0	14	325
SHL29AZ-2.1E	JW393	2008 Aug	0.0	0.11	0.1	15	3.6	1.1	14	254
SHL29AZ-2.2I	JW393	2008 Aug	0.1	0.09	0.1	14	9.2	1.5	32	281
SHL29AZ-2.3C	JW393	2008 Aug	0.0	0.02	0.2	13	5.8	1.3	18	433
SHL29AZ-3.1C	JW393	2008 Aug	0.0	3.41	0.1	15	7.0	1.4	14	259
SHL29AZ-3.2C	JW393	2008 Aug	0.0	7.48	0.2	8	3.8	1.5	21	251
SHL29AZ-4.1C	***JW393***	***2008 Aug***	***0.1***	***19.50***	***0.2***	***12***	***23.7***	***9.1***	***80***	***245***
SHL29AZ-4.2E	JW393	2008 Aug	0.0	0.75	0.1	12	4.2	1.2	17	242
SHL29AZ-5.1C	JW393	2008 Aug	0.1	37.52	0.1	10	4.7	1.6	21	337
SHL29AZ-5.2E	JW393	2008 Aug	0.0	16.21	0.2	10	4.3	1.4	14	230
SHL29AZ-6.1C	***JW393***	***2008 Aug***	***0.8***	***560.86***	***0.6***	***19***	***127.5***	***5.1***	***1059***	***1658***
SHL29AZ-6.2E	JW393	2008 Aug	0.0	12.67	0.1	13	3.9	1.1	14	285
SHL29AZ-6.3I	JW393	2008 Aug	0.0	22.21	0.1	10	3.7	5.9	18	264
SHL29AZ-7.1C	JW393	2008 Aug	0.0	12.68	0.0	14	6.4	4.8	25	392
SHL29AZ-7.2I	JW393	2008 Aug	0.0	59.68	0.1	9	4.1	1.3	13	385
SHL29AZ-7.3E	JW393	2008 Aug	0.0	12.39	0.1	11	4.4	1.8	16	280
SHL29AZ-8.1C	JW393	2008 Aug	0.1	129.58	0.1	11	4.2	1.3	14	756
SHL29AZ-8.2E	JW393	2008 Aug	0.0	39.87	0.1	9	3.9	1.2	15	356
SHL29AZ-9.1C	JW393	2008 Aug	0.1	25.05	0.1	10	11.3	1.9	28	346
SHL29AZ-9.2E	JW393	2008 Aug	0.0	17.45	0.1	12	4.8	1.2	14	303
SHL29Z-1.1C	***JW478***	***2010 May***	***0.365***	***23.9***	***0.2***	***9***	***25.4***		***31***	***814***
SHL29Z-2.1I	JW478	2010 May	0.018	19.2	0.1	8	1.6		4	248
SHL29Z-3.1C	JW478	2010 May	0.012	4.5	0.1	6	1.8		5	221
SHL29Z-4.1C	***JW478***	***2010 May***	***0.118***	***19.6***	***0.1***	***8***	***9.4***		***18***	***248***
SHL29Z-5.1C	JW478	2010 May	0.007	3.3	0.0	8	1.5		5	314
SHL29Z-5.2E	JW478	2010 May	0.005	4.2	0.0	5	1.5		5	147

Spot ID	Mount	Date Analyzed	Li ppm (est)	Be ppm (est)	B ppm (est)	F ppm (est)	Na ppm (est)	Mg ppm (est)	Al ppm (est)	P ppm
SHL29Z-6.1C	JW478	2010 May	0.040	12.4	0.1	7	1.4		6	314
SHL29Z-6.2I	JW478	2010 May	0.005	11.9	0.1	6	1.7		5	235
SHL29Z-7.1C	***JW478***	***2010 May***	***0.067***	***5.6***	***0.2***	***6***	***44.1***		***54***	***311***
SHL29Z-8.1C	***JW478***	***2010 May***	***0.003***	***2.8***	***0.1***	***5***	***10.9***		***13***	***229***
SHL29Z-8.2I	JW478	2010 May	0.000	3.3	0.0	4	1.2		3	135
SHL29Z-9.1C	JW478	2010 May	0.000	0.2	0.0	2	1.2		4	325
SHL29Z-10.1C	JW478	2010 May	0.000	1.5	0.0	3	1.2		4	368
SHL29Z-10.2I	JW478	2010 May	0.000	0.3	0.0	2	1.3		5	173
SHL29Z-11.1C	JW478	2010 May	0.010	0.1	0.0	3	6.7		9	257
SHL29Z-11.2I	JW478	2010 May	0.009	1.5	0.1	8	1.6		4	212
SHL29Z-12.1C	***JW478***	***2010 May***	***0.025***	***277.5***	***0.1***	***6***	***3.3***		***18***	***1961***
SHL29Z-13.1C	JW478	2010 May	0.045	26.3	0.3	10	1.6		5	387
SHL29Z-14.1C	JW478	2010 May	0.017	4.1	0.1	9	4.9		53	307
SHL29Z-14.2I	JW478	2010 May	0.034	12.1	0.1	8	2.2		9	172
SHL29Z-15.1I	JW478	2010 May	0.017	5.1	0.1	5	1.8		7	262
SHL29Z-16.1I	JW478	2010 May	0.007	1.4	0.0	5	1.7		6	224
SHL30-1.1C	JW443	2009 Dec	0.035	0.00	0.1	8	6.3		24	127
SHL30-1.2R	JW443	2009 Dec	0.000	0.00	0.1	14	6.0		16	219
SHL30-2.1C	JW443	2009 Dec	0.010	0.00	0.0	5	5.2		15	335
SHL30-2.2R	JW443	2009 Dec	0.006	0.00	0.1	8	6.6		21	277
SHL30-3.1C	JW443	2009 Dec	0.005	0.00	0.0	11	7.4		20	172
SHL30-3.2I	JW443	2009 Dec	0.003	0.00	0.1	8	6.4		23	235
SHL30-3.3I	JW443	2009 Dec	0.004	0.00	0.1	8	6.1		18	325
SHL30-3.4R	***JW443***	***2009 Dec***	***0.003***	***0.00***	***0.1***	***5***	***10.9***		***39***	***259***
SHL30-4.1I	JW443	2009 Dec	0.001	0.00	0.1	11	6.0		19	88
SHL30-4.2C	JW443	2009 Dec	0.004	0.00	0.1	10	5.7		23	256
SHL30-4.3R	JW443	2009 Dec	0.004	0.00	0.1	8	4.9		17	230
SHL30-5.1C	JW443	2009 Dec	0.003	0.00	0.1	7	7.1		24	277
SHL30-5.2T	JW443	2009 Dec	0.006	0.00	0.1	10	5.6		18	271

Spot ID	Mount	Date Analyzed	Li ppm (est)	Be ppm (est)	B ppm (est)	F ppm (est)	Na ppm (est)	Mg ppm (est)	Al ppm (est)	P ppm
SHL30-6.1I	JW443	2009 Dec	0.005	0.00	0.1	7	6.0		17	346
SHL30-7.1C	JW443	2009 Dec	0.031	0.00	0.0	7	5.9		23	266
SHL30-7.2R	JW443	2009 Dec	0.005	0.00	0.1	5	8.5		21	272
SHL30-7.3R	JW443	2009 Dec	0.000	0.00	0.1	10	4.9		16	286
SHL30-8.1C	JW443	2009 Dec	0.000	0.04	0.0	18	5.8		19	1231
SHL30-8.2T	JW443	2009 Dec	0.001	0.00	0.0	10	4.7		23	179
SHL30-9.1C	JW443	2009 Dec	0.001	0.04	0.1	6	5.2		17	1018
SHL30-10.1C	JW443	2009 Dec	0.006	0.00	0.1	10	5.4		21	253
SHL30-10.2I	JW443	2009 Dec	0.008	0.00	0.0	9	7.3		17	172
SHL30-10.3R	JW443	2009 Dec	0.007	0.00	0.1	5	7.6		21	245
SHL30-12.1C	JW443	2009 Dec	0.001	0.00	0.1	4	5.8		23	257
SHL30-12.2I	JW443	2009 Dec	0.004	0.00	0.0	7	4.8		14	272
SHL30-11.1C	JW443	2009 Dec	0.060	0.00	0.0	6	7.3		27	268
SHL30-11.2T	***JW443***	***2009 Dec***	***0.016***	***0.01***	***0.1***	***10***	***82.9***		***312***	***267***
SHL30-13.1C	JW443	2009 Dec	0.026	0.00	0.0	6	13.1		27	389
SHL30-13.2T	JW443	2009 Dec	0.004	0.00	0.0	6	6.8		37	252
SHL30-14.1C	JW443	2009 Dec	0.002	0.00	0.1	5	4.8		30	240
SHL30-14.2T	JW443	2009 Dec	0.006	0.00	0.0	5	6.9		19	104
SHL33-1.1C	JW443	2009 Dec	0.017	15.44	0.1	12	5.8		22	1009
SHL33-1.2R	JW443	2009 Dec	0.005	0.22	0.0	9	5.1		23	361
SHL33-2.1E	JW443	2009 Dec	0.000	0.00	0.0	19	5.0		29	242
SHL33-2.2I	JW443	2009 Dec	0.004	0.00	0.1	6	5.4		24	145
SHL33-3.1C	JW443	2009 Dec	0.001	0.06	0.0	15	5.2		22	1345
SHL33-3.2T	JW443	2009 Dec	0.002	0.02	0.1	1	4.4		27	177
SHL33-4.1T	JW443	2009 Dec	0.119	0.01	0.1	7	5.8		23	307
SHL33-4.2C	***JW443***	***2009 Dec***	***0.054***	***0.01***	***0.1***	***11***	***6.4***		***20***	***123***
SHL34Z-1.1C	JW392	2008 Aug	0.001	0.00000	0.1	12	1.9	0.5	14	298

Spot ID	Mount	Date Analyzed	Li ppm (est)	Be ppm (est)	B ppm (est)	F ppm (est)	Na ppm (est)	Mg ppm (est)	Al ppm (est)	P ppm
SHL34Z-1.2I	JW392	2008 Aug	0.002	0.00443	0.1	11	2.4	0.7	14	326
SHL34Z-1.3E	JW392	2008 Aug	0.005	0.03861	0.1	8	4.4	0.7	15	415
SHL34Z-2.1I	JW392	2008 Aug	0.034	0.00872	0.1	18	1.9	0.7	19	416
SHL34Z-3.1I	JW392	2008 Aug	0.007	0.00211	0.2	21	6.9	1.2	30	228
SHL34Z-3.2I	JW392	2008 Aug	0.003	0.00000	0.1	11	2.6	0.7	32	223
SHL34Z-3.3E	JW392	2008 Aug	0.017	0.00215	0.1	12	3.0	0.9	20	307
SHL34Z-4.1E	JW392	2008 Aug	0.013	0.01024	0.1	11	5.6	1.1	58	447
SHL34Z-4.2C	JW392	2008 Aug	0.013	0.00400	0.1	12	2.1	0.7	14	262
SHL34AZ-1.1I	JW393	2008 Aug	0.0	0.00363	0.1	9	3.8	1.4	23	225
SHL34AZ-1.2E	JW393	2008 Aug	0.0	0.00000	0.0	10	2.7	0.6	17	251
SHL34AZ-2.1E	JW393	2008 Aug	0.2	0.00000	0.1	11	3.8	1.5	13	350
SHL34AZ-2.2I	JW393	2008 Aug	0.0	0.00346	0.1	10	3.9	0.9	11	322
SHL34AZ-3.1E	JW393	2008 Aug	0.0	0.00174	0.1	5	3.6	2.0	19	335
SHL34AZ-3.2IE	JW393	2008 Aug	0.0	0.00531	0.1	10	2.9	1.0	18	228
SHL34AZ-3.3I	JW393	2008 Aug	0.0	0.00000	0.1	7	4.3	1.2	20	185
SHL34AZ-4.1I	JW393	2008 Aug	0.1	0.49652	0.1	8	4.4	1.5	18	357
SHL34AZ-5.1I	JW393	2008 Aug	0.0	0.00331	0.1	12	8.5	1.6	26	389
SHL34AZ-6.2I	JW393	2008 Aug	0.0	0.00166	0.1	14	3.9	1.3	12	423
SHL34AZ-7.1I	JW393	2008 Aug	0.0	0.01023	0.2	8	3.8	1.3	13	426
SHL34AZ-7.2E	JW393	2008 Aug	0.0	0.00661	0.0	13	5.2	1.3	16	476
SHL34AZ-8.1I	JW393	2008 Aug	0.1	0.00160	0.1	12	3.4	1.1	13	322
SHL34AZ-9.1I	JW393	2008 Aug	0.0	0.00166	0.1	7	3.4	1.2	44	359
SHL34AZ-10.1I	JW393	2008 Aug	0.0	0.01036	0.1	8	4.9	1.2	15	319
SHL34AZ-11.1I	JW393	2008 Aug	0.0	0.00163	0.1	8	10.8	1.7	49	426
SHL34AZ-11.2E	JW393	2008 Aug	0.0	0.01446	0.1	10	3.2	1.2	14	288
SHL34AZ-12.1I	JW393	2008 Aug	0.0	0.00318	0.1	8	2.8	0.8	8	292
SHL36E-1.1I	JW443	2009 Dec	0.002	0.00	0.0	8	3.1		16	275
SHL36E-1.2C	JW443	2009 Dec	0.081	0.01	0.0	4	9.0		32	363

Spot ID	Mount	Date Analyzed	Li ppm (est)	Be ppm (est)	B ppm (est)	F ppm (est)	Na ppm (est)	Mg ppm (est)	Al ppm (est)	P ppm
SHL36E-1.3I	JW443	2009 Dec	0.003	0.00	0.0	6	4.3		16	337
SHL36E-1.4R	JW443	2009 Dec	0.002	0.01	0.0	5	7.0		17	245
SHL36E-2.1C	JW443	2009 Dec	0.007	0.00	0.0	11	4.0		15	566
SHL36E-2.2T	JW443	2009 Dec	0.003	0.04	0.0	12	3.4		15	295
SHL36E-3.1C	***JW443***	***2009 Dec***	***0.167***	***0.15***	***0.2***	***15***	***187.4***		***718***	***1444***
SHL36E-3.2I	JW443	2009 Dec	0.018	0.01	0.0	10	3.3		15	303
SHL36E-3.3T	JW443	2009 Dec	0.009	0.01	0.0	9	6.9		20	271
SHL36E-4.1C	JW443	2009 Dec	0.001	0.00	0.1	5	3.9		22	330
SHL36E-4.2T	JW443	2009 Dec	0.001	0.01	0.1	5	10.5		18	329
SHL36E-5.1C	JW443	2009 Dec	0.000	0.01	0.0	5	4.0		26	320
SHL36E-6.1R	JW443	2009 Dec	0.042	0.00	0.0	5	6.3		18	315
SHL36E-6.2C	JW443	2009 Dec	0.004	0.00	0.0	6	17.3		22	365
SHL36E-7.1I	JW443	2009 Dec	0.003	0.01	0.1	6	4.9		16	301
SHL36E-7.2R	JW443	2009 Dec	0.000	0.00	0.0	3	5.3		16	216
SHL36E-8.1C	JW443	2009 Dec	0.004	0.00	0.1	8	4.3		14	391
SHL36E-8.2R	JW443	2009 Dec	0.003	0.01	0.1	4	5.6		19	331
SHL36E-9.1C	***JW443***	***2009 Dec***	***0.103***	***0.20***	***0.1***	***13***	***29.3***		***114***	***1460***
SHL36E-9.2R	JW443	2009 Dec	0.000	0.02	0.1	7	5.5		18	435
SHL36E-10.1I	***JW443***	***2009 Dec***	***0.120***	***0.02***	***0.0***	***4***	***17.4***		***55***	***459***
SHL36EX-11.1C	***JW443***	***2009 Dec***	***0.029***	***0.01***	***0.2***	***15***	***18.0***		***64***	***1944***
SHL36E-11.2I	JW443	2009 Dec	0.084	0.01	0.2	12	9.9		49	1212
SHL36E-11.3R	JW443	2009 Dec	0.000	0.00	0.1	4	4.6		18	364
SHL36E-12.1C	JW443	2009 Dec	0.007	0.01	0.1	5	5.6		19	533
SHL36E-12.2R	JW443	2009 Dec	0.001	0.00	0.1	10	5.8		19	370
SHL36E-12.3R	JW443	2009 Dec	0.003	0.01	0.1	7	5.7		21	313
SHL36E-13.1I	JW443	2009 Dec	0.004	0.01	0.1	7	5.3		17	326
SHL36E-13.2R	JW443	2009 Dec	0.004	0.00	0.0	6	4.9		22	302
SHL36E-14.2C	JW443	2009 Dec	0.004	0.09	0.1	7	5.4		16	1273
SHL36E-14.3I	JW443	2009 Dec	0.006	0.00	0.0	4	5.8		18	398
SHL36E-14.1T	JW443	2009 Dec	0.008	0.02	0.1	6	4.4		45	334

Spot ID	Mount	Date Analyzed	Li ppm (est)	Be ppm (est)	B ppm (est)	F ppm (est)	Na ppm (est)	Mg ppm (est)	Al ppm (est)	P ppm
SHL37P-1.1C	JW443	2009 Dec	0.040	0.00	0.0	17	5.9		24	256
SHL37P-1.2I	JW443	2009 Dec	0.002	0.01	0.1	4	3.9		17	267
SHL37P-1.3R	JW443	2009 Dec	0.013	0.00	0.0	9	3.4		14	281
SHL37P-2.1C	JW443	2009 Dec	0.000	0.00	0.0	10	3.9		20	295
SHL37P-2.2I	JW443	2009 Dec	0.003	0.04	0.1	12	3.6		15	244
SHL37P-2.3R	JW443	2009 Dec	0.001	0.02	0.0	12	4.0		16	211
SHL37P-14.1C	JW443	2009 Dec	0.010	0.00	0.1	9	6.2		28	331
SHL37P-14.2R	JW443	2009 Dec	0.005	0.00	0.1	9	3.8		18	321
SHL37P-3.1C	JW443	2009 Dec	0.016	0.00	0.1	16	4.2		17	197
SHL37P-3.2I	***JW443***	***2009 Dec***	***1.593***	***0.04***	***0.3***	***16***	***452.0***		***387***	***141***
SHL37P-3.3R	JW443	2009 Dec	0.003	0.03	0.1	13	3.8		16	285
SHL37P-4.1R	JW443	2009 Dec	0.005	0.07	0.0	8	3.5		16	507
SHL37P-4.2C	JW443	2009 Dec	0.004	0.00	0.0	8	10.6		15	191
SHL37P-4.3I	JW443	2009 Dec	0.002	0.01	0.0	10	4.6		19	219
SHL37P-5.1C	JW443	2009 Dec	0.046	0.01	0.1	13	25.3		72	394
SHL37P-5.2I	JW443	2009 Dec	0.037	0.00	0.1	6	31.5		31	337
SHL37P-5.3T	***JW443***	***2009 Dec***	***0.121***	***0.00***	***0.1***	***16***	***75.2***		***94***	***204***
SHL37P-6.1I	JW443	2009 Dec	0.000	0.00	0.1	14	4.2		18	350
SHL37P-6.2C	JW443	2009 Dec	0.019	0.00	0.1	12	6.5		23	443
SHL37P-6.3R	JW443	2009 Dec	0.000	0.00	0.0	9	4.8		18	214
SHL37P-7.1R	JW443	2009 Dec	0.003	0.06	0.1	9	3.9		19	299
SHL37P-7.2C	JW443	2009 Dec	0.001	0.10	0.1	12	4.4		17	419
SHL37P-7.3T	JW443	2009 Dec	0.002	0.14	0.2	9	7.1		26	248
SHL37P-7.4C	JW443	2009 Dec	0.009	0.05	0.1	5	4.9		21	222
SHL37P-8.1I	JW443	2009 Dec	0.000	0.00	0.0	9	4.3		15	150
SHL37P-8.2C	***JW443***	***2009 Dec***	***0.055***	***0.48***	***0.1***	***6***	***4.7***		***26***	***2009***
SHL37P-8.3R	JW443	2009 Dec	0.006	0.01	0.1	9	3.9		17	294
SHL37P-15.1C	JW443	2009 Dec	0.005	0.03	0.1	8	4.6		25	226
SHL37P-15.2T	JW443	2009 Dec	0.012	0.16	0.0	11	4.5		74	323
SHL37P-9.2R	JW443	2009 Dec	0.008	0.01	0.0	8	3.8		15	240

Spot ID	Mount	Date Analyzed	Li ppm (est)	Be ppm (est)	B ppm (est)	F ppm (est)	Na ppm (est)	Mg ppm (est)	Al ppm (est)	P ppm
SHL37P-9.1C	JW443	2009 Dec	0.003	0.01	0.1	11	6.5		23	97
SHL37P-10.2R	JW443	2009 Dec	0.003	0.19	0.1	11	4.7		14	213
SHL37P-10.1I	JW443	2009 Dec	0.008	0.03	0.1	19	5.4		16	118
SHL37P-11.1C	***JW443***	***2009 Dec***	***0.123***	***0.01***	***0.1***	***24***	***34.5***		***70***	***366***
SHL37P-11.2I	JW443	2009 Dec	0.005	0.00	0.0	11	4.9		19	404
SHL37P-11.3I	JW443	2009 Dec	0.002	0.00	0.1	18	5.3		20	234
SHL37P-11.4R	***JW443***	***2009 Dec***	***0.003***	***0.00***	***0.1***	***17***	***8.3***		***327***	***371***
SHL37P-12.1C	JW443	2009 Dec	0.016	0.00	0.0	10	4.8		16	348
SHL37P-12.2I	***JW443***	***2009 Dec***	***0.226***	***0.05***	***0.1***	***12***	***147.9***		***167***	***474***
SHL37P-12.3T	JW443	2009 Dec	0.002	0.04	0.1	13	20.4		35	323
SHL37P-13.1C	JW443	2009 Dec	0.075	0.36	0.1	13	5.7		22	632
SHL37P-13.2T	JW443	2009 Dec	0.213	1.21	0.1	2	6.7		162	257
SHL0849AZ-1.1I	JW414	2009 Jan	0.044	51.71	0.0	20	8.5	2.2	46	581
SHL0849AZ-1.2E	JW414	2009 Jan	0.011	36.97	0.1	14	2.4	0.5	29	463
SHL0849AZ-2.1E	JW414	2009 Jan	0.016	5.67	0.1	10	2.4	0.6	25	351
SHL0849AZ-3.1E	JW414	2009 Jan	0.065	2.43	0.1	20	5.5	1.6	23	401
SHL0849AZ-4.1E	JW414	2009 Jan	0.006	0.03	0.1	16	3.1	0.5	43	377
SHL0849AZ-4.2C	JW414	2009 Jan	0.014	0.19	0.1	17	3.3	0.6	24	444
SHL0849AZ-4.3E	JW414	2009 Jan	0.005	0.06	0.1	15	2.9	0.5	25	353
SHL0849AZ-5.1I	JW414	2009 Jan	0.020	8.28	0.0	16	3.8	0.5	31	365
SHL0849AZ-6.1I	***JW414***	***2009 Jan***	***0.073***	***7.45***	***0.0***	***14***	***5.2***	***0.8***	***40***	***576***

Spot ID	Mount	Date Analyzed	Li ppm (est)	Be ppm (est)	B ppm (est)	F ppm (est)	Na ppm (est)	Mg ppm (est)	Al ppm (est)	P ppm
SHL0849AZ-7.1C	JW414	2009 Jan	0.057	5.21	0.1	19	4.3	2.0	39	619
SHL0849AZ-8.1E	JW414	2009 Jan	0.044	2.69	0.0	14	2.7	0.9	22	603
SHL0849AZ-9.1E	JW414	2009 Jan	0.071	0.96	0.1	11	2.5	0.9	21	508
SHL0849AZ-9.2I	JW414	2009 Jan	0.009	0.75	0.1	13	2.9	0.7	28	240
SHL0849AZ-10.1C	JW414	2009 Jan	0.016	2.00	0.0	11	2.8	0.8	30	375
SHL0849AZ-11.1I	JW414	2009 Jan	0.001	0.07	0.0	12	2.5	0.3	34	250
SHL0849AZ-11.2E	JW414	2009 Jan	0.021	1.46	0.1	14	3.3	0.5	27	263
SHL0849AZ-12.1E	JW414	2009 Jan	0.023	52.65	0.0	10	2.2	0.6	20	461
SHL0849AZ-12.2C	***JW414***	***2009 Jan***	***0.075***	***1.81***	***0.1***	***17***	***55***	***3.2***	***38***	***374***
SHL0849AZ-13.1E	JW414	2009 Jan	0.020	16.75	0.3	49	7.7	1.3	48	182
SHL0849AZ-13.2I	JW414	2009 Jan	0.014	1.90	0.1	22	2.4	0.6	17	244
SHL0849AZ-13.3C	***JW414***	***2009 Jan***	***0.238***	***16.81***	***0.1***	***23***	***21***	***5.6***	***67***	***321***
SHL49AZ-14.1C	JW414	2009 Jan	0.046	0.16	0.1	18	3.8	0.9	35	662
SHD9-1.1R	JW443	2009 Dec	0.007	0.33	0.0	8	4.2		20	177
SHD9-2.1R	JW443	2009 Dec	0.003	0.41	0.0	19	5.2		21	384
SHD9-2.2C	JW443	2009 Dec	0.014	92.71	0.1	20	5.5		42	868

Spot ID	Mount	Date Analyzed	Li ppm (est)	Be ppm (est)	B ppm (est)	F ppm (est)	Na ppm (est)	Mg ppm (est)	Al ppm (est)	P ppm
SH325.2-1.1DGZT	JW309	2007 May		7.84	0.14	14.7			26.9	372
SH325.2-1.2MGZC	JW309	2007 May		7.26	0.07	13.8			9.6	398
SH325.2-1.3LGZI]	JW309	2007 May		15.48	0.04	13.7			18.8	238
SH325.2-2.1MGZC	JW309	2007 May		10.20	0.07	14.2			12.7	232
SH325.2-2.2LGZI	JW309	2007 May		2.32	0.05	9.9			11.5	117
SH325.2-3.1LGC	***JW309***	***2007 May***		***19.31***	***0.09***	***11.1***			***46.0***	***370***
SH325.2-3.2DGZE	JW309	2007 May		28.34	0.06	8.7			12.7	274
SH325.2-4.1DGZE	***JW309***	***2007 May***		***0.85***	***0.06***	***8.9***			***11.3***	***432***
SH325.2-4.2MGC	***JW309***	***2007 May***		***0.37***	***0.07***	***14.5***			***29.9***	***368***
SH325.2-5.1MGZE	JW309	2007 May		11.79	0.05	9.1			11.2	428
SH325.2-5.2DGZI	***JW309***	***2007 May***		***22.29***	***0.07***	***9.6***			***10.9***	***418***
SH325.2-5.3DGZE	***JW309***	***2007 May***		***23.16***	***0.03***	***10.6***			***11.6***	***338***
SH325.2-6.1MGT	JW309	2007 May		1.29	0.05	8.4			21.1	134
SH325.2-6.2MGI	JW309	2007 May		1.16	0.06	8.2			18.9	65
SH325.2-7.1LGZT	JW309	2007 May		30.85	0.06	11.0			21.1	299
SH325.2-7.2DGZT	JW309	2007 May		6.61	0.07	13.3			12.2	155
SH325.2-	JW309	2007 May		29.09	0.07	12.9			21.0	287

Spot ID	Mount	Date Analyzed	Li ppm (est)	Be ppm (est)	B ppm (est)	F ppm (est)	Na ppm (est)	Mg ppm (est)	Al ppm (est)	P ppm
7.3LGZC										
SH325.2-8.1MGZE	JW309	2007 May		10.65	0.05	13.3			14.6	289
SH325.2-8.2MGZC	JW309	2007 May		21.22	0.24	13.0			58.6	475
SH325.2-8.3DGZT	JW309	2007 May		2.28	0.05	10.3			13.9	261
SH325.2-9.1MGC	JW309	2007 May		11.41	0.05	8.8			17.8	426
SH325.2-10.1MGZI	JW309	2007 May		56.02	0.07	7.0			12.3	411
SH325.2-11.1DGZE	***JW309***	***2007 May***		***1.67***	***2.02***	***453.8***			***414.7***	***426***
SH325.2-11.1MGC	***JW309***	***2007 May***		***0.44***	***0.20***	***77.7***			***63.2***	***408***
SH325.2-12.1MGZT	JW309	2007 May		0.00	0.07	10.4			10.1	135
SH325.2-12.2MGZI	***JW309***	***2007 May***		***0.00***	***0.06***	***113.8***			***9.5***	***504***
SH325.2-13.1DGZT	JW309	2007 May		0.00	0.07	15.7			14.1	201
SH325.2-13.1T	***JW309***	***2007 May***		***0.02***	***0.06***	***51.8***			***14.3***	***75***
Z484A-10.1C	JP04	2008 Jan	0.0	0.01	0.022	12	3.0	0.6	14	291
Z484A-10.2IR	JP04	2008 Jan	0.0	0.12	0.033	8	5.0	2.3	9	388
Z484A-10.3T	JP04	2008 Jan	0.0	0.02	0.018	11	3.1	0.9	8	263
Z484A-12.1I	JP04	2008 Jan	0.0	0.35	0.178	15	4.3	2.1	10	271
Z484A-12.2EM	JP04	2008 Jan	0.0	0.00	0.184	7	2.9	5.5	10	71
Z484A-12.3T	JP04	2008 Jan	0.0	0.01	0.038	9	3.0	1.3	13	150
Z484A-14.1C	***JP04***	***2008 Jan***	***0.0***	***13.34***	***0.124***	***4***	***4.0***	***1.2***	***13***	***1929***

Spot ID	Mount	Date Analyzed	Li ppm (est)	Be ppm (est)	B ppm (est)	F ppm (est)	Na ppm (est)	Mg ppm (est)	Al ppm (est)	P ppm
Z484A-16.1C	JP04	2008 Jan	0.0	0.01	0.022	5	5.9	1.0	13	233
Z484A-16.2I	JP04	2008 Jan	0.0	0.26	0.026	4	4.2	2.1	9	303
Z484A-17.1C	JP04	2008 Jan	0.0	1.02	0.048	9	3.4	1.5	11	445
Z484A-17.2T	JP04	2008 Jan	0.0	0.08	0.023	8	1.6	0.7	8	281
Z484A-18.1C	JP04	2008 Jan	0.0	0.02	0.045	6	2.3	0.6	9	128
Z484A-18.2IR	JP04	2008 Jan	0.0	0.01	0.022	4	3.4	1.1	9	157
Z484A-19.1T	JP04	2008 Jan	0.0	0.06	0.025	2	2.5	0.8	9	210
Z484A-19.2C	JP04	2008 Jan	0.0	0.04	0.007	4	2.9	1.3	12	250
Z484A-19.3IR	JP04	2008 Jan	0.0	0.06	0.030	1	4.8	0.7	9	252
Z484A-19.4IR	JP04	2008 Jan	0.0	0.12	0.010	5	2.3	0.9	8	244
Z484A-2.1T	JP04	2008 Jan	0.0	0.09	0.036	14	4.1	1.2	13	335
Z484A-2.2C	JP04	2008 Jan	0.0	0.48	0.034	11	2.2	0.7	7	412
Z484A-4.1I	***JP04***	***2008 Jan***	***0.0***	***39.69***	***0.055***	***12***	***4.0***	***2.2***	***26***	***2143***
Z484A-4.2T	JP04	2008 Jan	0.0	0.02	0.020	16	3.2	1.1	13	181
Z484A-5.1I	***JP04***	***2008 Jan***	***0.0***	***0.02***	***0.025***	***11***	***16.0***	***0.6***	***28***	***356***
Z484A-8.1I	***JP04***	***2008 Jan***	***0.4***	***27.51***	***1.221***	***11***	***702.5***	***4.3***	***1856***	***1659***
Z484A-8.2I	JP04	2008 Jan	0.0	2.16	0.030	11	2.5	0.8	12	716

Spot ID	Mount	Date Analyzed	S ppm	Cl ppm (est)	K ppm (est)	Ca ppm (est)	Sc ppm	Ti48/Ti49	Ti48 ppm	Ti49 ppm
SHL3Z-1.1DI	JW414	2009 Jan	0.6		1.3	2.1	70	13.3	7.0	7.1
SHL3Z-1.2LC	JW414	2009 Jan	0.8		1.5	2.2	70	14.0	8.1	7.8
SHL3Z-1.3DI	JW414	2009 Jan	2.1		11.4	3.2	29	15.1	3.4	3.1
SHL3Z-1.4DR	JW414	2009 Jan	0.9		1.5	2.5	84	14.0	6.1	5.9
SHL3Z-2.1DC	JW414	2009 Jan	0.9		1.9	3.7	154	14.2	6.0	5.7
SHL3Z-2.2LR	***JW414***	***2009 Jan***	***1.5***		***6.3***	***19.0***	***112***	***13.0***	***5.2***	***5.3***
SHL3Z-3.1LC	***JW414***	***2009 Jan***	***0.3***		***18.9***	***4.6***	***85***	***13.3***	***3.7***	***3.7***
SHL3Z-3.2DI	JW414	2009 Jan	0.9		2.4	3.2	513	13.7	10.4	10.3
SHL3Z-3.3LR	JW414	2009 Jan	0.6		1.5	2.8	171	12.7	2.8	3.0
SHL3Z-4.1LR	JW414	2009 Jan	0.3		2.1	3.5	156	14.7	4.9	4.5
SHL3Z-4.2LI	JW414	2009 Jan	0.6		1.2	2.6	109	12.8	5.0	5.3
SHL3Z-4.3LC	JW414	2009 Jan	0.6		1.1	2.6	160	12.6	2.5	2.7
SHL3Z-5.1DC	JW414	2009 Jan	0.9		1.2	2.9	102	14.2	3.3	3.1
SHL3Z-5.2LR	JW414	2009 Jan	1.1		1.4	3.1	87	14.1	4.8	4.6
SHL3Z-6.1DI	JW414	2009 Jan	0.3		1.5	3.4	103	14.9	3.7	3.4
SHL3Z-6.2LC	***JW414***	***2009 Jan***	***1.5***		***15.2***	***4.4***	***130***	***13.9***	***4.1***	***3.9***
SHL3Z-6.3DE	JW414	2009 Jan	0.6		0.7	1.8	81	14.1	3.7	3.5
SHL3Z-7.1LR	JW414	2009 Jan	0.5		1.4	4.0	98	13.9	2.4	2.3
SHL3Z-7.2DI	***JW414***	***2009 Jan***	***0.3***		***10.2***	***5.0***	***109***	***14.5***	***3.2***	***3.0***
SHL3Z-7.3LC	***JW414***	***2009 Jan***	***0.6***		***10.4***	***3.9***	***40***	***14.0***	***5.7***	***5.5***
SHL3Z-8.1LC	JW414	2009 Jan	0.3		1.9	3.1	154	13.3	5.4	5.5
SHL3Z-8.2I	JW414	2009 Jan	0.0		1.8	2.8	221	13.0	4.2	4.3
SHL3Z-8.3LC	***JW414***	***2009 Jan***	***0.6***		***12.1***	***3.9***	***207***	***13.2***	***5.9***	***6.0***
SHL3Z-8.4DI	***JW414***	***2009 Jan***	***0.9***		***54.8***	***7.4***	***176***	***13.5***	***6.7***	***6.7***
SHL3Z-9.1DI	JW414	2009 Jan	1.1		1.9	3.5	164	14.7	6.1	5.6
SHL3Z-9.2LC	JW414	2009 Jan	1.1		1.8	3.0	156	13.6	7.5	7.4
SHL3Z-9.3LI	JW414	2009 Jan	0.0		1.6	3.5	165	13.2	4.7	4.8
MSHL3Z-1.1DGI	JW309	2007 May	0.4	1.12		3.07	418	13.2	20.1	20.7

Spot ID	Mount	Date Analyzed	S ppm	Cl ppm (est)	K ppm (est)	Ca ppm (est)	Sc ppm	Ti48/Ti49	Ti48 ppm	Ti49 ppm
MSHL3Z-1.2MGI	JW309	2007 May	0.5	0.00		2.16	136	13.5	3.5	3.5
MSHL3Z-2.1MGZC	***JW309***	***2007 May***	***1.6***	***4.17***		***12.60***	***139***	***13.6***	***5.5***	***5.5***
MSHL3Z-2.2DGZI	JW309	2007 May	1.0	1.02		1.97	85	13.9	5.4	5.3
MSHL3Z-3.1DGZT	JW309	2007 May	2.5	17.98		3.44	101	12.9	6.0	6.4
MSHL3Z-3.2LGZE	JW309	2007 May	1.1	2.16		2.14	120	14.2	4.1	3.9
MSHL3Z-3.3DGC	JW309	2007 May	0.8	0.00		2.49	257	13.0	6.1	6.4
MSHL3Z-4.1MGI	JW309	2007 May	1.7	0.00		1.86	154	13.9	4.8	4.7
MSHL4Z-1.1DGZE	JW309	2007 May	0.7	0.00		1.86	73	12.6	3.9	4.2
MSHL4Z-1.2MGZI	JW309	2007 May	0.6	0.00		1.56	154	13.8	7.8	7.7
MSHL4Z-10.1MGT	JW309	2007 May	1.2	0.00		1.49	158	13.2	6.6	6.8
MSHL4Z-10.2MGZC	JW309	2007 May	0.8	1.20		2.37	108	15.2	6.3	5.6
MSHL4Z-10.3DGZIT	JW309	2007 May	0.4	0.00		1.86	275	13.6	14.9	14.8
MSHL4Z-11.1DGZI	JW309	2007 May	2.1	1.12		1.79	134	13.4	6.0	6.1
MSHL4Z-11.2DZIT	JW309	2007 May	0.2	3.36		1.70	196	14.2	9.5	9.1
MSHL4Z-12.1MGI	JW309	2007 May	2.5	0.00		2.58	81	13.3	3.3	3.3
MSHL4Z-2.1DGZI	JW309	2007 May	1.1	0.00		2.17	61	12.4	3.4	3.7
MSHL4Z-2.2MGZI	JW309	2007 May	0.8	1.23		1.54	146	13.6	5.3	5.3
MSHL4Z-2.3DGZE	JW309	2007 May	1.2	0.00		1.78	88	13.2	3.1	3.2
MSHL4Z-3.1DGZT	JW309	2007 May	0.4	0.00		1.72	178	13.3	6.4	6.6
MSHL4Z-3.2MGZE	JW309	2007 May	1.0	1.16		2.11	130	13.1	3.9	4.1
MSHL4Z-10.2MGZC	JW309	2007 May	0.8	1.20		2.37	108	15.2	6.3	5.6
MSHL4Z-10.3DGZIT	JW309	2007 May	0.4	0.00		1.86	275	13.6	14.9	14.8
MSHL4Z-11.1DGZI	JW309	2007 May	2.1	1.12		1.79	134	13.4	6.0	6.1
MSHL4Z-5.1DGZT	JW309	2007 May	0.4	0.00		1.67	66	14.2	3.0	2.9
MSHL4Z-5.2MGZE	JW309	2007 May	0.8	1.15		1.80	150	14.1	4.4	4.3
MSHL4Z-5.3MGI	JW309	2007 May	1.8	0.00		1.59	36	14.0	2.0	1.9
MSHL4Z-6.1MGT	JW309	2007 May	0.2	2.44		2.00	130	13.8	4.2	4.1
MSHL4Z-6.2MGI	JW309	2007 May	1.0	0.00		1.91	98	13.9	3.4	3.3
MSHL4Z-7.1MGZT	JW309	2007 May	3.4	243.96		4.85	131	13.3	10.4	10.6

Spot ID	Mount	Date Analyzed	S ppm	Cl ppm (est)	K ppm (est)	Ca ppm (est)	Sc ppm	Ti48/Ti49	Ti48 ppm	Ti49 ppm
MSHL4Z-7.2LGC	JW309	2007 May	0.6	0.00		1.74	167	14.0	11.5	11.2
MSHL4Z-7.3DGI	JW309	2007 May	0.8	1.15		1.77	205	13.6	18.2	18.2
MSHL4Z-8.1MGZT	JW309	2007 May	1.2	2.43		1.62	106	13.1	4.2	4.3
MSHL4Z-8.2DGZI	JW309	2007 May	1.4	0.00		1.64	100	13.6	4.1	4.0
MSHL4Z-8.3MGZI	JW309	2007 May	0.8	0.00		1.76	89	13.9	2.9	2.8
MSHL4Z-9.1MGZT	JW309	2007 May	0.4	0.00		1.31	171	13.7	5.7	5.7
MSHL4Z-9.2LGC	JW309	2007 May	0.2	1.16		1.82	129	15.1	3.4	3.1
MSHL4Z-9.3MGZT	JW309	2007 May	1.3	1.11		2.05	97	13.8	4.9	4.8
SHL5Z-1.1C	JW364	2008 Jan	0.2		0.7	1.8	113	13.4	4.0	4.1
SHL5Z-2.1I	JW364	2008 Jan	0.7		7.9	2.6	52	13.7	4.6	4.6
SHL5Z-2.2T	JW364	2008 Jan	0.0		0.4	1.2	188	14.0	7.8	7.6
SHL5Z-3.1C	JW364	2008 Jan	0.3		0.7	1.4	117	13.2	4.0	4.1
SHL5Z-3.2E	JW364	2008 Jan	0.0		1.1	1.9	146	13.3	6.8	7.0
SHL5Z-4.1C	JW364	2008 Jan	1.5		6.7	4.8	138	13.0	9.6	10.1
SHL5Z-4.2T	JW364	2008 Jan	0.2		1.9	4.7	125	13.2	6.9	7.1
SHL5Z-5.1T	JW364	2008 Jan	0.8		2.0	4.8	91	13.9	6.5	6.4
SHL5Z-5.2C	***JW364***	***2008 Jan***	***1.0***		***75.7***	***13.8***	***212***	***13.7***	***35.5***	***35.3***
SHL5Z-6.1C	***JW364***	***2008 Jan***	***1.1***		***1.8***	***5.3***	***623***	***13.4***	***28.3***	***29.0***
SHL5Z-6.2T	JW364	2008 Jan	0.9		1.8	4.4	61	13.7	3.9	3.9
SHL5Z-6.3I	JW364	2008 Jan	0.4		1.8	4.3	113	14.1	4.4	4.2
SHL5Z-7.1C	***JW364***	***2008 Jan***	***1.6***		***54.7***	***14.1***	***95***	***14.3***	***7.3***	***7.0***
SHL5Z-7.2T	JW364	2008 Jan	0.8		3.8	4.6	78	14.3	3.9	3.7
SHL5Z-8.1T	JW364	2008 Jan	0.9		2.2	4.6	101	13.5	7.4	7.6
SHL5Z-8.2C	JW364	2008 Jan	0.8		2.6	4.6	224	14.1	8.0	7.7
SHL5Z-1.1T	JW365	2008 Jan	0.6		0.6	3.6	72	14.6	5.4	4.9
SHL5Z-1.2I	***JW365***	***2008 Jan***	***1.1***		***16.0***	***4.7***	***122***	***13.0***	***6.0***	***6.2***
SHL5Z-2.1C	JW365	2008 Jan	1.5		2.9	3.7	146	13.8	4.1	4.0
SHL5Z-2.2E	JW365	2008 Jan	1.1		0.6	3.2	124	13.9	5.5	5.3

Spot ID	Mount	Date Analyzed	S ppm	Cl ppm (est)	K ppm (est)	Ca ppm (est)	Sc ppm	Ti48/Ti49	Ti48 ppm	Ti49 ppm
SHL5Z-3.1C	JW365	2008 Jan	0.0		1.9	2.2	120	14.5	4.4	4.1
SHL5Z-3.2R	JW365	2008 Jan	1.6		0.6	2.1	117	13.0	10.4	10.8
SHL5Z-4.1C	JW365	2008 Jan	1.1		1.1	2.4	178	14.0	5.7	5.4
SHL5Z-4.2T	JW365	2008 Jan	1.5		7.8	3.4	186	13.6	7.4	7.3
SHL5Z-5.1C	JW365	2008 Jan	1.0		0.5	2.2	142	14.0	4.8	4.6
SHL5Z-5.2T	JW365	2008 Jan	2.4		0.8	2.5	230	13.5	11.7	11.7
SHL5Z-6.1C	***JW365***	***2008 Jan***	***1.0***		***11.4***	***2.9***	***179***	***13.5***	***9.8***	***9.8***
SHL5Z-6.2T	JW365	2008 Jan	1.0		0.4	2.0	55	13.6	5.3	5.2
SHL5Z-7.1T	JW365	2008 Jan	1.5		1.0	3.6	147	13.2	5.7	5.8
SHL5Z-7.2C	JW365	2008 Jan	0.5		0.8	2.5	125	12.2	5.2	5.8
SHL5Z-8.1I	JW365	2008 Jan	0.5		0.5	1.3	240	13.6	11.4	11.2
SHL5Z-8.2C	JW365	2008 Jan	0.9		2.9	2.4	105	13.3	4.9	4.9
SHL5Z-8.3T	JW365	2008 Jan	1.3		0.6	2.2	166	13.8	7.2	7.0
SHL5Z-9.1T	JW365	2008 Jan	1.4		0.5	2.2	263	13.4	11.3	11.2
SHL5Z-9.2I	JW365	2008 Jan	2.2		1.2	2.8	137	13.0	7.2	7.4
SHL5Z-9.3I	JW365	2008 Jan	0.5		0.4	2.1	310	13.4	10.3	10.3
SHL0821Z-1.1E	JW414	2009 Jan	1.4		3.1	5.8	117	12.8	6.3	6.6
SHL0821Z-1.2C	***JW414***	***2009 Jan***	***0.5***		***140.8***	***4.5***	***95***	***13.9***	***6.4***	***6.2***
SHL0821Z-2.1E	JW414	2009 Jan	0.9		2.4	2.3	52	12.0	6.6	7.5
SHL0821Z-2.2I	JW414	2009 Jan	0.3		1.9	2.4	170	13.3	5.2	5.3
SHL0821Z-3.1E	JW414	2009 Jan	0.3		6.7	2.6	84	13.7	4.9	4.8
SHL0821Z-3.2I	JW414	2009 Jan	1.1		2.4	3.2	48	14.4	2.4	2.3
SHL0821Z-4.1E	JW414	2009 Jan	0.5		1.3	3.1	77	14.1	5.3	5.0
SHL0821Z-4.2C	JW414	2009 Jan	1.1		1.9	3.2	125	15.2	3.8	3.4
SHL0821Z-5.1E	***JW414***	***2009 Jan***	***0.8***		***5.2***	***325.9***	***64***	***13.5***	***10.7***	***10.7***
SHL0821Z-5.2I	***JW414***	***2009 Jan***	***1.8***		***1012.5***	***9.0***	***37***	***13.5***	***27.5***	***27.5***
SHL0821Z-6.1E	JW414	2009 Jan	0.6		1.2	2.2	48	14.0	9.7	9.3
SHL0821Z-6.2I	JW414	2009 Jan	0.8		3.5	3.7	116	13.4	17.5	17.6
SHL0821Z-7.1C	JW414	2009 Jan	1.7		1.7	3.7	87	13.8	10.0	9.8

Spot ID	Mount	Date Analyzed	S ppm	Cl ppm (est)	K ppm (est)	Ca ppm (est)	Sc ppm	Ti48/Ti49	Ti48 ppm	Ti49 ppm
SHL0821Z-7.2I	JW414	2009 Jan	0.5		1.1	2.3	42	13.8	8.1	7.9
SHL0821Z-7.3R	JW414	2009 Jan	0.0		2.0	2.7	61	14.0	15.6	15.0
SHL0821Z-8.1C	***JW414***	***2009 Jan***	***1.1***		***13.3***	***3.2***	***162***	***10.8***	***4.4***	***5.5***
SHL0821Z-8.2I	JW414	2009 Jan	0.8		1.3	2.4	152	12.6	6.1	6.6
SHL0821Z-8.3I	JW414	2009 Jan	0.3		1.2	2.5	213	12.5	4.2	4.6
SHL0821Z-9.1I	JW414	2009 Jan	1.1		0.9	2.0	91	13.4	16.0	16.1
SHL0821Z-9.2E	JW414	2009 Jan	0.3		1.2	2.4	37	13.3	8.6	8.7
SHL0821Z-10.1I	JW414	2009 Jan	0.3		0.9	1.8	112	13.0	17.1	17.8
SHL0821Z-11.1E	JW414	2009 Jan	0.8		1.4	3.1	96	15.4	3.9	3.4
SHL0821Z-11.2C	JW414	2009 Jan	1.7		1.1	2.3	214	12.5	5.9	6.4
SHL0821Z-12.1C	JW414	2009 Jan	1.1		1.3	7.4	290	13.7	26.9	26.6
SHL0821Z-12.2E	JW414	2009 Jan	0.3		3.1	3.0	171	12.8	7.4	7.8
SHL0821Z-13.1C	JW414	2009 Jan	0.5		7.2	3.3	127	14.5	4.6	4.2
SHL0821Z-13.2I	JW414	2009 Jan	0.8		1.2	2.6	214	14.0	18.1	17.4
SHL0821Z-13.3E	JW414	2009 Jan	0.8		1.4	3.1	61	14.1	11.1	10.6
SHL26C-1.1C	JW443	2009 Dec			6.4	8.1	116	13.4	5.4	5.6
SHL26-1.2R	JW443	2009 Dec			0.3	2.7	125	14.4	4.6	4.4
SHL-26C-2.1C	JW443	2009 Dec			0.2	1.9	51	11.9	1.6	1.8
SHL-26C-2.2R	JW443	2009 Dec			0.3	2.6	142	13.6	5.3	5.5
SHL26C-3.1R	JW443	2009 Dec			0.5	4.7	193	13.2	14.5	15.3
SHL26C-3.2C	JW443	2009 Dec			0.8	5.7	173	14.1	8.6	8.5
SHL26C-4.1C	***JW443***	***2009 Dec***			***17.9***	***8.1***	***43***	***14.8***	***3.2***	***3.0***
SHL26C-4.2T	JW443	2009 Dec			0.4	2.5	161	12.4	4.3	4.8
SHL26C-5.1T	JW443	2009 Dec			5.5	4.5	128	14.5	5.9	5.7
SHL26C-5.2I	JW443	2009 Dec			0.5	3.9	136	12.5	6.0	6.7
SHL26C-5.3C	JW443	2009 Dec			0.6	3.3	121	12.3	4.0	4.6
SHL26C-6.1C	***JW443***	***2009 Dec***			***14.4***	***3.2***	***108***	***14.7***	***3.7***	***3.5***
SHL26C-6.2I	JW443	2009 Dec			1.3	3.0	124	13.8	5.7	5.7
SHL26c-7.1C	JW443	2009 Dec			8.5	3.5	87	14.3	3.1	3.0

Spot ID	Mount	Date Analyzed	S ppm	Cl ppm (est)	K ppm (est)	Ca ppm (est)	Sc ppm	Ti48/Ti49	Ti48 ppm	Ti49 ppm
SHL26C-7.2T	JW443	2009 Dec			0.5	3.3	147	12.8	4.2	4.5
SHL26C-8.1C	JW443	2009 Dec			0.5	3.7	115	13.3	3.0	3.1
SHL26C-8.2R	JW443	2009 Dec			0.3	2.5	92	13.5	2.4	2.5
SHL26C-9.1C	JW443	2009 Dec			0.3	2.6	218	12.6	10.6	11.8
SHL26C-9.2I	JW443	2009 Dec			0.4	2.6	120	15.7	5.7	5.1
SHL26C-9.3R	JW443	2009 Dec			1.0	2.5	99	12.6	3.4	3.8
SHL26C-9.4R	JW443	2009 Dec			4.4	2.5	124	13.8	3.3	3.4
SHL26C-10.1C	JW443	2009 Dec			0.3	2.8	130	15.4	3.3	3.0
SHL26C-10.2I	JW443	2009 Dec			0.4	2.8	179	13.3	7.4	7.7
SHL26c-10.3R	JW443	2009 Dec			0.8	5.1	182	13.2	7.0	7.4
SHL26C-11.1C	JW443	2009 Dec			1.0	7.2	168	14.4	6.5	6.3
SHL26C-12.1C	JW443	2009 Dec			1.8	5.5	137	13.3	3.6	3.8
SHL26C-12.2I	JW443	2009 Dec			0.7	5.5	196	14.6	5.8	5.6
SHL26C-13.1C	JW443	2009 Dec			0.7	5.4	150	13.6	4.0	4.1
SHL26c-13.2R	JW443	2009 Dec			0.8	6.0	129	13.6	3.4	3.5
SHL26C-14.2I	JW443	2009 Dec			0.6	5.1	357	13.2	19.0	20.1
SHL26C-14.1I	JW443	2009 Dec			0.8	5.7	93	13.2	2.7	2.8
SHL26C-14.3R	JW443	2009 Dec			0.6	4.6	130	11.7	3.7	4.4
SHL26C-15.1I	JW443	2009 Dec			0.7	5.4	398	13.4	7.5	7.8
SHL26C-15.2I	JW443	2009 Dec			0.8	6.0	147	13.5	6.0	6.2
SHL26C-15.3C	JW443	2009 Dec			0.8	5.2	128	12.5	3.2	3.6
SHL29AZ-1.1T	JW392	2008 Aug	0.7		1.4	3.2	122	12.2	4.2	4.7
SHL29AZ-1.2C	JW392	2008 Aug	0.5		3.3	5.8	390	13.8	18.6	18.1
SHL29AZ-1.3I	JW392	2008 Aug	0.2		0.7	1.3	23	14.3	1.7	1.6
SHL29AZ-2.1E	JW392	2008 Aug	0.7		0.9	2.2	141	13.4	4.4	4.4
SHL29AZ-2.2E	JW392	2008 Aug	0.7		0.6	1.6	76	14.4	3.7	3.5
SHL29AZ-2.3I	***JW392***	***2008 Aug***	***1.7***		***10.6***	***9.7***	***41***	***14.4***	***10.4***	***9.7***
SHL29AZ-2.4I	JW392	2008 Aug	0.7		0.9	2.4	47	12.9	10.9	11.3
SHL29AZ-3.1C	JW392	2008 Aug	0.7		1.0	1.8	125	14.8	4.7	4.3

Spot ID	Mount	Date Analyzed	S ppm	Cl ppm (est)	K ppm (est)	Ca ppm (est)	Sc ppm	Ti48/Ti49	Ti48 ppm	Ti49 ppm
SHL29AZ-3.2IE	JW392	2008 Aug	0.2		0.5	1.6	122	15.2	4.7	4.2
SHL29AZ-3.3IE	JW392	2008 Aug	0.5		0.6	1.6	155	13.8	6.8	6.7
SHL29AZ-3.4E	JW392	2008 Aug	0.2		0.7	2.0	109	14.2	3.8	3.6
SHL29AZ-1.1C	JW393	2008 Aug	1.0		3.3	4.0	98	11.4	3.2	3.8
SHL29AZ-1.2E	JW393	2008 Aug	0.9		0.6	2.8	154	13.4	7.6	7.6
SHL29AZ-2.1E	JW393	2008 Aug	0.4		0.8	2.7	131	13.0	6.2	6.4
SHL29AZ-2.2I	JW393	2008 Aug	0.2		3.2	3.6	142	12.4	4.9	5.3
SHL29AZ-2.3C	JW393	2008 Aug	0.5		1.2	3.7	147	15.2	4.1	3.6
SHL29AZ-3.1C	JW393	2008 Aug	0.4		1.7	3.2	102	16.4	3.7	3.0
SHL29AZ-3.2C	JW393	2008 Aug	0.2		0.8	2.6	90	12.5	3.5	3.7
SHL29AZ-4.1C	***JW393***	***2008 Aug***	***0.2***		***6.2***	***7.6***	***106***	***12.7***	***7.3***	***7.7***
SHL29AZ-4.2E	JW393	2008 Aug	0.2		0.7	2.8	64	14.6	4.2	3.9
SHL29AZ-5.1C	JW393	2008 Aug	0.5		1.4	3.6	45	12.7	5.5	5.8
SHL29AZ-5.2E	JW393	2008 Aug	0.5		1.8	3.7	118	13.6	4.5	4.5
SHL29AZ-6.1C	***JW393***	***2008 Aug***	***0.7***		***251.1***	***21.6***	***392***	***13.3***	***36.8***	***37.1***
SHL29AZ-6.2E	JW393	2008 Aug	1.1		0.7	3.0	105	13.5	4.9	4.9
SHL29AZ-6.3I	JW393	2008 Aug	0.1		1.2	4.6	117	13.0	3.7	3.8
SHL29AZ-7.1C	JW393	2008 Aug	0.9		1.3	4.0	195	13.9	5.5	5.3
SHL29AZ-7.2I	JW393	2008 Aug	0.9		0.8	2.7	244	14.1	9.8	9.3
SHL29AZ-7.3E	JW393	2008 Aug	0.8		0.7	4.0	150	12.5	5.5	5.9
SHL29AZ-8.1C	JW393	2008 Aug	0.6		0.7	3.0	246	13.9	9.5	9.1
SHL29AZ-8.2E	JW393	2008 Aug	0.4		0.7	2.9	172	14.8	9.2	8.4
SHL29AZ-9.1C	JW393	2008 Aug	0.0		1.6	4.3	162	14.0	8.2	7.9
SHL29AZ-9.2E	JW393	2008 Aug	0.2		0.9	3.3	156	13.7	5.5	5.4
SHL29Z-1.1C	***JW478***	***2010 May***			***13.39***	***17.1***	***142***	***13.8***	***3.1***	***3.1***
SHL29Z-2.1I	JW478	2010 May			0.32	1.8	130	14.8	4.9	4.5
SHL29Z-3.1C	JW478	2010 May			0.32	1.6	103	13.4	3.1	3.2
SHL29Z-4.1C	***JW478***	***2010 May***			***25.83***	***2.3***	***144***	***14.4***	***4.6***	***4.4***
SHL29Z-5.1C	JW478	2010 May			0.30	2.1	115	13.6	2.5	2.5

Spot ID	Mount	Date Analyzed	S ppm	Cl ppm (est)	K ppm (est)	Ca ppm (est)	Sc ppm	Ti48/Ti49	Ti48 ppm	Ti49 ppm
SHL29Z-5.2E	JW478	2010 May			0.28	1.7	54	12.3	2.3	2.6
SHL29Z-6.1C	JW478	2010 May			0.30	1.6	158	15.0	3.3	3.0
SHL29Z-6.2I	JW478	2010 May			0.35	2.3	129	11.9	4.9	5.6
SHL29Z-7.1C	***JW478***	***2010 May***			***23.31***	***6.9***	***122***	***16.0***	***9.8***	***8.2***
SHL29Z-8.1C	***JW478***	***2010 May***			***3.38***	***2.7***	***98***	***12.3***	***3.7***	***4.1***
SHL29Z-8.2I	JW478	2010 May			0.22	1.3	111	15.8	2.3	2.0
SHL29Z-9.1C	JW478	2010 May			0.29	1.3	142	14.1	3.5	3.4
SHL29Z-10.1C	JW478	2010 May			0.25	1.6	178	13.9	4.8	4.7
SHL29Z-10.2I	JW478	2010 May			0.29	1.6	60	12.3	2.9	3.2
SHL29Z-11.1C	JW478	2010 May			1.80	3.7	95	13.9	3.1	3.0
SHL29Z-11.2I	JW478	2010 May			0.32	2.1	135	14.0	5.3	5.1
SHL29Z-12.1C	***JW478***	***2010 May***			***0.21***	***7.3***	***354***	***13.4***	***28.9***	***29.1***
SHL29Z-13.1C	JW478	2010 May			0.33	2.5	52	13.4	26.8	27.1
SHL29Z-14.1C	JW478	2010 May			4.00	4.4	127	14.2	4.2	4.0
SHL29Z-14.2I	JW478	2010 May			1.89	2.0	81	13.0	4.6	4.8
SHL29Z-15.1I	JW478	2010 May			0.27	2.2	134	14.0	7.2	7.0
SHL29Z-16.1I	JW478	2010 May			0.28	1.9	71	13.6	4.3	4.3
SHL30-1.1C	JW443	2009 Dec			7.5	7.9	62	14.9	3.2	3.0
SHL30-1.2R	JW443	2009 Dec			0.9	6.5	143	13.0	4.9	5.3
SHL30-2.1C	JW443	2009 Dec			0.9	6.5	203	13.2	10.1	10.7
SHL30-2.2R	JW443	2009 Dec			1.2	8.2	102	13.7	4.1	4.1
SHL30-3.1C	JW443	2009 Dec			1.2	8.7	101	13.6	2.6	2.6
SHL30-3.2I	JW443	2009 Dec			1.4	9.3	130	13.8	5.9	6.0
SHL30-3.3I	JW443	2009 Dec			1.1	7.8	194	13.0	7.4	7.9
SHL30-3.4R	***JW443***	***2009 Dec***			***13.9***	***7.5***	***139***	***16.7***	***4.4***	***3.7***
SHL30-4.1I	JW443	2009 Dec			1.0	8.3	45	14.3	2.0	2.0
SHL30-4.2C	JW443	2009 Dec			0.9	6.6	127	13.4	4.2	4.4
SHL30-4.3R	JW443	2009 Dec			0.8	6.6	169	12.7	6.2	6.8
SHL30-5.1C	JW443	2009 Dec			1.4	9.2	136	14.7	5.3	5.0

Spot ID	Mount	Date Analyzed	S ppm	Cl ppm (est)	K ppm (est)	Ca ppm (est)	Sc ppm	Ti48/Ti49	Ti48 ppm	Ti49 ppm
SHL30-5.2T	JW443	2009 Dec			1.0	7.0	113	14.1	6.0	5.9
SHL30-6.1I	JW443	2009 Dec			1.1	6.4	162	13.5	4.1	4.2
SHL30-7.1C	JW443	2009 Dec			1.4	6.7	108	12.4	4.3	4.8
SHL30-7.2R	JW443	2009 Dec			1.1	7.5	123	13.5	3.8	4.0
SHL30-7.3R	JW443	2009 Dec			0.9	7.0	181	12.9	7.4	8.0
SHL30-8.1C	JW443	2009 Dec			1.2	8.4	586	14.2	17.4	17.1
SHL30-8.2T	JW443	2009 Dec			1.0	7.6	54	12.1	4.1	4.7
SHL30-9.1C	JW443	2009 Dec			1.2	7.2	518	14.7	13.5	12.9
SHL30-10.1C	JW443	2009 Dec			1.2	7.5	121	15.4	4.1	3.7
SHL30-10.2I	JW443	2009 Dec			1.1	8.1	100	14.0	4.1	4.1
SHL30-10.3R	JW443	2009 Dec			1.6	7.7	151	13.3	5.5	5.8
SHL30-12.1C	JW443	2009 Dec			1.1	8.2	127	12.9	3.6	3.9
SHL30-12.2I	JW443	2009 Dec			0.9	6.1	190	13.5	5.6	5.8
SHL30-11.1C	JW443	2009 Dec			8.4	7.0	120	14.3	4.0	4.0
SHL30-11.2T	***JW443***	***2009 Dec***			***17.4***	***20.5***	***161***	***13.4***	***7.7***	***8.0***
SHL30-13.1C	JW443	2009 Dec			3.8	7.8	174	13.5	5.6	5.9
SHL30-13.2T	JW443	2009 Dec			9.0	7.0	175	13.6	7.2	7.4
SHL30-14.1C	JW443	2009 Dec			0.9	6.2	93	13.2	8.8	9.3
SHL30-14.2T	JW443	2009 Dec			2.0	7.2	39	14.1	2.0	1.9
SHL33-1.1C	JW443	2009 Dec			1.1	8.8	631	13.6	15.0	15.5
SHL33-1.2R	JW443	2009 Dec			0.9	7.9	136	13.8	7.6	7.7
SHL33-2.1E	JW443	2009 Dec			0.8	8.5	67	13.2	11.2	11.8
SHL33-2.2I	JW443	2009 Dec			1.2	8.2	45	13.6	10.1	10.4
SHL33-3.1C	JW443	2009 Dec			1.0	10.2	560	13.8	22.1	22.3
SHL33-3.2T	JW443	2009 Dec			1.1	9.1	58	13.7	3.1	3.1
SHL33-4.1T	JW443	2009 Dec			1.0	9.0	113	15.0	5.9	5.5
SHL33-4.2C	***JW443***	***2009 Dec***			***1.2***	***12.6***	***90***	***13.9***	***11.4***	***11.5***

Spot ID	Mount	Date Analyzed	S ppm	Cl ppm (est)	K ppm (est)	Ca ppm (est)	Sc ppm	Ti48/Ti49	Ti48 ppm	Ti49 ppm
SHL34Z-1.1C	JW392	2008 Aug	1.0		0.6	1.9	109	14.3	3.3	3.1
SHL34Z-1.2I	JW392	2008 Aug	0.3		0.6	2.5	171	13.6	6.3	6.2
SHL34Z-1.3E	JW392	2008 Aug	0.8		1.2	2.5	251	13.5	5.1	5.1
SHL34Z-2.1I	JW392	2008 Aug	0.5		0.6	2.1	139	13.9	18.7	18.0
SHL34Z-3.1I	JW392	2008 Aug	1.6		2.8	3.8	59	14.1	8.6	8.2
SHL34Z-3.2I	JW392	2008 Aug	1.0		0.8	2.3	52	13.7	9.0	8.8
SHL34Z-3.3E	JW392	2008 Aug	0.5		1.0	2.6	129	13.9	4.3	4.2
SHL34Z-4.1E	JW392	2008 Aug	0.5		4.5	3.7	238	13.2	9.0	9.1
SHL34Z-4.2C	JW392	2008 Aug	0.5		0.6	2.0	96	13.9	13.8	13.3
SHL34AZ-1.1I	JW393	2008 Aug	1.1		0.7	3.5	147	13.4	7.0	7.0
SHL34AZ-1.2E	JW393	2008 Aug	0.0		0.5	1.6	217	14.0	10.2	9.8
SHL34AZ-2.1E	JW393	2008 Aug	0.8		1.0	2.9	166	14.2	6.4	6.0
SHL34AZ-2.2I	JW393	2008 Aug	0.2		0.9	2.5	118	13.1	5.5	5.6
SHL34AZ-3.1E	JW393	2008 Aug	1.7		1.0	2.8	202	13.3	6.7	6.8
SHL34AZ-3.2IE	JW393	2008 Aug	1.0		0.6	2.8	80	14.1	13.9	13.2
SHL34AZ-3.3I	JW393	2008 Aug	0.6		1.0	2.4	59	13.6	10.6	10.4
SHL34AZ-4.1I	JW393	2008 Aug	0.4		1.1	3.3	115	14.1	3.7	3.6
SHL34AZ-5.1I	JW393	2008 Aug	0.2		2.3	3.8	163	13.5	6.2	6.1
SHL34AZ-6.2I	JW393	2008 Aug	0.4		0.8	3.6	120	13.3	19.3	19.6
SHL34AZ-7.1I	JW393	2008 Aug	0.2		0.6	3.1	129	13.7	12.9	12.6
SHL34AZ-7.2E	JW393	2008 Aug	0.4		1.1	22.9	160	14.1	17.4	16.6
SHL34AZ-8.1I	JW393	2008 Aug	0.2		0.6	3.1	81	13.4	15.6	15.6
SHL34AZ-9.1I	JW393	2008 Aug	0.4		0.6	3.6	164	13.3	15.3	15.4
SHL34AZ-10.1I	JW393	2008 Aug	0.4		2.0	3.2	102	14.2	6.1	5.8
SHL34AZ-11.1I	JW393	2008 Aug	0.4		5.6	4.5	179	13.0	6.5	6.7
SHL34AZ-11.2E	JW393	2008 Aug	0.2		0.6	3.2	106	13.5	4.9	4.9
SHL34AZ-12.1I	JW393	2008 Aug	0.0		1.2	2.4	104	13.8	17.8	17.3
SHL36E-1.1I	JW443	2009 Dec			0.7	6.1	139	13.8	5.9	6.0

Spot ID	Mount	Date Analyzed	S ppm	Cl ppm (est)	K ppm (est)	Ca ppm (est)	Sc ppm	Ti48/Ti49	Ti48 ppm	Ti49 ppm
SHL36E-1.2C	JW443	2009 Dec			1.9	7.7	151	13.9	6.4	6.4
SHL36E-1.3I	JW443	2009 Dec			0.7	6.5	117	13.8	5.4	5.4
SHL36E-1.4R	JW443	2009 Dec			1.0	8.9	139	11.6	3.8	4.6
SHL36E-2.1C	JW443	2009 Dec			0.8	7.3	237	14.6	6.7	6.4
SHL36E-2.2T	JW443	2009 Dec			0.6	5.8	159	14.0	7.6	7.6
SHL36E-3.1C	***JW443***	***2009 Dec***			***294***	***54***	***338***	***13.9***	***25***	***25***
SHL36E-3.2I	JW443	2009 Dec			0.9	6.8	67	12.2	5.5	6.3
SHL36E-3.3T	JW443	2009 Dec			1.6	8.4	105	14.1	6.9	6.8
SHL36E-4.1C	JW443	2009 Dec			0.8	5.9	112	14.8	4.2	3.9
SHL36E-4.2T	JW443	2009 Dec			1.1	7.8	148	14.0	9.1	9.0
SHL36E-5.1C	JW443	2009 Dec			0.8	7.5	147	11.7	4.4	5.2
SHL36E-6.1R	JW443	2009 Dec			2.3	7.0	165	13.2	6.5	6.9
SHL36E-6.2C	JW443	2009 Dec			1.8	9.3	169	12.9	6.3	6.8
SHL36E-7.1I	JW443	2009 Dec			0.9	6.9	204	14.7	5.8	5.5
SHL36E-7.2R	JW443	2009 Dec			1.2	7.3	146	12.7	5.1	5.6
SHL36E-8.1C	JW443	2009 Dec			0.9	5.8	211	13.0	5.0	5.3
SHL36E-8.2R	JW443	2009 Dec			0.9	6.9	103	13.5	5.2	5.4
SHL36E-9.1C	***JW443***	***2009 Dec***			***51.7***	***14.5***	***783***	***13.8***	***22.7***	***22.9***
SHL36E-9.2R	JW443	2009 Dec			1.0	7.7	170	13.1	4.9	5.2
SHL36E-10.1I	***JW443***	***2009 Dec***			***13.0***	***8.4***	***229***	***13.4***	***8.9***	***9.4***
SHL36EX-11.1C	***JW443***	***2009 Dec***			***1.6***	***18.8***	***383***	***13.6***	***17.9***	***18.4***
SHL36E-11.2I	JW443	2009 Dec			3.4	12.7	285	13.1	9.2	9.8
SHL36E-11.3R	JW443	2009 Dec			0.8	6.8	173	14.0	7.4	7.4
SHL36E-12.1C	JW443	2009 Dec			2.2	7.0	235	13.3	6.1	6.4
SHL36E-12.2R	JW443	2009 Dec			0.8	6.5	167	14.3	4.3	4.2
SHL36E-12.3R	JW443	2009 Dec			1.1	7.9	193	11.1	5.6	7.0
SHL36E-13.1I	JW443	2009 Dec			0.9	6.9	235	13.4	6.4	6.6
SHL36E-13.2R	JW443	2009 Dec			0.8	6.7	123	13.6	3.3	3.3
SHL36E-14.2C	JW443	2009 Dec			0.8	6.6	575	14.0	18.4	18.4
SHL36E-14.3I	JW443	2009 Dec			0.8	6.4	198	14.5	6.5	6.3
SHL36E-14.1T	JW443	2009 Dec			0.9	5.0	228	13.3	7.4	7.7

Spot ID	Mount	Date Analyzed	S ppm	Cl ppm (est)	K ppm (est)	Ca ppm (est)	Sc ppm	Ti48/Ti49	Ti48 ppm	Ti49 ppm
SHL37P-1.1C	JW443	2009 Dec			1.0	6.9	140	12.2	5.0	5.8
SHL37P-1.2I	JW443	2009 Dec			0.8	5.5	152	13.9	5.5	5.5
SHL37P-1.3R	JW443	2009 Dec			0.6	4.5	167	13.2	6.7	7.1
SHL37P-2.1C	JW443	2009 Dec			0.8	6.1	120	13.4	3.6	3.8
SHL37P-2.2I	JW443	2009 Dec			0.8	5.6	101	14.5	4.7	4.6
SHL37P-2.3R	JW443	2009 Dec			0.7	5.2	111	12.6	3.7	4.1
SHL37P-14.1C	JW443	2009 Dec			0.6	4.9	128	13.4	5.5	5.7
SHL37P-14.2R	JW443	2009 Dec			0.8	6.3	190	13.9	7.4	7.4
SHL37P-3.1C	JW443	2009 Dec			0.8	7.1	74	13.3	12.9	13.5
SHL37P-3.2I	***JW443***	***2009 Dec***			***230.5***	***17.2***	***52***	***15.5***	***4.2***	***3.8***
SHL37P-3.3R	JW443	2009 Dec			0.8	6.0	179	12.8	5.0	5.5
SHL37P-4.1R	JW443	2009 Dec			0.7	5.9	275	14.1	13.5	13.3
SHL37P-4.2C	JW443	2009 Dec			0.7	5.6	110	13.8	2.9	2.9
SHL37P-4.3I	JW443	2009 Dec			0.9	6.0	101	13.2	3.3	3.5
SHL37P-5.1C	JW443	2009 Dec			15.1	9.6	178	14.8	9.1	8.5
SHL37P-5.2I	JW443	2009 Dec			1.2	5.9	92	13.5	5.4	5.5
SHL37P-5.3T	***JW443***	***2009 Dec***			***79.8***	***12.8***	***95***	***14.2***	***4.2***	***4.2***
SHL37P-6.1I	JW443	2009 Dec			0.9	7.0	120	12.2	3.2	3.6
SHL37P-6.2C	JW443	2009 Dec			1.7	6.2	161	14.3	4.5	4.4
SHL37P-6.3R	JW443	2009 Dec			0.8	6.6	127	13.6	4.5	4.6
SHL37P-7.1R	JW443	2009 Dec			0.7	5.8	119	12.0	2.8	3.3
SHL37P-7.2C	JW443	2009 Dec			0.8	6.0	161	13.3	3.9	4.1
SHL37P-7.3T	JW443	2009 Dec			5.7	8.7	70	13.9	3.3	3.3
SHL37P-7.4C	JW443	2009 Dec			1.1	7.1	78	12.5	2.4	2.7
SHL37P-8.1I	JW443	2009 Dec			0.8	5.3	89	15.0	2.6	2.4
SHL37P-8.2C	***JW443***	***2009 Dec***			***0.8***	***7.5***	***673***	***13.7***	***31.9***	***32.7***
SHL37P-8.3R	JW443	2009 Dec			0.8	6.5	119	15.1	4.4	4.1
SHL37P-15.1C	JW443	2009 Dec			0.9	7.3	112	14.5	3.6	3.4
SHL37P-15.2T	JW443	2009 Dec			3.6	12.9	172	15.1	16.1	14.9

Spot ID	Mount	Date Analyzed	S ppm	Cl ppm (est)	K ppm (est)	Ca ppm (est)	Sc ppm	Ti48/Ti49	Ti48 ppm	Ti49 ppm
SHL37P-9.2R	JW443	2009 Dec			0.7	4.7	104	13.9	4.4	4.4
SHL37P-9.1C	JW443	2009 Dec			2.5	6.7	37	14.7	6.6	6.3
SHL37P-10.2R	JW443	2009 Dec			0.9	5.6	136	14.2	4.7	4.6
SHL37P-10.1I	JW443	2009 Dec			1.4	6.4	64	15.7	2.9	2.5
SHL37P-11.1C	***JW443***	***2009 Dec***			***28.8***	***13.4***	***128***	***13.4***	***7.4***	***7.7***
SHL37P-11.2I	JW443	2009 Dec			0.8	6.5	142	10.6	5.3	7.0
SHL37P-11.3I	JW443	2009 Dec			1.0	7.2	139	14.1	5.5	5.4
SHL37P-11.4R	***JW443***	***2009 Dec***			***105.0***	***27.1***	***144***	***12.6***	***12.3***	***13.6***
SHL37P-12.1C	JW443	2009 Dec			0.8	6.2	137	12.7	6.1	6.7
SHL37P-12.2I	***JW443***	***2009 Dec***			***89.9***	***16.9***	***168***	***13.6***	***9.5***	***9.8***
SHL37P-12.3T	JW443	2009 Dec			8.2	7.2	123	13.0	5.3	5.7
SHL37P-13.1C	JW443	2009 Dec			1.1	7.7	261	14.4	9.5	9.2
SHL37P-13.2T	JW443	2009 Dec			2.6	9.7	159	13.8	10.2	10.3
SHL0849AZ-1.1I	JW414	2009 Jan	0.6		4.0	6.8	173	14.7	18.2	16.7
SHL0849AZ-1.2E	JW414	2009 Jan	0.6		0.7	2.4	150	13.9	17.4	16.9
SHL0849AZ-2.1E	JW414	2009 Jan	0.9		0.9	2.0	119	13.1	14.8	15.3
SHL0849AZ-3.1E	JW414	2009 Jan	0.9		0.9	2.3	128	14.2	15.2	14.4
SHL0849AZ-4.1E	JW414	2009 Jan	0.8		1.4	3.1	107	12.8	15.0	15.8
SHL0849AZ-4.2C	JW414	2009 Jan	1.4		1.6	3.1	164	13.7	22.5	22.2
SHL0849AZ-4.3E	JW414	2009 Jan	0.5		1.5	3.1	122	13.4	18.1	18.3
SHL0849AZ-5.1I	JW414	2009 Jan	0.0		1.4	2.9	134	13.7	16.3	16.0
SHL0849AZ-6.1I	***JW414***	***2009 Jan***	***0.8***		***17.4***	***2.2***	***188***	***13.7***	***18.9***	***18.6***
SHL0849AZ-7.1C	JW414	2009 Jan	1.5		1.7	4.6	184	13.7	17.4	17.1
SHL0849AZ-8.1E	JW414	2009 Jan	0.3		1.2	2.2	201	13.5	28.4	28.3
SHL0849AZ-9.1E	JW414	2009 Jan	0.9		1.2	2.9	172	13.9	23.7	23.0
SHL0849AZ-9.2I	JW414	2009 Jan	0.8		1.2	2.8	93	13.0	12.8	13.4
SHL0849AZ-10.1C	JW414	2009 Jan	1.1		1.4	2.4	131	13.0	15.4	16.0
SHL0849AZ-11.1I	JW414	2009 Jan	0.3		1.0	1.8	70	13.3	11.3	11.4
SHL0849AZ-11.2E	JW414	2009 Jan	0.8		1.3	2.4	94	14.1	14.3	13.7

Spot ID	Mount	Date Analyzed	S ppm	Cl ppm (est)	K ppm (est)	Ca ppm (est)	Sc ppm	Ti48/Ti49	Ti48 ppm	Ti49 ppm
SHL0849AZ-12.1E	JW414	2009 Jan	0.0		0.8	1.9	144	12.9	15.8	16.6
SHL0849AZ-12.2C	***JW414***	***2009 Jan***	***3.7***		***12.1***	***9.5***	***126***	***13.2***	***18.9***	***19.4***
SHL0849AZ-13.1E	JW414	2009 Jan	1.8		2.7	5.9	83	15.4	3.8	3.3
SHL0849AZ-13.2I	JW414	2009 Jan	0.9		0.8	1.9	69	14.3	4.0	3.8
SHL0849AZ-13.3C	***JW414***	***2009 Jan***	***0.8***		***6.1***	***3.6***	***172***	***14.1***	***10.5***	***10.1***
SHL49AZ-14.1C	JW414	2009 Jan	0.3		1.5	3.7	213	13.8	20.7	20.3
SHD9-1.1R	JW443	2009 Dec			0.7	6.5	58	10.6	3.6	4.8
SHD9-2.1R	JW443	2009 Dec			0.9	7.0	148	12.8	9.7	10.6
SHD9-2.2C	JW443	2009 Dec			0.8	8.4	225	13.6	26.4	27.1
SH325.2-1.1DGZT	JW309	2007 May	1.3	1		4.3	96	13.4	3.7	3.7
SH325.2-1.2MGZC	JW309	2007 May	0.6	0		1.6	140	14.1	3.9	3.7
SH325.2-1.3LGZI]	JW309	2007 May	0.9	1		2.0	118	12.8	6.4	6.8
SH325.2-2.1MGZC	JW309	2007 May	0.9	1		1.9	91	13.5	5.4	5.4
SH325.2-2.2LGZI	JW309	2007 May	0.9	0		1.9	47	13.2	2.0	2.1
SH325.2-3.1LGC	***JW309***	***2007 May***	***0.9***	***9***		***3.2***	***144***	***13.3***	***6.1***	***6.3***
SH325.2-3.2DGZE	JW309	2007 May	2.2	9		2.2	119	14.0	6.0	5.9
SH325.2-4.1DGZE	***JW309***	***2007 May***	***0.0***	***2***		***1.6***	***189***	***13.7***	***10.5***	***10.5***
SH325.2-4.2MGC	***JW309***	***2007 May***	***1.0***	***3***		***2.8***	***134***	***14.3***	***10.4***	***9.9***
SH325.2-5.1MGZE	JW309	2007 May	1.1	0		2.1	127	13.1	3.5	3.6
SH325.2-5.2DGZI	***JW309***	***2007 May***	***0.5***	***0***		***2.0***	***149***	***12.6***	***4.7***	***5.0***
SH325.2-5.3DGZE	***JW309***	***2007 May***	***0.9***	***0***		***2.0***	***118***	***12.9***	***4.7***	***4.9***
SH325.2-6.1MGT	JW309	2007 May	2.3	39		1.9	48	13.7	7.4	7.3
SH325.2-6.2MGI	JW309	2007 May	0.4	1		2.1	46	13.1	5.5	5.7
SH325.2-7.1LGZT	JW309	2007 May	0.8	0		3.1	130	14.0	7.1	6.9
SH325.2-7.2DGZT	JW309	2007 May	0.6	1		1.8	34	14.3	2.2	2.1
SH325.2-7.3LGZC	JW309	2007 May	0.6	1		2.4	108	12.8	7.4	7.9
SH325.2-8.1MGZE	JW309	2007 May	1.5	0		1.9	120	13.0	4.8	5.0

Spot ID	Mount	Date Analyzed	S ppm	Cl ppm (est)	K ppm (est)	Ca ppm (est)	Sc ppm	Ti48/Ti49	Ti48 ppm	Ti49 ppm
SH325.2-8.2MGZC	JW309	2007 May	0.7	0		2.5	154	13.6	7.2	7.2
SH325.2-8.3DGZT	JW309	2007 May	0.9	3		1.9	75	13.6	4.8	4.8
SH325.2-9.1MGC	JW309	2007 May	1.1	0		2.1	131	13.6	5.4	5.4
SH325.2-10.1MGZI	JW309	2007 May	0.4	1		1.8	199	13.4	10.2	10.3
SH325.2-11.1DGZE	***JW309***	***2007 May***	***1.6***	***19***		***34.8***	***36***	***13.5***	***71.9***	***72.4***
SH325.2-11.1MGC	***JW309***	***2007 May***	***1.3***	***6***		***39.0***	***48***	***13.9***	***16.4***	***16.0***
SH325.2-12.1MGZT	JW309	2007 May	1.2	1		1.9	39	13.5	7.4	7.4
SH325.2-12.2MGZI	***JW309***	***2007 May***	***2.3***	***123***		***225.1***	***18***	***14.1***	***5.8***	***5.5***
SH325.2-13.1DGZT	JW309	2007 May	0.6	1		2.3	18	13.3	16.9	17.2
SH325.2-13.1T	***JW309***	***2007 May***	***0.8***	***1***		***2.6***	***32***	***13.8***	***9.4***	***9.3***
Z484A-10.1C	JP04	2008 Jan	0.7		1.2	1.5	104	13.7	3.3	3.2
Z484A-10.2IR	JP04	2008 Jan	0.4		1.6	2.9	209	13.1	4.2	4.3
Z484A-10.3T	JP04	2008 Jan	0.0		1.5	1.6	119	13.6	4.2	4.1
Z484A-12.1I	JP04	2008 Jan	0.4		1.4	2.1	40	13.8	25.1	24.5
Z484A-12.2EM	JP04	2008 Jan	0.7		1.3	1.7	12	15.5	4.5	3.9
Z484A-12.3T	JP04	2008 Jan	1.1		1.5	2.1	46	13.1	3.2	3.3
Z484A-14.1C	***JP04***	***2008 Jan***	***0.5***		***0.9***	***2.0***	***512***	***13.5***	***24.5***	***24.4***
Z484A-16.1C	JP04	2008 Jan	1.3		1.1	1.7	85	13.5	3.6	3.6
Z484A-16.2I	JP04	2008 Jan	1.2		1.9	3.8	173	13.5	5.6	5.5
Z484A-17.1C	JP04	2008 Jan	1.9		1.4	1.2	226	13.6	10.1	9.9
Z484A-17.2T	JP04	2008 Jan	0.0		0.9	0.8	91	13.8	4.2	4.1
Z484A-18.1C	JP04	2008 Jan	1.6		2.4	1.2	51	15.0	1.9	1.7
Z484A-18.2IR	JP04	2008 Jan	0.8		1.6	1.3	115	13.7	3.2	3.1
Z484A-19.1T	JP04	2008 Jan	0.4		1.1	1.5	99	13.3	3.1	3.1
Z484A-19.2C	JP04	2008 Jan	1.6		1.3	3.0	100	13.8	5.0	4.8
Z484A-19.3IR	JP04	2008 Jan	1.4		0.8	1.2	113	12.9	4.7	4.9
Z484A-19.4IR	JP04	2008 Jan	0.4		1.1	1.3	165	13.3	4.4	4.4
Z484A-2.1T	JP04	2008 Jan	0.9		2.7	1.5	129	14.6	10.5	9.7
Z484A-2.2C	JP04	2008 Jan	0.8		2.3	1.5	155	13.5	7.1	7.1

Spot ID	Mount	Date Analyzed	S ppm	Cl ppm (est)	K ppm (est)	Ca ppm (est)	Sc ppm	Ti48/Ti49	Ti48 ppm	Ti49 ppm
Z484A-4.1I	***JP04***	***2008 Jan***	***0.4***		***1.5***	***2.9***	***776***	***13.3***	***34.6***	***34.8***
Z484A-4.2T	JP04	2008 Jan	0.4		1.7	1.0	68	13.8	4.6	4.5
Z484A-5.1I	***JP04***	***2008 Jan***	***0.4***		***12.6***	***2.6***	***140***	***13.1***	***4.3***	***4.4***
Z484A-8.1I	***JP04***	***2008 Jan***	***1.5***		***1153.8***	***100.6***	***590***	***13.6***	***38.8***	***38.4***
Z484A-8.2I	JP04	2008 Jan	0.8		0.9	1.8	309	13.8	10.1	9.7

Spot ID	Mount	Date Analyzed	V ppm (est)	Cr ppm (est)	Mn ppm (est)	Fe ppm	Ge ppm (est)	Y ppm	Nb ppm	La ppm	Ce ppm
SHL3Z-1.1DI	JW414	2009 Jan	0.19	0.06	0.05	0.9	0.3	752	3	0.015	14
SHL3Z-1.2LC	JW414	2009 Jan	0.27	0.05	0.05	4.4	0.3	966	3	0.007	14
SHL3Z-1.3DI	JW414	2009 Jan	0.07	0.07	0.19	28	0.2	395	4	0.012	8
SHL3Z-1.4DR	JW414	2009 Jan	0.01	0.01	0.05	4.3	***0.1***	694	3	0.005	8
SHL3Z-2.1DC	JW414	2009 Jan	0.04	0.06	0.06	1.1	0.4	1376	4	0.005	15
SHL3Z-2.2LR	***JW414***	***2009 Jan***	***0.03***	***0.03***	***5.73***	***225***	***0.2***	***990***	***4***	***0.050***	***13***
SHL3Z-3.1LC	***JW414***	***2009 Jan***	***0.03***	***0.10***	***0.06***	***1.9***	***0.2***	***648***	***1***	***0.017***	***8***
SHL3Z-3.2DI	JW414	2009 Jan	0.49	0.07	0.06	1.2	0.4	7023	81	0.005	76
SHL3Z-3.3LR	JW414	2009 Jan	0.06	0.05	0.02	0.7	0.3	3012	23	0.015	19
SHL3Z-4.1LR	JW414	2009 Jan	0.03	0.08	0.04	1.0	0.2	1202	6	0.010	15
SHL3Z-4.2LI	JW414	2009 Jan	0.05	0.06	0.04	0.9	0.3	712	2	0.005	9
SHL3Z-4.3LC	JW414	2009 Jan	0.02	0.08	0.05	1.1	0.2	947	3	0.007	5
SHL3Z-5.1DC	JW414	2009 Jan	0.03	0.06	0.05	6.2	0.3	198	4	0.000	1
SHL3Z-5.2LR	JW414	2009 Jan	0.03	0.06	0.02	1.0	***0.3***	912	7	0.007	19
SHL3Z-6.1DI	JW414	2009 Jan	0.02	0.07	0.04	0.8	0.4	1122	7	0.005	16
SHL3Z-6.2LC	***JW414***	***2009 Jan***	***0.04***	***0.06***	***1.31***	***154***	***0.1***	***935***	***2***	***0.030***	***9***
SHL3Z-6.3DE	JW414	2009 Jan	0.02	0.03	0.02	0.7	0.2	773	5	0.005	15
SHL3Z-7.1LR	JW414	2009 Jan	0.02	0.04	0.05	1.8	0.2	643	5	0.007	5
SHL3Z-7.2DI	***JW414***	***2009 Jan***	***0.02***	***0.04***	***0.12***	***9.4***	***0.4***	***836***	***7***	***0.005***	***10***
SHL3Z-7.3LC	***JW414***	***2009 Jan***	***1.64***	***0.03***	***0.22***	***31.1***	***0.4***	***924***	***2***	***0.037***	***15***
SHL3Z-8.1LC	JW414	2009 Jan	0.05	0.07	0.03	0.9	***0.2***	962	5	0.007	12
SHL3Z-8.2I	JW414	2009 Jan	0.01	0.06	0.02	0.7	0.3	1528	14	0.000	12
SHL3Z-8.3LC	***JW414***	***2009 Jan***	***0.03***	***0.08***	***0.26***	***55***	***0.1***	***1328***	***8***	***0.007***	***16***
SHL3Z-8.4DI	***JW414***	***2009 Jan***	***0.15***	***0.08***	***0.30***	***14***	***0.1***	***1513***	***15***	***0.103***	***15***
SHL3Z-9.1DI	JW414	2009 Jan	0.07	0.07	0.09	6.1	0.3	639	8	0.005	3
SHL3Z-9.2LC	JW414	2009 Jan	0.02	0.08	0.03	0.8	0.3	899	4	0.007	6
SHL3Z-9.3LI	JW414	2009 Jan	0.03	0.08	0.03	1.0	0.1	1394	7	0.002	12
MSHL3Z-1.1DGI	JW309	2007 May	2.6		4.86	15.00	0.2	7270	15	0.074	92
MSHL3Z-1.2MGI	JW309	2007 May	0.7		2.42	5.18	0.2	991	3	0.025	7

MSHL3Z-2.1MGZC	***JW309***	***2007 May***	***1.1***	***5.34***	***21.27***	***0.2***	***1330***	***7***	***0.177***	***12***
MSHL3Z-2.2DGZI	JW309	2007 May	1.0	0.57	1.37	0.2	730	6	0.013	17
MSHL3Z-3.1DGZT	JW309	2007 May	1.4	1.36	7.22	0.2	999	7	0.051	18
MSHL3Z-3.2LGZE	JW309	2007 May	0.9	3.20	38.24	0.2	767	3	0.039	7
MSHL3Z-3.3DGC	JW309	2007 May	1.1	1.00	3.02	0.2	1852	6	0.020	9
MSHL3Z-4.1MGI	JW309	2007 May	0.7	1.39	2.65	0.3	815	2	0.021	8
MSHL4Z-1.1DGZE	JW309	2007 May	1.2	0.76	1.2	0.3	615	4	0.006	15
MSHL4Z-1.2MGZI	JW309	2007 May	2.3	0.43	1.5	0.1	909	4	0.013	14
MSHL4Z-10.1MGT	JW309	2007 May	1.9	0.72	1.7	0.2	1044	4	0.013	17
MSHL4Z-10.2MGZC	JW309	2007 May	2.6	2.29	39.6	0.2	709	2	0.105	12
MSHL4Z-10.3DGZIT	JW309	2007 May	4.2	0.60	3.5	0.3	2417	9	0.013	40
MSHL4Z-11.1DGZI	JW309	2007 May	1.4	0.50	1.8	0.1	764	2	0.028	9
MSHL4Z-11.2DZIT	JW309	2007 May	2.8	0.63	1.7	0.1	1454	5	0.013	21
MSHL4Z-12.1MGI	JW309	2007 May	1.0	0.91	1.4	0.2	360	1	0.020	6
MSHL4Z-2.1DGZI	JW309	2007 May	1.3	0.70	1.5	0.2	444	2	0.012	12
MSHL4Z-2.2MGZI	JW309	2007 May	1.6	0.90	9.5	0.2	977	5	0.022	16
MSHL4Z-2.3DGZE	JW309	2007 May	0.8	0.75	1.2	0.2	599	3	0.005	12
MSHL4Z-3.1DGZT	JW309	2007 May	1.6	1.46	4.0	0.3	1302	6	0.046	27
MSHL4Z-3.2MGZE	JW309	2007 May	2.0	0.85	3.3	0.2	906	2	0.029	11
MSHL4Z-10.2MGZC	JW309	2007 May	2.6	2.29	39.6	0.2	709	2	0.105	12
MSHL4Z-10.3DGZIT	JW309	2007 May	4.2	0.60	3.5	0.3	2417	9	0.013	40
MSHL4Z-11.1DGZI	JW309	2007 May	1.4	0.50	1.8	0.1	764	2	0.028	9
MSHL4Z-5.1DGZT	JW309	2007 May	0.8	0.66	0.8	0.3	508	3	0.009	12
MSHL4Z-5.2MGZE	JW309	2007 May	1.5	0.59	1.1	0.3	938	5	0.006	17
MSHL4Z-5.3MGI	JW309	2007 May	0.5	0.61	0.6	0.2	193	1	0.015	5
MSHL4Z-6.1MGT	JW309	2007 May	1.6	0.89	0.8	0.2	951	5	0.014	19
MSHL4Z-6.2MGI	JW309	2007 May	0.7	0.77	1.8	0.1	431	1	0.008	6
MSHL4Z-7.1MGZT	JW309	2007 May	5.7	1.95	19.2	0.1	1072	4	0.583	22
MSHL4Z-7.2LGC	JW309	2007 May	2.6	1.11	9.1	0.2	1306	2	0.031	18
MSHL4Z-7.3DGI	JW309	2007 May	4.8	1.01	4.9	0.1	2319	6	0.019	43
MSHL4Z-8.1MGZT	JW309	2007 May	1.4	0.67	1.2	0.2	864	5	0.010	19

MSHL4Z-8.2DGZI	JW309	2007 May	1.8		0.87	4.0	0.2	776	5	0.015	27
MSHL4Z-8.3MGZI	JW309	2007 May	0.6		0.70	1.8	0.1	678	2	0.004	8
MSHL4Z-9.1MGZT	JW309	2007 May	1.6		0.56	2.6	0.2	1176	6	0.008	22
MSHL4Z-9.2LGC	JW309	2007 May	1.2		0.76	2.2	0.2	797	2	0.013	9
MSHL4Z-9.3MGZT	JW309	2007 May	1.3		0.80	1.4	0.2	728	4	0.017	18
SHL5Z-1.1C	JW364	2008 Jan	0.04	0.0	0.03	0.7	0.2	1023	6	0.013	29
SHL5Z-2.1I	JW364	2008 Jan	0.05	0.1	0.19	18.4	0.2	539	3	0.071	27
SHL5Z-2.2T	JW364	2008 Jan	0.07	0.0	0.04	1.2	0.4	1077	4	0.005	16
SHL5Z-3.1C	JW364	2008 Jan	0.07	0.0	0.08	8.7	0.2	679	1	0.026	9
SHL5Z-3.2E	JW364	2008 Jan	0.08	0.0	0.08	17.9	0.2	889	3	0.005	16
SHL5Z-4.1C	JW364	2008 Jan	0.09	0.1	0.10	16.0	0.3	1128	3	0.020	17
SHL5Z-4.2T	JW364	2008 Jan	0.07	0.1	0.11	13.7	***0.3***	702	2	0.010	10
SHL5Z-5.1T	JW364	2008 Jan	0.04	0.1	0.08	2.1	***0.1***	642	3	0.009	15
SHL5Z-5.2C	***JW364***	***2008 Jan***	***0.35***	***0.1***	***1.84***	***142***	***0.3***	***7310***	***21***	***0.584***	***202***
SHL5Z-6.1C	***JW364***	***2008 Jan***	***0.46***	***0.1***	***1.98***	***322***	***0.3***	***14683***	***24***	***0.167***	***350***
SHL5Z-6.2T	JW364	2008 Jan	0.03	0.1	0.10	2.3	***0.1***	531	2	0.005	12
SHL5Z-6.3I	JW364	2008 Jan	0.06	0.1	0.06	1.8	0.3	798	3	0.015	15
SHL5Z-7.1C	***JW364***	***2008 Jan***	***0.04***	***0.1***	***0.79***	***49***	***0.2***	***688***	***3***	***0.207***	***17***
SHL5Z-7.2T	JW364	2008 Jan	0.03	0.1	0.08	1.4	0.3	584	3	0.005	14
SHL5Z-8.1T	JW364	2008 Jan	0.04	0.1	0.11	2.1	0.2	584	2	0.007	9
SHL5Z-8.2C	JW364	2008 Jan	0.10	0.1	0.08	4.1	0.2	1029	2	0.021	12
SHL5Z-1.1T	JW365	2008 Jan	0.03	0.06	0.09	1.3	0.1	507	2	0.000	14
SHL5Z-1.2I	***JW365***	***2008 Jan***	***0.17***	***0.08***	***0.37***	***30.5***	***0.2***	***1104***	***3***	***0.169***	***16***
SHL5Z-2.1C	JW365	2008 Jan	0.07	0.09	0.11	99.4	0.1	968	4	0.021	14
SHL5Z-2.2E	JW365	2008 Jan	0.05	0.07	0.07	5.5	0.2	665	2	0.008	9
SHL5Z-3.1C	JW365	2008 Jan	0.02	0.04	0.08	0.9	0.1	546	1	0.011	7
SHL5Z-3.2R	JW365	2008 Jan	0.09	0.06	0.07	6.6	0.1	848	2	0.028	12
SHL5Z-4.1C	JW365	2008 Jan	0.17	0.08	0.06	2.0	0.2	1634	2	0.034	25
SHL5Z-4.2T	JW365	2008 Jan	0.07	0.07	0.16	5.6	0.2	1044	4	0.160	17
SHL5Z-5.1C	JW365	2008 Jan	0.02	0.05	0.08	1.1	***0.1***	594	1	0.010	7

SHL5Z-5.2T	JW365	2008 Jan	0.06	0.05	0.06	2.9	0.2	1728	6	0.005	27
SHL5Z-6.1C	***JW365***	***2008 Jan***	***0.19***	***0.06***	***1.74***	***287.1***	***0.2***	***1498***	***3***	***0.033***	***25***
SHL5Z-6.2T	JW365	2008 Jan	0.06	0.07	0.07	10.1	0.2	332	1	0.007	8
SHL5Z-7.1T	JW365	2008 Jan	0.04	0.05	0.07	5.1	0.2	883	3	0.030	13
SHL5Z-7.2C	JW365	2008 Jan	0.04	0.07	0.09	1.3	0.2	562	1	0.014	8
SHL5Z-8.1I	JW365	2008 Jan	0.12	0.07	0.07	3.4	0.1	1903	7	0.007	32
SHL5Z-8.2C	JW365	2008 Jan	0.06	0.09	0.08	5.6	0.3	491	1	0.008	7
SHL5Z-8.3T	JW365	2008 Jan	0.06	0.03	0.09	1.4	0.1	1050	3	0.006	16
SHL5Z-9.1T	JW365	2008 Jan	0.11	0.05	0.08	3.1	0.3	2063	9	0.013	37
SHL5Z-9.2I	JW365	2008 Jan	0.04	0.07	0.07	1.7	0.2	972	3	0.009	21
SHL5Z-9.3I	JW365	2008 Jan	0.13	0.06	0.06	7.7	0.2	2338	5	0.022	39
SHL0821Z-1.1E	JW414	2009 Jan	0.13	0.07	0.05	5.7	0.4	726	4	0.024	11
SHL0821Z-1.2C	***JW414***	***2009 Jan***	***0.09***	***0.07***	***0.21***	***9.8***	***0.2***	***597***	***3***	***0.074***	***9***
SHL0821Z-2.1E	JW414	2009 Jan	0.08	0.04	0.08	1.9	0.3	389	2	0.031	7
SHL0821Z-2.2I	JW414	2009 Jan	0.11	0.06	0.04	1.2	0.3	1165	6	0.011	17
SHL0821Z-3.1E	JW414	2009 Jan	0.05	0.04	0.05	2.4	0.2	560	3	0.059	16
SHL0821Z-3.2I	JW414	2009 Jan	0.01	0.06	0.05	1.1	0.2	239	1	0.016	4
SHL0821Z-4.1E	JW414	2009 Jan	0.05	0.06	0.05	1.0	0.1	435	1	0.004	7
SHL0821Z-4.2C	JW414	2009 Jan	0.03	0.06	0.04	0.9	0.2	481	1	0.012	6
SHL0821Z-5.1E	***JW414***	***2009 Jan***	***0.10***	***0.04***	***0.63***	***3.2***	***0.2***	***521***	***2***	***2.183***	***15***
SHL0821Z-5.2I	***JW414***	***2009 Jan***	***0.15***	***0.07***	***0.93***	***81***	***0.2***	***495***	***1***	***0.217***	***10***
SHL0821Z-6.1E	JW414	2009 Jan	0.11	0.07	0.02	0.5	0.2	475	1	0.007	11
SHL0821Z-6.2I	JW414	2009 Jan	0.78	0.06	0.03	0.7	0.2	1781	2	0.063	23
SHL0821Z-7.1C	JW414	2009 Jan	0.08	0.07	0.03	0.8	0.2	951	2	0.014	2
SHL0821Z-7.2I	JW414	2009 Jan	0.03	0.05	0.03	0.6	0.2	188	1	0.007	1
SHL0821Z-7.3R	JW414	2009 Jan	0.25	0.07	0.04	0.7	0.2	286	1	0.004	7
SHL0821Z-8.1C	***JW414***	***2009 Jan***	***0.06***	***0.07***	***0.36***	***113***	***0.1***	***990***	***3***	***0.135***	***15***
SHL0821Z-8.2I	JW414	2009 Jan	0.05	0.07	0.03	0.7	0.2	811	3	0.004	12
SHL0821Z-8.3I	JW414	2009 Jan	0.06	0.04	0.04	0.7	0.2	1555	12	0.009	27
SHL0821Z-9.1I	JW414	2009 Jan	0.76	0.03	0.04	0.4	0.2	1187	1	0.025	14
SHL0821Z-9.2E	JW414	2009 Jan	0.10	0.06	0.04	0.5	0.3	289	1	0.005	7

SHL0821Z-10.1I	JW414	2009 Jan	0.38	0.05	0.02	0.4	0.1	703	2	0.010	13
SHL0821Z-11.1E	JW414	2009 Jan	0.06	0.06	0.03	0.7	0.2	871	6	0.004	24
SHL0821Z-11.2C	JW414	2009 Jan	0.07	0.04	0.02	1.2	0.3	1202	2	0.014	13
SHL0821Z-12.1C	JW414	2009 Jan	0.14	0.09	0.09	4.9	0.2	1718	6	0.259	34
SHL0821Z-12.2E	JW414	2009 Jan	0.14	0.07	0.05	1.4	0.1	950	4	0.017	16
SHL0821Z-13.1C	JW414	2009 Jan	0.10	0.08	0.11	6.2	0.1	711	1	0.079	9
SHL0821Z-13.2I	JW414	2009 Jan	0.26	0.07	0.05	2.6	0.3	1616	4	0.013	31
SHL0821Z-13.3E	JW414	2009 Jan	0.06	0.06	0.04	2.7		192	2	0.004	6
SHL26C-1.1C	JW443	2009 Dec				2.3		989	4	0.024	13
SHL26-1.2R	JW443	2009 Dec				0.8		887	5	0.010	14
SHL-26C-2.1C	JW443	2009 Dec				1.8		600	5	0.010	6
SHL-26C-2.2R	JW443	2009 Dec				0.7		1063	4	0.020	16
SHL26C-3.1R	JW443	2009 Dec				2.2		1680	6	0.017	28
SHL26C-3.2C	JW443	2009 Dec				2.3		826	2	0.026	10
SHL26C-4.1C	***JW443***	***2009 Dec***				***3.1***		***236***	***1***	***0.040***	***5***
SHL26C-4.2T	JW443	2009 Dec				0.7		1304	10	0.018	33
SHL26C-5.1T	JW443	2009 Dec				3.5		861	4	0.194	17
SHL26C-5.2I	JW443	2009 Dec				0.8		689	2	0.023	9
SHL26C-5.3C	JW443	2009 Dec				0.8		550	2	0.022	7
SHL26C-6.1C	***JW443***	***2009 Dec***				***0.7***		***777***	***2***	***0.022***	***10***
SHL26C-6.2I	JW443	2009 Dec				1.1		864	4	0.026	15
SHL26c-7.1C	JW443	2009 Dec				1.7		478	2	0.023	7
SHL26C-7.2T	JW443	2009 Dec				0.7		887	4	0.019	13
SHL26C-8.1C	JW443	2009 Dec				0.8		958	3	0.026	13
SHL26C-8.2R	JW443	2009 Dec				0.7		602	3	0.027	8
SHL26C-9.1C	JW443	2009 Dec				3.2		2253	5	0.042	15
SHL26C-9.2I	JW443	2009 Dec				1.4		976	6	0.028	29
SHL26C-9.3R	JW443	2009 Dec				0.5		840	5	0.020	21
SHL26C-9.4R	JW443	2009 Dec				1.6		762	3	0.034	10
SHL26C-10.1C	JW443	2009 Dec				0.7		697	2	0.025	8
SHL26C-10.2I	JW443	2009 Dec				0.6		1093	4	0.018	14

SHL26c-10.3R	JW443	2009 Dec				1.0		1056	3	0.022	14
SHL26C-11.1C	JW443	2009 Dec				3.8		971	2	0.082	12
SHL26C-12.1C	JW443	2009 Dec				1.2		818	2	0.028	10
SHL26C-12.2I	JW443	2009 Dec				1.6		1232	6	0.031	21
SHL26C-13.1C	JW443	2009 Dec				1.2		575	2	0.032	7
SHL26c-13.2R	JW443	2009 Dec				1.3		607	2	0.042	8
SHL26C-14.2I	JW443	2009 Dec				4.1		3091	10	0.036	55
SHL26C-14.1I	JW443	2009 Dec				1.2		486	2	0.028	8
SHL26C-14.3R	JW443	2009 Dec				1.0		748	2	0.032	**11**
SHL26C-15.1I	JW443	2009 Dec				1.6		4042	21	0.043	52
SHL26C-15.2I	JW443	2009 Dec				1.4	0.3	837	3	0.025	13
SHL26C-15.3C	JW443	2009 Dec				1.5	0.2	731	2	0.023	10
SHL29AZ-1.1T	JW392	2008 Aug	0.04	0.11	0.09	1.5	0.3	832	4	0.012	12
SHL29AZ-1.2C	JW392	2008 Aug	2.17	0.07	0.16	38	0.3	3732	11	0.041	65
SHL29AZ-1.3I	JW392	2008 Aug	0.02	0.07	0.06	1.7	0.2	146	1	0.004	3
SHL29AZ-2.1E	JW392	2008 Aug	0.07	0.10	0.09	0.7	***0.3***	845	3	0.009	13
SHL29AZ-2.2E	JW392	2008 Aug	0.04	0.08	0.05	1.0	0.2	528	2	0.005	13
SHL29AZ-2.3I	***JW392***	***2008 Aug***	***0.59***	***0.11***	***0.61***	***249***	***0.3***	***834***	***1***	***0.092***	***11***
SHL29AZ-2.4I	JW392	2008 Aug	1.35	0.11	1.04	3.9	0.3	1628	1	0.040	15
SHL29AZ-3.1C	JW392	2008 Aug	0.09	0.08	0.09	3.9	0.3	836	3	0.024	15
SHL29AZ-3.2IE	JW392	2008 Aug	0.04	0.07	0.08	1.1	0.1	718	3	0.021	12
SHL29AZ-3.3IE	JW392	2008 Aug	0.12	0.08	0.08	1.7	0.3	1027	4	0.003	15
SHL29AZ-3.4E	JW392	2008 Aug	0.04	0.14	0.05	1.5	0.1	737	3	0.003	12
SHL29AZ-1.1C	JW393	2008 Aug	0.02	0.10	0.15	16.7	0.2	621	3	0.027	8
SHL29AZ-1.2E	JW393	2008 Aug	0.04	0.06	0.05	1.4	0.2	1153	5	0.003	21
SHL29AZ-2.1E	JW393	2008 Aug	0.07	0.07	0.07	0.6	0.2	739	3	0.003	10
SHL29AZ-2.2I	JW393	2008 Aug	0.14	0.08	0.09	8.0	0.2	1029	5	0.006	15
SHL29AZ-2.3C	JW393	2008 Aug	0.08	0.08	0.08	4.6	0.3	795	2	0.006	10
SHL29AZ-3.1C	JW393	2008 Aug	0.06	0.04	0.09	9.6	***0.3***	566	2	0.014	9
SHL29AZ-3.2C	JW393	2008 Aug	0.03	0.07	0.04	2.7	0.3	679	4	0.085	14

SHL29AZ-4.1C	***JW393***	***2008 Aug***	***0.07***	***0.07***	***0.80***	***127.6***	***0.3***	***863***	***5***	***0.167***	***14***
SHL29AZ-4.2E	JW393	2008 Aug	0.03	0.08	0.06	2.5	0.2	452	2	0.008	11
SHL29AZ-5.1C	JW393	2008 Aug	2.67	0.08	0.05	1.5	***0.3***	1620	2	0.082	13
SHL29AZ-5.2E	JW393	2008 Aug	0.05	0.07	0.07	2.2	0.2	791	4	0.026	14
SHL29AZ-6.1C	***JW393***	***2008 Aug***	***0.39***	***0.07***	***1.91***	***57.8***	***0.2***	***11621***	***29***	***0.701***	***232***
SHL29AZ-6.2E	JW393	2008 Aug	0.04	0.04	0.10	1.5	0.1	791	4	0.005	18
SHL29AZ-6.3I	JW393	2008 Aug	0.05	0.07	0.38	18.3	0.2	1122	4	0.024	17
SHL29AZ-7.1C	JW393	2008 Aug	0.15	0.10	0.16	26.5	0.2	926	2	0.028	10
SHL29AZ-7.2I	JW393	2008 Aug	0.11	0.08	0.03	4.0	0.1	1758	5	0.006	33
SHL29AZ-7.3E	JW393	2008 Aug	0.05	0.08	0.04	1.2	0.2	920	4	0.005	16
SHL29AZ-8.1C	JW393	2008 Aug	0.05	0.09	0.08	4.5	0.3	3355	6	0.011	41
SHL29AZ-8.2E	JW393	2008 Aug	0.05	0.07	0.04	1.9	0.2	1264	4	0.005	19
SHL29AZ-9.1C	JW393	2008 Aug	0.02	0.08	0.13	7.2		1065	4	0.055	16
SHL29AZ-9.2E	JW393	2008 Aug	0.09	0.08	0.05	1.2		988	5	0.011	15
SHL29Z-1.1C	***JW478***	***2010 May***				***10.8***		***2388***	***24***	***0.026***	***17***
SHL29Z-2.1I	JW478	2010 May				0.5		761	4	0.004	13
SHL29Z-3.1C	JW478	2010 May				0.5		452	2	0.001	7
SHL29Z-4.1C	***JW478***	***2010 May***				***2.3***		***859***	***4***	***0.003***	***17***
SHL29Z-5.1C	JW478	2010 May				0.4		797	3	0.004	10
SHL29Z-5.2E	JW478	2010 May				0.3		365	3	0.005	9
SHL29Z-6.1C	JW478	2010 May				0.5		585	2	0.002	9
SHL29Z-6.2I	JW478	2010 May				0.4		612	3	0.003	8
SHL29Z-7.1C	***JW478***	***2010 May***				***28.4***		***609***	***4***	***0.188***	***11***
SHL29Z-8.1C	***JW478***	***2010 May***				***56.4***		***383***	***4***	***0.009***	***5***
SHL29Z-8.2I	JW478	2010 May				0.3		500	4	0.003	6
SHL29Z-9.1C	JW478	2010 May				0.5		840	2	0.009	11
SHL29Z-10.1C	JW478	2010 May				0.8		823	2	0.004	10
SHL29Z-10.2I	JW478	2010 May				0.2		385	2	0.005	11
SHL29Z-11.1C	JW478	2010 May				3.8		456	2	0.003	5
SHL29Z-11.2I	JW478	2010 May				1.4		704	3	0.013	13
SHL29Z-12.1C	***JW478***	***2010 May***				***10.7***		***7326***	***10***	***0.103***	***106***
SHL29Z-13.1C	JW478	2010 May				0.5		1124	2	0.013	12

SHL29Z-14.1C	JW478	2010 May	31.6	562	3	0.244	9
SHL29Z-14.2I	JW478	2010 May	0.8	510	3	0.004	11
SHL29Z-15.1I	JW478	2010 May	1.8	672	3	0.006	10
SHL29Z-16.1I	JW478	2010 May	0.7	507	3	0.007	14
SHL30-1.1C	JW443	2009 Dec	2.1	347	2	0.038	6
SHL30-1.2R	JW443	2009 Dec	1.3	786	3	0.036	12
SHL30-2.1C	JW443	2009 Dec	1.6	1507	5	0.024	19
SHL30-2.2R	JW443	2009 Dec	1.7	987	6	0.037	20
SHL30-3.1C	JW443	2009 Dec	1.7	613	2	0.021	9
SHL30-3.2I	JW443	2009 Dec	2.4	835	3	0.027	13
SHL30-3.3I	JW443	2009 Dec	1.5	1199	5	0.022	16
SHL30-3.4R	***JW443***	***2009 Dec***	***2.9***	***925***	***5***	***0.030***	***21***
SHL30-4.1I	JW443	2009 Dec	1.5	209	1	0.036	4
SHL30-4.2C	JW443	2009 Dec	1.4	454	2	0.024	4
SHL30-4.3R	JW443	2009 Dec	1.1	864	3	0.037	11
SHL30-5.1C	JW443	2009 Dec	1.8	727	2	0.023	9
SHL30-5.2T	JW443	2009 Dec	7.0	809	4	0.028	22
SHL30-6.1I	JW443	2009 Dec	2.4	794	3	0.035	14
SHL30-7.1C	JW443	2009 Dec	2.7	857	2	0.026	**12**
SHL30-7.2R	JW443	2009 Dec	2.0	611	2	0.037	**8**
SHL30-7.3R	JW443	2009 Dec	1.4	1159	4	0.035	17
SHL30-8.1C	JW443	2009 Dec	11.2	6595	11	0.033	86
SHL30-8.2T	JW443	2009 Dec	2.0	300	2	0.024	7
SHL30-9.1C	JW443	2009 Dec	4.4	4930	10	0.041	74
SHL30-10.1C	JW443	2009 Dec	2.3	568	2	0.057	7
SHL30-10.2I	JW443	2009 Dec	2.2	580	2	0.037	10
SHL30-10.3R	JW443	2009 Dec	1.6	849	4	0.041	14
SHL30-12.1C	JW443	2009 Dec	1.6	546	1	0.035	7
SHL30-12.2I	JW443	2009 Dec	1.3	976	4	0.024	15
SHL30-11.1C	JW443	2009 Dec	1.3	882	2	0.034	13
SHL30-11.2T	***JW443***	***2009 Dec***	***6.2***	***962***	***4***	***0.028***	***16***

SHL30-13.1C	JW443	2009 Dec				2.2		1297	3	0.050	19
SHL30-13.2T	JW443	2009 Dec				3.7		1051	3	0.016	16
SHL30-14.1C	JW443	2009 Dec				1.1		709	1	0.029	9
SHL30-14.2T	JW443	2009 Dec				1.5		218	2	0.042	**5**
SHL33-1.1C	JW443	2009 Dec				5.4		5638	17	0.055	154
SHL33-1.2R	JW443	2009 Dec				2.4		1241	9	0.032	37
SHL33-2.1E	JW443	2009 Dec				1.8		464	2	0.038	9
SHL33-2.2I	JW443	2009 Dec				2.1		680	2	0.028	11
SHL33-3.1C	JW443	2009 Dec				11.9		5621	12	0.072	53
SHL33-3.2T	JW443	2009 Dec				2.2		373	2	0.026	10
SHL33-4.1T	JW443	2009 Dec				2.2	0.2	766	5	0.041	19
SHL33-4.2C	***JW443***	***2009 Dec***				***6.9***	***0.3***	***1505***	***4***	***1.306***	***225***
SHL34Z-1.1C	JW392	2008 Aug	0.03	0.04	0.04	0.7	0.1	622	2	0.011	7
SHL34Z-1.2I	JW392	2008 Aug	0.12	0.10	0.07	0.7	0.1	1414	6	0.000	21
SHL34Z-1.3E	JW392	2008 Aug	0.01	0.10	0.06	0.7	0.4	1468	8	0.025	23
SHL34Z-2.1I	JW392	2008 Aug	0.49	0.05	0.09	0.8	0.3	2368	3	0.058	29
SHL34Z-3.1I	JW392	2008 Aug	0.25	0.12	0.12	1.6	0.2	975	2	0.020	16
SHL34Z-3.2I	JW392	2008 Aug	0.07	0.10	0.07	1.1	0.3	335	1	0.010	7
SHL34Z-3.3E	JW392	2008 Aug	0.07	0.10	0.08	2.2	0.3	762	4	0.003	16
SHL34Z-4.1E	JW392	2008 Aug	0.04	0.03	0.16	6.4		1663	8	0.048	29
SHL34Z-4.2C	JW392	2008 Aug	0.60	0.07	0.05	0.8		1500	2	0.034	15
SHL34AZ-1.1I	JW393	2008 Aug	0.01	0.02	0.04	0.7	0.1	573	2	0.034	10
SHL34AZ-1.2E	JW393	2008 Aug	0.27	0.04	0.04	0.7	0.2	532	3	0.005	9
SHL34AZ-2.1E	JW393	2008 Aug	0.16	0.08	0.08	1.0	0.2	1107	6	0.005	22
SHL34AZ-2.2I	JW393	2008 Aug	0.12	0.08	0.07	1.1	0.1	1196	11	0.013	20
SHL34AZ-3.1E	JW393	2008 Aug	0.04	0.08	0.12	1.4	0.1	1212	4	0.008	18
SHL34AZ-3.2IE	JW393	2008 Aug	0.32	0.07	0.13	3.4	0.1	1278	2	0.070	16
SHL34AZ-3.3I	JW393	2008 Aug	0.36	0.06	0.07	0.5	0.3	301	1	0.005	6

SHL34AZ-4.1I	JW393	2008 Aug	0.03	0.06	0.11	1.8	0.1	1016	2	0.050	15
SHL34AZ-5.1I	JW393	2008 Aug	0.24	0.08	0.08	2.1	0.4	1316	7	0.049	24
SHL34AZ-6.2I	JW393	2008 Aug	0.46	0.07	0.06	0.6	0.2	2527	4	0.077	27
SHL34AZ-7.1I	JW393	2008 Aug	0.75	0.06	0.06	0.4	0.2	2296	3	0.072	33
SHL34AZ-7.2E	JW393	2008 Aug	0.43	0.06	0.09	1.2	0.1	1812	5	0.082	32
SHL34AZ-8.1I	JW393	2008 Aug	1.06	0.05	0.05	0.5	0.2	1880	3	0.042	17
SHL34AZ-9.1I	JW393	2008 Aug	0.19	0.06	0.13	2.8	0.2	764	2	0.083	22
SHL34AZ-10.1I	JW393	2008 Aug	0.03	0.09	0.10	0.9	0.2	820	7	0.016	18
SHL34AZ-11.1I	JW393	2008 Aug	0.20	0.06	0.18	4.6	0.2	1465	9	0.053	30
SHL34AZ-11.2E	JW393	2008 Aug	0.04	0.09	0.07	0.9	0.2	686	3	0.012	16
SHL34AZ-12.1I	JW393	2008 Aug	0.78	0.05	0.05	0.4	0.2	1789	3	0.049	20
SHL36E-1.1I	JW443	2009 Dec				1.6		965	4	0.014	14
SHL36E-1.2C	JW443	2009 Dec				5.0		751	2	0.033	**9**
SHL36E-1.3I	JW443	2009 Dec				1.3		1189	8	0.021	32
SHL36E-1.4R	JW443	2009 Dec				1.7		1104	6	0.019	14
SHL36E-2.1C	JW443	2009 Dec				1.8		2469	6	0.036	33
SHL36E-2.2T	JW443	2009 Dec				1.8		1212	5	0.031	20
SHL36E-3.1C	***JW443***	***2009 Dec***				***328***		***7270***	***31***	***0.060***	***125***
SHL36E-3.2I	JW443	2009 Dec				2.6		1506	5	0.023	32
SHL36E-3.3T	JW443	2009 Dec				3.2		1033	6	0.058	**25**
SHL36E-4.1C	JW443	2009 Dec				1.2		764	2	0.036	8
SHL36E-4.2T	JW443	2009 Dec				1.9		1081	4	0.026	15
SHL36E-5.1C	JW443	2009 Dec				2.3		682	2	0.027	6
SHL36E-6.1R	JW443	2009 Dec				2.1		1261	6	0.036	20
SHL36E-6.2C	JW443	2009 Dec				3.8		796	2	0.097	9
SHL36E-7.1I	JW443	2009 Dec				1.7		1228	6	0.022	18
SHL36E-7.2R	JW443	2009 Dec				1.8		877	5	0.033	13
SHL36E-8.1C	JW443	2009 Dec				1.6		1621	11	0.035	22
SHL36E-8.2R	JW443	2009 Dec				1.6		1055	7	0.041	29
SHL36E-9.1C	***JW443***	***2009 Dec***				***8.3***		***9596***	***19***	***0.057***	***194***
SHL36E-9.2R	JW443	2009 Dec				1.6		2310	29	0.027	24

SHL36E-10.1I	***JW443***	***2009 Dec***	***11.0***	***1613***	***5***	***0.161***	***22***
SHL36EX-11.1C	***JW443***	***2009 Dec***	***59.7***	***3488***	***6***	***0.042***	***9***
SHL36E-11.2I	JW443	2009 Dec	43.8	2032	5	0.054	9
SHL36E-11.3R	JW443	2009 Dec	1.7	1475	8	0.030	25
SHL36E-12.1C	JW443	2009 Dec	8.8	1318	4	0.047	13
SHL36E-12.2R	JW443	2009 Dec	1.9	846	2	0.024	10
SHL36E-12.3R	JW443	2009 Dec	2.0	1239	7	0.027	21
SHL36E-13.1I	JW443	2009 Dec	2.4	1683	6	0.030	73
SHL36E-13.2R	JW443	2009 Dec	2.8	827	3	0.022	13
SHL36E-14.2C	JW443	2009 Dec	6.3	6701	13	0.038	115
SHL36E-14.3I	JW443	2009 Dec	2.1	1496	5	0.038	23
SHL36E-14.1T	JW443	2009 Dec	3.3	1693	10	0.050	24
SHL37P-1.1C	JW443	2009 Dec	1.9	907	3	0.052	**13**
SHL37P-1.2I	JW443	2009 Dec	1.5	867	5	0.020	15
SHL37P-1.3R	JW443	2009 Dec	1.2	967	4	0.037	**16**
SHL37P-2.1C	JW443	2009 Dec	1.5	616	1	0.040	**7**
SHL37P-2.2I	JW443	2009 Dec	1.3	669	4	0.034	**12**
SHL37P-2.3R	JW443	2009 Dec	1.2	667	3	0.032	12
SHL37P-14.1C	JW443	2009 Dec	1.9	831	2	0.032	10
SHL37P-14.2R	JW443	2009 Dec	1.7	1423	6	0.023	26
SHL37P-3.1C	JW443	2009 Dec	1.4	1217	2	0.042	7
SHL37P-3.2I	***JW443***	***2009 Dec***	***11***	***345***	***1***	***0.032***	***6***
SHL37P-3.3R	JW443	2009 Dec	1.3	1105	6	0.024	19
SHL37P-4.1R	JW443	2009 Dec	2.7	2202	9	0.033	39
SHL37P-4.2C	JW443	2009 Dec	1.3	724	4	0.027	8
SHL37P-4.3I	JW443	2009 Dec	1.3	664	2	0.036	10
SHL37P-5.1C	JW443	2009 Dec	3.4	1736	10	0.067	31
SHL37P-5.2I	JW443	2009 Dec	2.7	979	6	0.057	29
SHL37P-5.3T	***JW443***	***2009 Dec***	***6.1***	***618***	***4***	***0.059***	***13***
SHL37P-6.1I	JW443	2009 Dec	1.5	870	3	0.036	11
SHL37P-6.2C	JW443	2009 Dec	2.1	868	2	0.024	9

SHL37P-6.3R	JW443	2009 Dec				1.4		713	3	0.023	11
SHL37P-7.1R	JW443	2009 Dec				1.5		650	2	0.026	8
SHL37P-7.2C	JW443	2009 Dec				1.4		1130	3	0.042	**16**
SHL37P-7.3T	JW443	2009 Dec				12		692	4	0.037	15
SHL37P-7.4C	JW443	2009 Dec				1.6		476	2	0.039	6
SHL37P-8.1I	JW443	2009 Dec				1.5		526	2	0.024	7
SHL37P-8.2C	***JW443***	***2009 Dec***				***14***		***15548***	***25***	***0.108***	***339***
SHL37P-8.3R	JW443	2009 Dec				1.7		1050	8	0.026	**19**
SHL37P-15.1C	JW443	2009 Dec				1.6		456	2	0.035	**6**
SHL37P-15.2T	JW443	2009 Dec				26		1126	5	0.038	18
SHL37P-9.2R	JW443	2009 Dec				1.4		633	4	0.028	17
SHL37P-9.1C	JW443	2009 Dec				6.4		600	1	0.056	30
SHL37P-10.2R	JW443	2009 Dec				1.4		727	3	0.017	11
SHL37P-10.1I	JW443	2009 Dec				2.2		362	2	0.038	5
SHL37P-11.1C	***JW443***	***2009 Dec***				***19***		***826***	***3***	***0.137***	***13***
SHL37P-11.2I	JW443	2009 Dec				1.5		1182	9	0.016	37
SHL37P-11.3I	JW443	2009 Dec				1.8		778	3	0.022	13
SHL37P-11.4R	***JW443***	***2009 Dec***				***454***		***1079***	***7***	***0.231***	***33***
SHL37P-12.1C	JW443	2009 Dec				2.0		912	3	0.036	11
SHL37P-12.2I	***JW443***	***2009 Dec***				***6.3***		***1259***	***14***	***0.047***	***29***
SHL37P-12.3T	JW443	2009 Dec				2.1		1019	7	0.041	17
SHL37P-13.1C	JW443	2009 Dec				3.8		2161	6	0.032	32
SHL37P-13.2T	JW443	2009 Dec				20		1005	5	0.086	24
SHL0849AZ-1.1I	JW414	2009 Jan	0.28	0.09	0.08	23.6	0.3	2565	7	0.102	24
SHL0849AZ-1.2E	JW414	2009 Jan	0.32	0.05	0.04	11.0	0.2	2119	5	0.051	21
SHL0849AZ-2.1E	JW414	2009 Jan	0.26	0.06	0.05	18.2	0.3	1766	5	0.053	20
SHL0849AZ-3.1E	JW414	2009 Jan	0.24	0.05	0.02	16.0	0.3	1797	5	0.059	21
SHL0849AZ-4.1E	JW414	2009 Jan	0.16	0.07	0.07	7.1	0.2	865	3	0.048	8
SHL0849AZ-4.2C	JW414	2009 Jan	0.23	0.08	0.05	9.7	0.2	1981	5	0.076	17
SHL0849AZ-4.3E	JW414	2009 Jan	0.26	0.09	0.03	6.8	0.3	1150	5	0.009	14
SHL0849AZ-5.1I	JW414	2009 Jan	0.20	0.06	0.04	11.0	0.3	1810	4	0.039	19

SHL0849AZ-6.1I	***JW414***	***2009 Jan***	***0.38***	***0.05***	***0.05***	***26.1***	***0.3***	***2886***	***8***	***0.086***	***30***
SHL0849AZ-7.1C	JW414	2009 Jan	0.28	0.06	0.06	51.4	0.2	2811	8	0.066	33
SHL0849AZ-8.1E	JW414	2009 Jan	0.53	0.07	0.05	34.4	0.3	2589	12	0.014	38
SHL0849AZ-9.1E	JW414	2009 Jan	0.36	0.07	0.04	31.0	0.1	2192	9	0.026	34
SHL0849AZ-9.2I	JW414	2009 Jan	0.10	0.05	0.05	18.6	0.3	1109	4	0.030	16
SHL0849AZ-10.1C	JW414	2009 Jan	0.26	0.05	0.05	21.8	0.3	1855	3	0.053	19
SHL0849AZ-11.1I	JW414	2009 Jan	0.09	0.06	0.03	1.3	0.3	442	2	0.009	6
SHL0849AZ-11.2E	JW414	2009 Jan	0.23	0.05	0.05	12.6	0.2	1192	3	0.034	13
SHL0849AZ-12.1E	JW414	2009 Jan	0.21	0.05	0.03	18.7	0.2	2239	6	0.069	24
SHL0849AZ-12.2C	***JW414***	***2009 Jan***	***0.31***	***0.11***	***0.05***	***22.7***	***0.3***	***1845***	***4***	***0.145***	***15***
SHL0849AZ-13.1E	JW414	2009 Jan	0.01	0.11	0.04	2.0	***0.1***	405	2	0.007	8
SHL0849AZ-13.2I	JW414	2009 Jan	0.02	0.04	0.02	1.2	0.5	563	3	0.005	16
SHL0849AZ-13.3C	***JW414***	***2009 Jan***	***0.09***	***0.07***	***0.28***	***62.1***	***0.3***	***1228***	***5***	***0.009***	***18***
SHL49AZ-14.1C	JW414	2009 Jan	0.34	0.07	0.04	26.2	0.2	3148	8	0.073	35
SHD9-1.1R	JW443	2009 Dec				2.9		335	3	0.036	8
SHD9-2.1R	JW443	2009 Dec				10.3		1289	5	0.053	20
SHD9-2.2C	JW443	2009 Dec				14.7		4964	11	0.044	45
SH325.2-1.1DGZT	JW309	2007 May	1.5		1.18	8.41	0.2	933	5	0.016	29
SH325.2-1.2MGZC	JW309	2007 May	1.8		0.67	11.22	0.2	792	2	0.014	9
SH325.2-1.3LGZI]	JW309	2007 May	4.4		0.82	10.97	0.2	693	3	0.019	10
SH325.2-2.1MGZC	JW309	2007 May	1.5		1.07	16.43	***0.3***	696	3	0.014	14
SH325.2-2.2LGZI	JW309	2007 May	0.7		1.86	5.79	0.2	304	1	0.012	6
SH325.2-3.1LGC	***JW309***	***2007 May***	***3.6***		***4.74***	***51.77***	***0.2***	***956***	***3***	***0.082***	***14***
SH325.2-3.2DGZE	JW309	2007 May	1.4		0.98	6.62	***0.1***	882	6	0.021	28
SH325.2-4.1DGZE	***JW309***	***2007 May***	***3.1***		***0.94***	***73.37***	***0.3***	***1793***	***8***	***0.030***	***32***
SH325.2-4.2MGC	***JW309***	***2007 May***	***6.8***		***3.82***	***52.42***	***0.3***	***1061***	***3***	***0.121***	***15***
SH325.2-5.1MGZE	JW309	2007 May	1.3		1.16	25.53	***0.3***	841	2	0.015	10
SH325.2-5.2DGZI	***JW309***	***2007 May***	***1.6***		***1.37***	***98.64***	***0.2***	***1106***	***2***	***0.019***	***13***
SH325.2-5.3DGZE	***JW309***	***2007 May***	***1.3***		***0.93***	***69.22***	***0.2***	***1073***	***7***	***0.012***	***21***

SH325.2-6.1MGT	JW309	2007 May	3.2		0.66	9.76	0.1	176	1	0.054	5
SH325.2-6.2MGI	JW309	2007 May	1.1		0.89	7.25	0.1	108	1	0.026	4
SH325.2-7.1LGZT	JW309	2007 May	2.1		0.85	2.72	0.2	936	4	0.005	21
SH325.2-7.2DGZT	JW309	2007 May	1.5		0.66	1.25	0.3	399	3	0.004	8
SH325.2-7.3LGZC	JW309	2007 May	3.5		1.39	11.49	0.2	960	5	0.030	16
SH325.2-8.1MGZE	JW309	2007 May	1.4		0.70	10.46	0.2	870	4	0.008	13
SH325.2-8.2MGZC	JW309	2007 May	21.1		2.60	39.48	0.2	1372	4	0.035	22
SH325.2-8.3DGZT	JW309	2007 May	1.2		0.77	2.31	0.2	599	3	0.020	15
SH325.2-9.1MGC	JW309	2007 May	2.4		1.74	5.27	***0.1***	876	2	0.062	12
SH325.2-10.1MGZI	JW309	2007 May	3.1		2.25	10.86	0.1	1535	5	0.018	21
SH325.2-11.1DGZE	***JW309***	***2007 May***	***187.5***		***168.59***	***252.38***	***0.7***	***1579***	***14***	***55.626***	***299***
SH325.2-11.1MGC	***JW309***	***2007 May***	***49.2***		***3.49***	***20.48***	***0.3***	***1183***	***5***	***3.649***	***74***
SH325.2-12.1MGZT	JW309	2007 May	5.4		0.65	0.72	0.3	779	8	0.008	76
SH325.2-12.2MGZI	***JW309***	***2007 May***	***4.2***		***7.40***	***2.24***	***0.2***	***413***	***3***	***13.974***	***70***
SH325.2-13.1DGZT	JW309	2007 May	7.2		0.74	2.18	0.3	502	8	0.016	76
SH325.2-13.1T	***JW309***	***2007 May***	***11.5***		***2.21***	***5.48***	***0.4***	***207***	***3***	***0.696***	***37***

Z484A-10.1C	JP04	2008 Jan	0.01	0.03	0.06	0.7	0.2	523	1	0.006	7
Z484A-10.2IR	JP04	2008 Jan	0.05	0.04	0.08	1.0	0.3	1457	9	0.003	19
Z484A-10.3T	JP04	2008 Jan	0.04	0.08	0.06	0.6	0.1	837	4	0.006	17
Z484A-12.1I	JP04	2008 Jan	0.76	0.05	0.07	0.8	0.2	1243	1	0.012	12
Z484A-12.2EM	JP04	2008 Jan	0.05	0.05	0.07	8.6	***0.1***	135	1	0.010	6
Z484A-12.3T	JP04	2008 Jan	0.05	0.06	0.06	0.7	0.2	263	1	0.007	6
Z484A-14.1C	***JP04***	***2008 Jan***	***0.32***	***0.07***	***0.19***	***6.5***	***0.3***	***8195***	***35***	***0.142***	***435***
Z484A-16.1C	JP04	2008 Jan	0.01	0.07	0.07	2.8	0.2	353	1	0.015	5
Z484A-16.2I	JP04	2008 Jan	0.05	0.05	0.08	0.8	0.2	1105	5	0.004	20
Z484A-17.1C	JP04	2008 Jan	0.10	0.04	0.13	26.8	0.1	1656	8	0.024	31
Z484A-17.2T	JP04	2008 Jan	0.06	0.04	0.05	0.6	0.2	788	5	0.010	22
Z484A-18.1C	JP04	2008 Jan	0.02	0.05	0.08	0.5	0.2	685	2	0.003	5
Z484A-18.2IR	JP04	2008 Jan	0.02	0.03	0.06	0.5	0.2	639	3	0.004	13
Z484A-19.1T	JP04	2008 Jan	0.06	0.07	0.06	0.5	0.2	594	3	0.008	11
Z484A-19.2C	JP04	2008 Jan	0.02	0.04	0.06	0.7	0.2	578	1	0.010	7

Z484A-19.3IR	JP04	2008 Jan	0.04	0.03	0.08	1.2	0.1	810	3	0.027	15
Z484A-19.4IR	JP04	2008 Jan	0.05	0.04	0.05	0.7	0.2	1062	6	0.007	21
Z484A-2.1T	JP04	2008 Jan	0.03	0.03	0.11	5.9	***0.2***	1097	3	0.103	20
Z484A-2.2C	JP04	2008 Jan	0.10	0.03	0.07	1.1	0.2	1301	7	0.003	26
Z484A-4.1I	***JP04***	***2008 Jan***	***0.65***	***0.04***	***0.75***	***24.4***	***0.1***	***12080***	***30***	***0.133***	***241***
Z484A-4.2T	JP04	2008 Jan	0.04	0.07	0.05	0.9	***0.2***	406	2	0.015	10
Z484A-5.1I	***JP04***	***2008 Jan***	***0.04***	***0.09***	***0.17***	***4.0***	***0.1***	***793***	***3***	***0.087***	***11***
Z484A-8.1I	***JP04***	***2008 Jan***	***0.23***	***0.06***	***4.74***	***214.8***	***0.2***	***9306***	***34***	***0.560***	***192***
Z484A-8.2I	JP04	2008 Jan	0.12	0.06	0.19	11.8	0.2	2722	11	0.041	53

Spot ID	Mount	Date Analyzed	Pr ppm	Nd ppm	Sm ppm	Eu ppm	Gd ppm	Tb ppm	Dy ppm	Ho ppm	Er ppm	Tm ppm	Yb ppm	Lu ppm
SHL3Z-1.1DI	JW414	2009 Jan	0.026	0.59	1.33	0.328	13	5.16	57	28	139	32	307	59
SHL3Z-1.2LC	JW414	2009 Jan	0.105	0.70	2.19	0.535	22	7.97	89	38	188	42	368	70
SHL3Z-1.3DI	JW414	2009 Jan	0.034	0.13	0.61	0.226	7	2.65	28	13	75	19	185	41
SHL3Z-1.4DR	JW414	2009 Jan	***0.018***	0.51	1.94	0.739	20	6.57	74	26	110	23	193	36
SHL3Z-2.1DC	JW414	2009 Jan	0.067	0.74	2.80	1.474	31	10.84	122	50	235	52	470	92
SHL3Z-2.2LR	***JW414***	***2009 Jan***	***0.060***	***0.30***	***1.43***	***0.735***	***19***	***7.38***	***97***	***36***	***170***	***40***	***347***	***67***
SHL3Z-3.1LC	***JW414***	***2009 Jan***	***0.117***	***0.66***	***1.72***	***1.500***	***15***	***4.71***	***55***	***22***	***94***	***22***	***182***	***37***
SHL3Z-3.2DI	JW414	2009 Jan	0.084	1.04	7.08	3.201	129	59.05	723	278	1230	249	1943	309
SHL3Z-3.3LR	JW414	2009 Jan	0.009	0.37	2.17	0.574	36	18.67	242	112	542	132	1202	218
SHL3Z-4.1LR	JW414	2009 Jan	0.051	0.33	1.25	0.722	20	8.22	103	42	209	50	446	89
SHL3Z-4.2LI	JW414	2009 Jan	0.058	0.28	1.00	0.711	13	5.03	54	25	125	30	278	58
SHL3Z-4.3LC	JW414	2009 Jan	0.025	0.17	0.94	0.537	13	6.24	79	34	165	40	352	67
SHL3Z-5.1DC	JW414	2009 Jan	0.017	0.07	0.28	0.133	5	2.60	23	8	24	4	29	4
SHL3Z-5.2LR	JW414	2009 Jan	***0.048***	0.51	1.91	1.024	23	8.04	84	33	154	33	297	58
SHL3Z-6.1DI	JW414	2009 Jan	0.074	0.34	2.18	0.937	26	9.94	123	42	192	41	345	65
SHL3Z-6.2LC	***JW414***	***2009 Jan***	***0.095***	***0.42***	***1.61***	***0.836***	***18***	***7.14***	***79***	***34***	***164***	***38***	***351***	***71***
SHL3Z-6.3DE	JW414	2009 Jan	0.044	0.35	1.39	0.703	15	5.79	71	29	122	28	248	48
SHL3Z-7.1LR	JW414	2009 Jan	0.047	0.12	0.90	0.374	11	4.97	64	23	112	24	212	41
SHL3Z-7.2DI	***JW414***	***2009 Jan***	***0.039***	***0.18***	***1.01***	***0.644***	***16***	***6.85***	***87***	***31***	***147***	***33***	***285***	***52***
SHL3Z-7.3LC	***JW414***	***2009 Jan***	***0.048***	***0.88***	***2.66***	***0.525***	***26***	***8.57***	***105***	***37***	***162***	***34***	***266***	***45***
SHL3Z-8.1LC	JW414	2009 Jan	***0.063***	0.34	1.39	0.779	16	6.66	86	34	180	42	386	78
SHL3Z-8.2I	JW414	2009 Jan	0.032	0.27	1.87	0.781	29	11.80	138	59	280	64	527	97
SHL3Z-8.3LC	***JW414***	***2009 Jan***	***0.049***	***0.41***	***1.73***	***1.213***	***22***	***9.34***	***130***	***48***	***247***	***57***	***498***	***96***
SHL3Z-8.4DI	***JW414***	***2009 Jan***	***0.106***	***0.59***	***2.09***	***1.003***	***31***	***12.84***	***159***	***59***	***280***	***60***	***489***	***88***
SHL3Z-9.1DI	JW414	2009 Jan	0.032	0.30	0.74	0.286	7	3.17	46	22	126	32	329	68
SHL3Z-9.2LC	JW414	2009 Jan	0.143	0.77	2.16	0.917	20	7.62	90	35	165	39	325	63
SHL3Z-9.3LI	JW414	2009 Jan	0.041	0.48	2.04	0.888	25	10.07	120	51	249	57	498	94
MSHL3Z-1.1DGI	JW309	2007	0.341	8.71	24.37	15.473	219	71.37	714	261	932	174	1304	218

		May 2007												
MSHL3Z-1.2MGI	JW309	May	0.040	0.36	1.32	0.705	16	6.62	82	35	168	38	346	67
		2007												
MSHL3Z-2.1MGZC	***JW309***	***May***	***0.034***	***0.53***	***2.14***	***1.045***	***26***	***10.23***	***121***	***51***	***225***	***50***	***432***	***82***
		2007												
MSHL3Z-2.2DGZI	JW309	May	0.072	0.43	1.75	0.980	17	5.81	65	27	119	27	240	49
		2007												
MSHL3Z-3.1DGZT	JW309	May	0.068	0.55	1.96	1.223	23	7.88	89	36	159	35	306	59
		2007												
MSHL3Z-3.2LGZE	JW309	May	0.076	0.20	1.03	0.646	13	5.20	63	28	134	31	287	59
		2007												
MSHL3Z-3.3DGC	JW309	May	0.108	1.16	4.91	2.229	52	18.37	179	67	262	52	437	79
		2007												
MSHL3Z-4.1MGI	JW309	May	0.073	0.46	1.34	1.082	17	6.31	74	31	152	34	322	66
		2007												
MSHL4Z-1.1DGZE	JW309	May	0.083	0.40	1.45	0.812	16	5.46	59	23	110	24	217	43
		2007												
MSHL4Z-1.2MGZI	JW309	May	0.087	0.56	1.56	1.074	18	6.66	78	33	160	36	325	69
		2007												
MSHL4Z-10.1MGT	JW309	May	0.061	0.54	1.90	1.275	22	8.09	93	39	177	40	339	69
		2007												
MSHL4Z-10.2MGZC	JW309	May	0.094	0.59	1.70	0.903	15	5.50	61	25	122	28	263	55
		2007												
MSHL4Z-10.3DGZIT	JW309	May	0.090	1.21	4.60	3.123	59	20.74	233	91	395	82	686	131
		2007												
MSHL4Z-11.1DGZI	JW309	May	0.084	0.41	1.27	0.854	14	5.21	63	27	128	30	273	57
		2007												
MSHL4Z-11.2DZIT	JW309	May	0.072	0.66	2.18	1.581	30	11.41	133	55	254	55	477	95
		2007												
MSHL4Z-12.1MGI	JW309	May	0.104	0.18	0.55	0.373	6	2.24	26	12	56	14	138	31
		2007												
MSHL4Z-2.1DGZI	JW309	May	0.069	0.26	0.81	0.532	9	3.26	37	16	75	17	163	35

MSHL4Z-2.2MGZI	JW309	2007 May 2007	0.059	0.48	1.46	0.858	18	6.92	84	36	174	40	352	73
MSHL4Z-2.3DGZE	JW309	May 2007	0.047	0.30	1.05	0.535	12	4.35	52	22	104	23	210	43
MSHL4Z-3.1DGZT	JW309	May 2007	0.041	0.67	2.28	1.296	25	9.35	112	49	229	52	470	96
MSHL4Z-3.2MGZE	JW309	May 2007	0.097	0.64	1.97	0.991	19	6.86	78	33	156	35	317	65
MSHL4Z-10.2MGZC	JW309	May 2007	0.094	0.59	1.70	0.903	15	5.50	61	25	122	28	263	55
MSHL4Z-10.3DGZIT	JW309	May 2007	0.090	1.21	4.60	3.123	59	20.74	233	91	395	82	686	131
MSHL4Z-11.1DGZI	JW309	May 2007	0.084	0.41	1.27	0.854	14	5.21	63	27	128	30	273	57
MSHL4Z-5.1DGZT	JW309	May 2007	0.063	0.27	0.83	0.502	11	3.89	47	19	91	20	184	38
MSHL4Z-5.2MGZE	JW309	May 2007	0.059	0.47	1.49	0.711	16	6.35	77	35	161	38	344	72
MSHL4Z-5.3MGI	JW309	May 2007	0.063	0.07	0.27	0.162	3	1.38	16	7	36	9	83	17
MSHL4Z-6.1MGT	JW309	May 2007	0.076	0.42	1.58	0.854	19	7.09	84	34	162	37	326	65
MSHL4Z-6.2MGI	JW309	May 2007	0.049	0.23	0.83	0.553	7	2.79	33	15	73	18	173	40
MSHL4Z-7.1MGZT	JW309	May 2007	0.205	1.12	2.50	1.762	25	8.57	97	39	171	37	327	66
MSHL4Z-7.2LGC	JW309	May 2007	0.095	2.08	4.45	3.075	33	10.63	117	47	219	49	442	93
MSHL4Z-7.3DGI	JW309	May 2007	0.124	1.74	6.67	5.181	71	22.72	233	87	370	76	639	120
MSHL4Z-8.1MGZT	JW309	May 2007	0.098	0.40	1.61	0.810	19	6.93	79	33	152	33	303	59
MSHL4Z-8.2DGZI	JW309	May	0.084	0.32	1.83	0.979	18	6.35	71	30	144	33	310	61
MSHL4Z-8.3MGZI	JW309	2007	0.063	0.39	1.17	0.597	12	4.54	57	24	121	28	278	57

MSHL4Z-9.1MGZT	JW309	May 2007 May 2007	0.079	0.55	1.77	1.038	22	8.06	101	43	212	49	453	92
MSHL4Z-9.2LGC	JW309	May 2007	0.043	0.36	1.40	0.671	15	5.65	68	29	138	33	296	61
MSHL4Z-9.3MGZT	JW309	May	0.088	0.43	1.42	0.860	15	5.52	63	27	126	29	261	53
SHL5Z-1.1C	JW364	2008 Jan	0.028	0.49	2.17	1.107	28	9.97	111	41	200	44	180	37
SHL5Z-2.1I	JW364	2008 Jan	0.101	0.54	0.93	0.551	22	7.05	71	10	109	23	195	35
SHL5Z-2.2T	JW364	2008 Jan	0.037	0.53	2.05	1.199	24	9.20	112	42	224	50	449	86
SHL5Z-3.1C	JW364	2008 Jan	0.042	0.55	1.65	1.047	17	6.05	70	27	144	33	316	65
SHL5Z-3.2E	JW364	2008 Jan	0.038	0.54	1.90	1.074	22	8.29	99	36	196	46	405	79
SHL5Z-4.1C	JW364	2008 Jan	0.054	0.89	2.91	1.948	29	9.82	112	40	212	48	441	87
SHL5Z-4.2T	JW364	2008 Jan	***0.025***	0.36	1.34	0.804	16	5.95	72	26	140	32	283	55
SHL5Z-5.1T	JW364	2008 Jan	***0.022***	0.41	1.64	0.877	18	6.26	67	24	109	24	201	38
SHL5Z-5.2C	***JW364***	***2008 Jan***	***1.911***	***30.66***	***57.41***	***28.788***	***361***	***96.32***	***869***	***282***	***1107***	***211***	***1597***	***257***
SHL5Z-6.1C	***JW364***	***2008 Jan***	***1.114***	***25.34***	***79.45***	***45.684***	***756***	***215.76***	***2011***	***590***	***2320***	***419***	***3009***	***473***
SHL5Z-6.2T	JW364	2008 Jan	***0.013***	0.29	0.91	0.475	11	4.21	49	20	97	22	197	39
SHL5Z-6.3I	JW364	2008 Jan	0.013	0.35	1.48	0.845	18	6.74	80	30	162	38	347	68
SHL5Z-7.1C	***JW364***	***2008 Jan***	***0.079***	***0.84***	***2.03***	***1.115***	***17***	***6.05***	***69***	***25***	***127***	***30***	***271***	***54***
SHL5Z-7.2T	JW364	2008 Jan	0.019	0.30	1.28	0.627	16	5.59	63	23	108	24	213	40
SHL5Z-8.1T	JW364	2008 Jan	0.090	0.35	1.21	0.726	13	4.40	55	21	115	27	243	50
SHL5Z-8.2C	JW364	2008 Jan	0.083	0.79	2.17	1.509	20	7.04	84	34	173	40	370	77
SHL5Z-1.1T	JW365	2008 Jan	0.023	0.26	1.16	0.584	12	3.94	46	19	87	19		
SHL5Z-1.2I	***JW365***	***2008 Jan***	***0.087***	***1.15***	***3.34***	***1.461***	***30***	***10.23***	***111***	***44***	***196***	***43***	***373***	***74***
SHL5Z-2.1C	JW365	2008 Jan	0.024	0.45	1.93	0.953	23	7.97	92	37	169	37	328	67
SHL5Z-2.2E	JW365	2008 Jan	0.021	0.44	1.29	0.671	12	4.59	53	24	110	24	215	46
SHL5Z-3.1C	JW365	2008 Jan	0.015	0.31	1.15	0.689	11	3.81	47	19	96	22	204	44
SHL5Z-3.2R	JW365	2008 Jan	0.031	0.47	1.56	0.962	17	6.54	80	35	169	39	347	73
SHL5Z-4.1C	JW365	2008 Jan	0.153	3.16	7.60	3.453	65	20.94	219	78	345	71	593	111
SHL5Z-4.2T	JW365	2008 Jan	0.044	0.65	2.15	1.153	24	9.21	110	42	207	45	388	74

SHL5Z-5.1C	JW365	2008 Jan	***0.026***	0.31	1.14	0.572	11	4.35	50	21	102	23	212	42
SHL5Z-5.2T	JW365	2008 Jan	0.051	0.93	3.18	2.104	43	15.44	182	69	335	71	610	118
SHL5Z-6.1C	***JW365***	***2008 Jan***	***0.136***	***1.93***	***5.01***	***3.409***	***42***	***13.87***	***151***	***56***	***273***	***60***	***522***	***103***
SHL5Z-6.2T	JW365	2008 Jan	0.016	0.23	0.70	0.421	8	2.65	29	12	54	12	106	22
SHL5Z-7.1T	JW365	2008 Jan	0.019	0.39	1.56	0.856	19	6.82	80	33	153	34	288	58
SHL5Z-7.2C	JW365	2008 Jan	0.024	0.38	1.40	0.851	16	5.66	65	25	129	30	277	59
SHL5Z-8.1I	JW365	2008 Jan	0.041	0.88	3.12	1.818	39	14.52	168	72	311	65	548	106
SHL5Z-8.2C	JW365	2008 Jan	0.019	0.24	0.83	0.493	9	3.48	40	18	88	21	197	43
SHL5Z-8.3T	JW365	2008 Jan	0.032	0.47	1.86	1.139	22	8.16	97	40	184	40	351	70
SHL5Z-9.1T	JW365	2008 Jan	0.054	0.92	3.29	1.938	41	15.60	193	79	351	76	640	123
SHL5Z-9.2I	JW365	2008 Jan	0.026	0.64	2.23	1.302	25	8.91	108	43	210	47	419	84
SHL5Z-9.3I	JW365	2008 Jan	0.031	1.77	5.64	3.752	60	21.01	243	95	459	99	867	175
SHL0821Z-1.1E	JW414	2009 Jan	0.058	0.39	1.04	0.631	12	4.77	52	25	114	27	239	48
SHL0821Z-1.2C	***JW414***	***2009 Jan***	***0.032***	***0.34***	***0.96***	***0.499***	***11***	***4.40***	***52***	***22***	***115***	***27***	***250***	***52***
SHL0821Z-2.1E	JW414	2009 Jan	0.033	0.27	0.80	0.386	8	2.89	33	14	64	15	141	29
SHL0821Z-2.2I	JW414	2009 Jan	0.039	0.51	2.03	0.891	21	7.97	104	42	212	50	467	94
SHL0821Z-3.1E	JW414	2009 Jan	0.039	0.54	1.42	0.675	13	4.48	49	19	94	22	203	41
SHL0821Z-3.2I	JW414	2009 Jan	0.031	0.08	0.42	0.241	4	1.60	23	9	45	12	114	26
SHL0821Z-4.1E	JW414	2009 Jan	0.077	0.39	0.93	0.403	9	3.40	41	16	78	19	165	34
SHL0821Z-4.2C	JW414	2009 Jan	0.072	0.23	0.71	0.536	10	3.78	44	17	89	22	210	43
SHL0821Z-5.1E	***JW414***	***2009 Jan***	***0.347***	***2.35***	***1.54***	***0.730***	***13***	***4.27***	***47***	***20***	***97***	***22***	***206***	***42***
SHL0821Z-5.2I	***JW414***	***2009 Jan***	***0.097***	***0.91***	***1.86***	***1.049***	***15***	***4.50***	***46***	***18***	***85***	***20***	***173***	***34***
SHL0821Z-6.1E	JW414	2009 Jan	0.081	0.41	0.98	0.589	10	3.69	42	17	78	18	161	32
SHL0821Z-6.2I	JW414	2009 Jan	0.215	3.59	7.71	3.694	66	19.43	175	72	287	55	433	77
SHL0821Z-7.1C	JW414	2009 Jan	0.065	1.14	2.86	0.406	21	7.27	88	34	168	38	332	63
SHL0821Z-7.2I	JW414	2009 Jan	0.031	0.08	0.36	0.084	3	1.29	17	7	36	8	80	17
SHL0821Z-7.3R	JW414	2009 Jan	0.084	0.20	0.64	0.401	8	2.57	30	11	52	11	96	17
SHL0821Z-8.1C	***JW414***	***2009 Jan***	***0.039***	***0.51***	***1.56***	***0.803***	***21***	***8.15***	***90***	***41***	***197***	***45***	***399***	***79***
SHL0821Z-8.2I	JW414	2009 Jan	0.038	0.41	1.38	0.935	15	5.71	69	30	148	34	313	64
SHL0821Z-8.3I	JW414	2009 Jan	0.070	0.53	2.13	0.752	26	10.83	133	59	296	69	611	116
SHL0821Z-9.1I	JW414	2009 Jan	0.159	2.25	5.34	2.468	42	12.91	135	49	197	39	308	55

SHL0821Z-9.2E	JW414	2009 Jan	0.039	0.16	0.63	0.371	5	1.83	25	11	47	12	105	23
SHL0821Z-10.1I	JW414	2009 Jan	0.065	0.53	1.75	0.842	16	5.56	61	28	118	25	218	41
SHL0821Z-11.1E	JW414	2009 Jan	0.046	0.43	1.92	0.887	21	7.30	84	33	152	35	310	60
SHL0821Z-11.2C	JW414	2009 Jan	0.040	0.80	2.43	1.346	22	8.68	104	44	203	46	426	88
SHL0821Z-12.1C	JW414	2009 Jan	0.993	14.26	18.59	11.434	92	24.09	219	66	263	52	419	75
SHL0821Z-12.2E	JW414	2009 Jan	0.052	0.57	1.46	0.997	18	7.42	89	36	173	38	336	67
SHL0821Z-13.1C	JW414	2009 Jan	0.062	0.35	1.26	0.658	13	5.18	63	26	125	29	260	51
SHL0821Z-13.2I	JW414	2009 Jan	0.050	1.60	3.55	2.088	38	13.42	160	60	274	60	501	97
SHL0821Z-13.3E	JW414	2009 Jan		0.61	1.15	0.957	10	2.60	23	7	30	6	54	10
SHL26C-1.1C	JW443	2009 Dec		0.48	1.65	0.851	17		72		144		266	52
SHL26-1.2R	JW443	2009 Dec		0.50	1.63	0.899	20		89		177		339	64
SHL-26C-2.1C	JW443	2009 Dec		0.04	0.52	0.225	7		36		77		168	35
SHL-26C-2.2R	JW443	2009 Dec		0.37	1.64	0.924	17		84		177		371	79
SHL26C-3.1R	JW443	2009 Dec		0.94	2.93	2.440	39		138		240		451	90
SHL26C-3.2C	JW443	2009 Dec		0.80	2.06	1.238	15		70		130		280	59
SHL26C-4.1C	***JW443***	***2009 Dec***		***0.15***	***0.40***	***0.287***	***5***		***21***		***45***		***118***	***25***
SHL26C-4.2T	JW443	2009 Dec		0.54	2.38	1.230	28		128		222		429	81
SHL26C-5.1T	JW443	2009 Dec		1.50	1.77	0.871	17		68		135		274	55
SHL26C-5.2I	JW443	2009 Dec		0.29	1.33	0.783	13		63		137		291	59
SHL26C-5.3C	JW443	2009 Dec		0.29	1.07	0.632	10		45		99		225	48
SHL26C-6.1C	***JW443***	***2009 Dec***		***0.42***	***1.41***	***0.880***	***19***		***80***		***162***		***340***	***71***
SHL26C-6.2I	JW443	2009 Dec		0.50	1.43	0.787	16		71		150		329	70
SHL26c-7.1C	JW443	2009 Dec		0.27	0.80	0.487	8		38		78		179	36
SHL26C-7.2T	JW443	2009 Dec		0.37	1.40	0.824	16		79		157		334	69
SHL26C-8.1C	JW443	2009 Dec		0.69	2.23	1.328	21		75		139		272	53
SHL26C-8.2R	JW443	2009 Dec		0.19	1.05	0.479	13		52		106		227	46
SHL26C-9.1C	JW443	2009 Dec		1.87	5.55	2.712	70		225		307		468	86
SHL26C-9.2I	JW443	2009 Dec		0.60	2.48	1.525	24		92		163		326	65
SHL26C-9.3R	JW443	2009 Dec		0.44	1.46	0.695	20		67		135		282	60
SHL26C-9.4R	JW443	2009 Dec		0.27	1.11	**0.480**	13		57		112		226	46
SHL26C-10.1C	JW443	2009 Dec		0.28	1.16	0.643	12		60		123		286	59

SHL26C-10.2I	JW443	2009 Dec		0.42	1.72	1.078	20		99		199	440	84
SHL26c-10.3R	JW443	2009 Dec		0.46	1.76	1.086	17		91		190	385	78
SHL26C-11.1C	JW443	2009 Dec		0.72	2.49	1.339	24		97		187	368	73
SHL26C-12.1C	JW443	2009 Dec		0.38	1.23	0.733	13		63		132	300	62
SHL26C-12.2I	JW443	2009 Dec		0.40	1.76	0.996	19		104		217	477	95
SHL26C-13.1C	JW443	2009 Dec		0.36	1.08	0.839	13		65		135	302	62
SHL26c-13.2R	JW443	2009 Dec		0.26	1.07	0.624	11		50		108	240	51
SHL26C-14.2I	JW443	2009 Dec		1.63	6.89	5.139	78		339		551	980	181
SHL26C-14.1I	JW443	2009 Dec		0.21	0.87	0.509	10		52		117	272	57
SHL26C-14.3R	JW443	2009 Dec		0.31	1.45	**0.870**	**14**		**70**		137	314	60
SHL26C-15.1I	JW443	2009 Dec		1.67	9.55	2.567	112		467		742	1231	207
SHL26C-15.2I	JW443	2009 Dec	0.091	0.42	1.43	0.980	15		78		157	339	70
SHL26C-15.3C	JW443	2009 Dec	0.038	0.38	1.27	0.823	13		67		136	326	66
SHL29AZ-1.1T	JW392	2008 Aug	0.048	0.40	1.55	0.705	17	6.11	70	29	133	30	
SHL29AZ-1.2C	JW392	2008 Aug	0.124	3.34	9.58	6.605	89	31.37	341	127	528	106	891	149
SHL29AZ-1.3I	JW392	2008 Aug	0.009	0.05	0.18	0.110	2	0.87	11	5	26	7	62	14
SHL29AZ-2.1E	JW392	2008 Aug	***0.036***	0.41	1.20	0.813	14	5.65	67	31	150	35	332	68
SHL29AZ-2.2E	JW392	2008 Aug	0.028	0.27	1.16	0.639	12	4.43	48	19	92	20	177	36
SHL29AZ-2.3I	***JW392***	***2008 Aug***	***0.031***	***0.57***	***1.79***	***0.221***	***17***	***6.66***	***80***	***32***	***139***	***29***	***225***	***39***
SHL29AZ-2.4I	JW392	2008 Aug	0.110	2.35	5.97	0.649	49	16.72	174	65	278	53	402	67
SHL29AZ-3.1C	JW392	2008 Aug	0.013	0.32	1.20	0.708	14	6.01	72	31	156	37	337	69
SHL29AZ-3.2IE	JW392	2008 Aug	0.058	0.32	1.14	0.655	12	4.33	57	25	125	29	277	59
SHL29AZ-3.3IE	JW392	2008 Aug	0.020	0.37	1.68	1.051	19	7.86	97	40	195	43	382	75
SHL29AZ-3.4E	JW392	2008 Aug	0.111	0.46	1.46	0.771	15	5.98	68	28	133	30	272	52
SHL29AZ-1.1C	JW393	2008 Aug	0.063	0.24	0.79	0.502	11	4.03	52	22	111	26	269	57
SHL29AZ-1.2E	JW393	2008 Aug	0.110	0.66	1.79	1.231	23	8.46	101	41	199	46	418	86
SHL29AZ-2.1E	JW393	2008 Aug	0.047	0.45	1.13	0.725	14	5.19	62	27	135	30	270	59
SHL29AZ-2.2I	JW393	2008 Aug	0.110	0.40	1.56	0.843	18	7.61	92	39	190	45	406	80
SHL29AZ-2.3C	JW393	2008 Aug	0.059	0.42	1.36	0.689	16	6.05	72	29	133	32	270	55
SHL29AZ-3.1C	JW393	2008 Aug	***0.046***	0.31	1.03	0.601	10	3.85	47	20	106	27	258	54

SHL29AZ-3.2C	JW393	2008 Aug	0.112	0.41	1.28	0.657	14	5.36	64	26	120	27	248	50
SHL29AZ-4.1C	***JW393***	***2008 Aug***	***0.105***	***0.42***	***1.44***	***0.694***	***16***	***6.36***	***79***	***32***	***160***	***37***	***335***	***69***
SHL29AZ-4.2E	JW393	2008 Aug	0.059	0.29	0.84	0.591	10	3.46	39	16	78	18	166	36
SHL29AZ-5.1C	JW393	2008 Aug	***0.225***	3.06	5.55	1.002	44	14.79	164	63	267	51	393	69
SHL29AZ-5.2E	JW393	2008 Aug	0.086	0.34	1.45	0.842	16	6.57	70	29	148	33	308	63
SHL29AZ-6.1C	***JW393***	***2008 Aug***	***1.502***	***36.24***	***86.16***	***40.038***	***645***	***172.80***	***1526***	***464***	***1685***	***296***	***2127***	***353***
SHL29AZ-6.2E	JW393	2008 Aug	0.085	0.40	1.79	0.943	19	6.79	75	29	137	31	263	52
SHL29AZ-6.3I	JW393	2008 Aug	0.065	0.74	2.48	1.205	26	8.96	101	41	191	43	388	77
SHL29AZ-7.1C	JW393	2008 Aug	0.099	0.59	2.07	1.424	20	7.88	96	38	215	53	513	110
SHL29AZ-7.2I	JW393	2008 Aug	0.070	0.93	3.45	2.833	39	14.13	163	63	302	65	586	113
SHL29AZ-7.3E	JW393	2008 Aug	0.093	0.39	1.26	0.829	15	6.18	76	33	164	39	354	76
SHL29AZ-8.1C	JW393	2008 Aug	0.210	2.88	9.98	5.820	99	33.41	341	121	484	95	755	136
SHL29AZ-8.2E	JW393	2008 Aug	0.088	0.66	2.26	1.277	24	9.49	112	47	218	48	424	86
SHL29AZ-9.1C	JW393	2008 Aug		0.68	1.79	1.142	21	8.07	93	39	187	43	381	77
SHL29AZ-9.2E	JW393	2008 Aug		0.53	1.65	0.908	19	7.25	88	36	178	40	375	75
SHL29Z-1.1C	***JW478***	***2010 May***		***0.56***	***2.42***	***0.520***	***35***	***16.46***	***217***	***90***	***444***	***107***		
SHL29Z-2.1I	JW478	2010 May		0.41	1.28	0.713	16	5.46	66	28	131	32	280	59
SHL29Z-3.1C	JW478	2010 May		0.24	0.86	0.618	9	3.13	40	16	89	21	203	44
SHL29Z-4.1C	***JW478***	***2010 May***		***0.58***	***1.55***	***0.928***	***17***	***6.26***	***71***	***30***	***149***	***36***	***322***	***68***
SHL29Z-5.1C	JW478	2010 May		0.32	1.07	0.638	14	5.41	62	27	136	31	299	63
SHL29Z-5.2E	JW478	2010 May		0.16	0.73	0.341	8	2.88	31	13	62	14	128	26
SHL29Z-6.1C	JW478	2010 May		0.30	1.00	0.788	10	3.96	49	21	106	26	251	56
SHL29Z-6.2I	JW478	2010 May		0.37	1.04	0.678	11	4.58	54	23	110	25	232	48
SHL29Z-7.1C	***JW478***	***2010 May***		***0.85***	***1.24***	***0.656***	***11***	***4.19***	***51***	***21***	***107***	***25***	***246***	***53***

SHL29Z-8.1C	***JW478***	***2010 May***	***0.19***	***0.67***	***0.418***	***7***	***2.54***	***30***	***13***	***69***	***18***	***181***	***42***
SHL29Z-8.2I	JW478	2010 May	0.13	0.62	0.426	8	3.17	43	18	95	23	219	47
SHL29Z-9.1C	JW478	2010 May	0.40	1.21	0.715	14	5.17	62	28	131	31	303	63
SHL29Z-10.1C	JW478	2010 May	0.43	1.45	0.929	15	5.46	66	28	140	33	310	66
SHL29Z-10.2I	JW478	2010 May	0.17	0.69	0.433	8	3.00	35	14	68	16	148	32
SHL29Z-11.1C	JW478	2010 May	0.24	0.68	0.454	9	3.09	39	17	87	21	204	45
SHL29Z-11.2I	JW478	2010 May	0.37	1.23	0.809	13	4.88	58	25	127	30	276	59
SHL29Z-12.1C	***JW478***	***2010 May***	***36.77***	***68.50***	***35.024***	***420***	***106.94***	***927***	***291***	***1064***	***198***	***1513***	***254***
SHL29Z-13.1C	JW478	2010 May	1.68	3.94	0.771	34	10.69	115	45	187	39	301	54
SHL29Z-14.1C	JW478	2010 May	0.62	0.98	0.629	12	4.05	48	22	108	27	246	54
SHL29Z-14.2I	JW478	2010 May	0.35	0.83	0.541	10	3.76	47	19	99	24	234	49
SHL29Z-15.1I	JW478	2010 May	0.37	1.09	0.800	12	4.83	58	24	115	26	237	50
SHL29Z-16.1I	JW478	2010 May	0.27	1.18	0.740	13	4.26	50	19	87	20	179	37
SHL30-1.1C	JW443	2009 Dec	0.18	0.54	0.333	7		34		78		173	37
SHL30-1.2R	JW443	2009 Dec	0.26	1.26	0.902	13		74		154		346	68
SHL30-2.1C	JW443	2009 Dec	0.68	2.54	1.571	28		145		270		550	105
SHL30-2.2R	JW443	2009 Dec	0.46	1.90	1.040	22		94		172		345	65
SHL30-3.1C	JW443	2009 Dec	0.23	0.94	0.554	9		50		107		260	54
SHL30-3.2I	JW443	2009 Dec	0.46	1.68	**0.935**	20		88		166		339	67

SHL30-3.3I	JW443	2009 Dec	0.52	2.52	1.272	23	121	237	488	94
SHL30-3.4R	***JW443***	***2009 Dec***	***0.38***	***1.95***	***0.921***	***19***	***94***	***166***	***342***	***66***
SHL30-4.1I	JW443	2009 Dec	0.07	0.35	0.270	3	20	44	112	23
SHL30-4.2C	JW443	2009 Dec	0.18	0.72	0.490	8	43	87	208	45
SHL30-4.3R	JW443	2009 Dec	0.38	1.42	0.892	14	77	166	346	69
SHL30-5.1C	JW443	2009 Dec	0.86	2.25	1.325	19	71	129	260	54
SHL30-5.2T	JW443	2009 Dec	0.52	2.13	1.195	18	83	154	333	65
SHL30-6.1I	JW443	2009 Dec	0.32	1.42	0.771	15	82	172	400	80
SHL30-7.1C	JW443	2009 Dec	1.02	2.94	1.378	21	95	169	351	67
SHL30-7.2R	JW443	2009 Dec	0.35	1.06	0.793	12	63	125	275	55
SHL30-7.3R	JW443	2009 Dec	0.55	2.03	1.168	20	109	220	456	88
SHL30-8.1C	JW443	2009 Dec	5.13	18.74	10.601	179	683	986	1499	261
SHL30-8.2T	JW443	2009 Dec	0.18	0.65	0.384	7	29	57	120	25
SHL30-9.1C	JW443	2009 Dec	4.27	16.35	8.319	152	607	802	1148	184
SHL30-10.1C	JW443	2009 Dec	0.39	1.00	0.687	10	50	101	234	50
SHL30-10.2I	JW443	2009 Dec	0.35	1.19	0.735	11	53	117	279	57
SHL30-10.3R	JW443	2009 Dec	0.44	1.51	1.066	18	91	181	398	78
SHL30-12.1C	JW443	2009 Dec	0.31	1.14	0.670	12	59	113	250	51
SHL30-12.2I	JW443	2009 Dec	0.38	1.55	0.872	17	98	190	391	75
SHL30-11.1C	JW443	2009 Dec	1.03	3.24	1.601	26	121	220	457	88
SHL30-11.2T	***JW443***	***2009 Dec***	***0.41***	***1.51***	***1.003***	***17***	***94***	***182***	***390***	***74***
SHL30-13.1C	JW443	2009 Dec	1.52	4.03	1.939	29	121	233	502	97
SHL30-13.2T	JW443	2009 Dec	0.48	1.86	1.243	19	109	201	416	79
SHL30-14.1C	JW443	2009 Dec	1.49	2.99	2.165	19	76	133	262	51
SHL30-14.2T	JW443	2009 Dec	0.08	0.29	0.227	**3**	22	42	95	19
SHL33-1.1C	JW443	2009 Dec	5.12	18.44	11.261	178	627	925	1451	251
SHL33-1.2R	JW443	2009 Dec	0.96	3.82	2.042	34	134	228	449	86
SHL33-2.1E	JW443	2009 Dec	0.55	1.60	0.868	11	49	88	172	33
SHL33-2.2I	JW443	2009 Dec	1.64	3.69	1.736	23	69	119	226	42
SHL33-3.1C	JW443	2009 Dec	8.35	20.90	12.082	156	643	929	1479	248
SHL33-3.2T	JW443	2009 Dec	0.24	0.72	0.426	8	32	66	148	31

SHL33-4.1T	JW443	2009 Dec	0.051	0.46	2.09	1.124	18		77		141		301	61
SHL33-4.2C	***JW443***	***2009 Dec***	***0.019***	***20.55***	***13.31***	***8.310***	***46***		***121***		***244***		***719***	***154***
SHL34Z-1.1C	JW392	2008 Aug	0.015	0.29	0.89	0.544	10	4.04	49	22	112	26	171	33
SHL34Z-1.2I	JW392	2008 Aug	0.029	0.56	2.19	1.035	23	9.75	118	51	249	56	502	101
SHL34Z-1.3E	JW392	2008 Aug	0.030	0.62	2.52	0.873	30	11.33	139	60	262	57	495	87
SHL34Z-2.1I	JW392	2008 Aug	0.241	3.94	9.74	4.940	84	26.40	262	97	392	75	582	102
SHL34Z-3.1I	JW392	2008 Aug	0.151	2.45	3.90	2.217	28	8.71	88	35	167	38	345	69
SHL34Z-3.2I	JW392	2008 Aug	0.041	0.33	0.77	0.530	7	2.38	27	12	60	15	145	30
SHL34Z-3.3E	JW392	2008 Aug	0.000	0.35	1.74	0.678	19	7.24	83	31	139	29	245	43
SHL34Z-4.1E	JW392	2008 Aug		0.93	3.05	1.509	37	13.91	162	64	276	55	452	82
SHL34Z-4.2C	JW392	2008 Aug		2.50	5.87	2.452	47	15.79	165	64	263	51	409	74
SHL34AZ-1.1I	JW393	2008 Aug	0.165	1.58	2.41	1.751	17	5.26	54	21	88	18	246	52
SHL34AZ-1.2E	JW393	2008 Aug	0.069	0.45	0.94	0.731	9	3.64	46	19	99	23		
SHL34AZ-2.1E	JW393	2008 Aug	0.054	0.65	2.66	1.246	28	10.42	114	43	182	37	303	57
SHL34AZ-2.2I	JW393	2008 Aug	0.056	0.43	2.35	1.413	29	10.91	118	44	206	45	386	73
SHL34AZ-3.1E	JW393	2008 Aug	0.051	0.55	2.08	0.966	26	9.99	113	46	210	44	376	72
SHL34AZ-3.2IE	JW393	2008 Aug	0.179	2.52	5.43	2.341	41	12.87	135	51	211	41	329	60
SHL34AZ-3.3I	JW393	2008 Aug	0.039	0.18	0.71	0.350	7	2.39	28	11	53	12	101	20
SHL34AZ-4.1I	JW393	2008 Aug	0.082	0.91	2.50	1.403	24	8.29	94	38	181	41	373	74
SHL34AZ-5.1I	JW393	2008 Aug	0.075	0.54	1.82	0.997	23	9.39	113	48	249	58	524	107
SHL34AZ-6.2I	JW393	2008 Aug	0.216	3.71	8.53	4.596	87	28.24	295	104	442	83	666	115
SHL34AZ-7.1I	JW393	2008 Aug	0.266	4.73	10.42	4.527	74	23.24	236	89	365	77	637	116
SHL34AZ-7.2E	JW393	2008 Aug	0.107	1.20	3.76	1.987	45	15.72	174	69	318	65	548	103
SHL34AZ-8.1I	JW393	2008 Aug	0.141	2.89	5.81	2.703	48	16.42	189	73	325	65	514	91
SHL34AZ-9.1I	JW393	2008 Aug	0.141	2.89	4.85	3.821	34	9.65	86	29	125	24	200	38
SHL34AZ-10.1I	JW393	2008 Aug	0.028	0.54	1.71	0.951	17	6.27	74	30	147	32	310	62
SHL34AZ-11.1I	JW393	2008 Aug	0.101	0.67	2.73	1.262	32	11.68	137	56	245	53	458	88
SHL34AZ-11.2E	JW393	2008 Aug	0.047	0.51	1.80	0.644	16	5.86	64	25	104	21	177	34
SHL34AZ-12.1I	JW393	2008 Aug	0.155	3.31	6.80	3.483	60	19.36	201	74	306	61	470	84

SHL36E-1.1I	JW443	2009 Dec	0.45	1.40	0.880	16	76	164	380	79
SHL36E-1.2C	JW443	2009 Dec	0.55	1.73	1.135	15	69	137	319	66
SHL36E-1.3I	JW443	2009 Dec	0.58	2.19	1.238	28	114	208	423	82
SHL36E-1.4R	JW443	2009 Dec	0.45	1.65	0.903	20	86	188	445	91
SHL36E-2.1C	JW443	2009 Dec	2.35	6.90	3.447	60	197	328	619	122
SHL36E-2.2T	JW443	2009 Dec	0.63	1.99	1.300	25	117	214	449	88
SHL36E-3.1C	***JW443***	***2009 Dec***	***7.83***	***24.01***	***12.539***	***200***	***620***	***997***	***1818***	***340***
SHL36E-3.2I	JW443	2009 Dec	1.50	6.54	3.168	62	187	297	528	97
SHL36E-3.3T	JW443	2009 Dec	0.78	2.58	1.465	24	99	173	347	68
SHL36E-4.1C	JW443	2009 Dec	0.33	1.19	**0.712**	12	59	130	315	65
SHL36E-4.2T	JW443	2009 Dec	0.51	1.69	**1.223**	19	94	196	455	95
SHL36E-5.1C	JW443	2009 Dec	0.31	1.19	0.691	12	54	114	251	56
SHL36E-6.1R	JW443	2009 Dec	0.54	2.07	1.085	24	108	230	500	102
SHL36E-6.2C	JW443	2009 Dec	0.59	1.44	1.025	16	74	146	321	68
SHL36E-7.1I	JW443	2009 Dec	0.42	1.61	1.122	19	104	230	531	108
SHL36E-7.2R	JW443	2009 Dec	0.40	1.45	0.837	15	75	168	394	80
SHL36E-8.1C	JW443	2009 Dec	0.43	2.04	1.085	28	164	312	628	116
SHL36E-8.2R	JW443	2009 Dec	0.41	2.22	**1.136**	24	103	**186**	383	73
SHL36E-9.1C	***JW443***	***2009 Dec***	***10.61***	***37.78***	***21.046***	***348***	***1225***	***1458***	***1970***	***307***
SHL36E-9.2R	JW443	2009 Dec	0.34	2.39	1.393	40	222	436	844	154
SHL36E-10.1I	***JW443***	***2009 Dec***	***1.18***	***4.02***	***2.362***	***40***	***170***	***301***	***571***	***110***
SHL36EX-11.1C	***JW443***	***2009 Dec***	***0.90***	***3.56***	***0.845***	***42***	***327***	***712***	***1520***	***271***
SHL36E-11.2I	JW443	2009 Dec	0.69	2.21	0.423	26	192	469	1089	201
SHL36E-11.3R	JW443	2009 Dec	0.72	2.86	1.543	33	148	257	490	89
SHL36E-12.1C	JW443	2009 Dec	0.42	1.74	1.043	20	95	195	440	90
SHL36E-12.2R	JW443	2009 Dec	0.40	1.36	0.895	15	76	166	387	81
SHL36E-12.3R	JW443	2009 Dec	0.56	1.96	1.173	22	117	247	557	112
SHL36E-13.1I	JW443	2009 Dec	2.03	6.50	4.593	61	219	286	469	75
SHL36E-13.2R	JW443	2009 Dec	0.34	1.42	0.801	16	80	156	340	66
SHL36E-14.2C	JW443	2009 Dec	5.80	23.42	13.577	213	831	1141	1703	287
SHL36E-14.3I	JW443	2009 Dec	1.22	4.46	2.634	41	173	250	421	75
SHL36E-14.1T	JW443	2009 Dec	0.57	2.50	1.326	30	177	326	672	123

SHL37P-1.1C	JW443	2009 Dec	0.40	1.54	0.810	16	86	175	382	73
SHL37P-1.2I	JW443	2009 Dec	0.44	1.39	0.928	16	74	157	365	74
SHL37P-1.3R	JW443	2009 Dec	0.51	1.66	1.080	18	92	188	380	76
SHL37P-2.1C	JW443	2009 Dec	0.26	0.99	0.630	10	51	110	259	55
SHL37P-2.2I	JW443	2009 Dec	0.26	1.38	0.724	**13**	56	116	271	56
SHL37P-2.3R	JW443	2009 Dec	0.32	1.21	0.710	13	69	131	279	56
SHL37P-14.1C	JW443	2009 Dec	0.31	1.43	1.133	14	71	154	386	76
SHL37P-14.2R	JW443	2009 Dec	0.63	2.17	1.510	27	138	274	561	112
SHL37P-3.1C	JW443	2009 Dec	2.23	5.02	0.531	37	134	205	309	53
SHL37P-3.2I	***JW443***	***2009 Dec***	***0.23***	***1.06***	***0.508***	***10***	***48***	***86***	***187***	***36***
SHL37P-3.3R	JW443	2009 Dec	0.47	1.60	0.946	19	96	206	454	90
SHL37P-4.1R	JW443	2009 Dec	1.02	4.47	3.050	54	229	401	772	146
SHL37P-4.2C	JW443	2009 Dec	0.19	0.84	0.538	13	65	142	343	70
SHL37P-4.3I	JW443	2009 Dec	0.22	1.14	**0.631**	11	56	**109**	251	53
SHL37P-5.1C	JW443	2009 Dec	0.86	2.63	1.534	32	143	249	505	95
SHL37P-5.2I	JW443	2009 Dec	0.60	2.46	1.296	25	108	179	335	63
SHL37P-5.3T	***JW443***	***2009 Dec***	***0.33***	***1.12***	***0.647***	***11***	***58***	***125***	***298***	***60***
SHL37P-6.1I	JW443	2009 Dec	0.28	1.30	0.688	16	72	151	353	67
SHL37P-6.2C	JW443	2009 Dec	0.39	1.55	0.971	17	81	159	359	72
SHL37P-6.3R	JW443	2009 Dec	0.30	1.36	0.713	12	61	130	293	58
SHL37P-7.1R	JW443	2009 Dec	0.23	1.02	0.624	12	61	122	282	57
SHL37P-7.2C	JW443	2009 Dec	0.52	2.11	1.261	**22**	98	180	383	75
SHL37P-7.3T	JW443	2009 Dec	0.12	1.12	0.817	14	66	132	284	56
SHL37P-7.4C	JW443	2009 Dec	0.12	0.65	0.347	7	38	82	189	39
SHL37P-8.1I	JW443	2009 Dec	0.18	0.64	0.558	**8**	49	103	237	47
SHL37P-8.2C	***JW443***	***2009 Dec***	***23.21***	***84.95***	***44.002***	***831***	***2183***	***2224***	***2608***	***402***
SHL37P-8.3R	JW443	2009 Dec	0.27	1.93	1.338	**21**	104	194	417	79
SHL37P-15.1C	JW443	2009 Dec	0.23	0.84	0.532	7	36	78	194	42
SHL37P-15.2T	JW443	2009 Dec	0.56	1.73	1.047	20	92	194	435	90
SHL37P-9.2R	JW443	2009 Dec	0.22	1.43	0.857	15	67	122	267	52
SHL37P-9.1C	JW443	2009 Dec	3.79	5.95	3.438	31	79	102	188	34

SHL37P-10.2R	JW443	2009 Dec		0.29	1.16	0.776	13		71		149		352	68
SHL37P-10.1I	JW443	2009 Dec		0.14	0.55	0.329	6		36		75		179	35
SHL37P-11.1C	***JW443***	***2009 Dec***		***0.84***	***2.25***	***1.359***	***22***		***121***		***252***		***548***	***110***
SHL37P-11.2I	JW443	2009 Dec		0.92	3.94	1.828	35		151		248		465	85
SHL37P-11.3I	JW443	2009 Dec		0.25	1.22	0.847	14		70		146		317	68
SHL37P-11.4R	***JW443***	***2009 Dec***		***1.00***	***3.22***	***2.023***	***28***		***119***		***208***		***400***	***76***
SHL37P-12.1C	JW443	2009 Dec		0.33	1.40	0.967	15		86		173		387	78
SHL37P-12.2I	***JW443***	***2009 Dec***		***0.97***	***3.73***	***2.171***	***34***		***140***		***212***		***366***	***68***
SHL37P-12.3T	JW443	2009 Dec		0.46	1.80	1.086	24		110		199		388	74
SHL37P-13.1C	JW443	2009 Dec		1.26	5.67	3.803	57		244		376		640	112
SHL37P-13.2T	JW443	2009 Dec		0.54	1.51	1.135	19		104		195		401	74
SHL0849AZ-1.1I	JW414	2009 Jan	0.367	5.21	10.56	6.317	79	25.62	250	102	410	86	709	131
SHL0849AZ-1.2E	JW414	2009 Jan	0.256	4.11	8.71	5.150	69	22.26	229	82	364	77	629	114
SHL0849AZ-2.1E	JW414	2009 Jan	0.233	3.37	6.86	3.712	55	17.59	176	70	298	63	511	95
SHL0849AZ-3.1E	JW414	2009 Jan	0.203	3.49	7.35	4.183	57	17.99	188	74	310	68	548	104
SHL0849AZ-4.1E	JW414	2009 Jan	0.134	1.48	2.99	1.893	23	7.83	87	35	157	34	296	58
SHL0849AZ-4.2C	JW414	2009 Jan	0.253	3.14	8.01	4.755	62	20.61	225	79	367	77	653	117
SHL0849AZ-4.3E	JW414	2009 Jan	0.046	0.68	2.12	1.342	24	9.30	112	47	222	50	424	84
SHL0849AZ-5.1I	JW414	2009 Jan	0.172	4.01	7.78	3.722	60	19.45	213	73	328	71	580	107
SHL0849AZ-6.1I	***JW414***	***2009 Jan***	***0.309***	***5.17***	***11.90***	***7.031***	***98***	***32.20***	***346***	***115***	***523***	***111***	***903***	***162***
SHL0849AZ-7.1C	JW414	2009 Jan	0.312	5.53	11.69	6.307	89	28.65	282	110	454	98	806	149
SHL0849AZ-8.1E	JW414	2009 Jan	0.137	1.48	5.24	3.829	67	24.07	251	103	455	97	776	141
SHL0849AZ-9.1E	JW414	2009 Jan	0.082	1.75	5.41	3.198	58	20.47	240	91	408	86	695	131
SHL0849AZ-9.2I	JW414	2009 Jan	0.166	2.01	4.86	2.441	39	12.77	148	49	226	48	398	75
SHL0849AZ-10.1C	JW414	2009 Jan	0.214	3.35	7.45	4.334	59	18.92	200	74	321	68	572	106
SHL0849AZ-11.1I	JW414	2009 Jan	0.031	0.33	1.11	0.583	10	3.63	44	17	82	20	173	35
SHL0849AZ-11.2E	JW414	2009 Jan	0.181	2.59	5.38	2.675	39	13.12	141	49	220	48	389	71
SHL0849AZ-12.1E	JW414	2009 Jan	0.229	4.26	9.79	4.842	70	21.42	237	88	371	78	641	121
SHL0849AZ-12.2C	***JW414***	***2009 Jan***	***0.545***	***3.79***	***8.36***	***4.410***	***59***	***18.68***	***210***	***74***	***313***	***66***	***530***	***102***
SHL0849AZ-13.1E	JW414	2009 Jan	***0.042***	0.21	0.77	0.576	8	3.00	33	14	60	14	127	26
SHL0849AZ-13.2I	JW414	2009 Jan	0.043	0.34	1.36	0.713	13	4.15	49	21	94	21	196	40

SHL0849AZ-13.3C	***JW414***	***2009 Jan***	***0.016***	***0.58***	***1.92***	***1.173***	***24***	***9.31***	***113***	***45***	***214***	***51***	***440***	***90***
SHL49AZ-14.1C	JW414	2009 Jan	0.363	6.33	14.53	8.402	112	34.64	372	128	545	115	936	167
SHD9-1.1R	JW443	2009 Dec		0.18	0.68	0.494	7		30		56		121	25
SHD9-2.1R	JW443	2009 Dec		0.96	3.37	1.895	31		131		227		453	86
SHD9-2.2C	JW443	2009 Dec		7.68	24.24	16.083	185		608		752		1084	179
SH325.2-1.1DGZT	JW309	2007 May	0.076	0.48	1.81	0.950	21	7.72	86	35	159	35	323	64
SH325.2-1.2MGZC	JW309	2007 May	0.087	0.33	1.26	0.721	15	6.17	69	29	144	33	298	62
SH325.2-1.3LGZI]	JW309	2007 May	0.063	0.35	1.19	0.710	12	5.04	60	25	123	28	262	54
SH325.2-2.1MGZC	JW309	2007 May	***0.080***	0.36	1.50	0.870	15	5.71	64	25	120	27	246	50
SH325.2-2.2LGZI	JW309	2007 May	0.060	0.14	0.36	0.275	5	1.93	23	11	54	13	130	29
SH325.2-3.1LGC	***JW309***	***2007 May***	***0.056***	***0.51***	***1.74***	***0.886***	***20***	***7.13***	***86***	***37***	***173***	***40***	***364***	***72***
SH325.2-3.2DGZE	JW309	2007 May	***0.096***	0.50	2.01	1.351	20	6.94	81	32	159	36	345	70
SH325.2-4.1DGZE	***JW309***	***2007 May***	***0.077***	***1.09***	***3.20***	***1.946***	***35***	***13.26***	***153***	***65***	***299***	***66***	***608***	***121***
SH325.2-4.2MGC	***JW309***	***2007 May***	***0.096***	***0.79***	***2.03***	***1.121***	***22***	***7.87***	***93***	***38***	***181***	***42***	***375***	***78***
SH325.2-5.1MGZE	JW309	2007 May	***0.055***	0.37	1.30	0.706	15	5.80	72	30	148	35	326	68
SH325.2-5.2DGZI	***JW309***	***2007 May***	***0.100***	***0.98***	***2.52***	***1.405***	***23***	***8.32***	***94***	***39***	***180***	***42***	***387***	***80***
SH325.2-5.3DGZE	***JW309***	***2007 May***	***0.074***	***0.52***	***1.98***	***1.075***	***24***	***8.61***	***98***	***40***	***188***	***41***	***376***	***73***
SH325.2-6.1MGT	JW309	2007	0.064	0.18	0.46	0.320	4	1.23	14	6	30	7	66	15

		May 2007												
SH325.2-6.2MGI	JW309	May 2007	0.079	0.13	0.25	0.187	2	0.73	10	4	20	5	50	11
SH325.2-7.1LGZT	JW309	May 2007	0.079	0.62	1.96	1.268	21	7.16	84	34	166	38	354	73
SH325.2-7.2DGZT	JW309	May 2007	0.073	0.13	0.48	0.242	7	2.65	34	14	72	17	159	33
SH325.2-7.3LGZC	JW309	May 2007	0.076	0.49	1.83	1.047	21	7.62	92	36	180	41	376	76
SH325.2-8.1MGZE	JW309	May 2007	0.067	0.37	1.40	0.753	15	5.93	70	30	151	35	332	69
SH325.2-8.2MGZC	JW309	May 2007	0.071	1.16	3.30	1.606	29	10.36	118	49	223	50	466	96
SH325.2-8.3DGZT	JW309	May 2007	0.054	0.30	1.36	0.795	13	4.79	55	22	105	24	229	46
SH325.2-9.1MGC	JW309	May 2007	***0.078***	0.56	1.70	0.929	19	6.87	82	34	166	38	354	73
SH325.2-10.1MGZI	JW309	May 2007	0.040	0.71	2.25	1.640	31	12.17	140	59	268	59	510	101
SH325.2-11.1DGZE	***JW309***	***May 2007***	***14.681***	***118.08***	***63.86***	***21.319***	***140***	***29.43***	***218***	***65***	***250***	***54***	***448***	***86***
SH325.2-11.1MGC	***JW309***	***May 2007***	***0.780***	***8.88***	***9.70***	***3.561***	***55***	***14.86***	***142***	***47***	***192***	***38***	***299***	***51***
SH325.2-12.1MGZT	JW309	May 2007	0.071	0.97	2.27	1.133	18	6.23	70	29	144	33	294	58
SH325.2-12.2MGZI	***JW309***	***May 2007***	***0.860***	***6.12***	***2.24***	***0.927***	***12***	***3.44***	***39***	***15***	***70***	***16***	***144***	***28***
SH325.2-13.1DGZT	JW309	May 2007	0.092	0.88	1.81	0.566	15	4.66	49	19	88	19	166	30
SH325.2-13.1T	***JW309***	***May 2007***	***0.130***	***0.58***	***0.54***	***0.282***	***4***	***1.44***	***17***	***7***	***36***	***9***	***94***	***21***
Z484A-10.1C	JP04	2008 Jan	0.055	0.25	0.95	0.579	10	3.52	43	18	92	23	217	48
Z484A-10.2IR	JP04	2008 Jan	0.042	0.36	1.99	0.849	26	10.81	136	56	281	64	568	110

Z484A-10.3T	JP04	2008 Jan	0.042	0.35	1.40	0.808	16	6.39	75	31	148	34	308	63
Z484A-12.1I	JP04	2008 Jan	0.129	1.68	5.09	0.928	43	13.98	148	51	225	45	330	57
Z484A-12.2EM	JP04	2008 Jan	***0.025***	0.06	0.20	0.086	2	0.76	10	5	26	7	73	17
Z484A-12.3T	JP04	2008 Jan	0.027	0.14	0.59	0.330	6	1.95	25	10	48	11	106	22
Z484A-14.1C	***JP04***	***2008 Jan***	***0.898***	***16.81***	***37.05***	***20.718***	***274***	***82.75***	***833***	***310***	***1136***	***219***	***1651***	***284***
Z484A-16.1C	JP04	2008 Jan	0.056	0.18	0.67	0.365	5	1.99	25	11	56	14	133	32
Z484A-16.2I	JP04	2008 Jan	0.057	0.47	1.75	0.934	22	7.78	95	41	185	43	372	77
Z484A-17.1C	JP04	2008 Jan	0.061	0.84	2.87	2.105	32	11.97	140	60	270	61	545	110
Z484A-17.2T	JP04	2008 Jan	0.063	0.49	1.94	1.028	20	6.63	75	30	135	30	272	55
Z484A-18.1C	JP04	2008 Jan	0.013	0.13	0.89	0.563	12	4.73	59	26	119	28	255	53
Z484A-18.2IR	JP04	2008 Jan	0.038	0.23	1.17	0.630	15	5.48	68	28	136	31	281	57
Z484A-19.1T	JP04	2008 Jan	0.038	0.20	0.95	0.499	11	4.07	47	21	95	22	203	43
Z484A-19.2C	JP04	2008 Jan	0.067	0.82	1.77	1.158	14	4.55	50	21	96	22	203	44
Z484A-19.3IR	JP04	2008 Jan	0.034	0.39	1.26	0.754	13	5.03	63	29	132	31	289	63
Z484A-19.4IR	JP04	2008 Jan	0.038	0.40	1.66	0.880	18	7.26	93	40	203	49	449	94
Z484A-2.1T	JP04	2008 Jan	***0.099***	0.74	2.36	1.683	26	9.02	104	40	192	43	374	75
Z484A-2.2C	JP04	2008 Jan	0.053	0.61	2.55	1.516	29	10.25	121	49	221	50	437	87
Z484A-4.1I	***JP04***	***2008 Jan***	***0.800***	***16.84***	***51.44***	***29.412***	***526***	***157.85***	***1506***	***483***	***1805***	***317***	***2274***	***378***
Z484A-4.2T	JP04	2008 Jan	***0.026***	0.24	0.95	0.619	10	3.48	40	16	79	18	169	35
Z484A-5.1I	***JP04***	***2008 Jan***	***0.046***	***0.40***	***1.25***	***0.687***	***15***	***5.57***	***70***	***30***	***142***	***33***	***307***	***64***
Z484A-8.1I	***JP04***	***2008 Jan***	***1.141***	***20.49***	***53.34***	***33.431***	***457***	***128.35***	***1164***	***369***	***1282***	***227***	***1603***	***262***
Z484A-8.2I	JP04	2008 Jan	0.213	4.10	11.95	6.678	106	32.31	319	110	410	76	580	98

Spot ID	Mount	Date Analyzed	Hf ppm	Th ppm	U ppm
SHL3Z-1.1DI	JW414	2009 Jan	10772	106	327
SHL3Z-1.2LC	JW414	2009 Jan	11062	184	503
SHL3Z-1.3DI	JW414	2009 Jan	12944	148	787
SHL3Z-1.4DR	JW414	2009 Jan	11342	158	769
SHL3Z-2.1DC	JW414	2009 Jan	10834	101	544
SHL3Z-2.2LR	***JW414***	***2009 Jan***	***12063***	***48***	***355***
SHL3Z-3.1LC	***JW414***	***2009 Jan***	***11271***	***25***	***96***
SHL3Z-3.2DI	JW414	2009 Jan	13299	433	2783
SHL3Z-3.3LR	JW414	2009 Jan	17174	99	2798
SHL3Z-4.1LR	JW414	2009 Jan	12096	54	461
SHL3Z-4.2LI	JW414	2009 Jan	10383	27	225
SHL3Z-4.3LC	JW414	2009 Jan	13038	29	462
SHL3Z-5.1DC	JW414	2009 Jan	13233	5	930
SHL3Z-5.2LR	JW414	2009 Jan	12545	164	755
SHL3Z-6.1DI	JW414	2009 Jan	12757	270	1229
SHL3Z-6.2LC	***JW414***	***2009 Jan***	***11614***	***44***	***355***
SHL3Z-6.3DE	JW414	2009 Jan	11715	129	695
SHL3Z-7.1LR	JW414	2009 Jan	13510	62	648
SHL3Z-7.2DI	***JW414***	***2009 Jan***	***13336***	***66***	***659***
SHL3Z-7.3LC	***JW414***	***2009 Jan***	***10679***	***106***	***148***
SHL3Z-8.1LC	JW414	2009 Jan	10898	38	366
SHL3Z-8.2I	JW414	2009 Jan	13318	80	1006
SHL3Z-8.3LC	***JW414***	***2009 Jan***	***12332***	***53***	***568***
SHL3Z-8.4DI	***JW414***	***2009 Jan***	***14014***	***160***	***1391***
SHL3Z-9.1DI	JW414	2009 Jan	11923	55	699
SHL3Z-9.2LC	JW414	2009 Jan	9857	45	164
SHL3Z-9.3LI	JW414	2009 Jan	12566	58	557
MSHL3Z-1.1DGI	JW309	2007 May	9790	787	1732
MSHL3Z-1.2MGI	JW309	2007 May	12702	43	427

Spot ID	Mount	Date Analyzed	Hf ppm	Th ppm	U ppm
MSHL3Z-2.1MGZC	***JW309***	***2007 May***	***13020***	***73***	***591***
MSHL3Z-2.2DGZI	JW309	2007 May	11469	147	675
MSHL3Z-3.1DGZT	JW309	2007 May	11911	164	751
MSHL3Z-3.2LGZE	JW309	2007 May	12597	34	342
MSHL3Z-3.3DGC	JW309	2007 May	14195	99	819
MSHL3Z-4.1MGI	JW309	2007 May	10889	41	276
MSHL4Z-1.1DGZE	JW309	2007 May	13372	152	482
MSHL4Z-1.2MGZI	JW309	2007 May	10110	72	311
MSHL4Z-10.1MGT	JW309	2007 May	11473	91	345
MSHL4Z-10.2MGZC	JW309	2007 May	11481	90	296
MSHL4Z-10.3DGZIT	JW309	2007 May	10235	294	762
MSHL4Z-11.1DGZI	JW309	2007 May	9830	50	183
MSHL4Z-11.2DZIT	JW309	2007 May	10537	117	404
MSHL4Z-12.1MGI	JW309	2007 May	11470	19	118
MSHL4Z-2.1DGZI	JW309	2007 May	12310	84	272
MSHL4Z-2.2MGZI	JW309	2007 May	11801	63	307
MSHL4Z-2.3DGZE	JW309	2007 May	13033	50	292
MSHL4Z-3.1DGZT	JW309	2007 May	11841	202	663
MSHL4Z-3.2MGZE	JW309	2007 May	11186	70	326
MSHL4Z-10.2MGZC	JW309	2007 May	11481	90	296
MSHL4Z-10.3DGZIT	JW309	2007 May	10235	294	762
MSHL4Z-11.1DGZI	JW309	2007 May	9830	50	183
MSHL4Z-5.1DGZT	JW309	2007 May	13352	61	348
MSHL4Z-5.2MGZE	JW309	2007 May	12136	60	337
MSHL4Z-5.3MGI	JW309	2007 May	14096	12	102
MSHL4Z-6.1MGT	JW309	2007 May	12468	84	347
MSHL4Z-6.2MGI	JW309	2007 May	10807	21	131
MSHL4Z-7.1MGZT	JW309	2007 May	10872	102	316
MSHL4Z-7.2LGC	JW309	2007 May	7842	93	219

Spot ID	Mount	Date Analyzed	Hf ppm	Th ppm	U ppm
MSHL4Z-7.3DGI	JW309	2007 May	9547	267	491
MSHL4Z-8.1MGZT	JW309	2007 May	12359	184	556
MSHL4Z-8.2DGZI	JW309	2007 May	13547	158	662
MSHL4Z-8.3MGZI	JW309	2007 May	13261	40	321
MSHL4Z-9.1MGZT	JW309	2007 May	12635	94	455
MSHL4Z-9.2LGC	JW309	2007 May	11590	53	295
MSHL4Z-9.3MGZT	JW309	2007 May	11694	109	383
SHL5Z-1.1C	JW364	2008 Jan	11036	135	347
SHL5Z-2.1I	JW364	2008 Jan	11812	96	178
SHL5Z-2.2T	JW364	2008 Jan	12296	57	289
SHL5Z-3.1C	JW364	2008 Jan	12558	57	317
SHL5Z-3.2E	JW364	2008 Jan	12600	59	265
SHL5Z-4.1C	JW364	2008 Jan	10303	117	400
SHL5Z-4.2T	JW364	2008 Jan	10934	35	166
SHL5Z-5.1T	JW364	2008 Jan	10669	97	309
SHL5Z-5.2C	***JW364***	***2008 Jan***	***7964***	***2254***	***1319***
SHL5Z-6.1C	***JW364***	***2008 Jan***	***8377***	***3847***	***3284***
SHL5Z-6.2T	JW364	2008 Jan	12591	66	286
SHL5Z-6.3I	JW364	2008 Jan	13133	53	327
SHL5Z-7.1C	***JW364***	***2008 Jan***	***12002***	***107***	***374***
SHL5Z-7.2T	JW364	2008 Jan	13100	78	324
SHL5Z-8.1T	JW364	2008 Jan	10004	32	131
SHL5Z-8.2C	JW364	2008 Jan	9759	62	250
SHL5Z-1.1T	JW365	2008 Jan			
SHL5Z-1.2I	***JW365***	***2008 Jan***	***13280***	***128***	***515***
SHL5Z-2.1C	JW365	2008 Jan	13167	110	393
SHL5Z-2.2E	JW365	2008 Jan	10700	32	137
SHL5Z-3.1C	JW365	2008 Jan	11079	25	133

Spot ID	Mount	Date Analyzed	Hf ppm	Th ppm	U ppm
SHL5Z-3.2R	JW365	2008 Jan	9421	76	201
SHL5Z-4.1C	JW365	2008 Jan	12000	188	454
SHL5Z-4.2T	JW365	2008 Jan	12703	72	280
SHL5Z-5.1C	JW365	2008 Jan	11043	26	111
SHL5Z-5.2T	JW365	2008 Jan	11391	139	434
SHL5Z-6.1C	***JW365***	***2008 Jan***	***10954***	***142***	***334***
SHL5Z-6.2T	JW365	2008 Jan	10804	55	161
SHL5Z-7.1T	JW365	2008 Jan	11664	54	213
SHL5Z-7.2C	JW365	2008 Jan	10718	56	184
SHL5Z-8.1I	JW365	2008 Jan	10518	156	451
SHL5Z-8.2C	JW365	2008 Jan	11278	26	131
SHL5Z-8.3T	JW365	2008 Jan	11836	59	249
SHL5Z-9.1T	JW365	2008 Jan	11112	180	546
SHL5Z-9.2I	JW365	2008 Jan	10496	120	332
SHL5Z-9.3I	JW365	2008 Jan	9864	322	714
SHL0821Z-1.1E	JW414	2009 Jan	11233	44	241
SHL0821Z-1.2C	***JW414***	***2009 Jan***	***11971***	***52***	***332***
SHL0821Z-2.1E	JW414	2009 Jan	11418	25	132
SHL0821Z-2.2I	JW414	2009 Jan	12448	70	523
SHL0821Z-3.1E	JW414	2009 Jan	12654	112	426
SHL0821Z-3.2I	JW414	2009 Jan	12860	14	112
SHL0821Z-4.1E	JW414	2009 Jan	11357	23	102
SHL0821Z-4.2C	JW414	2009 Jan	10470	22	129
SHL0821Z-5.1E	***JW414***	***2009 Jan***	***9951***	***35***	***108***
SHL0821Z-5.2I	***JW414***	***2009 Jan***	***10191***	***31***	***62***
SHL0821Z-6.1E	JW414	2009 Jan	10103	30	73
SHL0821Z-6.2I	JW414	2009 Jan	8584	92	109
SHL0821Z-7.1C	JW414	2009 Jan	9550	58	207
SHL0821Z-7.2I	JW414	2009 Jan	10639	15	78

Spot ID	Mount	Date Analyzed	Hf ppm	Th ppm	U ppm
SHL0821Z-7.3R	JW414	2009 Jan	9055	11	25
SHL0821Z-8.1C	***JW414***	***2009 Jan***	***13153***	***92***	***437***
SHL0821Z-8.2I	JW414	2009 Jan	10278	45	229
SHL0821Z-8.3I	JW414	2009 Jan	14190	110	706
SHL0821Z-9.1I	JW414	2009 Jan	8818	50	73
SHL0821Z-9.2E	JW414	2009 Jan	10260	16	47
SHL0821Z-10.1I	JW414	2009 Jan	8558	25	58
SHL0821Z-11.1E	JW414	2009 Jan	13490	245	824
SHL0821Z-11.2C	JW414	2009 Jan	10229	75	373
SHL0821Z-12.1C	JW414	2009 Jan	7165	141	224
SHL0821Z-12.2E	JW414	2009 Jan	10399	65	243
SHL0821Z-13.1C	JW414	2009 Jan	11702	58	257
SHL0821Z-13.2I	JW414	2009 Jan	9470	132	315
SHL0821Z-13.3E	JW414	2009 Jan	8791	15	57
SHL26C-1.1C	JW443	2009 Dec	11905	55	261
SHL26-1.2R	JW443	2009 Dec	12125	71	315
SHL-26C-2.1C	JW443	2009 Dec	14769	23	201
SHL-26C-2.2R	JW443	2009 Dec	11843	70	340
SHL26C-3.1R	JW443	2009 Dec	8672	129	308
SHL26C-3.2C	JW443	2009 Dec	8110	39	125
SHL26C-4.1C	***JW443***	***2009 Dec***	***12785***	***22***	***152***
SHL26C-4.2T	JW443	2009 Dec	13729	275	937
SHL26C-5.1T	JW443	2009 Dec	12515	55	261
SHL26C-5.2I	JW443	2009 Dec	9936	45	200
SHL26C-5.3C	JW443	2009 Dec	10651	30	155
SHL26C-6.1C	***JW443***	***2009 Dec***	***11071***	***69***	***325***
SHL26C-6.2I	JW443	2009 Dec	11994	60	320
SHL26c-7.1C	JW443	2009 Dec	13506	32	178
SHL26C-7.2T	JW443	2009 Dec	12614	58	299

Spot ID	Mount	Date Analyzed	Hf ppm	Th ppm	U ppm
SHL26C-8.1C	JW443	2009 Dec	11656	65	251
SHL26C-8.2R	JW443	2009 Dec	15180	39	210
SHL26C-9.1C	JW443	2009 Dec	11791	212	549
SHL26C-9.2I	JW443	2009 Dec	12773	312	764
SHL26C-9.3R	JW443	2009 Dec	13750	190	580
SHL26C-9.4R	JW443	2009 Dec	12279	44	225
SHL26C-10.1C	JW443	2009 Dec	12112	35	199
SHL26C-10.2I	JW443	2009 Dec	11487	66	289
SHL26c-10.3R	JW443	2009 Dec	11239	57	276
SHL26C-11.1C	JW443	2009 Dec	10849	125	326
SHL26C-12.1C	JW443	2009 Dec	12236	49	254
SHL26C-12.2I	JW443	2009 Dec	12703	84	406
SHL26C-13.1C	JW443	2009 Dec	10751	40	189
SHL26c-13.2R	JW443	2009 Dec	11900	32	162
SHL26C-14.2I	JW443	2009 Dec	10504	416	988
SHL26C-14.1I	JW443	2009 Dec	13590	36	246
SHL26C-14.3R	JW443	2009 Dec	12049	62	283
SHL26C-15.1I	JW443	2009 Dec	14785	598	1731
SHL26C-15.2I	JW443	2009 Dec	11636	53	270
SHL26C-15.3C	JW443	2009 Dec	12000	42	230
SHL29AZ-1.1T	JW392	2008 Aug			
SHL29AZ-1.2C	JW392	2008 Aug	10506	434	1128
SHL29AZ-1.3I	JW392	2008 Aug	13865	9	95
SHL29AZ-2.1E	JW392	2008 Aug	11703	50	300
SHL29AZ-2.2E	JW392	2008 Aug	12513	87	326
SHL29AZ-2.3I	***JW392***	***2008 Aug***	***12930***	***114***	***287***
SHL29AZ-2.4I	JW392	2008 Aug	13101	227	492
SHL29AZ-3.1C	JW392	2008 Aug	12713	62	400
SHL29AZ-3.2IE	JW392	2008 Aug	10826	40	227

Spot ID	Mount	Date Analyzed	Hf ppm	Th ppm	U ppm
SHL29AZ-3.3IE	JW392	2008 Aug	10604	74	313
SHL29AZ-3.4E	JW392	2008 Aug	11980	51	246
SHL29AZ-1.1C	JW393	2008 Aug	11511	35	249
SHL29AZ-1.2E	JW393	2008 Aug	11088	98	396
SHL29AZ-2.1E	JW393	2008 Aug	10195	46	218
SHL29AZ-2.2I	JW393	2008 Aug	11407	66	372
SHL29AZ-2.3C	JW393	2008 Aug	11253	41	227
SHL29AZ-3.1C	JW393	2008 Aug	12252	36	227
SHL29AZ-3.2C	JW393	2008 Aug	13345	115	432
SHL29AZ-4.1C	***JW393***	***2008 Aug***	***13063***	***74***	***446***
SHL29AZ-4.2E	JW393	2008 Aug	11753	102	373
SHL29AZ-5.1C	JW393	2008 Aug	9417	133	198
SHL29AZ-5.2E	JW393	2008 Aug	12620	54	274
SHL29AZ-6.1C	***JW393***	***2008 Aug***	***6516***	***2880***	***2530***
SHL29AZ-6.2E	JW393	2008 Aug	12133	130	417
SHL29AZ-6.3I	JW393	2008 Aug	12890	72	387
SHL29AZ-7.1C	JW393	2008 Aug	10147	76	309
SHL29AZ-7.2I	JW393	2008 Aug	10844	182	532
SHL29AZ-7.3E	JW393	2008 Aug	10934	54	313
SHL29AZ-8.1C	JW393	2008 Aug	9319	299	698
SHL29AZ-8.2E	JW393	2008 Aug	10107	92	340
SHL29AZ-9.1C	JW393	2008 Aug	10566	79	335
SHL29AZ-9.2E	JW393	2008 Aug	11361	67	342
SHL29Z-1.1C	***JW478***	***2010 May***			
SHL29Z-2.1I	JW478	2010 May	10217	50	231
SHL29Z-3.1C	JW478	2010 May	10369	32	168
SHL29Z-4.1C	***JW478***	***2010 May***	***11186***	***62***	***284***
SHL29Z-5.1C	JW478	2010 May	11707	49	364
SHL29Z-5.2E	JW478	2010 May	13849	72	271

Spot ID	Mount	Date Analyzed	Hf ppm	Th ppm	U ppm
SHL29Z-6.1C	JW478	2010 May	10284	39	200
SHL29Z-6.2I	JW478	2010 May	9941	32	166
SHL29Z-7.1C	***JW478***	***2010 May***	***10489***	***89***	***260***
SHL29Z-8.1C	***JW478***	***2010 May***	***10271***	***24***	***155***
SHL29Z-8.2I	JW478	2010 May	12477	22	210
SHL29Z-9.1C	JW478	2010 May	11607	54	280
SHL29Z-10.1C	JW478	2010 May	9985	58	301
SHL29Z-10.2I	JW478	2010 May	12463	53	256
SHL29Z-11.1C	JW478	2010 May	11456	25	219
SHL29Z-11.2I	JW478	2010 May	10743	49	227
SHL29Z-12.1C	***JW478***	***2010 May***	***8178***	***1918***	***1590***
SHL29Z-13.1C	JW478	2010 May	8730	133	174
SHL29Z-14.1C	JW478	2010 May	10668	34	231
SHL29Z-14.2I	JW478	2010 May	10572	48	239
SHL29Z-15.1I	JW478	2010 May	10296	58	210
SHL29Z-16.1I	JW478	2010 May	12062	133	405
SHL30-1.1C	JW443	2009 Dec	14286	20	150
SHL30-1.2R	JW443	2009 Dec	13493	39	254
SHL30-2.1C	JW443	2009 Dec	11987	110	534
SHL30-2.2R	JW443	2009 Dec	15297	237	840
SHL30-3.1C	JW443	2009 Dec	15257	29	228
SHL30-3.2I	JW443	2009 Dec	12588	67	271
SHL30-3.3I	JW443	2009 Dec	11881	77	351
SHL30-3.4R	***JW443***	***2009 Dec***	***14125***	***108***	***511***
SHL30-4.1I	JW443	2009 Dec	14991	10	92
SHL30-4.2C	JW443	2009 Dec	12018	24	148
SHL30-4.3R	JW443	2009 Dec	11161	43	225
SHL30-5.1C	JW443	2009 Dec	11672	45	181
SHL30-5.2T	JW443	2009 Dec	12458	233	602

Spot ID	Mount	Date Analyzed	Hf ppm	Th ppm	U ppm
SHL30-6.1I	JW443	2009 Dec	12618	61	352
SHL30-7.1C	JW443	2009 Dec	12040	76	313
SHL30-7.2R	JW443	2009 Dec	12478	46	235
SHL30-7.3R	JW443	2009 Dec	12459	86	397
SHL30-8.1C	JW443	2009 Dec	12526	805	1690
SHL30-8.2T	JW443	2009 Dec	12630	42	178
SHL30-9.1C	JW443	2009 Dec	10874	632	1056
SHL30-10.1C	JW443	2009 Dec	12695	35	164
SHL30-10.2I	JW443	2009 Dec	12923	46	265
SHL30-10.3R	JW443	2009 Dec	13346	69	364
SHL30-12.1C	JW443	2009 Dec	12672	30	176
SHL30-12.2I	JW443	2009 Dec	11835	60	313
SHL30-11.1C	JW443	2009 Dec	12173	119	431
SHL30-11.2T	***JW443***	***2009 Dec***	***11437***	***94***	***370***
SHL30-13.1C	JW443	2009 Dec	12057	104	440
SHL30-13.2T	JW443	2009 Dec	11755	82	342
SHL30-14.1C	JW443	2009 Dec	9163	37	100
SHL30-14.2T	JW443	2009 Dec	14887	16	135
SHL33-1.1C	JW443	2009 Dec	10870	1098	2019
SHL33-1.2R	JW443	2009 Dec	12403	559	1311
SHL33-2.1E	JW443	2009 Dec	9656	20	47
SHL33-2.2I	JW443	2009 Dec	11348	45	76
SHL33-3.1C	JW443	2009 Dec	7741	481	1152
SHL33-3.2T	JW443	2009 Dec	13732	60	238
SHL33-4.1T	JW443	2009 Dec	12221	217	608
SHL33-4.2C	***JW443***	***2009 Dec***	***7532***	***1360***	***922***
SHL34Z-1.1C	JW392	2008 Aug	9071	62	164

Spot ID	Mount	Date Analyzed	Hf ppm	Th ppm	U ppm
SHL34Z-1.2I	JW392	2008 Aug	12166	90	570
SHL34Z-1.3E	JW392	2008 Aug	12624	98	409
SHL34Z-2.1I	JW392	2008 Aug	8351	131	156
SHL34Z-3.1I	JW392	2008 Aug	10471	105	180
SHL34Z-3.2I	JW392	2008 Aug	10266	18	54
SHL34Z-3.3E	JW392	2008 Aug	12973	99	301
SHL34Z-4.1E	JW392	2008 Aug	11144	133	359
SHL34Z-4.2C	JW392	2008 Aug	9003	65	115
SHL34AZ-1.1I	JW393	2008 Aug	13589	36	337
SHL34AZ-1.2E	JW393	2008 Aug			
SHL34AZ-2.1E	JW393	2008 Aug	11628	174	417
SHL34AZ-2.2I	JW393	2008 Aug	13387	230	1276
SHL34AZ-3.1E	JW393	2008 Aug	11299	86	302
SHL34AZ-3.2IE	JW393	2008 Aug	9504	59	89
SHL34AZ-3.3I	JW393	2008 Aug	9866	8	25
SHL34AZ-4.1I	JW393	2008 Aug	11739	88	378
SHL34AZ-5.1I	JW393	2008 Aug	12387	106	621
SHL34AZ-6.2I	JW393	2008 Aug	8683	143	176
SHL34AZ-7.1I	JW393	2008 Aug	8756	163	240
SHL34AZ-7.2E	JW393	2008 Aug	9627	228	390
SHL34AZ-8.1I	JW393	2008 Aug	8613	95	131
SHL34AZ-9.1I	JW393	2008 Aug	7936	262	243
SHL34AZ-10.1I	JW393	2008 Aug	12301	151	769
SHL34AZ-11.1I	JW393	2008 Aug	12827	254	790
SHL34AZ-11.2E	JW393	2008 Aug	11624	157	350
SHL34AZ-12.1I	JW393	2008 Aug	8636	93	126
SHL36E-1.1I	JW443	2009 Dec	12073	58	352
SHL36E-1.2C	JW443	2009 Dec	10838	50	226

Spot ID	Mount	Date Analyzed	Hf ppm	Th ppm	U ppm
SHL36E-1.3I	JW443	2009 Dec	13518	308	1004
SHL36E-1.4R	JW443	2009 Dec	15767	60	449
SHL36E-2.1C	JW443	2009 Dec	12482	184	661
SHL36E-2.2T	JW443	2009 Dec	12802	93	489
SHL36E-3.1C	***JW443***	***2009 Dec***	***8281***	***833***	***2057***
SHL36E-3.2I	JW443	2009 Dec	14113	363	482
SHL36E-3.3T	JW443	2009 Dec	13776	200	761
SHL36E-4.1C	JW443	2009 Dec	12507	33	267
SHL36E-4.2T	JW443	2009 Dec	11453	69	432
SHL36E-5.1C	JW443	2009 Dec	11782	24	163
SHL36E-6.1R	JW443	2009 Dec	13528	85	521
SHL36E-6.2C	JW443	2009 Dec	10991	51	230
SHL36E-7.1I	JW443	2009 Dec	13607	57	448
SHL36E-7.2R	JW443	2009 Dec	13163	49	348
SHL36E-8.1C	JW443	2009 Dec	13981	97	738
SHL36E-8.2R	JW443	2009 Dec	14821	273	1009
SHL36E-9.1C	***JW443***	***2009 Dec***	***12146***	***1907***	***2810***
SHL36E-9.2R	JW443	2009 Dec	17599	262	2414
SHL36E-10.1I	***JW443***	***2009 Dec***	***12486***	***161***	***555***
SHL36EX-11.1C	***JW443***	***2009 Dec***	***14804***	***64***	***534***
SHL36E-11.2I	JW443	2009 Dec	15765	51	455
SHL36E-11.3R	JW443	2009 Dec	13288	213	850
SHL36E-12.1C	JW443	2009 Dec	12212	64	375
SHL36E-12.2R	JW443	2009 Dec	12425	45	300
SHL36E-12.3R	JW443	2009 Dec	14260	75	513
SHL36E-13.1I	JW443	2009 Dec	12761	447	851
SHL36E-13.2R	JW443	2009 Dec	14050	53	355
SHL36E-14.2C	JW443	2009 Dec	9535	1028	1717
SHL36E-14.3I	JW443	2009 Dec	12040	127	374
SHL36E-14.1T	JW443	2009 Dec	13166	166	937

Spot ID	Mount	Date Analyzed	Hf ppm	Th ppm	U ppm
SHL37P-1.1C	JW443	2009 Dec	12258	64	345
SHL37P-1.2I	JW443	2009 Dec	11918	60	310
SHL37P-1.3R	JW443	2009 Dec	10810	69	302
SHL37P-2.1C	JW443	2009 Dec	11426	29	187
SHL37P-2.2I	JW443	2009 Dec	12278	80	391
SHL37P-2.3R	JW443	2009 Dec	12751	73	398
SHL37P-14.1C	JW443	2009 Dec	9538	58	244
SHL37P-14.2R	JW443	2009 Dec	12538	129	500
SHL37P-3.1C	JW443	2009 Dec	11874	155	327
SHL37P-3.2I	***JW443***	***2009 Dec***	***12879***	***27***	***149***
SHL37P-3.3R	JW443	2009 Dec	12690	71	399
SHL37P-4.1R	JW443	2009 Dec	10887	271	774
SHL37P-4.2C	JW443	2009 Dec	13872	32	348
SHL37P-4.3I	JW443	2009 Dec	13448	34	200
SHL37P-5.1C	JW443	2009 Dec	12792	127	563
SHL37P-5.2I	JW443	2009 Dec	12553	424	1171
SHL37P-5.3T	***JW443***	***2009 Dec***	***13147***	***51***	***312***
SHL37P-6.1I	JW443	2009 Dec	13290	57	366
SHL37P-6.2C	JW443	2009 Dec	11501	47	281
SHL37P-6.3R	JW443	2009 Dec	12692	38	229
SHL37P-7.1R	JW443	2009 Dec	12104	39	248
SHL37P-7.2C	JW443	2009 Dec	11866	85	422
SHL37P-7.3T	JW443	2009 Dec	14417	147	774
SHL37P-7.4C	JW443	2009 Dec	14632	21	188
SHL37P-8.1I	JW443	2009 Dec	13114	23	200
SHL37P-8.2C	***JW443***	***2009 Dec***	***7978***	***4526***	***3468***
SHL37P-8.3R	JW443	2009 Dec	13992	181	1121
SHL37P-15.1C	JW443	2009 Dec	11013	20	120
SHL37P-15.2T	JW443	2009 Dec	12466	71	400
SHL37P-9.2R	JW443	2009 Dec	11798	126	443

Spot ID	Mount	Date Analyzed	Hf ppm	Th ppm	U ppm
SHL37P-9.1C	JW443	2009 Dec	10360	178	259
SHL37P-10.2R	JW443	2009 Dec	11879	42	274
SHL37P-10.1I	JW443	2009 Dec	13151	21	149
SHL37P-11.1C	***JW443***	***2009 Dec***	***11007***	***153***	***684***
SHL37P-11.2I	JW443	2009 Dec	12554	513	1296
SHL37P-11.3I	JW443	2009 Dec	11385	53	257
SHL37P-11.4R	***JW443***	***2009 Dec***	***10986***	***419***	***880***
SHL37P-12.1C	JW443	2009 Dec	11278	64	338
SHL37P-12.2I	***JW443***	***2009 Dec***	***12285***	***375***	***1360***
SHL37P-12.3T	JW443	2009 Dec	12520	144	888
SHL37P-13.1C	JW443	2009 Dec	9989	206	608
SHL37P-13.2T	JW443	2009 Dec	12765	111	383
SHL0849AZ-1.1I	JW414	2009 Jan	7191	149	185
SHL0849AZ-1.2E	JW414	2009 Jan	8105	120	164
SHL0849AZ-2.1E	JW414	2009 Jan	8603	90	145
SHL0849AZ-3.1E	JW414	2009 Jan	8323	106	161
SHL0849AZ-4.1E	JW414	2009 Jan	7451	35	70
SHL0849AZ-4.2C	JW414	2009 Jan	7480	114	175
SHL0849AZ-4.3E	JW414	2009 Jan	8090	63	126
SHL0849AZ-5.1I	JW414	2009 Jan	8138	97	150
SHL0849AZ-6.1I	***JW414***	***2009 Jan***	***8072***	***195***	***252***
SHL0849AZ-7.1C	JW414	2009 Jan	7499	179	232
SHL0849AZ-8.1E	JW414	2009 Jan	7873	218	264
SHL0849AZ-9.1E	JW414	2009 Jan	8229	189	242
SHL0849AZ-9.2I	JW414	2009 Jan	8535	72	114
SHL0849AZ-10.1C	JW414	2009 Jan	8278	96	153
SHL0849AZ-11.1I	JW414	2009 Jan	8109	14	41
SHL0849AZ-11.2E	JW414	2009 Jan	8019	55	98
SHL0849AZ-12.1E	JW414	2009 Jan	8085	127	182

Spot ID	Mount	Date Analyzed	Hf ppm	Th ppm	U ppm
SHL0849AZ-12.2C	***JW414***	***2009 Jan***	***7600***	***87***	***139***
SHL0849AZ-13.1E	JW414	2009 Jan	11511	46	175
SHL0849AZ-13.2I	JW414	2009 Jan	11833	157	483
SHL0849AZ-13.3C	***JW414***	***2009 Jan***	***10729***	***97***	***497***
SHL49AZ-14.1C	JW414	2009 Jan	7514	223	261
SHD9-1.1R	JW443	2009 Dec	12150	55	230
SHD9-2.1R	JW443	2009 Dec	10311	234	576
SHD9-2.2C	JW443	2009 Dec	8693	148	294
SH325.2-1.1DGZT	JW309	2007 May	13040	326	899
SH325.2-1.2MGZC	JW309	2007 May	12091	48	281
SH325.2-1.3LGZI]	JW309	2007 May	10381	37	192
SH325.2-2.1MGZC	JW309	2007 May	11749	71	286
SH325.2-2.2LGZI	JW309	2007 May	13578	16	132
SH325.2-3.1LGC	***JW309***	***2007 May***	***12155***	***82***	***380***
SH325.2-3.2DGZE	JW309	2007 May	11818	249	660
SH325.2-4.1DGZE	***JW309***	***2007 May***	***10996***	***185***	***773***
SH325.2-4.2MGC	***JW309***	***2007 May***	***11326***	***117***	***475***
SH325.2-5.1MGZE	JW309	2007 May	12022	52	359
SH325.2-5.2DGZI	***JW309***	***2007 May***	***10932***	***73***	***357***
SH325.2-5.3DGZE	***JW309***	***2007 May***	***12819***	***160***	***845***
SH325.2-6.1MGT	JW309	2007 May	10319	21	78
SH325.2-6.2MGI	JW309	2007 May	11745	17	70
SH325.2-7.1LGZT	JW309	2007 May	11895	175	492
SH325.2-7.2DGZT	JW309	2007 May	16122	85	412
SH325.2-7.3LGZC	JW309	2007 May	11903	112	516
SH325.2-8.1MGZE	JW309	2007 May	11850	69	434
SH325.2-8.2MGZC	JW309	2007 May	11681	136	555

Spot ID	Mount	Date Analyzed	Hf ppm	Th ppm	U ppm
SH325.2-8.3DGZT	JW309	2007 May	12172	136	551
SH325.2-9.1MGC	JW309	2007 May	11541	86	421
SH325.2-10.1MGZI	JW309	2007 May	10001	121	417
SH325.2-11.1DGZE	***JW309***	***2007 May***	***11900***	***389***	***560***
SH325.2-11.1MGC	***JW309***	***2007 May***	***9466***	***131***	***84***
SH325.2-12.1MGZT	JW309	2007 May	11520	199	233
SH325.2-12.2MGZI	***JW309***	***2007 May***	***11377***	***121***	***155***
SH325.2-13.1DGZT	JW309	2007 May	11378	123	159
SH325.2-13.1T	***JW309***	***2007 May***	***11704***	***159***	***234***
Z484A-10.1C	JP04	2008 Jan	11487	28	181
Z484A-10.2IR	JP04	2008 Jan	14155	83	589
Z484A-10.3T	JP04	2008 Jan	12546	63	283
Z484A-12.1I	JP04	2008 Jan	10764	94	140
Z484A-12.2EM	JP04	2008 Jan	12805	118	577
Z484A-12.3T	JP04	2008 Jan	11994	30	157
Z484A-14.1C	***JP04***	***2008 Jan***	***8086***	***2285***	***1689***
Z484A-16.1C	JP04	2008 Jan	10360	19	108
Z484A-16.2I	JP04	2008 Jan	11454	83	383
Z484A-17.1C	JP04	2008 Jan	10852	157	597
Z484A-17.2T	JP04	2008 Jan	13158	217	660
Z484A-18.1C	JP04	2008 Jan	14967	24	376
Z484A-18.2IR	JP04	2008 Jan	13935	45	272
Z484A-19.1T	JP04	2008 Jan	13013	43	271
Z484A-19.2C	JP04	2008 Jan	10614	33	167
Z484A-19.3IR	JP04	2008 Jan	11143	62	295
Z484A-19.4IR	JP04	2008 Jan	13282	73	443
Z484A-2.1T	JP04	2008 Jan	10135	94	252
Z484A-2.2C	JP04	2008 Jan	12100	229	853
Z484A-4.1I	***JP04***	***2008 Jan***	***8610***	***3089***	***2713***

Spot ID	Mount	Date Analyzed	Hf ppm	Th ppm	U ppm
Z484A-4.2T	JP04	2008 Jan	12010	49	217
Z484A-5.1I	***JP04***	***2008 Jan***	***14018***	***74***	***391***
Z484A-8.1I	***JP04***	***2008 Jan***	***6217***	***2126***	***1830***
Z484A-8.2I	JP04	2008 Jan	9393	498	617

APPENDIX G

PRE AND POST TEST AND STUDENT HANDOUT FOR LABORATORY ACTIVITY

Pre/Post Test

1. What do we most commonly use to determine the absolute age of a rock or mineral?
   a) stratigraphic relations
   b) fossils
   c) radioactive decay

2. What controls how much decay occurs in any given radioactive system?
   a) the decay constant of the parent isotope
   b) the amount of parent
   c) the amount of time that has passed
   d) a & c
   e) a, b & c

3. True or False: The basic form of the decay equation is the same for different isotopic systems (i.e. U-Pb or K-Ar).
   a) true
   b) false

4. Consider the following diagrams, and imagine that each block represents a bucket containing some amount of a parent or daughter isotope. Both systems A & B are the same isotopes (U-Pb, for example) Considering a typical situation with no complexities, which has been decaying longer, parent A or B? Circle one.

Parent A **Daughter A** **Parent B** **Daughter B**

5. Give two conditions for which the answer you gave in 4 might be different.

6. On a scale of 1 to 10, 1 being least confident and 10 being completely confident, how confident are you in your understanding of radioactive decay and its use in dating?

Laboratory Activity: Radioactive Decay and Radiometric Dating

USEFUL TERMS & CONCEPTS

radioactive decay
decay constant
decay rate
half-life
parent isotope
daughter isotope

Instructions:

For the following activities, consider the shampoo in the upper beaker to be the parent isotope, and the shampoo in the lower beaker to be the daughter isotope. The size of the hole is proportional to the decay constant for the system.

Run 1:

- Place the beaker with the smaller diameter hole into the beaker stand, directly over the beaker with no hole.
- Insert the stopper into the hole.
- Pour 5 cm of shampoo into the upper beaker.
- Remove the stopper, allowing the shampoo to run into the lower beaker. One person be in charge of timing, and announce to the group each 30 second interval. Record the depth of shampoo in the upper beaker at each 30 second interval in the table below. Allow the experiment to run for 5 minutes, or until a majority of the shampoo has passed through.

Run 2:

- Clean out the lower beaker with the spatula (return all shampoo to the original beaker).
- Repeat the experiment with the upper beaker with the larger diameter hole and 5 cm of shampoo.

Run 3:

- Clean out the lower beaker with the spatula (return all shampoo to the original beaker).
- Repeat the experiment with the upper beaker with the smaller diameter hole and 8 cm of shampoo.

RUN 1:

Time (min)	Parent/Upper depth (cm)
0	
0.5	
1.0	
1.5	
2.0	
2.5	
3.0	
3.5	
4.0	
4.5	
5.0	
5.5	
6.0	

RUN 2:

Time (min)	Parent/Upper depth (cm)
0	
0.5	
1.0	
1.5	
2.0	
2.5	
3.0	
3.5	
4.0	
4.5	
5.0	
5.5	
6.0	

RUN 3:

Time (min)	Parent/Upper depth (cm)
0	
0.5	
1.0	
1.5	
2.0	
2.5	
3.0	
3.5	
4.0	
4.5	
5.0	
5.5	
6.0	

While one or two group members enter the data into excel (Data Synthesis step below), other members of the group can perform this task.

Set up to begin a run like RUN 1 again with 5 cm of parent and the smaller hole. Start the timer and remove the stopper. After several minutes at a time of your choosing (before the run has gone to completion), insert the stopper into the hole. Record the time that passed on an index card and turn it face down beside your setup. Leave the setup in this condition for now, while you complete the data synthesis.

Data Synthesis (in Excel):

For each run:

- Enter the data into excel in a form like the above tables.
- Create a line graph with time on the x axis and depth on the y axis.
- Add a trendline to the line representing the parent isotope, and show the equation… this is the decay equation for your system!! Use this to answer the questions below.

Questions:

1. Considering how the 3 runs varied and which were faster/slower, what 3 things determine how much decay occurs in an isotopic system?

2. For Run 1:
   a. What is the decay equation? _____
   b. What is the initial parent (N_0)? _____
   c. What is the decay constant (λ)? _____

3. For Run 2:
   a. What is the decay equation? _____
   b. What is the initial parent (N_0)? _____
   c. What is the decay constant (λ)? _____

4. For Run 3:
   a. What is the decay equation? _____
   b. What is the initial parent (N_0)? _____
   c. What is the decay constant (λ)? _____

5. Using the form of your 3 equations above, write a general decay equation, using "N" for "number of atoms", "N_0" for "initial number of atoms," using "λ" for the decay constant, and using "t" for 'time."

Radiometric Dating Activity:

Now, move one table clockwise. You are going to "date" the experiment of another group. Measure the amount of parent/daughter in these beakers. Using your equations from RUN 1 and what you just measured, calculate an age for this system. Turn over the index card and check your answer. You will have to rearrange your decay equation to solve for time (t).

Solve decay equation for time:

Calculated time: _____

Measured time (from card): _____

Synthesis Questions:

You know that the amount of shampoo moving through the hole increased with a larger hole and with more shampoo in the upper beaker. This means that the AMOUNT of radioactive decay increases with larger decay constant and with more initial parent. But you know that the RATE of decay is constant for any given isotope, as evidenced by the fact that any given isotope has a set half-life. Explain.

During these experiments, you always knew what the initial parent was. <u>For the next 3 questions</u>, consider how the system works if you don't know the amount of initial parent.

If you didn't know the amount of initial parent, how could you determine the age?

How would it affect the age determination if some of the daughter product was somehow lost from the rock or mineral? Think about how it would affect your date if some of the shampoo had leaked out of the lower beaker when you went to date someone else's experiment (not knowing the initial parent).

How would it affect the age determination if some daughter product already existed in the rock or mineral when it was formed? Think about how it would affect your date if there had initially been a centimeter or two of shampoo in the lower beaker when you went to date someone else's experiment (not knowing the initial parent).